Agronomy Research

Established in 2003 by the Faculty of Agronomy, Estonian Agricultural University

Aims and Scope:

Agronomy Research is a peer-reviewed international Journal intended for publication of broad-spectrum original articles, reviews and short communications on actual problems of modern biosystems engineering incl. crop and animal science, genetics, economics, farm- and production engineering, environmental aspects, agro-ecology, renewable energy and bioenergy etc. in the temperate regions of the world.

Copyright & Licensing:

Agronomy Research online:

Agronomy Research is available online at: https://agronomy.emu.ee/

Acknowledgement to Referees:

The Editors of *Agronomy Research* would like to thank the many scientists who gave so generously of their time and expertise to referee papers submitted to the Journal.

Abstracted and indexed:

SCOPUS, EBSCO, DOAJ, CABI Full Paper and Clarivate Analytics database: (Zoological Records, Biological Abstracts and Biosis Previews, AGRIS, ISPI, CAB Abstracts, AGRICOLA (NAL; USA), VINITI, INIST-PASCAL.)

Subscription information:

Institute of Technology, EMU
Fr.R. Kreutzwaldi 56,
51006 Tartu,
ESTONIA
e-mail: timo.kikas@emu.ee

Journal Policies:

Estonian University of Life Sciences, Latvia University of Life Sciences and Technologies, Vytautas Magnus University Agriculture Academy, Lithuanian Research Centre for Agriculture and Forestry, and Editors of *Agronomy Research* assume no responsibility for views, statements and opinions expressed by contributors. Any reference to a pesticide, fertiliser, cultivar or other commercial or proprietary product does not constitute a recommendation or an endorsement of its use by the author(s), their institution or any person connected with preparation, publication or distribution of this Journal.

ISSN 1406-894X

CONTENTS

Agronomy Research **22**(2), 733–749, 2024
https://doi.org/10.15159/AR.24.081

Assessment of salt resistance of some potato varieties by biochemical and RFLP markers

M.V. Badalyan[1], T.B. Aloyan[1,*], V.T. Dilanyan[1], S.A. Kharatyan[2], H.S. Martirosyan[1], A.J. Sahakyan[1], N.A. Sahakyan[1], A.Sh. Melikyan[1]

[1]Scientific Center of Agrobiotechnology, ANAU Armenian National Agrarian University, Teryan 74, AM0009 Yerevan, Armenia
[2]Scientific Centre for Risk Assessment and Analysis in Food Safety Area, 107/2 of Masis Highway, AM0071Yerevan, Armenia
[*]Correspondence: tatevaloyan22@gmail.com

Received: April 19th, 2024; Accepted: August 7th, 2024; Published: August 26th, 2024

Abstract. Continuous changes in climate, desertification, reduction of arable land, increase in salted land, in the conditions of continuous growth of the population, the problem of providing food and food security to humanity arises, the solution of which is one of the challenges of the 21st century that requires universal efforts. At the same time, abiotic stresses, which are the cause of 50% of global yield losses, are the motivation for the creation of new stress-resistant varieties of crops using modern technologies. The salt resistance of that idea as a physiological manifestation with a polygenic component is characteristic in the modern processes of selection management.

This work presents studies of salt tolerance of three valuable varieties of potatoes cultivated in Armenia, using biochemical and DNA-markers. Classical agronomic, molecular-biological, genetic-mathematical methods are used in the researches. In order to induce salt stress and provocation background in plants, 50, 100 and 150 mmol solutions of NaCl were used.

The results have shown that 11S-globulin of all varieties are polymorphic, forming different electrophoresis spectra and protein formulas. It is also evident that plants with different spectra of the same varieties react differently to salt stress. The DNA restriction regions of the salt-resistant variants are significantly longer than those of the non-salt-resistant forms. Thanks to the biochemical and RFLP markers, it has been possible to establish salt tolerance loci, to identify and list plants with a salt-tolerant spectrum of the same variety, which can be nominated as new salt-tolerant varieties for breeding stock producers.

Key words: DNA restriction fragment, electrophoresis spectrum, protein formula, restriction enzyme, salt stress.

INTRODUCTION

Abiotic stresses such as high temperature, drought, frost and salinity stress threaten agriculture, especially affecting yield. These factors are the main cause of crop loss worldwide, reducing more than 50% of the world's harvest (Boyer, 1982; Askari & Pepoyan, 2015; Bray et al., 2000; Sassine et al., 2022).

It is known that only 10% of the world's arable land is free from stress factors, 20% is exposed to mineral stress, 26% to drought and 15% to frost. 10% of the earth's surface is occupied by saline soils, the surface of which is especially large in dry zones. Also, it is considered that not less than 25%, maybe 50%, of the 270 million ha of irrigated land is secondary to salinization (Zhuchenko, 2001; Schroeder et al., 2013; Luo et al., 2017).

Soil salinization is one of the most common abiotic stresses in terms of negative impact on area and plant productivity (Munns & Tester, 2008). The factors that cause salinity are diverse and include not only the characteristics of soils and their composition, but also climate, terrain, and human activities. Besides, climate change brings predictions of the development of an undesirable situation (Novikova et al., 2021). Moreover, even such an agricultural approach as the use of fresh water from different sources for irrigation only exacerbates the problem, the solution of which is increasingly difficult (Pankova et al., 2017).

The effect of soil salinity on plant characteristics is diverse. It is expressed not only by changes in the biomass accumulation rate, the total and economic productivity of different crops, but also by the effect of physiology and biochemistry on the quality of the crop of plants (Parvaiz, 2008; Agarwal et al., 2013; Torabi, 2014; Sajyan et al., 2018).

Very often the cause of soil salinization is also improper irrigation, immoderate use of mineral fertilizers, constant growth of soil-soluble waste (Shrivastava & Kumar, 2015).

In the process of salinization, different salts accumulate in the soil, which are various combinations of Na^+, Mg^{2+}, Ca^{2+} cations and Cl^-, SO_4^{2-}, CO_3^{2-} anions, of which NaCl is of great importance due to its widespread scale and high concentration.

Large amounts of salts in the soil have a toxic effect on plants, even destructive.

As a result of salinization, water penetration becomes difficult, metabolism is disturbed. Due to the violation of nitrogen conversion, toxic substances, such as ammonia, accumulate in plants (Fricke, 2004). The harmful effect of salts first of all negatively affects the root system. Under the influence of salts, the transparency of the cytoplasm increases, transpiration becomes excessively intense. The harmful effect of salt concentrations in the soil is due to the high osmotic pressure caused by the excess of salts in the soil solutions and the associated water absorption difficulties (osmotic effect of salinization) (Munns & Tester, 2008). In connection with this, only those groups of plant organisms can develop regularly in the saline soils, in which the appropriate adaptation properties have been developed and strengthened under the influence of salinization in the process of evolution (Levy & Veilleux, 2007; Tian et al., 2022).

Salt tolerance is a physiological feature of halophytes in terms of obtaining water from soil solutions with high osmotic pressure, the protoplasm of such plants is endowed with high transparency for electrolytes (Levy & Veilleux, 2007; Munns & Tester, 2008; Shabala, 2013; Meng et al., 2018; Zhang et al., 2018; Han et al., 2023; Mann et al., 2023).

The most important physiological manifestation of salt tolerance is the accumulation of a large number of teratogenic substances (organic acids, sugars, etc.) in the cell sap (Fricke, 2004; Polle & Chen, 2015; Assaha et al., 2017; Shahid et al., 2020).

The composition of plants to survive under high NaCl concentrations is related to their ability to transport, partition, release and mobilize Na+ ions (Assaha et al., 2017; Alharbi et al., 2022; Wang et al., 2022).

It is obvious that salt tolerance of plants is a physiological process with multigenic manifestation, the basis of which is gene expression, during which the information of genes is transformed into a material performing a certain function, RNA or protein.

These genes that are up-regulated more than 5-fold under salt and stress may be AP2-EREBP (ATERF11, CBF4 / DREB1D, CBF1 / DREB1B, ATERF4 / RAP2.5, DREB2A, CBF1 /DREB1B, DREB12A), - Helix-Loop-Helix (bHLH) family (AtbHLH17), leucine buckle (AtbZIP55 / GBF3), C2H2 family (ZAT10, ZAT12 / RHL41, ZAT6 and ZAT102 / RHL41), heat stress (Home-Box7E) family.) and and, to the NAC family (ANAC036, ANAC029 / ATNAP, ANAC055 / ATNAC3, ANAC047, ANAC072 / RD26, ANAC002 / ATAF1, ANAC019 and ANAC032). These transcription factors are induced in response to salt stress signals transmitted through sensing and signalling molecules; then the complex gene regulatory systems consisting of transcription factors and other proteins that control the expression of many genes (Huang et al., 2006; James et al., 2006; Byrt et al., 2007; Møller et al., 2009; Shokri-Gharelo & Noparvar, 2018).

Armenia occupies not much of the north-eastern part of the Armenian volcanic highlands. In the territory of Armenia, the saline soils were formed in those parts of the Ararat plain, where the groundwater is mineralized and is on the surface of the soil (1–2 m) hectare (Manukyan & Karapetyan, 2011).

Their total area is about 29 thousand hectares. In the Ararat Valley, there are favorable soil and climate conditions for farming, particularly for the cultivation of vegetable crops, orchards and vineyards, and for obtaining a high and quality yield from them.

As a crop of global importance, potato occupies a key place in the fields of agriculture and culture of Armenia, earning the name second 'bread', as it is second only to cereals in terms of its gross output.

The commercial varieties of potatoes cultivated in Armenia are mainly imported from abroad and do not have much resistance to salt stress, which is often the reason for low yields.

It is obvious that the multigenic character of salt tolerance and the existence of new different types create difficulties in the breeding works carried out in that direction. In addition, the main emphasis was placed on useful economic characteristics (yield) in potato breeding works.

At the same time, it should be noted that imported potato varieties, even if they had highly expressed genes for salt tolerance, may not be expressed in case of changes in climatic conditions, and this is the main reason why salt-tolerant varieties should be created for specific agro-ecosystems. Moreover, the response of plants with different genotypes within the same variety to stress factors is incompletely studied or absent, which is important in the process of breeding in a very specific direction. Very often, organisms with the same genotype have different phenotypic manifestations depending on paratypic factors (Verhoeven et al., 2008).

Among the markers (phenotypic, protein or biochemical, cytogenetic, DNA or molecular) used for the assessment of genetic diversity of plants (Kanukova et al., 2019), due to their simplicity, efficiency, speed, availability and most importantly, high efficiency and applicability, protein and DNA markers were selected by us.

The electrophoretic spectrum and protein formula of 11S-globulin, a common and rather well-studied storage protein in dicotyledonous plants, was used as a protein marker. Proteins, as a result of the coding of genomic DNA loci, are not only not inferior in their molecular capabilities, but also very often have a number of advantages over other markers. They are based on multiple allelism of genes, hence polymorphism.

The study of the electrophoretic spectrum of 11S-globulin makes it possible to clarify the frequency of alleles and genotypes in populations, origin, genetic similarity, evolution, the level of manifestation of useful economic and biological traits, the degree of heterozygosity, etc., which can be applied in the fields of starting material evaluation, breeding, variety testing, seed production and genetic engineering (Konarev, 2007; Kononenko et al., 2019).

The RFLP (Restriction Fragment Length Polymorphism) DNA marker is used in our research as a DNA marker. The basis of the RFLP method is the separation of DNA restriction segments of different lengths by electrophoresis, which are generated when the double-stranded DNA molecule is cleaved by restriction enzymes. At the same time, the placement of restriction sites of the same enzyme in the DNA segment of different species or cultivars is different, or at the same time, it is polymorphic, which is a species characteristic and has a hereditary nature. The RFLP method provides an opportunity to construct a map of the restriction segments of the DNA of various organisms. The advantage of RFLP markers compared to other DNA markers is that the information contained in them can be used by cloning the corresponding restriction fragment of DNA. Moreover, the results of the analysis of the relevant segment can be used to obtain STS from the given segment of the genome. The construction of restriction maps also does not require prior cloning of the DNA under study.

In addition, in the DNA-bank or gene library of the 'Scientific Center of Agrobiotechnology' branch of the Armenian National Agrarian University /ANAU/, restriction fragments of the genomic DNA and genetic constructions of a number of valuable crops and their wild relatives are preserved, with the aim of obtaining new high-yielding and stress-resistant varieties and improving the existing ones using agrobacterial transformation (Badalyan et al., 2023).

In fact, plants with different genotypes of the same variety can show greater or lesser tolerance to salt stress. From that point of view, our studies aimed to identify the most stable genotypes of Impala, Madeline and Arizona potato varieties cultivated in Armenia under salt stress conditions of 50, 100 and 150 mmol of NaCl. The results will be used to obtain new salt-resistant potato varieties through agrobacterial transformation (cisgenesis) and to improve existing ones.

MATERIALS AND METHODS

Experiments and studies were carried out in 2021–2023, in the 'Scientific Center of Agrobiotechnology' branch of the ANAU. Impala, Arizona and Madeline varieties of potatoes (*Solanum tuberosum* L.), which are widely cultivated in Armenia, were used as a test sample. Experiments and researches were carried out in 4 stages.

First stage: Marking was carried out within each variety and formation of experimental groups. Randomly selected 500 plants (from each variety) certified according to the electrophoresis spectrum of the 11S-globulin storage protein, as a result forming experimental groups, each with 20 plants.

A number of crops, including potato tubers, also contain albumin, whose electrophoresis mobility (RF) is close to that of globulin and is often a source of confusion.

In order to disable the globulin, it was carried out:

- Cryoprecipitation – for this purpose, 10 parts of 0.2 M NaCl solution was added to 1 part of the sample and kept at 4 °C for 2 hours. Then cold distilled water was added

to the supernatant containing albumin and globulin at a ratio of 1:10 and stored in a refrigerator at 4 °C for 2 hours to precipitate globulin. Then the precipitate is dissolved in buffer (0.4 g Tris, 3 mL 1 M HCl, 1 g sodium dodecyl sulfate, 5 g sucrose, 18 g urea, 2.5 mL mercaptoethanol, 0.25 g bromophenol blue, and 100 mL distilled water), in a ratio of 1:1.

- Preparation of the gel – 12.5% resolving gel contains 12.5 g acrylamide, 0.25 g bisacrylamide, 4 g Tris, 0.1 g SDS, 0.3 g ammonium persulfate, 0.28 mL TEMED (per 100 mL gel). The pH of the solution was adjusted to 8.8 with 1 M HCl. The stacking gel (5%) contains 5 g acrylamide, 0.13 g bisacrylamide, 0.24 g Tris, 0.1 g SDS, 0.02 g ammonium persulfate, 0.15 mL TEMED (per 100 mL gel). The pH of the solution was adjusted to 6.8 with 1M HCl (Konarev, 2007).

Electrophoresis was carried out by the Davis method on a 12.5% polyacrylamide gel with Multigel-long phoresis apparatus of the German company Biometra (Table 1) (Davis, 1964).

Table 1. Necessary conditions for electrophoresis of 11S-globulin protein

Protein	Gel (%)	Gel length (cm)	Sample titer	Buffer		Current voltage (V)	Duration of phoresis (hour)
				Gel	Electrode		
11S-Globulin	12.5	12	1:1	0.05 M Tris HCl, pH = 8.8	0.025 M Tris-glycine, pH = 8.3	230	1.5

After completion of phoresis, the gel was fixed for 60 min in ethanol, acetic acid, distilled water solution (40:10:60), then it was stained with Kummas G-250 dye for 30–60 minutes, then it was washed 3 times with washing buffer (10% solution of acetic acid).

The results of phoresis were compared with the reference spectrum of 11S-globulin. The frequency of meeting of electrophoretic spectra was calculated as follows by formula $P_i = \frac{n}{N}$, where P_i is the frequency of the spectrum and n is the frequency of the spectrum the number of plants, N is the total number of investigated plants.

Second stage: According to the electrophoresis spectrum of 11S-globulin and the decoded protein formulas, further cultivation of experimental groups was carried out by *in vitro* cultivation (Murashige, 1974). Potato tubers have been planted in a 3:1 mixture of peat. After sufficient growth of the stems, the stems with 3–4 leaf buds were harvested. For the purpose of sterilization, the samples were washed in 70% alcohol for 1–2 minutes, after which were washed with sterile distilled water. Sterilized sprouts were crushed to 0.5–0.8 mm size and placed in test tubes containing 10 mL of MS and various growth promoters. Test tubes with samples were kept in the laboratory under conditions of 27 ± 2 °C and 16 hours a day be illuminated by fluorescent lamps (2,000–3,000 lux).

Third stage: The transplantation of *in vitro* grown plants was carried out in soil (peat, soil and sand: 3:1:3). Ten-twelve-day-old acclimatized plants were exposed to NaCl 50, 100, 150 mmol salt stress within two months. For each version of the saline situation were determined wet weight, dry weight, height, number of tubers, shoot weight, root weight. The plants were watered with different concentrations of NaCl solution at least 1 time a day, in principle, soil moisture should be 50–53%. The genetic-mathematical analysis of the data was performed using the SPSS Statistics software package.

Fourth stage: Molecular-biological researches were carried out. In order to obtain restriction of DNA and use it as an RFLP marker, from plants with different electrophoretic spectra of studied cultivars the following works were performed:

- The extraction of DNA – The extraction of total DNA from studied plants was carried out by the SDS method according to of the guide (Padutov et al., 2007).
- DNA concentration test – The concentration of DNA in the samples was determined with a NanoDrop One spectrophotometer.
- Restriction and ligerization – The restriction of total DNA was performed by preparing a restriction mixture, with the following composition: 2 µl 10x appropriate restriction buffer, 5 µl nucleic acids free deionized water, 2 µl DNA sample, 1 µl (5 units µl) restriction enzyme. The restriction mixture was incubated at 37 °C for 5 hours. Of necessity the restriction process was stopped by adding 1 µl of 0.5 M toluene B (pH = 7.5) to the restriction mixture adding. In order to determine the restriction sequence of DNA and make maps it necessary to cleave complementary DNA with two restriction enzymes, using by Tango universal buffer.
- Electrophoresis – Quantitative DNA's restriction fragments' electrophoretic separation was performed on a 0.8% agarose gel, by Biometra company's Compact M electrophoresis apparatus.

RESULTS AND DISCUSSION

As a cross-pollinated crop, the potato stands out to a high degree with diverse cultivars endowed with genetic and biochemical variation which are seen as complex populations.

According to F. Ayala (1984) the genetic diversity degree can be estimated if protein formulas and populations are known of their occurrence frequency (Ayala, 1984). Diversity of 11S-globulin as a protein biological specificity is manifested as a result of electrophoresis, where amount and electrophoretic mobility of polypeptides are depends on characteristics and origin of genotypes (Barta et al., 2003).

At this stage of research, we aimed to find out the genetic structure of the studied potato varieties according to the electrophoretic spectrum of 11S-globulin (protein formula), because thousands of European varieties and samples of potato have been identified in this way at the International Germplasm Center (Dementyeva, 2006; Ammarelou & Lamei, 2007; Bernal et al., 2019).

The 11S-gobulin electrophoresis spectrum of Impala, Arizona and Madeline potato cultivars was compared with the reference spectrum of 11S-globulin (Fig. 1).

As a result, the protein formulas of the mentioned varieties and their meeting frequency were decoded (Table 2).

The intensity of the protein formula of each polypeptide was evaluated with points: 3 is very intense, 1 is weakly intense.

In the case of Impala (Im) potato's variety, were recorded 4 different electrophoresis spectra of 11S-globulin, which were conventionally designated Im1, Im2, Im3 and Im4, the frequency of them is high (0.18–0.31). The variety is also distinguished by a high total number of polypeptides (48), of which 48% is rated as low intensity, 23% as intense and 29% as very intense (Table 2).

11S-globulin protein of Arizona (Az) potato variety in the selected group is forming 3 types of electrophoresis spectrum (Az1, Az2, Az3), the frequency of them is ranging

from 0.16 to 0.44, total polypeptides quantity is 18 (for each type 6), 2% of which were assessed as low, 55.5% were high and 22.5% – very high intensity.

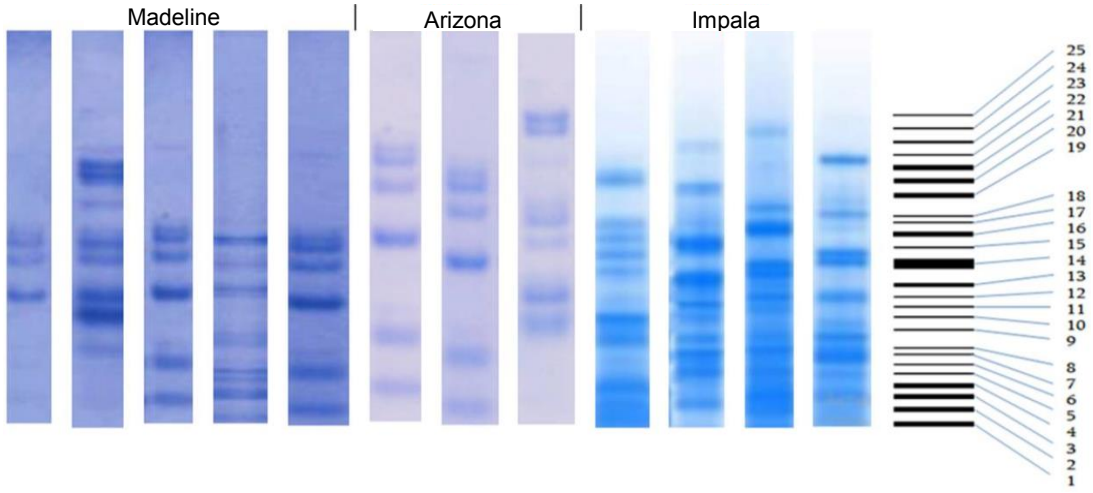

Figure 1. 11S-globulin electrophoretic spectrum of studied potato varieties according to the results of polyacrylamide gel electrophoresis.

The frequency of spectrum meeting in the selected group of Arizona potato variety was 44%, by the way, this index is the highest in the different electrophoresis types of all studied varieties (Table 2).

Table 2. Characterization of Impala, Arizona and Madeline potato cultivars by 11S-globulin electrophoresis spectrum

Varieties	Type of specrum	The frequency of meeting (n)	The number of fractions	Protein formula																							
				1	2	3	4	5	6	7	8	9	10	11	12	13	14	15	16	17	18	19	20	21	22	23	24	25
Impala (Im)	Im1	0.18	14	1	1	1		1	1	1		1	2		1		3	3	3	3			3					
	Im2	0.23	11		2			2			2	2	1	2		3		3		1		2			1		
	Im3	0.31	11		1	1		1			1	1		1	1	3	3				3						2	
	Im4	0.28	12	1		1		1		2		2		1	2		3	3	1		2			3				
Arizona (Az)	Az1	0.40	6				2					2								3			3		2	2	
	Az2	0.16	6		2					2							3				2	2	1					
	Az3	0.44	6									1			2					1	1						2	2
Madeline (Ma)	Ma1	0.28	6				1			1	1					3	2	2										
	Ma2	0.31	10			1						2		3	3		2	2			1		3	3			1	
	Ma3	0.11	7			2					2					3		2	2	2					1			
	Ma4	0.21	8	1		3		2	3			1				3	2			3								
	Ma5	0.09	8		2			2			1				3		3	3	2					1				

The 11S-globulin storage protein of the Madeline potato variety formed a 5-type spectrum in the electrophoresis field (Ma1, Ma2, Ma3, Ma4, Ma5) and the frequency of meetings this varies from 0.31 (Ma2) to 0.03 (Ma5). The total number of polypeptides was 39. The highest is 10 (Ma2), the lowest is 6 (Ma1), 28% of which were assessed as low, 38.5% as high, 33.5% as very high intensity (Table 2).

In recent years, studies based on protein markers at the A.G. Lorch Russian Potato Research Center prove that intervarietal differences in 11S-globulin spectra are clearly expressed, which makes it possible to easily distinguish the genetic diversity of the variety. In the same center, it was proved that most of the storage proteins present in tubers, due to differences in their molecular mass (35–78 kD), are considered to have slow and medium mobility. Moreover, plants with the same version of the electrophoretic spectrum also have phenotypic uniformity, except for those plants that have undergone somatic mutation and are distinguished not only by morphological indicators, but also by electrophoretic spectrum (Dementyeva, 2006).

In this regard, remarkable results were also recorded during the genotyping of other crops (Sayed Mohammad Reza Khoshroo, 2011; Mouzo et al., 2018; Nasrollahzadeh et al., 2023).

The highest frequency of the 11S-globulin electrophoresis spectrum of the potato varieties studied by us was recorded in the case of the Az3 version of the Arizona variety, it was 44%, and the lowest - in the case of the Ma5 version of the Madeline variety (9%) (Fig. 2).

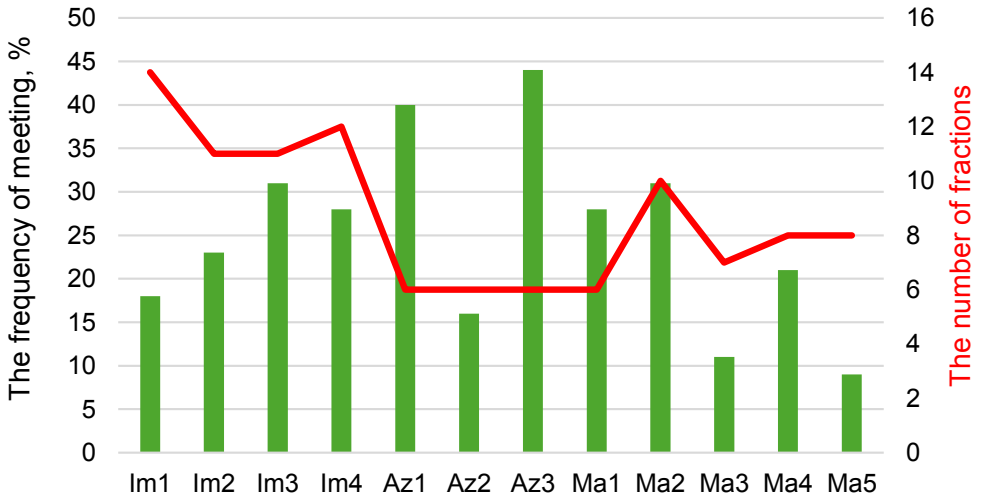

Figure 2. The frequency of meeting and number of fractions of different spectrums of potato varieties: Im 1–4 – Impala; Az 1–3 – Arizona; Ma 1–5 – Madeline.

It is obvious that in the process of evolution, plants have developed protective mechanisms against salt stress, the physiological manifestations of which have a multigenic arrangement (Askari et al., 2012; Askari & Pepoyan, 2015).

In higher plants and a number of microorganisms, the low level of Na^+ in the organism and the maintenance of the normal range of K^+/Na^+ ratio in the cytoplasm of the cells are necessary to increase the salt tolerance of plants (Ketehouli et al., 2019).

It has been established that stress proteins are active at the plasma membrane level (Horie et al., 2009), acting as transporters to remove Na^+ ions from leaves while increasing the movement of K^+ ions to cope with salt stress (Huang et al., 2006; James et al., 2006; Møller et al., 2009).

Several studies have shown that stress proteins are highly selective in transporting K^+ ions instead of Na^+ ions under salt stress conditions. Increasing calcium ion homeostasis helps maintain cytoplasmic properties and increase salt tolerance (Ardie et al., 2009; Bose et al., 2017).

The resistance of different genetic associations to salt stress within the same variety is due to the expression of genes responsible for this salt resistance (Zhang & Shi, 2013).

The studies at this stage aimed to clarify the response of different transplant plants of studied potato varieties to salt stress, taking into account a number of bio-economic characteristics.

From the results of our research, it becomes clear that different genetic associations of the studied potato varieties respond differently to salt stress, bringing some clarity to the circumstances in which the same variety exhibits different reaction rates to abiotic stresses.

Thus, among the plants with electrophoretic Im1, Im2, Im3, Im4 spectra of the Impala potato variety, the highest resistance was recorded in the case of the Im2 version in terms of all the characteristics studied at all stages of salt stress (Table 3).

Table 3. Effect of salt stress on plants with different 11S-globulin electrophoresis spectra of potato variety Impala. Numbers represent means ± standard errors

Impala	NaCl (mmol)	Wet weight (g)	Dry weight (g)	The height of plant (cm)	The number of tubers	The total weight of tuber (g)	The weight of shoot * (g)	The weight of root (g)
Im1	0	81.4 ± 06	15.5 ± 1.4	51.6 ± 0.44	7	63 ± 0.59	31 ± 0.08	8.44 ± 0.19
	50	50.7 ± 053	10.3 ± 0.8	24.7 ± 1.22	5	48 ± 0.67	17.5 ± 0.6	4.21 ± 0.7
	100	29.8 ± 1.48	7.23 ± 0.88	18.8 ± 1.55	2	15 ± 1.32	15.6 ± 1.16	3.91 ± 0.05
	150	10.4 ± 0.78	3.35 ± 1.14	14.2 ± 1.03	0	0	10.5 ± 0.41	1.1 ± 0.21
Im2	0	80.9 ± 0.53	15.31 ± 1.1	51.8 ± 0.29	7	63 ± 0.48	30.88 ± 1.13	8.19 ± 0.14
	50	62.8 ± 1.63	13.35 ± 1.3	42.5 ± 1.22	7	55 ± 1.31	25.1 ± 1.14	5.8 ± 2.8
	100	45.8 ± 0.65	11.55 ± 0.88	29.4 ± 1.66	4	28 ± 1.01	20.1 ± 1.33	3.9 ± 0.6
	150	34.5 ± 1.66	8.30 ± 0.94	18.8 ± 0.36	2	14 ± 1.14	16.6 ± 1.48	1.8 ± 0.1
Im3	0	81.0 ± 0.16	15.33 ± 1.6	50.9 ± 0.18	8	71 ± 0.41	31.8 ± 1.41	8.41 ± 0.19
	50	49.8 ± 0.43	9.68 ± 1.8	25.0 ± 1.13	5	43 ± 0.34	17.1 ± 0.9	4.26 ± 0.28
	100	30.1 ± 1.31	7.24 ± 1.16	19.0 ± 1.36	2	14.8 ± 1.63	15.4 ± 1.08	4.11 ± 0.13
	150	10.0 ± 0.18	3.36 ± 1.18	14.1 ± 1.14	0	0	10.1 ± 0.36	1.8 ± 0.18
Im4	0	81.3 ± 0.61	15.41 ± 1.4	51.1 ± 0.18	7	63 ± 0.43	31.4 ± 0.34	8.40 ± 0.18
	50	47.1 ± 1.36	9.11 ± 0.33	22.2 ± 1.63	4	33 ± 0.54	15.5 ± 0.48	3.91 ± 0.11
	100	26.6 ± 1.31	6.18 ± 1.41	16.2 ± 1.81	1	7.28 ± 0.18	13.4 ± 0.81	2.46 ± 0.24
	150	8.13 ± 0.43	4.36 ± 0.78	10.4 ± 0.31	0	0	7.84 ± 0.63	0.91 ± 0.14

Plants with Az1, Az2, Az3 electrophoretic spectra of Arizona variety showed the same level of trait reduction at all stages of salt stress. No special manifestations of salt resistance were observed in any of the variants (Table 4).

Table 4. The effect of salt stress on the electrophoretic difference of 11S-globulin of potato variety Arizona on plants with spectrum. Numbers represent means ± standard errors

Arizona	NaCl (mmol)	Wet weight (g)	Dry weight (g)	The height of plant (cm)	The number of tubers	The total weight of tubers (g)	The weight of shoot (g)	The weight of root (g)
Az1	0	88.4 ± 0.54	19.5 ± 1.21	48.8 ± 0.54	6	56 ± 1.34	26.16 ± 0.43	6.28 ± 0.18
	50	52.6 ± 1.24	12.34 ± 1.2	20.6 ± 1.12	4	33 ± 0.68	16.4 ± 0.72	3.66 ± 1.49
	100	85.2 ± 1.11	8.28 ± 1.48	16.8 ± 1.63	2	17 ± 0.68	13.3 ± 0.81	3.11 ± 0.36
	150	23.2 ± 0.71	4.85 ± 0.61	10.22 ± 0.43	0	0	11.0 ± 0.81	2.21 ± 0.32
Az2	0	87.8 ± 0.44	18.43 ± 2.16	48.91 ± 0.15	6	56 ± 1.41	25.8 ± 0.14	6.11 ± 0.14
	50	52.1 ± 1.14	11.93 ± 0.88	21.13 ± 1.34	4	32.95 ± 0.54	15.96 ± 0.61	3.13 ± 1.23
	100	34.64 ± 0.53	8.86 ± 1.13	17.0 ± 1.36	2	17.53 ± 0.86	12.95 ± 0.83	3.0 ± 0.66
	150	23.68 ± 0.43	4.17 ± 0.38	10.86 ± 0.94	0	0	10.96 ± 0.68	2.53 ± 0.49
Az3	0	88.83 ± 0.41	18.40 ± 1.63	48.1 ± 0.45	6	55.85 ± 1.33	25.0 ± 0.35	6.8 ± 0.71
	50	53.0 ± 1.04	12.93 ± 1.12	21.63 ± 1.12	4	33.48 ± 0.53	17.1 ± 0.57	3.15 ± 0.68
	100	34.88 ± 0.81	8.11 ± 1.63	16.54 ± 1.33	2	16.6 ± 0.35	13.53 ± 0.63	3.85 ± 0.66
	150	23.0 ± 0.63	4.43 ± 0.61	10.86 ± 0.38	0	0	11.35 ± 0.18	3.0 ± 0.22

Among the plants with electrophoretic spectra Ma1, Ma2, Ma3, Ma4, Ma5 of the Madeline variety, the highest indicators of resistance to salt stress of 50, 100, 150 mmol of NaCl were recorded in the case of the Ma5 variant (Table 5).

Table 5. Effect of salt stress on plants with different 11S-globulin electrophoresis spectrum of Madeline potato variety. Numbers represent means ± standard errors

Madeline	NaCl (mmol)	Wet weight (g)	Dry weight (g)	The height of plant (cm)	The number of tubers	The total weight of tubers (g)	The weight of shoot (g)	The weight of root (g)
Ma1	0	63.35 ± 0.67	16.21 ± 0.38	48.91 ± 0.45	4	35.54 ± 0.68	22.71 ± 0.84	5.88 ± 0.21
	50	51.61 ± 1.31	9.14 ± 0.81	23.68 ± 0.38	3	24.18 ± 0.17	21.5 ± 0.98	4.11 ± 0.38
	100	29.41 ± 0.32	5.39 ± 0.65	12.67 ± 1.18	1	7.84 ± 0.43	15.44 ± 0.64	3.45 ± 0.24
	150	17.44 ± 0.93	3.64 ± 0.38	9.18 ± 0.52	0	0	6.35 ± 0.26	1.58 ± 0.11
Ma2	0	62.88 ± 0.36	15.93 ± 0.51	48.11 ± 0.54	4	35.29 ± 0.44	21.89 ± 0.41	5.36 ± 0.38
	50	49.7 ± 1.32	9.65 ± 0.12	24.1 ± 0.76	3	24.64 ± 0.71	21.88 ± 0.28	3.91 ± 0.28
	100	30.11 ± 0.28	5.77 ± 0.54	12.91 ± 1.28	1	7.59 ± 0.16	16.18 ± 0.48	3.12 ± 0.13
	150	17.68 ± 1.33	3.51 ± 0.49	9.88 ± 0.7	0	0	6.53 ± 0.45	1.31 ± 0.14
Ma3	0	61.38 ± 0.39	15.48 ± 0.61	47.19 ± 0.14	3	26.29 ± 0.15	20.86 ± 0.71	5.11 ± 0.18
	50	48.36 ± 1.26	9.31 ± 0.13	23.18 ± 0.21	2	16.18 ± 0.13	19.64 ± 0.84	4.0 ± 0.13
	100	29.14 ± 0.21	5.11 ± 0.33	11.96 ± 1.01	0	0	15.96 ± 0.58	3.31 ± 0.26
	150	16.38 ± 0.16	2.99 ± 0.08	8.87 ± 0.21	0	0	6.14 ± 0.62	1.48 ± 0.27
Ma4	0	62.5 ± 0.66	15.21 ± 0.43	48.89 ± 0.16	4	35.51 ± 0.16	21.76 ± 0.41	5.81 ± 0.33
	50	49.6 ± 1.52	9.41 ± 0.84	22.86 ± 0.81	3	24.13 ± 0.73	20.89 ± 0.14	4.26 ± 0.36
	100	29.61 ± 0.38	5.13 ± 0.31	12.77 ± 1.13	1	7.68 ± 0.41	14.96 ± 0.63	3.16 ± 0.37
	150	17.13 ± 0.81	3.53 ± 0.44	9.18 ± 0.26	0	0	6.56 ± 0.46	1.38 ± 0.13
Ma5	0	63.84 ± 1.51	16.78 ± 1.11	48.53 ± 0.43	4	35.58 ± 0.36	23.9 ± 0.94	5.51 ± 0.76
	50	56.8 ± 1.23	14.22 ± 0.76	36.1 ± 0.84	4	34.86 ± 0.63	22.81 ± 1.31	4.13 ± 0.24
	100	33.68 ± 1.16	10.11 ± 0.34	22.18 ± 0.64	3	26.11 ± 0.48	16.87 ± 0.68	4.18 ± 0.16
	150	24.65 ± 1.05	8.18 ± 0.51	11.87 ± 0.35	2	13.16 ± 0.71	10.84 ± 1.11	2.65 ± 0.23

Similar results were also reported in the studies of A. Askari. The authors report that under salt stress conditions of 0, 50, 100, 150 mmol of NaCl, Sante, Arinda and Agria potato varieties showed significant intravarietal diversity in terms of a number of bio-economic traits (Askari et al., 2012; Askari & Pepoyan, 2015).

During the selection of breeding material resistant to salt stress, the results of the reaction norm of different fractions of the varieties studied under different concentrations of NaCl are undoubtedly important, considering the number and total weight of tubers as an important bio-economic characteristic (Fig. 3).

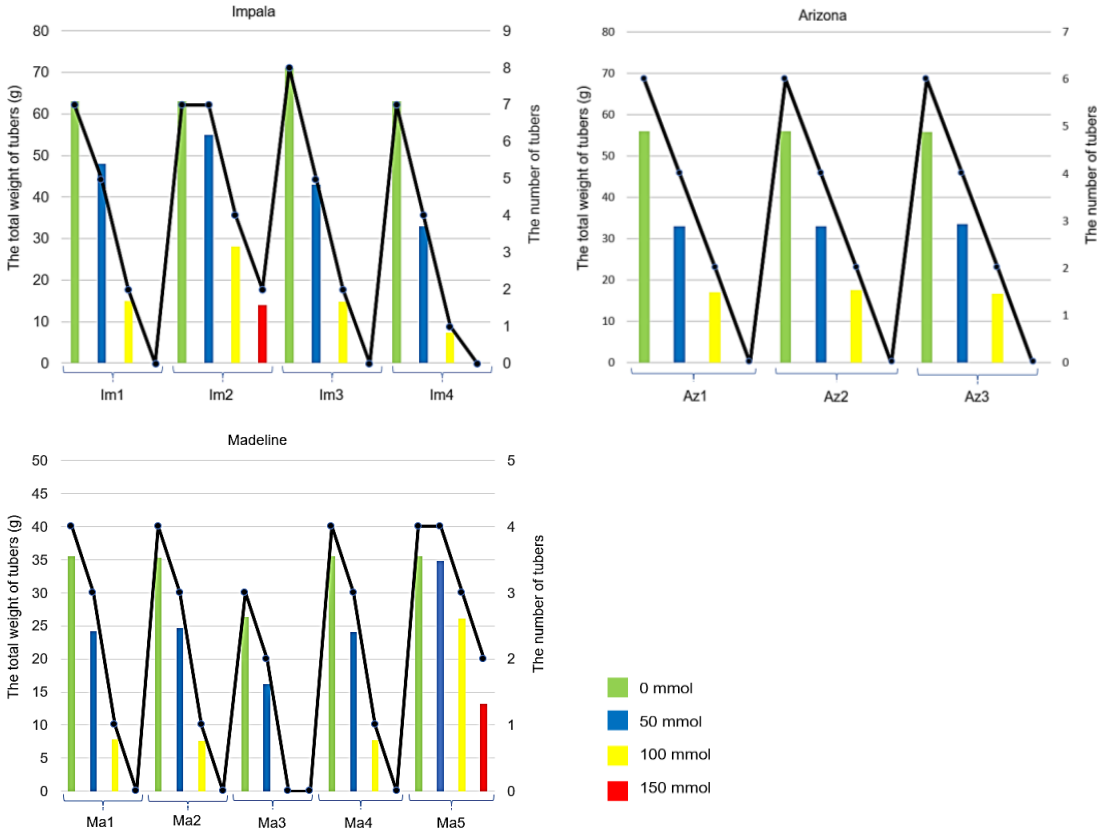

Figure 3. The effect of salt stress on the number and weight of tubers of different potato varieties according to protein spectra.

It is obvious that plant salt tolerance is a complex physiological process, which is regulated by many genes, or at the same time, it has a polygenic arrangement. By the way, as already mentioned, these genes have mutually complementary or additive effects. Therefore, in terms of a specific gene or group of genes selection is impossible, but their presence and location knowledge are very important for marker selection.

For detection the reaction of plants with different electrophoresis spectra of the storage protein 11S-globulin of potato varieties, DNA markers also have a big importance. There are many works aimed at the discovery of genes determining this or that characteristic of potatoes with the help of DNA markers (Shanina & Likhodeyevsky, 2021; Islam & Li, 2023). RFLP (restriction fragment length polymorphism) DNA markers were used in our research.

The study of the length of DNA restriction fragment (RFLP) enables the observation of genetic changes such as deletions and inversions, in which segments of DNA are shortened or lengthened due to the creation or elimination of corresponding sites (Beketova et al., 2021; Gavrilenko et al., 2021).

At this stage of the research, we aimed to construct genomic DNA restriction maps of the studied potato varieties and identify a direct relationship with salt tolerance in order to use it as a marker.

The total DNA restriction maps of plants (Im1, Im2, Im3, Im4) with different 11S-globulin electrophoresis spectra of Impala potato variety are shown in Fig. 4 (a, b, c).

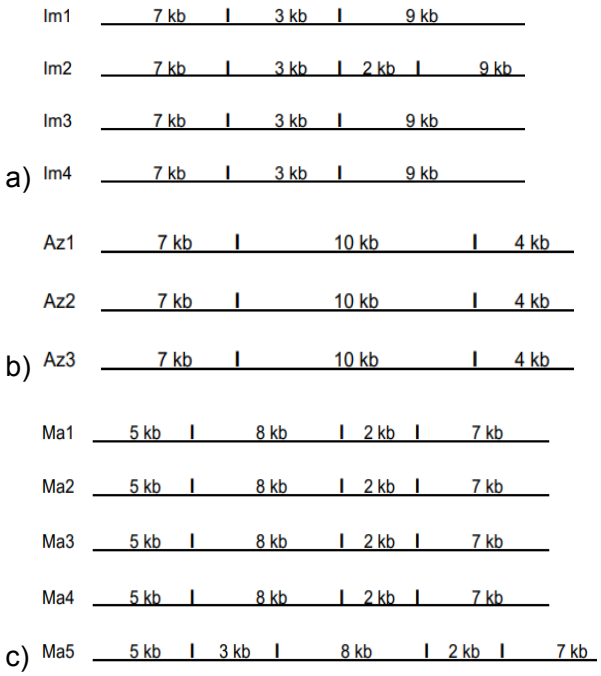

Figure 4. Quantitative DNA restriction fragment map of potato variety varieties according to RFLP analysis: a) Impala, b) Arizona, c) Madeline.

Analysis of DNA restriction maps shows that the total DNA of plants with Im1, Im2 and Im4 variants of the spectrum contains two restriction sites recognized by the *EcoR I* restriction enzyme, generating fragments of 7 and 9 kb in length. By the way, mentioned plants of variants showed similar results under salt stress conditions of 50, 100 and 150 mmol of NaCl (Table 2).

The total DNA of plants with an Im2 electrophoresis spectrum contains three restriction sites recognized by the *Eco*RI enzyme, generating fragments of 7, 3, 2, and 9 kb in length. In this variant, the genome contains a 2 kb mutational fragment, which absent in the restriction map of plants with other electrophoretic spectra. By the way, plants with the Im2 variant have all the characteristics under salt stress showed the highest stability in terms of. Most likely, the genes determining the stress resistance of the Impala potato variety is located in a 2 kb long DNA in the restriction section. Total DNA restriction fragment maps of plants (Az1, Az2, Az3) with different 11S-globulin electrophoresis spectra of Arizona potato variety are depicted in Fig. 4, b.

It is evident from the figure that the total DNA of all plants with different electrophoresis spectra contained 2 restriction sites recognizable by *Eco*RI restriction enzyme, generating restriction fragments of 7, 10 and 4 kb in length. Arizona potato variety Az1, Az2, Az3 variants had the same response to salt stress of 50, 100 and 150 mmol of NaCl, without giving an advantage to any variant. Apparently, the genes forming a certain natural resistance to salt stress are distributed in DNA sections of the specified size, not giving an advantage to any variant. The 11S-globulin electrophoresis spectrum of Madeline potato variety, maps of total DNA restriction segments of plants with variants Ma1, Ma2, Ma3, Ma4, Ma5 are shown in Fig. 4, c.

It is clear from the figure that the genomic DNA of plants with spectrum variants Ma1, Ma2, Ma3, Ma4 contains 3 restriction sites for recognition of the *Eco*RI enzyme, generating 4 restriction segments with lengths of 5, 8, 2 and 7 kb. By the way, the mentioned options plants under salt stress conditions of 50, 100 and 150 mmol of NaCl showed the same dynamics of decrease of the studied bio-economic features. The genomic DNA of plants with the Ma5 variant of the electrophoretic spectrum, in contrast to the other variants, contains 4 restriction sites recognizable by the *Eco*RI enzyme, generating fragments of 5, 3, 8, 2 and 7 kb in length.

From the restriction maps, it can be seen that there is a 3 kb long restriction fragment in the genome of plants of variant Ma5, which is absent in variants Ma1, Ma2, Ma3 and Ma4. It should be noted that the plants of this variant showed the highest resistance to salt stress and a small degree of reduction of the studied characteristics compared to plants of the same variety with other spectra. Most likely, the genes determining the salt tolerance of the Ma5 variant are located in the 3 kb DNA restriction region, which is absent in the other variants.

A group of scientists, while studying the genetic diversity of a number of potato varieties using DNA markers, came to the conclusion that there are always more regions and sites of different sizes in the DNA restriction maps of the most resistant variants to biotic and abiotic stresses. According to the authors, they are the result of aberrations and are directly related to stress resistance (Gavrilenko et al., 2021).

Professional literary sources document that the presence of deletions in the genome of the most stress-resistant forms within different varieties of both potatoes and a number of crops is an evolutionary progress and is directly related to the high expression of stress resistance genes (Bonierbale et al., 1988; Gebhardt et al., 1991, 1995; Pertuzé et al., 2002; Sharma et al., 2013; Gebhardt, 2023).

The results of our research prove that the addition of 2 and 3 kb segments in the DNA restriction maps of the most salt-resistant forms (Im2, Ma5) in different experimental groups of the studied potato varieties is directly related to stress resistance and can be used as markers in the identification of stress-resistant forms.

CONCLUSIONS

The studied potato varieties (Impala, Arizona, Madeline) are not genetically homogeneous. According to the electrophoresis spectrum and protein formula of the storage protein 11S-globulin, they are polymorphic, which is why they showed a different reaction rate to salt stress.

All described genetic associations had similar sizes of genomic DNA restriction fragments, except for the variants that showed the most pronounced salt tolerance.

The results of the research can be used as a guide in the breeding process, when obtaining new salt-resistant potato varieties and improving the existing ones.

REFERENCES

Agarwal, P.K., Shukla, P.S., Gupta, K. & Jha, B. 2013. Bioengineering for Salinity Tolerance in Plants: State of the Art. *Molecular Biotechnology* **54**(1), 102–123. doi: 10.1007/s12033-012-9538-3

Alharbi, K., Al-Osaimi, A.A. & Alghamdi, B.A. 2022. Sodium Chloride (NaCl)-Induced Physiological Alteration and Oxidative Stress Generation in *Pisum sativum* (L.): A Toxicity Assessment. *ACS Omega* **7**(24), 20819–20832. doi: 10.1021/acsomega.2c01427

Ammarelou, A. & Lamei, J. 2007. Study on Variation of Potato Varieties Using Electrophoretic Tuber Storage Proteins. *Pakistan Journal of Biological Sciences* **10**(18), 3195–3199. doi: 10.3923/pjbs.2007.3195.3199

Ardie, S.W., Xie, L., Takahashi, R., Liu, S. & Takano, T. 2009. Cloning of a high-affinity K+ transporter gene PutHKT2;1 from Puccinellia tenuiflora and its functional comparison with OsHKT2;1 from rice in yeast and Arabidopsis. *Journal of Experimental Botany* **60**(12), 3491–3502. doi: 10.1093/jxb/erp184

Askari, A. & Pepoyan, A. 2015. Increasing salinity tolerance in three potato (Solanum tuberosum L.) cultivares by transferring mtlD gene. *IJBPAS* **4**(3), 1013–1019.

Askari, A., Pepoyan, A. & Parsaeimehr, A. 2012. Salt Tolerance of Genetic Modified Potato (Solanum tuberosum) CV. Agria by Expression of a Bacterial MtLD Gene. *Advances in Agriculture & Botanics* **4**(1), 10–16.

Assaha, D., Ueda, A., Saneoka, H., Al-Yahyai, R. & Yaish, M.W. 2017. The Role of Na+ and K+ Transporters in Salt Stress Adaptation in Glycophytes. *Frontiers in Physiology* **8**. doi: 10.3389/fphys.2017.00509

Ayala, F. 1984. *Introduction to population and evolutionary genetics*. Moscow: Mir Publ., 230 pp. (in Russian).

Badalyan, M., Aloyan, T., Amirkhanyan, T., Dilanyan, V. & Melikyan, A. 2023. Efficacy of genetic transformation of *E. coli* field and reference (ATCC 8739) strains at different concentrations of $CaCl_2$ for creation of Gene libraries. *BIO Web of Conferences* **71**, 01082. doi: 10.1051/bioconf/20237101082

Barta, J., Curn, V. & Divis, J. 2003. Study of biochemical variability of potato cultivars by soluble protein, isoesterase, and isoperoxidase electrophoretic patterns. *Plant Soil. Environ* **49**(5), 230–236.

Beketova, M.P., Chalaya, N.A., Zoteyeva, N.M., Gurina, A.A., Kuznetsova, M.A., Armstrong, M., Hein, I., Drobyazina, P.E., Khavkin, E.E. & Rogozina, E.V. 2021. Combination Breeding and Marker-Assisted Selection to Develop Late Blight Resistant Potato Cultivars. *Agronomy* **11**(11), 2192. doi: 10.3390/agronomy11112192

Bernal, J., Mouzo, D., López-Pedrouso, M., Franco, D., García, L. & Zapata, C. 2019. The Major Storage Protein in Potato Tuber Is Mobilized by a Mechanism Dependent on Its Phosphorylation Status. *International Journal of Molecular Sciences* **20**(8), 1889. doi: 10.3390/ijms20081889

Bonierbale, M.W., Plaisted, R.L. & Tanksley, S.D. 1988. RFLP Maps Based on a Common Set of Clones Reveal Modes of Chromosomal Evolution in Potato and Tomato. *Genetics* **120**(4), 1095–1103. doi: 10.1093/genetics/120.4.1095

Bose, J., Munns, R., Shabala, S., Gilliham, M., Pogson, B. & Tyerman, S.D. 2017. Chloroplast function and ion regulation in plants growing on saline soils: lessons from halophytes. *Journal of Experimental Botany* **68**(12), 3129–3143. doi: 10.1093/jxb/erx142

Boyer, J.S. 1982. Plant Productivity and Environment. *Science* **218**(4571), 443–448. doi: 10.1126/science.218.4571.443

Bray, E., Bailey-Serres, J. & Weretilnyk, E. 2000. *Responses to abiotic stress. Biochemistry & molecular biology of plants* (R. Gruissem, W. and Jones, Ed.). American Society of Plant Physiologists, Rockville, 1158–1203.

Byrt, C.S., Platten, J.D., Spielmeyer, W., James, R.A., Lagudah, E.S., Dennis, E.S., Tester, M. & Munns, R. 2007. HKT1;5-Like Cation Transporters Linked to Na+ Exclusion Loci in Wheat, Nax2 and Kna1. *Plant Physiology* **143**(4), 1918–1928. doi: 10.1104/pp.106.093476

Davis, B.J. 1964. *Disc electrophoresis to human serum protein*. Ann. N.-Y. Acad. Sci., pp. 404–427.

Dementyeva, Z.A. 2006. Polymorphism of soluble potato tuber protein: potentials of their using for potato breeding and original seed production. *Polythematic Network Electronic Scientific Journal of Kuban State Agrarian University* **1**, 1–8 (in Russian).

Fricke, W. 2004. Rapid and tissue-specific changes in ABA and in growth rate in response to salinity in barley leaves. *Journal of Experimental Botany* **55**(399), 1115–1123. doi: 10.1093/jxb/erh117

Gavrilenko, T.A., Khiutti, A.V., Klimenko, N.S., Antonova, O.Y., Fomina, N.A. & Afanasenko, O.S. 2021. Phenotypic and DNA Marker-Assisted Characterization of Russian Potato Cultivars for Resistance to Potato Cyst Nematodes. *Agronomy* **11**(12), 2400. doi: 10.3390/agronomy11122400

Gebhardt, C. 2023. A physical map of traits of agronomic importance based on potato and tomato genome sequences. *Frontiers in Genetics* **14**. doi: 10.3389/fgene.2023.1197206

Gebhardt, C., Eberle, B., Leonards-Schippers, C., Walkemeier, B. & Salamini, F. 1995. Isolation, characterization and RFLP linkage mapping of a DNA repeat family of Solanum spegazzinii by which chromosome ends can be localized on the genetic map of potato. *Genetical Research* **65**(1), 1–10. doi: 10.1017/S001667230003295X

Gebhardt, C., Ritter, E., Barone, A., Debener, T., Walkemeier, B., Schachtschabel, U., Kaufmann, H., Thompson, R.D., Bonierbale, M.W., Ganal, M.W., Tanksley, S.D. & Salamini, F. 1991. RFLP maps of potato and their alignment with the homoeologous tomato genome. *Theoretical and Applied Genetics* **83**(1), 49–57. doi: 10.1007/BF00229225

Han, X., Yang, R., Zhang, L., Wei, Q., Zhang, Y., Wang, Y. & Shi, Y. 2023. A Review of Potato Salt Tolerance. *International Journal of Molecular Sciences* **24**(13), 10726. doi: 10.3390/ijms241310726

Horie, T., Hauser, F. & Schroeder, J.I. 2009. HKT transporter-mediated salinity resistance mechanisms in Arabidopsis and monocot crop plants. *Trends in Plant Science* **14**(12), 660–668. doi: 10.1016/j.tplants.2009.08.009

Huang, S., Spielmeyer, W., Lagudah, E.S., James, R.A., Platten, J.D., Dennis, E.S. & Munns, R. 2006. A Sodium Transporter (HKT7) Is a Candidate for Nax1, a Gene for Salt Tolerance in Durum Wheat. *Plant Physiology* **142**(4), 1718–1727. doi: 10.1104/pp.106.088864

Islam, M. & Li, S. 2023. Identifying Key Crop Growth Models for Rain-Fed Potato (Solanum tuberosum L.) Production Systems in Atlantic Canada: A Review with a Working Example. *American Journal of Potato Research* **100**(5), 341–361. doi: 10.1007/s12230-023-09915-5

James, R.A., Davenport, R.J. & Munns, R. 2006. Physiological Characterization of Two Genes for Na+ Exclusion in Durum Wheat, Nax1 and Nax2. *Plant Physiology* **142**(4), 1537–1547. doi: 10.1104/pp.106.086538

Kanukova, K.R., Gazaev, I.H., Sabanchieva, L.K., Bogotova, Z.I. & Appaev, S.P. 2019. DNA markers in crop production. *News of the Kabardin-Balkar Scientific Center of RAS* **6**(92), 220–232. doi: 10.35330/1991-6639-2019-6-92-220-232

Ketehouli, T., Idrice Carther, K.F., Noman, M., Wang, F.-W., Li, X.-W. & Li, H.-Y. 2019. Adaptation of Plants to Salt Stress: Characterization of Na+ and K+ Transporters and Role of CBL Gene Family in Regulating Salt Stress Response. *Agronomy* **9**(11), 687. doi: 10.3390/agronomy9110687

Konarev, V.G. 2007. *Molecular-biological studies of the gene pool of cultural plants in VIR (1967–2007).* (2nd ed.). VIR. Moscow, Russia.134 pp. (in Russian).

Kononenko, N.V, Dilovarova, T.A., Kanavsky, R.V, Lebedev, S.V, Baranova, E.N. & Fedoreeva, L.I. 2019. Evaluation of morphological and biochemical resistance parameters to chloride salination in different wheat genotypes. *RUDN Journal of Agronomy and Animal Industries* **14**(1), 18–39. doi: 10.22363/2312-797X-2019-14-1-18-39

Levy, D. & Veilleux, R.E. 2007. Adaptation of potato to high temperatures and salinity-a review. *American Journal of Potato Research* **84**(6), 487–506. doi: 10.1007/BF02987885

Luo, L., Zhang, P., Zhu, R., Fu, J., Su, J., Zheng, J., Wang, Z., Wang, D. & Gong, Q. 2017. Autophagy Is Rapidly Induced by Salt Stress and Is Required for Salt Tolerance in Arabidopsis. *Frontiers in Plant Science* **8**. doi: 10.3389/fpls.2017.01459

Mann, A., Lata, C., Kumar, N., Kumar, A., Kumar, A. & Sheoran, P. 2023. Halophytes as new model plant species for salt tolerance strategies. *Frontiers in Plant Science* **14**. doi: 10.3389/fpls.2023.1137211

Manukyan, R. & Karapetyan, F. 2011. *Agriculture with the basics of soil science* (Xachatryan O.M., Ed.). Yerevan, Armenia, ASAU publishing house. 218 pp. (in Armenian).

Meng, X., Zhou, J. & Sui, N. 2018. Mechanisms of salt tolerance in halophytes: current understanding and recent advances. *Open Life Sciences* **13**(1), 149–154. doi: 10.1515/biol-2018-0020

Møller, I.S., Gilliham, M., Jha, D., Mayo, G.M., Roy, S.J., Coates, J.C., Haseloff, J. & Tester, M. 2009. Shoot Na+ Exclusion and Increased Salinity Tolerance Engineered by Cell Type-Specific Alteration of Na+ Transport in Arabidopsis. *The Plant Cell* **21**(7), 2163–2178. doi: 10.1105/tpc.108.064568

Mouzo, D., Bernal, J., López-Pedrouso, M., Franco, D. & Zapata, C. 2018. Advances in the Biology of Seed and Vegetative Storage Proteins Based on Two-Dimensional Electrophoresis Coupled to Mass Spectrometry. *Molecules* **23**(10), 2462. doi: 10.3390/molecules23102462

Munns, R. & Tester, M. 2008. Mechanisms of Salinity Tolerance. *Annual Review of Plant Biology* **59**(1), 651–681. doi: 10.1146/annurev.arplant.59.032607.092911

Murashige, T. 1974. Plant propagation through tissue cultures. *Ann. Rev. Plant Physiology* **25**, 135–166.

Nasrollahzadeh, F., Roman, L., Skov, K., Jakobsen, L.M.A., Trinh, B.M., Tsochatzis, E.D., Mekonnen, T., Corredig, M., Dutcher, J.R. & Martinez, M.M. 2023. A comparative investigation of seed storage protein fractions: The synergistic impact of molecular properties and composition on anisotropic structuring. *Food Hydrocolloids* **137**, 108400. doi: 10.1016/j.foodhyd.2022.108400

Novikova, L. Yu., Chalaya, N.A., Sitnikov, M.N., Gorlova, L.M., Kiru, S.D. & Rogozina, E.V. 2021. Dynamics of tuber weight in early potato varieties in the contrasting weather conditions of the Northwestern Russia. *Agronomy Research* **19**(1), 185–198.

Padutov, V., Baranov, O. & Voropaev, E. 2007. *Methods of molecular genetic analysis*, 176 pp. https://www.studmed.ru/padutov-v-e-baranov-o-yu-voropaev-e-v-metody-molekulyarno-geneticheskogo-analiza_df2a10a241b.html (in Russian).

Pankova, E., Konyushkova, M. & Gorokhova, I. 2017. On the problem of soil salinity's evaluation and method of large-scale digital mapping of saline soils. *Ecosystems: Ecology and Dynamics* **1**(1), 26–54.

Parvaiz, S. 2008. Salt stress and phyto-biochemical responses of plants – a review. *Plant Soil Environ.* **54**(3), 89–99.

Pertuzé, R.A., Ji, Y. & Chetelat, R.T. 2002. Comparative linkage map of the Solanum lycopersicoides and S. sitiens genomes and their differentiation from tomato. *Genome* **45**(6), 1003–1012. doi: 10.1139/g02-066n

Polle, A. & Chen, S. 2015. On the salty side of life: molecular, physiological and anatomical adaptation and acclimation of trees to extreme habitats. *Plant, Cell & Environment* **38**(9), 1794–1816. doi: 10.1111/pce.12440

Sajyan, T., Shaban, N., Rizkallah, J. & Sassine, Y. 2018. Effects of Monopotassium-phosphate, Nano-calcium fertilizer, Acetyl salicylic acid and Glycinebetaine application on growth and production of tomato (Solanum lycopersicum) crop under salt stress. *Agronomy Research* **16**(3), 872–883. doi: 10.15159/AR.18.079

Sassine, Y., Sajyan, T.K., El Zarzour, A., Abdelmawgoud, A.M.R., Germanos, M. & Alturki, S.M. 2022. Integrative effects of biostimulants and salinity on vegetables: Contribution of bioumik and Lithovit®-urea50 to improve salt-tolerance of tomato. *Agronomy Research* **20**(4), 793–804. doi: 10.15159/AR.22.074

Sayed Mohammad Reza Khoshroo. 2011. Seed storage protein electrophoretic profiles in some Iranian date palm (Phoenix dactylifera L.) cultivars. *African Journal of Biotechnology* **10**(77). doi: 10.5897/AJB11.2726

Schroeder, J.I., Delhaize, E., Frommer, W.B., Guerinot, M. Lou, Harrison, M.J., Herrera-Estrella, L., Horie, T., Kochian, L.V., Munns, R., Nishizawa, N.K., Tsay, Y.-F. & Sanders, D. 2013. Using membrane transporters to improve crops for sustainable food production. *Nature* **497**(7447), 60–66. doi: 10.1038/nature11909

Shabala, S. 2013. Learning from halophytes: physiological basis and strategies to improve abiotic stress tolerance in crops. *Annals of Botany* **112**(7), 1209–1221. https://doi.org/10.1093/aob/mct205

Shahid, M.A., Sarkhosh, A., Khan, N., Balal, R.M., Ali, S., Rossi, L., Gómez, C., Mattson, N., Nasim, W. & Garcia-Sanchez, F. 2020. Insights into the Physiological and Biochemical Impacts of Salt Stress on Plant Growth and Development. *Agronomy* **10**(7), 938. doi: 10.3390/agronomy10070938

Shanina, E. & Likhodeyevsky, G. 2021. Evaluation of interspecific potato breeding material with a complex of genes of immunity to Potato virus Y using molecular markers. *Agronomy Research* **19**(1), 224–231. doi: 10.15159/AR.20.235

Sharma, S.K., Bolser, D., de Boer, J., Sønderkær, M., Amoros, W., Carboni, M.F., D'Ambrosio, J.M., de la Cruz, G., Di Genova, A., Douches, D.S., Eguiluz, M., Guo, X., Guzman, F., Hackett, C.A., Hamilton, J.P., Li, G., Li, Y., Lozano, R., Maass, A., … Bryan, G.J. 2013. Construction of Reference Chromosome-Scale Pseudomolecules for Potato: Integrating the Potato Genome with Genetic and Physical Maps. *G3 Genes|Genomes|Genetics* **3**(11), 2031–2047. doi: 10.1534/g3.113.007153

Shokri-Gharelo, R. & Noparvar, P.M. 2018. Molecular response of canola to salt stress: insights on tolerance mechanisms. *PeerJ*. **6**, e4822. doi: 10.7717/peerj.4822

Shrivastava, P. & Kumar, R. 2015. Soil salinity: A serious environmental issue and plant growth promoting bacteria as one of the tools for its alleviation. *Saudi Journal of Biological Sciences* **22**(2), 123–131. doi: 10.1016/j.sjbs.2014.12.001n

Tian, T., Wang, J., Wang, H., Cui, J., Shi, X., Song, J., Li, W., Zhong, M., Qiu, Y. & Xu, T. 2022. Nitrogen application alleviates salt stress by enhancing osmotic balance, ROS scavenging, and photosynthesis of rapeseed seedlings (Brassica napus). *Plant Signaling & Behavior* **17**(1). doi: 10.1080/15592324.2022.2081419

Torabi, M. 2014. Physiological and biochemical responses of plants to salt stress. *The 1st Intern. Conf. on New Ideas in Agricultural*, 1–25.

Verhoeven, K., Poorter, H., Nevo, E. & Biere, A. 2008. Habitat-specific natural selection at a flowering-time QTL is a main driver of local adaptation in two wild barley populations. *Molecular Ecology* **17**(14), 3416–3424. doi: 10.1111/j.1365-294X.2008.03847.x

Wang, C.-F., Han, G.-L., Qiao, Z.-Q., Li, Y.-X., Yang, Z.-R. & Wang, B.-S. 2022. Root Na+ Content Negatively Correlated to Salt Tolerance Determines the Salt Tolerance of Brassica napus L. Inbred Seedlings. *Plants* **11**(7), 906. doi: 10.3390/plants11070906

Zhang, J. & Shi, H. 2013. Physiological and molecular mechanisms of plant salt tolerance. *Photosynthesis Research* **115**(1), 1–22. doi: 10.1007/s11120-013-9813-6

Zhang, M., Cao, Y., Wang, Z., Wang, Z., Shi, J., Liang, X., Song, W., Chen, Q., Lai, J. & Jiang, C. 2018. A retrotransposon in an HKT1 family sodium transporter causes variation of leaf Na+ exclusion and salt tolerance in maize. *New Phytologist* **217**(3), 1161–1176. doi: 10.1111/nph.14882

Zhuchenko, A.A. 2001. *Adaptive Plant Breeding System, Tom 2*. Moscow, Russia, 785 pp. (in Russian).

Agronomy Research **22**(2), 750–773, 2024
https://doi.org/10.15159/AR.24.083

Structural-aggregate condition and utilization of productive water reserve depending on the tillage method of podzolized chernozem in agrocenosis

V. Bulgakov[1], I. Gadzalo[2], M. Chernovol[3], O. Demydenko[4], I. Holovach[1], Ye. Ihnatiev[5,6], O. Trokhaniak[1], V. Mitkov[6] and J. Olt[5,*]

[1]National University of Life and Environmental Sciences of Ukraine, 15 Heroyiv Oborony Str., UA03041 Kyiv, Ukraine
[2]National Academy of Agrarian Sciences of Ukraine, 9 Mykhailo Omelyanovych-Pavlenko Str., UA 01010 Kyiv, Ukraine
[3]Central Ukrainian National Technical University, University Ave., 8, UA25006 Kropivnitskyi, Kirovograd region, Ukraine
[4]Cherkasy State Agricultural Experimental Station National Scientific Centre, Institute of Agriculture of NAAS of Ukraine, 13 Dokuchaieva Str., Kholodnianske village, Cherkassy district, UA20731 Cherkassy region, Ukraine
[5]Estonian University of Life Sciences, Institute of Forestry and Engineering, 56 Kreutzwaldi Str., EE51006 Tartu, Estonia
[6]Dmytro Motornyi Tavria State Agrotechnological University, 66 Zhukovsky Str., UA69600 Zaporizhzhia, Ukraine
[*]Correspondence: jyri.olt@emu.ee

Received: May 17th, 2024; Accepted: August 5th, 2024; Published: August 26th, 2024

Abstract. The work established the features of formation of the structural-aggregate condition and determine the main patterns of the formation of spring productive water reserves and its consumption in a five-field crop rotation when cultivating winter wheat and spring cereal crops using different tillage methods (plowing, systematic surface tillage, No-till systems based on plowing and systematic surface tillage) of podzolized chernozem (black soil) in the conditions of the central part of the Forest-Steppe of Ukraine. Common research methods were applied: field, laboratory, mathematical, and comparative-computational. Analysis of the results showed that during surface treatment, water-resistant aggregates are enlarged into the most valuable fraction, which affects the more rational use of productive water reserves during the growth of crops in crop rotation. Under the No-till system (in years 2–3), there is an accumulation of productive moisture in the soil layer of 0–1 m by 8–12 mm more compared to conventional tillage, and relative to the water reserves in 2022, the water reserve in 2023 increased by +19.0 mm (after conventional tillage) and by +14.0 mm (under surface tillage). Under the no-till system, in June and July, the average productive water reserve for the years 2022–2023 was higher compared to conventional tillage by 5–10 mm and 7–10 mm, respectively, and compared to surface tillage by 10–12 mm and 18–21 mm, respectively. In 2023, the productive water reserve in July under the No-till system exceeded that under conventional tillage by 17 mm, and compared to surface tillage by 31 mm. This improvement in soil structure water resistance in June and July was due to the increase in the content of water-stable aggregates sized 3–0.5 mm.

Key words: conventional tillage, fractal dimension, surface tillage, structural condition, water resistance.

INTRODUCTION

The parameters of the physical structure are among the key rapidly changing properties of chernozem (black soil) in agroecosystems of the Forest-Steppe. When chernozem is plowed, there is a sharp change in its structural condition (Medvediev, 2016). Research conducted in the Forest-Steppe zone has established norms for changes in the physical properties of plowed chernozem and the maximum values of their indicators (Medvediev, 2012; Bulyhin et al., 2014; Medvediev et al., 2014). According to Medvediev (1990), reducing the depth and frequency of tillage or abandoning it altogether, practicing high agricultural culture with the application of organic fertilizers, and leaving crop residues in the field deteriorates the structural condition of chernozem under intensive tillage (plowing), while under minimum soil disturbance, the process of chernozem structure reproduction becomes actively sustainable. The structure of chornozem affects the carbon cycle (An et al., 2008; Jimenez et al., 2011), fertility, and humus regime (Garcia-Oliva et al., 2004) of chernozem in agroecosystems (Six et al., 2004). The fundamental properties of chornozem and the primary processes that determine its functions in agroecosystems depend on the proportion of large and small structural elements and water-resistant aggregates. Chernozems dominated by water-resistant macroaggregates contain more organic matter (Pirmoradian et al., 2005; Nichols & Toro, 2011; Nosko, 2017).

Water stability of soil structural aggregates is an important property from an agronomic perspective, but it does not provide a complete characterization of soil structure quality, as two soils with similar structures can be qualitatively different (Bulgakov et al., 2018; Ivanovs et al., 2020). This difference is determined by the intensity of agricultural use of chernozems, as soil structure water stability decreases with increasing anthropogenic load (Six et al., 2000; Gajic et al., 2006; Tkachenko et al., 2016). The most significant role in forming water-stable aggregates is attributed to mobile organic matter because easily mineralized organic substances (labile humic substances) play a significant role in forming water-stable structure (Chefetz et al., 2002; Zaryshnyak et al., 2016¸ Bulgakov et al., 2017).

The study of water stability in plowed chernozems is of great importance for assessing the resilience of soil structure to intensive agricultural impact, which depends on the cultivated crop, predecessor crop, soil tillage method, humus content, and application of organic and mineral fertilizers. The development and outfitting of modern machinery and tractor units to reduce agro-impact on chernozem soil structure is a relevant issue in contemporary soil-climatic conditions of the Ukrainian Forest-Steppe (Kosolap & Krotinov, 2011; Bulgakov et al., 2020; Bulgakov et al., 2021).

A compelling argument in favor of minimal tillage and No-till systems is the soil conservation effect, which is associated with the presence of a mulch layer on the field surface. This layer protects chornozem soils from strong winds and reduces their deflationary losses during prolonged use of intensive tillage technologies. Preservation of soil structure with the introduction of minimal tillage and No-till has been observed in soils of southern and central England, while the positive impact of No-till on aggregate stability and soil erosion resistance has been documented in France and other

Mediterranean countries (Medvediev, 2010). Implementation of No-till in the state of Mississippi (USA) has led to increased stability of air-dry aggregates, contributing to enhanced soil wind resistance (Rhoton, 2000).

An important characteristic of minimal tillage and No-till systems is their erosion-resistant soil structure and their resistance to deflation (wind erosion) (Baydyuk, 2004). The increase in the structural coefficient in the upper layers of chornozem soil under minimal tillage and No-till is associated with the enrichment of the soil environment with organic residues, along with the presence of microorganisms (fungi, bacteria, algae, etc.). These microorganisms bind elementary soil particles (ESPs) during their life processes, releasing polysaccharides and galacturonic acid polymers into the soil. These substances have an enhanced ability to bind ESPs together (Medvediev, 2008). Macrostructure parameters serve as an integral indicator characterizing erosion resistance, including the content of erosion-resistant aggregates larger than 0.25 mm and the mean weighted diameter of these aggregates (Hirte et al., 2017). The critical velocity of water flow that destroys erosion-resistant aggregates is proportional to the mean weighted diameter of these aggregates (Bardgett et al., 2014). Therefore, erosion resistance under No-till in the 0–0.1 m layer increases due to the formation of a soil environment saturated with surface organic residues and containing a large number of heterotrophic microorganisms. These microorganisms generate various adhesive substances, which participate in the formation of erosion-resistant aggregates, along with the formation of so-called labile humus, which has a high aggregation ability (Thorne, 2003; Medvediev, 2007).

The tillage method (plowing, surface tillage, No-till) of chornozem in crop rotation is one of the most important factors influencing fertility reproduction, growth and development, crop formation of agricultural crops. The improvement of tillage systems for chornozem, the reduction of energy costs, and the enhancement of its soil-protective properties are essential issues (Gassen & Gassen, 2004). Additionally, the adaptability to specific conditions, accumulation of spring water reserves, its preservation and expenditure, as well as the reproduction of agrophysical properties of chornozem, including its structural-aggregate composition, remain relevant tasks in agriculture in the central part of the Ukrainian Forest-Steppe region (Chornyi et al., 2012).

The aim of the research is to identify the peculiarities of forming the structural-aggregate state and to determine the fundamental patterns of spring productive water reserves and its consumption in a 5-field grain crop rotation when cultivating winter wheat and spring cereal crops using different cultivation methods (plowing, systematic surface tillage, No-till system based on plowing, and systematic surface tillage) of podzolized chornozem in the conditions of the central part of the Ukrainian Forest-Steppe region.

MATERIALS AND METHODS

The research was conducted at the experimental station of the Cherkasy Research Station of the Institute of Irrigated Agriculture of the National Academy of Agrarian Sciences of Ukraine under the conditions of a field stationary experiment established in 2010 (coordinates 49°56'46.1"N 32°07'02.1"E). The soil cover of the field is characterized

by strongly differentiated low-humus medium loamy podzolized chornozem on a carbonate loess (Polupan et al., 2005) or Chernic Phaeozems (Hyperhumic, Siltic, Calcaric, Cutanic, Episiltic, Sodic) according to WRB 2022. The humus content in the plowed horizon ranges from 2.58% to 3.08%, gradually decreasing with depth to 0.96% at a depth of one meter. According to the norms of agrophysical indicators developed over the previous 5 years of research, the podzolized chornozem meets the requirements for minimal tillage and special raw material zones for agricultural biologization (Fig. 1).

The research is conducted in a field stationary experiment to study the productivity of a 5-field grain-legume crop rotation, which includes: spring barley - peas - winter wheat - soybeans - spring wheat (Hordeum vulgare - Pisum sativum - Triticum aestivum - Glycine max - Triticum aestivum). The structure of the crop rotation is as follows: cereals - 60%, including: winter wheat - 20%; spring cereals - 40%; legumes (peas) - 20%; technical crops (soybeans) - 20%.

Figure 1. Location of the experimental site (coordinates 49°56'46.1"N 32°07'02.1"E).

The tillage system includes: 1) conventional tillage (plowing); 2) surface tillage for 8 years; 3) No-till alongside long-term conventional tillage and 6-year surface tillage at a depth of 10–12 cm. The fertilization system, in the context of the two cultivation systems, consists of: control (no fertilizers) and $N_{55}P_{55}K_{65}$, $N_{75}P_{65}K_{82}$ per hectare of crop rotation area.

The study investigated the impact of long-term use of different cultivation systems on the agrophysical and agrochemical condition of podzolized chornozem when transitioning to the No-till system with minimum tillage. It also examined the transition from systematic tillage and surface tillage to a specialized grain crop rotation, establishing the influence of transitional soil conditions on the productivity and quality of grain crops in a 5-field crop rotation.

Field stationary experiment layout:

1 – Systematic conventional tillage (plowing) from 10–12 cm to 22–25 cm depending on the crop in crop rotation;

2 – No-till system transitioning to minimal tillage (in 2021) after systematic plowing from 10–12 cm to 22–25 cm;

3 – No-till system of tillage through surface tillage at a depth of 10–12 cm for 6 years;

4 – Surface tillage at a depth of 10–12 cm for 8 years.

Fertilization system: $N_{75}P_{65}K_{82}$ per hectare of crop rotation area.

The analysis of the structural composition was conducted in the 0–0.3 m soil layer under all crops of the 5-field crop rotation at depths of 0–0.2 m and 0.2–0.3 m with fivefold repetition. The structural state was studied together with determining the structure density. The total humus content was determined by Tyurin's I.V. method in Simakov's M.V. modification (State standard of Ukraine, DSTU 4289:2004). The structural-aggregate composition was analyzed using the sieve method in Savinov's N.I. modification (DSTU 4744:2007) (State Standard of Ukraine, 2008), and soil structure stability was determined by I.M. Baksheev's method.

An important indicator of soil structure is the structural coefficient K_{st} (the ratio between the mass of agronomically valuable aggregates (0.25–10 mm) and the total mass of dust (less than 0.25 mm) and aggregates larger than 10 mm). This coefficient allows for a clearer assessment of the impact of different soil tillage methods.

Aggregate water stability is the ability of soil aggregates to resist the destructive action of water. Soils with high humus content have the greatest aggregate water stability. To determine the water stability of soil aggregates, the sieving method developed by Baksheev I.M. (Medvediev, 2008) was used. The C_{ws} criterion for soil water stability is determined by the following formula:

$$C_{ws} = \frac{A_{wet}}{A_{dry}}, \quad (1)$$

where A_{wet} – aggregates larger than 0.25 mm in wet sieving, %; A_{dry} – aggregates larger than 0.25 mm in dry sieving, %.

More than 600 soil samples were analyzed annually (5 agricultural crops; 4 types of soil treatment; 2 soil layers; 3 months of research; 5 repetitions along the diagonal of the experimental area).

Statistical calculations of the research results were conducted using the Analysis of Variance (ANOVA) method with the STATISTICA software, along with the application of non-parametric statistical methods, correlation analysis, factor analysis, and fractal analysis (Backhaus, 2008; Field, 2009).

In recent decades, methods of nonlinear dynamics, particularly fractal analysis, have been widely used for the processing and modeling of time series. The main task of fractal analysis is to determine the fractal dimension F_r and the Hurst exponent H_x of time series. It is known that the Hurst exponent is directly related to the fractal dimension F_r by the formula:

$$H_x = 2 - F_r, \quad (2)$$

where F_r is the measure of the roughness of the series (fractal dimension) and H_x is the Hurst exponent.

Mandelbrot used the Hurst coefficient to calculate the dimension of the probability space D_m as:

$$D_m = 1 / H_x, \quad (3)$$

The correlation ratio in this case is calculated by the following formula:

$$C_H = 2^{(2H-1)} - 1, \quad (4)$$

where C_H is the measure of correlation and H_x is the Hurst coefficient.

Amplitude range Δ_a is the difference between the highest and lowest values in a data set (Δ_a = max-min).

Normalized range is the relative range obtained by dividing the amplitude range by a certain characteristic of the distribution, allowing comparison of ranges across different data sets.

Quantile (L) is one of the numerical characteristics of random variables in mathematical statistics. Quantiles divide the range into certain portions. For example, $L_{0.25}$ means that 25% of the variable's values fall below this value.

RESULTS AND DISCUSSION

Research has shown that in the plow layer (0.22–0.25 m), the humus content ranges from 2.58% to 3.08% (according to the Tyurin method), gradually decreasing with depth to 0.92% at a depth of one meter. The sum of absorbed bases ranges from 25.1 to 27.8 mg-eq per 100 g of soil, hydrolytic acidity ranges from 1.87 to 2.22 mg-eq per 100 g of soil, pH of the salt extract ranges from 5.49 to 6.27 - soil to water ratio 1:2.5 (FAO, 2021). The base saturation degree is between 92.7% and 93.5%, the content of exchangeable phosphorus forms (according to the Truog method) is 9.5 mg per 100 g of soil, and exchangeable potassium (according to the Brovkin method) is 11.5 mg per 100 g of soil. The soil at the experimental site has the following morphological profile structure:

$H_{0–4}$ – sod, penetrated by plant roots;

$He_{5–47}$ – humus horizon, barely perceptibly eluvial, 5 YR 3/1, lumpy-powdery in structure, slightly dense, medium porosity, many plant roots, earthworm channels, filled burrows casts at the bottom of the horizon (5×6 cm), gradual transition in color;

$Hpi_{48–82}$ – transitional horizon, 5 YR 6/2, lumpy-granular in structure, medium porosity, earthworm channels, the transition is faintly visible in color, the transition line is wavy;

$Ph_{83–123}$ – transitional horizon, 7.5 YR 6/2, granular-lumpy in structure, dense (compacted), a few roots, gradual transition in color, the transition line is wavy;

$P(h)k_{123–190}$ – loess, 7.5 YR 6/4, earthworm channels, infilled large burrows, layers of carbonates, carbonates in mold form.

The distribution of structural components by size in the 0–0.3 m layer during dry sieving (Fig. 2) under different soil tillage methods is described by exponential equations. It has been determined that in the 0–0.2 m layer in April, with conventional tillage and surface tillage, the fractal dimension (F_r) was F_r = 1.40–1.42, while with the No-till system, F_r = 1.51–1.59, which is persistent in the first case and anti-persistent in the second (Table 1).

In the case of conventional tillage and surface tillage, the correlation between the fractal dimensions of structural components was at a low level (C_H = 0.12–0.15), while in No-till it was at a high level (C_H = 0.95–0.98), indicating the absence of soil's ability to maintain its structural integrity and stability over time in the first case and the presence of this ability in the second case. This is also supported by the degree of ruggedness of the components' redistribution series (D_m), which is ≥ 2.0 in the No-till system, whereas in conventional tillage and surface tillage, D_m is < 2.0.

In June, in the 0–0.2 m layer, the observed pattern of fractal assessment of structural components redistribution persisted. In surface tillage, the correlation value (C_H) doubled (C_H = 0.30), while in conventional tillage, it remained at the April level. The

constancy of the fractal assessment of structural components distribution in the No-till system indicates the stability of the soil's structural condition.

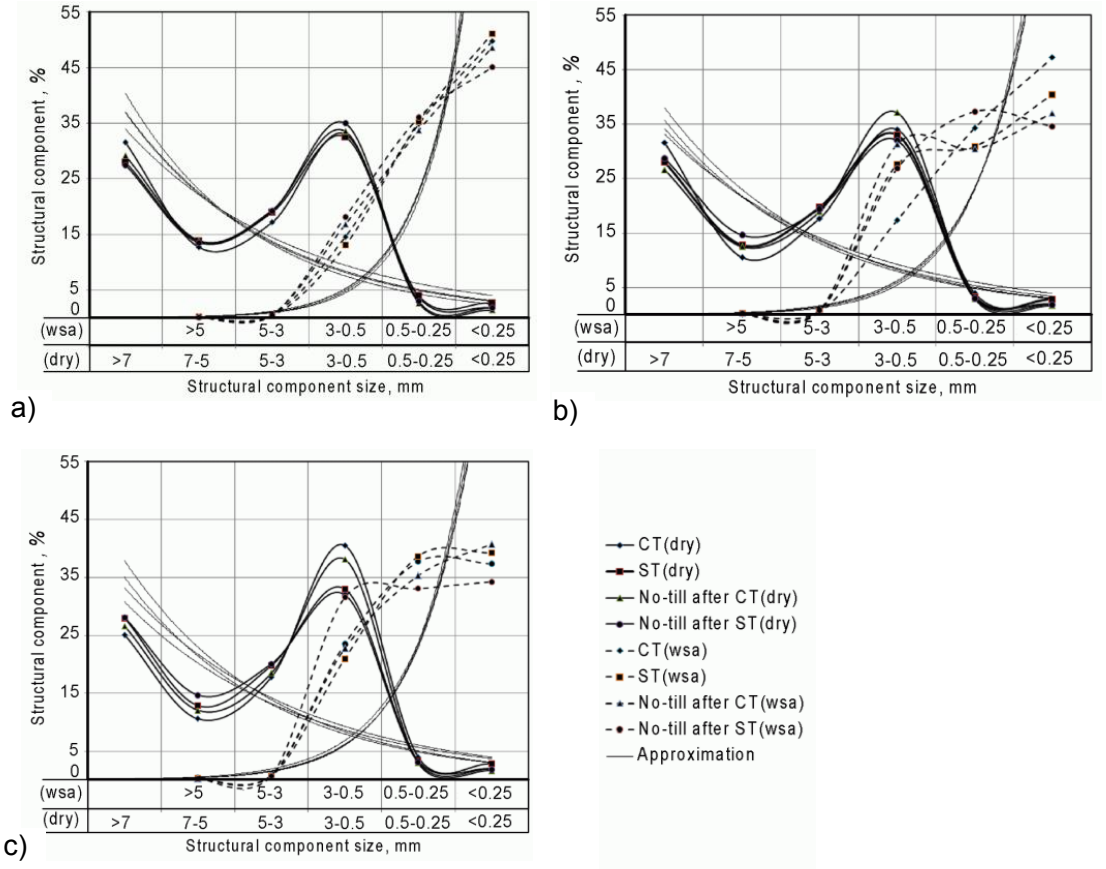

Figure 2. The influence of different tillage systems on the redistribution of structural components and water-stable aggregates in a five-field crop rotation on podzolized chornozem in the third year of implementation in the 0–0.3 m layer: a – April; b – June; c – July; (dry) – dry sieving; (wsa) – water-stable aggregates; (CT) – conventional tillage; (ST) – surface tillage.

In the 0.2–0.3 m layer in April, F_r was consistently above 1.4 regardless of the tillage method, indicating soil system disturbance. The D_m index was consistently above 2.0, and C_H ranged from 0.78 to 0.94, indicating dynamic redistribution of structural components by size. Plowing resulted in a more unstable structure with $F_r > 1.6$. In June, *Fr* was 1.46 under plowing, while under surface tillage and No-till systems, F_r approached 1.6. Furthermore, D_m was less than 2.0 under plowing but greater than 2.0 under surface tillage and No-till systems, leading to higher C_H values ranging from 0.86 to 0.98.

In July, the established pattern of fractal assessment of structural condition persisted: under surface tillage and No-till systems, the redistribution of components was persistent, while under plowing, it was anti-persistent. This means that in the former case, the soil system exhibited ability to maintain its structural integrity and stability over time, long-term memory, while in the latter case, it was unstable in terms of reproducing soil structure, characterized by redistribution of structural components by size during the spring-summer period.

Table 1. The influence of different tillage methods on the seasonal dynamics of fractal assessment of soil structure condition in the 0–0.3 m soil layer in the five-field crop rotation in the third year of the study

No.	Exponential equation, $Y = ae^{\pm bx}$	Fractal dimension, $Fr = 1+\|bx\|$	Hurst exponent, $H_x = -F$	Mandelbrot dimension, $Dm = 1: H_x$	Correlation relationship, $C_H = 2^{2H-1} - 1$
	April				
1	$Y = 60.6e^{-0.49x}$	1.49	0.51	1.96	+0.01
2	$Y = 51.89e^{-0.43x}$	1.43	0.57	1.76	+0.10
3	$Y = 60.8e^{-0.50x}$	1.50	0.49	2.00	+0.98
4	$Y = 70.55e^{-0.56x}$	1.56	0.44	2.25	+0.88
	June				
1	$Y = 54.1e^{-0.46x}$	1.46	0.54	1.85	+0.06
2	$Y = 50.7e^{-0.42x}$	1.42	0.58	1.72	+0.12
3	$Y = 62.9e^{-0.51x}$	1.51	0.51	2.00	+0.98
4	$Y = 58.7e^{-0.52x}$	1.51	0.48	2.00	+0.96
	July				
1	$Y = 46.9e^{-0.42x}$	1.42	0.58	1.72	+0.12
2	$Y = 50.7e^{-0.42x}$	1.42	0.58	1.74	+0.12
3	$Y = 62.6e^{-0.51x}$	1.51	0.40	2.00	+0.96
4	$Y = 57.3e^{-0.49x}$	1.49	0.51	1.96	+0.98

Note: 1. Conventional tillage (CT); 2. Surface tillage (ST); 3. No-till after CT; 4. No-till after ST.

The assessment of the structural organization based on the redistribution of structural components in the 0–0.3 m layer showed that in April, F_r under plowing, surface tillage, and No-till systems ranged from F_r = 1.43 to 1.56. D_m under plowing and surface tillage was < 2.0, while under the No-till system, D_m was > 2.0, influencing C_H, which ranged from C_H = 0.06 to 0.12 under surface tillage and plowing, while under the No-till system, C_H = 0.98. In July, the established pattern persisted, indicating higher dynamics in the formation of structural condition during dry sieving in the spring-summer period (Table 2).

In Table 2, the typification of components of the structural condition during dry sieving under different tillage methods for the spring-summer period is presented. Under plowing, the coefficient of variation of the content of dry aggregates sized 7–0.25 mm was 11%, under surface tillage 7.9%, and under the No-till system 9.1%, with average content in the 0–0.3 m layer of chornozem soil ranging from 69.9% to 71.5%. The normalized range varied from 4.4% to 2.0% under plowing and the No-till system, respectively. The coefficient of variation of the content of structural components sized 3–0.5 mm was 13.5% under plowing, 2.03% under surface tillage, and 7.65% under the No-till system, with average contents of 38%, 32.8%, and 34.8%, respectively. The normalized range of the mentioned fractions content was 6.5%, 0.8%, and 5.7%, respectively.

The coefficient of variation of the content of aggregates sized 1–0.25 mm was 31.9% under plowing, 24.8% under surface tillage, and 22.9% under the No-till system, with average contents ranging from 9.6% to 12.9%. Similarly, the coefficient of variation of the content of coarse aggregates (> 7–0.25 mm) was 11.9% under plowing, 5.7% under surface tillage, and 5.7% under the No-till system, with average contents ranging from 27.9% to 32.3%.

Table 2. Normalization of soil structural component parameters depending on the tillage method of the podzolized chornozem (soil layer 0–0.3 m) in a five-field crop rotation during the growing season of spring cereal crops and winter crops

Structural component parameters	Parameter value		Amplitude range Δ_a = max–min		Normalized range Δ_n: $\Delta_{50\%} = L_{0.75} - L_{0.25}$ $\Delta_{10\%} = L_{0.90} - L_{0.10}$				Coefficient of variation P, %
	%								
	mean	median	min	max	$L_{0.25}$	$L_{0.75}$	$L_{0.10}$	$L_{0.90}$	
	Conventional tillage (plowing)								
7–0.25 mm	71.5	72.9	66.8	75.8	69.2	73.6	66.8	75.8	4.32
7–5 mm	11.3	11.6	9.60	13.4	10.6	12.0	9.60	13.4	11.6
5–3 mm	17.6	17.4	16.8	18.8	17.0	17.8	16.8	18.8	4.40
3–0.5 mm	38.0	35.8	32.0	45.2	34.0	40.5	32.0	45.2	13.3
1–0.25 mm	12.9	12.4	8.00	21.5	10.8	13.5	8.00	21.5	31.9
*Non-valuable	27.8	26.8	24.2	33.2	26.0	30.8	24.2	33.2	11.9
K_{st}	2.63	2.77	2.01	3.32	2.25	2.88	2.01	3.32	16.4
**d, mm	4.31	4.18	3.50	5.30	3.89	4.81	3.50	5.30	14.7
	Surface tillage								
7–0.25 mm	67.9	69.0	64.3	69.8	66.8	69.1	64.3	69.8	2.83
7–5 mm	13.2	13.4	11.6	14.2	12.9	14.2	11.6	14.2	7.90
5–3 mm	19.5	19.8	18.2	21.0	18.6	19.8	18.2	21.0	5.22
3–0.5 mm	32.8	33.0	32.0	33.8	32.2	33.0	32.0	33.8	2.03
1–0.25 mm	10.4	9.60	8.10	16.3	9.00	10.4	8.10	16.3	24.8
Non-valuable	32.3	31.6	30.8	35.8	30.9	33.3	30.8	35.8	5.69
K_{st}	2.25	2.24	1.84	2.49	2.23	2.44	1.84	2.49	9.37
d, mm	4.68	4.64	4.29	4.97	4.55	4.91	4.29	4.97	5.13
	No-till								
7–0.25 mm	70.4	70.2	67.5	74.5	69.4	71.4	68.0	72.0	2.32
7–5 mm	13.5	13.7	11.4	15.4	12.8	14.4	11.4	15.4	9.05
5–3 mm	19.3	19.3	18.2	20.6	18.5	20.1	18.2	20.6	4.48
3–0.5 mm	34.8	33.8	31.8	38.4	32.1	37.8	31.8	38.4	7.65
1–0.25 mm	9.63	8.80	6.80	13.8	8.00	10.8	7.40	13.4	22.9
Non-valuable	29.5	29.6	25.5	32.5	28.3	30.1	27.5	32.0	5.69
K_{st}	2.52	2.44	2.10	3.63	2.32	2.66	2.13	2.86	13.9
d, mm	4.64	4.69	4.10	5.12	4.28	5.02	4.15	5.12	7.96

Note: * Non-valuable – agronomically non-valuable soil particles; **d – mean weighted diameter of soil structural aggregates; K_{st} – soil structure coefficient.

The soil structure coefficient, regardless of the tillage method, ranged from K_{st} = 2.25 to 2.63. However, the coefficient of variation was 16.4% under plowing, 9.4% under surface tillage, and 13.4% under the No-till system.

The coefficient of variation for the mean weighted diameter of structural components was 14.7% under plowing, 5.1% under surface tillage, and 7.9% under the No-till system, with average values of 4.31 mm, 4.68 mm, and 4.64 mm, respectively.

The median value under plowing was lower than the mean value, while under surface tillage and the No-till system, it exceeded the mean value and, to a greater extent, approached the upper typical value of the size of structural components. The normalized range of the mean weighted diameter of structural components was 0.92 mm under plowing, 0.36 mm under surface tillage, and 0.44 mm under the No-till system.

Practically, with almost identical levels of structural components in the soil layer 0–0.3 m under different tillage systems, the coefficient of variation of the main components of the structural state during dry sieving is 1.3–6.7 times higher under conventional tillage compared to surface tillage and the No-till system.

In the spring period, in the soil layer 0–0.2 m under conventional tillage, the amount of water-resistant aggregates < 0.25 mm was at the level of 48%, in the soil layer 0.2–0.3 m – 47.4%, and in the layer 0–0.3 m – 47.7%. Under surface tillage, it was 40.0%, 47.9%, and 44.0% respectively. With the No-till system under conventional tillage, the content of water-resistant aggregates < 0.25 mm was at 42.5%, 51.7%, and 45.1%, while with surface No-till tillage, it was 40.9% (0–0.2 m), 45.1% (0.2–0.3 m), and 43% (0–0.3 m). On average, in the soil layer 0–0.3 m, the amount of water-resistant aggregates > 0.25 mm was 52.3% under conventional tillage, which was 5.7% higher compared to surface tillage, 2.7% higher compared to No-till under conventional tillage, and 4.7% higher compared to No-till under surface tillage. The amount of aggregates sized 0.5–0.25 mm in the soil layer 0–0.2 m was the same regardless of the tillage method, ranging from 35.6% to 37.1%. In the soil layer 0.2–0.3 m, under conventional tillage and No-till systems, the amount of aggregates 0.5–0.25 mm was the same (31.8–32.6%), while under surface tillage, it reached 36% (see Table 3).

Table 3. The impact of tillage methods on the water stability of the soil structure in the 0–0.3 m layer of podzolized chornozem in a five-field grain crop rotation in the third year of implementation during the growing season of spring and winter cereals

Tillage method	Size of water-stable aggregates, mm							* C_{ws}	**d, mm
	> 3	3–0.5	1–0.5	0.5–0.25	< 0.25	0.5–0.25 to 1–0.5	> 0.25		
	April								
Conventional tillage (CT)	0.87	12.8	12.8	34.9	49.7	2.7	49.3	0.21	0.43
Surface tillage (ST)	0.60	13.4	13.4	37.9	46.4	2.8	49.2	0.22	0.41
No-till after CT	0.88	14.9	14.9	33.7	48.6	2.3	54.2	0.15	0.44
No-till after ST	0.73	16.7	16.7	36.1	45.0	2.2	56.1	0.16	0.44
Fallow	4.49	16.5	16.5	28.4	41.0	1.7	59.0	0.12	0.53
	June								
CT	0.95	14.0	14.0	34.3	47.2	2.46	52.8	0.23	0.46
ST	1.04	24.3	24.3	30.9	40.5	1.27	59.5	0.15	0.51
No-till after CT	1.26	27.1	27.1	30.4	34.6	1.12	65.4	0.13	0.54
No-till after ST	1.25	22.8	22.8	37.3	37.0	1.64	63.0	0.17	0.55
	July								
CT	1.44	19.5	19.5	37.7	37.3	1.93	62.7	0.19	0.49
ST	1.12	17.3	17.3	38.7	39.2	2.23	60.8	0.14	0.51
No-till after CT	1.16	18.4	18.4	35.3	40.8	1.92	59.2	0.19	0.52
No-till after ST	1.14	27.3	27.3	33.0	34.3	1.21	65.7	0.13	0.57

Note: *C_{ws} – water stability criterion; **d – mean weighted diameter of soil structural aggregates.

On average, in the 0–0.3 m soil layer, the content of water-stable aggregates sized 0.5–0.25 mm ranged from 34.2% to 35.8%. Valuable aggregates sized 3–0.5 mm in the 0–0.2 m soil layer were higher with surface tillage and No-till compared to plowing by 10% and 20.1–21.6%, respectively. Conversely, in the 0.2–0.3 m layer, plowing had more aggregates of this size by 3.3–3.8% compared to other cultivation methods.

In the 0–0.3 m soil layer, the average proportion of aggregates sized 3–0.5 mm was lowest with plowing (16.6%), while with surface tillage and No-till, it increased to 21.7% and 19.4–19.8%, respectively. In June (during the heading phase of spring and winter cereals), the distribution of water-stable aggregates slightly changed. The quantity of water-stable aggregates < 0.25 mm with plowing was higher compared to surface tillage by 5.5% (0–0.2 m), 8.2% (0.2–0.3 m), and by 4.5% (0–0.3 m). With No-till, the quantity of aggregates <0.25 mm was lower compared to plowing by 8.3–8.7% (0–0.2 m), 13–17% (0.2–0.3 m), and by 8.3–10.7% (0–0.3 m).

The highest quantity of water-stable aggregates sized 0.5–0.25 mm was observed with plowing and No-till using surface tillage, reaching 35.2–36.3% (0–0.2 m). Conversely, with surface tillage and No-till using plowing, the quantity of aggregates was lowest, being 8.8% less. In the soil layer 0.2–0.3 m, the content of aggregates sized 0.5–0.25 mm ranged from 31.4–33.2%, while in the 0–0.3 m layer, it ranged from 30.3–30.9% with surface tillage and No-till. However, with plowing, the content reached 34.3%.

The least amount of water-stable aggregates in the most valuable fraction (3–0.5 mm) was observed with plowing: 18.4% (0–0.2 m), 16.6% (0.2–0.3 m), and 19.5% (0–0.3 m). With surface tillage, there was an increase in the content of aggregates sized 3–0.5 mm compared to plowing by 12% (0–0.2 m), 7.2% (0.2–0.3 m), and 8.1% (0–0.3 m). Under the No-till system, the increase ranged from 9.4–14.7% (0–0.2 m), 11.0–13.7% (0.2–0.3 m), and 11.8–14.8% (0–0.3 m). This indicates an aggregation of water-stable aggregates into the most valuable fraction of water-stable aggregates.

During the ripening stage (July) of winter and spring cereals, the content of water-stable aggregates < 0.25 mm in the 0–0.2 m soil layer under plowing was 35.9%, while under surface tillage and the No-till system, their quantity increased by 5.1% and 6.8–7.2%, respectively. In the 0.2–0.3 m soil layer, the highest amount of non-valuable aggregates was observed under the No-till system with plowing, while in other variants, their quantity ranged from 35.4–38.8%. In the 0–0.3 m soil layer, the content of non-valuable aggregates ranged from 37.3–40.8%.

In July, there were more water-stable aggregates of 0.5–0.25 mm under plowing and surface tillage, while under the No-till system, the quantity of aggregates of this size was 4.5–5.0% lower. The highest amount of valuable water-stable aggregates (3–0.5 mm) was consistent across all tillage methods. Regarding the distribution of water-stable aggregates, a return to the distribution observed in April was noted, but the level of water stability of structure was higher under plowing, whereas under surface tillage and the No-till system, the water stability of the structure deteriorated slightly compared to its condition in June.

The normalization of parameters of water-stable structure in seasonal measurements revealed a significant influence of tillage methods on its condition. For instance, the average content of water-stable aggregates sized 3–0.5 mm was 19.5% under plowing, 21% under surface tillage, and 24.4% under the No-till system, which is 1.25 times higher (Table 4). The normalized range under plowing was Δ_n = 8.5%, while at No-till system, it was Δ_n = 11.8%, with higher values of interval limits by 1.06–1.6 times compared to plowing in the latter case.

Table 4. Normalization of parameters of water-stable structure components depending on the tillage method of podzolized chornozem (soil layer 0–0.3 m) in a five-field grain crop rotation during the growing season of spring and winter cereal crops

Structural component parameters	The content of water-stable aggregates %		Amplitude range: Δ_a = max-min		Normalized range Δ_n: $\Delta_{50\%} = L_{0.75} - L_{0.25}$ $\Delta_{10\%} = L_{0.90} - L_{0.10}$				Coefficient of variation P, %
	mean	median	min	max	$L_{0.25}$	$L_{0.75}$	$L_{0.10}$	$L_{0.90}$	
	Conventional tillage								
> 3 mm	1.11	1.05	0.64	1.96	0.92	1.08	0.64	1.96	34.7
3–0.5 mm	19.5	18.5	10.3	28.3	17.5	18.9	10.3	28.3	28.8
1–0.5 mm (a)	14.3	14.0	9.30	19.5	12.9	15.3	9.30	19.5	19.5
0.5–0.25 (b)	35.5	34.9	32.4	40.2	33.9	37.1	32.4	40.2	7.22
< 0.25 mm	44.9	47.2	35.9	52.0	40.0	49.7	35.9	52.0	13.1
b/a	2.57	2.47	1.95	4.00	2.41	2.63	1.95	4.00	23.2
> 0.25 mm	54.8	52.8	48.0	64.1	49.9	60.0	48.0	64.1	11.2
C_{ws}	0.21	0.22	0.17	0.24	0.19	0.23	0.17	0.24	13.0
d, mm	0.46	0.46	0.39	0.51	0.45	0.48	0.39	0.51	7.61
	Surface tillage								
> 3 mm	0.92	1.00	0.20	1.44	0.80	1.10	0.20	1.44	38.5
3–0.5 mm	20.9	21.2	13.2	30.5	15.3	23.8	13.2	30.5	27.7
1–0.5 mm (a)	17.8	17.3	9.40	26.8	13.4	21.0	9.40	26.8	31.1
0.5–0.25 (b)	35.3	36.0	29.5	41.0	33.2	37.9	29.5	41.0	10.5
< 0.25 mm	43.1	41.0	37.4	54.2	39.2	46.4	37.4	54.2	12.6
b/a	2.17	2.24	1.11	3.68	1.27	2.69	1.11	3.68	39.0
> 0.25 mm	56.5	59.0	46.3	62.6	52.1	60.8	46.3	62.6	10.3
C_{ws}	0.17	0.17	0.11	0.24	0.14	0.19	0.11	0.24	25.9
d, mm	0.47	0.49	0.38	0.53	0.44	0.51	0.38	0.53	11.1
	No-till								
> 3 mm	1.07	1.10	0.70	1.40	0.88	1.26	0.73	1.40	21.9
3–0.5 mm	24.4	26.6	13.1	34.8	18.5	30.3	14.6	31.6	27.3
1–0.5 mm (a)	21.3	22.9	12.9	29.7	16.6	26.0	13.2	28.9	26.6
0.5–0.25 (b)	34.3	34.5	29.5	39.8	31.8	36.1	30.4	39.5	8.83
< 0.25 mm	39.9	38.0	33.0	51.7	35.4	45.0	33.1	48.6	14.3
b/a	1.55	1.43	0.89	2.73	1.04	2.02	0.97	2.72	36.9
> 0.25 mm	60.7	62.0	54.0	67.0	56.1	64.6	54.2	66.9	7.78
C_{ws}	0.15	0.16	0.12	0.21	0.13	0.17	0.12	0.19	16.7
d, mm	0.51	0.52	0.42	0.58	0.44	0.55	0.44	0.57	10.6

Note: *C_{ws} – water stability criterion; **d – mean weighted diameter of soil structural aggregates.

The content of water-stable aggregates sized 3–0.5 mm, by the median, was lower than the mean under plowing, whereas under surface tillage and the No-till system, it was higher than the mean, indicating a tendency of the content of this fraction towards the upper typical value. The coefficient of variation of the content of the 3–0.5 mm fraction of water-stable aggregates was 28.8% under plowing and 27.3–27.6% under surface tillage and the No-till system, which is practically the same. The content of the 1–0.5 mm fraction of water-stable aggregates was 14.3% under plowing, 17.8% under

surface tillage, and 21.3% under the No-till system, which is 1.5 times higher. The normalized range of the content of this fraction of water-stable aggregates was $Δ_n$ = 2.4% under plowing, $Δ_n$ = 7.6% under surface tillage, and $Δ_n$ = 9.4% under the No-till system, with significantly higher (1.4–1.7 times) values of interval limits.

The coefficient of variation of the content of water-stable aggregates sized 1–0.5 mm was 19.5% under plowing, while under surface tillage and the No-till system, it increased to 26.6–31.1%, which is 1.36–1.6 times higher.

The average content of water-stable aggregates sized 0.5–0.25 mm, regardless of the tillage method, ranged from 34.3% to 35.5%. However, the median content of this fraction was lower than the average content under plowing, whereas under surface tillage and the No-till system, the median content exceeded the average. This indicates an increase in their content due to a decrease in the content of water-stable aggregates smaller than 0.25 mm. The coefficient of variation increased from plowing (7.22%) to surface tillage and the No-till system (8.8–10.5%).

The average ratio of water-stable aggregates sized 0.5–0.25 mm to 1.05 mm was 2.57 to 1 under plowing, 2.17 to 1 under surface tillage, and 1.55 to 1 under the No-till system, with an amplitude range of $Δ_a$=2.05 units (plowing), $Δ_a$ = 2.57 units (surface tillage), and $Δ_a$ = 1.84 units (No-till). The normalized range was $Δ_n$ = 0.22 (plowing), $Δ_n$ = 1.42 (surface tillage), $Δ_n$ = 0.98 (No-till), with lower values in the range of 1.3–2.32 interval values of the normalized interval.

The coefficient of variation (*P*) for ratio under plowing was at 23.2%, while under surface tillage and the No-till system, variability increased by 1.58–1.68 times, indicating an active process of rearrangement of water-stable aggregates from the 0.5–0.25 mm fraction to the 1–0.5 mm fraction.

The average content of water-stable aggregates larger than 0.25 mm under plowing was 54.8%, under surface tillage - 56.5%, and under the No-till system - 60.7%, which was higher compared to plowing by 5.9%. The content of this fraction of water-stable aggregates at the median under plowing was lower than the mean by 2%, while under surface tillage and the No-till system, it was higher by 2.5% and 1.3% respectively, indicating a tendency for the content of agronomically valuable aggregates under plowing to gravitate towards the lower typical value, while under surface tillage and the No-till system, it tends towards the upper typical value, leading to a decrease in the content of this fraction larger than 0.25 mm under plowing and an increase under surface tillage and the No-till system.

The coefficient of variation in the content of water-stable aggregates larger than 0.25 mm under plowing and surface tillage was 10.3–11.2%, while under the No-till system, it was 7.78%. Conversely, the content of water-stable aggregates smaller than 0.25 mm changed. The average content under plowing was 44.9%, while under the No-till system, it was 39.9%, which is 5% less. At the median, the content of non-valuable aggregates was higher than the mean under plowing, while under surface tillage and the No-till system, it was lower than the mean, indicating an increase in the former case and a decrease in the latter.

The mean value of the water stability index (C_{ws}) under plowing was $C_{ws} = 0.21$, under surface tillage $C_{ws} = 0.17$, and under the No-till system $C_{ws} = 0.15$. The median value of C_{ws} exceeded the mean under plowing, while under surface tillage and the No-till system, it remained at the mean level.

The normalized range of C_{ws} under plowing ranges from 0.04 to 0.07 units, under surface tillage from 0.05 to 0.13 units, and under the No-till system from 0.04 to 0.07 units. However, the interval values of the normalized ranges are lower.

The coefficient of variation under plowing was 13%, while under surface tillage it doubled, and under the No-till system, it increased by 1.29 times.

The decrease in the value of C_{ws} during surface tillage is associated with the aggregation of water-stable aggregates and their accumulation in fractions larger than 1 mm, which is linked to the increase in the fraction of 3–0.5 mm and the decrease in the ratio of fractions 0.5–0.25 mm to 1–0.5 mm, as shown above.

The average value of the mean weighted diameter of water-stable aggregates (d, mm) during conventional tillage was d= 0.46 mm, during surface tillage d = 0.47 mm, and during No-till d = 0.51 mm, which is 1.11 times higher.

The normalized indicators of the mean weighted diameter of water-stable aggregates were: 0.03–0.17 mm (CT), 0.07–0.15 mm (ST), and 0.11–0.13 mm (No-till), with higher values of the extreme interval values of the diameter size of water-stable aggregates. These values were 1.12–1.15 times higher in No-till compared to conventional tillage, with a coefficient of variation of 10.6–11.1% for surface tillage and No-till, and 7.61% for conventional tillage.

Calculations show that at conventional tillage, there were 11 significant correlation relationships ($R > \pm 0.7$) between indicators of soil structural condition and components of structural stability, comprising 9 pairs of strong positive correlations and 2 pairs of negative correlations. These correlations represent 11%, 9%, and 2% of the total number of pairwise correlations in the matrix field. Pairwise correlation coefficient calculations between components of soil structural condition revealed that in conventional tillage, there were 27 significant strong positive correlations (49%), 14 pairs of positive correlations (25.5%), and 13 pairs of negative correlations (23.6%). In surface tillage and No-till, there were 24 significant correlations (43.6%), 11 pairs of positive correlations (20%), and 13 pairs of negative correlations (23.7%). This indicates a nearly uniform soil structural condition in the 0–0.3 m layer of chornozem regardless of the tillage method.

In surface tillage, there were a total of 28 pairwise correlations (28%), with 12 positive correlations (12%) and 16 mutual correlations (16%). In the No-till system, there were 16 correlations (16%), comprising 9 positive correlations (9%) and 7 mutual correlations (7%) (Table 5).

The assessment of the water-resistant structure condition through paired correlations depending on the tillage method showed that with plowing, there were 15 significant correlation links ($R > \pm 0.7$) (42%), comprising 8 direct links (22%) and 7 inverse links (19%). With surface tillage, there were 21 links (58%), with 11 direct (31%) and 10 inverse (27.8%). In the No-till system, there were 23 links (63%), with 12 direct (33.3%) and 11 inverse (30.6%), respectively.

Table 5. The influence of different tillage methods on the coefficients of pairwise correlations between the parameters of the structural-aggregate state in the five-field grain crop rotation

	d, mm (dry)*	> 3 mm	3–0.5 mm	1–0.5 mm	0.5–0.25 mm	< 0.25 mm	X_5 to X_4	> 0.25 mm	C_{ws}	*d*, mm (wsa)**
	X_1	X_2	X_3	X_4	X_5	X_6	X_7	X_8	X_9	X_{10}
	No-till									
X_1	1.00	–0.81	–0.64	–0.54	0.25	0.65	0.63	–0.71	–0.15	–0.71
X_2		1.00	0.62	0.52	–0.28	–0.63	–0.61	0.66	0.21	0.82
X_3			1.00	0.95	–0.46	–0.90	–0.96	0.95	–0.33	0.89
X_4				1.00	–0.54	–0.87	–0.89	0.92	–0.51	0.83
X_5					1.00	0.12	0.57	–0.34	0.43	–0.24
X_6						1.00	0.77	–0.94	0.27	–0.92
X_7							1.00	–0.85	0.23	–0.82
X_8								1.00	–0.39	0.91
X_9									1.00	–0.11
X_{10}										1.00
	Surface tillage									
X_1	1.00	–0.65	–0.82	–0.74	0.32	0.75	0.64	–0.79	0.41	–0.88
X_2		1.00	0.60	0.56	–0.14	–0.72	–0.66	0.73	–0.52	0.87
X_3			1.00	0.98	–0.60	–0.77	–0.94	0.80	–0.60	0.86
X_4				1.00	–0.59	–0.77	–0.96	0.78	–0.63	0.82
X_5					1.00	–0.03	0.54	–0.04	–0.11	–0.23
X_6						1.00	0.78	–0.97	0.84	–0.91
X_7							1.00	–0.78	0.70	–0.82
X_8								1.00	–0.87	0.94
X_9									1.00	–0.71
X_{10}										1.00
	Conventional tillage (plowing)									
X_1	1.00	–0.35	–0.25	–0.13	–0.00	0.35	0.21	–0.42	–0.53	–0.47
X_2		1.00	0.90	0.44	–0.22	–0.80	–0.53	0.78	–0.11	0.82
X_3			1.00	0.71	–0.02	–0.87	–0.70	0.84	–0.32	0.86
X_4				1.00	0.17	–0.65	–0.88	0.61	–0.61	0.72
X_5					1.00	–0.36	0.26	0.40	–0.20	0.03
X_6						1.00	0.51	–0.99	0.35	–0.90
X_7							1.00	–0.46	0.51	–0.77
X_8								1.00	–0.28	0.88
X_9									1.00	–0.37
X_{10}										1.00

Note: *(dry) – dry sieving; ** (wsa) – water-stable aggregates; C_{ws} – water stability criterion; *d* – mean weighted diameter of soil structural aggregates.

In analyzing the components of the structural-aggregate state of chornozem using 17 quantitative variables, it was found that regardless of the tillage method, 3 factors were identified, accounting for: F_1 – 50–52%, F_2 – 22–25%, and F_3 – 11–17% of the total variance, totaling 74–75% of the variance across F_1–F_2. In terms of tillage systems: 86% – plowing, 91% – surface tillage, 80% – No-till system (Table 6).

Table 6. Factor loading of the components of the structural-aggregate composition depending on the tillage method of podzolized chornozem in a five-field crop rotation

	Conventional tillage (plowing)			Surface tillage			No-till		
	F_1	F_2	F_3	F_1	F_2	F_3	F_1	F_2	F_3
	Dry sieving								
7–0.25 mm	0.91	–0.37	–0.04	–0.66	–0.71	0.17	0.64	0.67	0.17
7–5 mm	–0.91	0.32	0.22	–0.61	0.30	–0.71	–0.09	–0.36	0.85
5–3 mm	–0.07	0.30	–0.33	0.24	–0.05	–0.93	–0.17	–0.47	0.75
3–0.5 mm	0.93	–0.26	–0.07	0.59	–0.32	0.66	0.21	0.46	–0.79
1–0.25 mm	0.49	–0.62	–0.33	0.53	0.31	0.56	0.75	0.30	–0.41
Non-valuable	–0.83	0.06	0.45	0.70	0.63	–0.31	–0.67	–0.62	–0.14
K_{st}	0.96	–0.23	–0.05	–0.20	–0.93	0.23	0.68	0.59	0.38
d, mm	–0.80	0.47	0.21	–0.82	0.35	–0.35	–0.90	–0.23	0.22
	Wet sieving								
> 3 mm	0.81	0.27	0.42	0.76	–0.39	0.08	0.84	0.10	–0.03
3–0.5 mm	0.75	0.52	0.32	0.96	0.10	0.07	0.86	–0.45	0.02
1–0.5 mm (a)	0.45	0.70	0.11	0.94	0.15	–0.01	0.79	–0.53	0.04
0.5–0.25 mm (b)	0.05	0.34	–0.89	–0.51	–0.72	–0.44	–0.39	0.23	0.46
b/a	–0.80	–0.55	0.11	–0.82	0.44	0.26	–0.83	0.41	–0.20
< 0.25 mm	–0.48	–0.51	–0.43	–0.95	–0.18	0.14	–0.83	0.38	0.11
> 0.25 mm	0.84	0.48	–0.18	0.85	–0.42	–0.25	0.87	–0.45	0.07
C_{ws}	0.16	–0.95	–0.04	–0.67	0.24	0.68	–0.03	0.74	0.08
d, mm	0.84	0.46	0.12	0.93	–0.36	0.01	0.89	–0.32	0.15
Expl.Var.	9.98	5.06	2.17	10.45	4.30	3.31	8.19	4.41	3.32
Prp.Total	0.50	0.25	0.11	0.52	0.22	0.17	0.41	0.22	0.17

There is a criterion of adequacy of the sample with respect to the factors, which makes it possible to characterize the degree of suitability of factor analysis to the given sample of quantitative indicators or variables (Kaiser-Meyer-Olkin test):

> 0.9 – unconditional adequacy;
> 0.8 – high adequacy;
> 0.7 – sufficient adequacy;
> 0.6 – satisfactory adequacy;
> 0.5 – low adequacy;
< 0.5 – lack of adequacy.

It was found that for plowing (F_1), there were 4 correlation coefficients > 0.9, 6 coefficients > 0.8, and 1 coefficients > 0.7. Out of these, 6 correlations were attributed to structural components, and 5 correlations were attributed to the components of water-resistant structure. Regarding F_2, a strong correlation was established with the group of water-resistant aggregates sized 1–0.5 mm ($R = 0.70$) and C_{ws} ($R = -0.95$). For F_3, the association was made with the fraction of water-resistant aggregates sized 0.5–0.25 mm ($R = -0.89$).

There were 33 correlation coefficients of low adequacy ($R < 0.05$) for F_1–F_3, which accounted for 71% of the total number of factor loadings.

For systematic surface tillage, regarding F_1, there were 9 correlation coefficients with $R = 0.7$–0.9 and 6 cases with $R = 0.5$–0.6. There were 2 correlation links of high adequacy level ($R = \pm 0.70$–0.82) related to the dry sieve fractionation, while there were

6 correlation links of unconditional and high adequacy related to the water-stable aggregates fraction, and 1 correlation link with a sufficient adequacy level.

Regarding factor F_2, there was a connection at the level of unconditional adequacy with K_{st}(dry), and at the level of sufficient adequacy with the fraction of aggregates 7–0.25 mm and 0.5–0.25 mm (wsa). For other variables (13 links), the connections were at a low adequacy level. For F_3, at the level of unconditional and sufficient adequacy, there were correlations with the fractions of aggregates 5–3 mm (wsa) and 7–5 mm (dry).

In surface tillage, there were 6 links of satisfactory adequacy ($R > 0.6$), which is 6 times more than in conventional tillage. There were 27 cases of low adequacy and its absence in surface tillage, which is 1.22 times less or 12% less compared to conventional tillage.

In the No-till system, regarding F_1, there were 9 cases of links with adequacy ranging from $R > 0.7$ to $R > 0.9$, and 3 cases with $R > 0.5$. Regarding F_2, there is one connection (C_{ws}) with sufficient adequacy, while there were four connections of satisfactory and low adequacy. In the No-till system, there were 5 cases of links with unconditional, high, and sufficient adequacy for dry sieve fractionation, while for water-stable aggregates fraction, there were 8 cases. Links with low adequacy and lack of adequacy accounted for 55% of the total, similar to surface tillage.

The consolidation of the components of the structural-aggregate composition of chornozem under different tillage systems is determined by links of sufficient to unconditional adequacy. In surface tillage and the No-till system, the same number of such links were created (13–14 cases), but in conventional tillage, the distribution ratio between components in dry and wet sieving was about 50% to 50%, while in surface tillage and the No-till system, the ratio was 1.3–1.6 to 1 in favor of water-stable aggregates. It is important to note the increase in links of satisfactory adequacy ($R > 0.6$), which were 5–6 times fewer in conventional tillage compared to surface tillage and the No-till system.

The principal component analysis revealed the main components of the structural-aggregate state, obtained under dry and wet sieving conditions, which determine the differences in soil structural condition under different tillage methods. Cluster analysis involves the use of distance matrices and the 'nearest neighbor' clustering algorithm to construct a dendrogram of grouping the components of the structural-aggregate composition under dry sieving and water erosion conditions (Vorobyov & Ladan, 2021).

The maximum cluster sizes are determined by half the distance between the most distant components based on the criterion $D_i < D_{max}/2$. The clustering results of the components of the structural-aggregate composition of leached chornozem, respectively, according to the distribution of dry structural aggregates and water-resistant aggregates, are shown in dendrograms (Fig. 3). Overall, the similarity measure based on the criterion of the largest cluster is 51.1% for plowing and surface treatment, and 48.8% for the No-till system (Fig. 3).

For plowing, three main clusters have been identified:

1. Cluster 1 – with the least dissimilarity (10.8%): d(dry), d(wsa), C_{ws}, K_{st}, > 3 mm (wsa), the ratio of 0.5–0.25 mm (wsa) to 1–0.5 mm (wsa);
2. Cluster 2 – with a similarity measure of 33.2% (7–5 mm (dry), 5–3 mm (dry), 1–0.5 mm (wsa), 1–0.25 mm (dry) и 3–0.5 mm (wsa));
3. Cluster 3 – with a similarity measure of 51.1% (3–0.5 mm (dry), 0.5–0.25 mm (wsa), non-valuable aggregates (dry)).

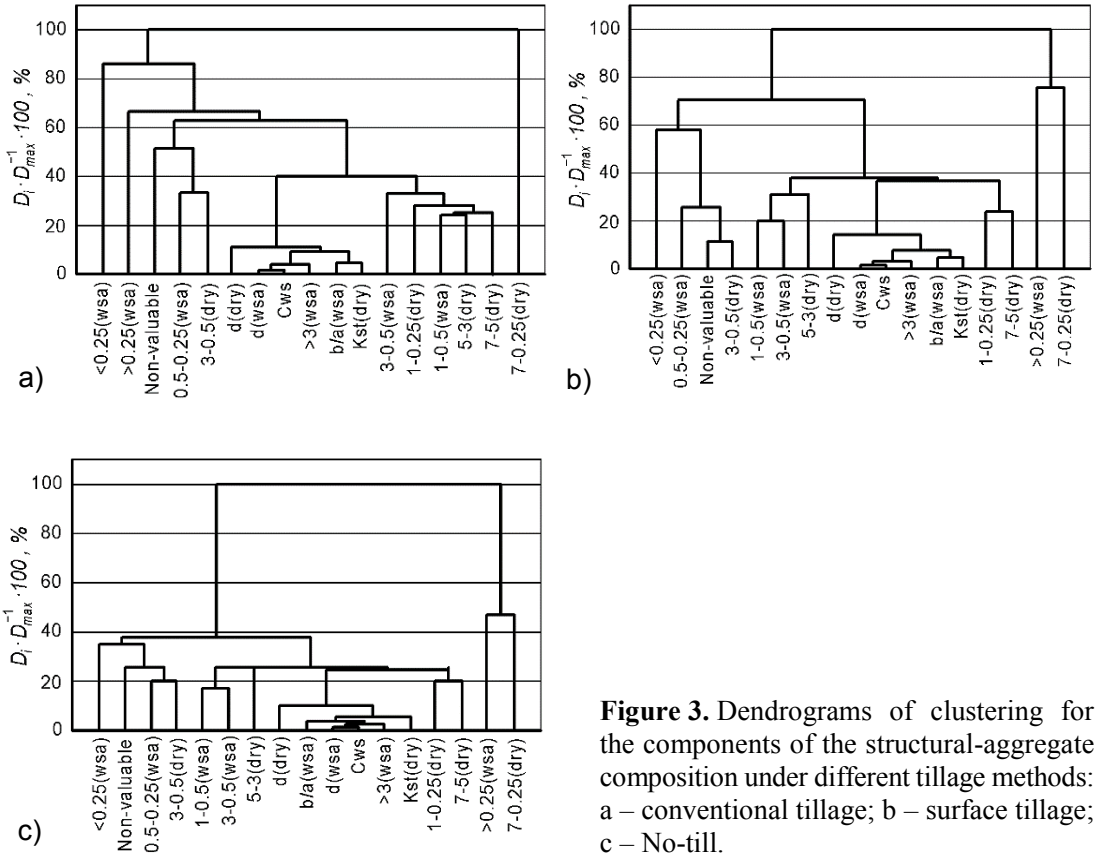

Figure 3. Dendrograms of clustering for the components of the structural-aggregate composition under different tillage methods: a – conventional tillage; b – surface tillage; c – No-till.

The similarity between clusters 1 and 2 was 40.5%, while between these clusters and cluster 3 it was 51.1%, which corresponds to the criterion of the maximum cluster. Beyond this point, further clustering loses its relevance. The identified fractions of 7–0.25 mm (dry), > 0.25 mm (wsa), and < 0.25 mm (wsa) stand out from the overall clustering of structural-aggregate components, indicating soil imbalance at the structural level as a system.

For surface tillage, the clustering of structural-aggregate state parameters follows a more complex pattern:

1. Cluster 1 – is similar to the cluster in conventional tillage, with increasing divergence up to 14.4%.
2. Cluster 2 – 1–0.5 mm (wsa), 3–0.5 mm (wsa), 5–3 mm (dry) – 19.4%.
3. Cluster 3 – 0.5–0.25 mm (wsa), non-valuable aggregates (dry) and 3–0.5 mm (dry) – 26.6%.
4. Cluster 4 – 1–0.25 m (dry) и 7–5 mm (dry).

The merging of these clusters occurs at a level of 37.5%, which is approximately 3% lower than in conventional tillage. The maximum criterion level of 51.1% excludes fractions > 0.25 mm (wsa) and 7–0.25 mm (dry) from the overall clustering, showing 86% similarity, and the fraction < 0.25 mm (wsa) with a 58.3% similarity level.

The decrease in the distance measure between clusters 1–3 compared to conventional tillage by about 3% indicates a certain stabilization of the soil structure under surface tillage.

In the No-till system, the clustering of soil structure elements during dry and wet sieving followed the same principle as surface tillage. Clusters 1–4 were merged at a level of 25.4%, which is 15.1% lower than in conventional tillage or approximately 1.6 times lower, and compared to surface tillage, it is 12.1% lower or approximately 1.48 times lower in total. At the similarity level of clustering features, 11 parameters (64.7%) were merged, whereas in conventional tillage, it was 6 parameters (35.3%), similar to surface tillage.

The maximum criterion value for the overall cluster in the No-till system was 48.8%. However, clusters 5 (< 0.25 mm (wsa), non-essential aggregates in dry sieving, 0.5–0.25 mm (wsa), 3–0.5 mm (dry)) and 6 (> 0.25 mm (wsa) and 7–0.25 mm (dry)) had distances of 38% and 46%, respectively, which did not exceed the value of the overall cluster (48.8%). This indicates that all components of the soil structure were involved in the overall clustering, which is a sign of optimization of the structural-aggregate state with the systematic use of the No-till system in the 5-field crop rotation.

The sustainable effect of using the No-till system is evident in the accumulation of mulch on the soil surface, which helps increase soil moisture content. With an increase in mulch mass from 1–2 t ha^{-1} to 8–10 t ha^{-1}, soil erosion losses are reduced. This is an effective way to increase soil moisture content, reduce the water consumption coefficient of crops, and reduce the consumption of productive water reserves for physical evaporation during the growing season of agricultural crops in a short rotation crop system (Tuure et al., 2021; Ye et al., 2024).

When creating a mulch layer on the soil surface, its influence is noted on both cultivated and uncultivated soil in preserving productive water reserves. It has been found that the content of productive water with No-till is higher than with soil tillage in 50% of cases, equal in 35%, and lower in 15%, which is associated with improved agrophysical indicators (Khera, 2006; Mulumba & Lal, 2008; Bhatt & Li et al., 2013; Blanco-Canqui & Ruis, 2018).

The impact of organic mulch on soil processes lies in improving parameters that contribute to its fertility, associated with the addition of additional organic matter and protection of the soil surface (Kibet et al., 2016¸ Vach et al., 2018). Negative assessments indicate soil compaction in the absence of tillage (Gozubuyuk et al., 2014), which is influenced by soil characteristics, climatic conditions, insufficient thickness or short duration of mulch use.

In semi-arid climates, soil water before autumn tillage was lower with tillage and shallow tillage at 22.4% and 12.8%, respectively, compared to No-till. However, three weeks after tillage, moisture levels were 21.1% and 14.3%, respectively. This can be explained by reduced evaporation and a 2.4 times increase in soil filtration coefficient due to increased vertical macropores (Dudchenko et al., 2014; Manushkina et al., 2020).

When comparing spring water reserves in 2023 to those in 2022, it was found that with tillage in the 0–1 m layer, there was a slight tendency towards accumulation, whereas with surface tillage over 7 years, water reserves in the 1 meter depth increased by 10 mm with growing water reserves in soil layers. With the No-till system, water reserves in the 1 meter depth relative to 2022 increased by 19 mm with a 13 mm increase in composite layers of soil thickness (0–0.5 mm) under plowing. Implementing No-till through surface tillage ensured an increase in water reserves in the 1 meter depth, reaching 14 mm.

In April 2022, the productive water reserves in the 0–1 m layer were at the same level regardless of tillage method, but with surface tillage, there was a decrease in productive water reserves by 8–10 mm. In June, water reserves in the 1 meter depth under the No-till system were higher by 7–9 mm, while in July, conversely, with plowing and surface tillage, moisture was higher by 5–7 mm. The expenditure of productive water reserves from the 1 meter depth for April–June increased with plowing by an average of 8–10 mm, while for June–July, it increased from plowing (–7.0 mm) to surface tillage (–16 mm) and the No-till system: –12.0 mm (with plowing) and –20 mm (with surface tillage). The expenditure of productive water reserves for April–July, regardless of the tillage method, was practically the same.

In 2023, the moisture expenditure for April–June with plowing was 120 mm with a ratio of expenditure from the sub-layers of 1.2 to 1. With the No-till system through plowing, the moisture expenditure was 112 mm (a decrease of 8 mm) with a ratio of expenditure of 1.64 to 1 (Table 7). With surface tillage and the No-till system through surface tillage, the moisture expenditure was 129–131 mm with a ratio of expenditure of 1.1 to 1. The highest water reserve was in June with the No-till system through plowing - 51 mm compared to 41 mm (tillage), 26 mm (surface tillage), and 42 mm (No-till through surface tillage).

Table 7. The impact of different tillage methods on the balance of productive water reserves in a 5-field crop rotation

Tillage method	Productive water reserves and consumption, mm					
	April	June	± April to June	July	± June to July	± April to July
	2022 year					
Conventional tillage (CT)	151.0	48.0	–103.0	41.0	–7.0	–110
No-till after CT	150.0	55.0	–95.0	43.0	–12.0	–107
Surface tillage (ST)	143.0	49.0	–94.0	33.0	–16.0	–110
No-till after ST	153.0	57.0	–96.0	37.0	–20.0	–116
	2023 year					
CT	161.0	41.0	–120.0	87.0	+46.0	–74.0
No-till after CT	167.0	55.0	–112.0	104.0	+49.0	–63.0
ST	157.0	26.0	–131.0	73.0	+46.0	–84.0
No-till after ST	171.0	42.0	–129.0	104.0	+62.0	–67.0
	2022–2023 years					
CT	156.0	45.0	–111.0	64.0	+19.0	–92.0
No-till after CT	160.0	55.0	–105.0	74.0	+19.0	–86.0
ST	150.0	38.0	–112.0	53.0	+15.0	–97.0
No-till after ST	162.0	50.0	–112.0	71.0	+21.0	–91.0
$LSD_{0.05}$	7.5	7.5	-	7.0	-	-

Note: (CT) – conventional tillage; (ST) – surface tillage.

The poorest water supply was observed with surface tillage – 26 mm with a layered distribution of 8 mm and 18 mm for ratios ranging from 0.4 to 1. The highest water supply was recorded with No-till under conventional tillage – 55 mm with a ratio of 0.36 to 1, with a water reserve in the 0.5–1 m layer of 41 mm, which is higher than with conventional tillage and No-till under surface tillage by 13 mm and 23 mm, respectively. Water intake during June–July with conventional tillage, No-till under conventional

tillage, and surface tillage was 46–49 mm, whereas with No-till under surface tillage, it was 62 mm. Kibet et al. (2016) came to similar results when studying the influence of long-term tillage when studying organic components in the soil and its structure on Typic Argiudoll. Accumulation of water occurred in the 0–0.5 m layer, increasing from conventional tillage to 56 mm (+10 mm) with No-till under surface tillage (Table 3).

The water reserve in July in the 0–1 m layer was highest with No-till – 104 mm, which is 17 mm more than conventional tillage and 31 mm more than surface tillage. Tuure et al. (2021) when studying and modeling the soil moisture content when mulching the soil surface with plant residues, confirms these results. Water consumption from the 0–1 m layer during the growing season with conventional tillage and surface tillage was: –74 mm and –84 mm, respectively, while with No-till it ranged from –63 mm to –67 mm, significantly lower by –9 mm and –19 mm.

On average for 2022–2023, the productive water reserves in the 0–1 m layer in April with conventional tillage and surface tillage were almost the same, while with No-till, water reserves were significantly higher (+10–12 cm). In June, the productive water reserve was highest with No-till and lowest with surface tillage (–15 mm). Ye et al. (2024) obtained similar results when studying moisture reserves in the soil during mulching, but he had different climatic conditions.

In July, the productive water reserve in the 1 meter layer with no-till was higher by 9–10 mm compared to conventional tillage, while with surface tillage, it was 11.0 mm lower. Water consumption from the productive water reserve during June–July was highest with No-till under surface tillage (+21.0 mm) compared to +15 mm with surface tillage. Water consumption with conventional tillage and No-till under conventional tillage was the same. Overall, water consumption from the productive water reserve during April–July, regardless of the tillage method, was consistent: 86–97 mm.

CONCLUSIONS

1. The normalization of water-resistant aggregates sized 3–0.5 mm showed that their content, as per the median, was lower than the mean value during plowing, while during surface tillage and No-till, conversely, it was higher than the mean value, indicating a tendency for the content of this fraction to approach the upper typical value or to increase. The most valuable fraction of water-resistant aggregates (3–0.5 mm) was least abundant during plowing: 18.4% (0–0.2 m), 19.5% (0–0.3 m). During surface tillage, the increase in the content of aggregates sized 3–0.5 mm relative to plowing was 12% (0–0.2 m) and 8.1% (0–0.3 m), while with No-till farming, it ranged from 9.4% to 14.7% (0–0.2 m) and 11.0% to 13% (0–0.3 m), indicating the aggregation of swater-resistant aggregates into the most valuable fraction of water-resistant aggregates, thereby influencing a more rational utilization of the productive water reserve during the crop growing period in the crop rotation.

2. No significant pairwise correlation links ($R > \pm 0.7$) were found between the mean-weighted diameter of dry aggregates and the components of water-resistant structure during conventional tillage, whereas during surface tillage, there were 7 such links, including 2 direct and 5 inverse correlations. Similarly, under the No-till system, there were 7 correlations, comprising 2 direct and 5 inverse correlations, indicating the subordination of water-resistant structure components to the structural composition during dry sieving through the mean-weighted diameter of dry structural aggregates. The

presence of inverse correlations of strong correlation indicates a high level of self-regulation of the structural-aggregate state compared to plowing during surface tillage and the No-till system.

3. Under the No-till system (after 2–3 years of implementation), there is an accumulation of productive soil water in the 0–1 m soil layer by 8–12 mm more compared to conventional tillage. Relative to the water reserves in 2022, the water stock increased by +19.0 mm (after plowing) and by +14.0 mm (under surface tillage) in 2023. This is associated with the formation of mulch layers on the field surface and the creation of vertical channels by earthworms and vertical macropores from the decomposition of roots, which are not disrupted by intensive tillage.

4. Under the No-till system, in June and July, the average productive soil water reserve was higher compared to conventional tillage by 5–10 mm and 7–10 mm, respectively, over the period of 2022–2023. In comparison to surface tillage, the difference was even greater, with increases of 10–12 mm and 18–21 mm, respectively. In 2023, the productive soil water reserve in July under the No-till system exceeded that of conventional tillage by 17 mm and surface tillage by 31 mm. This improvement in soil moisture retention in June–July is attributed to the increase in water-stable aggregates sized 3–0.5 mm.

REFERENCES

An, S.S., Huang, Y.M., Zheng, F.L. & Yang, J.G. 2008. Aggregate characteristics during natural revegetation on the loess plateau. *Pedosphere* **18**(6), 809–816.

Backhaus, K. 2008. Multivariate Analysemethoden. 12th Edition. *Berlin: Springer Verlag*, 575 pp.

Bardgett, R.D., Mommer, L. & De Vries, F.T. 2014. Going underground: root traits as drivers of ecosystem processes. *Trends Ecol. Evol*. **29**, 692–699. doi: 10.1016/j.tree.2014.10.006

Baydyuk, M.I. 2004. Features of cumulative soil formation under zero tillage of chornozems in the Donbass Steppe. *Abstract of dissertation for the degree of candidate of agricultural sciences*, Kharkiv, Ukraine, 19 pp. (in Ukrainian).

Bhatt, R. & Khera, K.L. 2006. Effect of tillage and mode of straw mulch application on soil erosion in the submontaneous tract of Punjab, India. *Soil and Tillage Research* **88**(1−2), 107−115.

Blanco-Canqui, H. & Ruis, S.J. 2018. No-tillage and soil physical environment. *Geoderma* **326**, 164−200.

Bulgakov, V., Adamchuk, V., Ivanovs, S. & Ihnatiev, Y. 2017. Theoretical investigation of aggregation of top removal machine frontally mounted on wheeled tractor. *Engineering for Rural Development* **16**, 273–280. doi: 10.22616/ERDev2017.16.N053

Bulgakov, V., Bonchik, V., Holovach, I., Fedosiy, I., Volskiy, V., Melnik, V., Ihnatiev, Y. & Olt, J. 2021. Justification of parameters for novel rotary potato harvesting machine. *Agronomy Research* **19**(2), 984–1007. doi: 10.15159/AR.21.079

Bulgakov, V., Kuvachov, V., Nozdrovický, L., Findura, P., Smolinskyi, S. & Ihnatiev, Y. 2018. The study of movement of the wide span tractor-based field machine unit with power method of its control. *Acta Technologica Agriculturae* **21**(4), 160–165. doi: 10.2478/ata-2018-0029

Bulgakov, V., Pascuzzi, S., Ivanovs, S., Santoro, F., Anifantis, A.S. & Ihnatiev, I. 2020. Performance assessment of front-mounted beet topper machine for biomass harvesting. *Energies* **13**(14), 3524. doi: 10.3390/en13143524

Bulyhin, S.Yu., Achasov, A.B., Achasova, A.O., Papchenko, O.V. & Panasenko, V.M. 2014. Evaluation and prediction system of land quality (state, concept and algorithms). Kyiv: *Ahrarna nauka*, 240 pp. (in Ukrainian).

Chefetz, B., Tarchitzky, J., Deshmukh, A.P., Hatcher, P.G. & Chen, Y. 2002. Structural characterization of soil organic matter and humic acids in particle_size fractions of an agricultural soil. *Soil Sci. Soc. Am. J.* **66**, 129–141. doi: 10.2136/sssaj2002.1290

Chornyi, S.G., Vydynivska, O.V. & Voloshenyuk, A.V. 2012. Quantitative assessment of the anti-erosion effectiveness of No-till technology in the conditions of the Southern Steppe of Ukraine. *Gruntoznavstvo* **13**(1–2), 38–47. (in Ukrainian).

Dudchenko, V.M., Krotinov, O.P., Kosolap, M.P. & Ivanyuk, M.F. 2014. Soil density under zero tillage (No-till) technology. *Kormy i Vyrobnytstvo* **79**, 28−34. (in Ukrainian).

FAO. 2021. Standard operating procedure for soil pH determination. Rome, 1–23.

Field, A. 2009. Discovering Statistics Using SPSS. Third Edition. *London: Sage*, 822 pp.

Gajic, B., Dugalic, G. & Diurovic, N. 2006 Comparison of soil , organic matter content aggregate composition and water stability of gleyic fluvisol from adjacent forest and cultivated areas. *Agronomy Research* **4**(2), 499–508.

Garcia-Oliva, F., Oliva, M. & Sveshtarova, B. 2004. Effect of soil macroaggregates crushing on C mineralization in a tropical deciduous forest ecosystem. *Plant and Soil* **259**(1–2), 297–305.

Gassen, D. & Gassen, F. 2004. Direct sowing – the road to the future. *Dnipro: Agrosoyuz*, 206 pp. (in Russian).

Gozubuyuk, Z., Sahin, U., Ozturk, I., Celik, A. & Adiguzel, M.C. 2014. Tillage effects on certain physical and hydraulic properties of a loamy soil under a crop rotation in a semi-arid region with a cool climate. *Catena* **118**, 195−205.

Hirte, J., Leifeld, J., Abiven, S. & Oberholzer, H.R. 2017. Overestimation of crop root biomass in field experiments due to extraneous organic matter. *Front Plant Sci.* **8**, 284. doi: 10.3389/fpls.2017.00284

Ivanovs, S., Bulgakov, V., Nadykto, V., Ihnatiev, Ye., Smolinskyi, S. & Kiernicki, Z. 2020. Experimental study of the movement controllability of a machine-and-tractor aggregate of the modular type. *INMATEH - Agricultural Engineering* **61**(2), 9–16. doi: 10.35633/inmateh-61-01

Jimenez, J.J., Lorenz, K. & Lal, R. 2011. Organic carbon and nitrogen in soil particle-size aggregates under dry tropical forests from Guanacaste, Costa Rica – Implications for within-site soil organic carbon stabilization. *Catena* **86**, 178–191.

Kibet, L.C., Blanco-Canqui, H. & Jasa, P. 2016. Long-term tillage impacts on soil organic matter components and related properties on a Typic Argiudoll. Soil and *Tillage Research* **155**, 78−84.

Kosolap, M.P. & Krotinov, O.P. 2011. No-till farming system. Kyiv: *Logos*, 352 pp. (in Ukrainian).

Li, S.X., Wang, Z.H., Li, S.Q., Gao, Y.J. & Tian, X.H. 2013. Effect of plastic sheet mulch, wheat straw mulch, and maize growth on water loss by evaporation in dryland areas of China. *Agricultural Water Management* **116**, 39−49.

Manushkina, T.M., Drobitko, A.V., Kachanova, T.V. & Geraschenko, O.A. 2020. Ecological features of No-till technology in the conditions of the southern Steppe of Ukraine. *Visnyk ahrarnoi nauky Prychornomoria* **4**, 47−53 (in Ukrainian).

Medvediev, V.V. 1990. Variability of optimal soil density and its causes. *Pochvovedenie* **5**, 20–31 (in Russian).

Medvediev, V.V. 2007. Interconnections between anthropogenic loads, soil degradation, and soil stability. *Visnyk ahrarnoi nauky* **8**, 49–55 (in Ukrainian).

Medvediev, V.V. 2008. Soil Structure (methods, genesis, classification, evolution, geography, monitoring, protection). Kharkiv: *13 Tipografiya*, 406 pp. (in Russian).

Medvediev, V.V. 2010. Zero tillage in European countries. *Kharkiv: EDUNA*, 202 pp. (in Ukrainian).

Medvediev, V.V., Plysko, I.V. & Bihun, O.N. 2014. Comparative characteristics of optimal and real parameters of Ukrainian chornozems. *Pochvovedenie* **10**, 1247–1261 (in Russian).

Medvediev, V.V. 2012. Physical degradation of soils, its diagnosis, distribution area and prevention measures. *Gruntoznavstvo* **13**(1–2), 5–22 (in Ukrainian).
Medvediev, V.V. 2016. Agrozem as a new 4-dimensional polygenic formation. *Gruntoznavstvo* **17**(1–2), 5–20 (in Ukrainian). doi: 10.15421/04160
Mulumba, L.N. & Lal, R. 2008. Mulching effects on selected soil physical properties. *Soil and Tillage Research* **98**(1), 106−111.
Nichols, K.A. & Toro, M. 2011. A whole soil stability index (WSSI) for evaluating soil aggregation. *Soil Till. Res.* **111**, 99–104.
Nosko, B.S. 2017. On the issue of the formation of the phosphate fund of soils. *Agrokhymiya i Gruntoznavstvo* **386**, 87–92 (in Ukrainian).
Pirmoradian, N., Sepaskhah, A.R. & Hajabbasi, M.A. 2005. Application of fractal theory to quantify soil aggregate stability as influenced by tillage treatments. *Biosyst. Eng.* **90**(2), 227–234.
Polupan, M.I., Solovei, V.B. & Velichko, V.A. 2005. Classification of soils of Ukraine. Kyiv: *Ahrarna nauka*, 300 pp. (in Ukrainian).
Rhoton, F.E. 2000. Inuence of Time on Soil Response to No-till Practices. *Soil Sci. Soc. Am. Journal* **64**, 700–710.
Six, J., Bossuyt, H., Degryze, S. & Denef, K. 2004. A history of research on the link between (micro) aggregates, soil biota, and soil organic matter dynamics. *Soil Till. Res.* **79**, 7–31.
Six, J., Elliott, E.T & Paustian, K. 2000 Soil Macroaggregate Turnover and Microaggregate Formation: A Mechanism for C Sequestration under No-Tillage Agriculture. *Soil Biology and Biochemistry* **32**, 2099**–**2103. doi: 10.1016/S0038-0717(00)00179-6
State Standard of Ukraine DSTU 4744:2007. 2008. Soil quality. Determination of the structural-aggregate composition by the sieve method according to N.I. Savvinov's modification. Introduced on January 1, 2008. Kyiv. 12pp. (in Ukrainian).
Thorne, M.E. 2003. No-till spring cereal cropping systems reduce wind erosion susceptibility in the wheat/fallow region of the Pacific Northwest. *Journal of the Soil and Water Conservation Society* **58**(5), 250–257.
Tkachenko, M.A., Havrishko, O.S., Habel, F.Y. & Olifir, Yu.M. 2016. Structural-aggregate state of gray forest surface-ogley soil under different land use. *Mizhvidomchyi tematychnyi naukovyi zbirnyk "Zemlerobstvo"* **1**, 25–31 (in Ukrainian).
Tuure, J., Räsänen, M., Hautala, M., Pellikka, P., Mäkelä, P.S.A. & Alakukku, L. 2021. Plant residue mulch increases measured and modelled soil moisture content in the effective root zone of maize in semi-arid Kenya. *Soil and Tillage Research* **209**, 104945. doi: 10.1016/j.still.2021.104945
Vach, M., Hlisnikovsky, L. & Javurek, M. 2018. The Effect of Different Tillage Methods on Erosion. *Agriculture (Pol'nohospodarstvo)* **64**(1), 28−34.
Vorobyov, N.I. & Ladan, S.S. 2021. Cluster analysis of statistical profiles of spatial distribution of humus. *Plodorodiye* **5**, 33−36.
Ye, L., Xu, Y., Zhu, G., Zhang, W. & Jiao, Y. 2024. Effects of Different Mulch Types on Farmland Soil Moisture in an Artificial Oasis Area. *Land* **13**(1), 34. doi:10.3390/land13010034
Zaryshnyak, A.S., Baliuk, S.A. & Lisovoy, M.V. 2016. Stationary field test-trials of Ukraine: register of certificates. Kharkiv: *Smuhasta Typohrafiya*, 265 pp. ISBN 617-7387-31-1(IC15467). (in Ukrainian).
WRB. 2022. *World Reference Base for Soil Resources. International soil classification system for naming soils and creating legends for soil maps. 4th edition.* Vienna, Austria, International Union of Soil Sciences (IUSS), 1–236.

Agronomy Research **22**(2), 774–793, 2024
https://doi.org/10.15159/AR.24.067

Advancing circular bioeconomy: trends, clusters, and roadmaps in biofuel production and waste valorisation

Y. Chernysh[1,2], V. Chubur[1] and H. Roubik[1,*]

[1]Czech University of Life Sciences Prague, Faculty of Tropical AgriSciences, Department of Sustainable Technologies, Kamýcká 129, CZ16500 Prague, Czech Republic
[2]Sumy State University, Faculty of Technical Systems and Energy Efficient Technologies, Department of Ecology and Environmental Protection Technologies, 116, Kharkivska Str., UA40007 Sumy, Ukraine
[*]Correspondence: roubik@ftz.czu.cz

Received: January 31st, 2024; Accepted: May 24th, 2024; Published: July 16th, 2024

Abstract. Today, one of the important tasks of bioeconomy development is waste management based on the principles of environmental management and bioenergy production. In the context of this issue, this review focusses on the analysis of current trends in biofuel production that involve sustainable feedstocks and the valorisation of waste into useful bioproducts in agriculture. The scientometric method included the use of Scopus and Web of Science databases to compare the coverage of the research topic with keyword chain optimization. In addition, bioinformational databases was used to support the involvement of secondary raw materials in the bioprocessing cycle. The implementation of the research objectives resulted in the identification of bioeconomy clusters that emphasize the importance of developing specific regional circular bioeconomy strategies while avoiding 'one-size-fits-all' solutions for individual sectoral technologies. An example of bioeconomy development in the world is bioenergy. The structure of bioenergy has been analysed. A roadmap for biotechnology modernisation was proposed using the example of anaerobic waste conversion process as part of the implementation of a circular bioeconomy. The stages of the roadmap for the modernisation of bioenergy technologies were analysed within the framework of the sectoral implementation of the circular bioeconomy. The efficiency indicators for the implementation of bioeconomy in agricultural production have been determined. In addition, an important direction unifying anaerobic technologies with the agricultural sector is the enrichment of digestates with macro and microelements, which is possible due to mineral additives, for example, phosphogypsum. This direction was also considered from the point of view of environmental safety.

Key words: bioeconomy, renewable energy, agricultural production, waste recycling.

INTRODUCTION

When discussing economic development with a focus on biotechnology, emphasis is placed on circular bioeconomy as a thermodynamic approach to the instability of the economic process based on the concept of entropy. McDougal (2022) presents a model of bioenergetic evolution at the planetary level that implies that, in theory, significant

public investment in terrestrial solar generation may be required to realise a planetary energy transition and prevent ecological collapse. This demonstrates the importance of energy for economic evolution at the planetary level. Leff (2021) demonstrates a nongentropic productivity that the authors claim mobilises the ecological organisation of life on the planet based on an alternative production paradigm. This ecotechnological paradigm increases the biosphere's production of natural use values by converting solar energy into biomass generated by photosynthesis and symbiogenesis, with a technological system designed to increase this potential, utilising and limiting entropic decay, rooting sustainable livelihoods in the cultural imagination. Additionally, cross-sector collaboration and regional incentives for waste management need to be implemented. The high costs associated with retrofitting biogas facilities, collecting and preprocessing raw materials, as well as developing downstream production processes for customers, could potentially impede the rapid integration of the concept of biowaste supply chain and its products into the market (Siegfried et al., 2023). The development of bioeconomy based on sectoral integration of bioproducts of different target orientation is of strategic importance for the leading economies of the world (China, USA, Germany, Sweden, etc.). At the same time, bioenergy is increasingly being demanded as a branch of applied development and participation as a stable raw material base for various types of waste (Hu et al., 2023, Moustakas et al., 2023).

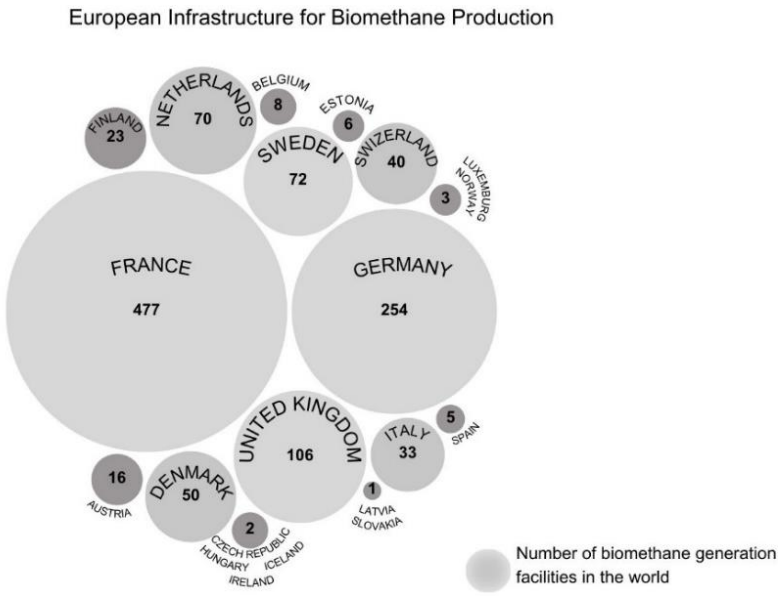

Figure 1. Biomethane production projects in the world (based on Statistical information sourced from IEA Bioenergy).

According to the data compiled, the diagram shown in Fig. 1 illustrates the countries that are leading in the implementation of biomethane technologies. France, with 477 projects, leads the chart, with biomethane used primarily by public authorities and companies, which currently represent the majority of biomethane consumers, primarily using it as a transportation fuel (European Biogas Association, 2017).

Germany, with 254 biomethane projects, is second, with biomethane primarily used for electricity production in combined heat and power (CHP) plants, and its use as fuel is indirectly supported and developing (European Biogas Association, 2020). The United Kingdom, which has 106 biomethane projects, involves most of these projects being connected to gas distribution networks (Green Gas Certification, 2024). Sweden, the Netherlands, Denmark, and Finland are among the countries with well-developed biomethane technologies, with biomethane projects in these countries accounting for about a quarter of their biogas plants. Governments around the world are supporting this trend, furthering the development of the biomethane sector.

Despite the fact that biomethane is currently not regulated at the European level, some countries, such as Germany, have introduced legislation that regulates the introduction of biomethane mesh. At the initial stage, when the first biomethane plants were built in Germany, there was no such legislation in the country. The first innovative plants were established by agreement between the main stakeholders, such as the biogas plant operator, the natural gas network operator, and the authorities (Thrän et al., 2023).

It should be emphasised that in Ukraine, only a small number of companies (up to 2% of the total) have the opportunity to implement biomethane (BM) projects with a capacity of 100 m^3 h^{-1} of biogas or more, using only waste from their own production. To a greater extent, these are large-scale poultry farms, sugar, and distilleries. The possibility of implementing large-scale projects (2,000 m^3 h^{-1} of biogas or more) using the raw materials of a single enterprise is limited to single examples. On the basis of this, promising BM production projects may be those that combine the fermentation of waste from several enterprises and/or plant material. A large-scale increase in biomethane production requires the use of part of agricultural land to grow plant material (Geletukha et al., 2022).

Biological waste is a source of environmental pollution and a significant repository of valuable resources because of the large amount of organic and biodegradable components it contains that can be reused. Recycling biological waste into resources through bioprocessing can help reduce carbon emissions and the growing environmental problems associated with solid waste (Mishra et al., 2023). Continuous innovation and research into large-scale fermentation processes are needed to make this technology more economically feasible and competitive, while providing global markets with an ever growing and more diverse range of high value biobased products (Verardi et al., 2023).

Therefore, this study focusses on reviewing trends in the development of biofuel potential as a branch of the bioeconomy with a focus on the recycling of wastes. The following objectives of the study were achieved:

- Bioeconomy strategy for the growth of industrial sectors
- Biowaste as a sustainable feedstock for energy production within the framework of bioeconomy promotion
- Evaluation of a mineral additive phosphogypsum for use in bioproduction.

MATERIALS AND METHODS

Life cycle assessments are an important tool for comparing a new biorefinery concept with landfill disposal. Specifying the environmental impacts of anaerobic digestion plants on individual substrate types, the impacted stations are shown in Fig. 2.

Canva, as a user-friendly graphic design software that offers a wide array of features to create visually engaging content, allowed us to create informative maps, incorporating key data, and trends related to the bioenergy sector. The software was used to develop visually appealing maps that effectively communicate the data collected during the bibliometric analysis of relevant bioenergy data.

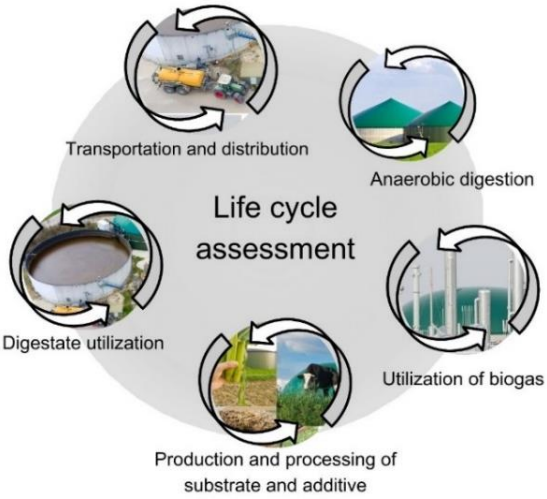

Figure 2. Life cycle assessment steps for organic waste utilisation through anaerobic digestion to biogas production (based on Ugwu et al., 2022).

Analytical tools of scientometric databases in the analysis of trends in the development of bioenergy technologies of anaerobic fermentation

To optimise analytical research, the Scopus and WoS database platforms have a set of various online tools that can be used to analyse publication activity in the field of anaerobic fermentation for bioproducts.

To identify emerging research trends, various combinations of keywords were used, including energy bioeconomy; waste bioprocessing bioeconomy; biofuel waste bioeconomy; anaerobic digestion bioeconomy; biodiesel bioeconomy; biogas bioeconomy; Life Cycle Assessment Bioeconomy; Bioinformation databases.

Using the analytical tools of the Scopus and WoS databases, it is possible to work with charts based on bibliographic data according to categories:

- number of published works by years (Fig. 3a);
- distribution of publications by publications indexed by the database;
- number of thematic publications among authors and organizations;
- quantitative distribution of published documents by territorial principle (Fig. 3, b);
- comparison of institutions that provide funding for research (Fig. 3, c);
- distribution of documents by type and field of knowledge to which the text belongs.

The total number of publications in databases amounted to 2,456 papers. The field of bioenergy, as a major component of the development of the bioeconomy, began to actively gain momentum in publications starting from 2015. At that time, the importance of opportunities offered by a sustainable bioeconomy became important. Since 2019,

there has been a threefold increase in the number of publications on this subject, peaking in 2022 with the registration of 514 scientific papers per year (Fig. 3, a). Research and development in this area are actively continuing to make progress.

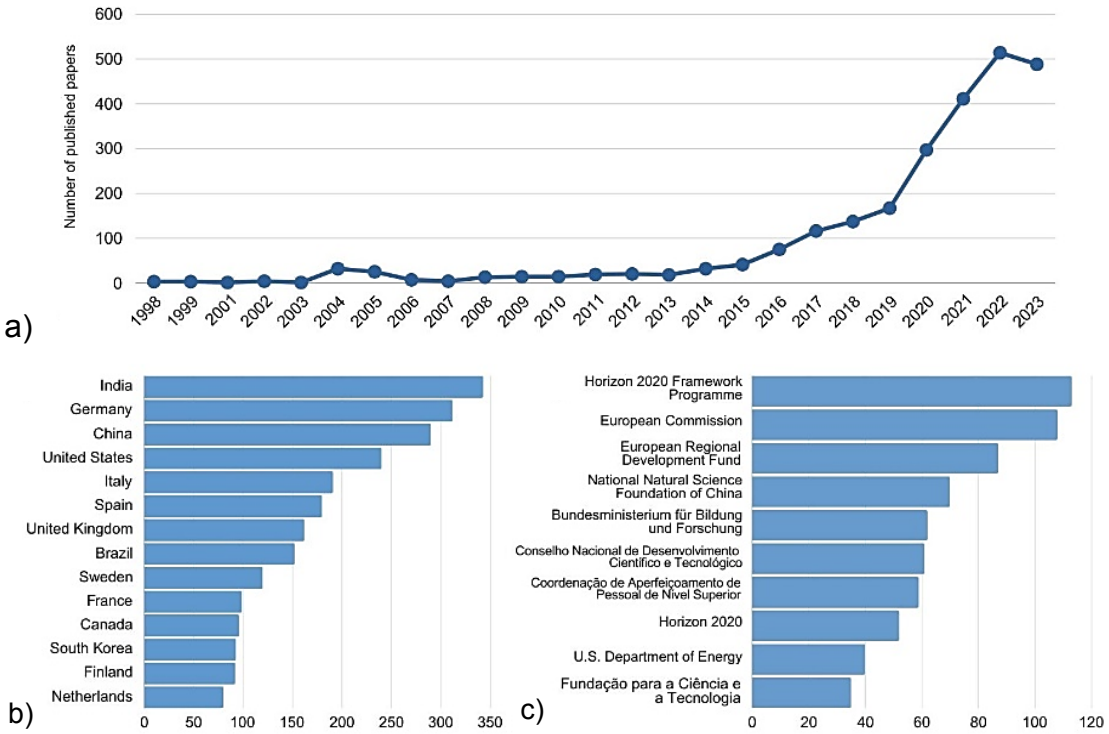

Figure 3. Bibliometric data processing: a) Number of articles published by year; b) Distribution of published papers by territorial scope; c) Comparison of institutions that provide research funding.

In terms of the geographical distribution of publication activity (Fig. 3, b), most of the research in this area is conducted by scientists from Indian, German scientific academies, demonstrating more than 300 published studies each. At the same time, China and the United States exhibit comparable levels of activity, each accounting for more than 200 publications. This indicates their significant contribution to the progress and development of the bioenergy sector.

However, most of the research funding comes from funds from the European Union (Fig. 3, c). In addition, leading positions are held by specialists from Italy, Spain, the UK, and other EU countries (Fig. 3, b).

It is worth noting that the types of documents are dominated by articles related to such fields of knowledge as environmental sciences and energy, as well as engineering, including chemical engineering, which means that most of the publications are aimed at improving the environmental situation by comprehensively solving several problems at once - utilisation of organic waste and obtaining alternative sources of fuel from biomass.

Use of bioinformatic electronic databases: KEGG database, BacDive and EAWAG-BBD

Bioinformatics databases have a narrow specialisation for microbiologists. The main aspects that were taken into account when using them in this work include the ability to analyse the metabolic pathways of microorganisms associated with the utilisation of the mineral components of phosphogypsum.

One of the most known and extensive databases for gene networks, metabolic and signalling pathways is KEGG PATHWAY. A special option of the database interface allows you to customise the diagram for a specific type of organism, and the number of species depends on how universal the biological process is displayed in the diagram. The KEGG REST API allows you to perform and run queries on the information available in the KEGG database (Kanehisa et al., 2017).

KEGG REACTION serves as the database for chemical reactions found in metabolic maps and distinctive enzymatic reactions, each with its unique identification number in the database (Shulipa et al., 2020).

Using the EAWAG-BBD bioinformation electronic database. Methane, a biogenic gas, is biologically produced from carbon dioxide through methanogenesis, involving 2-electron reductions. Methanogens worldwide generate 1,015 grammes of methane annually, according to the EAWAG-BBD. The interconnectedness of methanogenesis and methanotrophy plays a crucial role in the Earth's C1 metabolic cycle, facilitating the transformation and cycling of C1 compounds. According to Shulipa et al. (2020), this process involves the breakdown and assimilation of C1 fragments by various microorganisms, contributing to the dynamics of the global C1 cycle. The study of these reactions elucidates the principles of biocatalysis, which are essential for understanding the processes of chemical production and biodegradation of environmental contaminants. This includes detailed insights into the metabolic pathways, the chemicals involved at each stage, the microorganisms responsible for these transformations, as well as the relevant enzymes and genetic information (About the EAWAG Biocatalysis, 2014).

The BacDive bioinformation database offers a comprehensive repository of information on bacteria and archaea, supporting research into biodiversity among these organisms. This resource is particularly valuable for identifying species that play roles in the anaerobic digestion process, facilitating the search for data on their optimal cultivation conditions in technological applications. The BacDive platform also allows for the exploration of nutrient media, including those with varying compositions of trace elements (BacDive Dashboard, 2022). Additionally, it provides access to taxonomic directories and tools to determine the locations of inoculum selection and analyse their adaptive capacity to changing environmental conditions.

RESULTS AND DISCUSSION

Bioeconomy strategy for the growth of industrial sectors

Biotechnology as a tool for achieving economic realisation has its own sectoral division for application in various economic spheres.

According to the international classification, biotechnologies have been established to be distinguished by colour: green (agricultural and environmental biotechnology, including the production of biofuels and biofertilizers); red (biopharmaceuticals, biodiagnostics); white (industrial biotechnology); blue (marine biotechnology, aquaculture); gold (bioinformatics, nanobiotechnology); brown (biotechnology for deserts and arid areas); grey (bioprocesses and fermentation); black (bioterrorism, biological weapons) (Barcelos et al., 2018).

The diversity observed in bioeconomic cluster settings highlights the importance of developing specific regional circular bioeconomy strategies, taking into account local strengths and weaknesses, while avoiding 'oneshot' solutions for individual industry technologies. In addition, research into product and technology design, together with end-of-life strategies for bioproducts, are important elements of the systems. To optimise the potential, clear time-bound milestones are needed that not only promote the development of the bioeconomy as a whole, but also focus on enabling technologies and cascade pathways that promise the greatest potential for utilisation and emission reductions (OECD et al., 2009). It is gradually expanding its sphere of influence on the economies of different countries. Its influence is projected to increase globally starting in 2030 (Fig. 4).

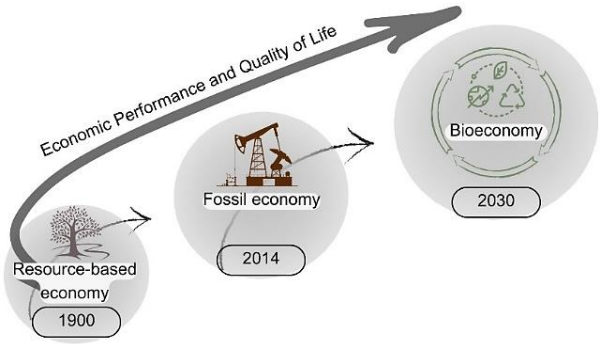

Figure 4. The bioeconomy will be the next wave of economy.

The global dynamics of biotechnology sector development is shown in Fig. 5.

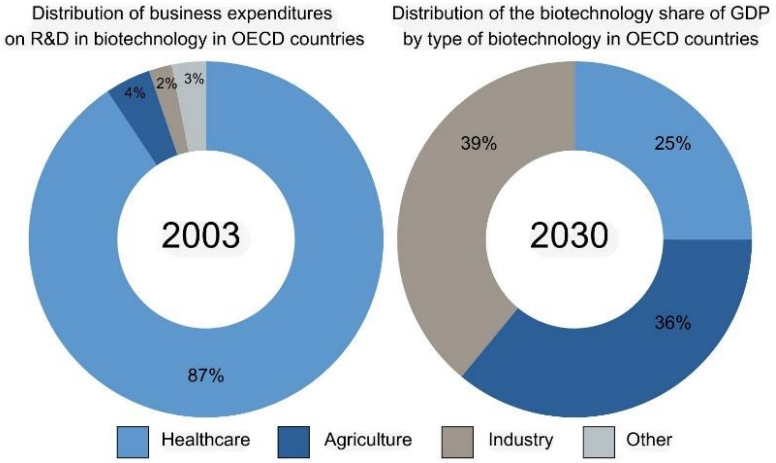

Figure 5. Comparative diagram of the distribution of business R&D expenditures and GDP share by type of biotechnology.

The circular economy aims to change the classical linear model of production by focussing on products and services that minimise waste and other types of pollution. The interdependence between the bioeconomy, green economy, and circular economy is shown in Fig. 6.

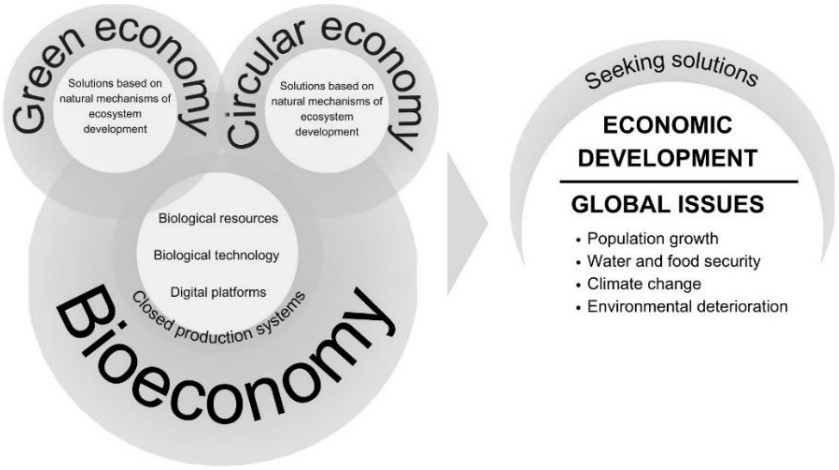

Figure 6. Diagram of dependencies between different economic concepts.

One example of the development of the bioeconomy in the world is bioenergy. Its structure is shown in Fig. 7. Experts estimate that proven oil reserves last for 40–50 years; gas reserves for 80 years; and coal reserves for about 400 years (Statistical Review of World Energy, 2021). Furthermore, the trend of rising gas prices over the past 10 years has increased rapidly, which is an economic prerequisite for the active development of bioenergy.

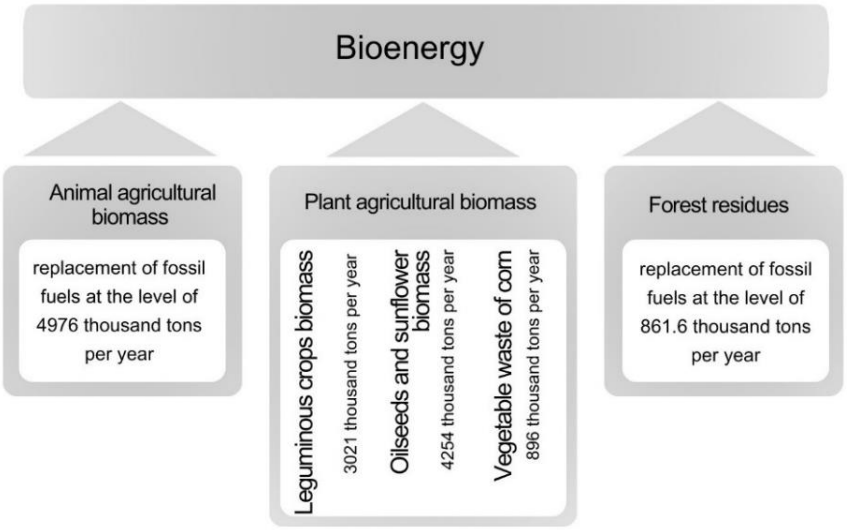

Figure 7. Structure of bioenergy.

Efficiency of sustainable development of the bioeconomy:

– environmental efficiency: minimizing the impact of production processes on the environment; promoting the conservation and restoration of biodiversity in agricultural landscapes; promoting the conservation and restoration of soil fertility; protecting water resources from pollution.

– economic efficiency: gradual increase in the natural productivity of agrocenoses and soils; reduction of production costs due to the refusal to use expensive chemicals and reduction of energy intensity of production; increase in product competitiveness;

– social efficiency: creation of additional jobs in rural areas; creation of new prospects for small and medium-sized farms.

The basis of domestic agricultural development's environmental policy should be rooted in ensuring its environmental safety through the adoption of green production practices. The greening of agricultural production should be understood as a process that involves combining and cooperating a set of innovative technologies in the sectors aimed at economic growth of the industry and environmental protection as interdependent and complementary elements of strategic agricultural development, which will guarantee high quality food to the population. The sustainable development of agriculture based on the green economy is possible through the use of alternative technologies that are environmentally friendly and ensure increased productivity in harmony with the ecosystem (Gollier et al., 2019). The effectiveness of the implementation of the green economy in agricultural production is confirmed by the following performance indicators:

– reduction of soil structure and compaction through agrotechnical measures;
– scientifically based application of agricultural land reclamation;
– reduction of nutrient losses in the soil;
– reducing chemical load through the use of environmentally friendly fertilisers;
– use of scientifically based crop rotations;
– introduction of environmentally friendly biologically based crop production technologies;
– introducing environmental certification and environmental labelling.

Biowaste as a sustainable feedstock for energy production within the framework of bioeconomy promotion

In general, the application of life cycle assessment to waste management systems has great potential, especially to support the decisions of planners and companies involved in waste collection, transportation, and disposal.

The principles of bioeconomy encourage the sustainable use of recycled nutrients and the transformation of conventional systems into sustainable ones to minimise environmental impacts. Thus in Fritzen Cidón et al. (2023) is presented how bioeconomy principles are applied for socio-ecological benefits to Brazilian organic farmers (in the region of Vale do Rio do Sinos, Rio Grande do Sul). The bioeconomic principles applied by Brazilian organic farmers have had a positive socio-ecological impact. Nevertheless, there is still a need for more assistance in the bioeconomy approach, adoption of cleaner technologies and independence of external suppliers without organic guarantees.

The idea of clean and affordable renewable energy sources has led the industry to focus on the development of biorefineries for a sustainable bioeconomy in Dvoretsky et al. (2022). Therefore, microalgae characterised by versatile metabolism, hold significant potential for the generation of beneficial substances across a range of applications, including pharmaceuticals, food and feed supplements for animals and fish, materials, biofertilizers, and biofuels.

Lignocellulosic biomass (LCB) is considered as a widely available and stable feedstock for biofuel production, with Yadav et al. (2023) emphasizing that through the implementation of diverse conversion technologies, an integrated LCB bioprocessing platform can be established, embodying the principles of a 'circular bioeconomy'.

Several technical challenges must be considered to ensure the sustainability of the biofuel economy for commercialisation (Hasan et al., 2023).

The primary commercial challenge in biofuel production is the high cost of production, which directly affects the price of the fuel. In addition to reducing the cost of biofuels, technological advancements are playing a crucial role in decreasing production costs, leading to biofuels becoming a prominent source of renewable energy. Therefore, the development of advanced biodiesel and bioethanol production technologies is imperative to increase the production of biofuels.

Infrastructure development is a challenge to the growth of the biofuel economy. The tendency of the public to transition from fossil fuels (gasoline and diesel) to biofuels in the road transportation sector is important for the successful implementation.

Enhancing farming practices to increase feedstock quality and yields, as well as appropriate infrastructure, including electricity, roads and water, also require further development.

The advancement of the bioenergy economy requires overcoming several challenges related to competition for agricultural land, rising food prices, difficulties in technological progress, and obstacles in infrastructure development (Hasan et al., 2023).

Many studies focus on a limited set of indicators that do not cover the full range of impact categories in understanding the 'Bioeconomic Footprint'. Furthermore, the majority of research is concentrated either on partial industry coverage within the bioeconomy or on assessing the overall economic impact without disaggregating sectors based on biotechnology (Sinkko et al., 2023).

The specificity of certain research focuses also prevails in a number of studies. For example, Cao et al. (2023) summarise recent advances in the application of biofertilizers derived from microalgae in agriculture. This represents a particular area within the agricultural sector, contributing to the development of the circular bioeconomy concept and the goals of sustainable development.

Additionally, anaerobic digestion can be used as a part of a larger bioprocessing system for the production of biofuels, biochemicals and fertilisers, potentially playing a central role in the emerging circular bioeconomy. It is necessary to assess long-term impacts and explore potential accumulations of specific undesired substances. In general, environmental risks are highly dependent on the input feedstock and the digestate produced. Comprehensive purification processes must be developed, as they can both minimise risks and improve economic prospects (Feng et al., 2023).

Another aspect of the bioeconomy that should be discussed is the impact on adaptation to climate change. The reliance on imported fossil resources in the face of current geopolitical challenges has led to significant increases in operational costs for

many European companies and municipalities. Seruga et al. (2023) show that using municipal biowaste methanogenesis to generate electricity is associated with a 25.3–26.6% reduction in CO2 emissions compared to a baseline scenario with conventional electricity generation. This reduction is attributed to the fact that CO_2 emissions from renewable sources, including biogas combustion, are not included in the emissions trading quota rules. However, the average national emissions factors used in this calculation are relatively high when compared to the reduction factors stipulated by the Directive (EU) 2018/2001 of the European Parliament and Council, dated December 11, 2018, on the promotion of the use of energy from renewable sources. It is important to emphasise that biological waste, unlike energy crops, is considered a sustainable feedstock for biogas and one of the priority areas for bioeconomy development.

In general, the agricultural support system in developed market economies is largely associated with state price regulation, including the establishment of maximum and minimum price thresholds and the setting of indicative or conditional pricing. Such regulatory measures are implemented through the buying or selling of goods (known as commodity intervention). In addition, EU agricultural policy uses such a tool as quotas to regulate the agricultural market. Its essence lies in the fact that maintaining prices for products leads to their overproduction, so quotas are introduced for the production of certain types of products (milk, sugar, alcohol, starch) in order to maintain high domestic prices, prevent overproduction, and reduce costs from the EU budget (EU budget: the Common Agricultural Policy beyond 2020, 2018).

The Fig. 8 groups the main factors influencing the process of biowaste valorisation taking into account the environmental factor, based on data from Mishra et al. (2023).

Figure 8. Environmental factors of waste valorisation in bioprocesses.

There are several significant obstacles associated with the boundaries of the LCA system that continue to pose challenges for biowaste management. In Mishra et al. (2023) The concept of 'waste to wealth' aims to create a future sustainable lifestyle where waste is valued for its environmental benefits and the development of new technologies, livelihoods and jobs.

We propose a roadmap for technology modernisation based on the example of the anaerobic waste conversion process as part of the implementation of the circular bioeconomy (Fig. 9).

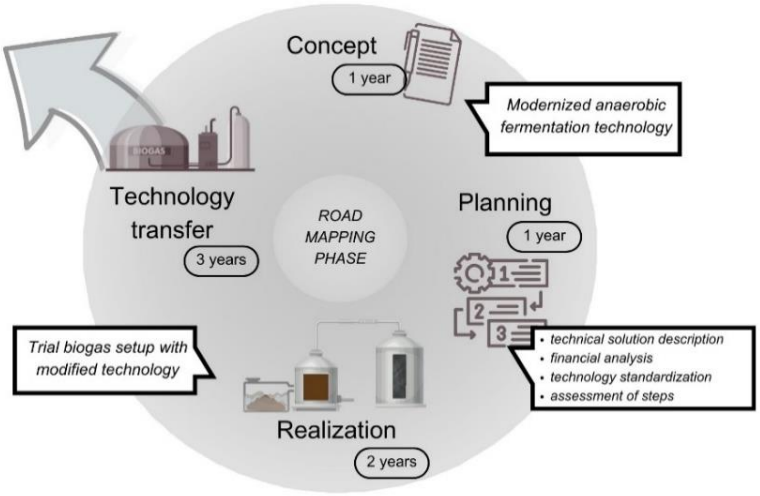

Figure 9. Phases of the roadmap for the modernisation of bioenergy technologies in the sectoral implementation of the principles of circular bioeconomy.

The first step is to identify the biotechnology sector for implementation, with a review and search for innovative solutions for implementation. The next stage is the development of a technological solution with visualisation of the necessary equipment. This phase involves conducting initial pilot experiments and modelling the results on the basis of the data obtained. Based on the results of successful process modelling, the finished concept is transferred to the planning stage before its full-scale implementation and direct implementation in the field of application, in our example, in the field of renewable energy with organic waste processing (Barretti et al., 2021; Luz et al., 2021). However, there are many challenges that need to be addressed to make biowaste fermentation (sustainable feedstock) sustainable for the commercial production of value-added products such as biofuels and biochemicals. More detailed determination of the optimal operating conditions for enzymes and fermenting microorganisms is needed, as well as the effect of biostimulant additives on their metabolic activity. Integrated microbial and enzyme engineering is a powerful approach to improve the efficiency of fermentation processes by improving the tolerance of microorganisms and enzymes to different pH and temperature conditions. Another important aspect is the scale-up of the fermentation process, which is also related to the evaluation of return on investment. which is important for the development of economically and environmentally sustainable processes. In addition, the properties and supply of raw materials, as well as the availability of skilled labour, must be considered (Verardi et al., 2023).

Evaluation of a mineral additive phosphogypsum for use in bioproduction

Phosphogypsum consists primarily of calcium sulphate dihydrate ($CaSO_4 \cdot 2H_2O$) and contains impurities of undecomposed phosphate, phosphoric salts and silicates. The amount of impurities present is influenced by factors such as the mineral composition of

the feedstock, production efficiency and equipment serviceability, as well as technological discipline, etc.

The results of the X-ray microanalysis of the phosphogypsum sample are shown in Table 1.

Phosphogypsum, containing calcium, phosphorus, sulphur, and various microelements, can be used for the chemical reclamation of soils, including those with Sandy compositions. Its utilization enhances the soil's physical properties, primarily through the enrichment with Ca^{2+} cations, as indicated (Nayak et al., 2013).

Table 1. Chemical composition of phosphogypsum (dried at 333 K)

Type of green area	% of total weight
CaO	38.73
SO_3	39.22
SiO_2	1.79[2]
P_2O_5	0.45[2]

In samples of phosphogypsum taken directly from the production process, the following metals were detected by XRF analysis (in % of total weight) Fe (0.010%), Ni (0.001%), Cu (0.003%).

In our previous studies (Plyatsuk & Chernish, 2014), phosphogypsum was used as a low-soluble sulphur-containing mineral additive in the process of biosulfide utilisation of biowaste, which is consistent with the studies of other authors Bounaga et al. (2022).

The use of phosphogypsum in the biowaste treatment process has the following advantages

- cheap raw material base (sustainable feedstock);
- significant prevalence of this type of waste;
- enrichment with microelements;
- sulphur compounds contained in PG can be freely used by sulphate reducers as a mineral substrate for their growth and hydrogen sulphide formation, due to the high affinity of microbial cells for sulphate/sulfite ions;
- reducing the technogenic load of phosphogypsum waste on the environment.

Mechanisms of transition of HM from organomineral complexes to the liquid phase:

- In the process of mineralisation, metal-organic complexes are transformed into soluble simple organic compounds under the influence of a biological agent and HM ions are released into solution;
- HMs that form salts with compounds of the organic component of sediments are exchanged for $Ca2^{+}$ on the surface of calcium material, such as phosphogypsum, by the mechanism of ion exchange. Thus, this leads to the formation of calcium compounds with organic structures of biowaste.

After the transition to the liquid phase, the HM ions interact with biogenic hydrogen sulphide. Hydrogen sulphide serves as a strong reducing agent, which contributes to the reduction of HM to reductive forms.

It should be noted that sulphate reducers are also present in the association of microorganisms during anaerobic digestion. Several works consider the competitive interrelationships of sulphate-reducing bacteria and methanogenic archaea (Oliveira et al., 2021; Sela-Adler et al., 2021). However, *sulphate-reducing* bacteria and *methanogens* may also be present in symbiotic relationships. Therefore, this work substantiated that through L-cysteine, methane metabolism participated in the sulphide consumption process, which is involved in cysteine and methionine metabolism,

promoted the direct reaction of sulphide formation and regulated environmental conditions (pH and S_2 concentration) for the symbiosis of sulphate reducers and methanogens (Shi et al., 2020). Consequently, the system was searched and the pathways for methane and sulphur metabolism were identified, as shown in Fig. 10.

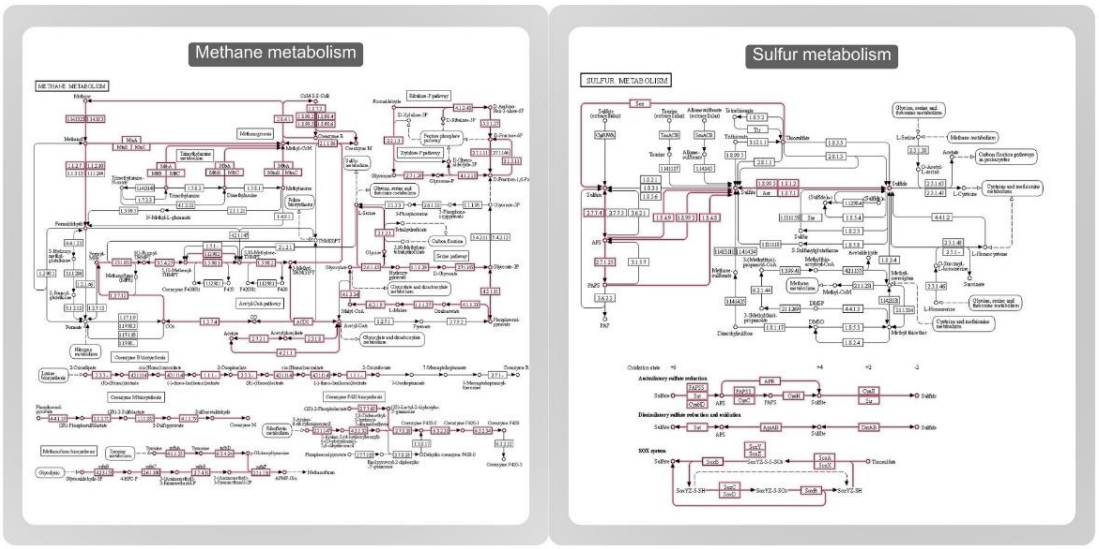

Figure 10. Search for dominant methanogenic species on the interactive map of methane production and sulphur metabolism. (based on KEGG PATHWAY: map00680; KEGG PATHWAY: map00920).

Fig. 10 delineates the crucial mechanisms by which methane and sulphur are metabolised within the microbial community, highlighting the pivotal roles of methanotrophs, methanogens, and methylotrophs in the carbon cycle. Methanotrophs are shown as the primary consumers of methane, whereas methanogens are depicted as the producers of methane through anaerobic processes, utilizing three distinct pathways, with CoM serving as the essential methyl carrier. These include the conversion of CO_2 to methane, methanol to methane, and acetate to methane. Furthermore, Fig. 10 demonstrates how the methane oxidation processes in methanotrophs and methylotrophs produce formaldehyde, which is then funnelled into three separate pathways for energy production and biosynthesis, including the metabolism of trimethylamine by methylotrophs (KEGG PATHWAY: map00680). With respect to sulphur metabolism, the diagram outlines its significance in the global sulphur cycle, illustrating both the assimilatory pathway, which incorporates sulphate reduction for amino acid synthesis without releasing sulphide, and the dissimilatory pathway, where sulphate serves as a terminal electron acceptor in anaerobic organisms, leading to the production of inorganic sulphide. The early stages of both pathways involve the activation of sulphate. Additionally, Fig. 10 shows the SOX system for sulphur oxidation, present in various bacteria and archaea, including those that oxidise sulphur compounds through photosynthesis. It also touches upon chemolithoautotrophic sulphur oxidizers that may invert the enzymes for dissimilatory sulphur reduction, creating a pathway for sulphur oxidation (KEGG PATHWAY: map00920).

The following is a text map of the methanogenesis pathways (Fig. 11), which outlines how a specific organism initiates the pathway, with later stages conducted by additional organisms. For more in-depth information regarding specific compounds or reactions, interactive links are accessible through a 40k graphical format map hosted on the KEGG database. Additionally, the map delves into the role of microorganisms in the dissimilatory reduction of sulphate, providing essential insights necessary for understanding the impact of phosphogypsum as a mineral supplement in optimising the anaerobic digestion process.

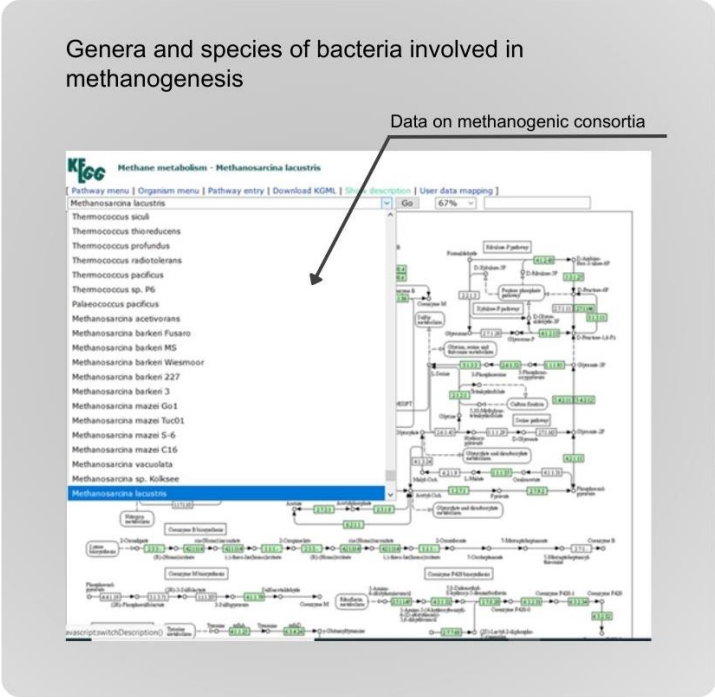

Figure 11. Web page displaying the necessary types and species of bacteria involved in the process of methanogenesis in a unified community (based on KEGG PATHWAY: map00680).

Thus metabolic pathways of sulphur-reducing microorganisms were analysed according to the KEGG database, BacDive, EAWAG-BBD, and their species were grouped, which can be effectively used for the detoxification of industrial wastewater and sewage sludge in the process of their anaerobic digestion with the addition of phosphogypsum (Table 2).

General view of the reaction of precipitation of heavy metal ions by hydrogen sulphide

$$b1_S SH^- + b1_{Me} Me^{n+} + b1_{SO} SO_4^{2-} \rightarrow b1_{MeS} MeS + b1_H H_2O, \qquad (1)$$

where $b1_S, b1_{Me}, b1_{SO}, b1_{MeS}, b1_H$ are stoichiometric coefficients; Me^{n+} is ions Cd^{2+}, Cu^{2+}, Fe^{2+}, Fe^{3+}, Zn^{2+}, Cr^{3+}, Ni^{2+}.

The main organic substrate at the final stage of organic matter decomposition is acetate. If the anaerobic oxidation of organic matter is not complete, acetic acid accumulates as the final product and the environment in the bioreactor is acidified.

Additionally, during sulfidogenesis, a biological reduction of phosphates occurs, which has been confirmed by previous studies (Plyatsuk & Chernish, 2014):

$$Fe_3(PO_4)_2 + 3SO_4^{2-} + 6C_{org} \rightarrow 3FeS \downarrow + 2PO_4^{3-} + 6CO_2, \quad (2)$$

where C_{org} is organic substrate.

Table 2. Characteristics of sulphur-reducing microorganisms

Species	Temperature range	Note	Link
Desulfovibrio	mesophilic	Desulfobaculum senezii CVL (species Desulfovibrio senezii) is an anaerobe, mesophilic bacterium that was isolated from solar saltern	https://bacdive.dsmz.de/strain/4136
Desulfonema	mesophili	Desulfonema ishimotonii DSM 9680 is an anaerobe, mesophilic bacterium that was isolated from marine mud	https://bacdive.dsmz.de/strain/3991
Desulfo-microbium	mesophilic	Desulfomicrobium aestuarii ADR26 is an anaerobe, mesophilic bacterium that was isolated from sediments	https://bacdive.dsmz.de/strain/4061
Desulforhabdus	mesophilic	Desulforhabdus amnigena ASRB1 is an anaerobe, mesophilic bacterium that was isolated from sludge, UASB reactor	https://bacdive.dsmz.de/strain/16675
Desulfomonile	mesophilic	Desulfomonile tiedjei DCB-1 is an anaerobe, mesophilic bacterium that was isolated from sewage sludge	https://bacdive.dsmz.de/strain/16666
Desulfarculus	mesophilic	Desulfarculus baarsii Konstanz is an anaerobe, mesophilic bacterium that was isolated from ditch mud	https://bacdive.dsmz.de/strain/17627
Desulforegula	mesophilic	Desulforegula conservatrix Mb1Pa is an anaerobe, mesophilic bacterium that was isolated from sediment from a shallow freshwater eutrophic lake	https://bacdive.dsmz.de/strain/3992

In this process, phosphate and hydrophosphate anions bind to Ca2+ cations to form various modifications of calcium phosphates, which precipitate due to their low water solubility. Additionally, part of the phosphate ions is displaced from the biotechnology system when it passes into the liquid phase. This also corresponds to the results obtained by other authors (Matsuura et al., 2021, Diao et al., 2023).

During the precipitation of hydrogen sulphide and HM ions in the form of sulphur, the microbial community works stably (Diao et al., 2023; Qin et al., 2024; Melgaço et al., 2020).

In the process of such treatment, a number of biochemical transformations of the components of the waste mixture occur, which is consistent with other research findings (Matsuura et al., 2021; Almuslamawy et al., 2023; Bounaga et al., 2023):

– biological reduction of phosphates, with a significant portion of the released phosphate ions chemically bonding with calcium and partially passing into the liquid phase;

– calcium carbonate is formed due to the release of carbon dioxide in the system;

– during the breakdown of protein compounds, ammonia is released and combined with sulfate ions, forming ammonium sulfate;

– complex compounds with HM (HM salts with organic compounds) are destroyed in the course of microbiological processes, HM ions pass into the liquid phase, where they interact with biogenic hydrogen sulphide to form stable metal sulphide compounds.

The prospect of industrial implementation in the field of integrated processing of persistent raw materials (biowaste and phosphogypsum) is one of the directions of the realisation of the sectoral bioeconomy. In our further research, we will develop a methodology of synergy of these wastes (as sustainable feedstock) on the basis of biochemical processes of their joint processing with the possibility of implementation in bioenergy and agriculture.

CONCLUSIONS

The analysis focusses into global advancements in bioeconomy development, particularly within the bioenergy sector. A breakdown of the bioenergy structure is provided, along with a proposed roadmap for the modernisation of biotechnology, exemplified by the anaerobic digestion process, aimed at promoting the principles of circular bioeconomy. Additionally, the integration of anaerobic digestion into broader bioprocessing systems is explored, highlighting its role in biofuel, biochemical and fertiliser production within the circular bioeconomy framework.

The stages of this modernisation roadmap are examined within the implementation of sectoral circular bioeconomy, focussing on efficiency indicators relevant to the integration of bioeconomy practices into agricultural production.

Furthermore, attention is drawn to a vital synergy between anaerobic technologies and the agricultural sector: the enrichment of digestates with essential macro- and microelements facilitated by mineral additives. Utilisation of the compositions of the components of phosphogypsum by various microorganisms is assessed through bioinformation databases, underscoring the importance of environmental sustainability in this context. In further studies, the application of phosphogypsum in bioprocesses will be deepened by biotesting. Possible applications of nanomaterials will also be considered.

ACKNOWLEDGEMENTS. This project ‘Phosphogypsum as a mineral resource for bioprocesses’ has received funding through the MSCA4Ukraine project, which is funded by the European Union (Yelizaveta Chernysh). Furthermore, this research was supported by BIOECO-UP project (Interreg Central Europe) and CEE2ACT (no. 101060280) projects.

REFERENCES

About the EAWAG Biocatalysis 2014. http://eawag-bbd.ethz.ch/aboutBBD.html. Accessed 13.10.2023.

Almuslamawy, H.A.J., Aldhrub, A.H.A., Ahmed, S.A. & Mouhamad, R.S. 2023. Microbial Simultaneous Eradication from Wastewater of Sulphate and Heavy Metals. *Asian Journal of Water, Environment and Pollution* **20**(3), 85–90. https://doi.org/10.3233/AJW230041

BacDive Dashboard 2022. https://bacdive.dsmz.de/dashboard. Accessed 23.10.2023.

Barcelos, M.C.S., Lupki, F.B., Campolina, G.A., Nelson, D.L. & Molina, G. 2018. The colors of biotechnology: general overview and developments of white, green and blue areas. *FEMS Microbiology Letters* **365**(21). doi:10.1093/femsle/fny239

Barretti, B.R.V., Kloth, M., Sydney, A.C.N., Lacerda, L.G., de Carvalho, J.C., Woiciechowski, A.L., Soccol, C.R. & Sydney, E.B. 2021. Recovery and valorization of CO_2 from the organic wastes fermentation. In *Valorization of Agri-Food Wastes and By-Products*, pp. 947–962. Elsevier. doi: 10.1016/B978-0-12-824044-1.00019-2

Bounaga, A., Alsanea, A., Danouche, M., Rittmann, B.E., Zhou, C., Boulif, R., Zeroual, Y., Benhida, R. & Lyamlouli, K. 2023. Effect of alkaline leaching of phosphogypsum on sulfate reduction activity and bacterial community composition using different sources of anaerobic microbial inoculum. *Science of The Total Environment* **904**, 166296. doi: 10.1016/j.scitotenv.2023.166296

Bounaga, A., Alsanea, A., Lyamlouli, K., Zhou, C., Zeroual, Y., Boulif, R. & Rittmann, B.E. 2022. Microbial transformations by sulfur bacteria can recover value from phosphogypsum: A global problem and a possible solution. *Biotechnology Advances* **57**, 107949. doi: 10.1016/j.biotechadv.2022.107949

Cao, T.N.-D., Mukhtar, H., Le, L.-T., Tran, D.P.-H., Ngo, M.T.T., Pham, M.-D.-T., Nguyen, T.-B., Vo, T.-K.-Q. & Bui, X.-T. 2023. Roles of microalgae-based biofertilizer in sustainability of green agriculture and food-water-energy security nexus. *Science of The Total Environment*, **870**, 161927. doi: 10.1016/j.scitotenv.2023.161927

Diao, C., Ye, W., Yan, J., Hao, T., Huang, L., Chen, Y., Long, J., Xiao, T. & Zhang, H. 2023. Application of microbial sulfate-reduction process for sulfate-laden wastewater treatment: A review. *Journal of Water Process Engineering* **52**, 103537. doi: 10.1016/j.jwpe.2023.103537

Dvoretsky, D.S., Temnov, M.S., Markin, I.V., Ustinskaya, Y. & Es'kova, M.A. 2022. Problems in the Development of Efficient Biotechnology for the Synthesis of Valuable Components from Microalgae Biomass. *Theoretical Foundations of Chemical Engineering* **56**(4), 425–439. doi:10.1134/S0040579522040224

EU budget: the Common Agricultural Policy beyond 2020. FAO. Home | Food and Agriculture Organization of the United Nations. 2018. https://www.fao.org/family-farming/detail/en/c/1137763/ Accessed: 21.08.2023.

European Biogas Association. All lights are green for renewable gas in France. 2017. https://www.europeanbiogas.eu/8789/. Accessed 2.04.2024.

European Biogas Association. Mapping the state of play of biomethane in Europe. 2020. https://www.europeanbiogas.eu/8789/. Accessed 2.04.2024.

Feng, L., Aryal, N., Li, Y., Horn, S.J. & Ward, A.J. 2023. Developing a biogas centralised circular bioeconomy using agricultural residues - Challenges and opportunities. *Science of The Total Environment* **868**, 161656. doi: 10.1016/j.scitotenv.2023.161656

Fritzen Cidón, C., Schreiber, D. & Schmitt Figueiró, P. 2023. Bioeconomics applied to organic agriculture enhance social and environmental impact of Brazilian properties. *Environment, Development and Sustainability*. doi: 10.1007/s10668-023-03718-8

Geletukha, G.G., Kucheruk, P.P. & Matveev, Y.B. 2022. Prospects for the production and use of biomethane in Ukraine. BAU Analytical Note. 11. Available at https://uabio.org/wp-content/uploads/2022/09/UA-Position-paper-UABIO-29.pdf (in Ukrainian).

Gollier, C. 2019. Valuation of natural capital under uncertain substitutability. *Journal of Environmental Economics and Management* **94**, 54–66. doi: 10.1016/j.jeem.2019.01.003

Green Gas Certification. Green Gas Production. 2024. https://www.europeanbiogas.eu/8789/. Accessed 2.04.2024.

Hasan, M., Abedin, M.Z., Amin, M.B.A., Nekmahmud, Md. & Oláh, J. 2023. Sustainable biofuel economy: A mapping through bibliometric research. *Journal of Environmental Management* **336**, 117644. doi: 10.1016/j.jenvman.2023.117644

Hu, Y., Du, H., Xu, L., Liang, C., Zhang, Y., Sun, Z., Lin, C.S.K., Wang, W. & Qi, W. 2023. Life cycle environmental benefits of recycling waste liquor and chemicals in the production of lignocellulosic bioethanol. *Bioresource Technology* **390**, 129855. doi: 10.1016/j.biortech.2023.129855

Kanehisa, M., Furumichi, M., Tanabe, M., Sato, Y. & Morishima, K. 2017. KEGG: new perspectives on genomes, pathways, diseases and drugs. *Nucleic Acids Research* **45**(D1), 353–361. doi:10.1093/nar/gkw1092

KEGG: Kyoto Encyclopedia of Genes and Genomes. KEGG PATHWAY: map00680. https://www.kegg.jp/entry/map00680. Accessed 2.04.2024.

KEGG: Kyoto Encyclopedia of Genes and Genomes. KEGG PATHWAY: map00920. https://www.kegg.jp/entry/map00920. Accessed 2.04.2024.

Konstantinidis, K.T. 2021. Metagenomic insights into the effect of sulfate on enhanced biological phosphorus removal. *Applied Microbiology and Biotechnology* **105**(5), 2181–2193. doi: 10.1007/s00253-021-11113-4

Leff, E. 2021. Bioeconomics, Negentropic Productivity and Eco-social Sustainability. In: *Political Ecology. Palgrave Macmillan, Cham*. doi: 10.1007/978-3-030-63325-7_9

Luz, F.G.G., Hájek, M., Rozenský, L. & Alves de Castro, M.C.A. 2021. Processing of biomethane for electricity production as a sustainable way to treat municipal organic solid waste: A case study of the Corumbataí river basin region. *BioResources* **16**(3), 5601–5617.

McDougal, T.L. 2022. The bioeconomics of planetary energy transitions – a theoretical note. *Economics of Peace and Security Journal*, EPS Publishing, **17**(2), 5–18. doi:10.15355/epsj.17.2.5

Melgaço, L.A. de O., Quites, N.C. & Leão, V.A. 2020. Uso do fosfogesso como fonte de sulfato para bactérias redutoras de sulfato em um reator contínuo de leito fluidizado. *Engenharia Sanitaria e Ambiental* **25**(1), 157–165. doi: 10.1590/s1413-4152202020180007

Mishra, B., Mohanta, Y.K., Reddy, C.N., Reddy, S.D.M., Mandal, S.K., Yadavalli, R. & Sarma, H. 2023. Valorization of agro-industrial biowaste to biomaterials: An innovative circular bioeconomy approach. *Circular Economy***2**(3), 100050. doi: 10.1016/j.cec.2023.100050

Moustakas, K., Loizidou, M., Klemes, J., Varbanov, P. & Hao, J.L. 2023. New developments in sustainable waste-to-energy systems. *Energy* **284**, 129270. doi: 10.1016/j.energy.2023.129270

Nayak, A.K., Mishra, V.K., Sharma, D.K., Jha, S.K., Singh, C.S., Shahabuddin, M. & Shahid, M. 2013. Efficiency of Phosphogypsum and Mined Gypsum in Reclamation and Productivity of Rice–Wheat Cropping System in Sodic Soil. *Communications in Soil Science and Plant Analysis* **44**(5), 909–921. doi: 10.1080/00103624.2012.747601

OECD. The Bioeconomy to 2030. Designing a Policy Agenda. Main Findings and Policy Conclusions. 2009. https://www.oecd.org/sti/futures/long-termtechnologicalsocietalchallenges/thebioeconomyto2030designingapolicyagenda.htm. Accessed 09.07.2023.

Oliveira, C.A., Fuess, L.T., Soares, L.A. & Damianovic, M.H. R.Z. 2021. Increasing salinity concentrations determine the long-term participation of methanogenesis and sulfidogenesis in the biodigestion of sulfate-rich wastewater. *Journal of Environmental Management* **296**, 113254. doi: 10.1016/j.jenvman.2021.113254

Plyatsuk, L. & Chernish, E. 2014. Intensification of Anaerobic Microbiological Degradation of Sewage Sludge and Gypsum Waste Under Bio-Sulfidogenic Conditions, *The Journal of Solid Waste Technology and Management* **1**(February), 10–23. doi: 10.5276/JSWTM.2014.10

Qin, R., Dai, X., Xian, Y., Zhou, Y., Su, C., Chen, Z., Lu, X., Ai, C. & Lu, Y. 2024. Assessing the effect of sulfate on the anaerobic oxidation of methane coupled with Cr(VI) bioreduction by sludge characteristic and metagenomics analysis. *Journal of Environmental Management* **349**, 119398. doi: 10.1016/j.jenvman.2023.119398

Sela-Adler, M., Ronen, Z., Herut, B., Antler, G., Vigderovich, H., Eckert, W. & Sivan, O. 2017. Co-existence of Methanogenesis and Sulfate Reduction with Common Substrates in Sulfate-Rich Estuarine Sediments. *Frontiers in Microbiology* **8**. doi: 10.3389/fmicb.2017.00766

Seruga, P., Krzywonos, M., den Boer, E., Niedźwiecki, Ł., Urbanowska, A. & Pawlak-Kruczek, H. 2022. Anaerobic Digestion as a Component of Circular Bioeconomy—Case Study. *Approach. Energies* **16**(1), 140. doi: 10.3390/en16010140

Shi, X., Gao, G., Tian, J., Wang, X.C., Jin, X. & Jin, P. 2020. Symbiosis of sulfate-reducing bacteria and methanogenic archaea in sewer systems. *Environment International* **143**, 105923. doi: 10.1016/j.envint.2020.105923

Shulipa, Ye.O., Chernysh, Ye.Yu., Plyatsuk, L.D. & Fukui, M. 2020. Ontological Tools in Anaerobic Fermentation Technologies: Bioinformation Database Applications. *Journal of Engineering Sciences* **7**(1), H1–H8. doi: 10.21272/jes.2020.7(1).h1

Siegfried, K., Günther, S., Mengato, S., Riedel, F. & Thrän, D. 2023. Boosting Biowaste Valorisation – Do We Need an Accelerated Regional Implementation of the European Law for End-of-Waste? *Sustainability* **15**(17), 13147. doi: 10.3390/su151713147

Sinkko, T., Sanyé-Mengual, E., Corrado, S., Giuntoli, J. & Sala, S. 2023. The EU Bioeconomy Footprint: Using life cycle assessment to monitor environmental impacts of the EU Bioeconomy. *Sustainable Production and Consumption* **37**, 169–179. doi: 10.1016/j.spc.2023.02.015

Statistical Review of World Energy. 2021. https://www.bp.com/content/dam/bp/business-sites/en/global/corporate/pdfs/energy-economics/statistical-review/bp-stats-review-2021-full-report.pdf. Accessed 28.08.2023.

Thrän, D., Deprie, K., Dotzauer, M., Kornatz, P., Nelles, M., Radtke, K.S. & Schindler, H. 2023. The potential contribution of biogas to the security of gas supply in Germany. *Energy, Sustainability and Society* **13**(1), 12. doi: 10.1186/s13705-023-00389-1

Ugwu, S.N., Harding, K. & Enweremadu, C.C. 2022. Comparative life cycle assessment of enhanced anaerobic digestion of agro-industrial waste for biogas production. *Journal of Cleaner Production* **345**, 131178. doi: 10.1016/j.jclepro.2022.131178

Verardi, A., Sangiorgio, P., Blasi, A., Lopresto, C.G. & Calabrò, V. 2023. Bioconversion of Crop Residues Using Alternative Fermentation-Based Approaches. *Frontiers in Bioscience-Elite* **15**(3), 17. doi: 10.31083/j.fbe1503017

Yadav, A., Sharma, V., Tsai, M.-L., Chen, C.-W., Sun, P.-P., Nargotra, P., Wang, J.-X. & Dong, C.-D. 2023. Development of lignocellulosic biorefineries for the sustainable production of biofuels: *Towards circular bioeconomy. Bioresource Technology* **381**, 129145. doi: 10.1016/j.biortech.2023.129145

Agronomy Research **22**(2), 794–814, 2024
https://doi.org/10.15159/AR.24.058

Innovative approach to real-time diagnostic of bolted joints and elastic couplings to prevent their fractures

D. Gorbacovs*, P. Gavrilovs, J. Eiduks and M. Gailis

Riga Technical University, Faculty of Mechanical Engineering, Department of Railway Engineering, Transport and Aeronautics, LV-1048 Riga, Latvia
*Correspondence: dmitrijs.gorbacovs@edu.rtu.lv

Received: October 10th, 2023; Accepted: April 3rd, 2024; Published: June 27th, 2024

Abstract. Failure of fasteners can lead to undesirable consequences. Fatigue failure of machine parts is difficult to predict and prevent. Vehicles and agricultural machinery include various systems such as engine, transmission, and many other systems that are fixed and connected using fasteners. Without a doubt, the performance of an individual system depends on the design of its kernel. But for the system to work, it must be properly fixed. Premature failure of bolts is subject of interest of engineers.
The purpose of this study is to identify the causes of the failure of the fixing bolts and develop device and algorithm for early detection of conditions that might lead to bolt failure. The experimental data is collected analysing bolts and elastic couplings of electric passenger trains.
Laboratory studies included the measurement of tensile strength, hardness, microanalysis of the metal structure and chemical analysis of failed old and new bolts. The authors present various visual and numerical results from this study. It also provides detailed conclusions about the causes of failure and recommendations for the selection of bolts for critical mechanical connections under dynamic loads and variable temperatures.
The authors have developed a device that can be used in mechanical engineering, shipbuilding and other industries to control the deformation, vibration and shocks acting on a bolted joint. This device for monitoring the load and vibrations of bolted connections allows to constantly collect and analyse data during the operation of the vehicle in order to reduce the number of unscheduled repairs of vehicles due to its damage, as well as to reduce the number of accidents or other incidents. The authors also have developed a method and algorithm for calculating and evaluating the influence of external factors on the shell of a rubber-cord coupling. The study is based on statistical, material, and mathematical analysis of unexpected failures of rubber couplings. A numerical analysis of the operating conditions of the couplings before failure was performed.
The results obtained are encouraging and prove that the use of an impact force measuring device and real-time data analysis can be cost-effective and can eliminate the problem of bolt and elastic coupling failure in one go, as well as reduce the cost of operating and repairing vehicles.

Key words: rubber cord coupling, fastening bolt, metal structure, chemical composition, hardness, static stress.

INTRODUCTION

In assembly structures, bolts are used as fastening elements to connect various parts and elements, which, in turn, can be part of any mechanisms and devices. Bolts are widely used in almost any production and the construction of almost all engineering structures. Fastening bolt connections allow easily and quickly connect the parts of assembly structures, in the construction of buildings, for connecting parts in cars, airplanes, railway rolling stock, pipelines, for fastening various structures, in the assembly of complex machines and equipment used in industry, as well as in everyday life.

On the other hand, the bolts that are used to fasten various structures and aggregates of the railway rolling stock work in quite severe conditions. So, when working on railway rolling stock, the fastening bolts are subjected to static, dynamic, as well as impact loads, and as a result of the action of impact loads, the strength capacity of the bolt material is exhausted over time. During the further actions of shock loads, microcracks gradually occur and develop in the bolts, and finally grow into cracks. They become stress concentrators and, due to the increasing weakening of the cross-section of the bolts, microcracks and cracks increase, and the bolts become the site of final fracture of the rubber cord coupling attachment. Rubber cord couplings operate under dynamic load conditions with high force and vibration loads, which can cause system resonance.

In order to reduce the failure rate of the rubber cord coupling mounting bolts, a solution to the failure problem of the M24 bolts must be found. For these purposes, it is proposed to create a device that allows you to monitor the impact force received by the rubber cord coupling bolts, and with the introduction of this device into operation, to achieve a reduction in the number of failures during the inter-repair period.

Many international scientific researchers dealt with the problems of researching the destruction of bolts.

In the scientific work (Grigorenko et al., 2014), the reasons for the destruction of M14 bolts made of steel 30ХГСА with a protective cadmium coating were investigated. The chemical and phase compositions, microstructure and fractures were studied to establish the causes of the destruction of bolts made of 30ХГСА steel. As a result of the analysis, the reasons for the destruction of the bolts were determined and recommendations were given for their elimination.

The paper also considers medium-carbon structural steels showing propensity to the delayed destruction at static loadings below yield point in conditions of cyclic (daily and seasonal) temperature changes.

In the scientific work (Grigorenko et al., 2018) various types of fractures of 30ХГСА steel samples with zinc-based coatings are considered, and also operational fractures of 30ХГСА steel fasteners are analyzed, the reasons of workability loss of destroyed parts are established, the mechanisms of fatigue and grain boundary brittle fracture of 30ХГСА steel samples are studied by raster electronic microscopy methods. The carried out researches of parts made of 30ХГСА steel allowed to allocate the basic reasons of the destruction of fasteners during operation. The majority of cases of details destruction is connected with the development of fatigue cracks formed due to the presence of scratches on the surface from machining, dents or embedded particles from sandblasting, as well as friction during operation. On the basis of the conducted researches recommendations on elimination of factors contributing to fracture of 30ХГСА steel samples are given.

The paper (Sapalov & Panfjerova, 2016) analyzes the measurement results of high-strength bolts strength properties with a portable hardness tester used during inspection of structures with the results obtained using a stationary hardness tester.

The researches of properties of high-strength bolts by means of various testing methods confirmed the admissibility and correctness of their strength properties determination in the process of structures examination by portable hardness tester provided that the device is preliminary corrected on comparative results of direct and indirect values.

The scientific paper (Sirokih, 2005) describes the experiment and its subsequent repetition in numerical simulation. The experiment consisted in stretching the friction connection of plates with different arrangement of bolts in the cross-section. Based on the results of the experiments stress distribution plots were obtained in the plate, near the holes and directly in the places of the weakened section, were obtained. a numerical model was created, boundary conditions are assigned, and a load was applied. Experiment and numerical simulation showed good convergence of experimental and calculated results. In conclusion, the author gives recommendations on the design of friction joints in the calculation systems.

In the paper (Zhang et al., 2021) is made an attempt to describe the decline in fatigue life of an aluminum alloy structure containing bolted joints under the conjoint influence of an aggressive aqueous environment and loading that is essentially cyclic in nature. The method proposed in this study provides a convincing approach for reliable estimation of life, or endurance, of an aluminum alloy structure containing joints.

The paper (Yingnan et al., 2020) proposes a cogging high-strength bolt composite joint (C-HSB joint), and introduces its main components and assembly methods.

In the paper (Desai et al., 2021) authors have developed methodology to predict the bolts loosening in dynamic condition using vibration data.

A lot of works are devoted to the rubber-cord couplings.

In the paper (Korneeva et al., 2016) the finite-element research of the intense deformed condition of the highly elastic flat coupling at the shaft axial offset and small twisting angles is presented.

In the paper (Evdokimov & Shikhnabieva, 2017) the results of experimental studies of stress–strain behavior during hardening stages, as well as the stabilization and strength degradation of the rubber-cord shells during the static loading mode have been given.

The paper (Vinogradov, 2016) gave the dynamic and static elastic characteristics of couplings and drive containing the coupling with rubber-cord shells.

In the paper (Klimentyev et al., 2015) advantages of rubber as a construction material are considered. Method of calculation such basic characteristics as the geometric dimensions, static deflection, natural frequencies, stiffness, vibration isolation and damping properties of rubber-cord cushions working under pressure is described. Rubber-cord cushions most typical use as shock absorbers, antivibration mounts, flexible couplings, flexible hoses and pipe work are presented.

The paper (Tribel'skii & Zubarev, 2008) a solution of the steady thermoelastic problem is proposed, taking account of the dependence of the elastic and thermophysical constants of the material on the temperature and strain.

However, analyzing the research and methods of the authors listed above, no answers were found to the following questions, how to predict the cause of failure of a bolted connection and a rubber-cord coupling. An algorithm for early detection of conditions that can lead to failure of these nodes is not explored. The articles did not present detailed studies on bolted connections; issues such as the effect of hardness on a bolted connection were not considered. Issues such as determining the chemical composition of new and old bolts, the influence of loads, and temperature were not considered. In the works discussed above, the factors that affect the operation of the rubber-cord coupling were not considered; there was no numerical analysis. However, premature failure of both the bolts and the rubber-cord coupling is an important factor in any installation and is the subject of research. Analyzing the above articles, it can be seen that the problems of failure, both of bolted connections, and the failure of the cord coupling, took place separately.

The authors propose to consider a common assembly, a rubber-cord coupling and its fastening bolts, and offer a technical solution that will allow to monitor the common node during operation. This idea was not chosen by chance. This will be discussed further.

Answer (1). In addition to standardised, generally accepted research methods, the article proposes innovative approaches that will reduce the number of rubber-cord couplings and its fastening bolts failures. This problem is solved by two new innovative research methods using an impact vibration device:

1. Determination of the shock and vibration load to which the rubber-cord coupling mounting bolts are exposed.
2. The influence of resonant frequencies on a rubber-cord coupling.

For example, on the Latvian Railway, a similar rubber-cord coupling is used on rolling stock, in particular on electric trains. The collection of statistical data was carried out. According to the data obtained, it was found that, the problem of wrinkling of the rubber cord bolts in the period from 2015 to 2021 has become predominant for all EMU trains. In the analysis of unscheduled repairs, the information of the Technical Department of the railway company JSC 'Pasažieru vilciens' was used on the basis of data on unscheduled repairs of EMU trains from which traction drive damage was identified for the period from 2015 to 2021 (Summary of non-scheduled repairs of electric trains…, 2021). Of the total number of unscheduled repairs, which amounted to 385 cases, the largest number of 180 cases was damage to the rubber-cord coupling bolts. The destruction of the rubber-cord fastening bolts is on average more than 49% of the total number of malfunctions in the traction gear. Failure of the rubber-cord coupling bolts occurred in the range of mileage of motor cars from 1628 to 256,646 km. Failure rate depends on a number of random factors and is actually a random variable.

Rubber cord couplings operate under dynamic load conditions with high force and vibration loads. Bolts, which are used to fasten various structures and aggregates of railway rolling stock, work in quite severe conditions. So, when working on the railway rolling stock, static, dynamic, as well as shock loads are applied to the fastening bolts, and as a result of the impact loads, the strength capacity of the bolt material is exhausted over time (Evdokimov & Shikhnabieva, 2017).

The breaking of four bolts out of eight may cause the rupture of the rubber-cord coupling and the ejection of the inner flange, which may cause damage to the track, the part of the rolling stock of EMU trains (rolling gear), the mechanical equipment of the

electric train or the car body. The disc of the inner flange can also get into the cabin of the car through the viewing hatch, causing damage to the cabin and even injury to the passengers, (Fig. 1).

This case took place on the Latvian Railway, when during the movement of an electric train, 5 bolts securing a rubber-cord coupling broke. As a result, the half-disk fastening the rubber-cord coupling flew into the car interior, breaking the protective grille and piercing the inspection hatch of the motor car (Fig. 1).

Figure 1. Ejection of the flange of the rubber-cord coupling in the passenger compartment.

Operating experience in electric train traction drives shows that using a rubber cord coupling due to its durability and reliability ascpect, these elements (coupling and its fastening bolts) are one of the weakest elements in the electric train traction equipment.

In connection with this, the problem of failures of rubber-cord couplings and their fastening bolts requires investigation of the causes of failures.

The failure data of the rubber cord coupling and its fastening bolts for the period from 2012 to 2021 are shown in (Fig. 2).

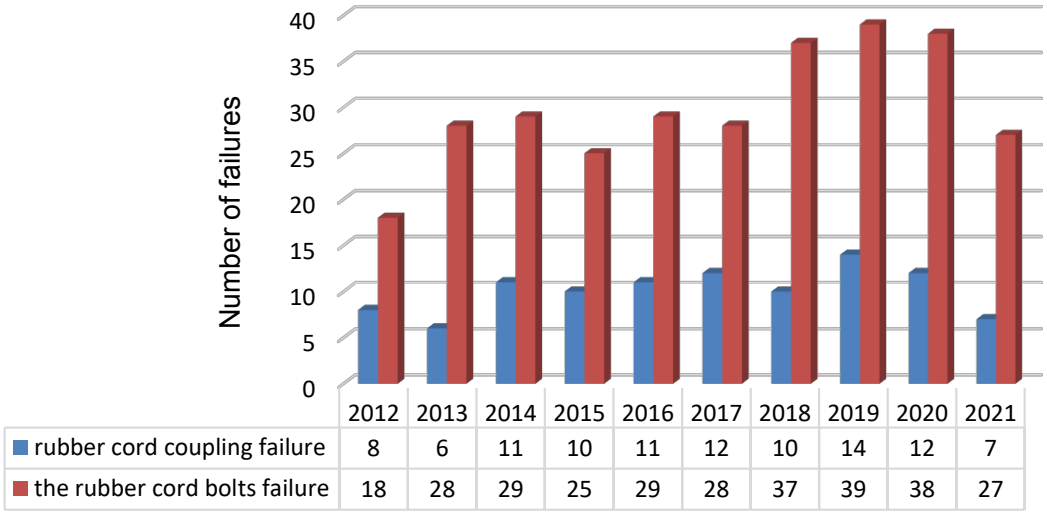

	2012	2013	2014	2015	2016	2017	2018	2019	2020	2021
rubber cord coupling failure	8	6	11	10	11	12	10	14	12	7
the rubber cord bolts failure	18	28	29	25	29	28	37	39	38	27

Figure 2. ER2 and ER2T Rubber cord coupling and rubber cord coupling bolt failures.

MATERIALS AND METHODS

To determine the causes of bolt disintegration, check the compliance of the samples with the requirements of ISO 898-1:2013 and EN 10083-3:2007-01 standards for 4Cr41 grade steel was done. Bolt samples, which were dismantled from ER2 and ER2T series motorcars, with numbers No. 1, No. 2, No. 3, No. 4 were chosen for research objects, as well as one sample of a new bolt with No. 5. The operating time of the car (number of days) and its mileage were taken into account.

Table 1. Data on the performance of bolts

Sample No.	Operating time days	Mileage, km
No. 1	201	59,348
No. 2	160	64,078
No. 3	43	17,124
No. 4	408	114,400
No. 5	new bolt -	-

The research was carried out in the laboratory of the Riga Technical University in the following directions:

1. determination of hardness;
2. chemical composition analysis.

The data on the mileage and the service life of the bolts in the railcars are shown in (Table 1).

Determination of hardness

In the laboratory of the Riga Technical University, steel hardness was tested according to the Brinell scale (HB) (Taylor et al., 2021) using the device 'MIC 10' (Kuzu et al., 2021). In order to obtain greater accuracy of the experiment, measurements were made at 5 points along the entire cross-section of the samples. The dependence of the hardness HB on the mileage of the bolts is shown on the graph of (Fig. 3).

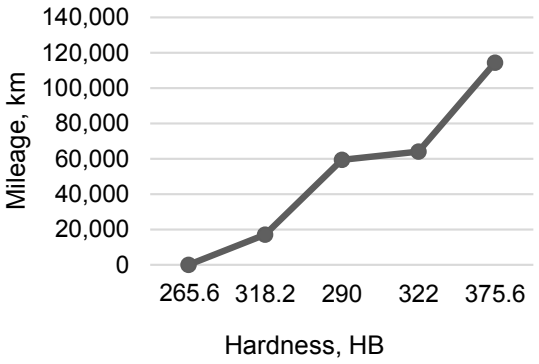

Figure 3. The hardness of the coupling bolts dependence on the mileage.

According to the results of the graph, we can see that the hardness of the coupling bolts increases with increasing mileage, i.e. the material of the bolts became stronger. The term hardness of a metal is a characteristic that describes its resistance to destruction upon contact with a harder element. An increase in metal hardness is usually associated with an increase in brittleness and a decrease in the ductility of the metal (Boguslavskij, 2016). This is explained by the fact that the atoms introduced into it form a chemical bond with the metal atoms and this significantly complicates the sliding of some planes of the densely packed structure of the metal along other planes, which determines the malleability of pure metals. At the same time, the presence of embedded atoms does not have a significant effect on the electrical conductivity of metals. This means that the intervening atoms little change the nature of the chemical bond between metal atoms (Slejbo, 2005). It can be assumed that over time there is an increase in fragility and a decrease in ductility, resulting in its fracture.

Chemical composition analysis

According to the results of determining the chemical composition of steel, it was found that:

steel grade of sample No. 1 – not determined;
steel grade of sample No. 2 – 34Cr4;
steel grade of sample No. 3 – not determined;
steel grade of sample No. 4 – not determined;
steel grade of sample No. 5 – 34Cr4.

During the investigation of the chemical composition of the steel, the following inconsistencies with the requirements of the standard EN 10083-3:2007-01 were discovered.

The carbon (C) content in four samples is less than the norm and amounts to:
for sample No. 2 – 0.366%;
for sample No. 3 – 0.261%;
for sample No. 4 – 0.316%;
for sample No. 5 – 0.322%;
however, in sample No. 1, the carbon content exceeds the norm and is 0.505%.

According to the requirements of the EN 10083-3:2007-01 standard, the carbon content in steel for the manufacture of bolts for fastening rubber-cord couplings must be in the range of 0.38–0.45%, which corresponds to steel grade 4Cr41. However, studies show that the material of the steel grade differed from the standard. As the amount of carbon in the steel decreases, its plasticity improves and rigidity (impact resistance) increases. As the carbon content in the steel increases, the hardness, strength and rigidity of the steel increases, the yield strength σ_t and tensile strength σ_s also increase, but at the same time plasticity and impact resistance decrease, and machinability and weldability also deteriorate (Zadel et al., 1985; Birjukov et al., 1986).

Harmful impurities of phosphorus and sulphur were found in the material of the bolts during the research process. The percentage of phosphorus (P) in sample No. 1 is – 0.125%; in sample No. 2 – 0.0050%, in sample No. 3 – 0.0813%, in sample No. 4 – 0.0898%, in sample No. 5 – 0.0671%. In four samples, the phosphorus content significantly exceeds the norms set by the EN 10083-3:2007-01 standard, which should be less than 0.025%.

As you know, phosphorus is one of the harmful impurities of steel, the source of which is charge materials, mainly cast iron. It is capable of dissolving in significant quantities in ferrite, which leads to distortion of the crystal lattice. At the same time, there is an increase in tensile strength and yield strength, a decrease in ductility and viscosity. An increase in phosphorus content causes an increase in the cold brittleness threshold and a decrease in the work of crack development.

Phosphorus is highly susceptible to segregation, which leads to a sharp decrease in viscosity in the central part of the ingot. Currently, there is no technology for deep purification of steel from phosphorus (Bhadeshia & Honeycombe, 2017).

Accordingly, the question arises of how increased hardness and an increase in harmful impurities in the metal affect the performance of the bolt and what measures can be proposed to identify them at an early stage, before it breaks.

The investigation of the causes of disintegration of the bolts of the rubber cord coupling fastening M24 bolts was carried out in the RTU laboratory in the following directions:

1. determination of the type and nature of disintegration in three specimens under static loading;

2. determination of the type and nature of disintegration for three specimens under cyclic loading.

Determining the type and nature of decomposition under static loading

In order to determine the type and nature of the disintegration stress, three samples of M24 bolts were tested in the RTU laboratory: No. 6; No. 7; No. 8 static tests for breakage. Bolt samples were taken from rail cars with the following mileage data:

Sample No. 6 mileage – 214,596 km;

Sample No. 7 mileage – 105,764 km;

Sample No. 8 without mileage (zero mileage).

The tests were performed in the RTU laboratory using a Zwick/Roell Z600 electromechanical testing machine with a load increase rate of 1 mm per minute. 1 mm was not chosen by chance – the minimum tensile load of the installation.

Determining the type and nature of decomposition under cyclic loading

In order to determine the type and nature of the bolt M24 decomposition, cyclic tests were carried out on three samples of the bolt numbered No. 9; No. 10; No. 11 (stretching and unloading – 10 tests and 11 tests for stretching the sample until decomposition) considering three different mileage ranges:

Sample No. 9 with mileage 22,543 km;

Sample No. 10 with mileage 155,365 km;

Sample No. 11 with mileage 210,298 km.

A stress cycle is understood as a set of varying stress values in one period of change. Cyclic tests were performed in the RTU laboratory using a Zwick/Roell Z60010 electromechanical testing machine with progressive loading and unloading. Load levels respectively: 25 kN; 50 kN; 75 kN 100 kN; 125 kN; 150 kN; 175 kN; 200 kN; 225 kN; 250 kN; decomposition. The speed of increasing the load is 7 mm per minute (Fig. 4). The rate of increase in load of 7 mm is the maximum tensile load.

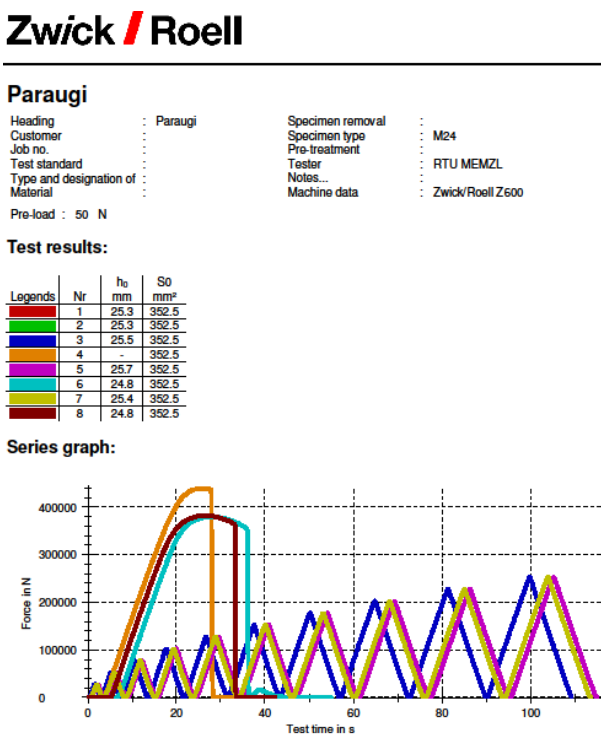
Zwick / Roell

Paraugi

Heading	: Paraugi	Specimen removal	:
Customer	:	Specimen type	: M24
Job no.	:	Pre-treatment	:
Test standard	:	Tester	: RTU MEMZL
Type and designation of Material	:	Notes...	:
		Machine data	: Zwick/Roell Z600

Pre-load : 50 N

Test results:

Legends	Nr	h_0 mm	S0 mm²
	1	25.3	352.5
	2	25.3	352.5
	3	25.5	352.5
	4	-	352.5
	5	25.7	352.5
	6	24.8	352.5
	7	25.4	352.5
	8	24.8	352.5

Series graph:

Figure 4. Bolts decomposition diagrams.

According to the test results it was found that the fractures of all the samples occurred at the connection point of the bolts with the insert, without cupped fracture. According to the test results, the fatigue decomposition of the samples was found as a result of the accumulation of defects from

the action of shock vibration load. Müller & Choteborský (2016) have shown that the temperature of the specimens influenced the impact strength, the toughness and the maximum deformation of the adhesives. To carry out diagnostics of bolted connections in real time, a shock vibration device was designed and developed.

The purpose of the invention is to create a device for monitoring the impact and vibration force of bolt fastenings, which would make it possible to constantly accumulate and analyze data on the impact force perceived by the bolts during the operation of the vehicle in order to reduce the number of unplanned repairs of rolling stock of railway transport or vehicles of other industries due to its damage, as well as to reduce the number of accidents or other accidents (Stauffer, 2004). As a result, the costs of operating and repairing vehicles will be reduced. The block diagram of the invented device is shown in (Fig. 5).

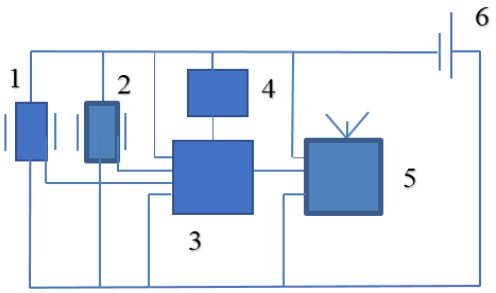

Figure 5. Block diagram of the invented device: 1 – vibration sensor; 2 – shock sensor; 3 – microcontroller; 4 – memory module; 5 – data transmission unit; 6 – power supply unit.

The purpose of the invention is achieved as follows: the device for monitoring the impact and vibration force of bolt fasteners consists of a housing, inside which the following elements are installed: a vibration sensor (4) and an impact sensor (5), a microcontroller (6), a data transmission unit (7) and a power supply unit (8). A piezo-accelerometer can be used as a vibration sensor (4) and shock sensor (5) – sensors that convert the value of vibration or shock force into an electric signal (Leonardson & MacGugan, 1994; Komorska, 2011).

When processing the information and finding that the allowable load on the rubber-cord coupling fastening bolts has been exceeded several times, the decision to replace the bolts was made in more than 10 cases during week. Thus, unplanned repairs due to damage to bolts and other components of the vehicle have been prevented. Putting the invented device into operation will allow obtaining objective data on the impact force and vibration loads on the bolts. Accumulating information and processing it regularly can prevent damage to rubber-cord coupling bolts and, accordingly, reduce the number of unplanned repairs of electric trains. The invention can be used in any type of railway rolling stock, as well as metro cars. The invented device can be used in mechanical engineering, shipbuilding and other industries to control the defect of bearings, deviations of shafts, the condition of transmission gears and other structures on which the fixing bolts are subjected to deformation forces. If, when processing the information received from the invented device during technical maintenance (or restoration repair), it is found that the allowable loads have been exceeded many times, then the bolts must be replaced with new ones. Thus, the need to perform unplanned repairs due to bolt damage, which are associated with large financial costs for the company, is avoided.

Shock vibration device testing

After a test using an impact stand, the impact load was determined in the railway undertaking AS ‘Pasažieru vilciens’. In order to do this, it was necessary to determine the impact force F, which is received by the bolts when the motor car passes the rail

joints. The impact force F, which is absorbed by the bolts of the rubber cord coupling, is determined according to the formula (1), in order to determine it, it is necessary to determine the acceleration with which the motor car passes the rail joint. For this purpose, we use the empirical formula (2).

$$F = \omega_r \cdot q \quad (1)$$

where q – half the mass of the wheelset, t; ω_r – the acceleration with which a car passes a rail joint, m s^{-2}.

$$\omega_r = \left[2 + 0.13\frac{V}{\sqrt[3]{(2q)^2}}\right] \cdot g \quad (2)$$

where V – car speed, km h^{-1}; q – half the mass of the wheelset, kg; g – gravitational acceleration, 9.81 m s^{-2}.

The data of acceleration and impact force calculations are presented in (Table 2).

Table 2. Acceleration and impact load calculation data

Car speed V, km h^{-1}	Acceleration of the wheelset ω_r, m s^{-2}	Impact force F, N
20	28.122	42,183
40	36.624	54,936
60	45.126	67,689
80	53.628	80,442
100	62.13	93,195
120	70.632	105,948

Further, in order to determine the impact load, tests of the disintegration load of the rubber cord coupling fixing bolts were carried out in the JSC 'Pasažieru vilciens' company, in which the developed impact vibration device was used, with different, but close to the calculated data of the impact force F. The experimental data was shown in (Table 3).

Table 3. Testing the impact vibration device on the bench

Trial No.	Quantity of bolts, pcs	The size of the impact force, F, N	Quantity of blows, pcs.	Impact level size, cond. units
1	16	20,000	1,000	305–317
2	16	40,000	730	329–338
3	16	60,000	467	354–362
4	16	80,000	354	383–395
5	16	100,000	136	418–430

Analyzing bolt impact test data, it was found that with an impact force equal to:

• 20,000 N (2 tons) – bolts do not break;

• 40,000 N (4 tons) – after the 730th impact, one bolt broke;

• 60,000 N (6 tons) – after the 467th impact, one bolt disintegrated, but after 500 hits the other bolt was found to have disintegrated during the inspection of the bolts.

• 80,000 N (8 tons) – after the 354th impact, one bolt disintegrated, but after 360 impacts, the disintegration of the second bolt was found during the inspection of the bolts;

• 100,000 N (10 tons) – after the 136th impact, it was found that two bolts were subject to disintegration at once, after testing of 150 impacts, it was found that disintegration took place in two more bolts, which are critical in operation.

Metallographic analysis of bolts subjected to impact force from 20,000 N (sample 12, a, b); 80,000 N (sample 13, a, b) and 100,000 N (sample 14, a, b) is shown in (Figs. 6–8).

Metallographic analysis confirmed the formation of critical defects and cracks is shown in (Figs. 6–8) in the microstructure at different values of the impact force, which caused the bolt to disintegrate. Müller (2017) has shown that adding the filler into the resin changed a fracture surface. An analysis of a scanning electron microscopy (SEM) proved a good wettability of the filler, the resin and the adhesive bonded material (a structural carbon steel S235J0). A crack propagation was concentrated around the filler B112 (151.59 ± 53.04 μm), namely at higher value of the loading speed, i.e. 10 mm min^{-1}. The crack propagation is a consequence of this.

To check the shock vibration load received by the rubber cord coupling bolts, a shock vibration device was installed on the rubber cord coupling flange. The installation location of the device is shown in (Fig. 9). The operation test of the shock vibration device was performed on electric train motor car No. 7118-10 starting from 15.04.2023.

To check the shock vibration load received by the rubber cord coupling bolts, a shock vibration device was installed on the rubber cord coupling flange. The installation location of the device is shown in (Fig. 9). The operation test of the shock vibration device was performed on electric train motor car No. 7118-10 starting from 15.04.2023. coupling bolts, a shock vibration device was installed on the rubber cord coupling flange. The installation location of the device is shown in (Fig. 9). The operation test of the shock vibration device was performed on electric train motor car No. 7118-10 starting from 15.04.2023.

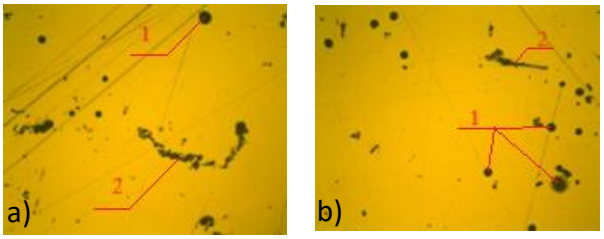

Figure 6. Metallographic analysis after 360 impacts with a force of 20000 N, magnification –x50, sample 12: 1 – inclusion; 2 – craks.

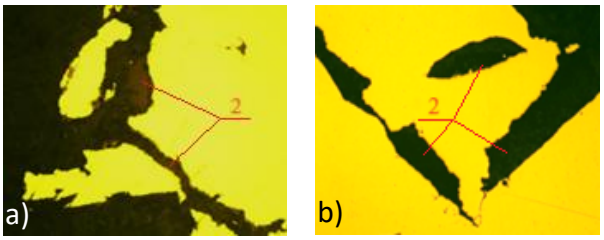

Figure 7. Metallographic analysis after 360 impacts with a force of 80000 N, magnification – x50, sample 13: 2 – craks.

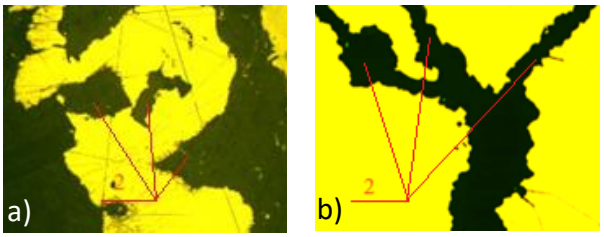

Figure 8. Metallographic analysis after 360 impacts with a force of 100000 N, magnification – x50, sample 14: 2 – craks.

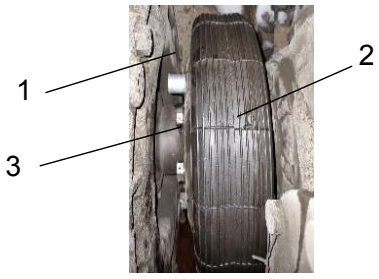

Figure 9. Placement of the impact monitoring device for bolted anchorages and rubber cord coupling: 1 – impact monitoring device; 2 – rubber cord coupling; 3 – fastening bolts.

Answer (3). Since all trains are used on the same identical directions and routes with a daily mileage of an average of 500 km per day, car 7118-10 was randomly selected for research. Based on data on the mileage of cars, where mileage not exceed more than 100 thousand km from repair (the standard mileage to the scheduled repair is 240 thousand km ± 10%), in order to monitor on daily basis the shock and vibration load during 6 months. The mileage of car 7118-10 from the scheduled repair at the time of installation of the shock-vibration device was 55 thousand km.

Answer (2). The device was used to test shock and vibration loads and control resonant frequencies during operation of a motor car in operation (on the line). Over the course of 6 months, the shock and vibration load was monitored under operating conditions of Latvian railway with daily shock load monitoring in order to ensure trouble-free operation of rolling stock and improve the quality of service and transportation of passengers.

The results obtained from the impact monitoring device for bolted anchorages and rubber cord are shown in (Fig. 10).

(Fig. 10) shows the amplitudes of vibrations (in conventional units) taken from the vibration sensor while the motor car is moving. Measurements were carried out throughout the day (24 hours). As can be seen from the graph, the amplitude of the vibration was at around 280 conventional units. However, 3 cases were recorded when the amplitude of oscillations reached up to 300 conventional units. The maximum amplitude of oscillations was 396 conventional units. The mileage of the car is 486 km.

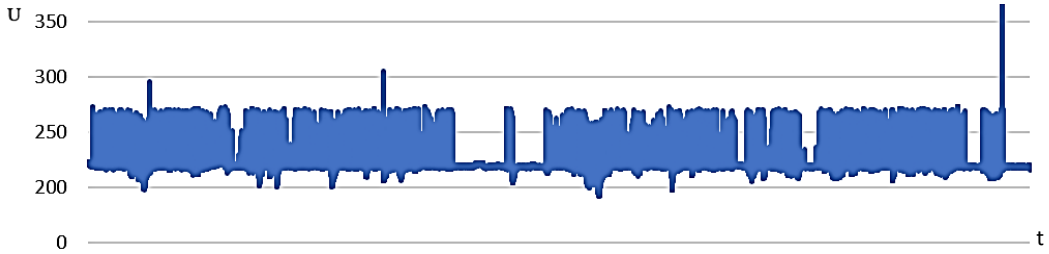

Figure 10. Shock vibration load graph for one working day.

Once a month, when the motor car reaches 10–15 thousand km mileage, one bolt was dismantled for metallographic analysis. The purpose of the metallographic analysis is to detect and confirm the existence of defects and microcracks in the microstructure at certain and determined impact loads and at a known distance of the motorcar bolts. The data of the study of the performance of bolts using an impact monitoring device for bolted anchorages and rubber cord coupling were shown in (Table 4).

Table 4. Impact load determination.

Sample No.	M24 bolt performance indicators				
	Mileage, km	The size of the shock sensor readings, cond. units			
		300–330	331–360	361–390	391–420
15	12,682	52	14	3	0
16	25,632	116	21	1	2
17	38,850	187	33	1	1
18	52,512	236	42	5	0
Critical level	264,000	700	250	150	40

During the monitoring, the maximum impact vibration level of the impact load is 396 conditional units.

Knowing the maximum value of the shock-vibration load to which the fastening bolts of rubber-cord couplings can be subjected, it is proposed to collect data on the shock-vibration loads. When the maximum impact load ascertained during operation of the rubber-cord couplings fastening bolts is reached, it is proposed to carry out measures for their replacement. This significantly reduces the likelihood of bolt failures and the associated need to perform unscheduled repairs of units, which entails a significant reduction in the costs for the company.

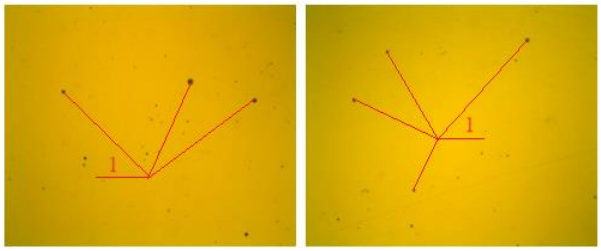

Figure 11. Bolt sample 15 metallographic analysis, mileage 12,882 km.

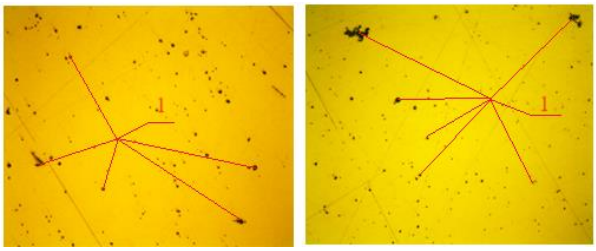

Figure 12. Bolt sample 18 metallographic analysis, mileage 52,512 km.

For metallographic analysis, bolts with mileage of 12,682 km and 52,512 km were taken. The results of metallographic analysis of bolt samples 15 and 18 are shown in (Figs. 11, 12).

The results of the metallographic analysis showed the gradual formation of defects in the microstructure, (Figs. 11, 12, poz. 1).

Frequency analysis of rubber cord coupling

The critical-frequencies of the coupling depend on the rigidity - the fastening method and on the mass of the coupling. For this purpose, we use the empirical formula (3) (Myakishev & Bukhovtsev, 2004).

$$w = (\frac{K}{M})^{0.5} \quad (3)$$

where K – coupling stiffness, N m^{-1}; M – coupling mass = 9.24 kg.

Based on the results of studies of 40 resonant frequencies, it was found that the total contribution of the coupling mass in these vibrations reaches 61.8% in the axial direction of the coupling, 50% in the vertical and horizontal radial directions. Since the total part of the mass of the coupling involved in the oscillations is greater than 60%, the further participation of the mass is not significant and therefore we stop at

Table 5. Summarized critical-frequency results

Number of test	Critical-oscillation frequency, Hz	Coupling mass participation coefficients by axles		
		X	У	Z
1	54.87	**0.5719**	$1.28 \cdot 10^{-6}$	$8.34 \cdot 10^{-9}$
2	56.27	**0.0194**	$2.66 \cdot 10^{-6}$	$3.23 \cdot 10^{-6}$
3	56.37	**0.0260**	$1.97 \cdot 10^{-8}$	$5.89 \cdot 10^{-7}$
11	88.25	$1.82 \cdot 10^{-8}$	**0.0533**	**0.3882**
12	88.36	$2.14 \cdot 10^{-9}$	**0.3881**	**0.0532**
22	126.05	$4.85 \cdot 10^{-7}$	**0.0511**	**0.0028**
23	126.22	$1.89 \cdot 10^{-7}$	**0.0048**	**0.0484**

the first 40 frequencies. We distinguish the main masses involved in the formation of oscillation modes. A summary table of resonance frequencies with the largest coupling mass contribution is shown in the (Table 5).

These fluctuating masses represent a portion of the energy that acts on the coupling shell and can cause its damage (Medvecka-Benova et al., 2015). For the largest masses specified in in the (Table 5), histogram was created a histogram of mass participation in fluctuations in each direction, shown on (Fig. 13).

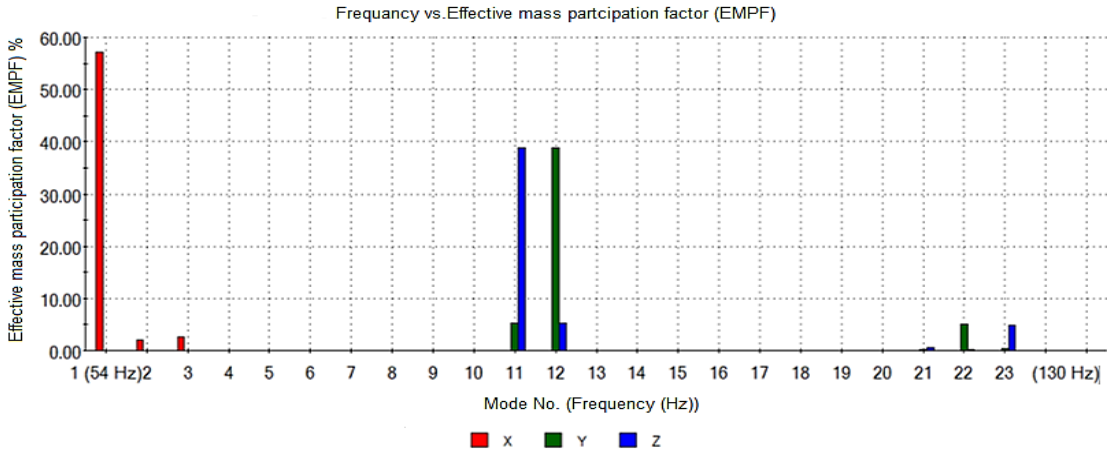

Figure 13. Histogram representing the mass participation in the oscillations.

To estimate the total mass participation coefficient from the oscillation frequencies, created a graph of the total mass participation (Fig. 14).

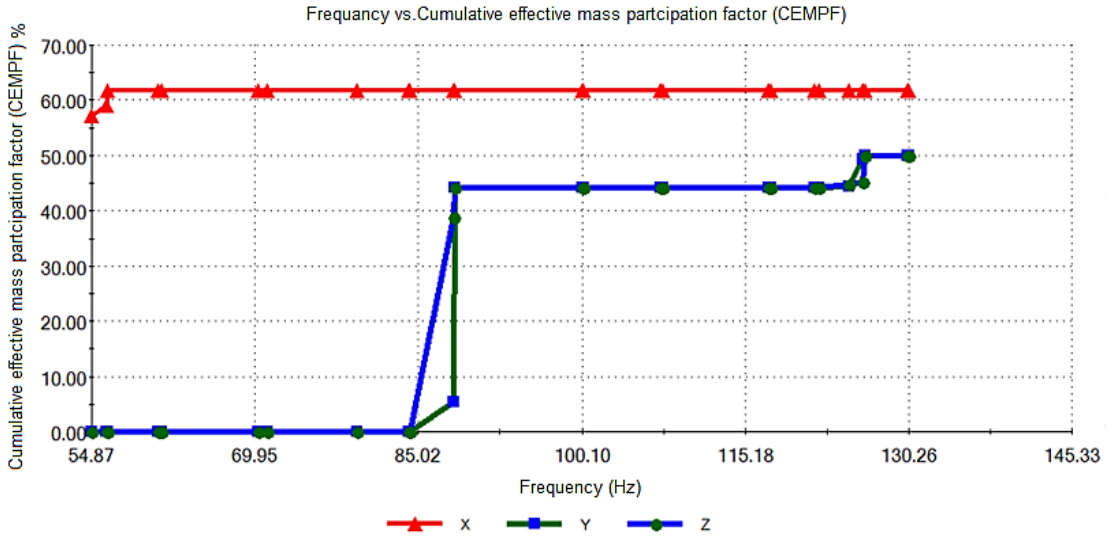

Figure 14. A graph showing the overall coefficient of mass participation as a function of the oscillation frequencies.

As a result of the analysis of the histograms (Figs. 13, 14), we determine the main vibration modes corresponding to the frequencies with the largest coupling mass, and

the mass participation indicates which frequency modes are the most dangerous (Sheshenin et al., 2021).

As can be seen on the (Fig. 15), the first and main form of oscillation at 54.87 Hz with the largest part of the mass of the coupling 57.19% loads the side wall of the coupling shell in the axial direction. The loaded zone coincides with the coupling failure zone during operation.

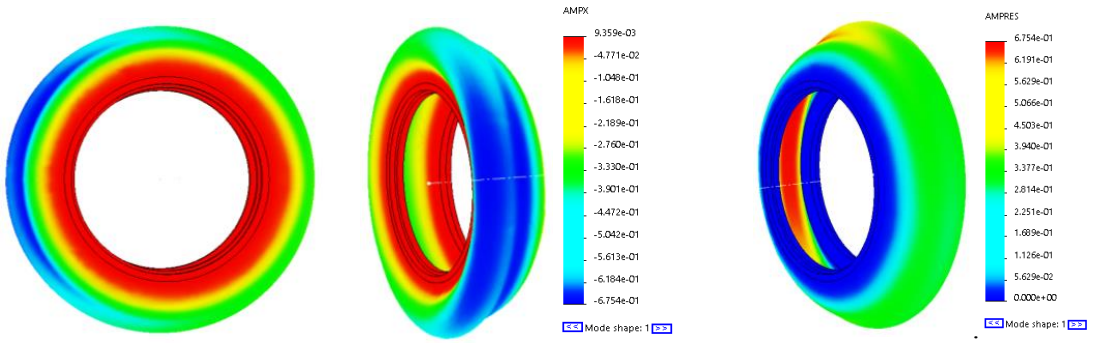

Figure 15. Coupling vibration along the X axis at frequency of 54.87 Hz.

As can be seen on (Figs. 16, 17), the shape of the oscillation at the frequencies of 88.25 Hz and 88.36 Hz with the largest part of the mass of the coupling, 38.82% and 38.81%, respectively, directed in the radial, horizontal and vertical directions, stretches the upper surface and the side of the coupling shell in the radial direction. During operation, the stressed areas partially coincide with the area of coupling damage.

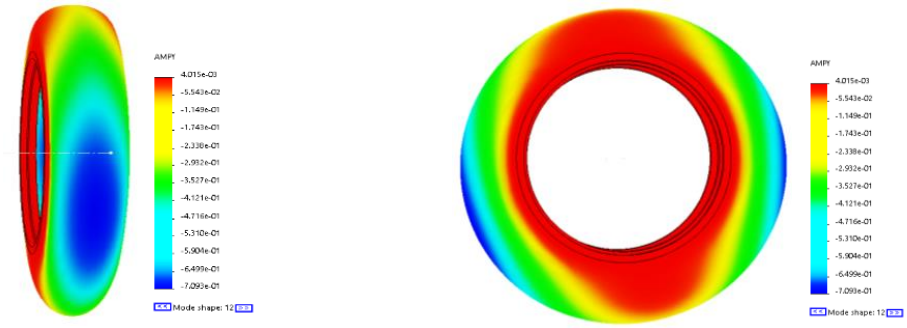

Figure 16. Coupling vibrations along the Y axis at frequency of 88.25 Hz.

At frequencies 56.37 Hz, 56.27 Hz, 126.05 Hz and 126.22 Hz, the coupling loses its stability, however the mass contribution at these frequencies is not significant and the place where the coupling is attached to the flanges is not under stress. At resonance frequencies of 56.37 Hz, 56.27 Hz, 126.05 Hz and 126.22 Hz, no more than 5% of the mass of the rubber cord coupling participates and its contribution does not affect the oscillations.

Using Solid Works software critical (dangerous) frequencies to which rubber-cord couplings may be exposed during operation were identified. In turn, use a shock-vibration device is proposed to collect data on the real frequencies to which the coupling

(or other unit) is exposed during operation. Shock and vibration load data is monitored in real time and stored on a server that can be accessed via the Internet.

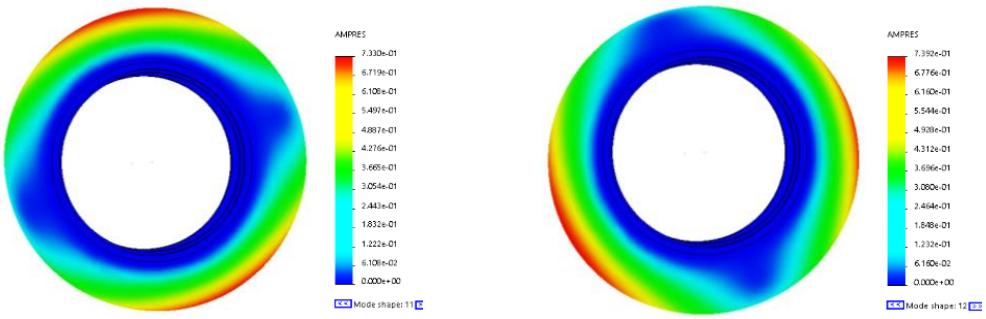

Figure 17. Coupling vibrations along the Z axis at frequency of 88.36 Hz.

The initial moment of resonance of the rubber cord coupling was determined using a impact monitoring device for bolted anchorages and rubber-cord coupling. The value of the oscillation frequency can be determined for individual stages of movement at a known speed. The results for different speed ranges for the 1 s period are shown in (Figs. 18–21).

Figure 18. Study of resonance frequencies at speed of 10–20 km h^{-1}.

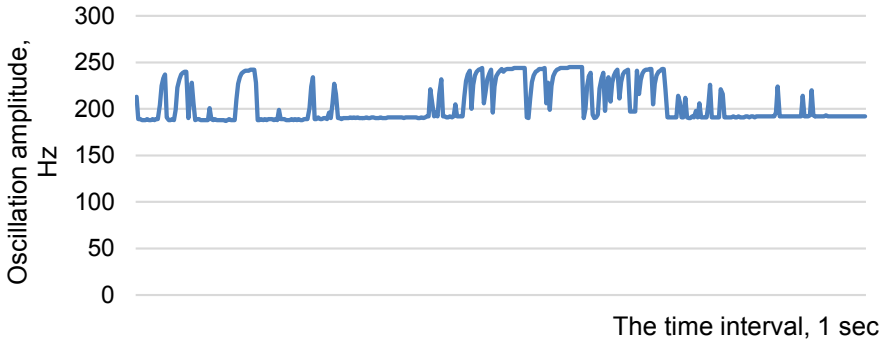

Figure 19. Study of resonance frequencies at speed of 40–60 km h^{-1}.

According to the results of the analysis of (Figs. 16–21), the oscillation frequencies to which the rubber cord coupling is exposed at different speeds from 20 to 120 km h^{-1} were determined and found:

- at a speed of 20–100 km h^{-1} resonance does not occur in the system;
- at speeds in the range of 110–120 km h^{-1} resonances occur periodically in the system and the frequency range in which the couplings operates is 53–57 Hz.

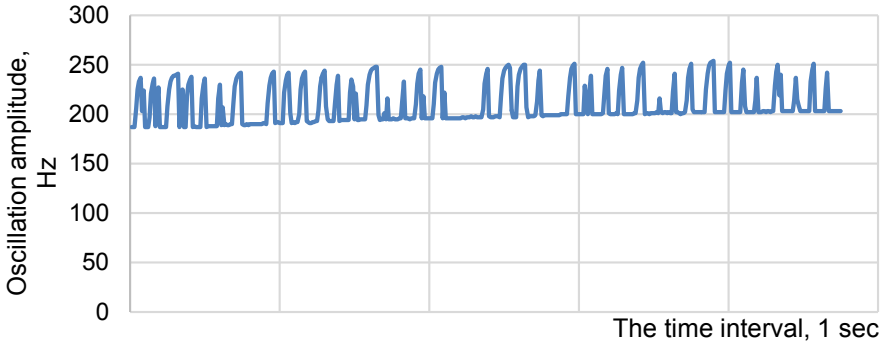

Figure 20. Study of resonance frequencies at speed of 80–100 km h^{-1}.

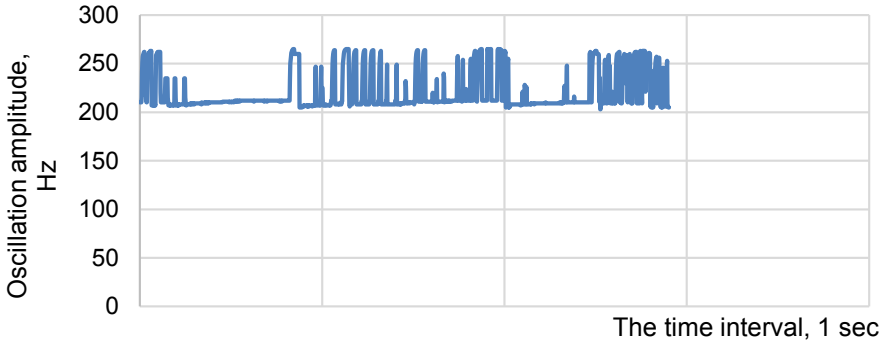

Figure 21. Study of resonance frequencies at speed of 110–120 km h^{-1}.

The critical resonance frequency of the oscillation determined by SolidWorks is 54.85 Hz along the X-axis. This means that the rubber cord coupling resonance may happenat the most dangerous resonant frequency.

RESULTS AND DISCUSSION

Metallographic analysis revealed a large number of non-metallic impurities in all samples. Decomposition of M24 bolts during service can often start from initial defects of metallurgical origin caused by non-metallic impurities. Which, with the increase in the life of the bolt (mileage), increase in number and size, which later cause fractures.

The implementation of the impact-vibration force monitoring device in service provided objective information on the impact loads perceived by the bolts for fastening the rubber cord coupling.

If, during technical maintenance, based on the data collected from the device, it is found that the level of permissible loads exceeds the critical level, then the M24 bolts of the rubber cord coupling must be replaced with new ones. Thus, it eliminates the need to perform unplanned repairs of the M24 bolts of the rubber cord coupling due to disintegration, which calls for large financial investments. In the future, the finished

product can be offered to European and other countries by installing the impact vibration device on railway rolling stock and metro cars or using it in other industries. In addition, this invention can be applied in mechanical engineering, aircraft construction, shipbuilding and other fields to control the technical condition of bolts and flexible coupling. Answer (4) having a certain set of shock-vibration load data in real time, it is possible to make adjustments to the repair system for servicing the rubber-cord coupling and its fastening bolts or other technical equipment, which is subject to shock-vibration loads. This means a change from a system of planned preventative repairs to repairs based on actual conditions.

According to the analysis of the stresses acting on the rubber cord coupling in different operating modes, calculated in the Solid Works program, it was found that at a speed above 110 km h^{-1} (1,673 rpm), the stress spreads throughout the cross section of the coupling.

As a result of the analysis of the first 40 frequencies, the critical frequencies and oscillation modes of the coupling shell were found. The calculated load of the coupling cover zones coincides with the damage zones of the coupling in service. Answer (4) knowing the most dangerous frequencies to which rubber-cord couplings can be exposed, it is proposed to use a shock-vibration device to collect data on the real frequencies to which the coupling (or other unit) is exposed under operating conditions. Answer (4) Knowing the most dangerous frequencies to which rubber-cord couplings can be exposed, it is proposed to use a shock-vibration device to collect data on the actual frequencies to which the coupling (or other unit) is exposed in operation.

To reduce the risk of damage to the coupling housing, it is necessary to prevent long-term operation of the coupling at the calculated critical frequencies – 54.87 Hz; 88.2 Hz; 88.36 Hz.

Answer (4). If values of resonant frequencies are coinciding with identified critical values, it is necessary to take measures to prevent the rubber-cord coupling from operating at dangerous frequencies or to accelerate their passage. This way it is possible significantly reduce the likelihood of rubber-cord couplings failure and the need for unscheduled repairs associated with replacing the coupling. All of the above measures lead to a cost reduction for the company.

Answer (4). Using the impact vibration device, it is possible constantly accumulate and analyse data on the impact force in order to reduce the number of unplanned repairs of railway rolling stock or other industries vehicles due to their damage, as well as to reduce the number of accidents or other incidents.

The results of the calculations in the SolidWorks program package confirmed that the most stressed area of the coupling is its wall 10–20 mm distance from the outer diameter of the mounting disc. This area is mainly loaded with loads from the shaft deviation and from the maximum moment at the beginning of the movement.

Usage of the impact monitoring device for bolted anchorages and rubber cord coupling and the methodology will give the following results. The costs for unplanned repairs will be eliminated, however the human factor still must be taken into account. The costs will be related only to the implementation of the impact vibration device. Data on unplanned repair costs and the impact monitoring device for bolted anchorages and rubber cord coupling implementation and operation are presented in (Table 6).

Answer (5) According to (Table 6) result data in the example of JSC ‘Pasažieru vilciens’, a company that operates electric trains, implementation of the device would be

done for all EMU trains, and the implementation costs would not exceed 15 thousand Euros, then the costs would be repaid within 2 years (the use of the device becomes profitable) due to the reduction in the number of unplanned repairs, and in the 3rd year, the company will have a profit of no less than 15 thousand. Euro (article Mihailovs et al., 2021).

Table 6. Comparison of costs for unplanned repairs and implementation of impact monitoring device

The name of the unplanned repair	One unplanned repair, EUR	Unplanned repairs during 10 years, EUR	Implementation of impact monitoring devices, EUR
Replacement of rubber-cord coupling bolts	429	103,895	15,000
Replacement of rubber cord coupling	575	58,842.28	

Answer (5) The impact vibration force monitoring device provided objective information on the impact loads perceived by the rubber cord coupling fastening bolts, and its serial introduction into operation makes possible monitoring of the rubber cord coupling and their fastening bolts technical condition and prevent unplanned repairs due to bolt damage.

CONCLUSIONS

Based on the experiments conducted, it was proved that the failures of the rubber cord coupling fastening bolts are related to the disintegration processes due to fatigue from the accumulation of defects in the microstructure as a result of exposure to impact loads, which is confirmed by metallographic analysis.

According to the results of the experiments, the critical value of the impact load was determined, and the load on the rubber-cord coupling fastening bolts exceeding several times the allowable values were found.

The implementation of the impact-vibration force monitoring device provided objective information on the impact loads perceived by the M24 bolts used for the rubber cord coupling fastening. Its serial introduction into operation makes possible to monitor the technical condition of rubber cord couplings fastening bolts.

If, during maintenance, the data collected from the device shows that the level of permissible loads exceeded the critical level, then the M24 bolts of the rubber cord coupling must be replaced by new ones. Thus, it eliminates the need to perform unplanned repairs of the rubber cord coupling due to M24 bolts disintegration, which requires large financial inputs.

When studying the influence of resonance frequencies, the stress zones of the rubber cord coupling were determined in the SolidWorks finite element modeling software, and it was found that the critical frequencies of resonance are influencing coupling oscillations in X; Y; and Z-axes directions, involving a certain amount of coupling mass. The most dangerous resonance frequency is along the X axis, when more than 57% of the coupling's own mass participates in the oscillations. At this frequency, the coupling areas are subject to deformation and coincide with damage areas found in operation.

As a result of the vibration level monitoring, using the impact vibration device, the oscillation frequencies to which the rubber cord coupling is exposed at different speeds from 10 to 120 km h^{-1} are determined. It was established that resonances in the system periodically occur at speeds in the range of 110–120 km h^{-1} and the frequency range in which the coupling operates is 53–57 Hz. The critical resonance frequency of the oscillation determined by SolidWorks is 54.85 Hz along the X-axis.

Appearance of critical resonant frequencies 88.25 Hz; 88.36Hz along the Y and Z axes by a shock vibration device not ascertained. In order to reduce the risk of coupling breakdown, it is necessary to limit the long-term operation of the coupling at a speed of more than 110 km h^{-1} (1,700 rpm) due to the effects of the action of the resonant frequency.

The developed and tested shock vibration device was tested on the rolling stock. Using this device, the data of shock vibration load levels in real operating conditions were obtained. The shock-vibration control device provided objective information about vibration and shock loads. By introducing the shock-vibration monitoring device into serial operation, it is possible to predict a significant reduction in the number of unplanned repairs of motor cars, as well as to reduce the costs of motor car downtime. In addition, this invention can be applied in mechanical engineering, aircraft construction, shipbuilding and other fields to monitor the technical condition of bolts.

ACKNOWLEDGEMENTS. This work has been supported by the European Social Fund within the Project No 8.2.2.0/20/I/008 'Strengthening of PhD students and academic personnel of Riga Technical University and BA School of Business and Finance in the strategic fields of specialization' of the Specific Objective 8.2.2 'To Strengthen Academic Staff of Higher Education Institutions in Strategic Specialization Areas' of the Operational Programme 'Growth and Employment'.

REFERENCES

Bhadeshia, H. & Honeycombe, R. 2017. *Steels Microstructure and Properties*, Fourth edition, 2017, Elsevier Science, 488 pp.

Birjukov, I., Beljajev, A. & Ribnikov, E. 1986. *Traction transmissions of electric rolling stock of railways.* M.: Transport, 256 pp. (in Russian).

Boguslavskij, B.L. 2016. *Metalhead's Handbook*. Volume 2. Edition 3, 2016.

Desai, A., Telukala, H., Jadhav, S. & Kurna, S. 2021. Strength Evaluation and Validation of Structural Joints. *SAE Technical Paper* 2021-26-0315. https://doi.org/10.4271/2021-26-0315

EN 10083-3:2007-01 Technical delivery conditions for alloy steels English version of p. 54.

Evdokimov, A.P. & Shikhnabieva, T.S. 2017. Stress–strain behavior and specific friction of toric rubber-cord casings of flexible couplings. *Journal of Machinery Manufacture and Reliability* **46**(2), 1 March 2017, 199–203.

Grigorenko, V., Orlov, M., Morozova, L. & Zuravljeva, P. 2014. Investigation of static destruction of bolts made of 30khgsa steel under operating conditions. *Aviation materials and technologies* **S4**, 125–135 doi: 10.18577/2071-9140-2014-0-s4-125-135 (in Russian).

Grigorenko, V., Morozova, L. & Vinogradov, S. 2018. Features of the destruction of fasteners made of structural steel. *Scientific and Technical Journal "Proceedings of VIAM"*, 66–74. doi: 10.18577/2307-6046-0-4-66-74 (in Russian).

ISO 898-1:2013 *Mechanical properties of fasteners made of carbon steel and alloy steel*. Part 1: Bolts, screws and studs with specified property classes, 27 pp.

Klimentyev, E.V., Zvonov A.O. & Glazkova E.U. 2015. Rubber-cord cushions application in modern engeineeging. *FSUE "RPE "Progress"* Omsk, 55–68. doi:10.1109/Dynamics.2014.7005706

Komorska, I. 2011. *Vibroacoustic Diagnostic Model of the Vehicle Drive System*. Institute for Sustainable Technologies & National Research Institute, 130 pp. ISBN-10: 837789016X, ISBN-13: 978-8377890165.

Korneeva, V.S., Romanyukb, D.A., Korneeva, S.A., Russkiha, G.S. & Vaskovaa, M.V. 2016. Finite element research of rubber-cord flat coupling. *Procedia Engineering* 1**52**, 321–326. doi: 10.1016/j.proeng.2016.07.710

Kuzu, C., Pelit, E. & Meral, İ. 2021. A new design of Rockwell-Brinell-Vickers hardness standard machine at UME. *Acta IMEKO* **9**(5), 230–234.

Leonardson, R. & MacGugan, D. 1994. Design and fabrication of a commercial triaxial accelerometer. *Sensors* (Peterborough, NH), **11**(8), 22–23.

Medvecka-Benova, S., Mikova, L. & Kassay, P. 2015. Material prope rties of rubber-cord flexible element of pneumatic flexible coupling metallurgical. *Metabk* **54**(1), 194–196.

Mihailovs, F., Eiduks, J. & Gorbačovs, D. 2021. Reducing the Number of Unscheduled Repairs of Traction Gear of EMU Trains by Introducing Modern Technical Solutions. No: *10th International Scientific Conference "Rural Development. Challenges for Sustainable Bioeconomy and Climate Change"*, Lietuva, Vytautas Magnus University Academy of Agriculture, pp. 1–6.

Müller, M. & Choteborský, R. 2016. Impact strength behaviour of structural adhesives, *Agronomy Research* **14**(S1), 1078–1087.

Müller, M. 2017. Mechanical properties of resin reinforced with glass beads. *Agronomy Research* **15**(S1), 1107–1118.

Myakishev, V., Bukhovtsev, I. & Sotsky, B. 2014. *Physics.* 10th grade, textbook. Moscow, Enlightenment, 417 pp. (in Russian).

Sapalov, E. & Panfjerova, O. 2016. Study of strength characteristics of high strength bolts of destructive and non-destructive methods, 6. https://3minut.ru/images/PDF/2016/25/issledovanie-prochnostnykh-kharakteristik.pdf.

Sheshenin, S.V., Gritchenko, M.E. & Chistyakov, P.V. 2021. Averging the viscoelastic properties of a rubber-cord ply in a plane stress state. *Mechanics of composite materials*. **57**(4), 673 – 688. https://doi.org/10.22364/mkm.57.4.05.

Sirokih, A., Simulation of friction joints on high-strength bolts by the finite element method. Ufa State Petroleum Technological University, Ufa (Oil and Gas Business, 2005).

Slejbo, Y.N. 2005. *General chemistry*, 2005. Moscow, Academia, 447 pp.

Stauffer, J.-M.2004. Market opportunities for advanced MEMS accelerometers and overview of actual capabilities vs. required specifications. In *Proceedings of the IEE Xplore: Position Location and Navigation Symposium*, Monterey, CA, USA, 26–29 April 2004, pp. 78–82.

Summary of non-scheduled repairs of electric trains JSC 'Pasažieru vilciens' (2015–2021) (template FT-20) (in Latvian).

Taylor, J., Mehmanparast, A., Kulka, R., Moore, P., Farrahi, G.H. & Xu, L. 2021. Compact crack arrest testing and analysis of EH47 shipbuilding steel. *Theoretical and Applied Fracture Mechanics* **114**, art. no. 103004. www.elsevier.com/locate/tafmec

Tribel'skii, I.A. & Zubarev, A.V. 2008. Stress-strain state and thermal state of rubber-cord casings of highly elastic couplings. *Russian Engineering Research* **28**, 1159–1164.

Vinogradov, B.V. 2016. Flexible couplings with rubber-cord shells in dual pinion mill drives.

Yingnan, D., Weibing, X., Yanjiang, C., Jin, W. & Weiming, Y. 2020. Experimental research on seismic performance of precast cogging high-strength bolt composite joint and influence of its arrangement location. *Engineering Structures* **225**, 111294. https://doi.org/10.1016/j.engstruct.2020.111294

Zadel, H., Kogen-Dalin, V., Krimov, V. 1985. *Electrical Engineering*. Moscow: Higher School, 480 pp.

Zhang, W., Sheng-Li, Lv, Wang, Ji-Pu, Gao, X. & Srivatsan, T.S. 2021. Conjoint influence of environment and load on fatigue life of a bolted aluminum alloy structure. *AIP Advances* **11**, 075210. https://doi.org/10.1063/5.0058946

Agronomy Research **22**(2), 815–831, 2024
https://doi.org/10.15159/AR.24.065

Psychosocial risks for health care workers in rehabilitation centre

H. Kalkis*, Z. Roja and V. Metuma

University of Latvia, Raina blv. 19, LV-1050 Riga, Latvia
*Correspondence: henrijs.kalkis@lu.lv

Received: January 26th, 2024; Accepted: April 28th, 2024; Published: July 11th, 2024

Abstract. Psychosocial risks at work have a strong impact on workers in every economic field, especially in health care. The aim of this study was to analyze psychosocial risk impact on workers in 3 areas of work, including doctors or functional specialists, nurses and support staff at work for healthcare employees in one of Rehabilitation centers in Latvia. The Copenhagen Psychosocial Questionnaire was used to assess psychosocial risks at work. Main results show that the high scores for work atmosphere and social support from colleagues reflect the favourable social environment in the context of employee relationships, but doctors and functional specialists face significant psychosocial risks characterized by high quantitative and emotional demands, compounded by job insecurity and inadequate managerial support. Nurses contend with high physical and emotional risks influenced by unpredictable work patterns, unclear roles, and insufficient social support, while support staff confront high workload, role conflicts, and pervasive job insecurity, minimal recognition and unsupportive workplace atmospheres. In general critical aspects include work-life balance, appreciation and self-rated health are at work. Continuation of the research will be related to investigating the psychosocial risks with cognitive tests for each research group.

Key words: healthcare, employees, rehabilitation, center, psychosocial risks.

INTRODUCTION

Globally, over the last few decades, there has been a significant shift in the nature of employment from manual labour to knowledge work and cognitive requirements of work is becoming more important topic (Kalakoski, 2019). When cognitive demands increase and are not balanced with employees' abilities, employees' health suffers (Karasek, 1979; Johnson & Hall, 1988; Bakker & Demerouti, 2007). Today, psychosocial risks (PSR) at work are an integral part of everyday life in various professions. Many scientists in recent years have focused on the study of this problem on the employed (Leka, et al., 2015; Bliese, et al., 2017; Di Tecco, 2023). According to Eurostat data, in 2020, 58.5% of those employed in the health and social care sector reported the impact of psychosocial risks on their mental health (Eurostat, 2021). Similar results were obtained in the Third European Enterprise Survey on new and emerging risks (ESENER, 2019), where it was found that the impact of psychosocial risks on health and social care workers is much more frequent than on those employed in other

sectors. In a study comparing sectors in relation to the impact of psychosocial risks on employees it was concluded that high demands and insufficient resources are the highest in the health and social care sector (De Hert, 2020). Some authors when describing psychosocial risk factors at work, associate them with job demands (tasks attributable to effort) and work resources to achieve a goal (Schaufeli et al., 2009). The work strain in various work environments in most cases are related to psychosocial risk factors rather than with physical risk factors (Roja et al., 2017). Health care workers are exposed to various PSR at work: overtime work, overload at work, time limitation, insufficient length of rest breaks, unbalanced work-home life, shift work, violence and harassment at work, etc. (Scozzafave et al., 2019; Ruotsalainen et al. 2020). If an individual is unable to adapt to psychosocial risks and their effects persist, he or she may experience cognitive and emotional impairments, which are closely linked to the individual's mental health. Exposure to psychosocial risks can adversely affect an individual's attention (orientation and concentration), memory and thinking (reflection, reasoning, language, etc.), decision-making, etc. Modern technologies and complex work tasks require high concentration abilities from employees, which are mainly related to decision-making in limited time and necessary procedures (De Jonge & Dormann, 2003). Health care workers are often exposed to worries about making the wrong decision regarding a patient's health, which can end up in court (Stehman et al., 2019).

There is a complex interplay between the effects of psychosocial risks, their mitigating or aggravating factors and the resulting consequences (Okuhara et al., 2021). Among the most important mental health disorders of the last decade is occupational burnout, a syndrome provoked by prolonged exposure to stressors that causes emotional disturbances and has a significant impact on individuals' work performance (De Hert, 2022). Occupational burnout is not only a problem for the employees themselves, but also causes serious problems in the quality of patient care, increased likelihood of medical errors at work, etc. (West et al., 2006; Shanafelt et al., 2010).

Research into the causes of psychosocial risks and their interactions with other workplace risks is important for promoting the health of healthcare workers. Research has shown that a bio-psychosocial approach, which includes an analysis of psychosocial and human factors risks, is essential to assess the causes of work related musculo-skeletal disorders (WRMSDs) (Deeney & O'Sullivan, 2009; Roja et al., 2013). Psychosocial factors can also be a contributing factor to workplace safety incidents and accidents. Adverse social conditions at work, e.g. ineffective management approach, conflicts, etc., can provoke dangerous behaviours that can lead to an accident at work (Hassanzadeh-Rangi, et al., 2014). The study on the impact of working time risks on accident incidence found a correlation between excessive working hours and overtime work with accident incidence (Dembe et al., 2005; Hsu et al., 2019).

Health care is one of the leading sectors of the national economy in Latvia, where employees according to the official statistics make up 6.7% of all employees in the country. In 2022, the Latvian health and social care sector employed 59.8 thousand people. Of these, 51.2 thousand or 85.6% were women (Central Statistical Bureau of Latvia, 2023). According to the study, employees working in healthcare in Latvia experienced the following psychosocial risks: workplace bullying 9.5%, physical violence 6.4% and sexual harassment 2.9%. These rates are higher than the national average for all sectors, at 5.3%, 3.0% and 1.4% respectively. (Research 'Work conditions and risks in Latvia 2019–2021', 2023).

The aim of this study was to analyze psychosocial risk impact on workers in 3 areas of work, including doctors or functional specialists, nurses and support staff at work for healthcare employees in one of Rehabilitation centers in Latvia. The study involved 39 respondents. The representatives of the following professions took part in the survey: doctors or functional specialists – 24; nurses – 9; support staff – 6.

METHODS

The Copenhagen Psychosocial Questionnaire (Kristensen et al., 2005) from the Danish National Research Centre for the Working Environment was used to assess psychosocial risks at work. COPSOQ is an instrument for research, for the assessment of psychosocial conditions and health promotion at workplaces. It was developed by a group of researchers lead by Tage S Kristensen and Vilhelm Borg at the Danish National Research Centre for the Working Environment (1995–2007). The COPSOQ III short version questionnaire allows the identification and assessment of major psychosocial risks and is suitable for organisations of all sectors and sizes. The results are comparable between organisations (benchmarking) and the repeated assessment of these risks allows the effectiveness of preventive measures to be evaluated. The survey is organised anonymously. The COPSOQ III methodological instructions also provide guidelines for formulating response options using Likert scale. The scale is scored from 0 to 100, with the total value calculated as the average of the answers provided by the selected respondents (Llorens et al., 2019). Each question presents five potential responses. These responses are assigned to weights of 0, 25, 50, 75, and 100 respectively. The value of the scale is determined calculating average, resulting in a scale range from 0 to 100. If a respondent provides answers to less than half of the questions on the scale, their response is deemed missing. However, if answers are provided at least half of the questions, the scale value is computed as the average of their responses.

The short version of the COPSOQ III includes the following aspects of the psychosocial environment and risk groups: quantitative load, work pace, emotional load, impact on work process, job predictability, job perspective, job importance, appreciation, role clarity, role conflict, effectiveness of management approach, social support from supervisor, social support from colleagues, work atmosphere, job insecurity, insecurity about job conditions, job satisfaction, work-life balance, trust in management, and fairness. In addition to the questions in the short version of the COPSOQ III, the questionnaire includes contextual and selection criteria questions. The contextual questions were sex of the employee, age of the employee, occupational group of the employee, length of service.

The respondents were doctors and functional specialists, nurses (general nursing), medical support staff. Participants were informed about the confidentiality of the survey results, the processing of the data and that the data will only be used in aggregate form. The survey took place from 5 February to 15 November 2023, after pandemic COVID 19. Selection criteria were as follows: full consent to participate, full-time or part-time work, no mental health problems detected in the mandatory health check-up, recognition of psychosocial risks at work and ability to assess their impact.

Permission for the research was received from the Ethics committee of the University of Latvia on February 23, 2023, protocol No. 4.

The research study utilized Microsoft Excel 365 and SPSS 20 for data analysis. Data was collected and organized the with softwares and after also used for descriptive statistical processing. The combination of Excel for data collection and processing, and SPSS for data analysis, ensured the reliability and validity of the research findings.

RESULTS AND DISCUSSION

Questionnaire Results

The questionnaire was sent to 52 respondents. The study analysed 39 questionnaires or 75.0% of respondents (recognized as valid for the research), 13 questionnaires or 25.0% of respondents did not meet one or more of the defined selection criteria for study participants, the most frequent of which was that the employee did not recognise a deterioration in health related to psychosocial risk factors (8 cases). Table 1 summarises the profile data of the study participants.

Table 1. Profile of study participants

Variable	Features	People	Proportion, %
Gender of employee	Female	33	84.6
	Male	6	15.4
	TOTAL	39	100.0
Age group	Up to 24 years	1	2.6
	25 to 34 years	15	38.5
	35 to 44 years	6	15.4
	45 to 54 years	8	20.5
	55 to 64 years	8	20.5
	65 and over	1	2.6
	TOTAL	39	100.0
Occupational group	Doctors and functional specialists	24	61.5
	Nurse	9	23.1
	Support staff	6	15.4
	TOTAL	39	100.0
Length of service in the profession	Up to 2 years	2	5.1
	3 to 10 years	22	56.4
	11 to 20 years	10	25.6
	21 and over	5	12.8
	TOTAL	39	100.0

The study was carried out among 33 women, of whom 36.4% were aged 25–34, 12.1% were aged 35–44, 24.2% were aged 45–54 and 55–64, and on 3.0% was aged 65+. The average age of the female participants is 43.3 years. Eighteen (54.5%) of the participants are employed as doctors or functional specialists, 9 (27.3%) are nurses and 6 (18.2%) are in the support staff occupational group. 6.1% have been in the profession for 2 years, 54.5% for 3 to 10 years, 24.2% for 11 to 20 years and 15.2% for more than 21 years. Of the 6 men in the study, 16.7% was aged 24 years or younger, 50.0% were aged 25–34 years and 33.3% were aged 35–44 years. The average age of the male participants is 30.8 years. All men are employed as a doctor or functional specialist. 66.7% have been working in the profession for 3 to 10 years and 33.3% for 11 to 20 years. The average age of the participants (women and men) is 41.4 years. To summarise, the

average participant in the study is a woman aged between 25 and 34 years, who has been working in a doctor or functional specialist profession for between 3 and 10 years. According to the participant selection criteria, she is working full-time, has experienced a deterioration in health related to psychosocial risk factors and has not been diagnosed with a mental health-related illness.

According to Central Statistical Bureau (CSB) data, in 2022, 85.6% of employees in the health and social care sector in Latvia were women, which is in line with the data obtained in the study when comparing employees by gender. Similar results have been obtained in other countries, e.g. a study on professional burnout of doctors and its causes in Lithuania indicated that the population consisted of 65.7% women (Žutautienė et al., 2020), and in a study on psychosocial work environment factors in healthcare workers in Switzerland, 81% of 12754 respondents were women (Peter et al., 2022).

The majority of participants in the study are in the 25–34 age group (38.5%) and the 45–64 age group (41%), which is partly in line with the results of other studies around the world (Majority of health jobs, 2021).

Overall, authors conclude that the study predominantly involved female health care workers, reflecting main sector's gender distribution. All participants, primarily doctors and functional specialists, reported health deterioration due to psychosocial risk factors, despite no prior mental health-related diagnoses. It should be noted that the age distribution of employees is often influenced by the specific nature and scope of the organisation. The same could be said of the distribution of employees by occupational group, which depends very much on the specifics of the chosen organisation and/or the objectives of the study.

Results of the Copenhagen Psychosocial Survey

Transforming the respondents' answers according to the COPSOQ III survey methodology, the mean scores of the psychosocial environment aspects and assessment of risk groups included in the short version of the survey were calculated on a Likert scale, indicating the frequency of each aspect or the degree of agreement with the statement.

Aspects of the psychosocial environment and risk groups in each of the occupational groups represented by the respondents are shown in Tables 2 to Table 5.

To quantify workload, respondents had to answer the following questions: 'how often do you run out of time to complete all your work tasks?' and 'do you delay completing work tasks?' Table 2 shows that the responses have a relatively high standard deviation across all occupational groups, with a mean of 50 or more. Doctors and functional specialists are more likely to report a lack of time and/or delays in completing work tasks, and those in support professions are also close to this rating (56.77 ± 27.16 and 56.25 ± 37.12). The mean value of the quantitative workload assessment for nurses is slightly lower than for both of these occupational groups and is in line with the 'sometimes' in numerical value. This suggests that the workload for functional specialists/doctors and nurses is evenly distributed, and it should not affect the quality of patient care. Studies on psychosocial risks in healthcare showed a similar trend, with doctors (71.9 ± 13.9) scoring higher than nurses (66.5 ± 13.5) on quantitative workload (Kersten et al., 2014; Wagner et al., 2019). But our research results are not in line with studies by other authors, e.g. for nurses, a study on the relationship between quantitative workload (as understood by the COPSOQ III) and professional burnout found a

correlation between the two, i.e. an increase in quantitative workload leads to an increase in the incidence of professional burnout (Diehl et al., 2021). Despite the high quantitative workload scores of the employees in our study, this is not critical, but it is noteworthy. Often it can cause not only burnout at work, but also an imbalance between work and private life (Fuß et al., 2008).

To assess the pace of work, respondents answered the following questions: 'do you need to work very quickly?' and 'do you need to work at a high pace throughout the day?' Table 2 shows that for all occupational groups, the mean values exceed the quantitative workload estimates. The need to work quickly and/or at a high pace throughout the day is more common in support staff (77.08 ± 32.78) than in the other occupational groups, with lower scores for doctors and functional specialists (65.63 ± 17.58) and even lower scores for nurses (55.56 ± 16.17). This could be explained by the fact that there is a shortage of support staff in healthcare and often one person must do the work of 2–3 staff members. Investigation characterized by Royal College of Physicians (2015) has found similar results where investigation shows that staff are often exposed to fast-paced work that have a negative impact on work duties.

Table 2. Aspects of the psychosocial environment and risk groups: quantitative load, work pace, emotional load

Aspects of the psychosocial environment	Profession group	Min	Max	Mean	SD
Quantitative load	Doctor or functional specialist	0	100	56.77	27.16
	Nurse	0	100	50.00	32.08
	Support staff	0	100	56.25	37.12
Work pace	Doctor or functional specialist	25	100	65.63	17.58
	Nurse	25	75	55.56	16.17
	Support staff	25	100	77.08	32.78
Emotional load	Doctor or functional specialist	0	100	68.23	24.59
	Nurse	25	100	63.89	21.39
	Support staff	0	100	64.58	31.00

Min – minimal value; Max – maximal value; Mean – mean value; SD – standard deviation.

To assess emotional strain, respondents answered the following questions: 'do you have to deal with other people's personal problems at work?' and 'is your work emotionally demanding?' Table 2 shows that doctors, functional specialists and nurses are more likely to have aspects of the psychosocial environment related to emotional strain (68.23 ± 24.59 and 63.89 ± 21.39, respectively). In the support staff group, however, emotional strain scores are lower than work pace scores. The results are in line with the findings of other authors. For nurses and doctors, for example, in Germany, a similar tendency is observed for high emotional strain scores with scores of 64.4 ± 18.3 and 64.6 ± 16.5, respectively (Wagner et al., 2019). This proves that doctors or functional specialists and nurses often have to deal with personal problems of patients or patients' relatives, thus putting themselves under greater emotional strain. This is supported by other studies that those in charge who are in direct contact with people and who have a high level of responsibility for the work are also exposed to psychoemotional overload at the work (Pastare et al., 2020).

The analysis of the impact on work processes shows that doctors and functional specialists have the highest impact on work processes (63.54 ± 19.48); support staff have a slightly lower impact on decisions affecting work tasks; and nurses have the lowest impact (41.67 ± 12.50) on work processes among the occupational groups considered. This leads to the conclusion that there is a lack of attention to organisational culture, which in the long term can lead not only to stress-related health problems for support staff and nurses, but also to work ethics. This is in line with the literature that people who work in a friendly and team-focused environment feel less stressed. Workers in a creative and forward-thinking setting also experience lower stress levels. On the other hand, people in a strict and structured workplace tend to have higher stress. Employees from companies with a competitive, rational and logical approach also report higher stress levels (Marchand, 2013; Olynick & Li, 2020).

To assess the predictability of work, respondents were asked the following questions: 'at work, are you informed in good time about important decisions, changes, or future plans?' and 'do you receive all the information you need to do your job well?' The results show a relatively high level of job anticipation across all occupational groups studied. This indicates that there is a good flow of information in the organisation which also indicates a high working culture in the organisation. Nurses have particularly high job predictability, with a relatively low standard deviation of responses (70.83 ± 12.86). The lowest job predictability scores are for doctors and functional specialists (63.94 ± 17.03). The results are consistent with research on organisational change in hospitals (Ellis et al., 2023), which has shown that positive organisational culture and communication are essential for staff to be ready for change, increasing opportunities for organisational change and reducing staff burnout and disruption to patient care.

Comparing our results with studies on the impact of doctors and nurses on the work process (38.8 ± 20.8 and 36.3 ± 17.3, respectively) and on job predictability (52.5 ± 19.3 and 53.3 ± 16.4, respectively), it can be concluded that these criteria were more critically evaluated (Wagner et al., 2019). It should certainly be borne in mind here that the nature of the respondents' work plays an important role in the context of a number of factors. For example, whether the nurse works in a primary health care establishment or in a rehabilitation establishment, between which there are differences both in the patient profile and in the predominant tasks to be carried out.

To assess their job prospects, respondents were asked the following questions: 'do you have the opportunity to learn new skills at work?' and 'do you have the opportunity to use your skills or knowledge at work?' Table 3 shows that the highest scores for job prospects, i.e. the most opportunities to learn new skills and use their skills at work, with a relatively low standard deviation of responses, are found among doctors and functional specialists (80.21 ± 17.83), which is consistent with studies by other authors (Hillen et al., 2015). In our study the job prospects score is lower for support staff and even lower, with a relatively low standard deviation, for nurses (66.67 ± 34.27 and 59.79 ± 15.19, respectively). There is a significant difference between the job prospects of doctors and functional specialists and those of other occupational groups. It suggests that there are limited opportunities among mid- and lower-level medical staff to learn new and/or make full use of existing knowledge and skills at work, possibly due to a relatively higher level of routine in the job content, which is most likely determined by the specificities of the chosen organisation, which contradicts other authors' studies that, in the context of continuing education, it is very important for nurses, for example,

to be educated about the complexity of existing diseases and their specific features, and about the economic and psychosocial consequences of diseases in later life (Robertson et al., 1999). Many studies have shown that educating employees in the workplace improves mental health, sense of belonging, organisation and reduces psychological distress (Katona, 2022).

Table 3. Aspects of the psychosocial environment and risk groups: impact on the work process, work predictability, job prospects, importance of work, appreciation

Aspects of the psychosocial environment	Profession group	Min	Max	Mean	SD
Impact on the work process	Doctor or functional specialist	25	100	63.54	19.48
	Nurse	25	50	41.67	12.50
	Support staff	25	100	62.50	26.22
Work predictability	Doctor or functional specialist	25	100	60.94	17.03
	Nurse	50	100	70.83	12.86
	Support staff	25	100	64.58	27.09
Job prospects	Doctor or functional specialist	25	100	80.21	17.83
	Nurse	25	75	59.72	15.19
	Support staff	0	100	66.67	34.27
Importance of work	Doctor or functional specialist	50	100	85.42	14.59
	Nurse	50	100	88.89	18.16
	Support staff	75	100	87.50	13.69
Appreciation	Doctor or functional specialist	0	100	44.79	27.56
	Nurse	0	75	58.33	25.00
	Support staff	0	75	41.67	34.16

Min – minimal value; Max – maximal value; Mean – mean value; SD – standard deviation.

To assess the importance of the work, respondents had to answer the following question: 'is your work important?' Table 3 shows particularly high scores for job importance in all occupational groups, and in all cases with a relatively low standard deviation of responses. Nurses gave the highest job importance ratings (88.89 ± 18.16), while support staff gave slightly lower ratings (87.50 ± 13.69). The lowest job importance scores were found among doctors and functional specialists (85.42 ± 14.59). All the professions studied, despite being exposed to various psychosocial risks at work, high levels of responsibility at work, value work as very important. Both the chosen profession and a positive working environment could play an important role here, as evidenced by the respondents' answers. Some studies have also shown that healthcare workers such as nurses positively associate work environment with work importance (Al-Hamdan, 2017).

To measure appreciation, respondents were asked the following question: 'does management appreciate your work and give you recognition?' Table 3 shows that the highest appreciation scores are among nurses (58.33 ± 25.00), which is the only case among the occupational groups where the mean value exceeds 50 points. This suggests that the organisation needs to improve its approach to feedback and performance appraisal. Lower scores are observed among doctors and functional specialists (44.79 ± 27.56), and even lower among support staff (41.67 ± 34.16). It is proved that if workers tend to work closely with managers then they receive higher support and appraisal that can influence job outcomes and results (Göras et al., 2017).

To assess role clarity, respondents were asked the question: 'do you have clear objectives for your work?' Table 4 shows relatively high role clarity scores for all occupational groups surveyed, which is also likely to be related to the specialisation of the healthcare workforce. Nurses have a particularly high role clarity score (80.56 ± 27.32). The scores of doctors, functional specialists, and support staff are slightly lower, with identical mean values. This leads to the conclusion that there is a lack of clarity among employees about the purpose of the work and that the company's management does not pay enough attention to this issue. This is in line with the research of several authors who believe that if employees have clear goals, they know why and how to work and achieve them (Becker & Klimoski, 1989). Role clarity is an important driver of employee performance and has a positive impact on employee satisfaction (Whitaker et al., 2007). In a study on the role significance in small companies, the authors propose to clearly define employee roles, provide periodic objective feedback on performance, and reduce role conflict by setting clear goals for each role. (Thangavelu & Sudhahar, 2017).

Table 4. Aspects of the psychosocial environment and risk groups: role clarity, role conflict, effectiveness of management approach, social support from the manager, social support from colleagues, atmosphere at work

Aspects of the psychosocial environment	Profession group	Min	Max	Mean	SD
Role clarity	Doctor or functional specialist-	50	100	70.83	14.12
	Nurse	25	100	80.56	27.32
	Support staff	50	100	70.83	18.82
Role conflict	Doctor or functional specialist	0	100	45.31	25.61
	Nurse	0	50	15.28	15.19
	Support staff	0	100	45.83	42.42
Effectiveness of management approach	Doctor or functional specialist	0	75	55.21	27.75
	Nurse	25	100	62.50	17.68
	Support staff	25	100	58.33	24.62
Social support from the manager	Doctor or functional specialist	0	100	68.75	29.72
	Nurse	50	75	63.89	13.18
	Support staff	25	100	54.17	36.80
Social support from colleagues	Doctor or functional specialist	50	100	78.13	15.31
	Nurse	75	100	86.11	13.18
	Support staff	50	100	83.33	20.41
Atmosphere at work	Doctor or functional specialist	50	100	81.25	13.29
	Nurse	75	100	88.89	13.18
	Support staff	50	100	79.17	18.82

Min – minimal value; Max – maximal value; Mean – mean value;, SD – standard deviation.

To assess role conflict, respondents were asked the following questions: 'are there conflicting demands on you at work?' and 'do you tend to have work tasks that need to be done differently than usual?' Table 4 shows that the average value of the responses for all occupational groups involved in the study does not exceed 50 points, i.e. the incidence of role conflict is relatively low. The highest scores are for support staff (45.83 ± 42.42), with slightly lower scores for doctors and functional specialists (45.31 ± 25.61). Nurses score particularly low, with a relatively low standard deviation

(15.28 ± 15.19). In this case (conflicting demands), this reduces the causes of stress at work, but it also shows a certain monotony at work (tasks that must be done differently from usual). These results are in accordance with other findings that state that work-related psychosocial risk factors including quantitative demands workload, emotional demands, work pace and role conflicts have impact on stress levels and burnout syndrome (Freimann & Merisalu, 2015). The low scores for role conflict in our study might reduce the causes of stress at work but suggest a higher level of routine in the tasks of professionals such as nurses.

To assess the effectiveness of the management approach, respondents were asked the following questions: 'to what extent would you say that your line manager plans well?' and 'to what extent would you say that your line manager is able to deal with conflict situations?' The scores for the effectiveness of the management approach for the occupational groups in the study are above 50, indicating satisfactory management skills of line managers in the organisation. Nurses have the highest scores (62.50 ± 17.68), while support staff have slightly lower scores (58.33 ± 24.62). The lowest scores for management approach are for doctors and functional specialists (55.21 ± 27.75). It should be noted that feedback and collaboration with management very essential factors and it aligns with other findings that the management link with employees is the strongest if the employees are motivated for work, receive support from the management, participate in decision making, and if they are involved in the development and implementation of changes (Kalkis & Roja, 2016).

To assess the social support of managers, respondents had to answer the question: 'how often do you get help and support from your line manager when you need it?' The occupational groups involved in our study indicating that managers generally provide social support to employees on a regular basis. Several studies have also concluded that lack of management support is a factor that could lead to post-traumatic stress disorder, depression and anxiety in healthcare workers (Feingold et al., 2021). Another study shows that the risk of anxiety, depression, burnout is halved for healthcare workers if they are supported by management (Smallwood et al., 2021). The results of our study add to this evidence. Similar results were obtained also in a study of the mental health burden during the Covid 19 pandemic, where the authors concluded that if healthcare managers and organisations had provided adequate information, communication and support, the mental health burden could have been reduced early in the pandemic (Ralph, 2022).

To assess the social support of colleagues, respondents had to answer the following question: 'how often do you get help and support from your colleagues when you need it?' According to the survey results, the score for social support of colleagues is particularly high, above 75 (often), and no respondent scored below 50 *(sometimes*). This indicates a strong collegial relationship between the employees of the selected organisation. The average value is highest among nurses (86.11 ± 13.18) and slightly lower among support staff (83.33 ± 20.41). Several studies have indicated that working conditions (i.e. management and colleague support, workload) can influence the incidence of adverse events, as well as contribute to health problems caused by psychosocial risks, such as burnout syndrome, etc. (Jarrar, 2023).

To assess the atmosphere at work, respondents were asked the question: 'do you have a good relationship with your colleagues?' All occupational groups surveyed score particularly highly, with a relatively low standard deviation of over 75 points in all cases, and no respondent scoring below 50 points (sometimes). This reflects a favourable social environment in the organisation. The highest mean (almost 90 points) is observed for nurses (88.89 ± 13.18), slightly lower for doctors and functional specialists (81.25 ± 13.29). The lowest work atmosphere score, however, is above 75 for support staff (79.17 ± 18.82).

Table 5. Aspects of the psychosocial environment and risk groups: job insecurity, insecurity about working conditions, satisfaction with work, work-life balance, trust in management, fairness, self-assessment of health

Aspects of the psychosocial environment	Profession group	Min	Max	Mean	SD
Job insecurity	Doctor or functional specialist	0	100	42.19	33.08
	Nurse	0	75	38.89	28.73
	Support staff	0	100	70.83	33.43
Insecurity about working conditions	Doctor or functional specialist	0	100	32.29	31.69
	Nurse	0	75	41.67	27.95
	Support staff	0	100	50.00	41.83
Satisfaction with work	Doctor or functional specialist	50	100	68.75	16.89
	Nurse	75	75	75.00	0.00
	Support staff	50	100	62.50	20.92
Work-life balance	Doctor or functional specialist	0	100	52.08	28.17
	Nurse	25	100	54.17	17.68
	Support staff	0	100	62.50	37.69
Trust in management	Doctor or functional specialist	25	100	69.79	15.44
	Nurse	50	100	84.72	17.45
	Support staff	25	100	79.17	25.75
Fairness	Doctor or functional specialist	0	100	55.21	20.60
	Nurse	25	100	66.67	21.00
	Support staff	25	100	72.92	22.51
Self-assessment of health	Doctor or functional specialist	0	75	41.67	19.03
	Nurse	25	50	36.11	13.18
	Support staff	0	75	29.17	24.58

Min – minimal value; Max – maximal value; Mean – mean value; SD – standard deviation.

To assess job insecurity, respondents were asked the following questions: 'are you worried about being out of a job?' and 'if you are unemployed, are you worried about the difficulties you might have in finding another job?' Table 5 shows a relatively high standard deviation of responses across all occupational groups, most likely due to differences in individuals' self-assessment of their competitiveness in the labour market, but the average score for job insecurity among nurses (41.67 ± 27.95), doctors and functional specialists (32.29 ± 31.69) does not exceed 50 points. This is most likely due to the inherent labour shortage in the healthcare sector in Latvia, where skilled workers have less difficulty finding other jobs. In contrast, in the support staff group, where employees generally do not need special qualifications, which makes them less competitive on the labour market, the job insecurity score is critical, i.e. there is concern about potential job loss and/or difficulty in finding a new job.

To assess insecurity about working conditions, respondents had to answer the question: ‘are you worried about being transferred to another job against your will?’ Table 5 shows a relatively high standard deviation of responses across all occupational groups, which is most likely due to differences in individuals' perceptions of working conditions. Among doctors, functional specialists and nurses, the average score for job insecurity is below 50, which is most likely due to the specialisation of healthcare workers, which narrows the scope for job transfers. Support staff have a higher job insecurity score (50.00 ± 41.83), i.e. they are more worried about potential changes in their working conditions.

To measure job satisfaction, respondents had to answer the question: ‘how satisfied are you with your job overall?’ Nurses have the highest job satisfaction (75.00 ± 0.00) with a mean of 75 points, which corresponds to the numerical value of satisfied, and there is consistency between the answers, with no standard deviation. Doctors and functional specialists scored slightly lower (68.75 ± 16.89), while the lowest level of satisfaction was observed among support staff (62.50 ± 20.92), with a mean value above 50 (moderately satisfied).

To assess work-life balance, respondents were asked the following questions: ‘do you feel that your work consumes too much energy and that this has a negative impact on your private life?’ and ‘do you feel that your work takes up too much of your time and that it has a negative impact on your private life?’ Table 5 shows that all occupational groups have a mean value above 50 (rather), which indicates a moderate work-life imbalance among employees in the selected organisation. The highest mean value is observed among support staff 62.50 ± 37.69), slightly lower among nurses (54.17 ± 17.68), and lowest among doctors and functional specialists (52.08 ± 28.17). Other studies analysing the impact of the type of employment (full-time or part-time) of doctors on work-life balance have found that the differences in scores are not significant. This suggests that it is not only the factor of working time or time spent physically at work that has a negative impact on private life (Bodendieck et al., 2022), but also factors related to the content of the work (Fuß et al., 2008).

To assess trust in management, respondents had to answer the following questions: ‘does management trust employees to do their job well?’ and ‘can employees trust the information they receive from management?’ Relatively high scores on trust in management are found in all occupational groups, similar to or higher than the scores on the effectiveness of the management approach. Nurses have the highest scores (84.72 ± 17.45), but with a relatively low standard deviation of responses. Support staff have slightly lower scores (79.17 ± 25.75), and doctors and functional specialists have even lower scores (69.79 ± 15.44). Nevertheless, in all cases the score is above 50 (somewhat) and in two out of three cases it is above 75 (to a large extent), which indicates a favourable social environment in the organisation, also in the context of subordination.

To assess fairness in the organisation, respondents answered the following questions: ‘are conflicts handled fairly?’ and ‘are workloads distributed fairly?’ In all occupational groups, the average score is above 50 (more likely), indicating a favourable social environment in the organisation and a low risk of discrimination. The highest fairness scores are for support staff (72.92 ± 22.51) and lower for nurses (66.67 ± 21,00). The lowest fairness scores are among doctors and functional specialists (55.21 ± 20.60).

To self-assess their health status, respondents answered the question: ‘overall, how would you say your health status is?’ In all occupational groups, the average score is below 50, which corresponds to the numerical value of a ‘good’ answer. No respondent answered ‘excellent’. In general, respondents' self-assessment of their health is self-critical. The highest scores are for doctors and functional specialists (41.67 ± 19.03), the lowest for nurses (36.11 ± 13.18). Particularly low scores are seen among support staff (29.11 ± 24.58). Studies by other authors show similar results, i.e., the overall perception of quality of life for healthcare workers is moderate, overall stress levels are moderately elevated and most had average resources to cope with their duties (Kumar et al., 2018).

The aspects with a mean value of more than 75 points include job importance (86.54 ± 14.81), work atmosphere (82.69 ± 14.04), and social support from colleagues (80.77 ± 15.46). Critical aspects with a mean score just above or below 50 include work-life balance (54.17 ± 27.57), appreciation (47.44 ± 27.62), and self-rated health (38.46 ± 18.64). The moderate work-life imbalance found in the selected organisation is a psychosocial risk with a potentially high impact on employees' health. The relatively low appreciation score indicates a management approach that needs improvement in the context of performance appraisal and feedback. The relatively low self-assessment of health status identifies the importance of implementing health promotion activities in an organisation with a high potential for benefits for both employees and the organisation.

Overall, the research provides the importance of addressing psychosocial risks for healthcare employees in a chosen Rehabilitation Centre. Analysing the COPSOQ III survey highlights both organizational strengths and critical aspects within the work environment. While aspects such as job importance, work atmosphere, and social support from colleagues had high scores, significant psychosocial risks were identified for different occupational groups. These risks include high quantitative and emotional loads for doctors, work predictability issues for nurses, and role conflicts for support staff. The moderate work-life imbalance found in the selected organisation is a psychosocial risk with a potentially high impact on employees' health. The relatively low appreciation score indicates a management approach that needs improvement in the context of performance appraisal and feedback. The relatively low self-assessment of health status identifies the importance of implementing health promotion activities in an organisation with a high potential for benefits for both employees and the organisation. Authors of the study suggests that the Copenhagen Psychosocial Questionnaire short version is an effective tool for investigating these risks and highlights the need for future research focusing on cognitive tests to further understand and address these challenges.

CONCLUSIONS

Psychosocial risks are the most essential ones for healthcare employees in Rehabilitation Centre. Regardless of the occupational groups represented, looking at the COPSOQ III (short version) survey as a whole it is possible to distinguish between the strengths of the organisation and the critical aspects for those working in the organisation. The most important psychosocial risks of the work environment for doctors or functional specialists are high quantitative and emotional load that has been influenced by high impact on a work process, job prospects, importance of the work duties, lower social support from the managers, low self-assessment of health. But for nurses the main psychosocial risks relate to high physical and emotional load influenced

by work predictability factors, high importance of work, unclear roles, low social support form managers and colleagues, high job insecurity, low work-life balance, self-assessment and fairness factors. And for support staff main risks are concerned with high quantitative load and work pace, importance of work, lack of appreciation, role conflicts, low social support form managers and atmosphere at work, as well as high job insecurity and low satisfaction with work, weak self-assessment of health. Overall health assessment shows that the highest scores are among doctors and functional specialists, the lowest among nurses. Particularly low scores are found among support staff. The relatively high job importance probably reflects a high level of responsibility towards the job and confirms the assumption of a sense of mission inherent in healthcare workers. The high scores for work atmosphere and social support from colleagues reflect the favourable social environment in the context of employee relationships.

Limitations of the research included the relatively small sample size from one Rehabilitation Centre, which may limit the generalizability of the findings to other healthcare settings, but at the same time discussion of the research results provided valuable insights into the topic. Differences in organizational culture, management practices, and patient populations could influence the prevalence and impact of psychosocial risks.

The study suggests the need for further research using cognitive tests to better understand psychosocial risks for health care workers. Future studies should address these limitations to provide a more comprehensive understanding of the topic. Future research with larger, more diverse sample size and objective measures of data will help to further address findings and supplementing it with qualitative methods could provide a more comprehensive understanding. Authors will conduct longitudinal study to track the long-term effects of psychosocial risks on the health and well-being of healthcare workers in rehabilitation centres as well as compare psychosocial risks and their impact on healthcare workers across different types of healthcare settings, including hospitals.

REFERENCES

Bakker, A.B. & Demerouti, E. 2007. The Job Demands-Resources model: State of the art. *Journal of Managerial Psychology* **22**(3), 309–328.

Becker, T.E. & Klimoski, R.J. 1989. A field study of the relationship between the organisational feedback environment and performance at sport. *Personnel Psychology* **42**(**2**), 343–58.

Bliese, P.D., Edwards, J.R. & Sonnentag, S. 2017. Stress and well-being at work: a century of empirical trends reflecting theoretical and societal influences. *J. Appl. Psychol.* **102**, 389–402.

Central Statistical Bureau of Latvia. 2023. Statistical database Available at https://data.stat.gov.lv/pxweb/lv/OSP_PUB/START__EMP__NB__NBLA/?tablelist=true

De Hert, S. 2022. Burnout in Healthcare Workers: Prevalence, Impact and Preventative Strategies. Local and Regional Anesthesia, [online], Vol. **13**, pp. 171–183. Available at doi: 10.2147/LRA.S240564

De Hert, S. 2020. Burnout in healthcare workers: Prevalence, impact and preventative strategies. *Local and Regional Anesthesia* **13**, 171–183.

Deeney, C. & O'Sullivan, L. 2009. Work related psychosocial risks and musculoskeletal disorders: Potential risk factors, causation and evaluation methods Work **34**(2), 239–48

De Jonge, J. & Dormann, C. 2003. The DISC model: Demand-induced strain compensation mechanisms in job stress. In M.F. Dollard, A.H. Winefield, & H.R. Winefield (Eds.), Occupational stress in the service professions, CRC Press, pp. 43–74.

Dembe, A., Erickson, J., Delbos, R.G. & Banks, S. 2005. The Impact of Overtime and Long Work Hours on Occupational Injuries and Illnesses: New Evidence from the United States. *Occupational and environmental medicine* **62**. 588–97.

Di Tecco, C., Persechino, B. & Iavicoli, S. 2023. Psychosocial Risks in the Changing World of Work: Moving from the Risk Assessment Culture to the Management of Opportunities. *Med Lav.* **114**(2), e2023013. doi: 10.23749/mdl.v114i2.14362

Diehl, E., Rieger, S., Letzel, S., Schablon, A., Nienhaus, A., Escobar Pinzon, L.C. & Dietz, P. 2021. The relationship between workload and burnout among nurses: The buffering role of personal, social and organizational resources. *PLoS One* **16**(1). doi: 10.1371/journal.pone.0245798

Ellis, L.A., Tran, Y., Pomare, C., Long, J.C., Churruca, K., Saba, M. & Braithwaite, J. 2023. Hospital organizational change: The importance of teamwork culture, communication, and change readiness. *PubMed* **11**, 1089252, Feb 9. doi: 10.3389/fpubh.2023.1089252

Eurostat. 2021. Self-reported work-related health problems and risk factors - Key statistics. Available at: https://ec.europa.eu/eurostat/statistics-explained/index.php?title=Self-reported_workrelated_health_problems_and_risk_factors_-_key_statistics

ESENER. 2019. Third European Survey of Enterprises on New and Emerging Risks: Overview Report How European workplaces manage safety and health. Available at: https://osha.europa.eu/sites/default/files/esener-2019-overview-report.pdf

Feingold, J.H., Peccoralo, L., Chan, C.C., Kaplan, C.A, Kaye-Kauderer, H., Charney, D., Verity, J., Hurtado, A., Burka, L., Syed, S.A, Murrough, J.W., Feder, A., Pietrzak, R.H. & Ripp, J. 2021. Psychological Impact of the COVID-19 Pandemic on Frontline Health Care Workers During the Pandemic Surge in New York City. *Chronic Stress* **5**, Feb 1. doi: 10.1177/2470547020977891

Freimann, T. & Merisalu, E. 2015. Work-related psychosocial risk factors and mental health problems amongst nurses at a university hospital in Estonia: a cross-sectional study. *Scand. J. Public. Health* **43**(5), 447–52. doi: 10.1177/1403494815579477

Fuß, I., Nübling, M. & Hasselhorn, H.M. 2008. Working conditions and Work-Family Conflict in German hospital physicians: psychosocial and organisational predictors and consequences. *BMC Public Health* [online], Vol. **8**, art. 353.

Göras, C., Unbeck, M. & Nilsson, U. 2017. Ehrenberg A. Interprofessional team assessments of the patient safety climate in Swedish operating rooms: a cross-sectional survey. *BMJ Open.* **7**, e015607. doi: 10.1136/bmjopen-2016-015607

Al-Hamdan, Z., Manojlovich, M. & Tanima, B. 2017. Jordanian Nursing Work Environments, Intent to Stay, and Job Satisfaction. *J. Nurs. Scholarsh*. **49**(1), 103–110. doi: 10.1111/jnu.12265

Hassanzadeh-Rangi, N., Farshad, A., Khosravi, Y., Zare, G. & Mirkazemi, R. 2014. Occupational cognitive failure and its relationship with unsafe behaviors and accidents. *Int. J. Occup. Saf. Ergon* **20**(2), 265–71.

Hillen, H., Pfaff, H. & Hammer, A. 2015. The association between transformational leadership in German hospitals and the frequency of events reported as perceived by medical directors. *J. Risk Res*. **20**, 499–515.

Hsu, Y.S., Chen, Y.P. & Shaffer, M.A. 2019. Reducing work and home cognitive failures: the roles of workplace flextime use and perceived control. *J. Bus. Psychol*. **20**, 1–8.

Jarrar, M., Al-Bsheish, M., Albaker, W., Alsaad, I., Alkhalifa, E., Alnufaili, S., Almajed, N., Alhawaj, R., Al-Hariri, M.T., Alsunni, A.A., Aldhmadi, B.K. & Alumran, A. 2023. Hospital Work Conditions and the Mediation Role of Burnout: Residents and Practicing Physicians Reporting Adverse Events. *Risk Manag Healthc Policy* **16**, 1–13 doi: 10.2147/RMHP.S392523

Johnson, J.V. & Hall, E.M. 1988. Job Strain, Work Place Social Support, and Cardiovascular Disease: A Cross-Sectional Study of a Random Sample of the Swedish Working Population. *American Journal of Public Health* **78**, 1336–1342. doi: 10.2105/AJPH.78.10.1336

Kalakoski, V. 2019. Cognitive Ergonomics is a Matter of Cognitive Factors. *In ReCogErg@ ECCC*, pp. 46–51.

Kalkis, H. & Roja, Z. 2016. Strategic Model for Ergonomics Implementation in Operations Management. *J. Ergonomics* **6**, 173.

Karasek, Jr., R.A. 1979. Job Demands, Job Decision Latitude, and Mental Strain: Implications for Job Redesign. *Administrative Science Quarterly* **24**(2) 285–308. doi: 10.2307/2392498

Katona, C., Bíró, É., Vincze, S. & Kósa, K. 2022. On-the-job vocational traininsg of nonprofessional ethnic health workers of a primary health care team improves their sense of coherence. *Hum. Resour. Health*. **20**, 17. doi: 10.1186/s12960-021-00690-0

Kersten, M., Kozak, A., Wendeler, D., Paderow, L., Nübling, M. & Nienhaus, A. 2014. Psychological stress and strain on employees in dialysis facilities: a cross-sectional study with the Copenhagen Psychosocial Questionnaire. *J. Occup. Med. Toxicol.* **9**, 4 2014.

Kristensen, T.S, Hannerz, H., Hogh, A. & Borg, V. 2006. The Copenhagen Psychosocial Questionnaire - A tool for the assessment and improvement of the psychosocial work environment. *Scandinavian Journal of Work, Enviro* **31**(6), 438–49 doi: 10.5271/sjweh.948

Kristensen, T.S., Hannerz, H., Høgh, A. & Borg, V. 2005. The Copenhagen Psychosocial Questionnaire – a tool for the assessment and improvement of the psychosocial work environment. *Scandinavian Journal of Work, Environment & Health* **31**, 438–449.

Kumar, A., Bhat, P.S. & Ryali, S. 2018. Study of quality of life among health workers and psychosocial factors influencing it. *Ind. Psychiatry J.* **27**(1), 96–102. doi: 10.4103/ipj.ipj_41_18. PMID: 30416299; PMCID: PMC6198596

Leka, S., Jain, A., Iavicoli, S. & Di Tecco, C. 2015. An evaluation of the policy context on psychosocial risks and mental health in the workplace in the European Union: achievements, challenges, and the future. *BioMed Res*. Int. 2015, 213089. doi: 10.1155/2015/21 3089

Llorens, C., Navarro, A., Salas, S., Utzet, M. & Moncada, S. 2019. For better or for worse? Psychosocial work environment and direct participation practices. *Safety Science* **116**, 78–85. doi: 10.1016/j.ssci.2019.02.028

Majority of health jobs (Majority of health jobs held by women). 2021. Available at https://ec.europa.eu/eurostat/web/products-eurostat-news/-/edn-20210308-1

Marchand, A., Haines, V.Y. & Dextras-Gauthier, J. 2013. Quantitative analysis of organizational culture in occupational health research: a theory-based validation in 30 workplaces of the organizational culture profile instrument. *BMC Public Health* **13**, 1–11.

Okuhara, M., Sato, K. & Kodama, Y. 2021. The nurses' occupational stress components and outcomes, findings from an integrative review. *Nursing Open* Vol. **8**(5) [online], 2153–2174.

Olynick, J. & Li, H. 2020. Organizational culture and its relationship with employee stress, enjoyment of work and productivity. *Int. J. Psychol.* Stud.12, 14. doi: 10.5539/ijps.v12n2p14

Pastare, D., Roja, Z., Kalkis, H. & Roja, I. 2020. Psychosocial risks analysis for employees in public administration. *Agronomy Research* **18**(S1), 945–957. doi: 10.15159/AR.20.076

Peter, K.A., Golz, C., Bürgin, R.A., Nübling, M., Voirol, C., Zürcher, S.J. & Hahn, S. 2022. Assessing the psychosocial work environment in the health care setting: translation and psychometric testing of the French and Italian COPSOQ in a large sample of health professionals in Switzerland. *BMC Health Services Research* [online], Vol. **22**(1), art. 608. Available at: https://www.ncbi.nlm.nih.gov/pmc/articles/PMC9074249/

Ralph, J., Freeman, L.A., Ménard, A.D. & Soucie, K. 2022. Practical strategies and the need for psychological support: recommendations from nurses working in hospitals during the COVID-19 pandemic. *J Health Organ Manag*. **36**, 240–55. doi: 10.1108/JHOM-02-2021-0051

Research 'Work conditions and risks in Latvia 2019–2021' final report. 2023. Available: https://doi.org/10.25143/DARL-LV-2023

Robertson, E.M., Higgins, L., Rozmus, C. & Robinson, J.P. 1999. Association between continuing education and job satisfaction of nurses employed in long-term care facilities. *J Contin Educ Nurs.* **30**(3), 108–13. doi: 10.3928/0022-0124-19990501-06

Roja, Z., Kalkis, H., Roja, I., Zalkalns, J. & Sloka, B. 2017. Work strain predictors in construction work. *Agronomy Research* **15**(5), 2090–2099.

Roja, Z., Kalkis, V., Roja, I. & Kalkis, H. 2013. The effects of a medical hypnotherapy on clothing industry employees suffering from chronic pain. *J Occup Med Toxicol.* **8**, 25.

Royal College of Physicians. 2015. Work and well-being in the NHS: why staff health matters to patient care. Available at https://www.rcplondon.ac.uk/guidelines-policy/work-and-wellbeing-nhs-why-staff-health-matters-patient-care

Ruotsalainen, S., Jantunen, S. & Sinervo, T. 2020. Which factors are related to Finnish home care workers' job satisfaction, stress, psychological distress and perceived quality of care? - a mixed method study. *BMC Health Serv Res* **20**, 896. doi: 10.1186/s12913-020-05733-1

Schaufeli, W.B., Bakker, A.B. & Van Rhenen, W. 2009. How changes in job demands and resources predict burnout, work engagement, and sickness absenteeism. *Journal of Organizational Behavior* **30**, 893–917.

Scozzafave, M.C.S., Leal, L.A., Soares, M.I. & Henriques, S.H. 2019. Psychosocial risks related to the nurse in the psychiatric hospital and management strategies. *Rev Bras Enferm* [Internet]. **72**(4), 834–40. doi: 10.1590/0034-7167-2017-0311

Shanafelt, T.D., Balch, C., Bechamps, G., Russell, T., Dyrbye, L., Satele, D., Collicott, P., Novotny, P.J., Sloan, J. & Freischlag, J. 2010. Burnout and medical errors among American surgeons. *Ann Surg*. **251**, 1001–1002. doi: 10.1097/SLA.0b013e3181bfdab3

Smallwood, N., Pascoe, A., Karimi, L., Bismark, M. & Willis, K. 2021. Occupational Disruptions during the COVID-19 Pandemic and Their Association with Healthcare Workers' Mental Health. *Int J Environ Res Public Health.* **18**, 9263. doi: 10.3390/ijerph18179263

Stehman, C.R., Testo, Z., Gershaw, R.S. & Kellogg, A.R. 2019. Burnout, drop out, suicide: Physician loss in emergency medicine, part I. *Western Journal of Emergency Medicine* **20**, 485–494.

Thangavelu, A. & Sudhahar, C. 2017. Role clarity and job performance among the employees in small and medium IT industries. *Research on Humanities and Social Sciences* **7**(17), 6–10.

Wagner, A., Rieger, M.A., Manser, T., Sturm, H., Hardt, J., Martus, P., Lessing, C. & Hammer, A. 2019. Healthcare professionals' perspectives on working conditions, leadership, and safety climate: a cross-sectional study. *BMC Health Services Research* [online], Vol. **19**, art. 53.

West, C.P., Huschka, M.M., Novotny, P.J., Sloan, J.A., Kolars, J.C., Habermann, T.M. & Shanafelt, T.D. 2006. Association of perceived medical errors with resident distress and empathy: a prospective longitudinal study. *JAMA*. **296**, 1071–1078.

Whitaker, B., Dahling, J. & Levy, P. 2007. The development of a feedback environment and role clarity model of job performance. *Journal of Management* **33**, 570–591.

Žutautienė, R., Radišauskas, R., Kaliniene, G. & Ustinaviciene, R. 2020. The Prevalence of Burnout and Its Associations with Psychosocial Work Environment among Kaunas Region (Lithuania) Hospitals' Physicians. *International Journal of Environmental Research and Public Health* [online], Vol. **17**(10), art. 3739.

Agronomy Research **22**(2), 832–844, 2024
https://doi.org/10.15159/AR.24.095

Molecular characterization of new causative agents of root rot of wheat in Morocco

H. Khalifi[1,2,*], F. Bentata[1], J. Bouarda[1,2], A. El Aissami[3], I. Niya[1,5], A. Kahama Issa[1,2], I. Maafa[1,2], S. Hammoumi[1,2], S. Karim[1,4], M. Ibriz[2], K. Amrani Joutei[5], N. Brhadda[2], R. Ziri[2] and M. Labhilili[1,*]

[1]National Institute of Agricultural Research (INRA), Regional Research Center for Agricultural of Rabat, Av Mohamed Belarbi Alaoui, B.P. 6356, Institutes, Rabat, Morocco
[2]Laboratory of Plant and Animal Production and Agro-industry productions, Faculty of Science, Ibn Tofail University, Av l'université, Kenitra, Morocco
[3]Laboratory of Botany, Mycology and Environment, Faculty of Sciences of Rabat, Mohammed V University Rabat, Morocco
[4]Laboratory of Spectroscopy, Molecular Modeling, Materials, Nanomaterials, Water and Environment, Faculty of Sciences, Mohammed V University of Rabat, Av Ibn Battouta, BP1014, Agdal, Morocco
[5]Faculty of Sciences and technique of Fès, University of Sidi Mohammed Ben Abdellah, Fès, Morocco
[*]Correspondence: houdakhalifi96@gmail.com; mustapha.labhili@inra.ma

Received: August 25th, 2024; Accepted: October 10th, 2024; Published: October 22nd, 2024

Abstract. Most of the world's cereal-growing regions are severely constrained by root rots, crown rot and head blight brought on by *Fusarium spp*. In Morocco, yield losses due to root rots are not negligible and range from 12 to 14%. For this study, wheat root rot was surveyed in wheat fields from 2014 to 2019 in different regions of Morocco. Diseased plants are less vigorous, show progressive rotting of the root system and produce white or discolored heads containing stunted seeds. Therefore, the improvement of national production goes through the study of this disease on a deep level. To do this, 75 samples have been collected for the morphological study, which made it possible to identify the genus *Fusarium* present in the roots and the crown of the infected plant, and the molecular study made it possible to characterize the *Fusarium* species that are present in Moroccan wheat fields. Molecular identification revealed the presence of five *Fusarium* species, namely: *Fusarium culmorum*, which is noted as the dominant species in Morocco with a relative frequency of 21%, *F. graminearum, F. equiseti, F. avenaccum* and finally *F. sambucinum*, which represented a high rate in the Gharb region.

Key words: *Fusarium spp.*, molecular characterization, root rot, wheat.

INTRODUCTION

Important producers of mycotoxins, which contaminate food and may have an impact on consumers health, include *Fusarium* fungi (Moretti, 2009). These fungi can induce diseases that cause a crop to completely fail, for example, in the United States, losses have been estimated at close to 2.7 billion dollars (Gautam & Dill-Macky, 2011). This shows the devastating effect of their existence in plants, but the distribution and prevalence of these pathogenic species are determined by the host plant, the location of the region and the climatic conditions (Goldschmied-Reouven et al., 1993; Kvas et al., 2009; Ballois, 2012).

Accurate identification of this fungus is crucial for crop production in order to ensure that there are no such infections in the plants and that the finished product satisfies international standards for both consumption and sale. Some species have been shown to parasitize a variety of cultivated and wild plants, including cereals like wheat, barley, and corn (Landschoot et al., 2011). Wheat *Fusarium* wilt is the most common disease worldwide in all cereal-growing regions of temperate zones (Parry et al.,1995; Trottet et al., 2014). Multiple species of *Fusarium* are also responsible for *Fusarium* head blight (FHB) in cereal crops and also crown rot worldwide (Powell & Vujanovic, 2021; Erginbas-Orakci et al., 2016).

The need to identify strains and to attach names to them is stronger in *Fusarium*, than it is in any fungal genus (Leslie & Summerell, 2006). Thus, based on morphological, metabolic, and genetic data, the taxonomy of fungi has evolved, encompassing their classification, identification, and naming. However, due to species similarities and a lack of ability to differentiate between them, our understanding of *Fusarium* taxonomy is restricted (Chun et al., 2018).

The objective of this work is the use of new tools like molecular characterization to help the morphological characterization of *Fusarium spp.* populations collected in some wheat growing areas of Morocco.

MATERIALS AND METHODS

Isolation and multiplication of the fungus

75 diseased wheat plants were collected from four different areas in Morocco: Marchouch, Sidi Bettach, Jemaa Shaim and Gharb.

For the isolation of the causative agent of the disease, fragments of the roots and stems of wheat measuring 1 to 2 cm and showing characteristic lesions are treated. Typically, surface sterilization is conducted in 10% commercial bleach, then using 70% ethanol solution for 5 seconds. Samples are soaked in sterile water twice. Plant material is blotted dry and plated onto Potato Dextrose Agar (PDA) media (Leslie & Summerell, 2006).

Then, they were incubated at 25 ± 1 °C to promote the development of the fungi. For 4 days of incubation, the fragments were observed daily using a binocular loupe, to detect any development of mycelia and spores. For morphological identification, further culturing is required. Single spore isolation is the most accurate way to identify

Fusarium isolates and the process of this step is realized by carrying out successive subcultures. Multiplication is then achieved by successive transplanting.

Macroscopic study

Each *Fusarium* isolate was placed in the center of PDA plates and incubated at 25 ± 1 °C (3 replicates per isolate). Mycelial elongation was measured daily with a ruler at 90° angles on each plate. The radial growth rate (RGR) of the fungus, expressed in millimeters per day, corresponds to the mycelial elongation rate on a solid surface.

The macroscopic study was done after the 8th day of incubation on PDA. Observations were made regularly on the petri dishes to reveal the morphological diversity of the fungus based on cultural parameters described below.

- Aerial mycelia: Present/ Absent
- Density of mycelia/ Abundance: Low/ Medium/ High
- Appearance of mycelia: Cottony/ Fluffy/ Woolly
- Color: Topside of thallus/ Underside of thallus
- Growth rate: Too Slow / Slow/ Medium/ Fast

Microscopic study

Microscopic observations of the conidia were made by the 'scotch tape' technique: the scotch tape was pressed on the youngest part of the culture in order to collect conidia and then stuck on a slide containing a droplet of bromothymol blue. These slides were observed under an optical microscope. This way, we can observe the hypha, macroconidia, microconidia, sporodochia, and chlamydospores (Boa, 1998; Leslie & Summerell, 2006).

Molecular study of Moroccan isolates of *Fusarium spp.*

Fusarium species can be detected and quantified through nucleic acid-based assays (Polymerase chain reaction).

DNA extraction

The effective DNA extraction method used is the one created by Möller et al. (1992), primarily distinguished by the use of cethyltrimethyl ammonium bromide (CTAB). DNA purification was performed by adding RNase, then the genomic DNA quality test was evaluated on 1% agarose gel.

PCR amplification

Specific PCR primers have been selected to identify *Fusarium* species by amplifying the fragment of the translation elongation factor 1-alpha (EF-1α) gene.

The PCR amplification was performed in a final volume of 10 µl containing 1 µM of each primer, 1X PCR buffer, 0.5 units of MyTaq DNA polymerase (Bioline, Meridian Life Science, Memphis, USA) and 50 to 100 ng of DNA. Amplification was carried out for 25 cycles, respecting the primer hybridization temperature. The primers used for the analysis of *Fusarium* populations are shown in the following table (Table 1).

Table 1. Primers used in the molecular characterization

Locus	Sequence	Tm (°C)	Reference
175F	5' TTTTAGTGGAACTTCTGAGTAT 3'	53 °C	(Mishra et al., 2003)
430R	5' AGTGCAGCAGGACTGCAGC 3'		
FSF1	5' ACATACCTTTATGTTGCCTCG3'	60° C	
FSR1	5' GGAGTGTCAGACGACAGCT 3'		
FOF1	5' ACATACCACTTGTTGGCCTCG3'	65 °C	
FOR1	5'CGCCAATCAATTTGAGGAACG3'		
FEF1	5' CATACCTATACGTTGCCTCG3'	56 °C	
FER1	5' TTACCAGTAACGAGGTGTATG3'		
FAF1	5' AACATACCTTAATGTTGCCTCGG3'	64 °C	
FAR	5' ATCCCCAACACCAAACCCGAG3'		
FgAAGF	5' TGATCACGGCCAATGAAAAG 3'	65 °C	(Soo-hyung Lee et al., 2013)
FgAAGR	5' TCAGTGATTGCTCGGCAGTT 3'		

Analysis of amplification products

The amplification products were analyzed on a 6% acrylamide gel alongside a molecular weight marker 100-bp ladder (Promega, Madison, WI, USA). Subsequent visualization of DNA bands was achieved through Ethidium Bromide application at a concentration of 10 mg/ml, under UV light using Molecular Imager Gel Doc XR^+ System (BioRad, CA, United States). The gel photos were then analyzed by Image lab software. The identification results obtained were annotated in an Excel sheet.

RESULTS AND DISCUSSION

Morphological study of Fusarium isolates from the wheat plant

The 75 isolates from the collected wheat samples have been identified. Therefore, the macroscopic characters of the different isolates selected were studied on PDA. The isolates were subdivided into groups with different characteristics to show the variations obtained, Table 2 summarizes the results. The macroscopic study of the purified isolates revealed a morphological variability within our collection that has been classified into groups presented in Table 2. Thus, we have distinguished two types of thalli, downy and cottony. Diversity also affects the color of isolates; they were white, yellow, light pink, purple or brownish red. Some isolates were characterized by extremely abundant mycelium production with a very cottony appearance and different colors of the thallus. Another group presented a diversity of color and showed an abundant presence of mycelium with a cottony appearance, unlike other isolates, which were characterized by a fluffy or grazing appearance.

For the microscopic study, an observation of the isolates under an optical microscope enabled us to detect the presence of septate mycelia, macroconidia and microconidia. The observed macroconida were fusiform or sickle-shaped and very abundant.

From the macroscopic and microscopic observations, it was perceived that all the isolates belong to the genus *Fusarium*. In order to confirm this observation and to deduce the species of each isolate, an in-depth identification, by molecular means, was carried out.

Table 2. Summary of morphological description of *Fusarium* isolates

Group	Macroscopic observation	Macroscopic characters	Microscopic characters
A)	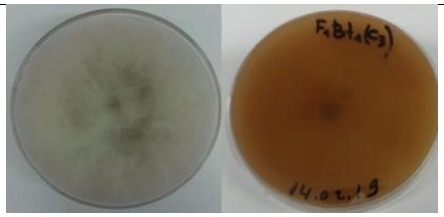	- White woolly colony - Yellow-orange reverse - Fast growth rate	- Thin and septate hyphae - Fusiform macroconidia - Oval microconidia
B)		- White fluffy flattened colony - Yellow-orange reverse - Medium growth rate	- Thin and septate hyphae - Fusiform macroconidia - Reniform microconidia
C)	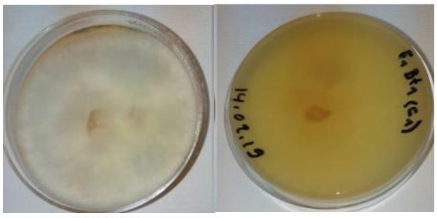	- White cottony colony - Yellow reverse - Medium growth rate	- Thin and septate hyphae - Sickle-shaped macroconidia - Reniform microconidia
D)	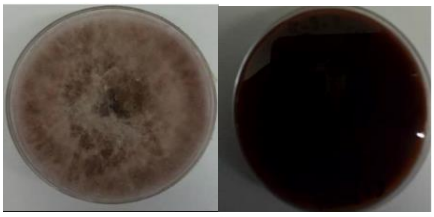	- Purple cottony colony - Dark brick-red reverse - Fast growth rate	- Thin and septate hyphae - Fusiform macroconidia - Oval microconidia
E)	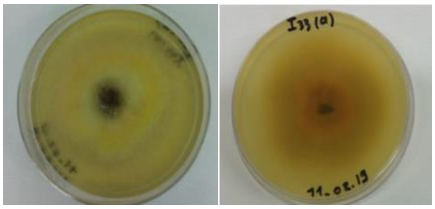	- Yellow fluffy flattened colony - Yellow reverse - Slow growth rate	- Thin and septate hyphae - Fusiform macroconidia - Reniform microconidia
F)		- Purple flattened colony - Purple reverse - Medium growth rate	- Thin and septate hyphae - Fusiform macroconidia - Reniform microconidia
G)		- White flattened colony - Orange reverse - Slow growth rate	- Thin and septate hyphae - Sickle-shaped macroconidia - Oval microconidia

Table 2 (continued)

H)	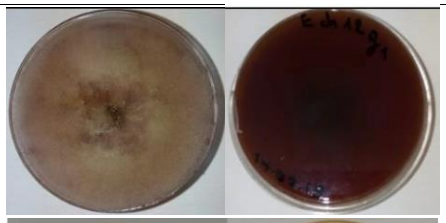	- Purple Woolly colony - Brick red reverse - Fast growth rate	- Thin and septate hyphae - Fusiform macroconidia - Reniform microconidia
I)	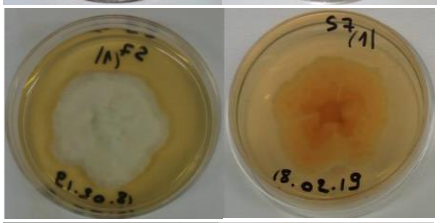	- White cottony colony - Yellow orange reverse - Slow growth rate	- Thin and septate hyphae - Fusiform macroconidia - Oval microconidia
J)	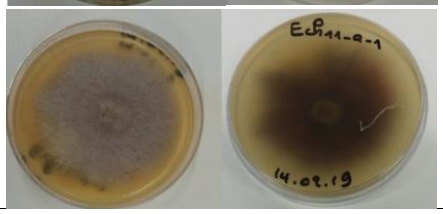	- Purple flattened colony - Dark purple reverse - Too slow growth rate	- Thin and septate hyphae - Fusiform macroconidia - Reniform microconidia

Molecular identification

Morphological characters, studied above, were not sufficient to distinguish *Fusarium* species due to morphological, colony and fructification similarities. DNA-derived molecular data can be very useful for the objective characterization of Fusarium. To this end, PCR was performed.

We succeeded in obtaining DNA with good quality, which was evaluated at 1% agarose gel, as shown in Fig. 1.

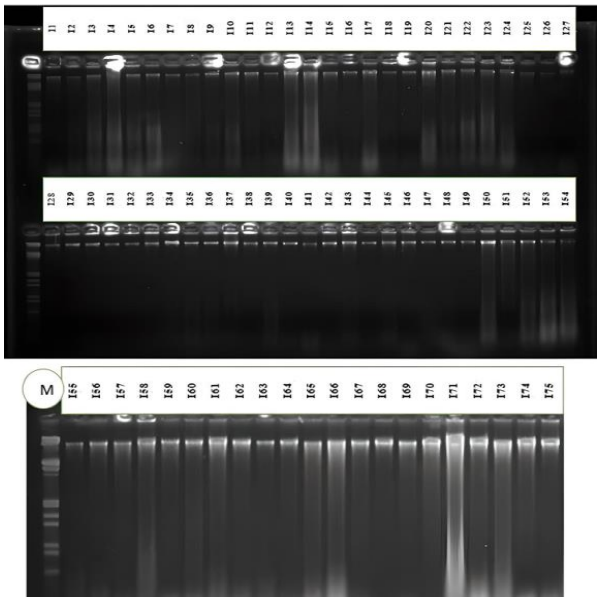

Figure 1. Electrophoretic profile of DNA quality test of 75 isolates of *Fusarium spp.* on 1% agarose gel.

DNA amplification by PCR

In this study, we were interested in the molecular characterization of several species of the causal fungus isolated from four different regions around the country. PCR amplification was carried out using 6 different markers, one for each distinct species. Analysis of the PCR products by acrylamide gel electrophoresis using the specific primers showed that the markers used produced interpretable profiles.

The electrophoretic profile of the *F. culmurum* specific primer 175F/430R (Fig. 2) shows the presence of PCR-amplified bands. This marker therefore identifies the isolates belonging to this species.

As for the other primers, the FgAAGF/FgAAGR primer shows clear bands corresponding to isolates identified as *F. graminearum* (Fig. 3).

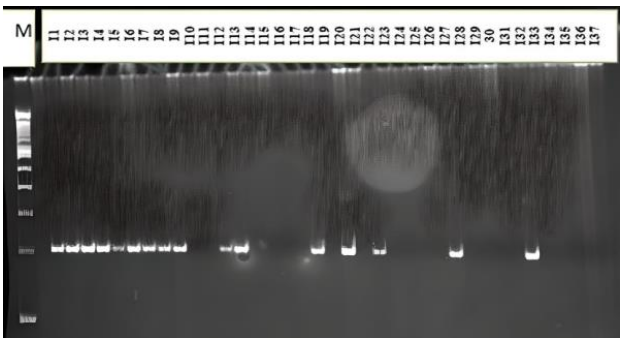

Figure 2. Electrophoretic DNA profile amplified by the 175F/430R primer; M, molecular-weight marker.

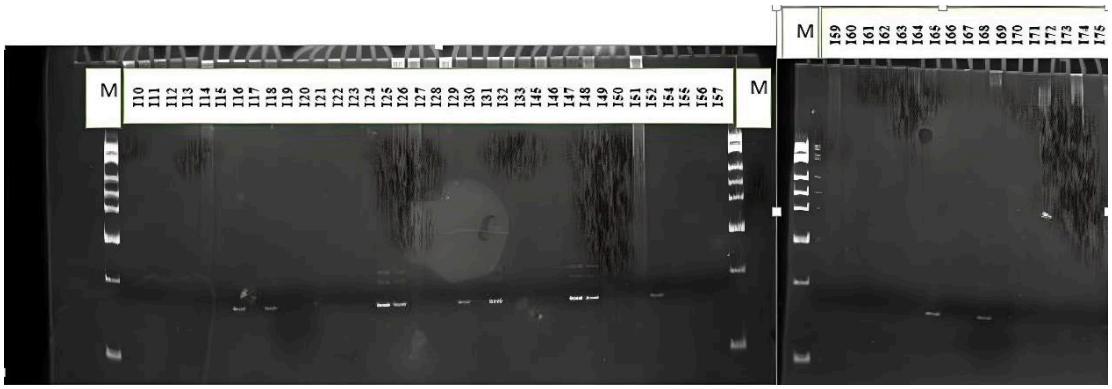

Figure 3. Electrophoretic DNA profile amplified by the FgAAGF/FgAAGRprimer; M, molecular-weight marker.

The primer pairs FSF1/FSR1, FAF1/FAR and FEF1/FER1 show clear amplifications for *F. sambucinum*, *F. avenaccum* and *F. equiseti* respectively (Fig. 4, Fig. 5 and Fig. 6).

This primer FOF1/FOR1 did not give any results when the isolates were analyzed by PCR technique, so none of the 75 samples corresponded to the species *F. oxysporum*.

In view of the results of molecular identification, five species belonging to the genus *Fusarium* were identified from a total of 75 isolates. *F. culmorum* is the most dominant species with a percentage of 31%, followed by *F. graminearum* (23%), *F. equisiti* (19%), *F. sambucinum* (17%) and finally *F. avenaccum* with a pourcentage of 10%. The *F. oxysporum*s pecific primer produced no matching isolates (Fig. 7).

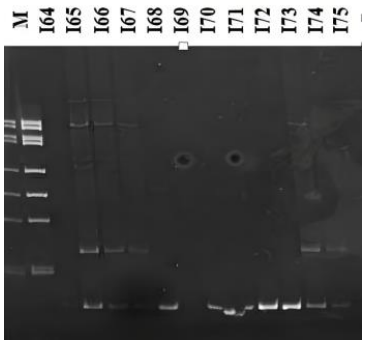

Figure 4. Electrophoretic DNA profile amplified by the FSF1/FSR1 primer; M, molecular-weight marker.

Marchouch region was characterized by the dominance of the species *F. culmorum* with a percentage of 40% followed by *F. equiseti* with the presence of 15%, then the species *F. graminearum* and *F. avenaccum* with respectively 12% and 9% (Fig. 5).

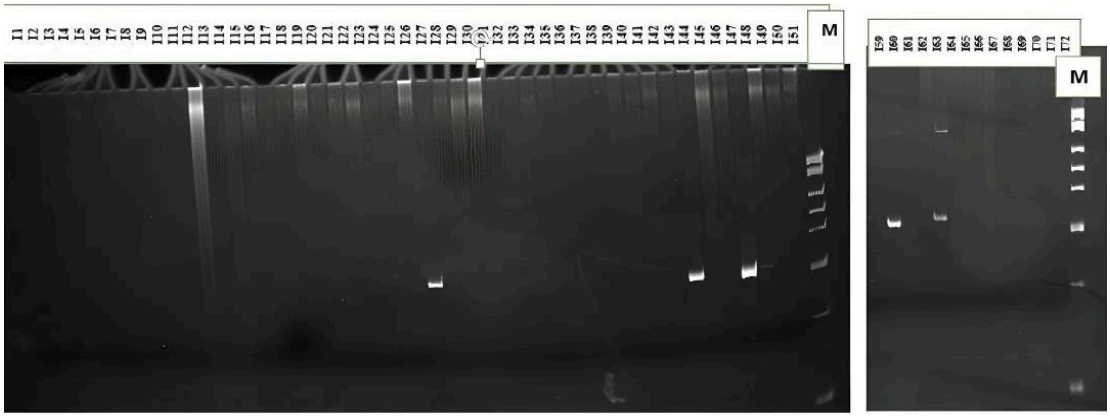

Figure 5. Electrophoretic DNA profile amplified by the FAF1/FAR1 primer; M, molecular-weight marker.

The region of Sidi Bettach was characterized by the presence of 3 *Fusarium* species named *F. equisiti, F. sambucinum and F. avenaccum* with a percentage of 18% each, while *F. culmorum*was presented only 9% of the total number of isolates (Fig. 5).

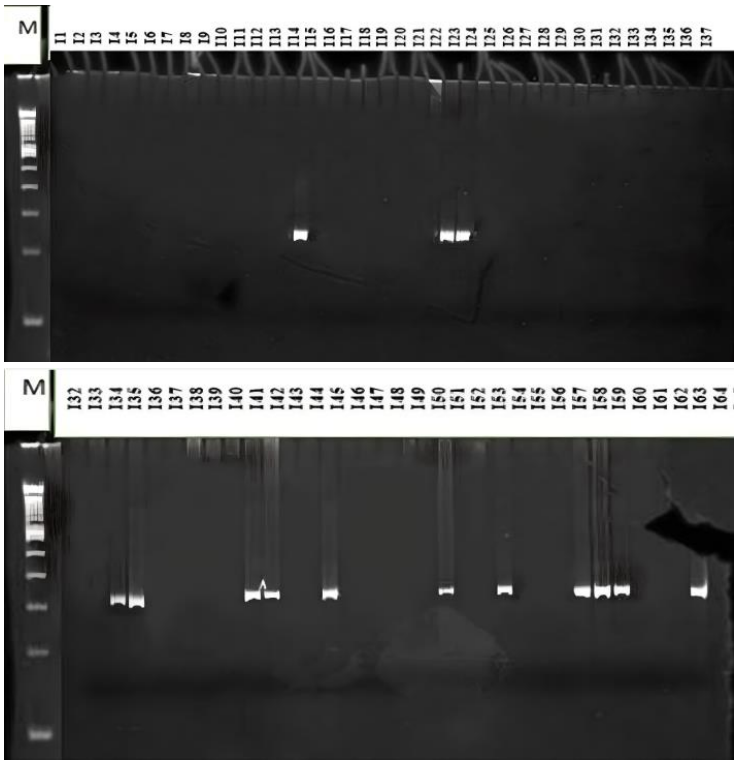

Figure 6. Electrophoretic DNA profile amplified by the FEF1/FER1primer; M, molecular-weight marker

For Jemaa Shaim region, like shown in Fig. 5, we have found a significant dominance of the species *F. graminearum* with a percentage of 42% while *F. culmorum* only has 17% and *F. equiseti* 8% of the *Fusarium* abundance. Unlike the other regions, Gharb region has a significant dominance of *F. sambucinum* species with a percentage of 37%, while *F. graminearum* and *F. equisti* presented 25% of the *Fusarium* abundance (Fig. 8).

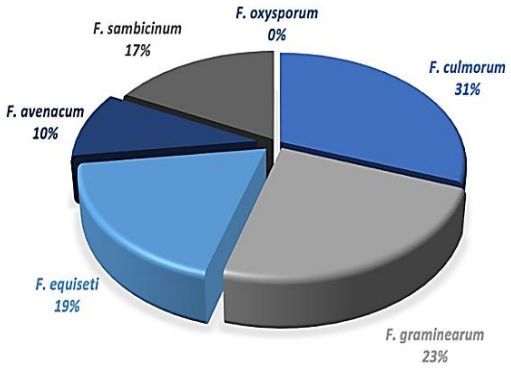

Figure 7. Percentages of identified *Fusarium* species in our population in all studied areas.

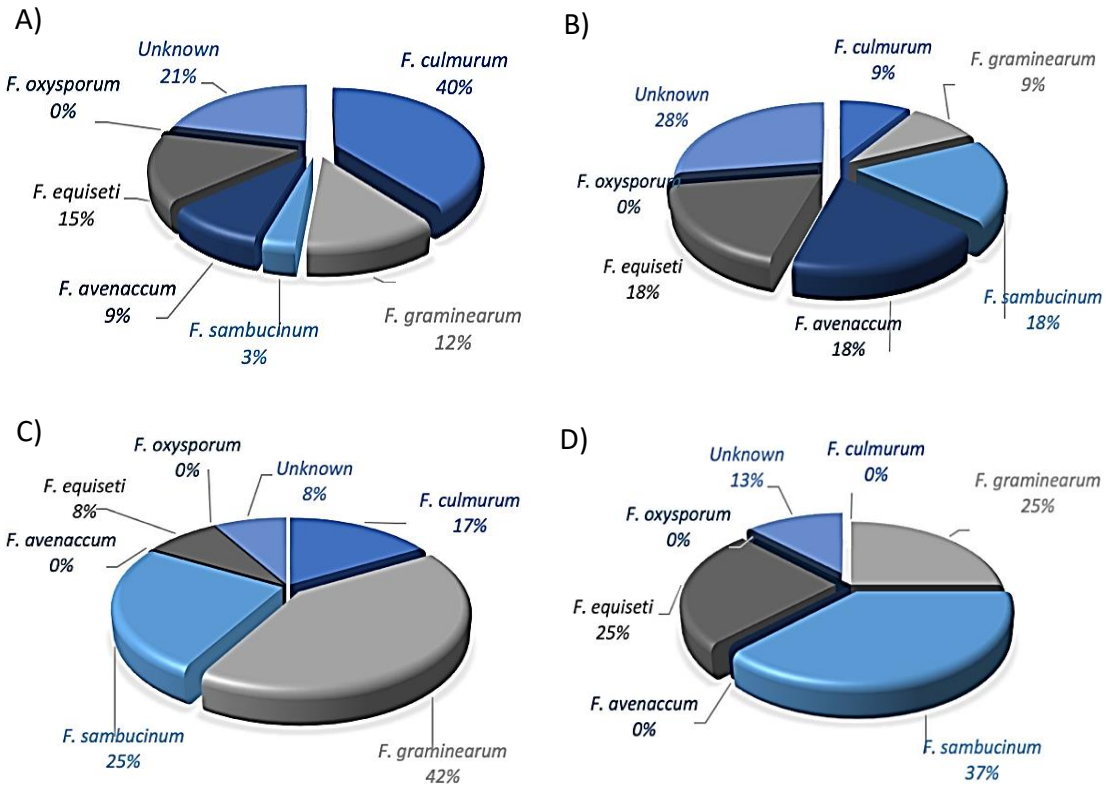

Figure 8. Percentages of identified *Fusarium* species in our population in every studied area; A: Marchouch / B: SidiBettach / C: JemaaShaim / D: Gharb.

Discussion

Abiotic and biotic stresses, climate change, and a scarcity of adequate farmland are just a few of the issues that consistently threaten wheat production. Integrated disease management, adaptation to abiotic stressors and warmer climates, and resource conservation must be combined to meet future demand (Simón et al., 2023).

The present work deals with the identification of *Fusarium* fungi affecting wheat. The fungi were present in different wheat fields, presumably different species were collected knowing that it is likely that a variety of wheat is attacked by one or more species of *Fusarium* pathogens (Alisaac & Mahlein, 2023).

Through the morphological study in this work, we found that there were isolates of the same species with different morphological traits that represent an intraspecific variability (Kulik et al., 2011) and other groups of isolates of different species presented similar characters, which is an accurate fact about *Fusarium* species according to multiple studies (Carreras-Villaseñor et al., 2022; James et al., 2022).

The morphological study alone was not sufficient to identify those species (Schollenberger et al., 2007; Nikitin et al., 2023). The vast and complicated morphological variability of *Fusarium* characteristics is also the reason why molecular technologies are required to specify the species and its traits (Xi et al., 2021).

The molecular study using the PCR technique allowed us to characterize some dominant *Fusarium* species in Morocco. For the first time, five species of genus *Fusarium* have been identified in this work within four wheat growing regions of Morocco.

It was shown that the identified species had different frequencies depending on the survey location. *F. culmorum* was the most common species in our isolates, which is supported by several studies over the years and in different countries (Smiley & Patterson, 1996; Fakhfakh et al., 2011; Yüksektepe et al., 2022). Although in other cases, a shift in the dominance of *F. culmorum* in favor of *F. graminearum* has also been observed (Francis & Burgess, 1977; Minnaar-Ontong et al., 2017). In our study *F. graminearum* was the second most common species, while *F. equiseti* and *F. sambucinum* were relatively present in all studied areas but with lower frequency and the least frequent species in this work was *F. avenaceum*.

F. graminearum was especially predominant in the Jemaa shaim region which represents the south of Morocco and is therefore considered an arid region. This species was the dominant by a relatively high percentage (42%). Its presence in this region is explained by its ability to survive in cold as well as dry regions in the world (Booth, 1971).

Even though Marchouch and Sidi Bettach areas have similar climate, which are part of the favorable regions in Morocco, but *F. culmorum* and *F. graminearum* presented higher frequencies in Marchouch than in SidiBettach (only 9% each in SidiBettach). This can be due to the difference in the host varieties and their different level of resistance to the fungi (Ghimire et al., 2022). It can be explained by genetic flow and selection pressure exercised on the genetic material, which didn't contain any source of resistance.

As for the Gharb region, *F. sambucinum* was predominant because of the presence of humidity on a wide variety of substrates (Leslie & Summerell, 2006), and it also proves that the cultivar, the environmental conditions and geographical locations play a key role in species distribution (Leslie & Summerell, 2006; Ghimire et al., 2022).

The last species is *F. avenaceum*, which was found only in the Marchouch region, a relatively favourable climate region than the other studied areas. This is in accordance with a study conducted in 2016, where it was stated that *F. avenaceum* can be found worldwide, but is more present in humid and cool climate areas (Stakheev et al., 2016). This geographic distribution is explained by environmental variables (Kakakhan & Shekhany, 2023).

Given the complexity of distribution of these fungi, a regular inventory of the species involved in wheat diseases is necessary in order to better control them. Detecting these pathogens is crucial to increasing food quality and quantity (Araújo et al., 2017). Studying these species and their mode of infection is essential to creating tolerant or resistant cultivars for a guaranteed wheat production (Wu et al., 2022; López-Moral et al., 2024).

Partially tolerant cultivars combined with cultural management techniques can effectively slow the spread of disease (Kazan & Gardiner, 2018), hence the importance of constantly aiming for the identification of resistant wheat cultivars. In addition to plant diseases, agriculture in Morocco faces many challenges, including limited water ressources and land fragmentation, that's why the country has increased its zero tillage area in order to have a conservative agriculture (OCP, 2018). Identifying the *Fusarium* species present in our fields is therefore an important step in helping the genetic breeder to produce disease-resistant varieties and to overcome the constraints of no till system.

CONCLUSIONS

Our work deals with the determination of the geographic and distribution importance of *Fusarium* species in Morocco. The application of molecular markers as a genetic study for analysis and identification of the causal species of wheat Fusariums.

Being able to identify the species present in Morocco, allows us to overcome the shortcomings of zero tillage and participate in breeding programs to release new varieties comprising resistant genes.

REFERENCES

Alisaac, E. & Mahlein, A.-K. 2023. Fusarium Head Blight on Wheat: Biology, Modern Detection and Diagnosis and Integrated Disease Management. *Toxins* **15**(3), 192. doi: 10.3390/toxins15030192

Araújo, N.A.F., Pasqual, M., Pio, L.A.S., Alves, E., de Matos Moura, N. & Costa, S. da S. 2017. Identification and aggressiveness of four isolates of Fusarium oxysporum f.sp. Cubense from Latundan banana in Brazil. *Journal of Phytopathology* **165**(4), 257–264. doi: 10.1111/jph.12557

Ballois, N. 2012. Characterisation of the diversity of Fusarium species and their mycotoxigenic potential on French cereals. Sciences de l'environment, Lorraine University. https://hal.univ-lorraine.fr/hal-02094098

Boa, E. 1998. Ainsworth and Bisby's Dictionary of the Fungi. *Plant Pathology* **47**(4), 541–541. doi: 10.1046/j.1365-3059.1998.0223b.x

Booth, C. 1971. *The Genus Fusarium*. Commonwealth Mycological Institute. Kew, Surrey, England, 237 pp.

Carreras-Villaseñor, N., Rodríguez-Haas, J.B., Martínez-Rodríguez, L.A., Pérez-Lira, A.J., Ibarra-Laclette, E., Villafán, E., Castillo-Díaz, A.P., Ibarra-Juárez, L.A., Carrillo-Hernández, E.D. & Sánchez-Rangel, D. 2022. Characterization of Two Fusarium solani Species Complex Isolates from the Ambrosia Beetle Xylosandrus morigerus. *Journal of Fungi* **8**(3), Article 3. doi: 10.3390/jof8030231

Chun, J., Oren, A., Ventosa, A., Christensen, H., Arahal, D.R., da Costa, M.S., Rooney, A.P., Yi, H., Xu, X.-W., De Meyer, S. & Trujillo, M.E. 2018. Proposed minimal standards for the use of genome data for the taxonomy of prokaryotes. *International Journal of Systematic and Evolutionary Microbiology* **68**(1), 461–466. doi: 10.1099/ijsem.0.002516

Erginbas-Orakci, G., Poole, G., Nicol, J.M., Paulitz, T., Dababat, A.A. & Campbell, K. 2016. Assessment of inoculation methods to identify resistance to Fusarium crown rot in wheat. *Journal of Plant Diseases and Protection* **123**(1), 19–27. doi: 10.1007/s41348-016-0001-8

Fakhfakh, M.M., Yahyaoui, A., Salah, R., Elias, E. & Daaloul, A. 2011. Identification and pathogenicity assessment of Fusarium spp. Sampled from durum wheat fields in Tunisia. *African Journal of Biotechnology* **10**, 6529–6539.

Francis, R.G. & Burgess, L.W. 1977. Characteristics of two populations of Fusarium roseum 'Graminearum' in Eastern Australia. *Transactions of the British Mycological Society* **68**(3), 421–427. doi: 10.1016/S0007-1536(77)80196-4

Gautam, P. & Dill-Macky, R. 2011. Type I host resistance and Trichothecene Accumulation in Fusarium-infected Wheat Heads. *American Journal of Agricultural and Biological Sciences* **6**(2), 231–241. doi: 10.3844/ajabssp.2011.231.241

Ghimire, B., Mergoum, M., Martinez-Espinoza, A.D., Sapkota, S., Pradhan, S., Babar, M.A., Bai, G., Dong, Y. & Buck, J.W. 2022. Genetics of Fusarium head blight resistance in soft red winter wheat using a genome-wide association study. *The Plant Genome* **15**(3), e20222. doi: 10.1002/tpg2.20222

Goldschmied-Reouven, A., Friedman, J. & Block, C.S. 1993. Fusarium species isolated from non-ocular sites: A 10 year experience at an Israeli general hospital. *CABI Databases*. https://www.cabidigitallibrary.org/doi/full/10.5555/19931215086

James, J.E., Santhanam, J., Zakaria, L., Mamat Rusli, N., Abu Bakar, M., Suetrong, S., Sakayaroj, J., Abdul Razak, M.F., Lamping, E. & Cannon, R.D. 2022. Morphology, Phenotype, and Molecular Identification of Clinical and Environmental Fusarium solani Species Complex Isolates from Malaysia. *Journal of Fungi* **8**(8), Article 8. doi: 10.3390/jof8080845

Kakakhan, H.S. & Shekhany, K.A.M. 2023. Molecular Detection of Fusarium species infected Corn in Kurdistan region-Iraq. Scopus, *Passer Journal of Basic and Applied Sciences* **5**(2), 224–230. doi: 10.24271/PSR.2023.375971.1190

Kazan, K. & Gardiner, D.M. 2018. Fusarium crown rot caused by Fusarium pseudograminearum in cereal crops: Recent progress and future prospects. *Molecular Plant Pathology* **19**(7), 1547–1562. doi: 10.1111/mpp.12639

Kulik, T., Pszczółkowska, A. & Łojko, M. 2011. Multilocus Phylogenetics Show High Intraspecific Variability within Fusarium avenaceum. *International Journal of Molecular Sciences* **12**(9), Article 9. doi: 10.3390/ijms12095626

Kvas, M., Marasas, W.F.O., Wingfield, B.D., Wingfield, M.J. & Steenkamp, E.T. 2009. Diversity and evolution of Fusarium species in the Gibberella fujikuroi complex. Scopus, *Fungal Diversity* **34**, 1–21.

Landschoot, S., Audenaert, K., Waegeman, W., Pycke, B., Bekaert, B., De Baets, B. & Haesaert, G. 2011. Connection between primary Fusarium inoculum on gramineous weeds, crop residues and soil samples and the final population on wheat ears in Flanders, Belgium. *Crop Protection* **30**(10), 1297–1305. doi: 10.1016/j.cropro.2011.05.018

Leslie, J.F. & Summerell, B.A. 2006. *The Fusarium Laboratory Manual*. doi: 10.1002/9780470278376.ch12

López-Moral, A., Antón-Domínguez, B.I., Lovera, M., Arquero, O., Trapero, A. & Agustí-Brisach, C. 2024. Identification and pathogenicity of Fusarium species associated with wilting and crown rot in almond (Prunus dulcis. *Scientific Reports* **14**(1), Article 1. doi: 10.1038/s41598-024-56350-5

Minnaar-Ontong, A., Herselman, L., Kriel, W.-M. & Leslie, J.F. 2017. Morphological characterization and trichothecene genotype analysis of a Fusarium Head Blight population in South Africa. *European Journal of Plant Pathology* **148**(2), 261–269. doi: 10.1007/s10658-016-1085-5

Mishra, P.K., Fox, R.T.V. & Culham, A. 2003. Development of a PCR-based assay for rapid and reliable identification of pathogenic Fusaria. *FEMS Microbiology Letters* **218**(2), 329–332. doi: 10.1111/j.1574-6968.2003.tb11537.x

Möller, E.M., Bahnweg, G., Sandermann, H. & Geiger, H.H. 1992. A simple and efficient protocol for isolation of high molecular weight DNA from filamentous fungi, fruit bodies, and infected plant tissues. *Nucleic Acids Research* **20**(22), 6115–6116.

Moretti, A. 2009. Taxonomy of Fusarium genus: A continuous fight between lumpers and splitters. *Zbornik Matice Srpske Za Prirodne Nauke* **117**. doi: 10.2298/ZMSPN0917007M

Nikitin, D.A., Ivanova, E.A., Semenov, M.V., Zhelezova, A.D., Ksenofontova, N.A., Tkhakakhova, A.K. & Kholodov, V.A. 2023. Diversity, Ecological Characteristics and Identification of Some Problematic Phytopathogenic Fusarium in Soil: A Review. *Diversity* **15**(1), Article 1. doi: 10.3390/d15010049

OCP. 2018. *Al Moutmir Initiative*. https://www.almoutmir.ma/en/ocp-al-moutmir

Parry, D.W., Jenkinson, P. & McLEOD, L. 1995. Fusarium ear blight (scab) in small grain cereals - A review. *Plant Pathology* **44**(2), 207–238. doi: 10.1111/j.1365-3059.1995.tb02773.x

Powell, A.J. & Vujanovic, V. 2021. Evolution of Fusarium Head Blight Management in Wheat: Scientific Perspectives on Biological Control Agents and Crop Genotypes Protocooperation. *Applied Sciences* **11**(19), Article 19. doi: 10.3390/app11198960

Schollenberger, M., Müller, H.-M., Rüfle, M., Terry-Jara, H., Suchy, S., Plank, S. & Drochner, W. 2007. Natural occurrence of Fusarium toxins in soy food marketed in Germany. *International Journal of Food Microbiology* **113**(2), 142–146. doi: 10.1016/j.ijfoodmicro.2006.06.022

Simón, M.R., Struik, P.C. & Börner, A. 2023. Editorial: Fungal wheat diseases: etiology, breeding, and integrated management, volume II. *Frontiers in Plant Science* **14**, 1247327. doi: 10.3389/fpls.2023.1247327

Smiley, R.W. & Patterson, L.M. 1996. Pathogenic fungi associated with Fusarium foot rot of winter wheat in the semiarid Pacific Northwest. *Plant Disease* **80**(8), 944–949.

Soo-hyung Lee, Jong-cheol Yoon, Seung-ho Lee, Teresa Lee, Jae-gi Ryu, & Mi-ja Kim. 2013. *Fine marker markers for lineage differentiation of red mold pathogens and methods for distinguishing lineages of red mold pathogens using these markers* (Patent KR101288510B1. https://patents.google.com/patent/KR101288510B1/ko (in Korean).

Stakheev, A.A., Khairulina, D.R. & Zavriev, S.K. 2016. Four-locus phylogeny of Fusarium avenaceum and related species and their species-specific identification based on partial phosphate permease gene sequences. *International Journal of Food Microbiology* **225**, 27–37. doi: 10.1016/j.ijfoodmicro.2016.02.012

Trottet, M., Atanosova-Penichon, V., Ferreyrolle, J., Gervais, L., Pinson-Gadais, L. & Roumet, P. 2014. Caractérisation de sources de résistance à la fusariose chez le blé dur. *Innovations Agronomiques* **35**, 173–180. doi: 10.17180/zz4f-se17

Wu, L., He, X., He, Y., Jiang, P., Xu, K., Zhang, X. & Singh, P. K. 2022. Genetic sources and loci for Fusarium head blight resistance in bread wheat. *Frontiers in Genetics* **13**, 988264. doi: 10.3389/fgene.2022.988264

Xi, K., Shan, L., Yang, Y., Zhang, G., Zhang, J. & Guo, W. 2021. Species Diversity and Chemotypes of Fusarium Species Associated With Maize Stalk Rot in Yunnan Province of Southwest China. *Frontiers in Microbiology* **12**. doi: 10.3389/fmicb.2021.652062

Yüksektepe, B., Sefer, Ö., Varol, G., Teker, T., Arslan, M., Çetin, B., Mert, F., Yörük, E. & Albayrak, G. 2022. Identification of Fusarium graminearum and Fusarium culmorum Isolates via Conventional and Molecular Methods. *Eur. J. Biol.* **81**(1), 107–116. doi: 10.26650/EurJBiol.2022.1078448

Agronomy Research **22**(2), 845–862, 2024
https://doi.org/10.15159/AR.24.091

The effect of storage conditions and packing materials on the quality properties of chicken eggs

A.J. Kryeziu[1], Xh. Ramadani[2,*], L. Hajra[1], M. Kamberi[1] and M. Zogaj[3]

[1]University of Prishtina 'Hasan Prishtina', Faculty of Agriculture and Veterinary, Department of Biotechnologyin Animal Science, Str. Lidhja e Pejës 34, XK10000 Prishtinë, Republic of Kosovo
[2]University of Prishtina 'Hasan Prishtina', Faculty of Agriculture and Veterinary, Department of Food Technology with Biotechnology, Str. Lidhja e Pejës 34, XK10000 Prishtinë, Republic of Kosovo
[3]University of Prishtina 'Hasan Prishtina', Faculty of Agriculture and Veterinary, Department of Plant Production, 34 Str. Tahir Zajmi, XK 10000 Prishtinë, Republic of Kosovo
*Correspondence: xhavit.ramadani@uni-pr.edu

Received: June 22nd, 2024; Accepted: September 23rd, 2024; Published: October 15th, 2024

Abstract. This study investigated how storing eggs in different packaging (unpackaged eggs-control, cardboard, styrofoam, plastic) and temperatures (4–6, 20–22 °C) for 28 days affects their quality. Eight eggs were analysed on days 0, 7, 14, 21, and 28 for each treatment. Storage temperature–ST, packaging material–PM, storage duration–SD, and their interaction encouraged egg weight loss–EWL ($P < 0.05$). The interaction of the three factors showed no significant difference in the EWL. Storage temperature significantly influenced ($P < 0.05$), eggshell thickness–EST, albumen index–AI, albumen pH–ApH, Haugh unit–HU, yolk height–YH, and yolk index– YI. Some parameters like egg weight–EW g, shape index–SI and albumen weight–AW g, changed significantly ($P < 0.05$) according to storage in different PM. The SI, eggshell weight–ESW g, EST, eggshell index–ESI, albumen ratio–AR, AI, ApH, HU, yolk weight–YW, yolk height–YH, YI, yolk colour–YC, and yolk:albumen–Y:A ratio changed during storage. The ST×SD was significant for EW, ESW g, EST, AW g, albumen ratio–AR, AI, ApH, HU, YW g, YH, and YI ($P < 0.05$). As a result of the PM×SD interaction, significant differences ($P < 0.05$) were observed in EW g ESW g, EST, AW g, and YI. A significant interaction effect of ST×PM×SD was found on AI, YH, and yolk pH–YpH ($P < 0.05$). The purpose of this research is to give an overview of the storage conditions in order to have good quality eggs.

Key words: chicken eggs, quality characteristics, packing material, storage duration and temperature.

INTRODUCTION

There is no doubt that eggs are an ideal food and an excellent source of high-quality protein, as well as essential vitamins and minerals. Eggs are also an affordable source of nutrients for a healthy diet and life. A previous study has shown that eggs play an important role in human nutrition, particularly for certain population such as the elderly,

pregnant woman, children, convalescents, and athletes (Miranda et al., 2015). On the other hand, if they are not stored in proper conditions, they can spoil and become a health hazard. Ensuring high egg quality is crucial for consumer satisfaction and the overall success of the egg industry. Today this industry faces several challenges related to ensuring and maintaining egg quality. Thus, Preisinger (2018) in his research described that one of the challenges of the poultry industry is to provide the consumer with eggs of the best possible quality.

Several factors influence the quality of table eggs, including the flock's age (Freitas et al., 2017), genotype, and raising system (Sokolowicz et al., 2018), methods of hen feeding (Anene et al., 2023), diet composition (Díaz-Echeverría et al., 2023) or the storage temperature and storage duration (Akyurek & Okur, 2009; Madrigal-Portilla et al., 2023; Murshed et al., 2023). Storage conditions play an important role in preserving the freshness and quality of eggs by influencing their appearance, weight, structure, taste, color, and nutritional value. Grashorn et al. (2016), also demonstrated that the main factors influencing internal egg quality are duration and temperature of storage, highlighting an important interaction between these two factors. Several authors have studied the effect of storage time and temperature on chicken egg quality. During storage, the egg begins to lose weight due to water evaporation through the membrane and pores of the shell. Based on previous studies (Wickramasinghe et al., 2013; Akter et al., 2014; Feddern et al., 2017; Martinez et al., 2021), egg weight loss increased, significantly. This decrease in weight is more pronounced in eggs stored at room temperature, achieving ~ 9% and for refrigerated eggs, this loss was only < 6% at the end of 9 weeks (Feddern et al., 2017). Storage temperature and storage duration affect the reduction of the albumen quality. This was found in the research of Jones et al. (2018) who recommended storing eggs at low temperatures to avoid problems of loss in albumen quality. Other significant ($P < 0.05$) changes that could be observed during storage time and temperature were demonstrated by Akter et al. (2014), for egg weight loss, specific gravity, Haugh Unit, pH of the albumen, albumen weight loss, increased pH of the yolk, yolk weight and percentage of yolk weight. A significant decrease in albumen, yolk, and shell weight was observed also by Murshed et al. (2023).

On the other hand, Wickramasinghe et al. (2013) studied the effect of packaging material that could be used with minimal changes in egg quality during storage at room temperature in Sri Lanka. In this case, the packaging material did not show significant changes for Haugh Unit, albumen pH, yolk pH, yolk color, and yolk index, while the effect was significant for weight loss (%) and air cell size at 32 °C.

In this regard, only a few studies have been published that have analysed egg quality during different egg storage conditions. Therefore, to further clarify this, our study aimed to determine the effects of storage temperature and duration, and packaging material on the quality of eggs during storage, until it reaches our table.

MATERIALS AND METHODS

Egg collection and preparation for storage

Three Hundred Twenty chicken eggs, collected on the day of laying, were obtained from laying hens kept in cage system, from Gjakova region and have been sent to the laboratory of the Faculty of Agriculture and Veterinary, University of Prishtina 'Hasan Prishtina', Prishtina, Kosovo. Table 1 gives the design of the experiment.

Egg storage methods description

The eggs storage methods consist of using three packing materials: cardboard, styrofoam, plastic boxes, and control (unpackaged eggs stored in glass shelf of refrigerator). Eggs packaged in each packaging material, which was closed, and stored in a refrigerator (Gorenje, Slovenia) at temperature 4–6 and at the counter at 20–22 °C. The eggs were weighed and analyzed at both storage temperatures: at the start (day 0), 7, 14, 21, and 28 days. The storage temperature was monitored daily through a digital thermometer (CombiSteel LCD Multi thermometer with ± 1 °C). Each egg was weighed with a digital analytical scale (KERN ALS 120-4N) with an accuracy of 0.01 g and the weight of each egg was recorded.

Table 1. Design of the experiment

Storage temperature, °C	Packing material	Storage duration, days				
		0	7	14	21	28
4–6 °C	Control Cardboard Styrofoam Plastic	Eight eggs for each treatment				
20–22 °C	Control Cardboard Styrofoam Plastic	Eight eggs for each treatment				

Egg weight loss

Egg weight loss was determined by weighing eggs individually at each storage time interval using a digital analytical scale with an accuracy of 0.01 g. All weights were expressed in grams and weight loss was determined as a percentage considering the difference between the initial egg weight and weight obtained at each time interval of storage, at both temperatures (4–6 °C and 20–22 °C) and in all types of packaging (cardboard, styrofoam, plastic boxes, and control). The egg weight losses (%) were calculated using the formula:

$$\textit{Weight loss}\ (\%) = [(\textit{Initial weight} - \textit{Final weight})/\textit{Initial weight}] \times 100. \quad (1)$$

External quality of chicken eggs

All external egg quality parameters (egg weight, shape index, eggshell weight, eggshell thickness, eggshell index, eggshell ratio, egg surface area and specific gravity) were evaluated on the collected day and weekly periods. The length and width of the egg was measured through a digital calliper. From these measurements was calculated egg shape index, according to the following equation:

$$\textit{Shape index} = (\textit{egg width}/\textit{egg length}) \times 100. \quad (2)$$

The surface area of the egg was calculated according to the following equation:

$$\textit{Egg surface area} = 3.9782 \times EW^{0.7056}\ \text{(Carter, 1975), EW-Egg weight.} \quad (3)$$

To calculate the specific gravity of the egg, we used the formula:

$$\textit{Specific gravity} = \textit{Egg weight}/\textit{Egg volume}. \quad (4)$$

The weight of the shell was measured using a digital analytical scale with an accuracy of 0.01 g. Meanwhile, the thickness of the shell was measured using a digital Verner calliper with an accuracy of 0.01 mm. The shell ratio was calculated by dividing the weight of the shell by the weight of the egg and multiplying by 100.The eggshell index was calculated according to the following equation:

$$\textit{Eggshell index} = (\textit{eggshell weight}/\textit{eggshell surface}) \times 100\ \text{(Ahmed et al., 2005)} \quad (5)$$

Internal quality of chicken eggs

To assess the effect of different storing condition on the internal quality of eggs (albumen weight, albumen ratio, yolk weight, yolk ratio, albumen, index, yolk index, albumen pH, yolk pH, Haugh unit, yolk colour and yolk:albumen ratio) each eggs were weightened and broken. After breaking the egg on the flat glass platform, the height of the dense albumen, the width and length of the albumen, the height of the yolk, and the width and length of the yolk were measured using a digital Vernier calliper. The intensity of the yellow colour was measured using the Roche paper color scale (1–15). In addition, the albumen was separated from the yolk, and their weights were measured. The weights of the albumen and yolk were recorded as absolute values, while the relative weights were calculated by dividing their absolute weight by the weight of the egg and expressed as a percentage. Through the pH meter (pH-mètre crison glp 21, developed and manufactured in Spain by Crison Instruments, S.A), was determined pH of the egg albumen and egg yolk. The Haugh unit was calculated after determining the egg weight and the height of the dense albumen. The following equation was used to calculate the Haugh unit:

$$Haugh\ Unit\ (HU) = 100\ log\ [h - 1.7W^{0.37} + 7.6] \text{ (Raymond Haugh, 1937)} \quad (6)$$

Statistical analysis

All data are presented as the mean of eight eggs and ± standard error of the mean (SEM). The collected data on various egg quality parameters were statistically analysed using JMP IN 7, statistical software (business unit of SAS). Tukey-Kramer HSD post hoc test was used to compare mean group differences. Differences in the mean were considered significant $P < 0.05$.

RESULTS AND DISCUSSION

The effect of storage temperature, packing material, storage duration and their interaction on egg weight and egg weight loss %

The effect of storage condition on the egg weight and egg weight loss are given in Table 2. The results of this research show that the no significant difference ($P > 0.05$) of storage temperature and storage duration was observed on egg weight. However, the type of packaging material has shown a significant influence ($P < 0.05$) on egg weight (g). This observation can be explained by the fact that the cardboard material serves as a favor for moisture absorption resulting in lower egg weight. The present finding is in line with the work of Akyurek & Okur (2009) and Martinez et al. (2021) who found that egg weight not affected ($P > 0.05$) by storage temperature, storage duration and their interaction, during 14, 10 days, respectively. Similar to our value was also reported Jin et al. (2011), who concluded that the storage duration for ten days did not affect the egg weight ($P > 0.05$) but observed significant difference ($P < 0.05$) of storage temperature on egg weight. Furthermore, the results obtained by Jin et al. (2011) showed that the interaction between storage temperature and storage duration did not affect egg weight. Yildirim (2017) studied the changes in quality characteristics during storage time of egg from layer hens fed diet supplemented with Panaxginseng Meyer leaf extract and found that the egg weight was not affected ($P > 0.05$) by storage times (28 days). When considering the interaction between ST × SD and PM × SD there were observed significant differences ($P = 0.0002$, $P = 0.0068$) in egg weight. While, the interaction

between ST × PM, as well as ST × PM × SD did not show any significant difference on egg weight ($P > 0.05$).

The mean values of EWL (%) were significantly influenced ($P < 0.05$) by storage temperature, storage duration, and packaging material (Table 2). The loss of weight and the expansion of the air cell occur due to water diffusion through the eggshell. The permeability of the eggshell is influenced by factors such as shell thickness, pore count, and the quality of the cuticle (Grashorn, et al., 2016). In our study the refrigerator demonstrated greater effectiveness in preserving the egg weight compared to ambient conditions. Significantly higher weight loss (1.98%) was observed in eggs stored at 20–22 °C than in eggs (0.93%) stored at 4–6 °C. This agrees with past works (Akyurek & Okur, 2009; Akter et al., 2014) that reported the room temperatures negatively affect ($P < 0.001$) EWL (%). Moreover, the decrease of egg weight in different storage temperature was also reported by Grashorn et al. (2016); Drabik et al. (2021); Martinez et al. (2021). These authors in their study concluded that the EWL (%) was significantly affected ($P < 0.001$) by storage temperature.

Table 2. Effect of storage temperature, packing material, storage duration and their interaction on egg weight loss, g and % (Mean ± SEM)

Treatments	Parameters		
	EW, g	EWL, g	EWL, %
Storage temperature, ºC			
20–22 °C	61.64 ± 0.47	1.25 ± 0.10^{a}	1.98 ± 0.16^{a}
4–6 °C	61.81 ± 0.59	0.58 ± 0.05^{b}	0.93 ± 0.08^{b}
Packing material, box			
Control	62.50 ± 0.78^{a}	1.10 ± 0.15^{a}	1.69 ± 0.22^{a}
Cardbox	59.93 ± 0.76^{b}	1.03 ± 0.13^{a}	1.70 ± 0.21^{a}
Styrofoam	62.54 ± 0.75^{a}	0.86 ± 0.10^{b}	1.36 ± 0.16^{b}
Plastic	61.94 ± 0.70^{a}	0.66 ± 0.10^{c}	1.06 ± 0.16^{c}
Storage duration, day			
7	62.07 ± 0.88	0.44 ± 0.03^{d}	0.72 ± 0.05^{d}
14	62.61 ± 0.90	0.89 ± 0.09^{c}	1.38 ± 0.13^{c}
21	62.24 ± 0.76	1.29 ± 0.09^{b}	2.07 ± 0.14^{b}
28	60.67 ± 0.82	1.94 ± 0.15^{a}	3.09 ± 0.23^{a}
P value			
ST	ns	< .0001	< .0001
PM	0.0264	< .0001	< .0001
SD	ns	< .0001	< .0001
ST × PM	ns	0.0019	0.0018
ST × SD	0.0002	< .0001	< .0001
PM × SD	0.0068	< .0001	< .0001
ST × PM × SD	ns	ns	ns

EW – Egg weight; EWL – Egg weight loss; ST – Storage temperature; PM – Packing material; SD – Storage duration, ns – non significant. ^{abcd}Means with different superscripts within the same column are significantly different at $P < 0.05$.

Table 2 shows that the type of packaging material has a significant effect on EWL percent ($P < 0.05$). The maximum EWL (%) were recorded at cardboard boxes (1.70%) and at control group (1.69%), compared to eggs stored in styrofoam and plastic packaging. This can happen because cardboard box has a higher potential to absorb

moisture. Also, this observation can be explained by the fact that the plastic and styrofoam material served as a barrier to moisture loss, resulting in lower EWL percentage (1.36% and 1.06%, respectively). Our results are somewhat in agreement with previous study reports in which significant changes ($P < 0.05$) of EWL percentage have also occurred on eggs stored as uncoated (control) (Jariyapamornkoon et al., 2023) and cardbox material (Wickramasinghe et al., 2013). In case of uncoated eggs showed significantly higher weight loss compared to coated eggs. It is important to note that similar results to ours, regarding the influence of packaging material on egg weight loss percentage ($P < 0.05$) have also been reported by Drabik et al. (2021). According to them the lowest percentage of egg weight losses were recorded at eggs stored in plastic boxes.

The study revealed that the EWL (%) was ($P < 0.05$) affected by storage duration. Similarly, to previous statement, interaction between ST × PM, ST× SD and PM × SD did affect ($P > 0.05$) the EWL percentage. There was no significant difference ($P > 0.05$) in EWL percentage when the three factors interacted (storage temperature, packing material and storage duration). Our study showed, as the storage time increases, changes occur in the weight and inside of the egg. Greatest weight loss was observed from day 21 to day 28 (1.02%). From the day 7–14, the egg had smaller weight loss by 0.66%. On the other hand, between days 14 and 21, the eggs experienced a 0.69% weight loss. This was due to the release of water from the egg albumen through the pores of the eggshell. This reality is supported by other researcher (Jin et al., 2011; Wickramasinghe et al., 2013; Grashorn, 2016; Martinez et al., 2021; Murshed et al., 2023; Jariyapamornkoon et al., 2023) who found that storage time significantly affected egg weight loss. Martinez et al. (2021) and Jin et al. 2011 reported similar results ($P < 0.05$) to our findings for the effect of interaction between storage duration and storage time in EWL (%). The results reported by Drabik et al. (2021) and Martinez et al. (2021) for the effect of interaction between ST × SD on egg weight losses is also similar to those derived from our research.

The effect of storage temperature, packing material, storage duration and their interaction on the external quality of eggs

The external quality of the egg and in particular the shell is very important for the processing industry and food safety. The results of external quality of chicken eggs were summarized in Table 3. The storage temperature, packing material, storage duration and interaction between them, had statistically no significant ($P > 0.05$) influence for shape index. Similar observation was also reported by Akyurek & Okur (2009); Yildirim (2017); Uyanga et al. (2020) and Murshed et al. (2023). They stated that storage duration for 14, 28, 10 and 30 days, respectively, did not significantly ($P > 0.05$) affected shape index. The results are in conformity also with the findings of Akter et al. (2014) who reported that shape index was not affected ($P > 0.05$) by storage temperature and storage duration. No significant difference ($P > 0.05$) of interaction between ST × SD and storage duration in shape index was also observed by other researcher (Akyurek & Okur, 2009). The changes of egg surface area (cm^{-2}) at eggs stored in refrigerator and those stored at room temperature was non–significantly ($P > 0.05$). Also, there were no significant changes to the ESA (cm^{-2}) even during storage and interaction of ST × PM, ST × SD, PM × SD and ST × PM × SD. Another researcher (Yildirim, 2017) was noticed similar trend in ESA (cm^{-2}) after storage duration. Meanwhile, the results of the packing material on the ESA (cm^{-2}) are at the limit of statistical significance ($P = 0.0452$). Our research shows (Table 3) that ST, PM and SD significantly influenced

($P < 0.05$) the specific gravity of eggs (ESG, g cm^{-3}). A slight decrease in ESG was recorded with increasing storage temperature from 4–6 to 20–22 °C (1.080 g cm^{-3}and 1.076 g cm^{-3} respectively). The egg specific gravity is a physical parameter related to the moisture loss from the egg or the weight of the egg. The higher ESG was recorded at eggs stored in plastic box (0.028, 0.005 and 0.003 score, respectively) compared with control, cardboard and styrofoam box. On the other hand, no similar finding obtained by Drabik et al. (2021), who explained that the packing material did not cause changes in egg specific gravity. A significant decrease of ESG ($P < 0.05$) was recorded with increasing in storage duration. The specific gravity of eggs was decreased from maximum of 1.104 g cm^{-3} recorded on the day of eggs collection to a minimum of 1.054 g cm^{-3} observed after 28 days' storage (Table 3). The interaction of ST × PM, ST × SD, PM × SD and ST × PM × SD on the specific gravity of the eggs was also significant ($P < 0.05$). Overall, the interaction between storage temperature, packaging material and storage duration creates a complex but crucial factor in maintaining egg quality. By understanding these interactions, we can ensure that optimal storage conditions positively affect specific gravity, thereby providing fresher and higher quality eggs for a longer period.

Table 3. Effect of storage temperature, packing material, storage duration and their interaction on external egg parameters (Mean ± SEM)

Treatments	Parameters		
	SI, %	ESA, cm^{-2}	ESG, g cm^{-3}
Storage temperature, °C			
20–22 °C	79.09 ± 0.51	72.84 ± 0.40	1.076 ± 0.02^{b}
4–6 °C	78.37 ± 0.24	72.95 ± 0.49	1.080 ± 0.02^{a}
Packing material, box			
Control	78.46 ± 0.35	73.54 ± 0.65	1.064 ± 0.02^{b}
Cardbox	77.89 ± 0.40	71.39 ± 0.64	1.087 ± 0.01^{ab}
Styrofoam	78.47 ± 0.41	73.58 ± 0.62	1.089 ± 0.02^{ab}
Plastic	80.08 ± 0.88	73.08 ± 0.58	1.092 ± 0.01^{a}
Storage duration, day			
0	80.30 ± 1.10	73.62 ± 0.74	1.104 ± 0.10^{a}
7	77.56 ± 1.10	73.18 ± 0.70	1.078 ± 0.02^{b}
14	79.05 ± 0.34	73.62 ± 0.74	1.061 ± 0.01^{c}
21	78.37 ± 0.43	73.34 ± 0.66	1.055 ± 0.01^{d}
28	78.36 ± 0.43	72.00 ± 0.69	1.054 ± 0.00^{d}
P value			
ST	ns	ns	< .0001
PM	ns	0.0452	0.0073
SD	ns	ns	< .0001
ST × PM	ns	ns	0.0065
ST × SD	ns	ns	< .0001
PM × SD	ns	ns	0.0033
ST × PM × SD	ns	ns	< .0001

SI – Shape index; ESA – Egg surface area; ESG – Egg specific gravity; ST – Storage temperature; PM – Packing material; SD – Storage duration. ^{abcdfgh}Means with different superscripts within the same column are significantly different at ($P < 0.05$).

External parameters of eggs, such as shape, surface area, thickness, etc. play a decisive role not only in determining the egg quality but also in consumer preference. Therefore, storage conditions, such as: temperature, packaging and storage duration can affect the external parameters of the eggs.

Besides the storage duration, the interaction between ST × SD, PM × SD and ST × PM× SD affected the ESW, g. Other factors (ST, PM and ST × PM) and their interaction did not affect the ESW, g. The results of our research, presented in Table 4, show that the SD has also affected EST and ESI. Our results are not in line with those of other authors (Murshed et al., 2023) who observed that the storage duration did not affect significantly ($P > 0.05$) eggshell weight. The longer eggs are stored the integrity of the eggshell may deteriorate slightly. This could happen because of the weakening of the eggshell structure or microcracks that develop over time, leading to a decrease in eggshell weight. Therefore, in present research, the decreasing of eggshell thickness is associated with changes in the eggshell weight during storage and with a decrease of the eggshell index.

Table 4. Effect of storage temperature, packing material, storage duration and their interaction on eggshell parameters (Mean ± SEM)

Treatments	Parameters			
	ESW, g	ESW, %	EST, mm	ESI
Storage Temperature (ST), °C				
20–22 °C	7.46 ± 0.06	12.13 ± 0.07	0.44 ± 0.01^{a}	10.24 ± 0.06
4–6 °C	7.52 ± 0.08	12.21 ± 0.11	0.51 ± 0.01^{b}	10.32 ± 0.08
Packing Material (PM), box				
Control	7.63 ± 0.08	12.25±0.11	0.49±0.02	10.38 ± 0.08
Cardbox	7.37 ± 0.10	12.31±0.11	0.47±0.02	10.32 ± 0.09
Styrofoam	7.39 ± 0.08	11.87±0.15	0.48±0.02	10.06 ± 0.11
Plastic	7.57 ± 0.10	12.24±0.13	0.46±0.02	10.36 ± 0.11
Storage duration (SD), day				
0	7.73 ± 0.13^{a}	12.48 ± 0.18	0.57 ± 0.02^{a}	10.56 ± 0.014^{a}
7	7.47 ± 0.09^{ab}	11.96 ± 0.12	0.59 ± 0.01^{a}	10.14 ± 0.09^{b}
14	7.54 ± 0.10^{ab}	12.16 ± 0.18	0.31 ± 0.02^{d}	10.30 ± 0.13^{ab}
21	7.28 ± 0.09^{b}	12.03 ± 0.12	0.51 ± 0.01^{b}	10.11 ± 0.09^{b}
28	7.44 ± 0.09^{ab}	12.21 ± 0.11	0.40 ± 0.01^{c}	10.27 ± 0.08^{ab}
P value				
ST	ns	ns	< .0001	ns
PM	ns	ns	ns	ns
SD	0.0203	ns	< .0001	0.0397
ST × PM	ns	ns	0.0092	ns
ST × SD	0.0378	ns	0.0013	ns
PM × SD	0.0038	ns	0.0062	ns
ST × PM × SD	0.0401	ns	ns	ns

ESW – Egg shell weight; EST – Egg shell thickness; ESI – Egg shell index; ST – Storage temperature; PM – Packing material; SD – Storage duration. ^{abcd}Means with different superscripts within the same column are significantly different at ($P < 0.05$).

At the end of the storage period, the eggshell thickness decreased by 29.82%. Similarly, Alshaikhi et al. (2020), Grashorn et al. (2016) and Sekeroglu et al. (2016) in their research found that the eggshell thickness was negatively influenced ($P < 0.05$) by storage duration. On the other hand, Murshed et al. (2023) reported that the storage

duration did not affect eggshell thickness ($P > 0.05$). Our results are in contrast with the findings of Lee et al. (2016), who reported that storage duration showed no significant effect on eggshell thickness. Our findings are in line with Martinez et al. (2021) and Camargo et al. (2021), who found significant difference for eggshell thickness during storage ($P < 0.05$). The decrease in eggshell index during storage (2.75%) may have been due to changes in ESW (g) and EST. The combined effects of ST × SD, PM × SD and ST × PM × SD (as shown in Table 4), significantly affected ($P < 0.05$) ESW (g). At the end of the storage period, the eggs stored at 4–6 °C, recorded a greater decrease of ESW (5.12%), compared to those that were stored for the same period of storage but at 20–22 °C (2.10%), respectively. Eggs stored in plastic box at the end of the storage period recorded a greater decrease in ESW (9.46%) compared to those stored in cardboard, styrofoam boxes and the control group, which recorded a decrease of ESW for 8.30, 3.24 and 6.81%. At the end of the storage period, the results of the present study showed (Table 4) that the eggs stored at 4–6 °C and packed in cardboard boxes recorded a greater decrease of ESW (19.08%), while the smallest decrease of ESW during storage (7.24%) was recorded in eggs stored at 20–22 °C and packed in plastic boxes. Moreover, EST was found to be statistically influenced ($P < 0.05$) by the interaction of ST × PM, ST × SD and PM × SD. Eggs of the control group, those in styrofoam, plastic and cardboard boxes, stored at 4–6 °C recorded 21.52, 10.00, 14.29 and 6.12% thicker eggshells compared to those stored at 20–22 °C. Eggs stored at 20–22 °C at the end of the storage period had 9.20% thinner shells compared to those stored at 4–6 °C. Martinez et al. (2021) have found a significant difference of interactions between ST × SD on eggshell thickness ($P < 0.001$). Our results are contrary to those of Grashorn et al. (2016) and Lee et al. (2016), who found that the eggshell thickness was not affected ($P > 0.05$) by interaction between ST × SD. At the end of the storage period (28 days), the eggs of the control group, those stored in styrofoam, plastic and cardboard boxes, recorded a decrease in eggshell thickness for 26.79, 36.80, 25.14 and 24.96%, respectively. In the case of our study, it can be assumed that eggshell weight can be an indicator of shell thickness and vice versa. The weight of the eggshell can influence the eggshell index because ESI is a calculated value that considers the ratio between shell weight and egg surface area, expressed as a percentage. A heavier eggshell generally contributes to a higher ESI, indicating a greater amount of eggshell material present. Kibala et al. (2018), in their study showed that eggshell thickness is closely related and is an indicator of other eggshell quality traits.

The effect of storage temperature, packing material, storage duration and their interaction on the internal quality of eggs

Inappropriate egg storage conditions can have negative effects on the freshness, structure and safety of chicken eggs, compromising their internal quality. Internal quality is assessed by albumen and yolk quality.

The present study (Table 5) shows that the storage temperature did not affect ($P > 0.05$) albumen weight and ratio. The AW, g from eggs stored at 20–22 °C decreased slightly (0.29%), but not significantly. This is not consistent with finding of Kim et al. (2024), who claimed that the storage temperature does affect albumen weight significantly ($P < 0.01$). Our results are in harmony with the Addo (2016), who presented the fact that the storage temperature did not affect significantly albumen ratio ($P > 0.05$) but interaction of different storage temperature and different storage duration significantly influenced

($P < 0.05$) albumen ratio. The albumen index was significantly ($P < 0.05$) affected by storage temperature. The eggs stored at 4–6 °C had a higher albumen index (41.37%) than those stored at 20–22 °C. Similar to our study, some researchers (Altunatmaz et al., 2020) found that the storage temperature negatively affects the albumen index ($P < 0.05$).

Table 5. Effect of storage temperature, packing material, storage duration and their interaction on egg albumen parameters (Mean ± SEM)

Treatments	Parameters				
	AW, g	AR, %	AI, %	ApH	HU
Storage Temperature, °C					
20–22 °C	38.35 ± 0.39	62.12 ± 0.25	2.65 ± 0.08^{b}	9.30 ± 0.02^{a}	59.48 ± 1.01^{b}
4–6 °C	38.46 ± 0.49	62.09 ± 0.29	4.52 ± 0.13^{a}	8.97 ± 0.03^{b}	74.46 ± 1.00^{a}
Packing Material, box					
Control	39.15 ±0.63^{a}	62.54 ± 0.37	3.55 ± 0.19	9.14 ± 0.04	69.10 ± 1.52
Cardbox	36.83 ± 0.59^{b}	61.36 ± 0.34	3.53 ± 0.19	9.17 ± 0.03	69.96 ± 1.41
Styrofoam	39.17 ± 0.67^{a}	62.48 ± 0.48	3.36 ± 0.20	9.10 ± 0.07	67.75 ± 1.56
Plastic	38.48 ± 0.56^{ab}	62.04 ± 0.29	3.88 ± 0.22	9.13 ± 0.03	70.16 ± 1.54
Storage Duration, day					
0	39.21 ± 0.67	63.10 ± 0.46^{a}	2.78 ± 0.11^{c}	8.91 ± 0.04^{b}	72.47 ± 0.40^{a}
7	39.03 ± 0.75	62.20 ± 0.40^{ab}	3.87 ± 0.20^{a}	9.13 ± 0.08^{a}	72.11 ± 0.57^{a}
14	38.76 ± 0.68	62.15 ± 0.46^{ab}	4.23 ± 0.22^{a}	9.20 ±0.04^{a}	71.36 ± 1.50^{a}
21	37.67 ± 0.69	61.97 ± 0.38^{ab}	3.78 ± 0.24^{ab}	9.22 ± 0.04^{a}	69.84 ± 1.97^{a}
28	37.36 ± 0.68	61.10 ± 0.37^{b}	3.25 ± 0.26^{bc}	9.21 ± 0.03^{a}	60.43 ± 2.28^{b}
P value					
ST	ns	ns	< 0.0001	< 0.0001	< 0.0001
PM	0.0242	ns	ns	ns	ns
SD	ns	0.0173	< 0.0001	< 0.0001	< 0.0001
ST × PM	ns	ns	ns	ns	ns
ST × SD	0.0004	0.0340	< 0.0001	0.0003	< 0.0001
PM × SD	0.0109	ns	ns	ns	ns
ST × PM × SD	ns	ns	0.0313	ns	ns

AW – Albumen Weight; AR – Albumen Ratio; AI – Albumen Index; ApH – Albumen pH; HU – Haugh Unit; ST – Storage temperature; PM – Packing material; SD – Storage duration. ^{abcdfgh}Means with different superscripts within the same column are significantly different at ($P < .05$).

Statistical analysis identified additional significant differences ($P < 0.05$) in eggs stored at different temperatures, specifically in albumen pH and Haugh Unit values. The ApH for eggs stored at higher temperatures was 0.33 unit higher or more alkaline than those stored at lower temperatures. Previous studies (Luo et al., 2020) also reported that albumen pH was significantly ($P < 0.05$) affected by storage temperature. After the laying of the egg, carbon dioxide begins to be released from the white, and when the eggs are stored at a higher temperature, the CO_2 release becomes more active. In this case, the egg albumen becomes more alkaline and can provide an antibacterial defence system (Guyot et al., 2016). The present study showed that the HU value was lower by 14.98 units or 20.12% in eggs stored at refrigerator temperature compared with those stored at room temperature. Similarly, Wlaźlak et al. (2024) observed significant influence ($P < 0.001$) of storage temperature on HU of duck eggs. They reported that the storing eggs at a higher (17 °C) temperature resulted in lower height of thick albumen a lower HU value (60.87) than the other stored in 7 °C (72.08). Although the weight of

albumen changed significantly ($P < 0.05$) with the change of packaging material, the changes of AR, AI, ApH and HU were not so large ($P > 0.05$). This is in line with the work of Drabik et al. (2021) who found that the type of packing material significantly ($P < 0.05$) contributed to the changes of albumen weight, g. It was also observed that the HU was better at eggs stored at plastic material (70.16), and the lowest value of HU registered at eggs of control group (69.10) but these changes were not significant ($P > 0.05$). A similar observation ($P > 0.05$) was also reported by another researcher (Drabik et al., 2021).

Our results regarding the influence of storage duration on albumen parameters are presented in Table 5. The main effect of storage duration on the AR, AI, ApH and HU were highly significant ($P < 0.05$), while on the AW were non-significant ($P > 0.05$). As the storage period changed, the albumen parameters also changed. Results showed that albumen ratio decreased by 1.44, 1.52, 1.81 and 3.22% after the first, second, third and fourth week, respectively. These differences were more noticeable after the first week, and between the third and fourth weeks (1.44 and 1.41%, respectively). Findings in our study showed that the albumen index changed significantly as a storage duration increased ($P < 0.05$). The AI in fresh eggs was 2.78%, increasing it to 3.25% at the end of storage period. This trend of increasing albumen index during the storage period in this study aligns with the findings of Ondrušíková et al. (2018), who also reported an increase in albumen index at the end of the fourth week (from 9.37 at fresh eggs to 10.47% at fourth week), at quail eggs. In their research the albumen index in the first, second and fourth weeks was higher (11.35, 10.19 and 10.47%), than at the beginning of the experiment (9.37%). The data regarding albumen pH presented in Table 5 revealed significant differences ($P < 0.05$) in pH with the storage duration. The pH value of the egg albumen increased from 8.91 to 9.21. These results agree with reports of Kocetkovs et al. (2022), who found the significant effect of storage duration on albumen pH. Egg albumen naturally becomes more alkaline (higher pH) as they age due to the loss of carbon dioxide and changes in the way proteins interact (Kocetkovs et al., 2022). Our data clearly demonstrates that the Haugh unit was influenced ($P < 0.05$) by storage duration. The results showed that the freshness of the eggs decreased drastically at the end of the storage period, resulting in a drop in HU from 72.47 to 60.43, making them unusable for the consumer. This is attributed to the continuous reduction of egg weight and albumen height. Our findings were also confirmed by Martinez et al. (2021), who reported that the storage duration significantly affected ($P < 0.05$) the HU, decreasing it from 101.63 to 79.17 after 10 days.

Our results show that the egg albumen parameters included in our research were not affected by the interaction between ST × PM. On this case, results recorded from our study are in contrast with the findings of Drabik et al. (2021), who reported significant influence ($P < 0.05$) of interaction between ST × PM on albumen weight and ratio and Haugh unit. But same as our results they did not find significant differences ($P = 0.136$) of these interaction on albumen pH. On the other hand, the interaction between ST × SD caused significant ($P < 0.05$) changes in all albumen parameters. At the end of the storage period (28 days), the albumen weight of eggs stored at 20–22 °C decreased progressively by 10.76%, while the albumen weight of eggs stored at 4–6 °C at the end of this period decreased by 5.59%. Albumen weight also decreased due to the interaction effects of PM × SD ($P < 0.05$). At the end of the storage period (28 days), greatest loss was recorded for eggs stored in cardboard boxes (14.29%). While eggs stored in plastic

boxes recorded lower weight loss of albumen (1.94%). The interaction between three factors (ST × PM × SD) changed the albumen index and these changes are significantly different ($P < 0.05$). The lower albumen index (1.91) observed at eggs stored in cardboard box, at 20–22 °C for 28 days.

The results of our research presented in Table 6 showed that the yolk height and yolk index were significantly influenced by storage temperature ($P < 0.05$). The yolk height of eggs stored at 20–22 °C was 17.18% lower compared to those stored at 4–6 °C.

Table 6. Effect of storage temperature, packing material, storage duration and their interaction on egg yolk parameters (Mean ± SEM)

Treatments	Parameters			
	YW, g	YW, %	YH, mm	YI, %
Storage Temperature, °C				
20–22 °C	15.83 ± 0.15	25.75 ± 0.23	13.84 ± 0.23	32.27 ± 0.68^{b}
4–6 °C	15.82 ± 0.16	25.70 ± 0.25	16.71 ± 0.19	42.26 ± 0.56^{a}
Packing Material, box				
Control	15.72 ± 0.24	25.21 ± 0.35	15.40 ± 0.32	37.54 ± 1.02
Cardbox	15.73 ± 0.22	26.32 ± 0.31	15.10 ± 0.34	36.78 ± 1.06
Styrofoam	15.98 ± 0.25	25.65 ± 0.40	15.04 ± 0.37	36.48 ± 1.13
Plastic	15.88 ± 0.16	25.72 ± 0.26	15.56 ± 0.42	38.27 ± 1.30
Storage Duration, day				
0	15.13 ± 0.28^{b}	24.42 ± 0.41^{b}	14.68 ± 0.26^{c}	36.08 ± 0.79^{bc}
7	16.11 ± 0.22^{a}	25.84 ± 0.36^{a}	16.72 ± 0.26^{a}	40.10 ± 0.77^{a}
14	15.94 ± 0.23^{a}	25.68 ± 0.36^{a}	16.18 ± 0.34^{ab}	39.57 ± 1.12^{a}
21	15.70 ± 0.19^{ab}	26.00 ± 0.35^{a}	15.60 ± 0.34^{bc}	37.83 ± 1.26^{ab}
28	16.26 ± 0.25^{a}	26.68 ± 0.33^{a}	13.20 ± 0.52^{d}	32.77 ± 1.77^{c}
P value				
ST	ns	ns	< 0.0001	< 0.0001
PM	ns	ns	ns	ns
SD	0.0094	0.0006	< 0.0001	< 0.0001
ST × PM	ns	ns	ns	0.0470
ST × SD	0.0360	ns	< 0.0001	< 0.0001
PM × SD	ns	ns	ns	0.0262
ST × PM × SD	ns	ns	0.0166	ns

YW – Yolk Weight; YH – Yolk Height; YI – Yolk Index.ST – Storage temperature; PM – Packing material; SD – Storage duration. ^{abcdfgh}Means with different superscripts within the same column are significantly different at ($P < 0.05$).

The eggs stored at a higher temperature resulted in a lower yolk index (32.27). The changes in YH and YI observed in our study are similar those noticed in previous studies (Feddern et al., 2017; Drabik et al., 2021). They reported that the storage temperature significantly affects yolk index ($P < 0.05$). The effect of storage temperature on YW, yolk pH, YC and Y:A ratio was found to be statistically insignificant ($P > 0.05$). In contrast to our results, Kim et al. (2024) reported that yolk weight, yolk ratio and yolk pH were affected by changing storage temperature ($P < 0.05$). Similar to our results they reported that yolk colour was not affected by storage temperature ($P > 0.05$). Also, Drabik et al. (2021) reported that the yolk weight was affected ($P < 0.05$) by storage temperature. No significant differences ($P > 0.05$) were observed in egg yolk parameters when considering the effect of storing in different packing material. Similarly, Drabik et

al. (2021) found a non-significant effect of packing in the YW, YR, YC and YI. Egg yolk parameters (except pH) changed significantly ($P < 0.05$) with increasing storage time. Yolk weight (g) has increased by 7.47% during the storage period (28 days), while the yolk ratio also increased from 24.42 to 26.68%. This effect has been previously discussed by Murshed et al. (2023), Wengerska et al. (2023) and Jin et al. (2011). In their research they found that the storage duration significantly affected ($P < 0.05$) yolk weight. Carvalho et al. (2023) and Adamski et al. (2017) reported that the yolk weight increased during storage because of water diffusion from albumen through the vitelline membrane into the yolk. But the storage period in their study did not affect ($P > 0.05$) yolk weight. The value of yolk height was increased by 13.90, 10.22 and 6.27% at day 7, 14 and 21, respectively. But at the end of storage period (day 28) the yolk height decreases by 10.08%. Some similar changes were found in the YI. The yolk index was increased at the end of the first week of storage (11.14%), while after the first week it again began to decrease. So, from 7–14, 14–24 and 21–28 the YI decrease by 1.32%, 4.40% and 13.32%. Moreover, this index recorded a decrease from 36.08 to 32.77 or 9.17% during all storage period (0–28 days). Other authors (Carvalho et al. 2023) also confirmed the influence of storage duration on yolk height and yolk index. In our case, a reduction in yolk height (from 14.68 to 13.20 mm) contributed to a lower yolk index (from 36.08 to 32.77%), and these changes were significant ($P < 0.05$).

The colour is an important sensory index of preserved eggs (Luo et al., 2020). The yolk colour was adversely affected by the length of storage, decreasing by 6.03%. Similar results were presented by other researcher (Murshed et al. 2023, Wengerska et al., 2023 and Lee et al., 2016) who showed significant changes in yolk colour depending of storage duration.

As observed in our research (Table 7) the duration of storage has an effect on Y:A ratio. This ratio increased by 12.58%. While not a definitive indicator, this is because albumen loses moisture more easily than yolk during storage, which can potentially affect the ratio. A higher Y:A ratio can generally indicate a higher concentration of nutrients in the egg yolk and making it more flavourful.

Interaction effects between ST × PM were significantly lower ($P < 0.05$) in terms of egg yolk index. The yolk index in the eggs of the control group, those packed in plastic, cardboard and styrofoam boxes and stored at a temperature of 20–22 °C was lower (33.16, 31.82, 32.21 and 31.89%) compared to the eggs stored at temperature 4–6 °C and that had the same storage packages (41.92, 44.72, 41.35 and 41.06%), respectively. There was no effect ($P > 0.05$) of ST × PM interaction on the YW (g and %), YH, YpH, YC and Y:A ratio. The same trend as our findings (except yolk index) were reported by Drabik et al. (2021), who confirm that the interaction between the ST × PM were not affected ($P < 0.05$) the change in the YW (g), YC and YpH.

In terms of egg yolk quality parameters (Table 6), it was found that the YW, YH and YI were significantly influenced ($P < 0.05$) by the interaction of ST × SD, while the other parameters (Table 6 and 7) yolk ratio, YpH, YC and Y:A ratio did not differ significantly ($P > 0.05$).

Eggs stored at 20–22 °C for 28 days showed a significant (8.38%) increase in yolk weight (from 14.79 to 16.03 g). While eggs stored at a temperature of 4–6 °C for the same storage period showed a 6.53% increase in yolk weight (from an initial value of 15.47 to 16.48 g). This indicates greater albumen degradation at higher temperatures, resulting in a higher capacity for the yolk to absorb moisture from the albumen. The

interaction between storage temperature and storage duration affected also yolk height, which is directly related to yolk index. In this study, eggs stored at a lower temperature at the end of the storage period resulted in an increase in yolk height from 14.65 to 16.25 mm (10.92%), while those stored for 28 days at a higher temperature, the height was reduced from 14.70 to 10.15 mm (30.95%). The same trend has occurred in the yolk index. After 28 days of storage at 4–6 °C, the eggs showed an increase (19.80%) of egg yolk index, while those stored at 20–22 °C resulted in a high decrease of this index by 33.22%, which directly related with their height and diameter. The results of the study conducted by Madrigal-Portilla et al. (2023), also proved that the interaction between storage duration and storage temperature does not lead to a significant change ($P > 0.05$) in the colour of the yolk.

Table 7. Effect of storage temperature, packing material, storage duration and their interaction on egg yolk pH, colour and yolk:albumen ratio (Mean ± SEM)

Treatments	Parameters		
	YpH	YC, Roche	Y:A
Storage Temperature, °C			
20–22 °C	6.29 ± 0.02	12.22 ± 0.06	41.65 ± 0.53
4–6 °C	6.36 ± 0.06	12.24 ± 0.05	41.65 ± 0.59
Packing Material, box			
Control	6.34 ± 0.08	12.18 ± 0.08	40.54 ± 0.81
Cardbox	6.32 ± 0.04	12.24 ± 0.09	43.10 ± 0.74
Styrofoam	6.38 ± 0.08	12.16 ± 0.07	41.39 ± 0.93
Plastic	6.25 ± 0.03	12.34 ± 0.09	41.59 ± 0.61
Storage Duration, day			
0	6.21 ± 0.10	12.77 ± 0.12^{a}	38.95 ± 0.91^{b}
7	6.41 ± 0.09	12.05 ± 0.03^{b}	41.74 ± 0.83^{a}
14	6.38 ± 0.03	12.17 ± 0.07^{b}	41.58 ± 0.89^{a}
21	6.28 ± 0.04	12.15 ± 0.07^{b}	42.15 ± 0.82^{a}
28	6.34 ± 0.03	12.00 ± 0.05^{b}	43.85 ± 0.81^{a}
P value			
ST	ns	ns	ns
PM	ns	ns	ns
SD	ns	< 0.0001	0.0020
ST × PM	ns	ns	ns
ST × SD	ns	ns	ns
PM × SD	ns	ns	ns
ST × PM × SD	0.0072	ns	ns

YpH – Yolk pH; YC – Yolk color; Y:A – Yolk:Albumen ratio; ST – Storage temperature; PM – Packing material; SD – Storage duration. ^{abcdfgh}Means with different superscripts within the same column are significantly different at ($P < 0.05$).

No significant differences ($P > 0.05$) were determined in YW (g and %), YH, YpH, YC and Y:A ratio, because of the interaction effect between PM × SD. This interaction showed its effect ($P < 0.05$) on the yolk index. On the seventh day of storage, the eggs of the control group recorded an increase in the yolk index from 38.56–42.48%, but at the end of the storage period YI decreased to 33.41%. The same trend has also occurred in the eggs placed in plastic box, where the yolk index on the seventh day marked an increase from 37.68 to 41.53%, while at the end of the storage period (28 days) the yolk

index decreased to 33.65%. In eggs stored in cardboard boxes at the end of the storage period YI decreased from 35.45 to 31.80%. The yolk index of eggs stored in styrofoam box, at the end of the storage period, recorded a decrease from 32.62 to 32.22% or 1.23%, respectively.

The yolk height of the eggs of the control group, those packed in cardboard, styrofoam and plastic boxes increased significantly by 7.89, 2.67, 18.48 and 15.58% during the storage periods at 4–6 °C. On the other hand, eggs stored at 20–22 °C resulted in a significant decrease in yolk height, with 30.26, 29.17, 26.39 and 15.00%, respectively. This decrease in the height of the yolk may occur due to the storage of eggs at high temperature, which affects the deterioration of the structure of the vitelline membrane (Bulut & Aygun, 2023).

This study discovered that the interaction between ST × PM × SD significantly affect ($P < 0.05$) YH and YpH. At the end of the storage period, eggs of the control group stored at 4–6 °C recorded a significant decrease in yolk pH from 7.23 to 6.19. Also, eggs placed in styrofoam boxes and stored at 4–6 °C, at the end of the storage period, showed a significant decrease in yolk pH from 7.06 to 6.49. While the eggs placed in plastic and cardboard boxes and stored at a temperature of 4–6 °C, did not record significant changes in yolk pH at the end of storage period. Regarding the eggs stored at 20–22 °C, in all forms of packaging (cardboard, styrofoam and plastic), including those of the control group, at the end of the storage period, the pH of the yolk increased from 6.04 to 6.43; 6.10 to 6.48; 6.14 to 6.24 and 6.13 to 6.28, respectively, but this increase was not significant. No recent data was found regarding the effect of storage temperature, storage duration and packing material on yolk height and yolk pH.

CONCLUSION

Based on the results reported herein, the main conclusion is that most influential factor is storage duration followed by storage temperature. The effect of storage duration is observed on almost all internal egg quality parameters, being most expressed after 14 days of storage. The study reconfirmed results of other studies related to negative effect of high storage temperature (20–22 °C), on critical egg quality parameters, such as egg weight loss, albumen index, pH, Haugh unit, yolk height, and yolk index. Packing material affected few external parameters and just albumen weight. However, further studies on the effects of storage condition (temperature and duration), different packing material and their interaction on egg quality are recommended.

REFERENCES

Adamski, M., Kuźniacka, J., Czarnecki, R., Kucharska-Gaca, J. & Kowalska, E. 2017. Variation in egg quality traits depending on storage conditions. *Polish Journal of Natural Science* **32**(1), 39–47.

Addo, A. 2016. *Impact of egg storage duration and storage temperature on egg quality, fertility, hatchability and chick quality, of naked neck chickens' egg*. A Master of Philosophy thesis, Department of Animal Science, Kwame Nkrumah University of Science and Technology, Kumasi, Ghana.

Ahmed, A.M.H., Rodriguez-Navarro, A.B., Vidal, M.L., Gautron, J., Garcia-Ruiz, J.M. & Nys, Y. 2005. Changes in eggshell mechanical properties, crystallographic texture andin

matrix proteins induced by moult in hens. *British Poultry Science* **46**(3), 268–279. doi: 10.1080/00071660500065425

Akter, Y., Kasim, A., Omar, H. & Sazili, A.Q. 2014. Effect of storage time and temperature on the quality characteristics of chicken eggs. J*ournal of Food, Agriculture & Environment* **12**(3&4), 87–92.

Akyurek, H. & Okur, A.A. 2009. Effect of storage time, temperature and hen age on egg quality in free-range layer hens. *Journal of Animal and Veterinary Advances* **8**(10), 1953–1958.

Alshaikhi, A.M., Abdullatif, A.A., Badwi, M.A. & Alsobayel, A.A. 2020. Effects of Storage Period, Marketing Channels and Season on Internal and External Quality of Commercial Table Eggs Marketed in Riyadh City (Saudi Arabia). *Brazilian Journal of Poultry Science* **23**(1), 001–010. dpi: 0.1590/1806-9061-2020-1334

Altunatmaz, S.S., Aksu, F., Bala, D.A., Akyazi, I. & Çelik, C. 2020. Evaluation of quality parameters of chicken eggs stored at different temperatures. *Kafkas Universitesi Veteriner Fakultesi Dergisi* **26**(2), 247–254. doi: 10.9775/kvfd.2019.22856

Anene, D.O., Akter, Y., Thomson, P.C., Groves, P. & O`Shea, C.J. 2023. Effect of restricted feeding on hen performance, egg quality and organ characteristics of individual laying hens. *Animal Nutrition* **14**, 141–151. doi: 10.1016/j.aninu.2023.05.001

Bulut, C. & Aygun, A. 2023. The Effect of Different Layer Genotypes Raised in The Free-range System on Egg Quality Storage at Different Temperatures. *Poultry Studies* **20**(2), 42–51. doi: 10.34233/jpr.1408022

Camargo, S.M.P., Ferrraz de Oliveira, N., Cordeiro, D.A., Freitas de Oliveira, H., Carvalho, D.P., Rocha, C.H.R., Racanicci, A.M.C., Barros de Carvalho, F. & Stringhini, J.H. 2021. Environment type and storage period on eggshell quality of laying hens at different ages. *Ciência Rural, Santa Maria* **52**(1). doi: 10.1590/0103-8478cr20200908

Carter, T.C. 1975. The hen's egg: A rapid method for routine estimation of flock means shell thickness. *British Poultry Science* **16**, 131–143.

Carvalho, D.C., Nunes, K.R.B., Gois, G.C., Moraes, E.A., Gonçalves-Gervásio, R.R., Borgers, M.C.R.Z., Rodrigues, R.T.S., Brito, C.O. 2023. Quality of Japanese quail eggs according to different storage periods and temperatures. *Acta Scientiarum Animal Sciences* **45**, e61040.

Díaz-Echeverría, V., F, Velmar-Chan, V., Santos-Ricalde, R.H., Segura-Correa, J.C., Pat-Ake, I., Chavarria-Diaz, A.C., Oros-Ortega, I., Casanova-Lugo, F., Cen Hoy, A. & Kim Barrera, C. 2023. Production and egg quality in chicken layers fed with Tithoniadiversifolia. *Veterinaria México OA* **10**. doi: 10.22201/fmvz.24486760e.2023.1133

Drabik, K., Próchniak, T., Spustek, D., Wengerska, K. & Batkowska, J. 2021. The Impact of package type and temperature on the changes in quality and fatty acidsprofile of table eggs during their storage. *Foods* **10**, 2047. doi: 10.3390/foods10092047

Feddern, V., Celant De Pra, M., Mores, R., Nicoloso, R.S., Coldebella, A. & Giovanni de Abreu, P. 2017. Egg quality assessment at different storage conditions, seasons and laying hen strains. *Ciência e Agrotecnologia* **41**(3), 322–333. doi: 10.1590/1413-70542017413002317

Freitas, L.C.S.R., Tinôco, I.F.F., Baêta, F.C., Barbari, M., Conti, L., Teles Júnior, C.G.S., Cândido, M.G.L., Morais, C.V. & Sousa, F.C. 2017. Correlation between egg quality parameters, housing thermal conditions and age of laying hens. *Agronomy Research* **15**(3), 687–693.

Grashorn, M., Juergens, A. & Bessei, W. 2016. Effects of storage conditions on egg quality. Lohman information **50**(1). https://lohmann-breeders.com/media/2020/08/VOL49-GRASHORN-Storage.pdf.

Guyot, N., Réhault-Godbert, S., Slugocki, C., Harichaux, G., Labas, V., Helloin, E. & Nys, Y. 2016. Characterization of egg white antibacterial properties during the first half of incubation: A comparative study between embryonated and unfertilized eggs. *Poultry Science* **95**(12), 2956–2970. doi: 10.3382/ps/pew271

Haugh, R. 1937. The Haugh Unit for Measuring Egg Quality. The U.S. Egg & Poultry Magazine, **43**, 552–555.

Jariyapamornkoon, N., Phongthajitr, C., Sritharet, N. & Sutthitham, W. 2023. Preservation of chicken egg quality using pectin derived fromwater hyacinth. *Applied Food Research* **3**. doi: 10.1016/j.afres.2023.100355

Jin, Y.H., Lee, K.T. & Han, Y.K. 2011. Effects of storage temperature and time on the quality of eggs from laying hens at peak production. *Asian-Australasian Journal of Animal Sciences* **24**(2), 279–284.

JMP–in 7.0 (1989–2004). The statistical Discovery SoftwareTM. SAS Institute.

Jones, D.R., Ward, G.E., Regmi, P. & Karcher, D.M. 2018. Impact of egg handling and conditions during extended storage on egg quality. *Poultry Science* **97**, 716–723. doi: 10.3382/ps/pex351

Kibala, L., Rozempolska-Rucinska, I., Kasperek, K., Zieba, G. & Lukaszewicz, M. 2018. Eggshell Qualities as Indicative of Eggshell Strength for Layer Selection. *Brazilian Journal of Poultry Science* **20**(1), 099–102. doi: 10.1590/1806-9061-2017-0590

Kim, Y.B., Lee, S.Y., Yum, K.H., Lee, W.T., Park, S.H., Lim, Y.H., Choi, N.Y., Jang, S.Y., Choi, J.S. & Kim, J.H. 2024. Effects of storage temperature and egg washing on egg quality and physicochemical properties. *Discover Applied Sciences* **6**(111). doi: 10.1007/s42452-024-05760-1

Kocetkovs, V., Radenkovs, V., Juhnevica-Radenkova, K. & Muizniece-Brasava, S. 2022. Variation in the Fatty Acid and Amino Acid Profiles of Pasteurized Liquid Whole Hen Egg Products Stored in Four Types of Packaging. *Animals* **12**(21), 2990. doi: 10.3390/ani12212990

Lee, M.H., Cho, E.J. & Sohn, S.H. 2016. The Effect of Storage Period and Temperature on Egg Quality in Commercial Eggs. *Korean Journal Poultry Science* **43**(1), 31–38. doi: 10.5536/KJPS.2016.43.1.31

Luo, W., Xue, H., Xiong, C., Li, J., Tu, Y. & Zhao, Y. 2020. Effects of temperature on quality of preserved eggs during storage. *Poultry Science* **99**(6), 3144–3157. doi: 10.1016/j.psj.2020.01.020

Madrigal-Portilla, J., Salas-Duran, C. & Macaya-Quiros, S. 2023. Effect of temperature and storage time on hen egg quality. *Agronomia Mesoamericana* **34**(2), 51223. doi: 10.15517/am.v34i2.51223 (in Spanish).

Martinez, Y., Soliz, N.D., Bejarano, M.A., Paz, A. & Valdivie, M. 2021. Effect of storage duration and temperature on daily changes in external and internal egg quality of eggs from Dekalb White laying hens. *European Poultry Science* **85**. doi: 10.1399/eps.2021.329

Miranda, J.M., Anton, X., Redondo-Valbuena, C., Roca-Saavedra, P., Rodriguez, J.A, Lamas, A., Franco, C.M. & Cepeda, A. 2015. Egg and egg-derived foods: effects on human health and use as functional foods. *Nutrients* **7**(1), 706–729. doi: 10.3390/nu7010706

Murshed, M., Qaid, M.M. & Gatasheh, M.K. 2023. The Effect of Storage Periods on the Internal and External Quality Characteristics of White and Brown–Shell Table Eggs in Saudi Arabia. *Indian Journal of Animal Research*. doi: 10.18805/IJAR.BF-1611

Ondrušíková, S., Nedomová, Š., Pytel, R., Cwiková, O. & Kumbár, V. 2018. Effect of different storage times on Japanese quail egg quality characteristics. *Slovak Journal of Food Science* **12**, 560–565.

Preisinger, R. 2018. Innovative layer genetics to handle global challenges in egg production. *British Poultry Science* **59**(1), 1–6. doi:10.1080/00071668.2018.1401828

Sekeroglu, A., Gök, H. & Duman, M. 2016. Effect of egg shell color and storage duration on the external and internal egg quality traits of ATAK-S layer hybrids. *Ciencia Investigacion Agraria* **43**(2), 327–335.

Sokolowicz, Z., Krawczyk, J. & Dykiel, M. 2018. The effect of the type of alternative housing system, genotype and age of laying hens on egg quality. *Annals of Animal Science* **18**(2)**,** 541–555. doi: 10.2478/aoas-2018-0004

Uyanga, V.A., Onagbesan, O.M., Oke, O.E., Abiona, J.A & Egbeyale, L.T. 2020. Influence of age of broiler breeder and storage duration on egg quality and blastoderm of Marshall broiler breeders. *Journal of Applied Poultry Research* **29**(3), 535–544. doi: 10.1016/j.japr.2020.03.001

Wengerska, K., Batkowska, J. & Drabik, K. 2023. The eggshell defect as a factor affecting the egg quality after storage. *Poultry Science* **102**(7), 102749. doi: 10.1016/j.psj.2023.102749

Wickramasinghe, H.K.J.P., Vidanarachchi, J.K., Himali, C.S.M. & Fernando, P.S. 2013. Effect of different packaging materials on quality characteristics of chicken eggs during storage at room temperature in Sri Lanka. 13th*ASEAN Food Conference*, 9–11 September 2013, Singapore.

Wlaźlak, S., Brzycka, Z., Ragus, W., Banaszak, M. & Grabowicz, M. 2024. Quality characteristics, lysozyme activity, and albumen viscosity of fresh hatching duck eggs after a week's storage at various temperatures. *Scientific Reports* **14**, 5616. doi: 10.1038/s41598-024-56351-4

Yildirim, A. 2017. Changes in quality characteristics during storage time of eggs from layer hens fed diet supplemented with Panaxginseng Meyer leaf extract. *Progress in Nutrition* **19**(2), 197–204. doi: 10.23751/pn.v19i2.4867

Agronomy Research **22**(2), 863–875, 2024
https://doi.org/10.15159/AR.24.056

Multi-criteria decision analysis of wood waste ash and glass foam: toward sustainable material selection for biomethanation

Z. Kusnere*, D. Lauka and K. Spalvins

Riga Technical University, Institute of Energy Systems and Environment, Azenes iela 12/1, LV 1048 Riga, Latvia
*Correspondence: zane.kusnere@rtu.lv

Received: February 1st, 2024; Accepted: June 7th, 2024; Published: June 20th, 2024

Abstract. The study examines the potential applications of wood waste ash and waste glass, by-products of various industrial processes, which have conventional applications such as composting and soil improvement. A new development, vulcanised wood ash material, is studied analysed, drawing parallels between its industrial production process and that of clay pellets. Vulcanised wood ash material and glass foam, which are characterised by advantageous chemical and physical properties, are proving to be versatile resources for various technical applications. Employing a systematic decision-making approach, the study utilises multi-criteria decision analysis and the Technique for Order of Preference by Similarity to Ideal Solution method to evaluate materials for biotrickling filter reactors in ex-situ biomethanation. The comparative analysis includes ash filter material, glass foam, and other industry alternatives, emphasising environmental impacts. The findings reveal expanded clay pellets as the most suitable carrier material, closely followed by polyurethane foam, while glass foam demonstrates remarkable performance despite ranking third. The innovative qualities of glass foam, such as high porosity and thermal insulation, position it as a viable option for biotrickling filter reactors, promoting sustainable practices and circular economy principles. However, further development is required to optimise vulcanised wood ash for biomethanation, potentially enhancing its efficiency through pH adjustment and porosity optimisation.

Key words: biomethanation, glass foam, glass waste material, mcda, TOSPIS, vulcanised wood ash material.

INTRODUCTION

Biogas upgrading is a growing concern due to rising production costs, necessitating technologies that achieve high efficiency with minimal energy consumption. Biotrickling filter reactors are one of the most promising biomethanation methods (Angelidaki et al., 2018; Baransi-Karkaby et al., 2020; Sieborg et al., 2020), with the carrier material in the reactor playing an important role in promoting methanogenesis efficiency (Kusnere et al., 2021). However, there is a need for more sustainable and cost-effective solutions. Industries are investigating alternative materials derived from various by-products to address this demand in order to comply with sustainable standards and achieve operational efficiency goals. The circular bioeconomy concept focuses on using

by-products from bioprocesses to generate new products, promoting resource efficiency and minimising waste. (Jensen et al., 2021).

The energy produced in industrialised countries is the future generation of electricity, anticipated to be generated from the combustion of waste and residues made from biomass. (Kalak, 2023). This transition underscores the critical role of efficient biomethanation processes in leveraging renewable energy sources effectively. Biomethanation, in particular, plays a dual role in energy production and storage, with emerging methods such as Power-to-Gas or, more specifically, Power-to-Methane offering innovative solutions (Götz et al., 2016; Ghaib & Ben-Fares, 2018; Daniarta et al., 2024). By converting surplus renewable energy into methane, biomethanation enables the storage and utilization of renewable energy resources, thereby bolstering grid stability and ensuring energy security. In the broader context of the green energy transition, biological methanation emerges as a pivotal technology for upgrading biogas and advancing sustainable energy practices (Gallo et al., 2016; Blanco & Faaij, 2018).

Given the shift towards renewable energy sources, there has been considerable focus on using biomass wastes for energy generation. Nevertheless, the management of biomass combustion leftovers, such as wood ash, poses significant difficulties due to its elevated ash concentration and the existence of heavy metals and inorganic compounds (Bachmaier et al., 2021). Not withstanding these difficulties, there is an increasing interest in investigating novel methods to reuse these by-products for sustainable energy use. Wood ash, a common by-product of biomass combustion operations, poses challenges for disposal due to its high ash percentage and the presence of heavy metals and inorganic compounds (Zhai et al., 2021). However, these substances can be recycled to enhance energy output and process efficiency (Demeyer et al., 2001; Kusnere et al., 2023b). The circular bioeconomy entails utilising by-products from bioprocesses to generate new products (Bharathiraja et al., 2017). Wood ash is energy waste with few application possibilities, such as forestry and soil amendment, (Zhai et al., 2021; Elliott et al., 2022), for example, it can serve as a mineral fertiliser that can be utilised to deacidify soil and replace calcium fertilisers (Stankowski et al., 2021). Developing novel materials like vulcanised wood ash and glass foam presents opportunities to repurpose wood ash waste and waste glass for biomethanation applications.

The study explores the potential applications of wood waste ash and glass waste, focusing on the innovative development of vulcanised wood ash material and glass foam material(‘Green Gravels’; Lauka et al., 2015). Specifically, the research delves into these materials' chemical and physical properties to identify prominent characteristics in selecting carrier materials for ex-situ biomethanation, a crucial parameter in biotrickling bioreactors (Jensen et al., 2021). To achieve this objective, multi-criteria decision analysis (MCDA) and the Technique for Order of Preference by Similarity to Ideal Solution method (TOPSIS) are employed to make systematic decisions. The research compares wood waste ash, glass foam, and other alternatives using predetermined criteria and data to provide insights into sustainable material selection for biomethanation processes.

MATERIALS AND METHODS

The research algorithm (Fig. 1) starts with literature analysis as a foundation for choosing alternatives and defining criteria. After defining criteria and choosing alternative materials, the decision making matrix is made where criteria weights are

calculated from an expert questionnaire. The study explores the complexities of MCDA, with a focus on the TOPSIS. Additionally, a sensitivity analysis is conducted to enhance the dependability of the findings.

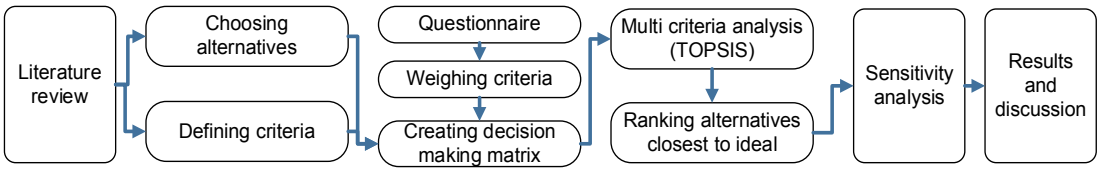

Figure 1. Research algorithm.

This research algorithm is used to rank the alternatives based on their performance against the defined criteria, ultimately leading to the selection of the most suitable material for *ex-situ* biomethanation.

Choosing alternatives

For the biomethanation in biotrickling filter reactors, choosing materials is a crucial aspect because their properties can influence microorganism growth (Jensen et al., 2021; Kusnere et al., 2023a). In this study, two packing materials derived from waste materials are chosen: filter material obtained from the bottom ash of wood chips (VAM) and material made from glass waste (GF). Two alternatives were chosen to be previously studied in the field (Ashraf et al., 2020). Expanded clay pellets (CP), such as Leca®, is a readily available, cost-effective natural material that has a wide range of uses in gardening and is now being utilised in construction (Rashad, 2018). In order to compare materials that have completely distinct origins and qualities, polyurethane foam (PUF) was selected. PUF, an artificial substance derived from fossil fuels, is characterised by its low cost, excellent porosity, and extensive surface area (Kusnere et al., 2021).

Selection of criteria

The chosen criteria are grouped into four groups of aspects - environmental aspects, economic aspects, technical aspects, and performance aspects. All criteria are quantitative, and data was collected from literature and previous studies (Kusnere et al., 2023b, 2023a).

Table 1. Criteria for multi-criteria analysis for material application in biomethanation

Criteria category	Criteria
Environmental aspects	Energy for production of the material °C
	Source of the raw material (fossil or not) 0–1 points
Economical aspects	Material costs EUR m^{-3}
	Material availability, Mt $year^{-1}$
Technical aspects	Material pH
	External porosity %
	Bulk density kg m^{-3}
	Specific surface area m^2 m^{-3}
Performance aspects	Average biomethane yield NmL $L_{material}^{-1}$
	Water retention %

Table 1 lists criteria for multi-criteria analysis for material application in biomethanation. The criteria were separated into four categories: environmental aspects,

economical aspects, technological aspects, and performance aspects. By analyzing these criteria, its is possible to determine the most suitable materials for biomethanation applications that strike a balance between environmental sustainability, economic viability, technical feasibility, and performance efficiency.

Weighing criteria

Multi-criteria matrixes weights for materials were based on expert evaluation. People who have studied or worked in biology, environmental engineering, biotechnology and chemistry, and civil, industrial, and mechanical engineering were targeted as potential experts. Together, thirty experts participated in the evaluation. Of these experts, 11 had doctoral degrees, 15 had master's degrees, and 4 had bachelor's degrees. Google Forms was used to perform the questionnaire. The weights for each criterion were established using a questionnaire-based method, in which participants assessed each criterion on a scale ranging from 1 to 5. The total of the ratings given to each criterion was divided by the total of the ratings given to all criteria. This algorithm ensured that the weights allocated to each criterion collectively totaled 1, so creating a normalised foundation for comparison and decision-making.

Evaluating materials using TOPSIS

To find the ideal solution closest to a favorable option, TOPSIS (Ishizaka & Nemery, 2013). Using this method, this approach utilises the numerical values of the previously defined criteria (Ishizaka & Nemery, 2013). The TOPSIS analysis involves a series of five consecutive processes that can be employed to calculate the closest to the ideal solution (Fig. 2).

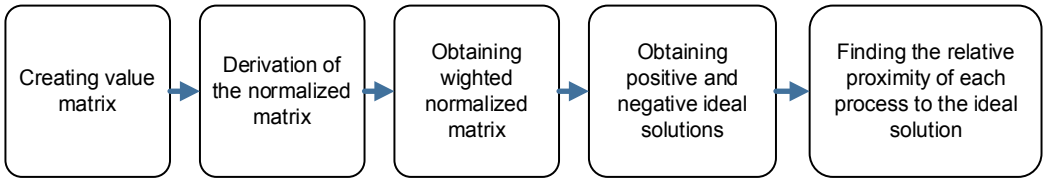

Figure 2. Toolbox for applying Technique of Order Preference Similarity to the Ideal Situation (TOPSIS) method.

At first, the matrix of values is created. It is based on chosen criteria. After constructing the matrix of values, a normalised matrix is formed by dividing each value by the sum of all square roots linked with the respective criterion, as calculated using Eq. (1).

$$r_{ai} = \frac{x_{ai}}{\sqrt{\sum_{a=1}^{n} x_{ai}^2}} \quad (1)$$

where r_{ai} – normalised value; x_{ai} – indicator value; i – criterion; a – alternative.

A weighted normalised matrix is created from normalised matrix values. Each rai value multiplied by w yields the weighted normalised matrix values. The sum of all criteria should be one. Once the weighted normalised matrix is obtained, the positive ideal and negative ideal solutions are identified. It is done by selecting the highest and lowest values from the previously calculated weighted normalised values. Subsequently, the numerical value of each alternative is measured in terms of its distance from both the

positive ideal solution and the negative ideal solution. Eq. (2) was applied to calculate the distance from the positive ideal solution, while Eq. (3) was used to find the distance from the negative ideal solution.

$$d_a^+ = \sqrt{\sum_i (v_i^+ - v_{ai})^2} \tag{2}$$

$$d_a^- = \sqrt{\sum_i (v_i^- - v_{ai})^2} \tag{3}$$

where d_a^+ – distance from the positive ideal solution; d_a^- – distance from the negative ideal solution; v_i^+ – positive ideal value; v_i^- – negative ideal value; v_{ai} – weighted value.

The relative proximity coefficient is calculated based on the distances determined from the positive and negative values using the given Eq. (4):

$$C_a = \frac{d_a^-}{d_a^+ + d_a^-} \tag{4}$$

where C_a – coefficient of relative proximity; d_a^+ – distance from the positive ideal solution; d_a^- – distance from the negative ideal solution.

The relative closeness coefficient ranges from zero to one, with a higher value indicating a more favourable alternative that can be regarded as more sustainable.

The values are subsequently employed to ascertain both positive and negative ideal values, which are then utilised to derive the relative proximity coefficient. A graph is used to illustrate the relative closeness coefficient in order to facilitate the analysis of the results.

Sensitivity analysis

After TOPSIS multi-criteria analysis, sensitivity analysis was performed to determine criteria stability. The sensitivity study illustrates how much the TOPSIS performance of each alternative changes when the criterion weight is altered. A matrix was developed for each criterion to display the relative proximity coefficient of each choice when the weighting is altered. The overall weighting of all criteria should be one, as specified. This means that modifying the weighting of one criterion distributes the remaining weighting value evenly among the remaining nine criteria. The weighted value of each criterion was changed from 0.1 to 0.9 in stages of 0.1. Eq. (5) determined the weighting of the remaining criteria, subtracting the criterion's value from one and dividing it by ten, which is the number of criteria. Thus, the remaining weighted value is spread equally among the criteria.

$$w = \frac{1 - w_0}{10} \tag{5}$$

where w – weight of each remaining criterion; w_0 – weight of sensitivity analysis criterion.

After the sensitivity analysis, graphics are constructed using the modified matrix of each criterion to demonstrate how the results ranking of the alternatives change due to the adjustment of criteria weights. According to the sensitivity analysis, the most suitable outcome has the most upward curves and adjusts well to criteria adjustments. The number of upward curves for each choice was deducted from the number of downward curves. The best option has the highest numerical result.

RESULTS AND DISCUSSION

Weights of criteria

The results obtained from the questionnaire were calculated to give the criteria weights. The results are shown in Table 2. The weights for each criterion were established using a questionnaire-based method, and the sum of all criteria weights is 1.

Table 2. Weights for criteria

Number of criterion	Criterion	Unit of measure	Weight
C1	Average biomethane yield	NmL $L_{material}^{-1}$	0.125
C2	Water retention %	%	0.084
C3	Energy for the production of the material	°C	0.102
C4	Raw material costs	EUR m^{-3}	0.112
C5	Material availability	t $year^{-1}$	0.101
C6	Source of the material	Points 0–1	0.091
C7	pH	0–14	0.099
C8	External porosity	%	0.099
C9	Bulk density	kg m^{-3}	0.081
C10	Specific surface area	m^2 m^{-3}	0.105

The average biomethane yield was given the highest weight of 0.125, reflecting its crucial role in determining the overall success of the material.

Analysis of TOPSIS Results

The results of the TOPSIS multi-criteria analysis calculations carried out to assess the materials for biomethanation against the stated are shown in Fig. 3.

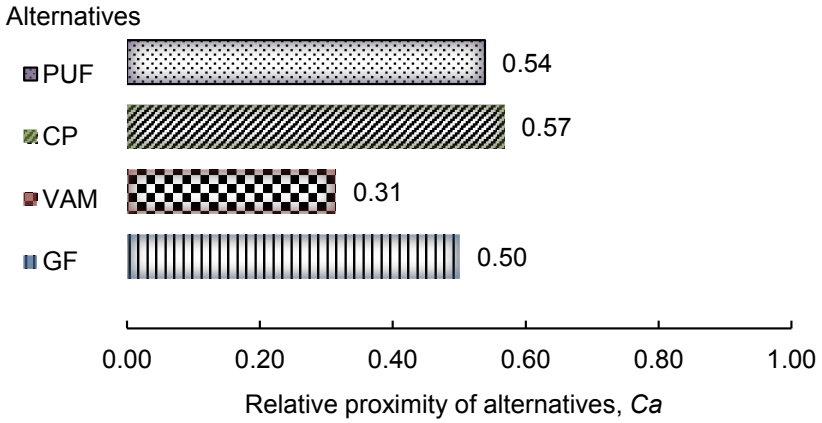

Figure 3. TOPSIS analysis results. The relative closeness coefficient ranges from zero to one, with a higher value indicating a more favorable alternative. PUF – polyurethane foam; CP – expanded clay pellets; VAM – vulcanised ash material; GF – glass foam.

Based on the coefficient of relative proximity values as shown in Fig. 3, it is evident that expanded clay pallets and polyurethane foam are the closest to the ideal result.

Among these alternatives, expanded clay pallets have a coefficient of 0.57, indicating that they are the most suitable carrier material for biomethanation according to the given criteria. However, it should be noted that the relative coefficient values are similar for two other alternatives – polyurethane foam and glass foam material. The value of PUF differs from CP by only 0.03, and GF comes in third, differing from CP by 0.07. The results show that the alternatives or materials whose values are closest to the ideal result. This means that polyurethane foam has good properties as a carrier material for ex-situ biomethanation. Nevertheless, it is evident that the values for glass foam products and clay pallets are very similar to those for PUF. This implies that the hierarchy of alternatives in the sustainability evaluation may fluctuate as the materials and their manufacturing methods progress.

Results of Sensitivity analysis

A criterion sensitivity analysis was conducted for all criteria within each aspect category to enhance clarity on the results. This analysis facilitated comprehension of the extent to which each criterion impacted the study's overall findings. By analysing several weight allocations for each criterion, the key parameters that have the most influence on determining the outcomes were successfully identified. The thorough examination improved the strength and dependability of conclusions, resulting in a more comprehensive comprehension of the research outcomes. Figs 4–13 show changes when criteria weights are changed and which alternatives have upward curves. Understanding the significance of these criteria enables the consideration of modifying materials and their parameters to better align with the selected application. If the criteria values may be enhanced to approach ideal values, the results will vary appropriately.

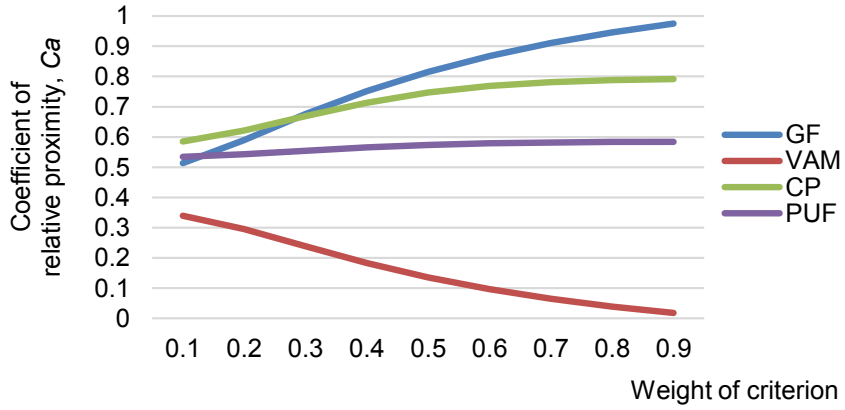

Figure 4. C1 – Changes in results by changing the weight of biomethane yield from 0.1 to 0.9 in stages of 0.1.

Figs 4 and 5 display the graphs of the alterations in the performance criteria. Fig. 4 illustrates the impact on results when the weighting of the biomethane yield criterion is altered, while Fig. 5 demonstrates the effect of changing the weighting of the water retention criterion. While the change in the relative proximity coefficients varies for all options, it is evident that the glass foam results increases for both criteria. This demonstrates that glass foam has the potential to be feasible option.

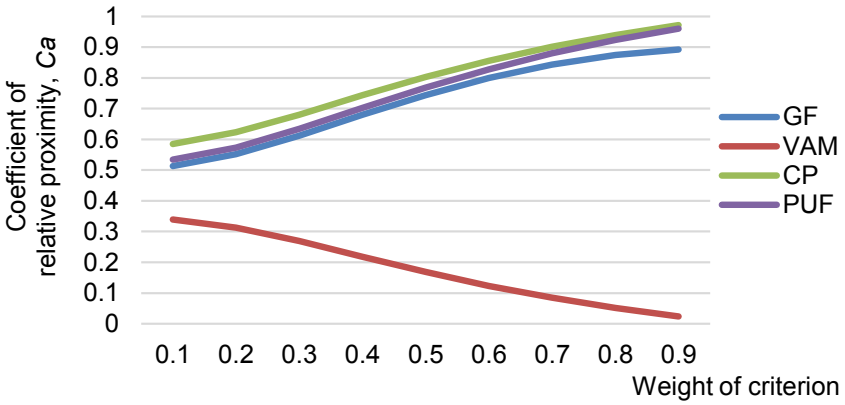

Figure 5. C2 – Changes in results by changing the weight of water retention from 0.1 to 0.9.

By increasing the criterion weighting of raw material costs value of expanded clay pellets decline dramatically (Fig. 6). However, by increasing the weight of material availability, the relative closeness coefficients of all alternatives drop, except expanded clay pellets (Fig. 7).

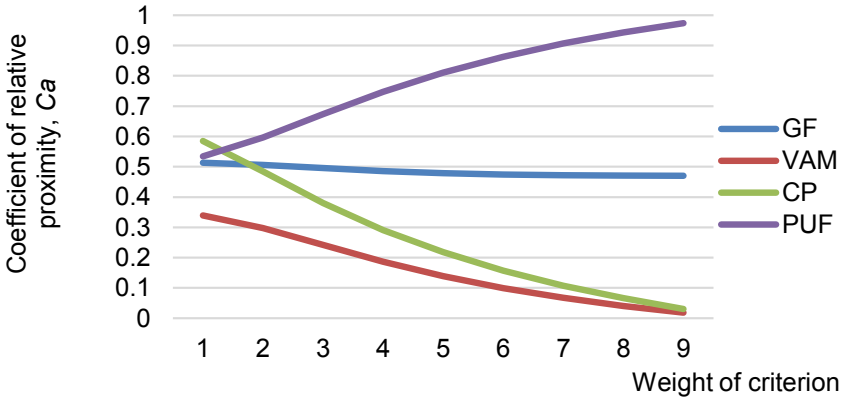

Figure 6. C3 – Changes in results by changing the weight of raw material costs from 0.1 to 0.9.

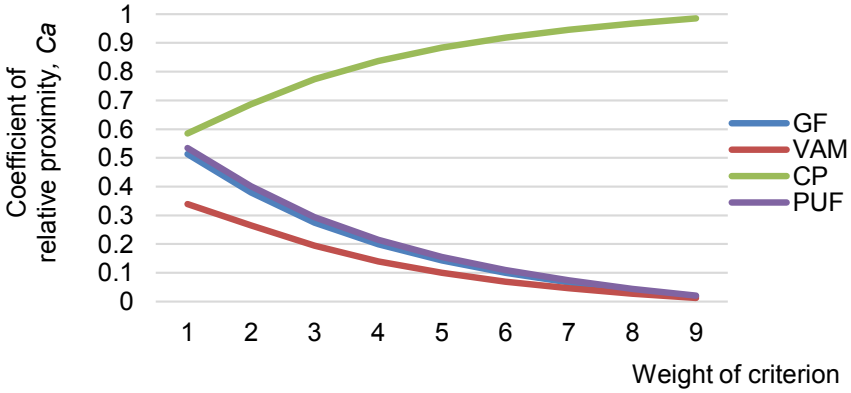

Figure 7. C4 – Changes in results by changing the weight of material availability from 0.1 to 0.9.

Reducing the importance of weight of energy for production of the material (as shown in Fig. 8) decreases the value all alternatives except polyurethane foam. The opposite results occur if the weight of source of material is increased (Fig. 9). The relative closeness coefficients of all alternatives drop, except polyurethane foam.

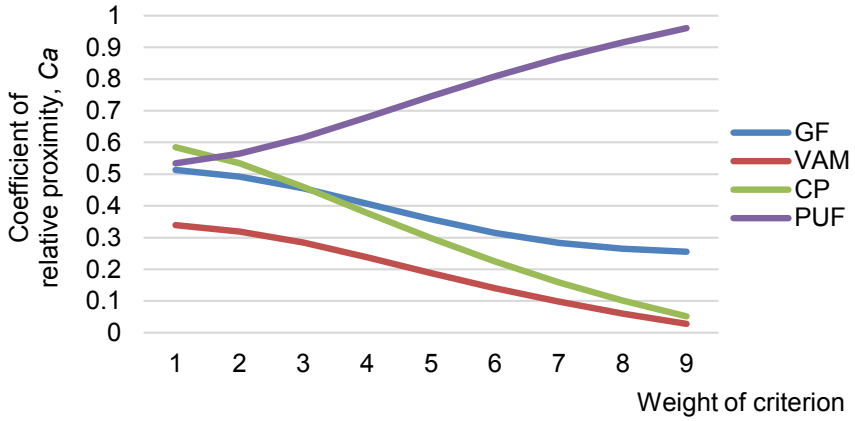

Figure 8. C5 – Changes in results by changing the weight of energy for production of the material from 0.1 to 0.9.

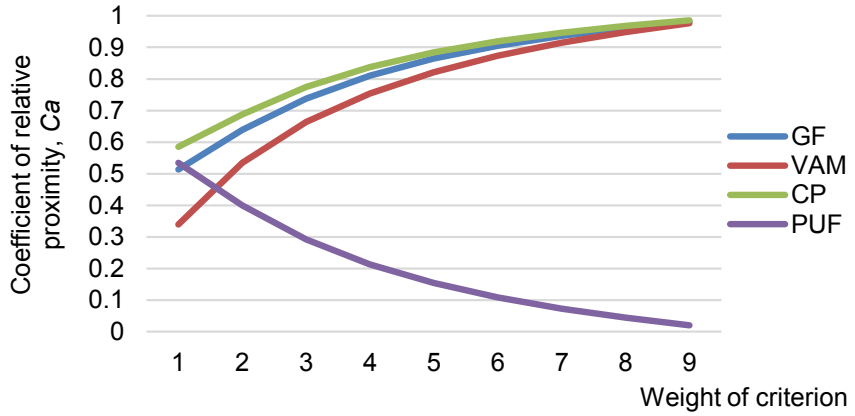

Figure 9. C6 – Changes in results by changing the weight of source of material from 0.1 to 0.9.

Figs 10–13 show changes in ranking alternatives if different technical criteria weights are changed. By increasing the weights of pH value, external porosity, bulk density, and specific surface area, polyurethane foam value increases, while vulcanised ash material decreases dramatically for all these criteria. These technical parameters could be improved for some of these materials in development.

Based on the sensitivity analysis, the optimal outcome shows the highest number of upward curves and demonstrates a strong ability to adapt to alterations in criteria. The number of positive curves for each option was subtracted from the number of negative slopes in Figs 4 to 13. The optimal choice has the greatest numerical outcome. This numerical outcome suggests that the optimal choice is most flexible and capable of promptly adjusting to variations in the weights assigned to different criteria.

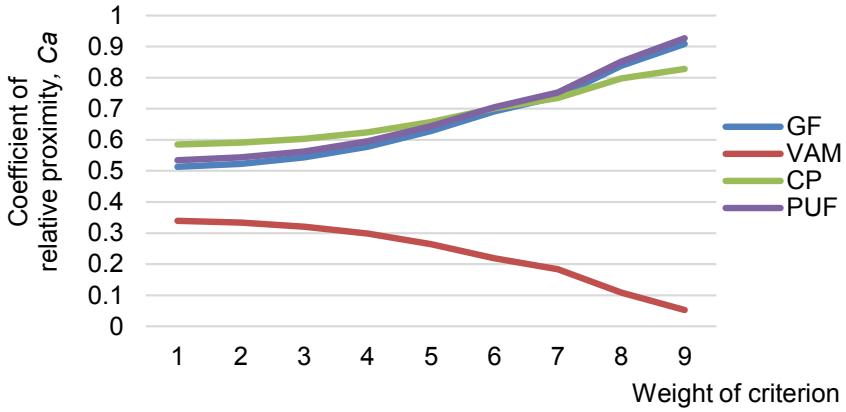

Figure 10. C7 – Changes in results by changing the weight of pH value from 0.1 to 0.9.

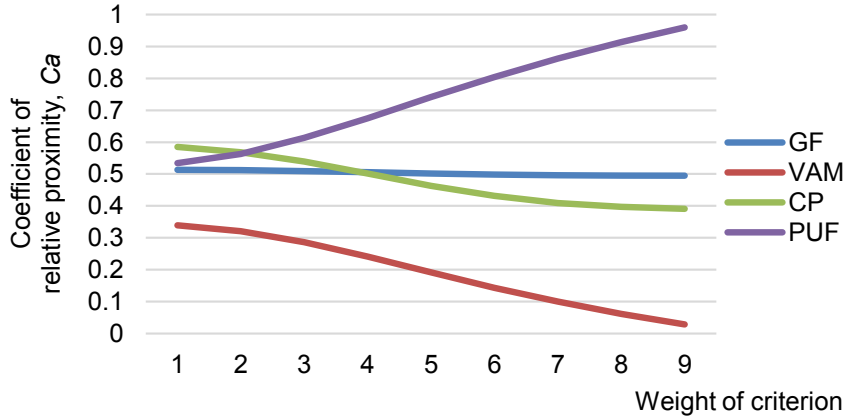

Figure 11. C8 – Changes in results by changing the weight of external porpsity from 0.1 to 0.9.

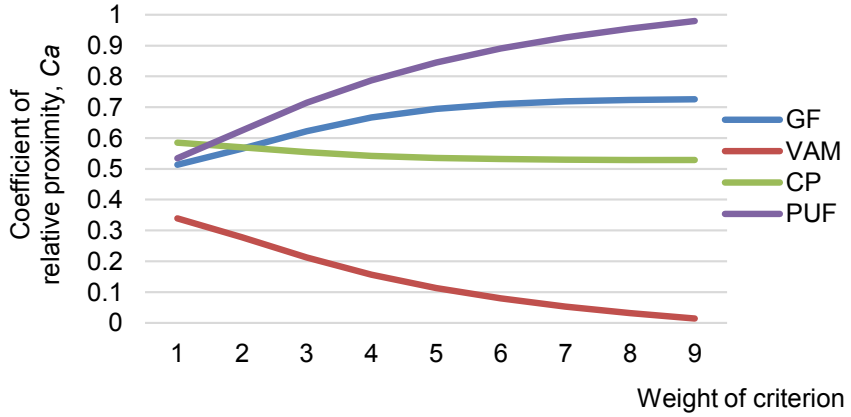

Figure 12. C9 – Changes in results by changing the weight of bulk density from 0.1 to 0.9.

Based on the sensitivity analysis, the optimal outcome shows the highest number of upward curves and demonstrates a strong ability to adapt to alterations in criteria. The number of positive curves for each option was subtracted from the number of negative

slopes in Figs 4 to 13. The optimal choice has the greatest numerical outcome. This numerical outcome suggests that the optimal choice is most flexible and capable of promptly adjusting to variations in the weights assigned to different criteria.

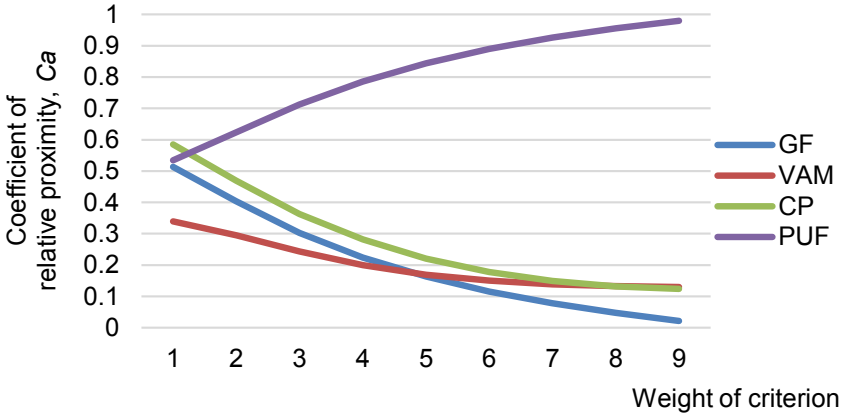

Figure 13. C10 – Changes in results by changing the weight of specific surface area from 0.1 to 0.9.

The sensitivity analysis results in Table 3 provide valuable insights into the performance of each alternative material. Polyurethane foam emerges as the top choice based on the number of upward curves and margin scores. Following closely behind are glass foam and expanded clay pellets, both showing promising results.

Table 3. Sensitivity analysis results

	Glass foam	Vulcanised ash material	Clay pellets	Polyurethane foam
Number of upward curves	4	1	4	8
Number of downward curves	6	9	6	2
Margin	-2	-8	-2	6

However, vulcanised ash material falls short in comparison, indicating that improvements are necessary in technical and performance aspects for it to be considered a viable option.

CONCLUSIONS

As part of a systematic decision-making approach, a multi-criteria decision analysis and the Technique for Order of Preference by Similarity to Ideal Solution method are used in this study to determine which of the chosen materials would be a better solution for biotrickling filter reactors used for ex-situ biomethanation. According to the coefficient of relative proximity values, it is clear that expanded clay pallets and polyurethane foam are the most similar to the ideal solution. CP have a coefficient of 0.57, which makes them the most appropriate carrier material for biomethanation based on the specified parameters. The disparity between PUF and CF is 0.03, while GF, ranking third, deviates from CP by 0.07. Among the four selected options, the PUF yields the most favorable outcomes in sensitivity analysis, showcasing its robust capacity to

adjust to changes in criteria weights. However, GF, made from recycled glass, also demonstrates exceptional performance. Glass foam can be considered an innovative concept for use as a carrier material for biomethanation. Furthermore, glass foam exhibits excellent properties such as high porosity, good thermal insulation, and low density, making it an ideal choice for biotrickling filter reactors. The utilisation of waste materials in ex-situ biomethanation, where it serves as a carrier material, not only enhances the overall efficiency of the process but also promotes sustainable practices. Moreover, the innovative quality of glass foam highlights the possibility of generating value from otherwise discarded resources following the ideas of a circular economy. Hence, due to its advantageous attributes and positive environmental impact, glass foam presents itself as an appropriate solution for biotrickling filter reactors.

Several undesirable characteristics and factors hinder using vulcanised wood ash as a filter material for biomethanation purposes. However, it is now undergoing development and can be enhanced to meet the requirements of biomethanation technology better. The vulcanised wood ash material has the potential to be selected for biomethanation by enhancing specific values. For instance, altering the pH value can improve microorganism growth and biomethane yield. Adding foaming agents can lead to changes in porosity, increasing specific surface area. This enhances the efficiency of the material. With further research and development, vulcanised wood ash material also has the potential to become a highly efficient and sustainable solution for biomethanation processes. Developing and improving innovative materials such as vulcanised wood ash and glass foam offers the possibility to reuse wood ash waste and waste glass for biomethanation purposes.

ACKNOWLEDGEMENTS. This work was supported by the European Social Fund within the Project No 8.2.2.0/20/I/008 ‘Strengthening of PhD students and academic personnel of Riga Technical University and BA School of Business and Finance in the strategic fields of specialisation’.

REFERENCES

Angelidaki, I., Treu, L., Tsapekos, P., Luo, G., Campanaro, S., Wenzel, H. & Kougias, P.G. 2018. Biogas upgrading and utilization: Current status and perspectives. *Biotechnol Adv* **36**, 452–466. doi: 10.1016/j.biotechadv.2018.01.011

Ashraf, M.T., Triolo, J.M. & Yde, L. 2020. Assay for Testing Packing Materials for Ex-situ Bio-methanation. *28th European Biomass Conference and Exhibition*, 317–321 https://doi.org/10.5071/28thEUBCE2020-2DO.4.1

Bachmaier, H., Kuptz, D. & Hartmann, H. 2021. Wood Ashes from Grate-Fired Heat and Power Plants: Evaluation of Nutrient and Heavy Metal Contents. *Sustainability* **13**, 5482. doi: 10.3390/su13105482

Baransi-Karkaby, K., Hassanin, M., Muhsein, S., Massalha, N. & Sabbah, I. 2020. Innovative ex-situ biological biogas upgrading using immobilized biomethanation bioreactor (IBBR). *Water Science and Technology* **81**, 1319–1328. https://doi.org/10.2166/wst.2020.234

Bharathiraja, B., Sridharan, S., Sowmya, V., Yuvaraj, D. & Praveenkumar, R. 2017. Microbial oil – A plausible alternate resource for food and fuel application. *Bioresource Technology* **233**, 423–432. doi: 10.1016/j.biortech.2017.03.006

Blanco, H. & Faaij, A. 2018. A review at the role of storage in energy systems with a focus on Power to Gas and long-term storage. *Renewable and Sustainable Energy Reviews* **81**, 1049–1086. doi: 10.1016/j.rser.2017.07.062

Daniarta, S., Sowa, D., Błasiak, P., Imre, A.R. & Kolasiński, P. 2024. Techno-economic survey of enhancing Power-to-Methane efficiency via waste heat recovery from electrolysis and biomethanation. *Renewable and Sustainable Energy Reviews* **194**, 114301. doi: 10.1016/j.rser.2024.114301

Demeyer, A., Nkana, J.C.V. & Verloo, M.G. 2001. Characteristics of wood ash and in¯uence on soil properties and nutrient uptake: an overview. *Bioresource Technology*. **77**, 287–295. doi: 10.1016/S0960-8524(00)00043-2

Elliott, A., Mahmood, T. & Kamal, A. 2022. Boiler ash utilization in the Canadian pulp and paper industry. *J Environ Manage* **319**, 115728. https://doi.org/10.1016/j.jenvman.2022.115728

Gallo, A.B., Simões-Moreira, J.R., Costa, H.K.M., Santos, M.M. & Moutinho dos Santos, E. 2016. Energy storage in the energy transition context: A technology review. *Renewable and Sustainable Energy Reviews* **65**, 800–822. doi: 10.1016/j.rser.2016.07.028

Ghaib, K. & Ben-Fares, F.-Z. 2018. Power-to-Methane: A state-of-the-art review. *Renewable and Sustainable Energy Reviews* **81**, 433–446. doi: 10.1016/j.rser.2017.08.004

Götz, M., Lefebvre, J., Mörs, F., McDaniel Koch, A., Graf, F., Bajohr, S., Reimert, R. & Kolb, T. 2016. Renewable Power-to-Gas: A technological and economic review. *Renewable Energy* **85**, 1371–1390. https://doi.org/10.1016/j.renene.2015.07.066

Green Gravels [WWW Document], n.d. URL https://gravels.ee/en/foam-glass-gravel/ (accessed 9.6.23).

Ishizaka, A. & Nemery, P. 2013. Multi-criteria Decision Analysis: Methods and Software. *John Wiley & Sons Ltd*., Chichester. doi:10.1002/9781118644898

Jensen, M.B., Poulsen, S., Jensen, B., Feilberg, A. & Kofoed, M.V.W. 2021. Selecting carrier material for efficient biomethanation of industrial biogas-CO2 in a trickle-bed reactor. *Journal of CO2 Utilization* **51**, 101611. doi: 10.1016/j.jcou.2021.101611

Kalak, T. 2023. Potential Use of Industrial Biomass Waste as a Sustainable Energy Source in the Future. *Energies* **16**, 1783. doi: 10.3390/en16041783

Kusnere, Z., Rupeika, D., Spalvins, K. & Mika, T. 2023a. Turning Trash into Treasure: The Use of Vulcanized Ash Filters and Glass Waste for Renewable Energy. *Environmental and Climate Technologies* **27**, 1049–1060. doi: 10.2478/rtuect-2023-0076

Kusnere, Z., Spalvins, K. & Bataitis, M. 2023b. Wood Ash Filter Material Characterization as a Carrier Material for *Ex-Situ* Biomethanation of Biogas in Biotrickling Filter Reactors. *Environmental and Climate Technologies* **27**, 92–102. https://doi.org/10.2478/rtuect-2023-0008

Kusnere, Z., Spalvins, K., Blumberga, D. & Veidenbergs, I. 2021. Packing materials for biotrickling filters used in biogas upgrading - biomethanation. *Agronomy Research* **19**, 819–833. doi: 10.15159/AR.21.082

Lauka, D., Pastare, L., Blumberga, D. & Romagnoli, F. 2015. Preliminary Analysis of Anaerobic Digestion Process using Cerathophyllumdemersum and Low Carbon Content Additives: A Batch Test Study. *Energy Procedia* **72**, 142–147. https://doi.org/10.1016/j.egypro.2015.06.020

Rashad, A.M. 2018. Lightweight expanded clay aggregate as a building material - An overview. *Construction and Building Materials* **170**, 757–775. doi: 10.1016/j.conbuildmat.2018.03.009

Sieborg, M.U., Jønson, B.D., Ashraf, M.T., Yde, L. & Triolo, J.M. 2020. Biomethanation in a thermophilic biotrickling filter using cattle manure as nutrient media. *Bioresource Technology Reports* **9**, 100391. doi: 10.1016/j.biteb.2020.100391

Stankowski, S., Chajduk, E., Osińska, B. & Gibczyńska, M. 2021. Biomass ash as a potential raw material for the production of mineral fertilisers. *Agronomy Research* **19**, 1999–2012. doi: 10.15159/AR.21.156

Zhai, J., Burke, I.T. & Stewart, D.I. 2021. Beneficial management of biomass combustion ashes. *Renewable and Sustainable Energy Reviews* **151**, 111555. doi: 10.1016/j.rser.2021.111555

Agronomy Research **22**(2), 876–886, 2024
https://doi.org/10.15159/AR.24.069

Production of simple sugars from olive grove pruning using acid pretreatment and enzymatic hydrolysis

N. Pedro[1,2,*], R. Bezerra[3,4], I. Fraga[3,4] and A.P. Duarte[5,6]

[1]Polytechnic University of Castelo Branco, Faculty of Agriculture, Department of Natural Resources and Sustainable Development, Quinta da Sra. de Miércoles, apartado 119, PT6001-909 Castelo Branco, Portugal
[2]QRural - Qualidade De Vida No Mundo Rural, Av. Pedro Álvares Cabral, n.º12, PT6000-084 Castelo Branco, Portugal
[3]UTAD - University of Trás-os-Montes and Alto Douro, Quinta de Prados, PT5000-801 Vila Real, Portugal
[4]CITAB - Centre for the Research and Technology of Agro-Environmental and Biological Sciences. UTAD, Quinta de Prados, PT5000-801 Vila Real, Portugal
[5]UBI - University Beira Interior. Convento de Sto. António, PT6201-001 Covilhã, Portugal
[6]CICS-UBI - Health Sciences Research Centre, University Beira Interior, Av. Infante D. Henrique, PT6200-506 Covilhã, Portugal
[*]Correspondence: npedro@ipcb.pt; lnova@ipcb.pt

Received: January 30th, 2024; Accepted: April 19th, 2024; Published: July 18th, 2024

Abstract. The purpose of this paper was to optimize the production of simple sugars from olive grove pruning (OGP) using acid pretreatment and enzymatic hydrolysis. This study was based on a model composition corresponding to a 34 orthogonal factorial design and employed the response surface methodology (RSM) to optimize the pretreatment and hydrolysis conditions, aiming to attain maximum glucose, xylose and arabinose extraction from cellulose and hemicellulose of biomass. The pretreatment operating conditions considered for optimization, were temperature (60–180 °C), residence time (30–120 min) and sulphuric acid concentration (0.5–5% w w^{-1}). Enzymatic hydrolysis experiments on solid fraction pretreated with diluted acid were performed at a solid concentration of 5% (w v^{-1}, based on dry weight), using 50 mM citrate buffer pH 4.8 with BSA at a concentration of 60 mg g^{-1} dry biomass. The reaction mixture was incubated at 50 °C for 174 h on an orbital shaker at 150 rpm. Three commercial enzyme preparations (cellulase complex, b-glucosidase and xylanase) were used in enzymatic saccharification. Total carbohydrate content of the initial biomass was 51.25% (in dry mass), of which glucose was the major constituent with 33.59%. Contents of lignin and extractable found in biomass were 24.96% and 15.84%, respectively. In this work, it was possible to extract 93.1% of the sugars present in the olive grove pruning, with pretreatments carried out for 102 min at 156 °C with a sulfuric acid load of 4.09% (w w^{-1}), followed by enzymatic hydrolysis performed for 174 h, with an enzyme loading of 18 PFU, 36 p-NPGU and 36 IU per gram of substrate.

Key words: acid hydrolysis, enzymatic hydrolysis, olive pruning, pretreatment, RSM, sugars.

INTRODUCTION

The production of sugars from lignocellulosic materials comprises two steps: pretreatment and enzymatic hydrolysis (Láinez et al., 2018; Nashiruddin et al., 2020). The pretreatment is an important step to reduce the recalcitrance of the biomass for the subsequent steps of enzymatic hydrolysis and fermentation (Zhu & Pan, 2010). This step, although essential, because without it the efficiency of enzymatic hydrolysis rarely exceeds 20%, is one of the most expensive steps for production of sugars from cellulosic wood materials due to energy consumption, the use of chemical substances, and the need to treat and reuse process water (Sun at al., 2016; Zhu & Pan, 2022).

The main purpose of acid pretreatment is to solubilize the hemicellulose fraction of biomass in order to make cellulose more accessible to enzymatic attack. Such pretreatments are usually accomplished with dilute acid (< 4% w w^{-1}), being the sulfuric acid the most widely used reagent. The application of dilute acid pretreatments appears as the most advantageous method for industrial applications being considered cheap and effective (Huang et al., 2021; Jehadin et al., 2021; Mankar at al., 2021). In addition to sulfuric acid, other pretreatments have been tested, such as hydrothermal, alkaline and oxidative (Woiciechowski at al., 2020; Sarker et al., 2021; Scapini et al., 2021; Zhou et al., 2023).

The hydrolysis of cellulose in lignocellulosic materials requires the application of three enzymatic components: endoglucanases, exoglucanases and β-glucosidases. The hydrolysis of hemicelluloses, due to their heterogeneity, with different sugar backbones with different backbone linkages and side groups, requires complex enzymatic systems. Improving this step of the process can be approached by increasing the accessibility of the substrate, as already mentioned, modifying its chemical structure, thus promoting the performance of the enzymes (Luo et al., 2019). The application of surfactants in lignocellulosic materials have been shown to promote a substantial increase of enzymatic hydrolysis efficiency (Zheng et al., 2021; Sánchez-Muñoz et al., 2022). In recent years new types of surfactants have emerged to improve enzymatic hydrolysis, such as proteins like the bovine serum albumin (BSA), one of the most used (Brondi et al., 2019), or polymers such as polyethylene glycol (PEG) (Nogueira et al., 2022).

Olive grove pruning waste is an agricultural residue widely available in Portugal. It is estimated that the amount of material produced annually from olive grove pruning could amount to 290,000 t per year.

The purpose of this paper was to optimize the acid pretreatment and hydrolysis process and investigate the effects of acid concentration, temperature and residence time on the production of sugars (glucose, xylose and arabinose) as well as on the formation of degradation products (furfural, 5-hydroxymethylfurfural and acetic acid).

The work carried out aims to increase the profitability of olive farms in Portugal by using residues from olive grove pruning, which are usually burned on farms, as a raw material, to produce added value compounds, such as ethanol, xylitol, lactic acid, among others.

MATERIALS AND METHODS

Olive tree pruning´s samples were collected and harvested on the farm of Higher School of Agriculture of Castelo Branco (GPS: 39.8197117, -7.4964662, Alt. 361 m). The raw material was collected after the olive grove pruning, consisting of small branches (diameter less than 4 cm) and fresh leaves.

Raw material analysis

The raw material was prepared for further analysis according with the standard NREL / TP-510-42620 (Hames et al., 2005), which defines a material particle size of 0.180 and 0.850 mm. For this purpose, the raw material was ground in a slide mill (Retch Mühle - West Germany) and subsequently sieved using 0.180 mm (80 mesh) and 0.500 (35 mesh) sieves in accordance with the specifications of the American Society for Testing and Materials (ASTM E1757-19).

The determination of the extractable content was carried out according to the Tappi 204 om-88 standard (Sithole et al., 1991).

The ash determination was performed in accordance with the standard NREL / TP-510-42622 (Sluiter et al., 2005) and the incineration was carried out in muffle furnace, using a temperature of 525 ± 25 °C.

The content of insoluble and soluble lignin was determined according to the standard NREL / TP-510-42618 (Sluiter et al., 2008a).

The concentration of total reducing sugars present in the solutions of the treated substrates was determined using the Miller method (Miller, 1959).

For the quantitative analysis of individual sugars and degradation products, a high-performance liquid chromatography apparatus (High-Performance Liquid Cromatography - HPLC) was used. For these analysis, an Aminex-87P column (Bio-Rad, Hercules, CA) was used to determine individual carbohydrates, namely glucose, xylose, galactose, arabinose and mannose, according to the standard NREL / TP-510-42618 (Sluiter et al., 2008a). The Aminex-87H column (Bio-Rad, Hercules, CA) was used for determining degradation products, namely acetic acid, formic acid, hydroxymethylfurfural (HMF) and furfural, following the standard NREL / TP-510-42623 (Sluiter et al., 2008b).

Pretreatment

Batch reactions were carried out under different operating conditions and a total of 34 runs, corresponding to the orthogonal factorial design, with different combinations of the variables were used, according to a central composite rotable design (CCDR) generated using Design Expert 7 Trial Version (Stat-Ease inc. minneapolis) (Table 1). The reaction media was sulfuric acid, in concentrations ranging from 0.5 to 5.00% (w w^{-1}, dry biomass), using a solid-liquid ratio of 1.0 g dried biomass/10 mL liquid on a final volume of 100 mL. The temperature ranged from 60 to 180 °C and reaction time from 30 to 120 min. Sulfuric acid in this pretreatment was added from a solution with a concentration of 5 g L^{-1} previously prepared. The dependent variable studied in the hydrolysate resulting from the pretreatment was the total reducing sugars content.

After this process, the material was washed with distilled water until the pH of the slurry became neutral (pH 7), to remove traces of acid and inhibitors, such as formic acid, which inactivates xylanase (Panagiotou, 2007). The solid residue resulting from pretreatment was used without drying in the subsequent phase of enzymatic hydrolysis, as drying can lead to the collapse of the pores of plant material, making enzymatic hydrolysis more difficult and consequently considerably reducing its yield. (Hendriks & Zeeman, 2009; Zhang et al., 2004).

Table 1. Test conditions tested in pre-treatment with sulfuric acid

Temperature (ºC)	Residence time (min.)	Sulfuric acid (% w w^{-1})	Runs/ Samples nº
60	75	2.75	2
84	48	1.41	2
84	102	1.41	2
84	48	4.09	2
84	102	4.09	2
120	75	0.50	2
120	30	2.75	2
120	75	2.75	6
120	120	2.75	2
120	75	5.00	2
156	48	1.41	2
156	102	1.41	2
156	48	4.09	2
156	102	4.09	2
180	75	2.75	2
	Total		34

Enzymatic hydrolysis

Enzymatic hydrolysis was performed at a solid concentration of 5% (w v^{-1}, based on dry weight), using 50 mM citrate buffer pH 4.8 with BSA at a concentration of 60 mg g^{-1} dry biomass. The reaction mixture was incubated at 50 °C for 174 h on an orbital shaker at 150 rpm (Ferreira et al., 2010; Wei et al., 2012).

For enzyme digestion three commercial enzyme from Novozymes (Denmark) were used. A cellulase complex with 148 FPU mL^{-1} (NS22086), a b-glucosidase with 426 p-NPGU mL^{-1} (NS22118) and a xylanase with 7498 IU mL^{-1} (NS22083).

In each hydrolysis assay, two enzymatic loads were tested, one with 18 FPU / 36 p-NPGU / 36 IU per gram of biomass and the other with 6 FPU / 12 p-NPGU / 12 IU per gram of biomass. The enzymatic load of b-glucosidase and xylanase was twice that of the cellulase complex to avoid inhibition caused by the accumulation of cellobiose. (Lloyd & Wyman, 2005; Wyman et al., 2005; Kumar & Wyman, 2009).

Samples were taken at incubation times of 0 (used as control), 2, 4, 6, 24, 48, 72 and 174 h. The enzymatic hydrolysis was stopped by immediate freezing on ice and centrifugation at 5,000 g, 4 °C for 10 min. The supernatants were separated for subsequent analytical characterization and stored at -20 °C until analysis. The analysis of sugars released during hydrolysis was carried out using the DNS method (Miller, 1959). All the assays were performed at least in triplicates.

RESULTS AND DISCUSSION

Characterization of the raw material

The chemical composition of the olive grove pruning biomass, is shown in Table 2. The HPLC analysis of the carbohydrates present in the biomass revealed a presence of 51.15% of sugars, these being constituted mostly by glucose (33.59%) and xylose (13.11%). Lignin is the second most significant component in the constitution of the material used, representing about 25% of its dry weight. The results obtained are similar to

those obtained by other authors for olive pruning characterisation (Ballesteros et al., 2011; Requejo et al., 2012; Barbanera et al., 2015; Díaz et al., 2023).

Table 2. Chemical composition of raw material

Composition	Quantities (%) ± SD [a]
Glucose	33.59 ± 2.25
Xilose	13.11 ± 1.02
Arabinose	4.55 ± 0.20
Galactose	n.d.
Manose	n.d.
Acetic acid	3.53 ± 0.43
Insoluble acid lignin	18.07 ± 0.33
Soluble acid lignin	6.89 ± 0.06
Extractables	15.84 ± 0.44
Ashes	3.76 ± 0.01

[a] Composition expressed on a dry basis; n.d. – not detect.

Pretreatment

Fig. 1 presents the chemical constitution of the hydrolysates, resulting from pretreatments with sulfuric acid, based on determinations carried out with HPLC. These results show that xylose and glucose were the sugars with the highest concentration in the hydrolysates. The highest sugar release rate for the hydrolysate, 29.9%, occurred in pretreatments carried out at a temperature of 156 °C, an acid concentration of 4.09% and a residence time of 48 min. As it can be seen, no large variations were recorded in the solubilization rates of glucose and xylose in pretreatments carried out at a temperature below 156 °C. Below this temperature value, glucose solubilization varied between 3.0% and 5.7%, and xylose solubilization between 3.8% and 7.1%. The greatest increase in glucose and xylose solubilization occurred, in pretreatments carried out at a temperature of 156 °C, when the acid load was increased from 1.41% to 4.09%. In this situation, glucose solubilization more than doubled, going from 5.7% to 12.2%, while there was a simultaneous increase in xylose solubilization from 7.1% to 13.1%. With an acid load of 4.09% it is possible to obtain solubilization rates of 100% of xylose and arabinose in pre-treatments carried out at 156 °C. Above this temperature, the release rates of these sugars decrease due to the formation of a greater quantity of degradation products.

These results are in line with those obtained by other authors. Wei and collaborators achieved an increase in glucose solubilization from 3% to 13% when the temperature increased from 140 °C to 170 °C, in pretreatments carried out with sulfuric acid using wheat straw as a substrate (Wei et al., 2012). Yat and collaborators also found, after carrying out pretreatments with sulfuric acid, at temperatures between 160 and 190 °C, maximum glucose solubilization of only 13%, concluding that acid pretreatments were not efficient in solubilizing this sugar. However, under the same conditions these authors achieved solubilizations of around 94% for xylose (Yat et al., 2008). Shen & Wyman also achieved similar xylose solubilization rates (93.1%) in pretreatments carried out with sulfuric acid on corn stover for 40 minutes, at 160 °C and with an acid load of 0.5% (w w^{-1}) (Yat et al., 2008; Shen & Wyman, 2011).

Fig. 1 also shows that the increase in concentrations of by-products (BP) and degradation products (DP) was directly related to the increase in temperature, acid concentration and time pretreament.

The BP and DP are produced, in greater quantities, in pretreatments carried out at temperatures equal to or greater than 156 °C. The production of BP and DP increases from 5.6 to 6.2% when we increase the temperature from 156 °C to 180 °C even using lower acid concentrations and shorter pretreatment times.

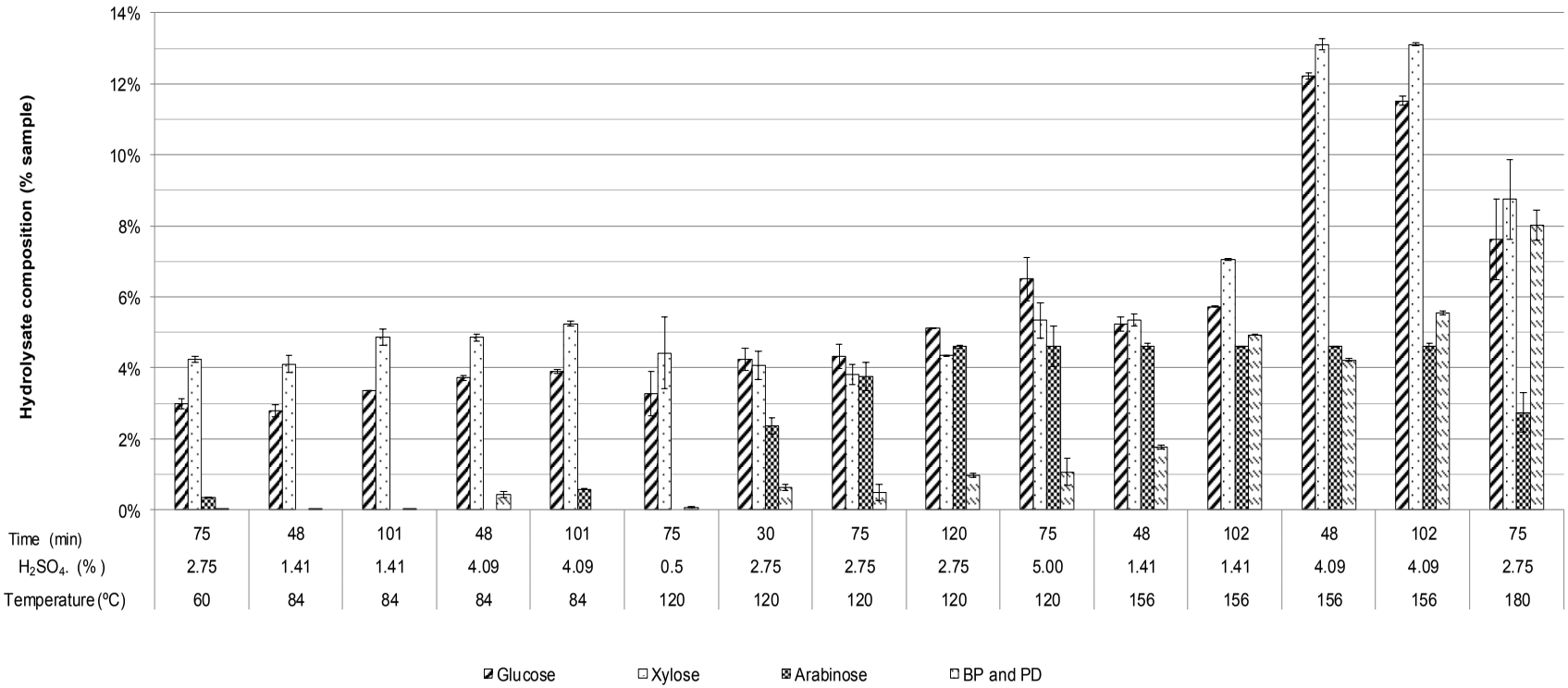

Figure 1. Chemical composition of hydrolysates resulting from pretreatment with sulfuric acid (in % of sample).

* BP – By-products; DP – Degradation Products.

At 156 °C the production of BP and DP increases with the acid concentration and pretreatment time. In this temperature class, pretreatments carried out for 48 min with an acid concentration of 1.41% produced 1.8% BP and PD. However, when are increased the pretreatment time to 102 min and the acid concentration to 4.09%, the formation of BP and DP rise to 5.6%.

Cara et al., in 2008, with olive tree pruning, obtained a xylose solubilization rate of 97.3% in pretreatments with sulfuric acid at 210 °C, with an acid load of 1.4% (w w^{-1}) and for 10 min. However, under these conditions the production of BP and DP were 10.4% (Cara et al., 2008).

Kim et al., in 2011, obtained a xylose removal rate of 87.4% from yellow poplar wood in pretreatments carried out at 160 °C, with 3.7% (w w^{-1}) oxalic acid for 40 min, in which the production of 5-HMF and furfural was 0.10 g L^{-1} and 0.66 g L^{-1}, respectively. However, when the pretreatment temperature was increased to 187 °C, even with a lower acid load of 2.5% (w w^{-1}) and for a shorter time, 30 min, the xylose removal rate increased to 96.3%, but the production of 5-HMF and furfural rise to 0.87 g L^{-1} and 4.15 g L^{-1}, respectively (Kim et al., 2011).

The inhibitors, especially furfural and 5-hydroxymethylfurfural, have a severe effect on the microorganisms used for the fermentation process including a breakdown of DNA and reduced RNA synthesis, resulting in hampered enzymatic activity (Solarte-Toro et al., 2019; Woiciechowski et al., 2020).

From the results expressed above, it can be conclude that the conciliation between the solubilization of hemicelluloses and a minimum production of degradation products can be achieved with pretreatment temperatures around 150–160 °C, even with higher acid loads.

Enzymatic hydrolysis

As it can be observed in Table 3, for the same enzymatic concentration, increasing any of the factors used, temperature, concentration and pretreatment duration, has a positive effect on the enzymatic hydrolysis (EH) promoting the sugar release rate (SRR).

Table 3. Enzymatic hydrolysis yield (% sugars present in the pretreated solid residues)

Pre-treatment conditions				Enzymatic hydrolysis time (h)				
A	B	C	Enzymatic load[1]	12	24	48	72	174
156	48	1.41	6-12-12	11.7 ± 0.5	18.5 ± 1.1	19.5 ± 0.4	21.5 ± 0.6	25.3 ± 0.7
156	48	1.41	18-36-36	19.4 ± 0.1	25.0 ± 0.5	28.5 ± 0.4	32.6 ± 0.2	40.8 ± 1.6
156	102	1.41	6-12-12	11.6 ± 0.6	17.6 ± 1.1	20.3 ± 0.4	21.8 ± 1.0	26.4 ± 0.3
156	102	1.41	18-36-36	19.9 ± 0.9	29.8 ± 0.1	30.8 ± 0.7	36.2 ± 0.3	46.9 ± 1.4
156	48	4.09	6-12-12	9.9 ± 0.8	17.8 ± 0.5	22.4 ± 0.3	24.3 ± 0.3	34.8 ± 1.5
156	48	4.09	18-36-36	18.5 ± 0.5	31.5 ± 1	38.7 ± 0.6	51.6 ± 0.2	70.9 ± 1.0
156	102	4.09	6-12-12	9.8 ± 0.2	19.0 ± 0.8	25.0 ± 0.5	30.9 ± 0.9	44.8 ± 0.5
156	102	4.09	18-36-36	23.4 ± 0.4	33.1 ± 1.0	46.9 ± 0.2	64.3 ± 0.7	84.4 ± 3.0
180	75	2.75	6-12-12	12.8 ± 0.5	22.5 ± 0.2	30.4 ± 0.6	38.9 ± 0.7	57.1 ± 0.6
180	75	2.75	18-36-36	28.8 ± 0.5	42.2 ± 1.6	54.5 ± 1.0	71.4 ± 1.0	83.6 ± 2.3

A – Temperature (ºC); B – Time (min); C – Concentration of H_2SO_4 (% w w^{-1}); [1] – Enzymatic load: FPU g^{-1} substrate – p-NPGU/g substrate – IU g-1 substrate.

After 72 h of reaction, the highest EH yield were achieved with pretreatments carried out at the highest temperature (180 °C), reaching a SRR of 67% in tests performed with 18 FPU, 36 p-NPGU and 36 IU per gram of substrate. The results obtained after 72 h of enzymatic hydrolysis are lower than those obtained by other authors, possibly due to the use of lower pretreatment temperatures in this study. Cara and collaborators, using the same raw material and the same time duration of EH, achieved a SRR of 76.5% from pretreatments carried out at 210 °C, with a 1.4% sulfuric acid for 10 min with a enzyme loading of 15 FPU and 15 IU per gram of substrate (Cara et al., 2008).

It can also be observed that the release rates did not stabilize after 72 h of reaction, continuing to increase in all tests carried out. With material resulting from pretreatments carried out at 156 °C, for 102 min and with 4.09% H_2SO_4, it was observed an increase of 20.7%, from 64.3% to 84.0%, in tests carried out between 72 h and 174 h of enzymatic reaction and with higher enzyme concentration (18 PFU per gram of substrate, 36 p-NPGU per gram of substrate and 36 IU per gram of substrate).

Overall process yields

The greatest amount of sugars released, considering the two stages of the process, pretreatment and enzymatic hydrolysis, was obtained with pretreatments carried out at 156 °C, with a sulfuric acid load of 4.09% and for 102 min. Under these conditions, during the pretreatment was possible to solubilize 29.18 g of sugars per 100 g of raw material. The enzymatic hydrolysis process that follows, after 72 h, was able to release 13.46 g of sugar per 100 g of raw material. The sum of sugars released in pretreatment and EH corresponds to 83,2% of sugars content in the sample (42.64 g of sugars per 100 g of raw material). Using 174 h in EH, the release of sugars increased to 18.54% leading to a combined yield of 93.1%, considering the two stages, corresponding this value to a release of 47.72 g of sugars per 100 g of raw material.

Cara and collaborators, obtained a maximum of 36.3 g of sugars per 100 g of raw material from pretreatments carried out at 180 °C, with a 1.4% sulfuric acid during 10 min and an enzymatic hydrolysis performed for 72 h, with an enzyme loading of 15 FPU and 15 IU per gram of substrate (Cara et al., 2008). Also, in a study performed by Martínez-Patiño and collaborators, it was obtained an overall yield of 39.8 g total sugars/ 100 g extracted from olive tree biomass, with pretreatments carried out at 160 °C, with 4.9% sulfuric acid and a residence time of 10 min, using an enzyme loading of 15 FPU and 15 IU per gram of substrate (Martínez-Patiño et al., 2017).

CONCLUSIONS

This work shows that residues from olive grove pruning, with a sugar content of 51.15%, can play a relevant role in sugar production, transforming waste from olive grove maintenance into raw material likely to generate wealth and employment.

In this work, it was possible to extract 93.1% of the sugars present in the olive grove pruning, with pretreatments carried out for 102 min at 156 °C with a sulfuric acid load of 4.09% (w w^{-1}), followed by enzymatic hydrolysis performed for 174 h, with an enzyme loading of 18 PFU, 36 p-NPGU and 36 IU per gram of substrate.

The yield obtained in this process opens possibilities for the use of this agricultural residue, currently without any commercial use, as raw material for the extraction of sugars and subsequent conversion into value-added products for the food, pharmaceutical and

fuel production industries, through production of ethanol, xylitol, lactic acid, and furfural (Gírio et al., 2010; Seidl & Goulart, 2016; Attard et al., 2020; Gonçalves et al., 2022).

ACKNOWLEDGEMENTS. This work is supported by National Funds by FCT - Portuguese Foundation for Science and Technology, under the project UIDB/04033/2020 (https://doi.org/10.54499/UIDB/04033/2020).

REFERENCES

ASTM E1757-19 2019. Standard Practice for Preparation of Biomass for Compositional Analysis. *Book of Standards* Volume: **05.06**. doi: 10.1520/E1757-19

Attard, T.M., Clark, J.H., & McElroy, C.R. 2020. Recent developments in key biorefinery areas. Current Opinion in Green and Sustainable' *Chemistry* **21**, pp. 64–74. Advance online publication. doi: 10.1016/j.cogsc.2019.12.002

Ballesteros, I., Ballesteros, M., Cara, C., Sáez, F., Castro, E., Manzanares, P., Negro, M.J. & Oliva, J.M. 2011. Effect of water extraction on sugars recovery from steam exploded olive tree pruning. *Bioresource technology* **102**(11), 6611–6616. doi: 10.1016/j.biortech.2011.03.077

Barbanera, M., Buratti, C., Cotana, F., Foschini, D., Lascaro, E. 2015. Effect of Steam Explosion Pretreatment on Sugar Production by Enzymatic Hydrolysis of Olive Tree Pruning. *Energy Procedia* **81**, 146–154, doi: 10.1016/j.egypro.2015.12.069

Brondi, M.G., Vasconcellos, V.M., Giordano, R.C. & Farinas, C. 2019. Alternative Low-Cost Additives to Improve the Saccharification of Lignocellulosic Biomass. *Appl Biochem Biotechnol* **187**, 461–473. doi: 10.1007/s12010-018-2834-z

Cara, C., Ruiz, E., Oliva, J.M., Sáez, F. & Castro, E. 2008. Conversion of olive tree biomass into fermentable sugars by dilute acid pretreatment and enzymatic saccharification. *Bioresource technology* **99**(6), 1869–1876. doi: 10.1016/j.biortech.2007.03.037

Díaz, M.J., Pedro, M.F. & Moya, M. 2023. Sequential Acid/Alkali Pretreatment for an Olive Tree Pruning Biorefinery. *Agronomy* **13**(11), 2682. doi: 10.3390/agronomy13112682

Ferreira, S., Gil, N., Queiroz, J.A., Duarte, A.P. & Domingues, F.C. 2010. Bioethanol from the Portuguese forest residue Pterospartum tridentatum – An evaluation of pretreatment strategy for enzymatic saccharification and sugars fermentation. *Bioresource Technology* **101**(20), 7797–7803. doi: 10.1016/j.biortech.2010.05.038

Gírio, F., Fonseca, C., Carvalheiro, F., Duarte, L., Marques, S. & Bogel-Łukasik, R. 2010. Hemicelluloses for fuel ethanol: A review. *Bioresource Technology* **101**(13), 4775–4800, ISSN 0960-8524, doi: 10.1016/j.biortech.2010.01.088

Gonçalves, M., Romanelli, J., Cansian, A., Pucci, E., Guimarães, J., Tardioli, P. & Saville, A. 2022. A review on the production and recovery of sugars from lignocellulosics for use in the synthesis of bioproducts. *Industrial Crops and Products* **186**, 115–213. doi: 10.1016/j.indcrop.2022.115213

Hames, B., Ruiz, R., Scarlata, C., Sluiter, A., Sluiter, J. & Templeton, D. 2005. Preparation of Samples for Compositional Analysis. *In Technical Report NREL/TP-510-42619* (NREL, ed.).

Hendriks, A.T.W.M. & Zeeman, G. 2009. Pretreatments to enhance the digestibility of lignocellulosic biomass. *Bioresource technology* **100**(1), 10–18. doi: 10.1016/j.biortech.2008.05.027

Huang, C., Liu, J., Geng, W., Wei, T. & Qiang, Y. 2021. A Review of Lignocellulosic Biomass Pretreatment Technologies. *Paper and Biomaterials* **6**(3), 61–76. doi: 10.1213/j.issn.2096-2355.2021.03.007

Jehadin, F., Rabeya, T. & Asad, M.A. 2021. Efficient conversion of cornstalk to bioethanol using dilute H_2SO_4 pretreatment. *Int. J. Energy Environ Eng.* **12**, 203–211. doi: 10.1007/s40095-020-00366-w

Kim, H., Lee, J., Jeffries, T. & Choi, I. 2011. Response surface optimization of oxalic acid pretreatment of yellow poplar (Liriodendron tulipifera) for production of glucose and xylose monosaccharides. *Bioresource Technology* **102**(2), 1440–1446. doi: 10.1016/j.biortech.2010.09.075

Kumar, R. & Wyman, C.E. 2009. Effect of additives on the digestibility of corn stover solids following pretreatment by leading technologies. *Biotechnology and bioengineering* **102**(6), 1544–1557. doi: 10.1002/bit.22203

Láinez, M., Ruiz, H.A., Castro-Luna, A.A. & Martínez-Hernández, S. 2018. Release of simple sugars from lignocellulosic biomass of Agave salmiana leaves subject to sequential pretreatment and enzymatic saccharification. *Biomass and Bioenergy* **118**, 133–140. doi: 10.1016/j.biombioe.2018.08.012

Lloyd, T.A. & Wyman, C.E. 2005. Combined sugar yields for dilute sulfuric acid pretreatment of corn stover followed by enzymatic hydrolysis of the remaining solids. *Bioresource Technology* **96**, 1967–1977. doi: 10.1016/j.biortech.2005.01.011

Luo, X., Liu, J., Zheng, P., Li, M., Zhou, Y., Liulian, H., Lihui, C. & Li, S. 2019. Promoting enzymatic hydrolysis of lignocellulosic biomass by inexpensive soy protein. *Biotechnol Biofuels* **12**, 51. doi: 10.1186/s13068-019-1387-x

Mankar, A., Pandey, A., Modak, A. & Pant, K. 2021. Pretreatment of lignocellulosic biomass: A review on recent advances. *Bioresource Technology* **334**. doi: 10.1016/j.biortech.2021.125235

Martínez-Patiño, J.C., Romero, I., Ruiz, E., Cara, C., Romero-García, J.M. & Castro, E. 2017. Design and optimization of sulfuric acid pretreatment of extracted olive tree biomass using response surface methodology. *BioRes*. **12**(1), 1779–1797. doi: 10.15376/biores.12.1.1779-1797

Miller, G.L. 1959. Use of Dinitrosalicylic Acid Reagent for Determination of Reducing Sugar. *Analytical Chemistry* **31**(3), 426–428. http://dx.doi.org/10.1021/ac60147a030

Nashiruddin, N.I., Manas, N.H.A., Rahman, R.A., Azelee, N.I.W., Dailin, D.J., Shaarani, S.M. 2020. Pretreatment and Enzymatic Hydrolysis of Lignocellulosic Biomass for Reducing Sugar Production. In: Zakaria, Z., Aguilar, C., Kusumaningtyas, R., Binod, P. (eds) Valorisation of Agro-industrial Residues – Volume **II**: Non-Biological Approaches. *Applied Environmental Science and Engineering for a Sustainable Future*. Springer, Cham. doi: 10.1007/978-3-030-39208-6_1

Nogueira, C., Padilha, C.E., Souza Filho, P. & Santos, S. 2022. Effects of the Addition of Poly(ethylene Glycol) and Non-ionic Surfactants on Pretreatment. Enzymatic Hydrolysis, and Ethanol Fermentation. *Bioenerg. Res.* **15**, 889–904. doi: 10.1007/s12155-021-10388-9

Panagiotou, G.L.O. 2007. Effect of compounds released during pretreatment of wheat straw on microbial growth and enzymatic hydrolysis rates. *Biotechnology and bioengineering* **96**(2), 250–258. doi: 10.1002/bit.21100

Requejo, A., Peleteiro, S., Garrote, G., Rodríguez, A. & Jiménez, L. 2012.'Biorefinery of olive pruning using various processes.' *Bioresource Technology* **111**, 301–307. doi: 10.1016/j.biortech.2012.01.156

Sánchez-Muñoz, S., Balbino, T.R., Oliveira, F., Rocha, T.M., Barbosa, F.G., Vélez-Mercado, M.I., Marcelino, P., Antunes, F., Moraes, E. & dos Santos, J. 2022. Surfactants, Biosurfactants, and Non-Catalytic Proteins as Key Molecules to Enhance Enzymatic Hydrolysis of Lignocellulosic Biomass. *Molecules* **27**(23), 8180. doi: 10.3390/molecules27238180

Sarker, T., Pattnaik, F., Nanda, S., Dalai, A.K., Meda, V. & Naik, S. 2021. Hydrothermal pretreatment technologies for lignocellulosic biomass: A review of steam explosion and subcritical water hydrolysis. *Chemosphere* **284**, 131372, doi: 10.1016/j.chemosphere.2021.131372

Scapini, T., Santos, M., Bonatto, C., Wancura, J., Mulinari, J., Camargo, A., Klanovicz, N., Zabot, G., Tres, M., Fongaro, G. & Treichel, H. 2021. Hydrothermal pretreatment of lignocellulosic biomass for hemicellulose recovery. *Bioresource Technology* **342**, 126033. doi: 10.1016/j.biortech.2021.126033

Seidl, P.R. & Goulart, A.K. 2016. Pretreatment processes for lignocellulosic biomass conversion to biofuels and bioproducts. *Curr Opin Green Sust.* **2**, 48–53. doi: 10.1016/j.cogsc.2016.09.003

Shen, J. & Wyman, C.E. 2011. A novel mechanism and kinetic model to explain enhanced xylose yields from dilute sulfuric acid compared to hydrothermal pretreatment of corn stover. *Bioresource technology* **102**(19), 9111–9120. doi: 10.1016/j.biortech.2011.04.001

Sithole, B.B., Vollstaedt, P. & Allen L.H. 1991. Comparison of Soxtec and Soxhlet systems for determining extractives content. *Tappi Journal*, pp. 187–191.

Sluiter, A., Hames, B., Ruiz, R., Scarlata, C., Sluiter, J. & Templeton, D. 2005. Determination of Ash in Biomass. In *Technical Report* NREL/TP-510-42622 (NREL, ed.).

Sluiter, A., Hames, B., Ruiz, R., Scarlata, C., Sluiter, J., Templeton, D. & Crocker, D. 2008a. Determination of Structural Carbohydrates and Lignin in Biomass. In *Technical Report* NREL/TP-510-42618 (NREL, ed.).

Sluiter, A., Hames, B., Ruiz, R., Scarlata, C., Sluiter, J. & Templeton, D. 2008b. Determination of Sugars, Byproducts, and Degradation Products in Liquid Fraction Process Samples. In *Technical Report* NREL/TP-510-42623 (NREL, ed.).

Solarte-Toro, J., Romero-García, J., Martínez-Patiño, J., Ruiz-Ramos, E., Castro-Galiano, E. & Cardona-Alzate, C. 2019. Acid pretreatment of lignocellulosic biomass for energy vectors production: A review focused on operational conditions and techno-economic assessment for bioethanol production. *Renewable and Sustainable Energy Reviews* **107**, 587–601. doi: 10.1016/j.rser.2019.02.024

Sun, S., Shaolong Sun, Sh., Cao, X. & Sun, R. 2016. The role of pretreatment in improving the enzymatic hydrolysis of lignocellulosic materials. *Bioresource Technology* **199**, 49–58. doi: 10.1016/j.biortech.2015.08.061

Wei, W., Wu, S. & Liu, L. 2012. Enzymatic saccharification of dilute acid pretreated eucalyptus chips for fermentable sugar production. *Bioresource Technology* **110**, 302–307. doi: 10.1016/j.biortech.2012.01.003

Woiciechowski, A., Neto, C., Vandenberghe, L., Neto, D., Sydney, A., Letti, L., Karp, S., Torres, L. & Soccol, C. 2020. Lignocellulosic biomass: Acid and alkaline pretreatments and their effects on biomass recalcitrance – Conventional processing and recent advances. *Bioresource Technology* **304**, 122848. doi: 10.1016/j.biortech.2020.122848

Wyman, C.E., Dale, B.E., Elander, R.T., Holtzapple, M., Ladisch, M.R. & Lee, Y.Y. 2005. Coordinated development of leading biomass pretreatment technologies. *Bioresource Technology* **96**, 1959–1966. doi: 10.1016/j.biortech.2005.01.010

Yat, S. C., Berger, A., Shonnard, D.R. 2008. 'Kinetic characterization for dilute sulfuric acid hydrolysis of timber varieties and switchgrass.' *Bioresource Technology* **99**(9), 3855–3863. doi: 10.1016/j.biortech.2007.06.046

Zhang, Y.H.P., Lynd, L.R. & Zhang, Y. 2004. Toward an aggregated understanding of enzymatic hydrolysis of cellulose: noncomplexed cellulase systems. *Biotechnology and bioengineering* **88**, 797. doi: 10.1002/bit.20282

Zheng, T., Jiang, J. & Yao, J. 2021. Surfactant-promoted hydrolysis of lignocellulose for ethanol production. *Fuel Processing Technology* **213**, 106660, doi: 10.1016/j.fuproc.2020.106660

Zhou, Z., Ouyang, D., Liu, D. & Zhao, X. 2023. Oxidative pretreatment of lignocellulosic biomass for enzymatic hydrolysis: Progress and challenges. *Bioresource Technology* **367**, 128208. doi: 10.1016/j.biortech.2022.128208

Zhu, J. & Pan, X. 2022. Efficient sugar production from plant biomass: Current status, challenges, and future directions. *Renewable and Sustainable Energy Reviews* **164**. doi: 10.1016/j.rser.2022.112583

Agronomy Research **22**(2), 887–897, 2024
https://doi.org/10.15159/AR.24.063

Genotype prediction in maize (*Zea mays* L.) progeny using different predictive models

A. Polyvanyi[1,*], A. Butenko[2], M. Mikulina[1], V. Zubko[1], S. Kharchenko[3], V. Dubovyk[4], O. Dubovyk[4] and B. Sarzhanov[1]

[1]Sumy National Agrarian University, Faculty of engineering and technology, Department of Agroengineering, H. Kondratieva Str. 160, UA40021 Sumy, Ukraine
[2]Sumy National Agrarian University, Faculty of agrotechnologies and natural resource management, Plant growing Department, H. Kondratieva Srt. 160, UA40021 Sumy, Ukraine
[3]Sumy National Agrarian University, Faculty of agrotechnologies and natural resource management, Department of Physical Education, H. Kondratieva Str. 160, UA40021 Sumy, Ukraine
[4]Sumy National Agrarian University, Faculty of agrotechnologies and natural resource management, Department of Biotechnology and chemistry, H. Kondratieva Str. 160, UA40021 Sumy, Ukraine
[*]Correspondence: polivanui1@gmail.com

Received: March 29th, 2024; Accepted: June 27th, 2024; Published: July 11th, 2024

Abstract. This study utilized two probabilistic methods, Gaussian Naive Bayes (GNB) and Logistic Regression (LR), to predict the genotypes of the offspring of two maize varieties: SC604 and KSC707, based on the phenotypic traits of the parent plant. The predictive performance of both models was evaluated by measuring their overall accuracy and calculating the area under receiver operating characteristic curve (AUC). The overall accuracy of both models ranged from 80% to 89%. The AUC values for the LR models were 0.88 or higher, while the GNB models had AUC values of 0.83 or higher. These results indicated that both models were successful in predicting the genetic makeup of the progeny. Furthermore, it was observed that both models were more accurate in predicting the SC604 genotype, which was found to be more consistent and predictable compared to the KSC707 genotype. A chi-square test was conducted to assess the similarity between the prediction results of the two models, revealing that both models had a similarly high likelihood of making accurate predictions in all scenarios.

Key words: Gaussian Naive Bayes (GNB), genotype prediction, Logistic Regression (LR), predictive models, *Zea mays* L.

INTRODUCTION

The implementation and development of learning algorithms have paved the way for novel approaches to data processing, information extraction, and decision-making. These algorithms have widespread applications across various fields of human activity, as evidenced by the abundance of literature on their development and use. Scientists

have devised an algorithm for the selection of genetic biomarkers and classification of subjects through the analysis of genome-wide single nucleotide polymorphism data. The algorithm demonstrated significantly improved classification accuracy in identifying biomarkers for Type 1 diabetes (Sambo et al., 2012).

Other researchers have used a naive Bayes classifier combined with small RNA deep sequencing statistics, as well as genomic signatures to recognize offspring microRNAs in different types of crops and herbs (Douglass et al., 2016). The classifier exhibited high accuracy in identifying microRNA for all four plants, as determined by the AUC's receiver operating characteristic curve. The values of the area under the receiver operating curve reported in the study range from 0.9750 to 0.9960, with the highest value being obtained for the identification of Arabidopsis microRNAs. These machine learning algorithms have been widely employed in the classification of various plant organisms as well. Typically, the identification of plants is based on leaf characteristics, such as their shape, color, and texture, which are unique to each plant species. Unlike flowers and fruits, plants maintain functional leaves throughout their lifespan (Siravenha & Carvalho, 2015).

Another group of scientists from China and the US created a probabilistic series of algorithms that endeavors to recognize underlying relationships in a set of data, employing image and data processing techniques to automatize herb classifying (Wu et al., 2007). This algorithm successfully classified 32 different herb species based on their visual characteristics with a greater than 90% accuracy rate. The authors found their algorithm to be both rapid and efficient in recognizing and classifying herbs.

In different years, many scientists were engaged in the development of an algorithm for the visual recognition of plants. One such research group, for example, created an algorithm that can differentiate weeds from two main crops - carrots and cabbage (Hemming & Rath, 2001). They initially used eight morphological features in combination with three color features, selecting the most relevant features to discriminate between the different plant species. The inclusion of color features improved classification accuracy, with the researchers reporting between 50% and 95% of crops being accurately classified. The average rate of successful classifying was 87% and 73% for cabbage and carrots, respectively.

Continuing research on this topic, another group of scientists from the University of Southern Denmark created a dataset representing visual features using distance data from images of seedlings of various plants (Giselsson et al., 2013). The researchers utilized a high-degree Legendre polynomial to fit the distance data and subsequently extracted the coefficients of the polynomial, which they referred to as the Legendre polynomial feature set. In addition, they collected another set of data, which they named the standard feature set. The data sets were then subjected to four classification algorithms. The researchers observed that the Legendre polynomial feature set exhibited a high degree of robustness, generating an accuracy rate of nearly 99% when used in conjunction with the classification algorithms. Conversely, the standard feature set yielded an accuracy rate of 87%. Despite these promising results, the researchers recommended further testing of the attribute data collection method to determine its true value.

A new method for data acquisition on leaf features has also been proposed previously (Siravenha & Carvalho, 2015; Änäkkälä et al., 2023; Esan et al., 2023). It includes contour-to-centroid distance and transforms the data using a fast Fourier transform. The authors of this method used a feature selection approach to reduce

dimensionality, which led to increased classification accuracy. Also, they employed various classification algorithms for plant identification, achieving classification accuracies ranging from 66% (with the C4.5 algorithm) to 98% (with the Pattern Net algorithm applied to main components). The field of phenotypic predictions for quantitative traits of sequenced whole genomes has seen significant advancement with the incorporation of learning algorithms and other statistical methods. Scientists from Fondazione Bruno Kessler, Italy, made a significant contribution to the development of this field with their research (Guzzetta et al., 2010). They outlined a learning process that uses a naive elastic network-based L1L2 regularization method to predict phenotypes. The effectiveness of this method was found to be highly accurate. Similarly, a group of Chinese scientists employed machine learning techniques to distinguish root traits that caused cultivar differentiation in a binomial environment (Zhao et al., 2016).

Lippert et al. (2017) and Dragov et al. (2023) developed models for phenotypic feature prediction and combined them into a singular machine learning model for genome re-identification. In all instances, various learning methods were utilized, each with satisfactory to excellent performance in prediction or classification. It should be noted, however, that no single machine-learning method is optimal for every circumstance, as each has its strengths and limitations (Kell et al., 2001; Hudzenko et al., 2023).

The exceptional proficiency of the algorithms in recognizing and grouping the subjects being examined led us to undertake a study that aims to forecast the genotypes of plants by examining the phenotypic traits of their parents. Furthermore, this study serves as a quantitative confirmation of the theory that GNB with continuous characteristics and LR are fundamentally identical, despite being generative and discriminative respectively (Ng & Jordan, 2001; Chen et al., 2019).

The present study incorporates a comprehensive analysis of the materials and methods used in its execution. This involved the procurement of all necessary materials, including instruments, equipment, and chemicals, from reputable sources. The methods employed in this study were carefully formulated and optimized to obtain the most accurate and reliable data possible. The techniques used were based on established protocols and were performed under standardized conditions to minimize experimental variability and ensure consistency. All procedures were documented in detail to facilitate reproducibility and ease of replication.

MATERIALS AND METHODS

Location of the Study

In May 2020, an experiment was conducted in the experimental field of Sumy National Agrarian University, located in the Sumy district of the Sumy region, which is part of the Forest-steppe zone of Ukraine. The soils on the experimental site were dark gray podzolized and fertilizers were added to the soil.

Plant Material

For this research, two genotypes of maize (*Zea mays* L.) were used: SC604 and KSC707. They differed in the color of their kernels, with SC604 having translucent, white kernels, and KSC707 having yellow kernels.

Selection Process

The SC604 genotype underwent a selection process spanning three cycles, to develop larger, wider leaves, an increased number of leaves, and taller plant structures. In contrast, the KSC707 genotype underwent random selection after each cycle.

Pollination Process

To obtain seeds from selected plants of each strain, pollination was carried out using bulk pollen harvested from male inflorescences of the same genotype. Controlled pollination was ensured by protecting the ear with a paper bag immediately after emergence.

Field Research Methods

The experiment involved planting seeds of fourth-generation parent plants and fifth-generation offspring plants of the two genotypes mentioned. It was conducted using a completely randomized design with two factors - genotype and generation. The experimental field was divided into two rows for each variety, with each row being 5 meters long, and separated by a distance of 0.9 meters. The plots were overseeded, and after three weeks of planting, the number of plants in each plot was thinned to 40,000 units per hectare. During silking, when almost half of the planted plants in the field developed silks, in order to obtain accurate data, we employed a series of measurements to determine various plant attributes for accurate data collection. We used a node-counting method to determine the number of leaves present (nl). Additionally, we measured the length and width of the ear leaf (el, ew), and the overall height of the experimental samples (hs), defined as the distance from the soil base to the apex of the m-inflorescence. To assess grain filling rate (gf), we used a linear coefficient derived from the orthogonal contrast of grain dry weight during the linear phase of the filling time, as part of a sequential selection process.

Prediction Methods

To predict the genotypes of the offspring, we utilized two classification techniques: the GNB and LR. The GNB algorithm was used to determine the probability of a progeny belonging to either the SC604 or KSC707 strain, based on attributes such as the number of leaves, length and width of the ear leaf and others. The probability model was simplified as follows:

$$\Pr(Class|P_1, P_2, \dots, P_5) = \Pr(Class) \times \prod_{i=1}^{5} \Pr(P_i|Class) \quad (1)$$

In this model, Class represents the class label (SC604 or KSC707) and P_1 is used to represent the attributes. The model calculates the posterior probability of a progeny's lineage by multiplying the prior probability of the class label with the conditional probabilities of the attributes associated with that class label. It is important to note that this model falls under the discriminative category for prediction or classification, unlike LR, which is generative.

To determine whether a progeny belongs to the KSC707 or SC604 genotypes, we used measurements from the parents of these genotypes to fit an LR model, following the methodology outlined by Tsangaratos & Ilia (2016). The model parameters were

estimated to compute the posterior probabilities of the progeny being classified into either the KSC707 or SC604 genotypes.

$$\Pr(Class|P_1, P_2, \dots, P_5) \quad (2)$$

The LR model assumes a parametric structure when the class variable is binomial, as shown by Ng & Jordan (2001):

$$\Pr(Class = "SC604"|P_1, P_2, \dots, P_5) = \frac{1}{1 + \exp(b_o + \sum_{i=1}^{5} b_i P_i)} \quad (3)$$

and

$$\Pr(Class = "KSC707"|P_1, P_2, \dots, P_5) = \frac{\exp(b_o + \sum_{i=1}^{5} b_i P_i)}{1 + \exp(b_o + \sum_{i=1}^{5} b_i P_i)} \quad (4)$$

Ng & Jordan (2001) demonstrated that the mathematical structure of Pr(Class|P_1, P_2,… P_5) employed by LR conforms exactly to the structure of a GNB classifier under the assumptions made. Furthermore, in the majority of cases, both methods yield comparable outcomes. It is pertinent to note that LR estimates the parameters of Pr(Class|P_1, P_2,… P_5) directly, whereas GNB estimates the parameters of Pr(Class) and Pr(P_1, P_2,… P_5|Class) directly.

In order to evaluate the proposition, that GNB and LR models yield identical outcomes (Ng & Jordan, 2001), we conducted a series of experiments. First, we created several sub-samples from the original dataset by iteratively excluding some attributes and then computed their main components. Next, we used both models to predict the offspring based on the conserved attributes or the respective main components of each dataset. The main components, which are an orthogonal conversion of the initial observations that maintain the total variance, are expected to eliminate any bias associated with the assumption of independence between attributes, compared to using the original variables. This approach is intended to help identify any such bias in the prediction results. We evaluated the relative significance of the characteristics in distinguishing between the two categories. We calculated several metrics, including precision, sensitivity, the maximum AUC of receiver operating characteristics and others for both models. We assessed each model's efficacy using both the accuracy and the AUC value. In our experiments, the SC604 genotype was defined as the positive class. All analyses were conducted using the R statistical software package (R Core Team, 2017).

RESULTS AND DISCUSSION

Kuhn (2015) in his study utilized the variable significance ranking technique to identify the most pertinent traits among the properties of the data set in distinguishing between the two genotypes. The analysis determined that *ew*, *gf*, and *hs* were the most crucial attributes, with respective significance values of 0.86, 0.83, and 0.74 on a 1-point scale. This conclusion was validated through the LR model, which also identified *ew*, *gf*, and *hs* as the most significant predictor variables in the data set, with p-values of 0.0395, 0.0475, and 0.05, respectively. Means and standard deviations for each of the five traits were calculated and displayed (Table 1), with the *nl* trait exhibiting minimal variability across generations and genotypes and ranking last in its capability to distinguish one genotype from another with a significance value of 0.58.

Table 1. Mean and standard deviation for the five parent-offspring properties considered

Attribute	Parent		Offspring	
	SC604	KSC707	SC604	KSC707
ew (cm)	9.71(0.60)	8.41(1.13)	9.52(0.66)	8.99(0.79)
el (cm)	88.45(6.55)	83.97(7.44)	90.12(5.11)	84.92(6.04)
nl (cm)	12.22(1.57)	12.13(1.08)	12.94(1.03)	12.31(1.21)
hs (cm)	236.73(24.12)	217.32(24.86)	232.10(21.34)	217.06(21.48)
gf ($mg \times d^{-1}$)	5.52(0.31)	5.05(0.35)	5.62(0.29)	5.17(0.39)

By utilizing diverse subsets of the original data set and their main components, we were able to predict the offspring of two parents. In the following, we will present the performance of both models on specific subsets (Table 2 and Table 3).

Table 2. Values of the confusion matrix of the LR and GNB models with subsets of the initial information and their respective main components

Data	Attribute	Model	Confusion Matrix			
			PT	NF	NT	PF
Initial data	(1) *ew*+*el*+*nl*+*hs*+*gf*	LR	27	3	24	6
		GNB	28	2	25	5
	(2) *ew*+*gf*+*hs*+*nl*	LR	28	2	23	7
		GNB	28	2	23	7
	(3) *ew*+*gf*+*hs*	LR	28	2	23	7
		GNB	28	2	24	6
	(4) *gf*+*hs*	LR	27	3	27	3
		GNB	25	5	28	2
	(5) *ew*+*gf*	LR	28	2	24	6
		GNB	27	3	24	6
Main component	$mc_1+mc_2+mc_3+mc_4+mc_5$ from (1)	LR	27	3	24	6
		GNB	27	3	23	7
	$mc_1+mc_2+mc_3+mc_4$ from (2)	LR	28	2	23	7
		GNB	29	1	20	10
	$mc_1+mc_2+mc_3$ from (3)	LR	28	2	23	7
		GNB	28	2	23	7
	mc_1+mc_2 from (4)	LR	27	3	27	3
		GNB	24	6	26	4
	mc_1+mc_2 from (5)	LR	28	2	24	6
		GNB	27	3	23	7

mc_i(i=1, 2,…,5) – main components; PT – positive true; NF – negative false; NT – negative true; and PF – positive false.

To compare the confusion matrices generated by the models on each subset, we conducted a Chi-square test (Agresti, 2007). The p-values resulting from the test of homogeneity of the confusion matrices ranged from 0.7812 to 1, indicating that the prediction performances of both models were very similar. GNB and LR are both models utilized to compute the conditional probability that an offspring belongs to a particular genotype. GNB updates prior knowledge from parents with current evidence of offspring, while LR estimates the parameters of the model with the parents' phenotypic values. Previously, scientists have already provided a comprehensive and refined demonstration

that, under certain conditions of a binary response variable (Y) with parameter π=Pr(Y="PositiveClass"), Gaussian distributed attributes (P_i) that are conditionally independent concerning Y, and $Pr(P_i|Y=y_k)\sim N(\mu_{ik},\sigma_i)$, the conditional probabilities under the GNB model can be expressed in parametric forms (Ng & Jordan, 2001).

$$\Pr(Class = "SC604"|P_1, P_2, \dots, P_5) = \frac{1}{1 + \exp(w_o + \sum_{i=1}^{5} w_i P_i)} \quad (5)$$

and

$$\Pr(Class = "KSC707"|P_1, P_2, \dots, P_5) = \frac{\exp(w_o + \sum_{i=1}^{5} w_i P_i)}{1 + \exp(w_o + \sum_{i=1}^{5} w_i P_i)} \quad (6)$$

where

$$w_i = \frac{\mu_{i0} - \mu_{i1}}{\sigma_i^2} \quad (7)$$

and

$$w_0 = \ln\frac{1-\pi}{\pi} + \sum_i \frac{\mu_{i1}^2 - \mu_{i0}^2}{2\sigma_i^2} \quad (8)$$

When the response variable has binary outcomes and the predictor variables are distributed according to a Gaussian distribution, the probabilities provided by LR remain identical. The numerical evidence obtained from the experiment supports the findings of other studies (Ng & Jordan, 2001; Bhowmik, 2015; Vasilaki et al., 2023). It is important to note that LR estimates the parameters for Pr(Class|Pi) directly, while GNB estimates the parameters for Pr(Class) and Pr(Pi|Class) directly.

Table 3. The predictive attributes of the LR and GNB models with subsets of the initial information and their respective main components

Data	Attribute	Model	*p*-value	Accuracy	AUC
Initial data	(1) *ew*+*el*+*nl*+*hs*+*gf*	LR	0.9710	0.84	0.88
		GNB		0.86	0.90
	(2) *ew*+*gf*+*hs*+*nl*	LR	1.000	0.83	0.91
		GNB		0.84	0.88
	(3) *ew*+*gf*+*hs*	LR	0.9886	0.85	0.90
		GNB		0.86	0.89
	(4) *gf*+*hs*	LR	0.8904	0.89	0.91
		GNB		0.88	0.90
	(5) *ew*+*gf*	LR	0.9822	0.85	0.89
		GNB		0.84	0.86
Main component	mc_1+mc_2+mc_3+mc_4+mc_5 from (1)	LR	0.9886	0.82	0.89
		GNB		0.83	0.83
	mc_1+mc_2+mc_3+mc_4 from (2)	LR	0.8196	0.85	0.91
		GNB		0.80	0.85
	mc_1+mc_2+mc_3 from (3)	LR	1.000	0.84	0.91
		GNB		0.84	0.88
	mc_1+mc_2 from (4)	LR	0.7812	0.89	0.90
		GNB		0.82	0.88
	mc_1+mc_2 from (5)	LR	0.9696	0.84	0.89
		GNB		0.82	0.88

mc_i(i=1, 2,…,5) – main components.

The findings indicate that logistic regression produced identical prediction outcomes, regardless of whether subsets of the initial data or their main components were utilized (Table 2 and Table 3). This consistency can be attributed to the logistic equation's right-hand side remaining consistent for both the original data and main components,

$$\frac{1}{1+\exp(\hat{\beta}_{obs}^{t}A)} = \frac{1}{1+\exp(\hat{\beta}_{pc}^{t}Z)}$$

which leads to:

$$\hat{\beta}_{obs}^{t}A = \hat{\beta}_{pc}^{t}Z \tag{9}$$

In this case, based on the initial data, $\hat{\beta}_{obs}^{t}$ is the vector of ERC (estimated regression coefficient) while A denotes the matrix composed of the subset of the original variables. On the other hand, the vector of ERC based on the main traits is $\hat{\beta}_{pc}^{t}$, and Z is the matrix of main traits that is derived from the subset of the primary data.

So,

$$\Pr(Class = "SC604"|P, \beta_{obs}) = \Pr(Class = "SC604"|Z, \beta_{pc})$$

and

$$\Pr(Class = "KSC707"|P, \beta_{obs}) = \Pr\big(Class = "KSC707"\big|Z, \beta_{pc}\big).$$

When utilizing GNB, it was observed that the confusion matrices derived from subsets of the original data and their main components were not consistently identical. However, the disparities did not prove to be of significant value, as all *p*-values were found to be greater than or equal to 0.7812.

The prediction performances of both models were highly commendable. When all available data were tested, the overall accuracy of predictions ranged from 80% to 89% (Table 3), with AUC values between 0.83 and 0.91. The models were notably more accurate in predicting SC604 genotypes than KSC707 genotypes, with lower specificity but higher sensitivity. This observation may be attributed to the structures of the SC604 and KSC707 populations and their respective development procedures. The SC604 population was developed using a selection process aimed at promoting wider and longer leaves, with increased leaf numbers and taller plants. The three cycles of selection likely contributed to the partial realization of that objective. The SC604 genotypes have progressively formed a more homogenous group that exhibits the distinctive traits selected for, except for *nl*. As a result, the accuracy of prediction in these models was higher.

To date, scientists have provided a lot of evidence to support the influence of selection on a hereditary trait (García-Ruiz et al., 2016; Kolesnikov et al., 2023). They have demonstrated that selection, whether natural or artificial, influences the expression of the gene(s) responsible for the development of a modified phenotype. A group of Chinese researchers has discovered that the regulation of maize leaf width is governed by dominant genes that are not linked to the gene(s) responsible for the control of maize leaf length (Wang et al., 2018). This discovery suggests that selection can be employed to modify the width of maize leaves without any direct effect on other canopy traits.

The present study confirms the hypothesis that the increase in maize leaf width and plant height of the SC604 genotype can be attributed to the direct impact of selection for wider leaves and taller plants. Consequently, these two traits have emerged as the most significant discriminating features between the two populations. The discrepancy in grain filling rate between the SC604 and KSC707 genotypes can be attributed to an indirect selection for canopy size. Conversely, the KSC707 genotypes were selected at random, resulting in larger trait variability and less homogeneity among individuals. The increased dispersion of the KSC707 strains led to reduced model specificity. Although some individuals of the KSC707 strains shared traits with the SC604 genotypes, the majority maintained their distinct traits and were accurately predicted by the models.

The tests assessing the genotypes of offspring primarily focused on parent-offspring resemblance. In models trained with the phenotypic values of parents, similar traits were identified in their progeny. The receiver operating characteristic's AUC from these tests, which utilized a single predictor variable, may serve as a reliable predictor of heritability. Wray et al. (2010) developed an equation correlating the maximum receiver operating characteristic's AUC with heritability and the prevalence of a given trait. Dreyfuss et al. (2012) noted in their study that the precision of a study reflects the heredity of the trait being evaluated. They added that the high heritability of a phenotypic trait resulted in greater prediction accuracy, while traits with low heritability had lower accuracy predictions, being more susceptible to environmental factors than genetic factors. This study considered numerous phenotypic traits in determining offspring genotypes. However, it was unclear whether the AUC value was a suitable estimator of heritability. In this study, we may consider the AUC value as an adequate indicator for measuring the similarity between parents and their offspring. As the AUC value increases, so does the level of resemblance between the two parties.

CONCLUSIONS

Using field data, we employed two different predictive models, LR and GNB, to determine the genotype of two distinct maize strains. The accuracy of our predictions ranged from 80% to 89%, with the AUC values of the receiver operating characteristic falling between 0.83 and 0.91. Our tests showed a high level of sensitivity, indicating a correct identification of the SC604 genotype, with a modal value of 0.91 for both GNB and LR. Conversely, specificity, defined as the correct identification of the KSC707 genotype, had a modal value of 0.74 for both GNB and LR. This discrepancy in sensitivity and specificity can be attributed to the varying structures of the two populations, rather than the quality of the tests themselves. Specifically, the SC604 population was more homogenous and easier to identify, while the KSC707 population was more diverse, with a large proportion of its progeny being misclassified as SC604 genotypes.

To conduct the genotype-prediction tests, various subsets of the data along with their corresponding main components were utilized. A Chi-square test was performed to compare the prediction results of the LR and GNB models for each data set. The outcome indicated that both models produced similar prediction performances. The results of our field research are consistent with the conclusions of the theoretical works of other scientists (Ng & Jordan, 2001; Bhowmik, 2015). When using LR, there was no difference in prediction results whether the subset of the data or its corresponding main

components were used. The main components preserved the overall fluctuation of the information, and the outcome of the matrix of data multiplied by the ERC's vector from a subset remained consistent with the product of the matrix of primary constituents and the vector of estimated coefficients from those components. When employing the GNB model, the predictive results with a subset of the data or the corresponding primary constituents did not invariably match. However, any differences found were not significant.

REFERENCES

Agresti, A. 2007. *An Introduction to Categorical Data Analysis.* (2nd ed.). John Wiley & Sons, 38 pp.

Änäkkälä, M.A., Lehtilä, A., Mäkelä, P. & Lajunen, A. 2023. Application of UAV multispectral imaging for determining the characteristics of maize vegetation. *Agronomy Research* **21**(2), 644–653.

Bhowmik, T.K. 2015. Naive Bayes vs Logistic Regression: theory, implementation and experimental validation. *Inteligencia Artificial. Revista Iberoamericana de Inteligencia Artificial* **18**(56), 14–30. doi: 10.4114/intartif.vol18iss56pp14–30

Chen, W., Yan, X., Zhao, Z., Hong, H., Bui, D.T. & Pradhan, B. 2019. Spatial prediction of landslide susceptibility using data mining–based kernel logistic regression, naive Bayes and RBFNetwork models for the Long County area (China). *Bulletin of Engineering Geology and the Environment* **78**, 247–266. doi: 10.1007/s10064–018–1256–z

Douglass, S., Hsu, S.W., Cokus, S., Goldberg, R.B., Harada, J.J. & Pellegrini, M. 2016. A naïve Bayesian classifier for identifying plant micro RNAs. *The Plant Journal* **86**(6), 481–492. doi: doi.org/10.1111/tpj.13180

Dragov, R., Taneva, K. & Bozhanova, V. 2023. Parametric and nonparametric stability of grain yield and grain protein content in durum wheat genotypes with various origins. *Agronomy Research* **21**(2), 693–710.

Dreyfuss, J.M., Levner, D., Galagan, J.E., Church, G.M. & Ramoni, M.F. 2012. How accurate can genetic predictions be?. *BMC Genomics* **13**(1), 1–8. doi: 10.1186/1471-2164-13-340

Esan, V.I., Sangoyomi, T.E., Ajayi, O.A., Christensen, M. & Ogunwole, J.O. 2023. Performance evaluation and variability analysis for morpho-physiological traits of orange fleshed tomato varieties introduced in Nigeria climatic conditions. *Agronomy Research* **21**(2), 711–727.

García-Ruiz, A., Cole, J.B., VanRaden, P.M., Wiggans, G.R., Ruiz-López, F.J. & Van Tassell, C.P. 2016. Changes in genetic selection differentials and generation intervals in US Holstein dairy cattle as a result of genomic selection. *Proceedings of the National Academy of Sciences* **113**(28), E3995–E4004. doi: 10.1073/pnas.1519061113

Giselsson, T.M., Midtiby, H.S. & Jørgensen, RN. 2013. Seedling discrimination with shape features derived from a distance transform. *Sensors* **13**(5), 5585–5602. doi: 10.3390/s130505585

Guzzetta, G., Jurman, G. & Furlanello, C. 2010. A machine learning pipeline for quantitative phenotype prediction from genotype data. *BMC Bioinformatics* **11**(8), 1–9. doi: 10.1186/1471-2105-11-S8-S3

Hemming, J. & Rath, T. 2001. PA—Precision agriculture: Computer-vision-based weed identification under field conditions using controlled lighting. *Journal of Agricultural Engineering Research* **78**(3), 233–243. doi: 10.1006/jaer.2000.0639

Hudzenko, V.M., Lysenko, A.A., Tsentylo, L.V., Demydov, O.A., Polishchuk, T.P., Khudolii, L.V., ... & Kozelets, H.M. 2023. Genotype by yield x trait (GYT) biplot analysis for the identification of the superior winter and facultative barley breeding lines. *Agronomy Research* **21**(2), 739–757.

Kell, D.B., Darby, R.M. & Draper, J. 2001. Genomic computing. Explanatory analysis of plant expression profiling data using machine learning. *Plant Physiology* **126**(3), 943–951. doi: 10.1104/pp.126.3.943

Kolesnikov, M., Gerasko, T., Paschenko, Y., Pokoptseva, L., Onyschenko, O. & Kolesnikova, A. 2023. Effect of water deficit on maize seeds (Zea mays L.) during germination. *Agronomy Research* **21**(1), 156–174.

Kuhn, M. 2015. Caret: classification and regression training. *Astrophysics Source Code Library*, ascl–1505.

Lippert, C., Sabatini, R., Maher, M.C., Kang, E.Y., Lee, S., Arikan, O., Harley, A., Bernal, A., Garst, P., Lavrenko, V., Yocum, K., Wong, T., Zhu, M., Yang, W.-Y., Chang, C., Lu, T., Lee, C.W.H., Hicks, B., Ramakrishnan, S., …, & Venter, J.C. 2017. Identification of individuals by trait prediction using whole-genome sequencing data. *Proceedings of the National Academy of Sciences* **114**(38), 10166–10171. doi: 10.1073/pnas.1711125114

Ng, A. & Jordan, M. 2001. On discriminative vs. generative classifiers: A comparison of logistic regression and naive Bayes. *Advances in neural information processing systems* **14**, 841–848.

R Core Team. 2021. R: A language and environment for statistical computing. *R Foundation for Statistical Computing* **14**, 841–848.

Sambo, F., Trifoglio, E., Di Camillo, B., Toffolo, G.M. & Cobelli, C. 2012. Bag of Naïve Bayes: biomarker selection and classification from genome-wide SNP data. *BMC Bioinformatics* **13**(14), 1–10. doi: 10.1186/1471–2105–13–S14–S2

Siravenha, A.C.Q. & Carvalho, S.R. 2015. Exploring the use of leaf shape frequencies for plant classification. In *2015 28th SIBGRAPI Conference on Graphics, Patterns and Images*, pp. 297–304. IEEE. doi: 10.1109/SIBGRAPI.2015.36

Tsangaratos, P. & Ilia, I. 2016. Comparison of a logistic regression and Naïve Bayes classifier in landslide susceptibility assessments: The influence of models complexity and training dataset size. *Catena* **145**, 164–179. doi: 10.1016/j.catena.2016.06.004

Vasilaki, C., Katsileros, A., Doulfi, D., Karamanos, A. & Economou, G. 2023. Evaluation of seven barley genotypes under water stress conditions. *Agronomy Research* **21**(1), 222–238.

Wang, B., Zhu, Y., Zhu, J., Liu, Z., Liu, H., Dong, X., Guo, J., Li, W., Chen, J., Gao, C., Zheng, X., Lizhu, E., Lai, J., Zhao, H. & Song, W. 2018. Identification and fine–mapping of a major maize leaf width QTL in a re-sequenced large recombinant inbred lines population. *Frontiers in Plant Science* **9**, 101. doi: 10.3389/fpls.2018.00101

Wray, N.R., Yang, J., Goddard, M.E. & Visscher, P.M. 2010. The genetic interpretation of area under the ROC curve in genomic profiling. *PLoS genetics* **6**(2), e1000864. doi: 10.1371/journal.pgen.1000864

Wu, S.G., Bao, F.S., Xu, E.Y., Wang, Y.X., Chang, Y.F. & Xiang, Q.L. 2007. A leaf recognition algorithm for plant classification using probabilistic neural network. In *2007 IEEE international symposium on signal processing and information technology*, pp. 11–16. IEEE. doi: 10.1109/ISSPIT.2007.4458016

Zhao, J., Bodner, G. & Rewald, B. 2016. Phenotyping: using machine learning for improved pairwise genotype classification based on root traits. *Frontiers in plant science* **7**, 1864. doi: 10.3389/fpls.2016.01864

Agronomy Research **22**(2), 898–912, 2024
https://doi.org/10.15159/AR.24.090

Effect of genotype x external environment interaction on the number of the kernel per ear of barley

V. Radic*, I. Komljenovic, S. Nastic and B. Petkovic

University of Banjaluka, Faculty of Agriculture, Bulevar Vojvode Petra Bojovica 1A, BA78000 Banjaluka, Bosnia and Herzegovina
*Correspondence: vojo.radic@agro.unibl.org

Received: May 24th, 2024; Accepted: September 3rd, 2024; Published: September 26th, 2024

Abstract. Genotype, external environment and their mutual interaction are determining or limiting a yield and barley tolerance to stressful conditions. This paper presents the results of a two-year study of nine selected genotypes at two localities. Aim of the investigation was determine which of the genotypes in the given production conditions gives the best results in the height and stability of yield. Based on the analysis of variance, *Duncan 's test* and interaction relations, a large variability between the examined genotypes was determined under the influence of different agroecological conditions of the locality, years of testing and their mutual interactions. All genotypes in this study achieved high yields. The highest total average yield from both localities and both years of testing was achieved by genotype 3 (8,767.99 kg ha^{-1}), and the lowest genotype 7 (6,075.85 kg ha^{-1}), which is significantly higher than the average yield in production in our country (3,150 kg ha^{-1}). This showed that, with the selection of quality genotypes, the application of quality agrotechnics in appropriate agroecological conditions, a higher yield can be achieved.

Key words: winter barley, selected genotype, interaction, cluster analysis.

INTRODUCTION

Due to its high polymorphism, barley belongs to the group of plants that are characterized by a high degree of plasticity, and because it can be grown in different climatic conditions, its distribution area is more significant than in other real cereals (Glamoclija, 2004). Widespread, despite different climatic conditions, indicates that the genetic pool of barley is rich in traits (genes) that allow wide adaptation to environmental conditions and good resistance to stress (Stanca et al., 2003). Drought is considered the main limiting environmental factor affecting crop productivity, including barley (Jana & Wilen, 2005). Therefore, drought due to low rainfall or high temperatures is one of the main problems underlying modern agriculture around the world, and is one of the most important environmental factors affecting plant growth, development and production. The most important environmental factors that affect the growth, development and production of plants (Hasanuzzaman et al., 2012; Hossain et al., 2012).

Genotypes tested in multiple environments often do not give the same rank in terms of yield, which is a consequence of the interaction of the genotype with the external environment. Interactions are the response of genotypes to changes in environmental conditions (Hühn, 1990; Kang, 1990). Without interaction, individual varieties would be grown in an extensive range, and yield trials to confirm the value of a particular genotype would be performed in only one location. Varieties with a smaller contribution to the interaction are less sensitive to changes in environmental conditions, so the values of the examined traits will not change much. Such varieties are stable. The ability of a variety to achieve high and stable yields is called adaptability (Ebdon & Gauch, 2002). Genetic variability plays a significant role in the adaptability of barley to the stress caused by the external environment and to the prevalence of barley in various climates (Cattivelli et al., 2002). At barley breeding and many aspects of barley research, the analysis of genotype-by-environment interactions (GEIs) is of primary importance, as it is also for other crops (Ceccarelli, 1996; Annicchiarico, 2002; Voltas et al., 2002). Crop improvement through breeding brings immense value relative to investment and offers a practical approach to improving food security (Tester & Langridge, 2010).

Kaydan & Yagmur, (2007) investigated yield and yield components in two years, (2004/05) and (2005/06), at one location in Van Province on 13 barley cultivars. The trials were set in a randomized block treatment in 4 replicates. The results showed significant differences at the tested traits among barley genotypes. The number of days to earing barley ranged from 179.3 to 189.7; the number of spikes per m^{-2} was 249.3–560.7; stem length 51.2–64.9 cm; ear length 5.83–7.26 cm; number of kernels per ear 16.32–20.24; kernel weight per ear 0.73–0.99 g; weight of 1,000 kernels 41.7–46.32 g; grain yield 197.3–319.7 kg ha^{-1} and harvest index ranged from 23.11% – 36.43%.

Pouraboughadareh et al. (2013) examined the tolerance of certain barley genotypes to water shortage in field conditions. The surveys were carried out at western Azerbaijan in two production years (2011 and 2012), on seven genotypes and five barley lines. The experiments were set in a randomized block treatment with four replicates, in conditions of lack of water and optimal conditions. Analysis of variance ($p \leq 0.01$) showed significant differences between genotypes and populations for all tested traits except for1,000 kernel weight. It showed significant effects of stress on water deficiency on all tested traits. The interaction of the stress effect from water deficiency x genotype was also significant ($p \leq 0.01$) for all examined traits (Kendal et al., 2019; Oral et al., 2019). Therefore, it is essential to develop high yield varieties which are physiologically and morphologically compatible with different environmental conditions (Kendal et al., 2019; Oral et al., 2019).

Karahan & Akgun (2020) of this study showed that the GYT approach puts too much weight on yield relative to other traits. However, this approach can be used in other crops studied based on multi-location, multi-years with multi-traits.

Arshadi et al. (2018) write that when it comes to the interaction between genotype and the environment, there are varieties with exceptional adaptability to smaller, homogeneous areas and varieties with a wide range of adaptation that can be grown in more expansive areas. Researchers often perform experiments in → an extensive range, and base their decision mainly on the average values of the genotype, neglecting the interaction (Babic, 2006). Ideal varieties are those with high grain yield and appropriate adaptability to various of environmental conditions (Dawson et al., 2007). Mirosavljevic et al. (2015) given the data, it can be concluded that in years with increased spring

precipitation, sowing of medium early and late varieties of winter barley allows better accumulation of dry matter, and higher grain yields are achieved.

It has long been recognized that wheat productivity and quality of seed vary considerably as a result of genotype, environment and their interaction, which describe most agronomic traits, their affectedness by the growing environment, as well as by genetic factors (Ahmadi et al., 2012; Doehlert & McMullen, 2000; Doehlert et al., 2001).

Previous research has been empirical and has not dealt much with the nature of genotype responses to external stress conditions. Basford & Cooper (1998) and Voltas et al. (2002) highlight two groups of methods on G × E interaction depending on the level of understanding of genotypes and external environments. The first group consists of empirical models that do not provide a biological basis for interpreting the interaction. This group includes a large number of regression models. The second group consists of analytical models that provide a biological basis for explaining the interaction and explain the interaction as a complex problem that is a function of many climatic, genetic, morphological, phenological and physiological variables. This group includes multivariate models. Of the climate variables, precipitation and temperature have the most significant influence on barley yield, so they are also the most responsible for the interaction in barley (Voltas et al., 1999).

The aim of this study is to single out superior genotypes by yield and examined yield components that show minimal interaction, ie. high stability, and as such recommended for expansion in production or as parental components in future breeding programs.

MATERIALS AND METHODS

Study area

Field trials were conducted during two years (2016/2017 and 2017/2018) at two locations: Gradiska (N 45°01′48′′; E 17°32′52′′) and Bijeljina (N 44°4′25′′; E 19°14′14′′) in dry farming conditions. Nine winter barley genotypes were included in the study using the *Randomized Complete Block Design method (RCBD)*.

Chemical analysis of the soil was done before setting up the experiment when soil samples were taken at both sites (Table 1). It can be seen from the attached that both plots were suitable for growing small grains or barley. The amounts of nutrients were equal at both sites in both examined years (162 kg ha^{-1} of pure N; 60 kg ha^{-1} P_20_5 and 60 kg ha^{-1} K_2O). After chemical analysis of the soil, it was determined that the needs for phosphorus and potassium were not met at any locality, that the examined genotypes were in different production conditions when it comes to the amount of nutrients in the soil.

Table 1. Data of chemical analyses of soil

	Depth of sampling	pH		humus	P_20_5	K_2O
Locality		H_20	KCl	%	$mg/_{100g}$	$mg/_{100g}$
Gradiska	0–30 cm	6.00	5.00	2.90	15.9	14.9
Bijeljina	0–30 cm	6.49	5.39	2.53	5.0	19.1

Experimental design and data collection

Data of climatic characteristics for both localities were processed through climatic diagrams according to *Walter* (Fig. 1) and (Fig. 2) with the aim of better overview and

comparison of these data. Fig. 1 shows the climate diagram for the Gradiska locality, which shows that the critical period for growing small grains in 2016/17 was during June.

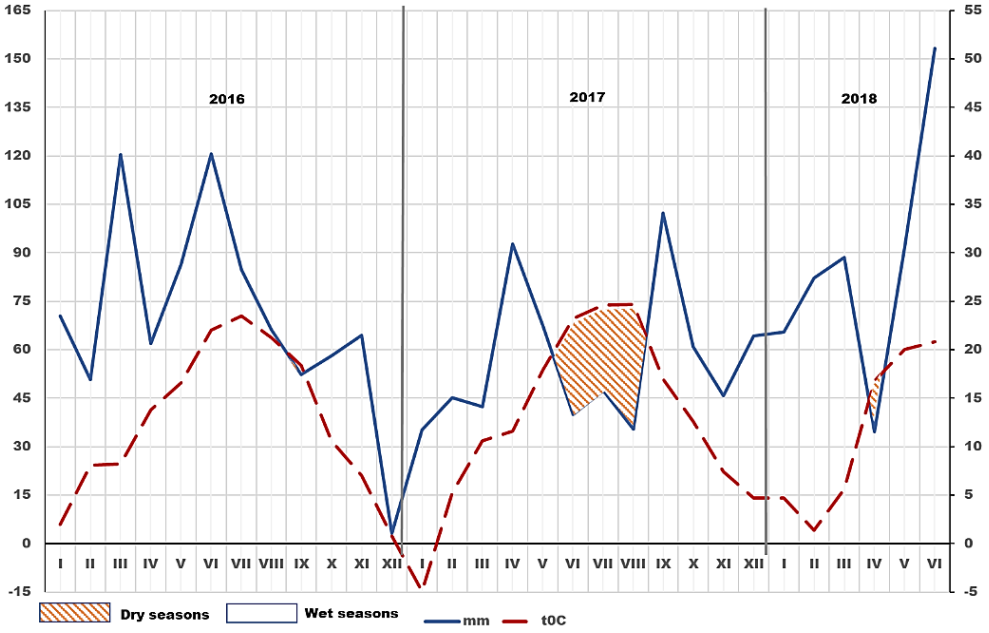

Figure 1. Climate diagram by *Walter* for Gradiska.

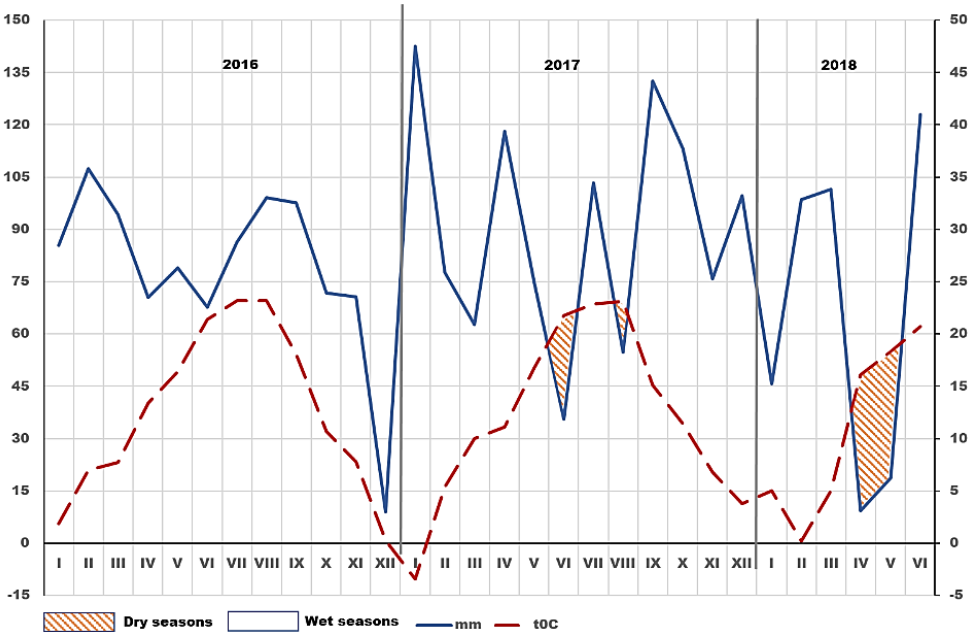

Figure 2. Climate diagram by *Walter* for Bijeljina.

When this is compared with the data from Fig. 2, which shows the climate diagram for the Bijeljina site, where it can be seen that in the same study year the drought period

lasted during May, June and July, it can be concluded that for 2016/17 the Gradiska site had better, ie. more humid production conditions. When analyzing the year 2017/18, the climate diagrams from both locations show that during the spring there was a period of drought. The drought period at the Bijeljina site lasted during April and at the Gradiska site significantly longer, during April, May and June. In the soil of the Gradiska locality, gravel is present, and the water seeps faster, therefore this locality had more arid production conditions to the Bijeljina locality.

The trials were set in two vegetation seasons by a randomized block system in four replications. The size of the experimental unit was 2 m^2 (2×1 m).

Measured parameters for cluster analysis are: number of sprouted plants m^2, number of overwintered plants per m^2, height of whole plant, ear length, number of grains per ear, grain weight per ear, total mass, grain yield, straw yield, harvest index, hectoliter kernel mass, seed germination energy, total germination, 1,000 kernel weight and protein content.

Analytical methods

Measurement results were statistically processed. The results of biometric measurements were processed by PC applications for Windows: *Statistical Package for Social Sciences*, *StatSoft Statistica* and *Excel*. The results of the studied properties were processed by analysis of variance (*ANOVA*) by a computational program using the *GLM* procedure. The *Duncan's Multiple Range Test (DMRT)* was used to determine the significance of differences between genotypes and their ranking for significance levels $R = 0.01$. Grouping of data of examined traits by similarity was performed based on hierarchical cluster analysis. The evaluation of the divergence of the tested material was performed using the *UPGMA (unweighted pair-group method using arithmetic averages)*.

RESULTS AND DISCUSSION

The number of grains per ear is a trait formed during the vegetative phase and depends on the environmental conditions in which the morphogenesis of generative organs takes place during the process of ontogenesis. Arisnabarreta & Miralles (2008a) consider that the critical period for grain formation in six-row forms is 30 days before flowering, and the number of fertile ear is affected by the amount of assimilates available to the ear in the early stages of its development, Arisnabarreta & Miralles (2008b).

Grain yield of barley is strongly positively correlated with the number of kernels per ear than with kernel size (Gallagher et al., 1975). The number of kernels per ear is a very important component of the yield that is formed during the vegetative phase and depends on the environmental conditions in which the morphogenesis of generative organs takes place during ontogenesis. The increase yield of barley is conditioned by the increase the number of grains per ear (Barczak & Majcherczak, 2009), and the high number of grains per ear can compensate for the reduced number of ears and plants per unit area (Schillinger, 2005).

Between two-row and six-row forms, a statistically significant difference was obtained in the average number of kernels per ear 27.5 versus 53.4. Similar results are obtained the other authors (Przulj et al., 2001; Zare et al., 2011; Przulj & Momcilovic,

2012). The number of kernels per ear is the most important criterion in breeding barley to increase yield (Dofing & Knight, 1994).

Observing the average values of the number of grains per ear of nine examined barley genotypes from Table 2, it is evident that for the 2016/17 examined year, the average value of all genotypes from the Gradiska locality is lower compared to the Bijeljina locality. Genotype 9, had the highest value of the tested trait for 2016/17 at both localities, while genotype 1, had the lowest value of this trait for the first examined year at the Gradiska locality, and genotype 7 at the Bijeljina locality.

Table 2. Average values of the number grain per spike

Year	2016/17			2017/18		
Genotype	Gradiska	Bijeljina	$\bar{x}$	Gradiska	Bijeljina	$\bar{x}$
1	21.4	25.8	23.6	21.3	23.7	22.5
2	48.5	50.0	49.2	32.1	38.8	35.4
3	39.3	54.2	46.7	31.3	41.0	36.1
4	23.8	27.8	25.8	22.9	27.5	25.2
5	22.6	27.2	24.9	22.0	22.3	22.2
6	26.4	29.8	28.1	21.9	28.8	25.3
7	22.8	23.5	23.1	20.7	22.3	21.5
8	48.1	48.4	48.2	35.3	51.2	43.3
9	**49.6**	**59.2**	**54.4**	**45.2**	**49.2**	**47.2**
$\bar{x}$	33.6	38.4	36.0	28.1	33.8	31.0

When looking at average values by genotypes for both locations for the first test year, it is seen that genotype 9 had the highest and genotype 7 and genotype 1, the lowest value of the tested trait. In 2017/18, the average number of grains per ear of all genotypes for the locality Gradiska was also lower compared to the locality Bijeljina.

The highest value of the examined trait for this production season also had genotype 9 and the lowest, at the locality Gradiska, genotype 7, and at the locality Bijeljina genotypes 7 and 5. According to the average values of this trait by genotypes for both locations, the highest average value per ear it had genotype 9 while the lowest value had genotype 7. From this, it can be concluded that genotype 9 showed the best characteristics for this trait for the examined years while genotype 7 showed the worst. In the 2016/17 examined year, the total average mean value of all genotypes of this trait for both localities was 36.0 and was is higher than the total average mean value of all genotypes of the same for the 2017/18 investigated year 31.0.

Al-Tabbal & Al-Fraihat (2012) on 86 barley genotypes had an average value of this trait of 51.9, the minimum mean value of the number of grains per spike was 36.7 and the maximum 73.3. In studies by Garcia de Moral et al. (2002) at six barley genotypes, the mean values of this trait ranged from 18.6 to 23.5 for two-row barley and from 26.1 to 37.6 for six-row barley per spike.

According to the analysis of variance for the number of grains per ear of nine barley genotypes for two localities and two examined years (Table 3), it was determined that year (A), location (B), genotype (C) and year x genotype interaction (AxC) had statistically highly significant influence ($p < 0.01$) on this examined property. The interaction of sites x genotype (BxC) and the interaction of years x sites x genotype (AxBxC) showed a statistically significant influence ($p < 0.05$) on the examined trait.

The year x location interaction factor (AxB) did not have a statistically significant effect on the number of grains per ear.

Table 3. Analyze variance of kernel number per ear of nine types of winter barley

Source of variations	SS	Df	MS	F
Treatment	19,885.6[a]	35	568.2	**31.7****
Year (A)	919.1	1	919.1	**51.2****
Location (B)	1,008.1	1	1,008.1	**56.2****
Genotype (C)	16,551.7	8	2,069.0	**115.3****
Year x Location (AxB)	8.5	1	8.5	0.5 [ns]
Year x Genotype (AxC)	679.3	8	84.9	**4.7****
Location x Genotype (BxC)	360.4	8	45.0	**2.5***
Year x Location x Genotype (AxBxC)	358.5	8	44.8	**2.5***
Error	1,937.8	108	17.9	
Total	183,199.6	144		

Significantly: $p < 0.01$**; $p < 0.05$*; ns no significantly.

Fig. 3 shows the results of the *Duncan test* in the differences in the range of grain number per ear between the examined years (factor A) for nine barley genotypes at two localities in the two examined years. The examined 2016/17 year (interval A) had a higher total average value of all genotypes from both localities of this examined trait compared to the total average value of all genotypes from both localities of the examined trait in 2017/18 (interval B). The graph shows that the *Duncan test* showed a statistically significant difference between the interval A and the interval B for factor A for the characteristic number of grains per ear.

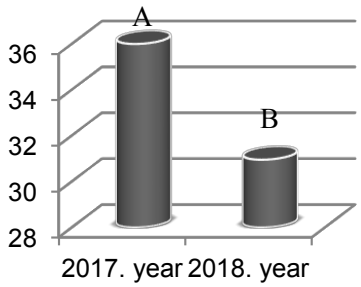

Figure 3. Differences in the range of the number of grains per class between the examined years (factor A).

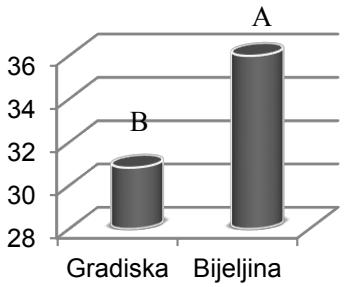

Figure 4. Differences in the range of the number of grains per class between the examined locations (factor B).

The total average value of all genotypes of the examined trait for the Gradiska locality was lower to the Bijeljina locality for both examined years. This can be seen from Fig. 4, where the total average value of the tested trait from Gradiška is marked by the interval B and the higher total average value from Bijeljina is marked by interval A. After comparing the differences of the number of grains per ear between the tested localities year, Duncan's test showed a statistically significant difference between the interval A and the interval B for factor B for the property number of grains per ear.

If we observe differences in the rank of the number of grains per ear between the examined genotypes (factor C), it is noticed that the results of the total mean values of the examined trait by genotypes, according to Duncan's test, are classified into five intervals (Fig. 5). Interval A belongs to genotype 9 which had the highest total average value of the examined trait and its mean value by localities in the two examined years for the number of grains per ear differs statistically significantly from other genotypes.

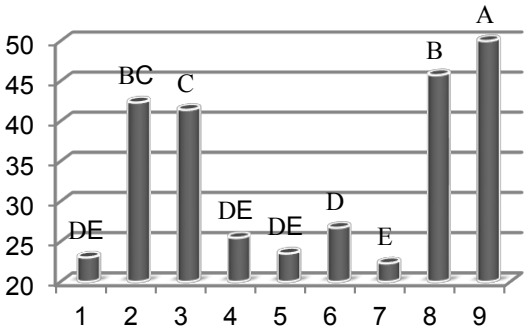

Figure 5. Differences in the range of number of grains per class between the examined nine genotypes (factor C).

Genotype 7, which had the lowest mean value of the tested trait, belongs to the interval E and there are no statistically significant differences between it, genotypes 1, 4 and 5. Between genotype 8 and genotype 2 there are no statistically significant differences in mean values of number of grains per ear as and between genotypes 2 and 3.

Genotypes interaciton

At the interaction of year x genotype for the trait number of grains per ear for examined genotypes, locations and years, Fig. 6 shows that during the first production year the average values of the number of grains per ear by genotypes were higher than in the second production year.

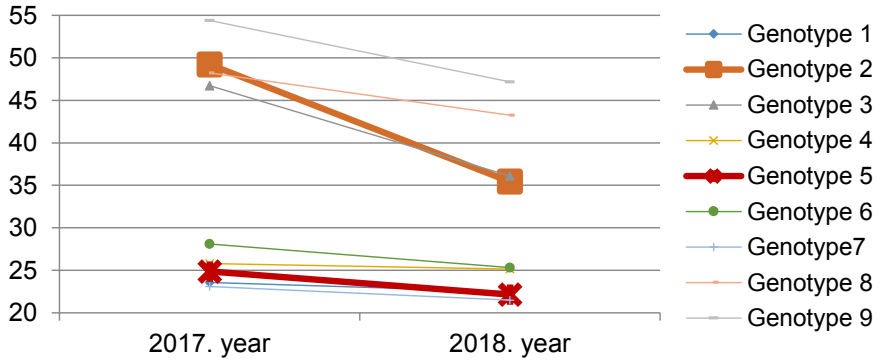

Figure 6. Number of grains per ear - interaction years of investigation x genotype.

Fig. 6 shows that in some genotypes, such as genotype 2 and genotype 3 visible large variation in mean values by localities, so the interaction of years x genotype had a statistically highly significant impact on them for the number of grains per ear. It can be noticed that genotype 4 has the opposite tendency of the mean value of ear length to the years of testing, and the mean values of the examined trait of genotype 5 also deviate from the central tendencies, so they have a strong influence of year x locality interaction. Genotype 9, with the highest mean value of the examined trait, does not interact with any mean value of other genotypes. Genotypes 1 and 5 interact with each other, looking

at the mean values of the examined trait by years, they have approximate values as genotype 7, but they do not interact with it. Genotypes 6 and 4 interact with each other and act independently of the values of other genotypes. Genotype 2 interacts with genotypes 8 and 3, while genotypes 8 and 3 do not interact and the year x genotype interaction is not statistically significant for the examined trait.

Fig. 7 shows that at the Gradiska locality the mean values of the number of grains per ear for the examined genotypes in the two-year period were lower in relation to the Bijeljina locality. Variations among the mean values of genotypes by localities were different. When observing the behavior of mean values of genotypes in interaction with localities, it is realized that genotype 9 had the highest mean value of the examined trait and does not interact with any mean value of another genotype. The lowest mean value by localities has genotype 7, which interacts with genotype 1 and genotype 5, and there is a statistically significant influence of the interaction of local x genotype on this trait in the mentioned genotypes.

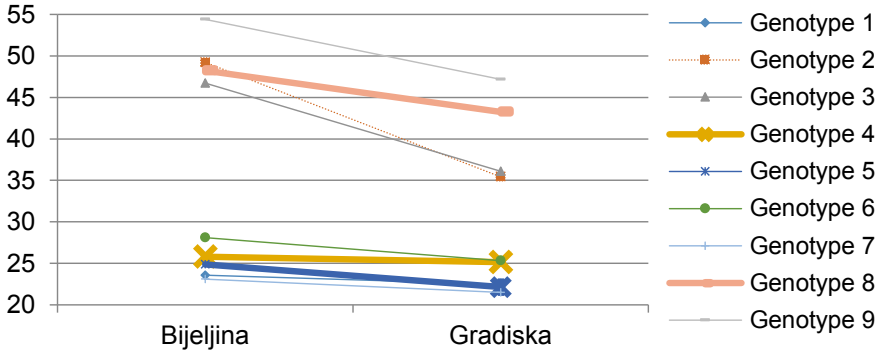

Figure 7. Number of kernels per ear - interaction locality x genotype.

The largest oscillations in the mean value of this trait show genotype 3, genotype 4, genotype 5 and genotype 8 whose mean values of the examined trait vary significantly by localities. Genotype 4 and genotype 6 have mean values of the number of grains per ear. They are also in interactions and have a statistically significant effect of locality x genotype interaction on this trait. There is no interaction with other values of the examined genotypes. The influence between them is not statistically significant. According to the mean values of the number of grains per ear, genotype 2 interacts with genotype 8 and genotype 3 and interacts locality x genotype. For this trait, the statistical difference between them is highly significant, and genotype 8 genotype 3 are not in interaction, and the interaction of locality x genotype between them is not statistically significant.

Fig. 8 shows the relationships between the examined genotypes in the interaction of years x locality x genotype. Table 2 shows that the highest mean value of the number of grains per ear of all genotypes was recorded at the locality Bijeljina 2016/17, then Bijeljina 2017/18, then Gradiska 2016/17 and the lowest at the locality Gradiska in the 2017/18 examined year. Figure 8 shows that the highest mean value of the examined trait was genotype 9 at the Bijeljina site in 2016/17, but the mean value from the Gradiska site in 2016/17 was higher compared to the same from the Bijeljina site in 2017/18. The mean value from the Gradiska 2017/18 locality differs significantly in this genotype

compared to other locations. Such a case also resulted in genotype 8, where the mean value of the number of grains per ear is significantly lower at the locality Gradiska 2017/18 compared to the mean values from other locations. The strong influence of the interaction and the influence of the locality on the examined property can be seen here.

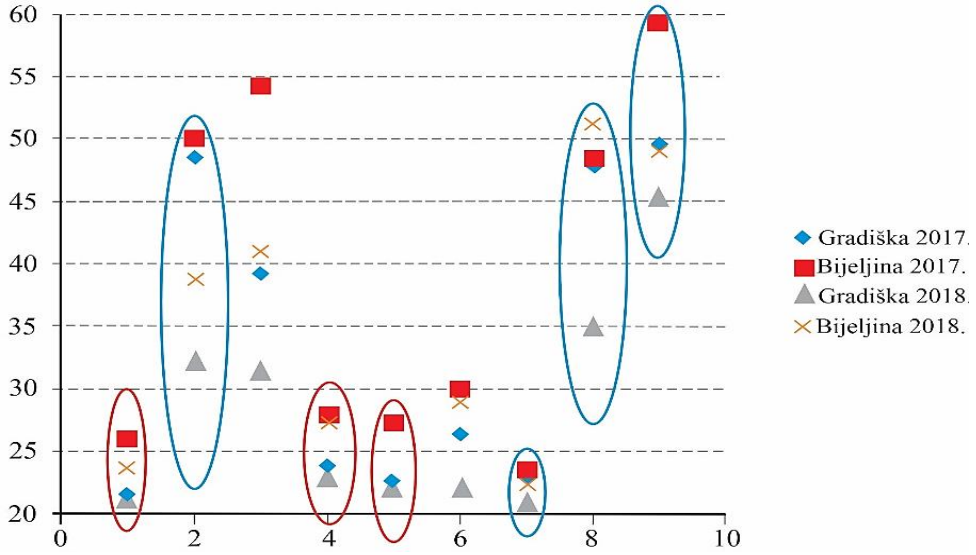

Figure 8. Number of kernel per ear- interaction of tested years x locality x genotype.

The opposite case is with genotype 1, genotype 4, genotype 5, genotype 6 and genotype 7 where the average values of the number of grains per ear from the locality Gradiska 2017/18 do not vary significantly compared to the mean values from other localities. Genotype 8 also deviates from other genotypes since the highest mean value of the examined trait was recorded at the Bijeljina locality in 2017/18, unlike other genotypes whose highest values of number of grains per ear were recorded at the Bijeljina 2016/17 locality. If you look at the mean values by genotypes, it can be seen that they can also be ranked into two groups. Genotype 1, genotype 4, genotype 5 and genotype 7 have approximate mean values of the tested trait for all localities and significant deviations from the average values of genotype 2, genotype 3, genotype 8 and genotype 9. From all the above we can see the strong influence of year x locality x genotype for the test trait.

Cluster analysis

Cluster analysis groups the examined genotypes by similarity based on the examined traits. Cluster analysis is the name for a group of multivariate techniques whose primary purpose is grouping based on certain characteristics that measurement objects possess.

The grouped observations should show a high internal similarity within each cluster as well as a high external difference between the derived clusters.

Fig. 9 shows the grouping by cluster analysis of nine barley genotypes at both localities in a two-year period based on the values of all examined traits. There is an evident existence of two large clusters. The first group consists of genotype 4 and genotype 7. The second group includes genotype 8 and genotype 9. The third group

includes genotype 2 and genotype 5, genotype 1 and genotype 6, which are further grouped into cluster number 1. Cluster number 2 includes only genotype 3 which means that the values of all examined traits of genotype 3 are different in relation to the same values of all other genotypes belonging to one cluster.

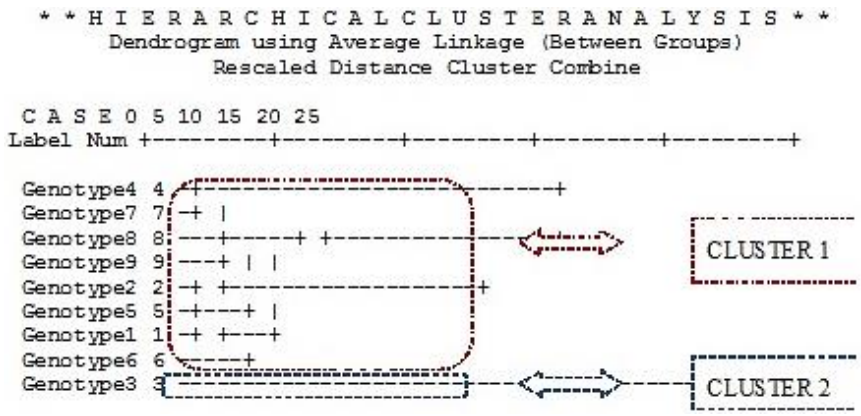

Figure 9. Cluster for nine barley genotypes at two localities in a two - year period.

The cluster of nine genotypes of barley at the Gradiska site in a two-year period based on the values of all examined traits is shown in Fig. 10. The presence of two main clusters can be observed here. The first group consists of genotypes gathered around the values of genotype 5, namely genotypes 1, 6, 5 and 4, and the second group consists of genotypes 7, 2 and 9. These groups are further grouped into cluster number 1. In cluster number 2 include genotype 3 and 8.

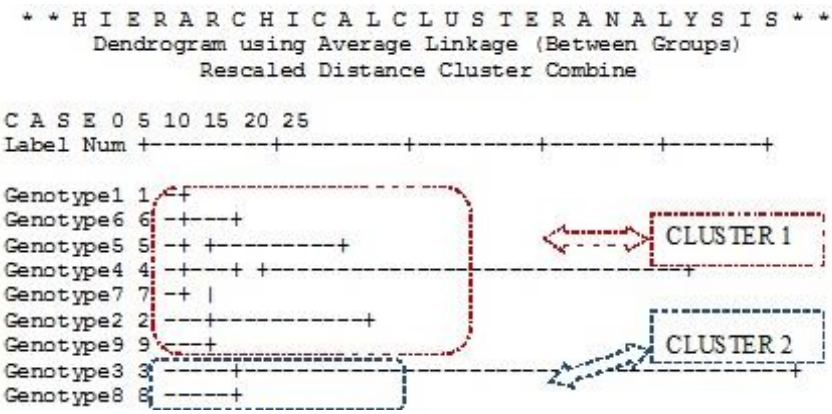

Figure 10. Cluster for nine barley genotypes at the Gradiska locality in a two - year period.

Fig. 11 shows a cluster of examined genotypes for the Bijeljina locality in a two-year period. The presence of two main clusters was observed here. Genotype 1 and genotype 9 have similar test values and belong to the same group while genotypes 5, 3 and 8 form a different group. These two groups are grouped into the first large cluster. Genotypes 2, 4 and 7 are grouped around the values of the examined traits of genotype 6 and form a second cluster.

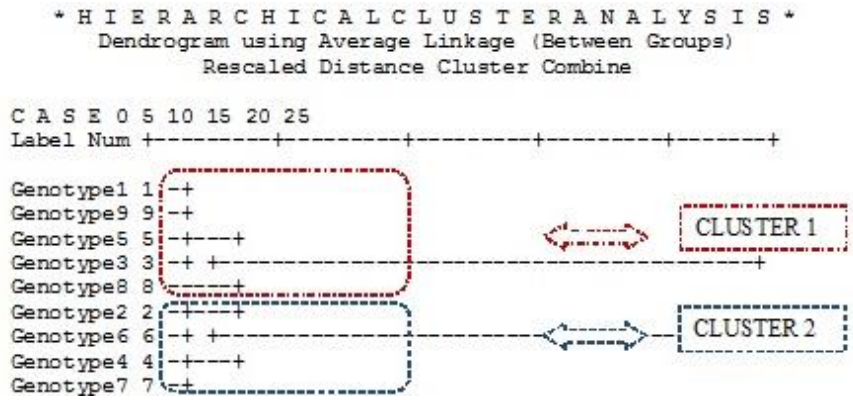

Figure 11. Cluster for nine barley genotypes at the Bijeljina locality in two years.

The cluster for nine barley genotypes at two localities for the first examined year is shown in Fig. 12. The first group is concentrated around the values of all examined traits of genotype 5. This group consists of genotypes 6, 7 and 4, which is the first cluster. The second group consists of genotypes 8, 9, 2 and 3 and the third, genotype 1. They are further grouped into cluster number 2.

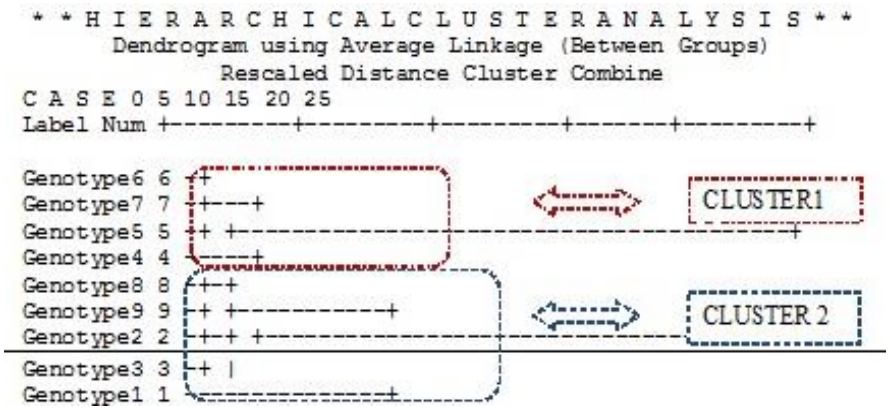

Figure 12. Cluster for nine barley genotypes at two localities in the 2016/17 vegetation seasons.

Fig. 13 shows the cluster for nine barley genotypes at two localities in the surveyed 2017/18. years. The presence of two clusters was noted. The first group according to the similarity of the values of all tested traits consists of genotypes 1, 8, 5 and 6, and the second genotypes 9, 2, 4 and 7. These two groups are combined into the main cluster no. 1. The second cluster belongs to genotype 3, which with its values of all examined traits, significantly deviates from the values of genotypes from cluster no.1.

From the cluster analysis, it can be concluded that genotype 5 is positioned quite well according to the examined values. This genotype on each chart belonged to the first cluster with higher values of the examined traits. This means that in the examined years and at the examined localities it showed standard values. Genotypes 4, 6 and 7 belonged to the first cluster on all graphs except the cluster for the Bijeljina locality, while genotype 9 was also positioned in the first cluster according to the localities in 2017/18. It was only positioned in the second cluster in 2016/17. Genotypes 2 and 8 varied a lot,

and genotype 3, according to the values of the examined traits, belongs to the second cluster on all graphs except for the locality of Bijeljina.

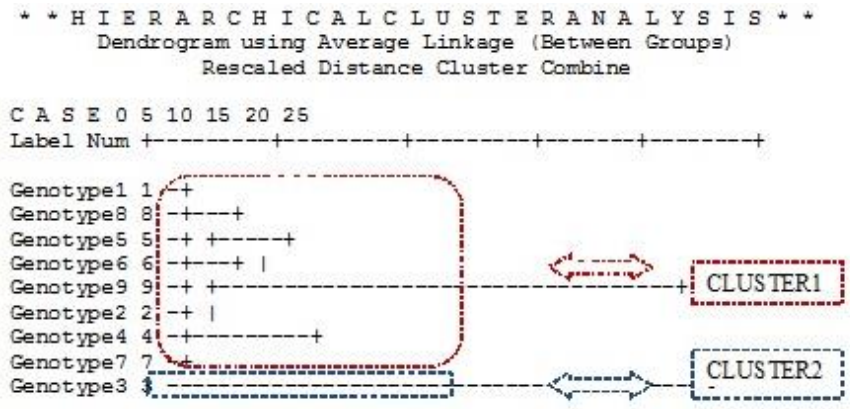

Figure 13. Cluster for nine barley genotypes at two localities in the 2017/18 vegetation Seasons.

CONCLUSIONS

The highest total average grain yield at both sites and both years of testing was achieved by genotype 3 (8,767.99 kg ha^{-1}), and the lowest genotype 7 (6,075.85 kg ha^{-1}), which is significantly higher than the average yield in production in our country (3150 kg ha^{-1}). This has shown that, with the selection of quality genotypes, the application of quality agrotechnics in our agroecological conditions, the yield can be raised.

The determined interaction parameters show no interaction relations between the examined years to individual localities. There is a statistically significant interaction relationship between location and genotype, as well as between location, genotype, and year. A highly significant interaction effect was observed between year and genotype.

UPDMA cluster analysis was used to construct a dendrogram which classified 9 genotypes into two main groups. Based on the cluster analysis, genotype 3 is separated into a separate cluster. The highest yield was achieved with this genotype, so it can be stated that in this way a genotype with better characteristics can be identified.

REFERENCES

Ahmadi, J., Mohammadi, A. & Mirak, T.N. 2012. Targeting Promising Bread Wheat (*Triticum aestivum* L.) Lines for Cold Climate Growing Environments Using AMMI and SREG GGE Biplot Analyses. *J. Agr. Sci. Tech*. **14**, 645–657.

Al-Tabbal, J. & Al-Fraihat, A. 2012. Genetic variation, heritability, phenotypic and genotypic correlation studies for yield and yield components in promising barley genotypes. *Journal of Agricultural Science* **4**(3), 193–210.

Annicchiarico, P. 2002. Genotype 9 Environment interactionschallenge and opportunities for plant breeding and cultivar recommendations. *FAO Plant production and protection paper*, 174.

Arisnabarreta, S. & Miralles, D.J. 2008a. Critical period for grain number establishment of near isogenic lines of two - and six - rowed barley. *Field Crops Res.* **107**, 196–202.

Arisnabarreta, S. & Miralles, D.J. 2008b. Radiation effects on potential number of grains per aer and biomass partitioning in two - and six - rowed near isogenic barley lines. *Field Crops Res.* **107**, 203–210.

Arshadi, A., Karami, E., Sartip, A., Zare, M. & Rezabakhsh, P. 2018. Genotypes performance in relation to drought tolerance in barley using multi-environment trials. *Agronomy Research* **16**, 1–17.

Babic, V. 2006. *Evaluation of genotype × environment interaction for grain yield of commercial ZP maize hybrids.* Master's thesis. University of Novi Sad. Procena interakcije genotip × sredina za prinos zrna komercijalnih ZP hibrida kukuruza. Magistarska teza. Univerzitet u Novom Sadu (in Serbian).

Barczak, B. & Majcherczak, E. 2009. Effect of varied fertilization with sulfur onselected spring barley yield structure components. *Journal of Central European Agriculture* **9(2008) No 4**, 777–784.

Basford, K.E. & Cooper, M. 1998. Genotype x environment interaction and some consideration of their implication for wheat breeding in Australia. *Australian Journal of Agricultural research* **49**, 153–174.

Cattivelli, L., Ceccarelli, S., Romagosa, I. & Stanca, M. 2002. *Abiotic stresses in barley: Problems and solution*. Barley: Production, Improvement and Uses, 282–302.

Ceccarelli, S. 1996. *Positive interpretation of genotype by environment interactions in relation to sustainability and biodiversity*. In: Cooper M, Hammer GL (eds) Plant adaptation and crop improvement. CABI, Wallingford, UK, 467–486.

Dawson, I.K., Guarino, L. & Jaenicke, H. 2007. Underutilised plant species: impacts of promotion on biodiversity: Position paper *No.* **2**. *The International Centre for Underutilised Crops*.

Doehlert, D.C. & McMullen, M.S. 2000. Genotypic and environmental effects on oat milling characteristics and groat hardness. *Cereal Chem* **77**, 148–154.

Doehlert, D.C., McMullen, M.S. & Hammond, J.J. 2001. Genotypic and environmental effects on grain yield and quality of oat grown in North Dakota. *Crop Sci.* **41**, 1066–1072.

Dofing, S. & Knight, C.W. 1994. Yield Component Compensation in Uniculm Barley Lines. *Agronmy Journal* **86**, 273–276.

Ebdon, J.S. & Gauch, H.G.Jr. 2002. Additive main effect and multiplicative interaction analysis of national turfgrass performance trials. *Crop sci.* **42**, 489–496.

Gallagher, J.N., Biscoe, P.V. & Scott, R.K. 1975. Barley and its environment V. stabillity of grain weight. *Journal of Applied* ***ECO-o1-2Y***, 19–336.

Garcia del Moral, L., Belen Garcia del Moral, M., Molina-Cano, J. & Slafer, G. 2002. Yield stability and development in two and six-rowed winter barleys under Mediterranean conditions. *Field Crops Research* **81**(2003), 109–119.

Glamoclija, D. 2004. *Posebno ratarstvo*. Draganic, 309 pp.

Hasanuzzaman, M., Hossain, M.A., Teixeira da Silva, J.A. & Fujita, M. 2012. *Plant response and tolerance to abiotic oxidative stress: antioxidant defense is a key factor* V. Bandi, A.K. Shanker, C. Shanker, M. Mandapaka (Eds.), *Crop Stress and its Management: Perspectives and Strategies. Springer,* The Netherlands, 261–315.

Hossain, A., Lozovskaya, M.V., Zvolinsky, V.P. & Tutuma, N.V. 2012. Effect of soil resources and climatic factors (temperature) on spring wheat and barley in the northern Bangladesh and southern Russia. *International scientific and practical conference on problems of environmental management and conservation of ecological balance in the arid zones‖. Salt Zaymische, Chorniarsky district, Astrakhan State, Russia, from 16–18 May. Hunt R.G.* (1978): Plant growth analysis. Edward Arnold

Hühn, M. 1990. *Nonparametric estimation and testing of genotype × enviroment interactin by ranks*. In: M.S. Kang (eds) Genotype by Enviroment Interaction and Plant Breeding. Louisiana State University Agricultural Center. USA, pp. 69–93.

Jana, S. & Wilen, R.W. 2005. *Breeding for abiotic stress tolerance in barley*. In: M. Ashraf, and P.J.C. Harris, eds. Abiotic Stresses. Plant Resistance Through Breeding and Molecular Approaches, pp. 491–511. Haworth Press, New York. Jones, H.G. (1983).

Kang, M.S. 1990. *Genotype by Enviroment Interaction and Plant reeding*. Louisiana State Univerity Agricultural Center, Baton Rouge, Louisiana, 221–243.

Karahan, T. & Akgun, I. 2020. Selection of barley (*Hordeum vulgare*) genotypes by GYT (genotype × yield × trait) biplot technique and its comparison with GT(genotype × trait). *Applied Ecology and Environmental Research* **18**(1), 1347–1359.

Kaydan, D. & Yagmur, M. 2007. A research on yield components of some two rowed barley varieties (*Hordeum vulgare* convar. *distichon)* in Van ecological conditions. *Journal of agricultural science* ISSN: 1300-7580, 269–278.

Kendal, E., Karaman, M., Tekdal, S. & Doğan, S. 2019. Analysis of promising barley (*Hordeum vulgare* L.) lines performance by AMMI and GGE biplot in multiple traits and environment. *Applied Ecology and Environmental Research* **17**(2), 5219–5233.

Mirosavljevic, M., Przulj, N., Momcilovic, V., Hristov, N. & Maksimovic, I. 2015. Dry matter accumulation and remobilization in winter barley as affected by genotype and sowing date. *Genetika* **47**(2), 751–763.

Oral, E., Kendal, E., Kilic, H. & Dogan, Y. 2019. Evolation barley genotypes in multi-environment trials by AMMI model and GGE biplot analysis. *Fresenius Environmental Bulletin* **28**(4A), 3186–3196.

Pouraboughadareh, A., Naghavi, M. & Khalili, M. 2013. Water deficit stress tolerance in some of barley genotypes and landraces under field conditions, *Not Sci Biol.* **5**(2), 249–255.

Przulj, N. & Momcilovic, V. 2012. Spring barley performances in the Pannonian zone. *Genetika* **44**(3), 499–512.

Przulj, N., Momcilovic, V. & Mladenov, N. 2001. Dynamics of grain filling of winter two-row barley. Proceedings of the Institute for Agriculture and Vegetables. Dinamika nalivanja zrna ozimog dvoredog jecma. *Zbornik radova Instituta za ratarstvo i povrtarstvo*, Novi Sad **35**, 175–184 (in Serbian).

Schillinger, W.F. 2005. Tillage method and sowing rate relations for dryland spring heat, barley and oat. *Crop Sci.* **45**, 2636–2643.

Stanca, A.M., Romagosa, I., Takeda, K., Lundborg, T., Terzi, V. & Cattivelli, L. 2003. *Diversity in abiotic stresses*. In R. von Bothmer, H. Knüpffer, T. Van Hintum and K. Sato (eds.). Diversity in Barley (*Hordeum vulgare* L.). *Elsevier*, Amsterdam, pp. 179–199.

Tester, M. & Langridge, P. 2010. Breeding Technologies to Increase *Crop Production in a Changing World. Science (American Association for the Advancement of Science)* **327**(5967), 818–822.

Voltas, J., van Eeuwijk, F.A., Igartua, E., Garcia del Moral, L.F., Molina-Cano, J.L., Romagosa, I. 2002. Genotype by environment interaction and adaptation in barley breeding: basic concepts and methods of analysis. In: Slafer, G.A., Molina-Cano, J.L., Savin, R., Araus, J.L. and Romagosa, I. (eds.). *Barley Science: Recent Advances from Molecular Biology to Agronomy of Yield and Quality*. Haworth Press, Binghamton, NY., pp. 205–241.

Voltas, J., van Eeuwijk, F.A., Sombrero, A., Lafarga, A., Igartua, E. & Romagosa, I. 1999. Integrating statistical and ecophysiological analysis of genotype by environment interaction for grain fi lling of barley in Mediterranean areas I. Individual grain weight. *Field Crop Res*. **62**, 63–74.

Zare, M., Azizi, M.H. & Bazrafshan, F. 2011. Effect of drought stress on some agronomic traits in ten barley (*Hordeum vulgare*) cultivars. *Tech. J. Eng. Pplied Sci*. **1**, 57–62.

Agronomy Research **22**(2), 913–938, 2024
https://doi.org/10.15159/AR.24.060

Herbicide-based selection of mutants for improved single cell protein synthesis: application and procedures

S. Raita, I. Berzina, Z, Kusnere*, M. Kalnins, I. Kuzmika and K. Spalvins

Riga Technical University, Institute of Energy Systems and Environment, Azenes street 12/1, LV 1048 Riga, Latvia
*Correspondence: zane.kusnere@rtu.lv

Received: January 29th, 2024; Accepted: June 14th, 2024; Published: July 9th, 2024

Abstract. Enhancement of industrially important microbial strains using random mutagenesis is widely used. Screening of potential mutants accelerates the selection of mutants with desired properties such as improved synthesis of lipids, carotenoids, enzymes, or increased tolerance to unfavourable conditions. However, random mutagenesis has not been used to improve protein biosynthesis in microorganisms, and a method for screening these mutants has not yet been developed. The present work reviews the new concept of using herbicides as tools for selecting mutant microorganisms with improved protein biosynthesis. Several pure herbicide substances are amino acid inhibitors whose specific action can be used as a selective pressure for screening protein-rich mutants. The article summarises information about thirteen amino acid inhibitors that inhibit microorganisms and provides data on applicable doses and specifics of use. The article contains mutagenesis protocols and mutant selection strategies, supplemented by theoretical considerations for practical application.

Key words: amino acid inhibitors, herbicide, mutagenesis, mutant selection, protein production, single cell protein.

INTRODUCTION

Agriculture and industrial by-products are commonly employed for energy production, and it is crucial to explore and exploit their potential to create higher-value products. Based on added value, the bioresource pyramid categorises products into energy, bulk chemicals, food, animal feed, special fibres, pharmaceuticals, and fine chemicals. Approximately 46% of the globally produced waste is organic, with food waste presenting a valuable resource (Chavan et al., 2022). Recovering and transforming food waste into high-value products can be more profitable and ecological than conventional processing, contributing to the transition to zero-waste management (Arnold, 2018; Narisetty et al., 2022).

One such higher-value product is microbial protein, called single-cell protein (SCP). SCP is an alternative protein source that offers a sustainable solution to reduce protein scarcity (Najafpour, 2007; FAO, 2020). Wider use of SCP, particularly in livestock and aquaculture feeds, could reduce the need for intensive farming and align with environmental strategies to reduce greenhouse gas emissions (European

Commission, 2012, 2019). Today, 1 in 3 people worldwide struggle with moderate to severe food insecurity, yet 33% of food produced is wasted (Arnold, 2018; United Nations, 2023). Using food waste as a feedstock to produce SCP would help provide a sufficient protein supply to meet growing demand. According to the United Nations Sustainable Development Goals 2023 report, since waste substrates can be used as raw materials, they will help solve current environmental problems (United Nations, 2023).

SCP technology has many advantages over conventional feed protein sources. It is acknowledged for its environmental friendliness, reduced water consumption, resilience to climatic conditions, smaller land requirements, and utilisation of agro-industrial by-products as feedstock (Singh & Mishra, 1995; García-Garibay et al., 2014; El-Sayed, 2020; Berzina et al., 2024). Although SCP production technologies have undergone extensive research and are steadily expanding in the market (Ritala et al., 2017; P&S Intelligence, 2018), there exists potential for further enhancing the properties of SCP-producing microorganisms. Improving and creating strains with superior characteristics can boost the competitiveness of the SCP and contribute to the advancement of a circular bioeconomy by maximising the efficient utilisation of available resources for high-value-added product production (Spalvins et al., 2021).

The present study proposes a new way to create mutant microorganisms with higher protein biosynthesis or an improved amino acid (AA) profile. We suggest using random mutagenesis followed by a screening of mutants in media supplemented with AA inhibitors. This concept is well known in the selection of mutant microorganisms with improved synthesis of fatty acids and carotenoids, where inhibition of the biosynthetic pathway of the target metabolite allowed the collection of overproducers (Ducrey Sanpietro & Kula, 1998; Atzmüller et al., 2019; Luna-Flores et al., 2022). Interestingly, the widely used random mutagenesis to improve the desired properties of strains is not used to create protein-synthesised mutants. Although there is evidence of the effect of random mutagenesis on increasing the protein content biomass of microalgae (Liu et al., 2015). Several herbicides are AA inhibitors, which can be a tool for selecting improved SCP-producing mutants. We assume that microbial cells that have undergone mutagenesis and are capable of growing in media in the presence of an herbicide concentration that inhibits 100% of the cells of the wild-type strain have a high probability of being protein overproducers.

The first part of the study summarises the results of inhibition of bacteria and fungi treated with commercial herbicides and pure active ingredients. Evaluation of microbial growth inhibition and the herbicide doses used are presented in 5 tables. The second part of the study presents protocols for the mutagenesis of microorganisms and subsequent screening of protein-synthesising mutants on selective media supplemented with AA inhibitors. The protocols and accompanying description of the screening procedure for potential mutants consider the details of working with treated yeast cells based on our experience creating SCP yeast mutants.

EFFECT OF HERBICIDES ON THE GROWTH OF BACTERIA AND FUNGI

Many studies report that AA inhibitors, which are the active ingredients of herbicides, affect the growth of microorganisms (Table 1–5). The main effect of different AA inhibitors for plants, algae, bacteria, yeast, and moulds is similar: to inhibit

the enzymatic activity responsible for the biosynthesis of AAs in cells (Kumada et al., 1993; Ravanel et al., 1998; Grant Pearce et al., 2017; Vallejo et al., 2017; Sardrood & Goltapeh, 2018; Lonhienne et al., 2020; Tall & Puigbò, 2020). These inhibitors can lead to AA starvation, suppression of cell growth, and death at specific concentrations. However, other cellular responses are also observed, such as a complete lack of inhibition or stimulation of growth in some species (Forlani et al., 1995; Grandoni et al., 1998; Xuedong et al., 2005¸ Halgren et al., 2011). The reasons for such reactions may lie in the individual characteristics of the species or strain of the microorganism and depend on environmental conditions and interactions in the microbiota (Vallejo et al., 2017; Nielsen et al., 2018). For example, the reason for the lack of inhibition may be associated with the activity of efflux pumps that release the herbicide from the cell or with a disruption of the transport system, such as a porin mutation (Thiour-Mauprivez et al., 2019). Stimulation of growth may be caused by the ability of the microorganism to use the herbicide as a source of carbon or phosphorus, which has been described in several studies (Xuedong et al., 2005; Wang et al., 2007; Łozowicka et al., 2021).

The sources of carbon and nitrogen in the medium directly influence the response of microorganisms to the presence of AA inhibitors (Schloss, 1990; Wang et al., 2012; Nielsen et al., 2018). Studies report that the inhibitory effect is observed in minimal media containing an inorganic nitrogen source and is absent in protein or AA-rich media. If an inhibited AA is subsequently added to the minimal medium, the inhibition of the microorganism is reversed (Schloss, 1990; Nielsen et al., 2018). Therefore, minimal media should be used to select protein-producing mutants. Interesting results were achieved in a study of the ability of soil bacterial isolates to degrade the herbicide tribenuron-methyl (TBM). Isolate of *Serratia marcesens* in the presence of glucose, glycerol, or sucrose contributed to the complete degradation of 0.5 g L^{-1} tribenuron-methyl in 3 days. Adding other carbon sources, such as sodium acetate, sodium succinate, sodium citrate, yeast extract, etc., supported the growth of the bacteria but did not affect the degradation of TBM. It was found that the bacteria could not use the inhibitor as a carbon source, and its degradation is associated with microbial activity of a different nature. It turned out that the degradation of TBM molecules occurred due to acid hydrolysis caused by short-chain fatty acids, fermentation products of glucose, sucrose, and glycerol (Wang et al., 2012). This is consistent with the finding of other studies that a pH decrease in a medium due to microbial metabolism causes some herbicide degradation (Braschi et al., 2000; Boschin et al., 2003). For example, the herbicide primisulfuron is stable in a neutral pH environment, but lowering the pH below six during fermentation resulted in acidohydrolysis (Braschi et al., 2000). Herbicides metsulfuron-methyl and chlorsulfuron are sensitive to a decrease in pH. Significant degradation of these herbicides is reported after 15–48 hours in acidic aqueous solutions with a pH value of 2–5 (PubChem, 2024a, 2024b, 2024c). In comparison, glyphosate and amitrole are stable to hydrolysis at pH 3–9 (PubChem, 2024d, 2024e). Therefore, the medium must be buffered at neutral pH or, if necessary, used at pH 6–8 when using AA inhibitors. The importance of a media composition and pH stability is highlighted in the study reporting the degradation of chlorsulfuron and metsulfuron-methyl by *Aspergillus niger* in a rich-nutrient buffered media but not in a minimal buffered media (Boschin et al., 2003).

In this article, we summarised the results of the inhibition of bacteria and fungi by AA inhibitors (Tables 1–5), selecting AA inhibitors with the best-ranked value according to multicriteria data analysis (MCDA) in our previous study (Berzina et al., 2024). The tables contain information about thirteen AA inhibitors (CAS number of the substance which AA inhibits), a list of bacteria (B) and fungi (F), concentrations of inhibitors, percentage of inhibition, or other effects. Data for both commercial herbicides and pure active components are summarised.

Glutamine AA inhibitors

L-methionine sulfoximine (MSO) and glufosinate-ammonium (GA) are inhibitors of glutamine synthetase, an enzyme involved in nitrogen metabolism and the synthesis of glutamine, purines, and pyrimidines. Glutamine is a precursor to the biosynthesis pathway of the AAs: arginine (Arg), proline (Pro) and aspartate (Asp), lysine (Lys), methionine (Met), threonine (Thr), and isoleucine (Ile) (Mowbray et al., 2014; Joo et al., 2018; Gong et al., 2020). The study (Hernandez & Mora, 1986) suggests that using sugars and a nitrogen source is a coordinated process in microbial cells. When ammonium assimilation and glutamine synthesis are impaired, a decrease in the rate of carbon catabolism is a natural outcome.

Table 1. Evaluation of microbial growth inhibition using herbicides and pure active components. Glutamine inhibitors

Herb.	Microorganism	Inhibition		References
		%	Conc, mg L^{-1}	
L-Methionine sulfoximine (CAS 15985-39-4)				
B	*Azospirillum brasilense*	100	5	(Van Dommelen et al., 2003)
	Mycobacterium tuberculosis	50	9.2	(Mowbray et al., 2014)
F	*Aspergillus niger*	0	360.5	(Ahuja & Punekar, 2008)
	Gibberella fujikuroi	Sign.	360.5	(Muñoz & Agosin, 1993)
Glufosinate ammonium (CAS 77182-82-2)				
B	*Mycobacterium tuberculosis*	50	0.3	(Mowbray et al., 2014)
F	*Aspergillus niger*	Sign.	30	(Ahuja & Punekar, 2008)
	Saccharomyces cerevisiae	55–63	10	(Vallejo et al., 2017)

Sign. – significant inhibition; B – bacteria; F – fungi.

Despite similar activity, GA appears to be a more effective microbial inhibitor than MSO (Table 1). For 50% growth inhibition of *Mycobacterium tuberculosis*, a concentration of 0.3 mg L^{-1} GA was required, while for MSO, the concentration was 9.2 mg L^{-1} (Mowbray et al., 2014). The fungus was less sensitive to these inhibitors; no inhibition of *Aspergillus nige*r growth was detected when treated with 360.5 mg L^{-1} MSO, although 30 mg L^{-1} GA caused significant inhibition, *A. niger* colony diameters decreased by approximately threefold in the presence of GA (Ahuja & Punekar, 2008). Vallejo et al. assessed the effect of 10 mg L^{-1} GA on the growth and metabolism of wine yeast *Saccharomyces cerevisiae* during fermentation. The presence of GA slowed down the rate of sugar metabolism, suppressed growth, and extended the lifespan of cells in the stationary phase. Biomass analysis showed an increase in AAs and polyamines in GA-treated cells compared to untreated cells. AAs such as Met, Ile, Leucine (Leu),

phenylalanine (Phe), tryptophan (Trp), tyrosine (Tyr), etc. were significantly higher in the treated biomass. At the same time, the values of glutamine and asparagine decreased, and Lys, Arg, Pro, and Asp did not differ from untreated cells. This is one of the first studies to report the adaptation of a microorganism to the damaging effects of a herbicide by increasing the biosynthesis of AAs (Vallejo et al., 2017).

Aromatic AA inhibitor

Glyphosate or N-(Phosphonomethyl)glycine is an inhibitor of aromatic amino acids phenylalanine (Phe), tryptophan (Trp), and tyrosine (Tyr) (Hertel et al., 2021). Table 2 shows the required concentrations of glyphosate to completely inhibit the growth of pathogenic or beneficial intestinal bacteria and several fungi. Concentrations refer to the weight of glyphosate active ingredient in the commercial herbicide per litre of media. It is estimated that 75–5,000 mg L^{-1} of glyphosate may be needed for complete inhibition of bacteria (Shehata et al., 2014) and up to 1,000 mg L^{-1} for fungi (Tahiri et al., 2022). However, it should be noted that the inhibitory effect of glyphosate is stronger in the commercial formulation (Braconi et al., 2006; Clair et al., 2012). Therefore, when using a pure substance, higher concentrations may be required.

Table 2. Evaluation of microbial growth inhibition using herbicides and pure active components. Aromatic amino acid inhibitor

Herb.	Microorganism	Inhibition		References
		%	Conc., mg L^{-1}	
Glyphosate (CAS 1071-83-6)				
B	*Bacillus* spp.	100	150–300	(Shehata et al., 2014)
	Bacteroides vulgatus	100	600	(Shehata et al., 2014)
	Bifidobacterium adolescentis	100	75	(Shehata et al., 2014)
	Campylobacter spp.	100	150	(Shehata et al., 2014)
	Clostridium spp.	100	1,200–5,000	(Shehata et al., 2014)
	Enterococcus faecalis	100	150	(Shehata et al., 2014)
	Escherichia coli	100	1,200	(Shehata et al., 2014)
	Escherichia coli	100	80–160	(Nielsen et al., 2018)
	Lactobacillus spp.	100	600	(Shehata et al., 2014)
	Riemerella anatipestifer	100	150	(Shehata et al., 2014)
	Salmonella spp.	100	5,000	(Shehata et al., 2014)
	Staphylococcus spp.	100	300	(Shehata et al., 2014)
F	*Geotrichum candidum*	100	1,000	(Tahiri et al., 2022)
	Penicillium digitatum	100	240	(Tahiri et al., 2022)
	Penicillium italicum	100	240	(Tahiri et al., 2022)

* Commercial herbicide was used; B – bacteria; F – fungi.

Aspartate-derived AA inhibitors

S-(2-aminoethyl)-L-cysteine (AEC), L-α-(2-aminoethoxyvinyl) glycine (AVG), and DL-propargylglycine (PAG) are aspartate-derived amino acid inhibitors (Table 3). AEC and AVG inhibit the biosynthesis of methionine (Met), lysine (Lys), threonine (Thr), and isoleucine (Ile), and PAG inhibits Met (Spalvins et al., 2021). The sensitivity of bacteria to the AEC inhibitor varies. Treatment of *Bacillus subtilis* with 1,000 mg L^{-1}

of inhibitor resulted in complete inhibition, while 3,000 mg L^{-1} caused 50% inhibition of *Brevibacterium flavum*. Interestingly, adding 3,000 mg L^{-1} L-threonine increased the inhibition of *B. flavum* from 50% to over 90% (Shiio, 1970). The effect of AEC on fungi has been poorly studied, and there is no data on a 100% inhibitory dose. Only one study reports that AEC inhibits yeast growth; however, the inhibition rate is too low; 83.3% of the yeast isolates were resistant to the inhibitor (Odunfa et al., 2001). Presumably, the sensitivity of bacteria to AEC is lower than fungi's. No inhibition or inhibition of up to 50% of bacteria was reported when treated with 590 mg L^{-1} AVG inhibitor (Halgren et al., 2011). In comparison, two species of fungi showed up to 80% inhibition at 0.3 mg L^{-1} commercial AVG inhibitor (Jin et al., 2004) and at 200 mg L^{-1} when using the pure substance (Al-Masri et al., 2006). It is worth noting that higher concentrations, such as 1 g L^{-1} or more, were not tested for this inhibitor. Therefore, it is expected that better inhibition may be achieved when using higher concentrations. For complete inhibition of *Fusarium oxysporum* fungi and the enzymatic activity of *Aspergillus flavipes* L-methioninase, about 1 g L^{-1} of PAG inhibitor is required (Jin et al., 2004; El-Sayed, 2011).

Table 3. Evaluation of microbial growth inhibition using herbicides and pure active components. Aspartate-derived amino acid inhibitors

Herb.	Microorganism	Inhibition		References
		%	Conc., mg L^{-1}	
S-(2-aminoethyl)-L-cysteine (CAS 2936-69-8)				
B	*Bacillus subtilis*	100	1,000	(Shiio, 1970)
	Brevibacterium flavum	50	3,000	(Shiio, 1970)
	Brevibacterium flavum	> 90	3,000*	(Shiio, 1970)
	Escherichia coli	100	1,000	(Shiio, 1970)
	Escherichia coli	100	1	(Ataide et al., 2007)
F	yeast, the species were not specified	16.7	200	(Odunfa et al., 2001)
DL-Propargylglycine (CAS 64165-64-6)				
B	*Porphyromonas gingivalis*	100	6.8	(Kandalam et al., 2018)
F	*Aspergillus flavipes*	98**	1,130	(El-Sayed, 2011)
	Fusarium oxysporum	61–93	1,000	(Jin et al., 2004)
L-α-(2-Aminoethoxyvinyl) glycine (CAS 49669-74-1)				
B	*Agrobacterium tumefaciens*	0	589.9	(Halgren et al., 2011)
	Bacillus megaterium	34–38	589.9	(Halgren et al., 2011)
	Erwinia amylovora	47–51	589.9	(Halgren et al., 2011)
	Escherichia coli	0	589.9	(Halgren et al., 2011)
	Pantoea agglomerans	0	589.9	(Halgren et al., 2011)
	Pectobacterium carotovorum	0	589.9	(Halgren et al., 2011)
	Pseudomonas spp.	0	589.9	(Halgren et al., 2011)
	Xanthomonas hortorum	0	589.9	(Halgren et al., 2011)
F	*Fusarium oxysporum*	24–81	0.29***	(Jin et al., 2004)
	Sclerotinia sclerotiorum	70–80	200	(Al-Masri et al., 2006)

* L-threonine supplementation; ** Enzyme L-methioninase inhibition; *** Commercial herbicide was used; B – bacteria; F – fungi.

Branched-chain AA inhibitors

Branched-chain AA inhibitors metsulfuron-methyl (MSM), sulfometuron-methyl (SMM), chlorsulfuron (CS), tribenuron-methyl (TBM), etc., belong to the group of sulfonylureas and imazapyr, imazapic, imazethapyr, and imazaquin, etc. belong to the group of imidazolinones. All of them inhibit the three AA isoleucine (Ile), leucine (Leu), and valine (Val). These inhibitors are considered the most effective herbicides required in micro-doses for complete inhibition of vegetation or microorganisms (Chen et al., 2009; Zabalza et al., 2013; Łozowicka et al., 2021; Berzina et al., 2024). SMM appears more effective than other sulfonylureases in inhibiting microorganisms (Table 4).

Table 4. Evaluation of microbial growth inhibition using herbicides and pure active components. Branched-chain amino acid inhibitors. Sulfonylureas

Herb.	Microorganism	Inhibition		References
		%	Conc., mg L^{-1}	
Metsulfuron-methyl (CAS 74223-64-6)				
B	*Arthrobacter crystallopoietes*	100	50	(Wang et al., 2007)
	Bacillus subtilis	50	11.9	(Kreisberg et al., 2013)
	Burkholderia spp.	50	1.19–47.7	(Kreisberg et al., 2013)
	Mycobacterium avium	> 90	286.0	(Zohar et al., 2003)
	Mycobacterium spp.	100	2.4–9.5	(Kreisberg et al., 2013)
	Pseudomonas aeruginosa	90	95.3	(Kreisberg et al., 2013)
F	*Candida mengyuniae* sp. nov.	50	> 5,000	(Chen et al., 2009)
	Candida shehatae	50	10	(Chen et al., 2009)
	Pichia farinosa	50	200	(Chen et al., 2009)
	Saccharomyces cerevisiae	50	5	(Chen et al., 2009)
	Williopsis saturnus	50	200	(Chen et al., 2009)
Sulfometuron-methyl (CAS 74222-97-2)				
B	*Burkholderia pseudomallei*	50	74.7–182.2	(Kreisberg et al., 2013)
	Mycobacterium avium	100	218.6	(Zohar et al., 2003)
	Mycobacterium spp.	100	0.6–4.4	(Grandoni et al., 1998)
	Pseudomonas spp.	50	22.8–74.7	(Kreisberg et al., 2013)
F	*Candida albicans*	80	12.5	(Kingsbury & McCusker, 2010)
	Saccharomyces cerevisiae	80	5	(Kingsbury & McCusker, 2010)
Chlorsulfuron (CAS 64902-72-3)				
B	*Agrobacterium tumefaciens*	Sign.	0.01–10	(Petrovickij-Angerer, 2009)
	Azospirillum lipoferum	S/g	1.1	(Forlani et al., 1995)
	Azotobacter chroococcum	0	1.1	(Forlani et al., 1995)
	Azotobacter spp.	Sign.	10	(Petrovickij-Angerer, 2009)
	Bacillus cereus	Sign.	1–10	(Petrovickij-Angerer, 2009)
	Bacillus spp.	0	1.1	(Petrovickij-Angerer, 2009)
	Bacillus subtilis	Sign.	0.001–10	(Forlani et al., 1995)
	Bradyrhizobium sp.	Sign.	0.001–10	(Petrovickij-Angerer, 2009)
	Brevundimonas vesicularis	0	1.1	(Forlani et al., 1995)
	Cronobacter sakazakii	0	1.1	(Forlani et al., 1995)

Table 4 (continued)

	Sinorhizobium meliloti	Sign.	0.001–10	(Petrovickij-Angerer, 2009)
	Enterobacter cloacae	0	1.1	(Forlani et al., 1995)
	Escherichia coli	Sign.	0.1–10	(Petrovickij-Angerer, 2009)
	Micrococcus luteus	Sign.	0.1–10	(Petrovickij-Angerer, 2009)
	Mycobacterium avium	85	357.8	(Zohar et al., 2003)
	Mycobacterium spp.	100	11.1–447.2	(Grandoni et al., 1998)
	Pantoea agglomerans	0	1.1	(Forlani et al., 1995)
	Pectobacterium carotovorum	Sign.	0.1–10	(Petrovickij-Angerer, 2009)
	Pseudomonas aeruginosa	Sign.	0.01–10	(Petrovickij-Angerer, 2009)
	Pseudomonas luteola	S/g	1.1	(Forlani et al., 1995)
	Rhizobium spp.	Sign.	0.001–10	(Petrovickij-Angerer, 2009)
	Serratia plymuthica	0	1.1	(Forlani et al., 1995)
	Sphingomonas paucimobilis	0	1.1	(Forlani et al., 1995)
	Stenotrophomonas maltophilia	0	1.1	(Forlani et al., 1995)
	Streptomyces griseus	Sign.	0.1–1	(Petrovickij-Angerer, 2009)
Tribenuron-methyl (CAS 101200-48-0)				
B	*Mycobacterium tuberculosis* (3 strains)	0	49.4	(Grandoni et al., 1998)
F	*Alternaria triticina*	50	239.5*	(Sameer, 2019)
	Pyrenophora tritici	50	238*	(Sameer, 2019)

* Commercial herbicide was used; B – bacteria; F – fungi; Sign. – Significant inhibition; S/g – Slow growth.

SMM's inhibition of some bacteria and fungi has been achieved at relatively low concentrations. CS had significant inhibition against a variety of bacteria, but the study was limited to a concentration of 10 mg L^{-1}, and higher concentrations were not tested (Petrovickij-Angerer, 2009). Another study used a concentration of 1.1 mg L^{-1} CS, which did not have an inhibitory effect on various bacteria and only caused significant inhibition for *Azospirillum lipoferum* (Forlani et al., 1995). No studies have been reported on the inhibition of fungi by a CS inhibitor. The inhibitory effect of MSM on bacteria and fungi has been described in several publications. The sensitivity of fungi to this inhibitor varies greatly. To achieve 50% inhibition of five yeast species, 5 to 200 mg L^{-1} of MSM was required, and for the resistant strain of *Candida mengyuniae,* more than 5 g L^{-1} (Chen et al., 2009).

Complete inhibition of bacteria was observed when using 300–400 mg L^{-1} imazapyr, while lower concentrations of 26.13 and 32.66 mg L^{-1} imazapyr and imazethapyr had no inhibitory effect (Table 5). However, such a small concentration prolonged the generation time of *Bacillus cereus* (Forlani et al., 1995; Xuedong et al., 2005) and *B. circulans* (Xuedong et al., 2005). Four yeast species that showed sensitivity to MSM were less sensitive to imazethapyr. For 50% inhibition, 100, 25, 40, and 25 times more imazethapyr were required for *Candida shehatae, Pichia farinosa, Saccharomyces cerevisiae*, and *Williopsis saturnus*, respectively (Chen et al., 2009).

Table 5. Evaluation of microbial growth inhibition using herbicides and pure active components. Branched-chain amino acid inhibitors. Imidazolinones

Herb.	Microorganism	Inhibition		References
		%	Conc., mg L^{-1}	
Imazapyr (CAS 81334-34-1)				
B	*Azospirillum lipoferum*	0	26.13	(Forlani et al., 1995)
	Azotobacter chroococcum	0	26.13	(Forlani et al., 1995)
	Bacillus cereus	100	300	(Forlani et al., 1995)
	Bacillus spp.	S/g	26.1	(Forlani et al., 1995)
	Bacillus spp.	0	26.13	(Xuedong et al., 2005)
	Brevundimonas vesicularis	0	26.13	(Forlani et al., 1995)
	Cronobacter sakazakii	0	26.13	(Forlani et al., 1995)
	Enterobacter cloacae	0	26.13	(Forlani et al., 1995)
	Mycobacterium spp.	0	32.66	(Grandoni et al., 1998)
	Pantoea agglomerans	0	26.13	(Forlani et al., 1995)
	Pseudomonas fluorescens	100	300–400	(Xuedong et al., 2005)
	Bacillus cereus	100	400	(Xuedong et al., 2005)
	Pseudomonas luteola	0	26.13	(Forlani et al., 1995)
	Serratia plymuthica	0	26.13	(Forlani et al., 1995)
	Sphingomonas paucimobilis	0	26.13	(Forlani et al., 1995)
	Stenotrophomonas maltophilia	0	26.13	(Forlani et al., 1995)
Imazethapyr (CAS 81335-77-5)				
B	*Azospirillum lipoferum*	0	28.93	(Forlani et al., 1995)
	Azotobacter chroococcum	0	28.93	(Forlani et al., 1995)
	Bacillus spp.	0	28.93	(Forlani et al., 1995)
	Bacillus subtilis	S/g	28.9	(Forlani et al., 1995)
	Brevundimonas vesicularis	0	28.93	(Forlani et al., 1995)
	Cronobacter sakazakii	0	28.93	(Forlani et al., 1995)
	Enterobacter cloacae	0	28.93	(Forlani et al., 1995)
	Mycobacterium spp.	0	36.17	(Grandoni et al., 1998)
	Pantoea agglomerans	0	28.9	(Forlani et al., 1995)
	Pseudomonas luteola	0	28.9	(Forlani et al., 1995)
	Serratia plymuthica	0	28.9	(Forlani et al., 1995)
	Sphingomonas paucimobilis	0	28.9	(Forlani et al., 1995)
	Stenotrophomonas maltophilia	0	28.9	(Forlani et al., 1995)
F	*Candida mengyuniae* sp. nov.	50	>5,000	(Chen et al., 2009)
	Candida shehatae	50	1,000	(Chen et al., 2009)
	Pichia farinosa	50	>5,000	(Chen et al., 2009)
	Saccharomyces cerevisiae	50	200	(Chen et al., 2009)
	Williopsis saturnus	50	5,000	(Chen et al., 2009)
Imazaquin (CAS 81335-37-7)				
B	*Arthrobacter crystallopoietes*	100	300	(Wang et al., 2007)
	Bacteria (not specified)	100	10	(Wang et al., 2007)

S/g – Slow growth; B – bacteria; F – fungi.

Most of the data in the tables is devoted to inhibiting pathogenic or soil bacteria and fungi. Pathogenic microorganisms have been reported to be less sensitive to the effects of AA inhibitors (Shehata et al., 2014). Therefore, it can be expected that herbicides may be more effective in inhibiting industrially important microorganisms. To summarise the data, concentrations of 0.01–1,000 mg L^{-1} should be used to determine each inhibitor's complete inhibition of the target microorganism. Subsequently, the tested concentrations can be reduced and narrowed around those mentioned in the literature to find the minimum concentration for full inhibition of the target microorganism.

APPLICATION OF MUTAGENESIS AND AMINO ACID INHIBITORS

Mutagenesis

Mutations are a natural process that occurs in all types of cells as a result of the influence of internal or external stimuli (Pacher & Puchta, 2017). Mutations in microbial cells create new genetic variations that allow them to survive and adapt to rapidly changing environments (Boyce, 2022). This knowledge has enabled the use of random mutagenesis to improve the productivity of commercially important microbial products (pigments, lipids, enzymes, surfactants, etc.) or increase tolerance to stressful conditions (Katre et al., 2017; Bouassida et al., 2018; Vasylkivska et al., 2020; Bleisch et al., 2022; Luna-Flores et al., 2022). Physical, chemical, or biological mutagenesis is widely used for these purposes (Bleisch et al., 2022).

Ultraviolet (UV) irradiation is a widely used physical mutagen (Yamada et al., 2017; Ardelean et al., 2018; Yu et al., 2020; Li et al., 2021). UV irradiation passes through cells, and both physical and chemical changes occur that can cause damage to cell structures such as membranes, enzymes, DNA, and others (Ho, 1975). UV light causes a mutation in which cytosine is modified to thymine by base substitutions at the dipyrimidine sites. UV irradiation also causes oxidative stress in cells by inducing the production of reactive oxygen species (ROS). ROS damages cellular DNA and can cause oxidative damage to DNA bases or even cause DNA breaks. It is known that some of these oxidative DNA and nucleotide damages can function as secondary mutagens. Therefore, it is possible to conclude that UV irradiation can induce specific primary DNA mutations and secondary mutations caused by oxidative stress (Ikehata & Ono, 2011). UV mutagenesis is a relatively simple and effective method for obtaining random mutations in the genome of a microorganism. It is worth noting that each microorganism requires a mutagenesis optimization step to determine the appropriate ratio of UV intensity to irradiation duration to achieve target cell mortality (Shibai et al., 2017; Suryadi et al., 2022).

Chemical mutagens can be divided into alkylating agents and base analogues (Leitão, 2012). Alkylating substances have a strong reaction with different matters and working with it should be done cautiously since they are toxic and have a similar effect to ionizing radiation. An example of such mutagen agents is ethyl methanesulfonate (EMS) and methylnitronitrosoguanidine (MNNG) (Manti & D'Arco, 2010). Alkylation of genetic material leads to the generation of triesters that degrade rapidly, producing alkyl groups that interfere with DNA replication. This process includes the hydrolysis of phosphate triesters, resulting in cleavage of the DNA backbone, and the alkylation of

nitrogenous bases, particularly guanine, which may lead to base-pairing errors during replication (Kodym & Afza, 2003). Other commonly used mutagens are the base analogue 5-bromouracil and nitric acid. The 5-bromouracil can form a base pair with adenine, one of the DNA bases, but also can unexpectedly convert to an isomer that binds to another nucleotide base - guanine, causing variation in a single DNA base pair which is called a transition mutation (Ross et al., 1987). Nitric acid influences both replicating and non-replicating DNA as well can induce the reversal of the mutant to the wild-type strain (Weiss, 2006).

Mutagenesis involves treating cells with a mutagen long enough to cause 50–95% cell death (Chumpolkulwong et al., 1997; Ang et al., 2019; Khan et al., 2020). It is necessary to find and choose an effective amount of mutagenic agent to mutate the target microorganism. The dose of mutagen may vary depending on the species, the time of mutagenesis, the environment temperature, and the composition of the medium. Therefore, preliminary tests are performed with different mutagens doses and exposure times to determine the optimal treatment of the target microorganism (Kodym & Afza, 2003; Demirkan & Özdemir, 2020). The next step is to incubate the cells in the dark for 24 hours and then plate them on the preferred selective medium. Improved strains can be selected using screening appropriate to the desired phenotype (Spencer & Spencer, 1996; Bleisch et al., 2022). Selective agents that exert specific pressure on cells are widely used to select mutants with desired properties. For example, the metabolic inhibitors diphenylamine, β-ionone, and antimycin A are used to select *P. rhodozyma* mutants with improved astaxanthin biosynthesis. Additionally, astaxanthin-producing mutants are selected by visual assessment of the size and colour of colonies on agar (An et al., 1989; Chumpolkulwong et al., 1997; Ducrey Sanpietro & Kula, 1998; Lin et al., 2012; Xie et al., 2014; Luna-Flores et al., 2022). The fatty acid inhibitors cerulenin, isoniazid, and triclosan are used to select mutants with increased lipid biosynthesis (Arora et al., 2020; Atzmüller et al., 2019; Katre et al., 2017). Furthermore, mutants with improved lipid synthesis can be screened using Sudan Black B stained cell microscopy, Nile red fluorescence microscopy, and spectrofluorimetry (Katre et al., 2017; Demirkan & Yıldırım, 2023).

Research on using random mutagenesis and selective agents to improve protein synthesis properties is limited. Significant improvements in protein biosynthesis have been reported in *Chlorella* sp. due to exposure to UV irradiation. Interestingly, the study aimed to improve biomass yield and lipid biosynthesis in microalgae, and the increase in protein content was determined by analysing the biochemical composition of biomass (Liu et al., 2015). In another study, UV irradiation successfully created *Bacillus megaterium* mutant with improved lysine biosynthesis (Li et al., 2015). Therefore, it can be assumed that random mutagenesis can be used to create protein-rich mutants. Further screening of mutants must be used since protein synthesis is a non-obvious phenotype, and selecting such mutants is challenging. Analysing the total protein content in all candidates that survived mutagenesis is not efficient because it is time-consuming and labour-intensive (Yu et al., 2020). Therefore, the use of selective pressure on protein synthesis by the AA inhibitor may be a good solution for effectively screening protein-rich mutants.

Mutagenesis using UV irradiation. A UV light source (254 nm) will be needed to perform mutagenesis with UV irradiation. The UV lamp should be turned on in the laminar flow hood 20 minutes before the start of treatment. Safety glasses should be worn during work to protect the eyes from UV light. The process steps listed below are designed for the yeast *Yarrowia lipolytica* (Winston, 2008; Atzmüller et al., 2019; Ozola, 2022):

1. Prepare an inoculum in a 50 mL flask in a universal yeast medium and incubate for 24 at 28 °C.
2. Collect 1 mL of the inoculum cell suspension and transfer it to a sterile 1.5–2 mL microcentrifuge tube.
3. Centrifuge cells at room temperature for 10–15 seconds using the 'pulse' function and decant the supernatant under aseptic conditions.
4. Resuspend the cells in 1 mL sterile distilled water, vortex, and centrifuge as described in step 3. Wash cells in sterile water twice.
5. Then, determine and dilute the cell concentration in the aqueous solution to obtain a concentration of 1.0×10^6 cells per mL.
6. Distribute the resulting suspension among sterile 1.5 mL tubes, each filled with 1 mL of the suspension (use enough tubes so that there is enough for the experiment and leave one tube that will not be treated. It will act as a control).
7. Place the vortex stand for microcentrifuge tubes 20 cm away from the UV lamp (the distance can also be optimised, with specific durations).
8. Treat the cells with UV light for different durations (e.g., 5, 10, 20, 30, 40, 50, and 60 seconds) while the tubes are vortexing at medium speed in the stand. For other microorganisms, a new combination of distance to the source and irradiation time should be selected to achieve the required percentage of cell mortality.
9. After treatment, dilute samples to 2,000 cells mL^{-1}. Plate 100 µL of each sample on agar in triplicate (respectively 200 cells per plate) and incubate at the microorganism's optimal temperature.
10. Count colony-forming units after 48–96 hours and determine the percentage of dead cells. Conditions that ensure the death of 50–95% of cells are recommended.

Notes: UV mutagenesis of cells can be performed on agar plates, considering the following features. Some components of the environment, such as vitamins, may be sensitive to UV irradiation. Treating cells with open plate lids is more practical, significantly reducing processing time.

Mutagenesis using MNNG. This MNNG mutagenesis protocol is based on methods described in the literature (Winston, 2008; Luna-Flores et al., 2022) and modified in our laboratory for mutagenesis of the red yeast *Phaffia rhodozyma* (Feldmane, 2023). These materials should be prepared in advance - universal yeast broth medium and agar plates, 0.1 M sterile citrate buffer (pH 5.5), and sterile 0.1 M phosphate buffer (pH 7.0). The half-life of EMS in water at pH 7.0 and 20 °C is 93 hours, and at 30 °C, the half-life is 26 hours. MNNG solution also is not stable for an extended period (Luna-Flores et al., 2022). Therefore, the mutagen solutions should be prepared before use and not stored (Kodym & Afza, 2003). It is also important to rinse and wipe all instruments, materials, and surfaces that were in contact with EMS mutagen after work with 5% sodium thiophosphate to inactivate it (Rowlands, 1984). The protocol includes step-by-step instructions for preparing microorganism cells for mutagenesis and subsequent plating:

1. Prepare an inoculum in a 50 mL flask in a universal yeast medium and incubate for 24–48 hours at 22 °C.

2. Transfer 1 mL of the inoculum cell suspension to a sterile 1.5–2 mL microcentrifuge tube. Centrifuge cells at room temperature for 10–15 seconds using the 'pulse' function. 20–22 °C will be the preferred centrifuging temperature for *P. rhodozyma* cells. Decant the supernatant and then resuspend the cells in 1 mL of sterile 0.1 M citrate buffer (pH 5.5). Wash cells in citrate buffer twice.

3. Prepare a 1.25 g L^{-1} (0.125%) MNNG solution using 0.005 g MNNG crystals. Dissolve them in 4 mL of sterile citrate buffer (pH 5.5). Vortex until the crystals are completely dissolved.

4. Dilute the MNNG solution to a concentration of 0.167 g L^{-1} (0.0167%). For example, transfer 200 µL of MNNG stock solution and 1,300 µL of citrate buffer into a 1.5–2 mL microcentrifuge tube.

5. Resuspend the washed cells without supernatant in 1 mL of MNNG solution (0.0167%) and incubate at 22 °C for 30 min. Gently shake the microcentrifuge tube a few times every 10 min to ensure that the cells are mixed evenly.

6. Centrifuge the cells and decant the MNNG solution, then wash them twice in 0.1 M phosphate buffer (pH 7.0).

7. To prepare the inoculum, resuspend all cells in approximately 15 mL of the universal yeast medium. Incubate cells overnight at 22 °C on an orbital shaker at 250 rpm.

8. The next day, dilute and count samples to 3,000 cells mL^{-1}. Plate 100 µL of each sample on agar in triplicate (300 cells per plate) and incubate at 22 °C.

9. Count colony-forming units after 48–96 hours and determine the percentage of dead cells. It is recommended that conditions ensure the death of 50–95% of cells.

Mutagenesis using EMS. This protocol is based on the method used by Luna-Flores et al. (Winston, 2008; Luna-Flores et al., 2022). These materials should be prepared in advance - medium plates, sterile 0.5 mM potassium phosphate buffer (pH 7.0), sterile 5% (w v^{-1}) sodium thiophosphate solution, and microbial medium. EMS concentration should be previously determined to cause 50–95% cell death in the test organism. All instruments, materials, and surfaces that were in contact with EMS mutagen after work should be treated with 5% sodium thiophosphate to inactivate the mutagen. In this description, the concentration was determined for the yeast strain *Phaffia rhodozyma* (Feldmane, 2023):

1. Prepare an inoculum in a 50 mL flask in a universal yeast medium and incubate for 24–48 hours at 22 °C.

2. Transfer 5 mL of inoculum to a sterile 50 mL centrifuge tube, then centrifuge the cells for 10 min at 1,800 × g, 22 °C. Decant the supernatant and add 5 mL of sterile 50 mM potassium phosphate buffer (pH 7.0).

3. Resuspend the cells then perform centrifugation as described in step 2. Repeat the washing twice.

4. Resuspend the cells in 5 mL potassium phosphate buffer and add 209 µL sterile EMS solution; the EMS concentration in the solution is 4%. Incubate the cells in this solution for 2 h at 22 °C on an orbital shaker at 250 rpm.

5. Then add 8 mL of sterile 5% (w v^{-1}) sodium thiophosphate solution to neutralise EMS, gently vortex and centrifuge the cells as described in step 3. with potassium phosphate buffer.

6. Wash the cells in potassium phosphate buffer twice.

7. To prepare the inoculum, resuspend all cells in approximately 15 mL of the universal yeast medium. Incubate cells overnight at 22 °C on an orbital shaker at 250 rpm.

8. The next day, dilute and count samples to 3,000 cells mL^{-1}. Plate 100 µL of each sample on agar in triplicate (300 cells per plate) and incubate at 22 °C.

9. Count colony-forming units after 48–96 hours and determine the percentage of dead cells. It is recommended that conditions ensure the death of 50–95% of cells.

Screening of mutants using AA inhibitors

Preparation of agar plates with AA inhibitors. The wild-type strain must be cultivated on selective agar with different inhibitor concentrations from 0.01 to 1,000 mg L^{-1} to determine the 100% cell inhibition dose. It should be noted that the selective agar does not have organic nitrogen in its composition, and the aqueous solubility of AA inhibitors is closely related to the pH of the solution. For example, the water solubility of sulfometuron-methyl at pH 5 is 0.00642 g L^{-1}, and at pH 8.6, it is 12.5 g L^{-1}, resulting in a 1947-fold increase in solubility with increasing pH (PubChem, 2024f). However, some AA inhibitors are practically insoluble in water; thus, they need to be dissolved in polar solvents. This study reports that the stock solution of the inhibitor imazaquin was prepared with methanol since its solubility in water is three times lower than in methanol (Wang et al., 2007; PubChem, 2024g). Polar organic solvents can also promote hydrolysis of herbicides such as chlorsulfuron, so it needs to be dissolved in dimethyl sulfoxide (DMSO) to prepare the stock solution (MedchemExpress, 2024; PubChem, 2024b). It is, therefore, important to study the available information on the properties of the inhibitor before preparing the solutions. The protocol for preparing an agar medium supplemented with 5 doses of inhibitor is as follows:

1. Prepare an AA inhibitor stock solution for the 420–540 mL of agar medium.

2. Sterilize the inhibitor stock solution using a membrane filter with a pore size of 0.22 µm.

3. Prepare 6 bottles of minimal agar medium for approximately 70–90 mL of medium for 6 plates each. Adjust pH to neutral and autoclave.

4. After sterilisation, cool the media to approximately 45–50 °C and add the required amount of inhibitor solution (add vitamins, salts, or antibiotics if necessary). Add AA inhibitor solution in different concentrations from 0.01 to 1,000 mg per litre of agar medium into 5 bottles.

5. Mix the agar thoroughly and carefully to avoid the formation of bubbles and pour into Petri plates.

6. Prepare an inoculum in a 50 mL flask in a universal yeast medium and incubate for 24–48 hours under optimal conditions.

7. Transfer 1 mL of the inoculum to a sterile 1.5–2 mL microcentrifuge tube. Centrifuge cells at room temperature for 10–15 seconds using the ‘pulse’ function.

8. Decant the supernatant and then resuspend the cells in 1 mL of 0.1 M phosphate buffer (pH 7.0). Wash the cells in phosphate buffer twice.

9. Prepare a cell suspension with 3,000 cells mL^{-1}. Plate 100 µL of cell suspension on agar in triplicate with 5 different concentrations of AA inhibitor and as a control on agar without inhibitor.

10. Incubate the plates for 2–7 days and count the surviving colonies to determine the approximate dose of complete inhibition. Repeat the test using narrow-range concentrations to find the minimum dose to completely inhibit the target microorganism.

Even though most inhibitor solutions can be stored at room temperature for 30 days, except for imazethapyr and imazapyr, these inhibitor solutions have a half-life of 2 and 6 days (PubChem, 2024c, 2024h), respectively, it is also better to store the solutions in the dark as they degrade rapidly in sunlight. All solutions can be stored in a freezer at -20 °C for 1 month or at -80 °C for 6 months ('MedChemExpress', 2024).

Selection of potential candidates on selective plates. When the needed dose for mutagen (~50–95% cell death) and inhibitor (100% inhibited growth) is found, these two factors should be combined. Plates with selective agar should be prepared so that there are at least three identical samples. In an experiment where mutagenesis is combined with an inhibition, many inhibitor concentrations should be tested. This will increase the chances of selecting potentially better mutants. For yeast, use a two-day-old inoculum and add 300 cells to each plate.

After incubation of the plates for two to three days, the potential mutant candidates are chosen and transferred to a new plate with the same inhibitor and concentration as the previous plate on which it was placed. The colonies can be selected by multiple strategies or characteristics: size, colour, growth speed, morphology, etc. When these candidates have grown on the new plates, those colonies that better fit the selection criteria should again be transferred to a regular agar plate, saved in storage, and further used in experiments. To determine whether mutant selection was successful chosen candidates should be used in a flask test obtaining biomass which can be used in detailed analyses. It is expected that the mutants will be able to synthesize more total protein or increase the synthesis of inhibitor-targeted AA.

As seen in Fig. 1. new mutants from the mutagenesis step should be placed in cold permanent storage. Although mutations will be inherited by the offspring of mutants, if possible, number of generations should be reduced as much as possible. The mutant microorganism has better chances to keep their gained quality if used under environmental conditions corresponding to employed selective stressors or, in this case, AA inhibitors (Lenski, 1991). Otherwise, those abilities can decline in time and may eventually be lost (Lenski, 1991; Peng & Liang, 2020). Other stressful environments can also promote oxidative stress to microorganisms that can damage DNA and trigger SOS response and adaptive mutation response (Peng & Liang, 2020). Genetic stability should be one of the factors that are tested after mutant creation by determining whether the new strain maintains obtained traits after multiple generations. It has been observed that strains can lose the ability to produce products upon repeated transfers in batch culture and the production rate can decrease during long-time fermentation (Peng & Liang, 2020). Therefore, it would be important to employ multiple preventive actions to maintain the enhanced abilities as long as possible for the mutant strain and not lose the newly acquired strain.

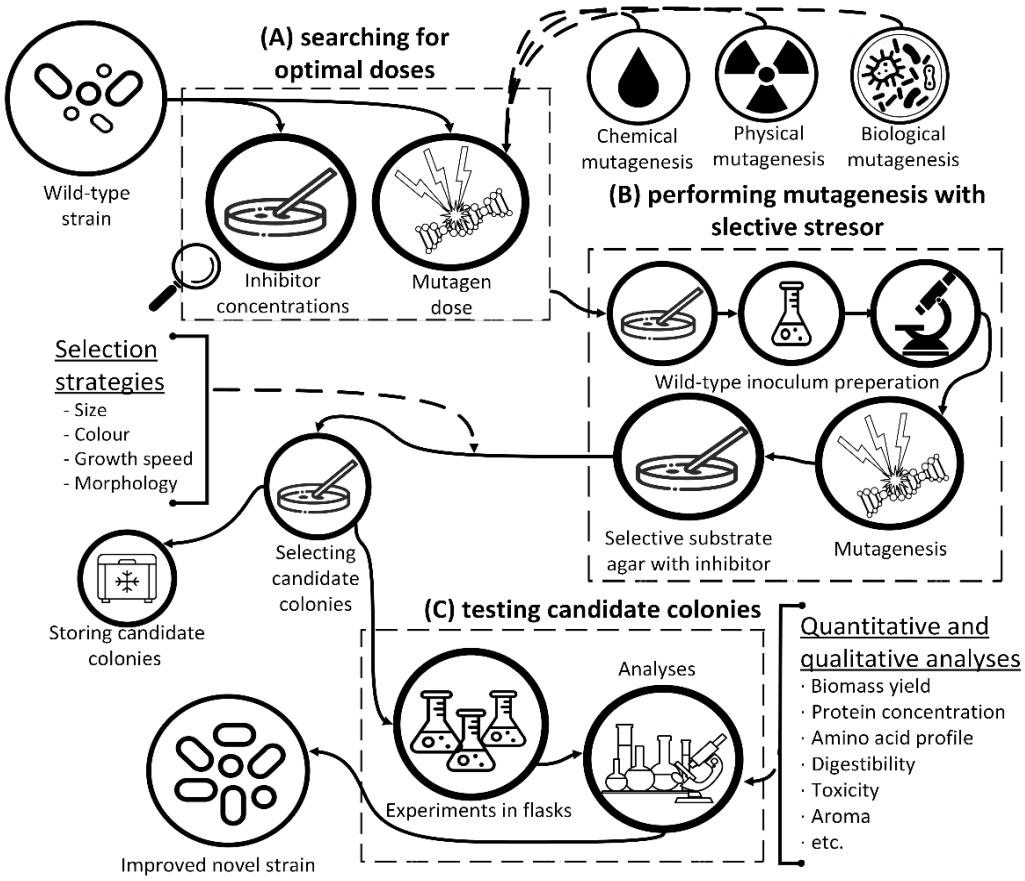

Figure 1. Process scheme for developing a novel mutant strain using mutagenesis and AA inhibitors.

In stage (A) (Fig 1, A), inhibition doses are searched where mutagenesis cell death is 50–90% and for AA inhibitor 100% growth inhibition. In stage (B) (Fig. 1, B), a wild-type strain inoculum is prepared to perform mutagenesis. Afterward, the cell aliquot with a concentration of 300 cells per 100 µL is inoculated on multiple selective substrate agar plates with AA inhibitors. Candidate colonies are selected after two to three days according to their size, colour, morphology, or other criteria and transferred on agar plates with the same properties as the previous one. When the new candidate colonies have grown, they are stored and used in experiments. In stage (C) (Fig. 1, C), the candidate colonies are used to perform experiments, which can take the form of, for example, flask tests where the candidates are compared to each other by determining which has higher quantitative properties, such as biomass yield or cell density. Later, gathered biomass can be used for further analysis where other quantitative and qualitative properties can be determined. According to the study results, the colonies with the best improved and desirable properties are considered new novel strains.

Determination of microbial growth inhibition using a microplate reader. An alternative approach to screening mutants on selective agar plates is to measure a cell suspension's optical density (OD) using a microplate reader. The use of 48-well or 96-well microplates increases screening throughput while reducing time and resource costs (Alcalde et al., 2005; Yu et al., 2020). However, OD measurements with a microplate

reader cannot distinguish between dead and viable cells. Therefore, cell counting at the end of cultivation is required (Hazan et al., 2012). The following protocol is applicable for screening potential mutants, where they are inoculated into a microplate after mutagenesis and placed in a medium supplemented with a selected inhibitor concentration.

1. Dissolve needed inhibitors.
2. Prepare optimal medium for the microorganism (buffered medium at 6–7 pH with inorganic nitrogen source should be used).
3. Divide the medium and add inhibitors in different concentrations determined previously. Use the 24-well, 48-well, or 96-well microplate with a working volume of 1mL, 0.5 mL, or 0.2 mL, respectively.
4. Inoculate each well of the triplet with an inoculum concentration of 1.0×10^6 cells mL^{-1} for each inhibitor dose.
5. Carefully fill the microplate with samples (each medium/inhibitor concentration should be done in triplicate).
6. Set the microplate reader to measure OD every hour and incubate the microplate at the optimal temperature with agitation for 48 to 120 hours.
7. Microscope and count the viable cells from each sample at the end of the test.
8. Based on the OD and number of cells, select the minimum concentration of inhibitor that completely inhibits the growth of the microorganism.

It is important to note that a significant portion of the inoculum cells may be lost after mutagenesis and buffer washing. Therefore, it is necessary to prepare a larger amount of inoculant, for example, 50–100 mL, depending on the cell density in the culture. This is necessary to subsequently be able to inoculate each well of the microplate with 1.0×10^7 cells per mL. Since, theoretically, after chemical mutagenesis, 10% of viable cells will remain in the inoculum. The optimal cell concentrations may vary depending on the microorganism and the used microplate reader. Consistency in the cell concentration directly inoculated into the microplate is crucial for identifying a complete growth-inhibiting inhibitor dose and seeding cells post-mutagenesis. Mutagenesis should be carried out on cells collected from the entire volume of the inoculum. Resuspend the cells in 5 mL of potassium phosphate as described in the EMS mutagenesis protocol and then follow the specified volumes of solutions. In the case of MNNG, it is necessary to increase the volumes of all solutions used in the protocol by at least five times. Further, all actions are performed according to the microplate protocol, with the only correction for the inoculation of cells in mL being ten times higher than that used in the previous test to search for a complete growth-inhibiting dose. After completing the microplate test, it is necessary to take samples from the wells with confirmed microbial growth for further inoculation into flasks for protein analysis from the collected biomass.

Estimated effectiveness and safety of AA inhibitors

Determining which of the mutagens (UV radiation, EMC, or MNNG) is more effective is difficult. Improved strains have been obtained using each of them, according to numerous publications (Lin et al., 2012; Katre et al., 2017; Arora et al., 2020; Bleisch et al., 2022; Demirkan & Yıldırım, 2023). However, a comparison of these three mutagens according to such criteria as methods probability of success, approximate induced mutation frequency, methods toxicity to environment, price of the required

amount of mutagen per run, etc., using the MCDA was rated higher for EMS and lower for MNNG (Berzina et al., 2024). It is worth noting that combining these mutagens leads to a more effective result (Agrawal et al., 2013; Kumar et al., 2015; Zhang et al., 2016; Gopinath et al., 2020). The effectiveness of AA inhibitors as a selective agent for screening protein-rich mutants can be assessed after experimental tests. On the other hand, a preliminary MCDA analysis of AA inhibitors according to criteria such as inhibition efficacy, inhibited EAA, possibility of false positive selection, price of inhibitor, etc., showed potentially the best inhibitors for bacteria and fungi. According to the analysis, glufosinate-ammonium, L-methionine sulfoximine, L-α-(2-aminoethoxyvinyl) glycine, and S-(2-aminoethyl)-L-cysteine are potentially the best AA inhibitors for both bacteria and fungi. However, considering the high cost of L-α-(2-aminoethoxyvinyl) glycine, using this AA inhibitor for mutant screening seems irrelevant (Berzina et al., 2024). Promising results were obtained in a study of the effects of herbicides on wine yeast. Biochemical analysis of *Saccharomyces cerevisiae* biomass treated with the inhibitor glufosinate-ammonium showed a significant increase in some essential AA compared to untreated biomass (Vallejo et al., 2017).

Currently, the mechanisms of AA inhibitors' action on the metabolic pathways of microorganisms have not been well studied to provide a clear understanding of the results of their use. The safety of feed containing mutant biomass previously treated with herbicide is controversial. It is known that herbicides such as glyphosate, glufosinate ammonium, sulfonylurea herbicides (Table 4), and imidazolinones (Table 5) selectively inhibit the amino acid biosynthesis pathway in plant, fungal, and insect cells, but not in animals and humans (Gupta, 2018; Thiour-Mauprivez et al., 2019). Studies report these herbicides' absence of mutagenicity and carcinogenicity, but they harm animal health at specific doses (Gupta, 2018; Thiour-Mauprivez et al., 2019; Berry, 2020; Peillex & Pelletier, 2020). DL-propargylglycine and L-methionine sulfoximine inhibit the amino acid biosynthetic pathway in animals. On the other hand, this effect of inhibitors can be used in therapy and minimisation of the consequences of several human diseases (Brusilow & Peters, 2017; Zhou et al., 2018). AA inhibitor S-(2-aminoethyl)-Lcysteine hydrochloride is an analogue of lysine and is completely safe for animals (Friedman & Gumbmann, 1981; Li et al., 2015). It can be concluded that the herbicide content in edible microbial biomass is not desirable. The safety of such mutants can be confirmed in the absence or acceptable levels of herbicides and their breakdown products in biomass using gas chromatographic analysis or another alternative technique. It is important to note that when using mutagens and AA inhibitors in research, the precautions specified by the manufacturer of the substances should be strictly followed and disposed of properly.

CONCLUSIONS

Many microorganisms, such as bacteria, fungi, and microalgae, are excellent SCP producers. Microbial growth rate, protein productivity, and protein quality are significant determining factors for the successful production of SCP on a commercial scale. Improved microbial strains capable of synthesising more proteins, mainly by increasing the content of amino acids that are limiting in traditional plant-based protein sources, will increase the potential of SCP and contribute to the commercial development of technology.

In the present study, we examined thirteen herbicides with the potential to exert selective pressure on mutant microbial strains to select improved SCP producers. Literature data are summarised in five tables and contain concentrations of herbicides inhibiting bacteria, yeast, and moulds. Microalgae, protists, and other microorganisms were not considered. However, the presented protocols may apply to additional inhibitory dose studies. The article contains protocols for random mutagenesis and describes the preparation of a selective medium for subsequent screening of mutants with desired properties on plates or with a microplate. The article is valuable for its detailed description of both critical aspects of the methodology and recommendations based on our experience working with AA inhibitors in the laboratory.

In the future, a series of experiments must be conducted to confirm the effectiveness of AA inhibitors in selecting protein-synthesizing mutants and the stability of the mutation. If the result is positive, the growing conditions must be optimised, and the quality of the biomass and protein, including its safety for use in feed or food, must be analysed. Thus, using this technology to create SCP-improved strains on a broad scale could reduce pressure on conventional protein production sectors such as agriculture and fishery.

ACKNOWLEDGEMENTS. The work has been developed by the Fundamental and Applied Research Project 'Herbicides as a tool for selection of edible protein-rich mutants', project No. lzp-2022/1-0126, funded by the Latvian Council of Science.

REFERENCES

Agrawal, R., Satlewal, A. & Verma, A.K. 2013. Development of a β-glucosidase hyperproducing mutant by combined chemical and UV mutagenesis. *3 Biotech* **3**, 381–388. doi: 10.1007/s13205-012-0095-z

Ahuja, M. & Punekar, N.S. 2008. Phosphinothricin resistance in *Aspergillus niger* and its utility as a selectable transformation marker. *Fungal Genetics and Biology* **45**, 1103–1110. doi: 10.1016/j.fgb.2008.04.002

Alcalde, M., Bulter, T., Zumárraga, M., García-Arellano, H., Mencía, M., Plou, F.J. & Ballesteros, A. 2005. Screening Mutant Libraries of Fungal Laccases in the Presence of Organic Solvents. *SLAS Discovery* **10**, 624–631. doi: 10.1177/1087057105277058

Al-Masri, M.I., Elad, Y., Sharon, A. & Barakat, R. 2006. Ethylene production by *Sclerotinia sclerotiorum* and influence of exogenously applied hormone and its inhibitor aminoethoxyvinylglycine on white mold. *Crop Protection* **25**, 356–361. doi: 10.1016/j.cropro.2005.05.010

An, G.-H., Schuman, D.B. & Johnson, E.A. 1989. Isolation of *Phaffia rhodozyma* Mutants with Increased Astaxanthin Content. *Applied and Environmental Microbiology* **55**, 116–124. doi: 10.1128/aem.55.1.116-124.1989

Ang, F.S., Khaw, S.Y., Few, L.L., See Too, W.C. & Chew, A.L. 2019. Isolation of a Stable Astaxanthin-Hyperproducing Mutant of *Xanthophyllomyces dendrorhous* Through Random Mutagenesis. *Applied Biochemistry and Microbiology* **55**, 255–263. https://doi.org/10.1134/S0003683819030025

Ardelean, A., Ardelean, I., Sicuia, O. & Cornea, C.P. 2018. Random- Mutagenesis in Photosynthetic Microorganisms Further Selected with Respect to Increased Lipid Content. *'Agriculture for Life Life for Agriculture' Conference Proceedings* **1**, pp. 501–507. doi: 10.2478/alife-2018-0079

Arnold, T. 2018. Bioeconomy, food and nutrition security Chapter 1, in: *Bioeconomy Challenges and Implementation: The European Research Organisations*' Perspective. Éditions Quæ, France. Available at https://pdfs.semanticscholar.org/130e/e0018196d4977ed9a3cafe14579cc0160492.pdf

Arora, N., Yen, H.-W. & Philippidis, G.P. 2020. Harnessing the Power of Mutagenesis and Adaptive Laboratory Evolution for High Lipid Production by Oleaginous Microalgae and Yeasts. *Sustainability* **12**, 5125. doi: 10.3390/su12125125

Ataide, S.F., Wilson, S.N., Dang, S., Rogers, T.E., Roy, B., Banerjee, R., Henkin, T.M. & Ibba, M. 2007. Mechanisms of Resistance to an Amino Acid Antibiotic That Targets Translation. *ACS Chemical Biology* **2**, 819–827. doi: 10.1021/cb7002253

Atzmüller, D., Hawe, F., Sulzenbacher, D. & Cristobal-Sarramian, A. 2019. Wheat straw and lipids: UV-mutagenized *Yarrowia lipolytica* for the conversion of wheat straw hydrolysate into lipids. *Agronomy Research* **17**, 2172–2179. doi: 10.15159/AR.19.197

Berry, C. 2020. Glyphosate and cancer: the importance of the whole picture. *Pest Management Science* **76**, 2874–2877. doi: 10.1002/ps.5834

Berzina, I., Raita, S., Kalnins, M., Kuzmika, I. & Spalvins, K. 2024. In search of the best technological solutions for creating edible protein-rich mutants: a multi-criteria analysis approach. *Agronomy Research* **22**(S1), 370–400. doi: 10.15159/AR.24.039

Bleisch, R., Freitag, L., Ihadjadene, Y., Sprenger, U., Steingröwer, J., Walther, T. & Krujatz, F. 2022. Strain Development in Microalgal Biotechnology—Random Mutagenesis Techniques. *Life* **12**, 961. doi: 10.3390/life12070961

Boschin, G., D'Agostina, A., Arnoldi, A., Marotta, E., Zanardini, E., Negri, M., Valle, A. & Sorlini, C. 2003. Biodegradation of Chlorsulfuron and Metsulfuron-Methyl by *Aspergillus niger* in Laboratory Conditions. *Journal of Environmental Science and Health, Part B* **38**, 737–746. doi: 10.1081/PFC-120025557

Bouassida, M., Ghazala, I., Ellouze-Chaabouni, S. & Ghribi, D. 2018. Improved Biosurfactant Production by *Bacillus subtilis* SPB1 Mutant Obtained by Random Mutagenesis and Its Application in Enhanced Oil Recovery in a Sand System. *Journal of Microbiology and Biotechnology* **28**, 95–104. doi: 10.4014/jmb.1701.01033

Boyce, K.J. 2022. Mutators Enhance Adaptive Micro-Evolution in Pathogenic Microbes. *Microorganisms* **10**, 442. doi: 10.3390/microorganisms10020442

Braconi, D., Sotgiu, M., Millucci, L., Paffetti, A., Tasso, F., Alisi, C., Martini, S., Rappuoli, R., Lusini, P., Sprocati, A.R., Rossi, C. & Santucci, A. 2006. Comparative Analysis of the Effects of Locally Used Herbicides and Their Active Ingredients on a Wild-Type Wine *Saccharomyces cerevisiae* Strain. *Journal of Agricultural Food Chemistry* **54**, 3163–3172. doi: 10.1021/jf052453z

Braschi, I., Pusino, A., Gessa, C. & Bollag, J.-M. 2000. Degradation of Primisulfuron by a Combination of Chemical and Microbiological Processes. *J. Agric. Food Chem.* **48**, 2565–2571. doi: 10.1021/jf990604q

Brusilow, W.S.A. & Peters, T.J. 2017. Therapeutic effects of methionine sulfoximine in multiple diseases include and extend beyond inhibition of glutamine synthetase. *Expert Opinion on Therapeutic Targets* **21**, 461–469. doi: 10.1080/14728222.2017.1303484

Chavan, S., Yadav, B., Atmakuri, A., Drogui, P., Tyagi, D. & Wong, J.W.C. 2022. Bioconversion of organic wastes into value-added products: A review. *Bioresource Technology* **344**. doi: 10.1016/j.biortech.2021.126398

Chen, B., Huang, X., Zheng, J.-W., Li, S.-P. & He, J. 2009. *Candida mengyuniae* sp. nov., a metsulfuron-methyl-resistant yeast. International *Journal of Systematic and Evolutionary Microbiology* **59**, 1237–1241. doi: 10.1099/ijs.0.004614-0

Chumpolkulwong, N., Kakizono, T., Nagai, S. & Nishio, N. 1997. Increased astaxanthin production by *Phaffia rhodozyma* mutants isolated as resistant to diphenylamine. *Journal of Fermentation and Bioengineering* **83**, 429–434. doi: 10.1016/S0922-338X(97)82996-0

Clair, E., Linn, L., Travert, C., Amiel, C., Séralini, G.-E. & Panoff, J.-M. 2012. Effects of Roundup® and Glyphosate on Three Food Microorganisms: *Geotrichum candidum*, *Lactococcus lactis* subsp. *cremoris* and *Lactobacillus delbrueckii* subsp. *bulgaricus*. *Curr Microbiol* **64**, 486–491. doi: 10.1007/s00284-012-0098-3

Demirkan, E. & Özdemir, K. 2020. Ethyl Methanesulfonate (EMS) Mutation for Hyper Protease Production by *Bacillus subtilis* E6-5 and Optimization of Culture Conditions. *Hacettepe Journal of Biology and Chemistry* **48**, 355–365. doi: 10.15671/hjbc.697070

Demirkan, E. & Yıldırım, İ. 2023. Screening of Lipid Production Capacities of *Bacillus* sp. Strains Isolated from Soil and Lipid Staining with Different Staining Techniques. A*fyon Kocatepe Üniversitesi Fen Ve Mühendislik Bilimleri Dergisi* **23**, 1094–1102. doi: 10.35414/akufemubid.1265060

Ducrey Sanpietro, L.M. & Kula, M.-R. 1998. Studies of astaxanthin biosynthesis in *Xanthophyllomyces dendrorhous* (*Phaffia rhodozyma*). Effect of inhibitors and low temperature. *Yeast* **14**, 1007–1016. doi: 10.1002/(SICI)1097-0061(199808)14:11<1007::AID-YEA307>3.0.CO;2-U

El-Sayed, A.-F.M. 2020. Nutrition and feeding, in: *Tilapia Culture*, Elsevier, pp. 135–172. https://doi.org/10.1016/B978-0-12-816509-6.00007-0

El-Sayed, A.S.A. 2011. Purification and characterization of a new L-methioninase from solid cultures of *Aspergillus flavipes*. *Journal of Microbiology* **49**, 130–140. doi: 10.1007/s12275-011-0259-2

European Commission, 2019. 2050 long-term strategy. https://climate.ec.europa.eu/eu-action/climate-strategies-targets/2050-long-term-strategy_en. Accessed 19.12.23.

European Commission, 2012. MEMO - Indirect Land Use Change (ILUC) (No. MEMO/12/787). Brussels. https://ec.europa.eu/commission/presscorner/detail/de/MEMO_12_787

FAO, 2020. Food Outlook – Biannual Report on Global Food Markets. doi: 10.4060/ca9509e

Feldmane, L. 2023. *Mutagenesis and property analysis of astaxanthin producing microorganism Phaffia rhodozyma*. Master's Thesis, Riga Technical University, Riga, Latvia, 71 pp.

Forlani, G., Mantelli, M., Branzoni, M., Nielsen, E. & Favilli, F., 1995. Differential sensitivity of plant-associated bacteria to sulfonylurea and imidazolinone herbicides. *Plant Soil* **176**, 243–253. doi: 10.1007/BF00011788

Friedman, M. & Gumbmann, M.R. 1981. Bioavailability of some Lysine Derivatives in Mice. *The Journal of Nutrition* **111**, 1362–1369. doi: 10.1093/jn/111.8.1362

García-Garibay, M., Gómez-Ruiz, L., Cruz-Guerrero, A.E. & Bárzana, E. 2014. Single Cell Protein: Yeasts and Bacteria, in: Encyclopedia of Food Microbiology: Second Edition. *Elsevier Inc.*, pp. 431–438. doi: 10.1016/B978-0-12-384730-0.00310-4

Gong, C., You, X., Zhang, S. & Xue, D. 2020. Functional Analysis of a Glutamine Biosynthesis Protein from a Psychrotrophic Bacterium, *Cryobacterium soli GCJ02*. *Indian Journal of Microbiology* **60**, 153–159. doi: 10.1007/s12088-020-00858-7

Gopinath, S., Venkataprasad, R., Rajnish, K.N., Datta, S. & Selvarajan, E. 2020. Enhancement of Serrapeptase Hyper Producing Mutant by Combined Chemical and UV Mutagenesis and its Potential for Fibrinolytic Activity. *Journal Pure and Applied Microbiology* **14**, 1295–1303. doi: 10.22207/JPAM.14.2.25

Grandoni, J.A., Marta, P.T. & Schloss, J.V. 1998. Inhibitors of branched-chain amino acid biosynthesis as potential antituberculosis agents. *Journal of Antimicrobial Chemotherapy* **42**, 475–482. doi: 10.1093/jac/42.4.475

Grant Pearce, F., Hudson, A.O., Loomes, K. & Dobson, R.C.J. 2017. Dihydrodipicolinate Synthase: Structure, Dynamics, Function, and Evolution, in: Harris, J.R., Marles-Wright, J. (Eds.), Macromolecular Protein Complexes, Subcellular Biochemistry. *Springer International Publishing*, Cham, pp. 271–289. doi: 10.1007/978-3-319-46503-6_10

Gupta, P.K. 2018. Toxicity of Herbicides, in: Veterinary Toxicology. *Veterinary toxicology,* pp. 553–567. doi: 10.1016/B978-0-12-811410-0.00044-1

Halgren, A., Azevedo, M., Mills, D., Armstrong, D., Thimmaiah, M., McPhail, K. & Banowetz, G. 2011. Selective inhibition of *Erwinia amylovora* by the herbicidally active germination-arrest factor (GAF) produced by *Pseudomonas* bacteria. *Journal of Applied Microbiology* **111**, 949–959. doi: 10.1111/j.1365-2672.2011.05098.x

Hazan, R., Que, Y.-A., Maura, D. & Rahme, L.G. 2012. A method for high throughput determination of viable bacteria cell counts in 96-well plates. *BMC Microbiol* **12**, 259. doi: 10.1186/1471-2180-12-259

Hernandez, G. & Mora, J. 1986. Glutamine Synthesis Regulates Sucrose Catabolism in *Neurosporu crussu*. *Journal of General Microbiology* **132**, 3315–3323. doi: 10.1099/00221287-132-12-3315

Hertel, R., Gibhardt, J., Martienssen, M., Kuhn, R. & Commichau, F.M. 2021. Molecular mechanisms underlying glyphosate resistance in bacteria. *Environmental Microbiology* **23**, 2891–2905. doi: 10.1111/1462-2920.15534

Ho, K.S.Y. 1975. Induction of DNA double-strand breaks by X-rays in a radiosensitive strain of the yeast *Saccharomyces cerevisiae*. *Mutation Research/Fundamental and Molecular Mechanisms of Mutagenesis* **30**, 327–334. doi: 10.1016/0027-5107(75)90003-2

Ikehata, H. & Ono, T. 2011. The Mechanisms of UV Mutagenesis. *Journal of Radiation Research* **52**, 115–125. doi: 10.1269/jrr.10175

Jin, J.-K., Adams, D.O., Ko, Y., Yu, C.-W. & Lin, C.-H. 2004. Aviglycine and propargylglycine inhibit conidial germination and mycelial growth of *Fusarium oxysporumf.* sp. *luffae*. *Mycopathologia* **158**, 369–375. doi: 10.1007/s11046-004-2225-6

Joo, H.K., Park, Y.W., Jang, Y.Y. & Lee, J.Y. 2018. Structural Analysis of Glutamine Synthetase from *Helicobacter pylori*. *Scientific Reports* **8**, 11657. https://doi.org/10.1038/s41598-018-30191-5

Kandalam, U., Ledra, N., Laubach, H. & Venkatachalam, K.V. 2018. Inhibition of methionine gamma lyase deaminase and the growth of *Porphyromonas gingivalis*: A therapeutic target for halitosis/periodontitis. *Archives of Oral Biology* **90**, 27–32. doi: 10.1016/j.archoralbio.2018.02.022

Katre, G., Ajmera, N., Zinjarde, S. & RaviKumar, A. 2017. Mutants of Yarrowia lipolytica NCIM 3589 grown on waste cooking oil as a biofactory for biodiesel production. *Microbial Cell Factories* **16**, 176. doi: 10.1186/s12934-017-0790-x

Khan, R.I., Mukhtar, H., Gohar, U.F. & Tahir, S.F. 2020. Random Mutagenesis of Endophytic Fungi for Enhanced Taxol Production: Enhancement of taxol production by random mutagenesis. Proceedings of the Pakistan Academy of Sciences: B. *Life and Environmental Sciences* **57**, 67–74.

Kingsbury, J.M. & McCusker, J.H. 2010. Homoserine Toxicity in *Saccharomyces cerevisiae* and *Candida albicans* Homoserine Kinase (thr1Δ) Mutants. *American society for microbiology* **9**. doi: 10.1128/ec.00044-10

Kodym, A. & Afza, R. 2003. Physical and Chemical Mutagenesis. *Methods in Molecular Biology* **236**, 189–204. doi: 10.1385/1-59259-413-1:189

Kreisberg, J.F., Ong, N.T., Krishna, A., Joseph, T.L., Wang, J., Ong, C., Ooi, H.A., Sung, J.C., Siew, C.C., Chang, G.C., Biot, F., Cuccui, J., Wren, B.W., Chan, J., Sivalingam, S.P., Zhang, L.-H., Verma, C. & Tan, P. 2013. Growth Inhibition of Pathogenic Bacteria by Sulfonylurea Herbicides. *Antimicrobial Agents and Chemotherapy* **57**, 1513–1517. doi: 10.1128/AAC.02327-12

Kumada, Y., Benson, D.R., Hillemann, D., Hosted, T.J., Rochefort, D.A., Thompson, C.J., Wohlleben, W. & Tateno, Y. 1993. Evolution of the glutamine synthetase gene, one of the oldest existing and functioning genes. *Proceedings of the National Academy of Sciences* **90**, 3009–3013. doi: 10.1073/pnas.90.7.3009

Kumar, A.K., Parikh, B.S., Singh, S.P. & Shah, D. 2015. Use of combined UV and chemical mutagenesis treatment of *Aspergillus terreus* D34 for hyper-production of cellulose-degrading enzymes and enzymatic hydrolysis of mild-alkali pretreated rice straw. *Bioresources and Bioprocessing* **2**, 35. doi: 10.1186/s40643-015-0062-8

Leitão, J.M. 2012. Chemical mutagenesis. Plant mutation breeding and biotechnology, *CABI Books,* 135–158. https://doi.org/10.1079/9781780640853.0135

Lenski, R.E. 1991. Quantifying Fitness and Gene Stability in Microorganisms. *Ecological Risks of Biotechnology* **1991**, 173–192. doi: 10.1016/B978-0-409-90199-3.50015-2

Li, Y., Li, J., Ye, Z. & Lu, L. 2021. Enhancement of angucycline production by combined UV mutagenesis and ribosome engineering and fermentation optimization in *Streptomyces dengpaensis* XZHG99T. *Preparative Biochemistry and Biotechnology* **51**, 173–182. doi: 10.1080/10826068.2020.1805754

Li, Y., Liu, B., Song, J., Jiang, C. & Yang, Q. 2015. Utilization of Potato Starch Processing Wastes to Produce Animal Feed with High Lysine Content. *Journal of Microbiology and Biotechnology* **25**, 178–184. doi: 10.4014/jmb.1404.04035

Lin, G., Bultman, J., Johnson, E.A. & Fell, J.W. 2012. Genetic Manipulation of *Xanthophyllomyces dendrorhous* and *Phaffia rhodozyma*, in: Barredo, J.-L. (Ed.), Microbial Carotenoids From Fungi: Methods and Protocols. *Humana Press*, Totowa, NJ, pp. 235–249. doi: 10.1007/978-1-61779-918-1_16

Liu, S., Zhao, Y., Liu, L., Ao, X., Ma, L., Wu, M. & Ma, F. 2015. Improving Cell Growth and Lipid Accumulation in Green Microalgae *Chlorella* sp. via UV Irradiation. *Applied Biochemistry and Biotechnology* **175**, 3507–3518. doi: 10.1007/s12010-015-1521-6

Lonhienne, T., Low, Y.S., Garcia, M.D., Croll, T., Gao, Y., Wang, Q., Brillault, L., Williams, C.M., Fraser, J.A., McGeary, R.P., West, N.P., Landsberg, M.J., Rao, Z., Schenk, G. & Guddat, L.W. 2020. Structures of fungal and plant acetohydroxyacid synthases. *Nature* **586**, 317–321. doi: 10.1038/s41586-020-2514-3

Łozowicka, B., Wołejko, E., Kaczyński, P., Konecki, R., Iwaniuk, P., Drągowski, W., Łozowicki, J., Tujtebajeva, G., Wydro, U. & Jablońska-Trypuć, A. 2021. Effect of microorganism on behaviour of two commonly used herbicides in wheat/soil system. *Applied Soil Ecology* **162**, 103879. doi: 10.1016/j.apsoil.2020.103879

Luna-Flores, C.H., Wang, A., von Hellens, J. & Speight, R.E. 2022. Towards commercial levels of astaxanthin production in *Phaffia rhodozyma*. *Journal of Biotechnology* **350**, 42–54. doi: 10.1016/j.jbiotec.2022.04.001

Manti, L. & D'Arco, A. 2010. Cooperative biological effects between ionizing radiation and other physical and chemical agents. Mutation Research/Reviews in Mutation Research, ESF-*EMBO Conference: Spatio-Temporal Radiation Biology: Transdisciplinary Advances for Biomedical Applications* **704**, 115–122. doi: 10.1016/j.mrrev.2010.03.005

Master of Bioactive Molecules. Inhibitors, Screening Libraries & Proteins [WWW Document], 2024. *MedchemExpress.* https://www.medchemexpress.com. Accessed 25.01.24.

MedchemExpress, 2024. Chlorsulfuron Herbicide *MedChemExpress* [WWW Document]. https://www.medchemexpress.com/chlorsulfuron.html. Accessed 25.01.24).

Mowbray, S., Kathiravan, M., Pandey, A. & Odell, L. 2014. Inhibition of Glutamine Synthetase: A Potential Drug Target in *Mycobacterium tuberculosis*. *Molecules* **19**, 13161–13176. doi: 10.3390/molecules190913161

Muñoz, G.A. & Agosin, E. 1993 Glutamine Involvement in Nitrogen Control of Gibberellic Acid Production in *Gibberella fujikuroi*. *Applied and Environmental Microbiology* **59**, 4317–4322. doi: 10.1128/aem.59.12.4317-4322.1993

Najafpour, G. 2007. Single-Cell Protein. *Biochemical Engineering and Biotechnology* 332–341. doi: 10.1016/B978-044452845-2/50014-8

Narisetty, G.V., Adlakha, N., Singh, N.K., Dalei, S., Prabhu, A.A., Nagarajan, S., Kumar, A.N. & Nagoth, J.A. 2022. Integrated Biorefineries for Repurposing of Food Wastes into Value-added Products. *Bioresource Technology* **363**, 127856. doi: 10.1016/j.biortech.2022.127856

Nielsen, L.N., Roager, H.M., Casas, M.E., Frandsen, H.L., Gosewinkel, U., Bester, K., Licht, T.R., Hendriksen, N.B. & Bahl, M.I. 2018. Glyphosate has limited short-term effects on commensal bacterial community composition in the gut environment due to sufficient aromatic amino acid levels. *Environmental Pollution* **233**, 364–376. doi: 10.1016/j.envpol.2017.10.016

Odunfa, S.A., Adeniran, S.A., Teniola, O.D. & Nordstrom, J. 2001. Evaluation of lysine and methionine production in some lactobacilli and yeasts from *Ogi*. *International Journal of Food Microbiology* **63**, 159–163. doi: 10.1016/S0168-1605(00)00320-2

Ozola, S. 2022. *Developing single cell protein producing microorganism mutants via UV irradiation*. Bachelor's Thesis, Riga Technical University, Riga, Latvia, 67 pp. (in Latvian).

Pacher, M. & Puchta, H. 2017. From classical mutagenesis to nuclease-based breeding – directing natural DNA repair for a natural end-product. *The Plant Journal* **90**, 819–833. doi: 10.1111/tpj.13469

Peillex, C. & Pelletier, M. 2020. The impact and toxicity of glyphosate and glyphosate-based herbicides on health and immunity. *Journal of Immunotoxicology* **17**, 163–174. doi: 10.1080/1547691X.2020.1804492

Peng, M. & Liang, Z. 2020. Degeneration of industrial bacteria caused by genetic instability. *World Journal of Microbiology and Biotechnology* **36**, 119. doi: 10.1007/s11274-020-02901-7

Petrovickij-Angerer, I. 2009. Herbicide-sensitivity of some microorganisms on the basis of the chlorsulfuron. Available in https://archive2020.szie.hu/file/tti/archivum/Angerer_PhD_Thesis.pdf

P&S Intelligence, 2018. Protein Extracts from Single Cell Protein Sources Market | Forecast Report 2023 [WWW Document]. https://www.psmarketresearch.com/market-analysis/protein-extracts-from-single-cell-protein-sources-market, Accessed 19.12.23).

PubChem, 2024a. Metsulfuron-methyl [WWW Document]. National Center for Biotechnology Information. https://pubchem.ncbi.nlm.nih.gov/compound/52999. Accessed 24.01.24.

PubChem, 2024b. Chlorsulfuron [WWW Document]. National Center for Biotechnology Information. https://pubchem.ncbi.nlm.nih.gov/compound/47491. Accessed 24.01.24.

PubChem, 2024c. Imazapyr [WWW Document]. National Center for Biotechnology Information. https://pubchem.ncbi.nlm.nih.gov/compound/54738. Accessed 24.01.24.

PubChem, 2024d. Glyphosate [WWW Document]. https://pubchem.ncbi.nlm.nih.gov/compound/3496. Accessed 24.01.24.

PubChem, 2024e. Amitrole [WWW Document]. National Center for Biotechnology Information. https://pubchem.ncbi.nlm.nih.gov/compound/1639. Accessed 24.01.24.

PubChem, 2024f. Sulfometuron-methyl [WWW Document]. National Center for Biotechnology Information. https://pubchem.ncbi.nlm.nih.gov/compound/52997. Accessed 25.01.24.

PubChem, 2024g. Imazaquin [WWW Document]. National Center for Biotechnology Information. https://pubchem.ncbi.nlm.nih.gov/compound/54739. Accessed 25.01.24.

PubChem, 2024h. Imazethapyr [WWW Document]. National Center for Biotechnology Information. https://pubchem.ncbi.nlm.nih.gov/compound/54740. Accessed 25.01.24.

Ravanel, S., Gakière, B., Job, D. & Douce, R. 1998. Cystathionine γ-synthase from *Arabidopsis thaliana*: purification and biochemical characterization of the recombinant enzyme overexpressed in *Escherichia coli*. *Biochemical Journal* **331**, 639–648. doi: 10.1042/bj3310639

Ritala, A., Häkkinen, S.T., Toivari, M. & Wiebe, M.G. 2017. Single cell protein-state-of-the-art, industrial landscape and patents 2001–2016. *Frontiers in Microbiology* **8**. doi: 10.3389/fmicb.2017.02009

Ross, L.S., Landman, O. & Little, J.G., 1987. Base analogue mutagenesis in yeast and its modulation by pyrimidine deoxynucleotide pool imbalances: incorporation of bromodeoxyuridylate and iododeoxyuridylate. *Current Genetics* **11**, 421–427. doi: 10.1007/BF00384602

Rowlands, R.T. 1984. Industrial strain improvement: mutagenesis and random screening procedures. *Enzyme and Microbial Technology* **6**, 3–10. doi: 10.1016/0141-0229(84)90070-X.

Sameer, W. 2019. Effect of herbicides on tan spot and leaf blight diseases of wheat leave. *Egyptian Journal of Plant Protection Research* **7**(4), 25–34. Available in https://www.researchgate.net/publication/339800376_EFFECT_OF_HERBICIDES_ON_TAN_SPOT_AND_LEAF_BLIGHT_DISEASES_OF_WHEAT_LEAVES

Sardrood, B.P. & Goltapeh, E. 2018. Weeds, Herbicides and Plant Disease Management, in: Lichtfouse, E. (Ed.), *Sustainable Agriculture Reviews* **31**, pp. 41–178. doi: 10.1007/978-3-319-94232-2_3

Schloss, J.V. 1990. Acetolactate synthase, mechanism of action and its herbicide binding site. *Pestic. Sci.* **29**, 283–292. doi: 10.1002/ps.2780290305

Shehata, A., Schrödl, W., Schledorn, P. & Krüger, M. 2014. Distribution of Glyphosate in Chicken Organs and its Reduction by Humic Acid Supplementation. *The Journal of Poultry Science* **51**, 333–337. doi: 10.2141/jpsa.0130169

Shibai, A., Takahashi, Y., Ishizawa, Y., Motooka, D., Nakamura, S., Ying, B.-W. & Tsuru, S. 2017. Mutation accumulation under UV radiation in *Escherichia coli. Scientific Reports* **7**, 14531. doi: 10.1038/s41598-017-15008-1

Shiio, I. 1970. Microbial production of L-lysine III. Production by mutants resistant to S-(2-aminoethyl)-L-cysteine. *The Journal of General and Applied Microbiology* **16**(5), 37 *Escherichia coli. Scientific Reports* 3–391.

Singh, A. & Mishra, P. 1995. Microbial production of single cell protein (SCP) and single cell oil (SCO). *Progress in Industrial Microbiology* **33**, 301–316. doi: 10.1016/S0079-6352(06)80051-2

Spalvins, K., Raita, S., Valters, K. & Blumberga, D. 2021. Improving single cell protein yields and amino acid profile via mutagenesis: review of applicable amino acid inhibitors for mutant selection. *Agronomy Research* **19**, 1285–1307. doi: 10.15159/AR.21.083

Spencer, J.F.T. & Spencer, D.M. 1996. Mutagenesis in Yeast, in: Yeast Protocols. *Methods in Molecular Biology **53***, Humana Press, 17–38. doi: 10.1385/0-89603-319-8:17

Suryadi, H., Irianti, M.I. & Septiarini, T.H. 2022. Methods of Random Mutagenesis of *Aspergillus* Strain for Increasing Kojic Acid Production. *Current Pharmaceutical Biotechnology* **23**, 486–494. https://doi.org/10.2174/1389201022666210615125004

Tahiri, N.E.H., Saghrouchni, H., Hamamouch, N., Khomsi, M.E., Alzahrani, A., Salamatullah, A.M., Badiaa, L. & Lrhorfi, L.A. 2022. Treatment with Glyphosate Induces Tolerance of Citrus Pathogens to Glyphosate and Fungicides but Not to 1,8-Cineole. *Molecules* **27**, 8300. doi: 10.3390/molecules27238300

Tall, T. & Puigbò, P. 2020. The Glyphosate Target Enzyme 5-Enolpyruvyl Shikimate 3-Phosphate Synthase (EPSPS) Contains Several EPSPS-Associated Domains in Fungi, *Proceedings* **76**(1), 6. doi: 10.3390/IECGE-07146

Thiour-Mauprivez, C., Martin-Laurent, F., Calvayrac, C. & Barthelmebs, L. 2019. Effects of herbicide on non-target microorganisms: Towards a new class of biomarkers? *Science of The Total Environment* **684**, 314–325. https://doi.org/10.1016/j.scitotenv.2019.05.230

United Nations, 2023. The Sustainable Development Goals Report 2023: Special Edition, The Sustainable Development Goals Report. *United Nations*. doi: 10.18356/9789210024914

Vallejo, B., Picazo, C., Orozco, H., Matallana, E. & Aranda, A. 2017. Herbicide glufosinate inhibits yeast growth and extends longevity during wine fermentation. *Scientific Reports* **7**, 12414. doi: 10.1038/s41598-017-12794-6s

Van Dommelen, A., Keijers, V., Wollebrants, A. & Vanderleyden, J. 2003. Phenotypic Changes Resulting from Distinct Point Mutations in the *Azospirillum brasilense glnA* Gene, Encoding Glutamine Synthetase. *Applied and Environmental Microbiology* **69**, 5699–5701. doi: 10.1128/AEM.69.9.5699-5701.2003

Vasylkivska, M., Branska, B., Sedlar, K., Jureckova, K., Provaznik, I. & Patakova, P. 2020. Phenotypic and Genomic Analysis of *Clostridium beijerinckii* NRRL B-598 Mutants with Increased Butanol Tolerance. *Frontiers Bioengineering and Biotechnology* **8**. doi: 10.3389/fbioe.2020.598392

Wang, N.-X., Tang, Q., Ai, G.-M., Wang, Y.-N., Wang, B.-J., Zhao, Z.-P. & Liu, S.-J. 2012. Biodegradation of tribenuron methyl that is mediated by microbial acidohydrolysis at cell-soil interface. *Chemosphere* **86**, 1098–1105. doi: 10.1016/j.chemosphere.2011.12.013

Wang, X., Liu, X., Wang, H. & Dong, Q. 2007. Utilization and degradation of imazaquin by a naturally occurring isolate of *Arthrobacter crystallopoietes*. *Chemosphere* **67**, 2156–2162. doi: 10.1016/j.chemosphere.2006.12.042

Weiss, B. 2006. Evidence for Mutagenesis by Nitric Oxide during Nitrate Metabolism in *Escherichia coli*. *Journal of Bacteriology* **188**, 829–833. doi: 10.1128/JB.188.3.829-833.2006

Winston, F. 2008. EMS and UV mutagenesis in yeast. *Current Protocols in Molecular Biology* **2008**(13), 13.3B. doi: 10.1002/0471142727.mb1303bs82

Xie, H., Zhou, Y., Hu, J., Chen, Y. & Liang, J. 2014. Production of astaxanthin by a mutant strain of *Phaffia rhodozyma* and optimization of culture conditions using response surface methodology. *Annals of Microbiology* **64**, 1473–1481. doi: 10.1007/s13213-013-0790-y

Xuedong, W., Huili, W. & Defang, F. 2005. Biodegradation of Imazapyr by Free Cells of *Pseudomonas fluorescene* Biotype II and *Bacillus cereus* Isolated from Soil. *Bulletin of Environmental Contamination Toxicology* **74**, 350–355. doi: 10.1007/s00128-004-0591-x

Yamada, R., Kashihara, T. & Ogino, H. 2017. Improvement of lipid production by the oleaginous yeast *Rhodosporidium toruloides* through UV mutagenesis. *World Journal of Microbiology and Biotechnology* **33**, 99. doi: 10.1007/s11274-017-2269-7

Yu, Q., Li, Y., Wu, B., Hu, W., He, M. & Hu, G. 2020. Novel mutagenesis and screening technologies for food microorganisms: advances and prospects. *Applied Microbiolohy and Biotechnology* **104**, 1517–1531. doi: 10.1007/s00253-019-10341-z

Zabalza, A., Zulet, A., Gil-Monreal, M., Igal, M. & Royuela, M. 2013. Branched-chain amino acid biosynthesis inhibitors: Herbicide efficacy is associated with an induced carbon–nitrogen imbalance. *Journal of Plant Physiology* **170**, 814–821. doi: 10.1016/j.jplph.2013.01.003

Zhang, C., Shen, H., Zhang, X., Yu, X., Wang, H., Xiao, S., Wang, J. & Zhao, Z.K. 2016. Combined mutagenesis of *Rhodosporidium toruloides* for improved production of carotenoids and lipids. *Biotechnol Lett* **38**, 1733–1738. doi: 10.1007/s10529-016-2148-6

Zhou, X., Tang, S., Hu, K., Zhang, Z., Liu, P., Luo, Y., Kang, J. & Xu, L. 2018. dl-Propargylglycine protects against myocardial injury induced by chronic intermittent hypoxia through inhibition of endoplasmic reticulum stress. *Sleep Breath* **22**, 853–863. doi: 10.1007/s11325-018-1656-0

Zohar, Y., Einav, M., Chipman, D.M. & Barak, Z. 2003. Acetohydroxyacid synthase from *Mycobacterium avium* and its inhibition by sulfonylureas and imidazolinones. *Biochimica et Biophysica Acta (BBA) - Proteins and Proteomics* **1649**, 97–105. doi: 10.1016/S1570-9639(03)00160-2

Agronomy Research **22**(2), 939–955, 2024
https://doi.org/10.15159/AR.24.094

An optimization model for evaluating the economic effect of foliar treatment with biostimulants on spring rape

A. Sarov[1,*], K. Kostenarov[2] and E. Tzvetanova[3]

[1]Institute of Agricultural Economics, Agricultural Academy, Department 'Economics and Management of Agriculture, Food and Agrarian Policy', Str., 'Tsarigradsko shose' No 125, block 1, BG1113 Sofia, Bulgaria
[2]New Bulgarian University, Department 'Economics', Ovcha Kupel 2, 21 Montevideo Blvd, BG1618 Sofia, Bulgaria
[3]New Bulgarian University, Department 'Administration and Management', Ovcha Kupel 2, 21 Montevideo Blvd, BG1618 Sofia, Bulgaria
[*]Correspondence: angel.sarov@gmail.com

Received: June 27th, 2024; Accepted: September 23rd, 2024; Published: October 21st, 2024

Abstract. The aim of the study is to evaluate the economic effect of foliar treatment with biostimulants: chitosan, vermicompost and vermicompost + nature-identical growth regulator on organic production of spring rape on organic production of spring rape. Two-years field trials were conducted using a block method with foliar treatment in 2 phenological phases (in rosette and flowering phase). The biological response of the culture at different doses of the biostimulators was investigated. The obtained primary results were used as input data for the construction of an economic-mathematical model for economic evaluation The treatment of spring rape with biostimulators has a positive effect on the yield of the crop. After that, a specific agricultural holding in the region is selected, which will serve as a model on which to construct the optimization model for evaluating the economic efficiency. In this farm, along with the intended crops in the production structure, spring canola is added - controls and treated with BS. The results are optimal after using chitosan in a dose of 500 mL daa^{-1}. The results of this research show the economic benefits of using biostimulants, which are extremely important for farmers. They are an alternative to the requirements of the European Union's Green Deal At the heart of the Green Deal is the Farm to Fork (F2F) and the 'Biodiversity Strategy' (BS) strategy, which was launched by the European Commission in May 2020 to achieve a fair, healthy and sustainable food system by 2030. Under the F2F strategy, there is a need to reduce reliance on pesticides and antimicrobials, reducing excess fertilization, increasing areas for organic farming, improving animal welfare and reducing biodiversity loss. With the announcement of the goals and intentions of the Green Deal and its manifestations in agriculture, preparations also began for preliminary assessments of the consequences and impact that it will have on the entire food chain and for its transposition into the Common Agricultural Policy. At the same time, science research on alternatives to traditional conventional technologies is increasing. The results of the studies also took into account a set of assumptions for simulations of farm incomes, production and product prices.

Key words: optimization model, economic effect, biostimulants, spring rape.

INTRODUCTION

The use of biostimulants (BS) in agriculture is a significant challenge for achieving the EU's Green Deal. The implementation of the objectives set in the Green Deal are expected to significantly affect the conservation of natural resources and biodiversity. The components of the European Green Deal are the 'Farm to Fork Strategy' and the 'Biodiversity Strategy'. The objectives of the Strategies aim to reduce the environmental and climate impact on the EU food system and strengthen its sustainability. Achieving the goals of the Green Deal will require a reorientation and restructuring of Bulgarian and European agriculture to replacing technological intensity with precise and intelligent new solutions The Roadmap and the Farm to Fork and Biodiversity strategies will have a tangible impact on the European economy, the food value chain and food security. Many policy papers and research studies discuss the expected effects and trade-offs of implementing the Green Deal principles on the EU crop and livestock sector (Bremmer et al., 2021; Jongeneel et al., 2021; Wesseler, 2022; Rosegrant et al., 2022; Hurduzeu et al., 2022; Rudnicki et al., 2023.

The announcement of the goals and intentions of the Green Deal and its manifestations in agriculture and preparations began for preliminary assessments of the consequences and its impacts on the entire food chain and its transposition to the Common Agricultural Policy (CAP). The main debates before economists are whether, after biostimulants increase the yield of a certain crop, will this lead to an increase in the profit of the particular farm?

The application of biostimulants has a positive effect on bulk density, porosity soil structure, and crop yields (Belcheva, 1989; Findura et al., 2022). Studies have shown that biostimulators have a beneficial effect on the weight of the root, the number of grains of grade, weight, and seed yield (Brown et al., 2015; Szczepanek et al., 2018). Scientific publications focusing on the effect on yield, biometry and efficiency of biostimulant application in agricultural crops are available (Grabowska et al., 2012; Nemes, 2020; Woziak et al., 2020; Li et al., 2022). Additionally, the effect on plant growth and tolerance to salt stress (Gedeon et al., 2022), improves tolerance to salinity (Campobenedetto et al., 2021), under abiotic stress conditions (Bulgari et al., 2019) and biochemical and economical effect of application biostimulants (Kocira et al., 2020), vegetative, physiological and reproductive attributes of tomato crops (Sassine et al., 2022), to stress resilience in nursery production, (Di Vaio et al., 2021), the effect on the productivity and quality indicators of green mass (Chernikova et al., 2021).

The aim of the study is to evaluate the economic effect of foliar treatment with biostimulants on organic production of spring rape. An optimization model based on linear programming is applied. The analyses of the scientific team are based on the hypothesis that it is possible to apply a given biostimulator to significantly increase the yield of spring rape per unit area, but not to increase the profit of the agricultural holding as a whole. Therefore, the usefulness of biostimulants is established in the development of optimization of the production structure of a selected agricultural holding. The research team accepts that those biostimulants that increase the economic efficiency of the farm are considered useful.

Currently known that the use of biostimulants may provide benefits in the cultivation of agricultural crops, but the economic results are not fully understood. The researchers limit themselves to presenting the increase in yield. Nowadays, it is even

more important to consider whether the use of biostimulants is economically effective for farmers and whether they will contribute to an increase in profit in general. Also, for the society, in addition to the economic aspects, the environmental benefits are also important.

Rapeseed (*Brassica napus*) is a widespread agricultural crop worldwide, due to its diverse application. The development of spring rape takes place in a shorter period of time, compared to winter oilseed rape, which is limiting for the yield potential, and the generative plants are formed at rather high temperatures.

MATERIALS AND METHODS

For primary data, the results obtained from the Agricultural Experiment Station (AES) are used, in an experimental field at the Institute of Agriculture and Seed Science (ASS) 'Obraztsov Chiflik' - Ruse at the Agricultural Academy, Sofia. In the two-year period 2021–2022, 7 plots of 10 square meters each were prepared, in which seeds of spring rapeseed (*Lakritz, Brassica Napus* L.) were planted. The choice of 7 plots is consistent with the condition that there is also 1 control plot for which three repetitions of three biostimulants (BS) with different concentration of active substance (Table 1) will be made for representativeness of the results. Spring rape was treated with products developed at the Institute of Cryobiology and Food Technologies (ICFT) at the Agricultural Academy, Sofia.

Table 1. Applied biostimulants and their concentration

Biostimulants	Description
BS1_CH	(GA) chitosan 500 mL daa^{-1}
BS2_2CH	(GA+GA) chitosan 2*500 mL daa^{-1}
BS3_V	(HA) vermicompost extract 500 mL ha^{-1}
BS4_2V	(HA + HA) vermicompost extract 2*500 mL daa^{-1}
BS5_VR	(HA_IA) vermicompost + nature-identical growth regulator 500 mL daa^{-1}
BS6_2VR	(HA_IA+ HA_IA) vermicompost + nature-identical growth regulator 2*500 mL daa^{-1}

Source: Institute of Cryobiology and Food Technology, Agricultural Academy, Sofia.

Spring rape was treated twice (in rosette and flowering phase). Harvesting of agricultural crops was done mechanized. Before sowing, all necessary agrotechnical measures have been observed. After obtaining the experimental results of the application of the different BS on spring rape in the experimental fields, they were automatically equated to 1 decare. After that, a specific agricultural holding in the region is selected, which will serve as a model on which to construct the optimization model for evaluating the economic efficiency. In this farm, along with the intended crops in the production structure, spring canola is added - controls and treated with BS. Based on experimental results obtained from 2021–2022 and the complex of additional factors, such as existing (available) resources: land, labor resources, mechanization, etc.; as well as the development of technical and economic standards (TES), the optimization model was developed.

Modeling is a categorical approach to studying complex problems that involves replacing the object with another similar to the original. We can construct this problem

in a system of linear dependencies. Solving agricultural economic problems involves constructing a system of linear equations.

They must correspond to agronomic dependencies, restrictions on crop rotation, cultivated land, etc. (Nikolov et al., 1994). The objective function gives an answer for the previously selected optimality criteria (min, max):

$$\begin{gathered} A_{11}X_1 + A_{12}X_2 + \cdots + A_{1n}X_n \leq B_1 \\ A_{21}X_1 + A_{22}X_2 + \cdots + A_{2n}X_n \geq B_2 \\ A_{m1}X_1 + A_{m2}X_2 + \cdots + A_{mn}X_n = B_1 \\ \hline F = C_1X_1 + C_2X_2 + \cdots + C_nX_n \rightarrow \max(\min)' \end{gathered} \quad (1)$$

where Xj – shows the size (magnitude) of activities or metrics; Aij and Cj – indicates the activities to be performed; Bi – means the number of resources available or the number of activities (constraints); the objective function F indicates the optimality criteria.

The economic-mathematical model (EMM) makes it possible to compare many possible solutions, from which to choose the most optimal one. In reality, however, it is quite difficult, and often even impossible, to account for the influence of the complex of all factors. Solving the present economic problem with the help of mathematical methods means to compose an economic-mathematical task. This task should be constructed according to a coordinate system that includes the most important dependencies with satisfactory accuracy.

Constructing the model

A. The unknowns are two groups:

The first group means the area of crops that are grown on the farm. These are wheat, corn, sunflower and canola. In canola, unknowns are added for the different BS and the control.

The second group includes unknowns, with the help of which the value indicators are determined. These are the so-called auxiliary unknowns and mean: gross output, variable costs, gross margin and the subsidies the farm receives.

B. Constrains

The constrains the field breeding activity block are generally divided into three groups.

I. Land use constrains

They provide the condition that the area of the crops included in the optimal production structure, which are grown on the respective land, is not more than the available area.

Mathematically, this group of restrictive conditions is formulated as follows:

$$\sum_{j \in Mi} x_{ji} \leq B_i \quad (2)$$

where Mi – set of the indices of the unknowns indicating the area of the j–th culture, on the i–th category of land, B_i – the available land category – i.

II. Constrains related to agrotechnical requirements for crop rotation

Correct crop rotation requires the establishment of a scientifically based ratio between the areas of autumn-winter crops with a fused surface and spring trench crops. For this purpose, two limiting conditions for the given field crop rotation are included in the task. They provide, respectively, a minimum and a maximum size of the areas with

autumn cereal crops, thus limiting the areas with spring trench crops. The constrains are formulated as follows:

a/ for a minimum amount of arable land with autumn cereal crops

$$\sum_{j \in M} x_j - \mathrm{k}' \sum_{j \in N} x_j \geq 0 \qquad (3)$$

b/ for maximum amount of arable land with autumn cereal crops with a combined surface

$$\sum_{j \in M} x_j - \mathrm{k}'' \sum_{j \in N} x_j \leq 0 \qquad (4)$$

where k′ – minimum relative share of the areas of autumn crops with a fused surface; k″ – maximum relative share of the areas of autumn crops with a fused surface; M – set of the indices of the unknowns x_j expressing the areas of autumn crops with a fused surface; N – set of the indices of the unknowns x_j expressing the area of all crops in the crop rotation.

c/ About the specific requirements of the sunflower for its inclusion in the crop rotation

$$x_j - \mathrm{k} \sum_{j \in N} x_j \leq 0 \qquad (5)$$

where k – coefficient denoting the maximum share of the sowing rotation area that can be occupied by the j-th crop; N – set of the indices of the unknowns x_j expressing the area of all crops in the crop rotation.

The requirement is formulated as follows: the sunflower area is less than or equal to one maximum percentage of the sowing turnover area.

III. Computational /auxiliary/ constraints

These constraints are formulated as follows:

$$\sum_{j \in M_1} f_{ij} x_j = x_i \qquad (6)$$

where M_1 – a set of indices of the unknowns, denoting the activities that influence the formation of the i-th value indicator x_i; f_{ij} – coefficient denoting the contribution of the j-th activity to the formation of the i-th value indicator.

The coefficients f_{ij} in the gross production limit are calculated on the basis of average yields and current prices, or on the basis of the standard gross production determined according to the EU methodology.

Connecting block

The calculation unknowns serve to establish the value indicators for the farm as a whole. They are: gross output, variable costs, gross margin, subsidies by type.

Constraints

I. On the balance of labor resources

The farm mainly grows mechanized commodity crops; therefore, the balance of labor resources will be carried out in general for the farm all year round. In addition to the man-hours of the permanent workers, the resources also include the temporary help that the farm can provide.

The mathematical formulation is as follows:

$$\sum_{j \in J} a_{dj} X_{dj} - \sum_{d \in D} Z_d X_d \leq 0 \quad (7)$$

where J – set of indices of the unknowns denoting cultures (activities), which require the input of the d-th category of labor; D – multiple of the category indexes permanently occupied; a_{dj} – labor cost in working days of the d-th labor category to perform the j-th activity; Z_d – number of working days that a permanently employed worker from the d-th labor category can work annually; X_d – number of people permanently employed in the d-th labor category

II. Auxiliary constraints

The constraints for the value indicators in general for the farm are:

$$\sum_{j \in M_2} x_j = x_i \quad (8)$$

where M_2 – a set of subscripts of the auxiliary unknowns in the connecting block denoting the magnitude of the i-th metric in the j-th division; x_i – the value of the i-th value indicator in general for the farm.

Objective function

The solution of the considered problem is carried out under the optimality criterion 'max gross margin and max profit'. It is expressed as follows:

$$\sum_{j \in M_3} x_j \rightarrow max \quad (9)$$

where M_3 – a set of the indices of the unknowns, signifying cultures and activities which contribute to the formation of the gross margin and profit; x_j – the size of the j-th activity.

The coefficients in front of the unknowns are as follows:

– commodity crops;

– the gross margin and profit per 1 area.

The assessment of the effect of biostimulants on the economic efficiency of the agricultural holding is a complex agrarian economic task. When compiling it, it is required to take into account the complex impact of many interrelated factors and conditions and the huge number of possible solutions in order to choose the best one.

Collection and processing of the necessary information for the development of an economic-mathematical task (EMT)

Conditions under which the agricultural holding functions

Those working in the relevant agricultural holding assisted in the collection of input data for the construction of the model.

The agricultural holding operates on the territory of the Ruse region. The topography of the area is predominantly low-lying and flat-hilly, which is suitable for agricultural development. The territories around the Danube River are characterized by high groundwater and alluvial-meadow soils, on which mainly vegetables, technical and fruit crops are grown, as well as deep subsoil and chernozem soils, suitable for the cultivation of cereals and technical crops, such as wheat, barley, rye, oats, corn, sunflower, canola, vines, perennials, late greens, beans, lentils, peas, etc.

The production activity of the farm mainly involves the cultivation of crop production - wheat, corn, sunflower. We are also adding the potential to grow spring canola. The farm owns 1,000 decares (daa) of its own land and can rent another 11,000 decares. Cultivable land falls into two soil types. Alluvial-meadow soil, which occupies 50%, and chernozem - 50%, respectively. This is a facilitating condition when reporting yields, because averaged data will be used. According to National Statistical Institute, Sofia, the average rent in the Ruse region for 2021 is BGN 58 daa^{-1}, but the owner has agreed with the landlord on BGN 55 daa^{-1}. There is no additional possibility of leasing land in the area because it is too limited as a productive resource. There are no hydromelioration facilities built on the land, which means that the crops are grown under non-irrigated conditions.

Wheat, sunflower, corn are grown on the arable land. According to data from the National Statistical Institute in Bulgaria for 2021–2022, the average prices of soft wheat are BGN 0.40 kg^{-1}, corn - BGN 0.40 kg^{-1}, sunflower - BGN 1.00 kg^{-1}. Rapeseed - BGN 0.93 kg^{-1}. Data from the Ministry of Agriculture and Food are used for the average costs in 2021–2022 for material costs, labor costs, mechanized services. The crops are grown organically, which means there is no cost of spraying with insecticides, fungicides and pesticides. For spring rape treated with biostimulants, we add costs for two sprays. According to our expert calculations, the price for the applied biostimulators is calculated at about BGN 5.00 daa^{-1}.

The farm employs six people, including: 4 tractor drivers with a gross salary of BGN 1,500 per month (BGN 1,8000 year per person). The manager and his wife perform administrative and management functions, additionally participating in the production process. In practice, 2 more workers should be accepted with a salary of BGN 1,500 (BGN 18,000 year per person); Salary costs are included as variable costs. They depend on the volume of work performed and change depending on the size of the cultivated land. The maximum number of permanent employees on the farm is 6 people.

According to the agronomic, technological and economic requirements, the following constrains are accepted:

• Autumn cereal crops under non-irrigated conditions should occupy no less than 45% and no more than 55% of the sowing rotation area.

• Sunflower should not occupy more than 17% of the crop rotation (1/6)

Agriculture received subsidies under Pillar 1 of the CAP as follows:

• BGN 21 daa^{-1} under SEPP. And support under the so-called 'green payments' BGN 10 daa^{-1}, or a total of BGN 31 daa^{-1}.

According to the preliminary data on the yields of agricultural crops in 2021–2022, Department of Agrostatistics, Ministry of Agriculture and Foods, the average yields in Bulgaria for the North-East region in 2021 are: wheat - 5,902 kg ha^{-1}, corn 5,892 kg ha^{-1}, rapeseed 2,845 kg ha^{-1}, sunflower 2,378 kg ha^{-1}.

In 2021–2022, in Bulgaria, the tendency for the areas to be predominantly fertilized with nitrogen fertilizers is maintained. Phosphorous and potassium fertilizers are used to a lesser extent. The use of combined mineral fertilizers is increasing. Chemical fertilizers are not used in agriculture. Therefore, we assume that the average crop yield is as follows: wheat - 2,900 kg ha^{-1}, corn 3,400 kg ha^{-1}, sunflower 1,900 kg ha^{-1}, experimental yield of spring rapeseed 1,220 kg ha^{-1}. In the development of IMT, the yield of rape and oats from the experimental experience (control and different BS) are applied. The

construction of the model uses two criteria - max gross margin and max profit. There were build two economic-mathematical models based on these criteria:

First task. A task with optimized production structure of a farm, considering the agrotechnical requirements for crop rotation. The solution gives the most optimal production structure under both criteria of **max gross margin and max profit**. It will allow obtaining a decision on how to optimally combine available resources (land, labor force, size of arable land) and farm constraints; what crops to produce; agrotechnical requirements; which biostimulants to apply; on which cultures and in what concentration to be applied BS; in which phase to treat them to achieve the highest economic effect.

Second task. There were set bounds for the minimal and maximum size of the arable land, including crops treated with biostimulants. The aim is to find an optimal solution, achieving **max gross margin** and **max profit.** The solution gives the optimal combination of the most economically effective productions. The result is the best combination of the available resources (land, labor resources, and various biostimulants), giving specific constraints. Also, what crop to produce and what agrotechnical requirements? All this achieves the highest economic effect.

Defined variables and constrains

The subjective restrictions shrink the possible solutions. This is because including more and more different group criteria in the model (e.g., land, crops, BS, land constraints, labor force, etc.) searches for a balance between the defined constraints and often leads to compromise solutions to the task.

Table 2. Variables with biostimulants treatment

Crop	Biostimulants (daa)						
	Control	BS1_CH	BS2_2CH	BS3_V	BS4_2V	BS5_VR	BS6_2VR
spring rape	x_4	x_5	x_6	x_7	x_8	x_9	x_{10}

Source: Authors' calculations.

The variables used to evaluate the BS effect on economic efficiency are presented in Tables 2 and 3. It is worth mentioning that the spring rape were treated with different BS in different concentrations (Table 2). In addition, it was used other factors such as other crops, resources (land, labor force), and financial indicators (gross margin, costs, profit) (Table 3).

Table 3. Other variables

Other crops (daa)		Resources		Finance (BGN)	
x_1	Wheat	x_{18}	Own arable land (daa)	x_{22}	Income
x_2	Corn	x_{19}	Rented arable land (daa)	x_{23}	Material costs
x_3	Sunflower	x_{20}	Permanently employed mechanics (number)	x_{24}	Labor costs
		x_{21}	Permanent employees (number)	x_{25}	Margin
				x_{26}	Gross margin
				x_{27}	Fixed costs
				x_{28}	Profit
				x_{29}	Profit with subsidies

Source: Authors' calculations.

Constrains

The constraints of the optimal plan are divided into three groups: land usage (Table 4); labor (Table 5); and supporting constrains (Table 6).

Table 4. First group of constrains related to the land usage (daa)

Constrains	Formula	
	Optimal production structure task (first)	Max and min area bounds task (second)
Area constrains (acres)	$x_1 + x_2 + x_3 + x_4 + x_5 + x_6 + x_7 + x_8 + x_9 + x_{10} = x_{18} + x_{19}$	$x_1 + x_2 + x_3 + x_4 + x_5 + x_6 + x_7 + x_8 + x_9 + x_{10} \leq x_{18} + x_{19}$
Constrain on rented area (daa)	$x_{19} = 11{,}000$	$x_{19} \leq 11{,}000$
Constrain on owned area (daa)	$x_{18} = 1{,}000$	
Autumn cereal crops, minimum 45% of the sowing area (daa)	$x_1 \geq 5{,}400$	
Autumn cereal crops, minimum 55% of the sowing area (daa)	$x_1 \leq 6{,}600$	
Sunflower, maximum 17% (1/6) of the sowing area (ha)	$x_3 \leq 2{,}040$	
Constrains on the land, using BS, minimum (daa)		$x_4 + x_5 + x_6 + x_7 + x_8 + x_9 + x_{10} \geq 3{,}360$
Constrains on the land, using BS, maximum (daa)		$x_4 + x_5 + x_6 + x_7 + x_8 + x_9 + x_{10} \leq 4{,}560$

Source: Authors' calculations.

Table 5. Second group of constrains related to the labor (number)

Constrains	Formula
Permanently employed mechanics (number)	$x_{20} = 4$
Permanent employees (number)	$x_{21} = 2$

Source: Authors' calculations.

Table 6. Third group of constrains, supporting (BGN)

Constrains	Formula
Income	$116x_1 + 136x_2 + 190x_3 + 133.52x_4 + 135.48x_5 + 120.08x_6 + 118.63x_7 + 115.79x_8 + 127.12x_9 + 115.95x_{10} = x_{22}$
Variable material costs	$27x_1 + 27x_2 + 26x_3 + 24.5x_4 + 39.5x_5 + 39.5x_6 + 39.5x_7 + 39.5x_8 + 39.5x_9 + 39.5x_{10} = x_{23}$
Labor costs	$x_{24} = 18{,}000x_{20} + 18{,}000x_{21}$
Fixed costs	$x_{27} = 55x_{19}$
Margin	$x_{25} = x_{22} - x_{23}$
Gross margin	$x_{26} = x_{22} - x_{23} - x_{24}$
Profit	$x_{28} = x_{22} - x_{23} - x_{24} - x_{27}$

Source: Authors' calculations.

RESULTS AND DISCUSSION

Results from an experimental field of the Institute of Agriculture and Seed Science 'Obraztsov Chiflik' - Ruse.

Table 7. Spring rape yield, harvest 2021–2022 (Average)

	Spring rape yield, harvest 2021					Spring rape yield, harvest 2022					Average 2021–2022
Biostimulant	1 rep (kg)	2 reps (kg)	3 reps (kg)	Av. (kg)	kg daa^{-1}	1 rep (kg)	2 reps (kg)	3 reps (kg)	Av. (kg)	kg daa^{-1}	kg daa^{-1}
Chitosan 500 mL daa^{-1}	1.30	1.28	1.26	1.28	128.0	1.45	1.40	1.38	1.45	141.0	134.50
Chitosan-2*500 mL daa^{-1}	1.25	1.30	1.24	1.26	126.3	1.35	1.25	1.29	1.35	129.7	127.98
Vermi compost extract 500 mL daa^{-1}	1.15	1.20	1.31	1.22	123.5	1.27	1.32	1.28	1.27	129.0	126.25
Vermicompost + nature-identical growth regulator 2*500 mL daa^{-1}	1.25	1.22	1.27	1.25	124.5	1.24	1.34	1.30	1.24	129.3	126.92
vermicompost extract 2*500 mL daa^{-1}	1.30	1.24	1.28	1.27	127.3	1.37	1.35	1.34	1.37	135.3	131.32
Vermicompost + nature-identical stretch regulator 500 mL daa^{-1}	1.23	1.22	1.24	1.23	122.7	1.30	1.27	1.28	1.30	128.3	125.52
Control	1.15	1.20	1.31	1.22	122.0	1.24	1.28	1.27	1.24	126.3	124.17

Source: The primary data from The Agricultural Experimental Station (AES) in a test (experimental) field at the Institute of Agriculture and Seed Science 'Obraztsov Chiflik' – Ruse, Agricultural Academy, 2021–2022.

Table 8. Biometrics - spring rape, 2021–2022

BS	Biometrics - spring rape, 2021					Biometrics - spring rape, 2022						
	plant height, cm	branches per 1 plant, no.	Beans in 1 plan, no.	weight of beans in 1 plant, gr.	seeds in 1 plan, no.	weight of seeds in 1 plant, gr.	plant height, cm	branches per 1 plant, no.	beans in 1 plan, no.	weight of beans in 1 plant, gr.	seeds in 1 plan, no.	weight of seeds in 1 plant, gr.
Chitosan 500 mL daa^{-1}	109.0	7.2	259.1	22.9	1,213.2	7.7	106.9	7.6	246.2	23.3	1,267.2	7.9
Chitosan - 2*500 mL daa^{-1}	110.0	6.9	246.8	22.4	1,118.1	6.9	110.4	7.2	260.8	23.4	1,220.7	7.5
Control	109.4	7.0	238.0	22.7	1,266.2	7.4	110.4	7.1	264.1	23.6	1,272.8	7.5
Vermi compost extract 500 mL daa^{-1}	109.4	7.1	248.2	22.6	1,265.0	7.6	110.5	7.2	252.3	23.5	1,256.3	7.5
Vermicompost + nature-identical growth regulator 2*500 mL daa^{-1}	111.6	7.1	248.1	22.6	1,236.9	7.5	110.2	6.8	243.8	22.1	1,244.7	7.5
Vermicompost + nature-identical stretch regulator 500 mL daa^{-1}	108.8	7.3	248.1	22.4	1,284.3	7.6	109.6	6.9	236.7	22.4	1,128.6	6.8
Vermicompost extract 2*500 mL daa^{-1}	110.8	6.9	247.9	22.2	1,232.0	7.6	107.6	6.8	264.7	24.3	1,316.9	8.2

Source: The primary data from The Agricultural Experimental Station (AES) in a test (experimental) field at the Institute of Agriculture and Seed Science 'Obraztsov Chiflik' – Ruse, Agricultural Academy, 2021–2022.

The primary data were collected from an experimental field of the Institute of Agriculture and Seed Science 'Obraztsov Chiflik' - Ruse, Agricultural Academy. Table 7 presents the yields of spring canola in three replications of the biostimulants at different concentrations of dry matter and the control for 2021–2022. Table 8 presents the biometric indicators after treatment with biostimulants, for 2021 and 2022, respectively.

Objective function

The objective function and the constrained values were added in the following linear programming model, using two optimal criteria - max gross margin and max profit.

$$F = 80x_1 + 102x_2 + 155x_3 + 100.02x_4 + 86.98x_5 + 71.58x_6 + 70.13x_7 + 67.29x_8 + 78.62x_9 + 71.05x_{10} - 18{,}000x_{20} - 18{,}000x_{21} \rightarrow \textbf{Max gross margin}, \quad (10)$$

$$F = 80x_1 + 102x_2 + 155x_3 + 100.02x_4 + 86.98x_5 + 71.58x_6 + 70.13x_7 + 67.29x_8 + 78.62x_9 + 71.05x_{10} - 18{,}000x_{20} - 18{,}000x_{21} - 55x_{19} + 31x_{18} + 31x_{19} \rightarrow \textbf{Max profit} \quad (11)$$

Task solution

Making a management decision is an extremely important and responsible task for agrarian entrepreneurs. The results obtained from the optimization are shown in tabular form as follows:

First option. In Table 9, the parameters of the solution of the objective function with optimization and maximum gross margin and maximum profit can be traced. The decision presents an option for crop rotation of the included agricultural crops with the use of different biostimulants, and with different concentration of active substance, with/without included CAP subsidy for the farm. The optimal solution of the task also includes the set precondition for dropping the requirement for the maximum size of cultivated land.

When constructing the production structure in the farm's crop rotation, the assumption is made that the own land of 1,000 decares (daa), and the leased land -11,000 decares, are used to their full capacity.

Solving the task gives an answer to the set parameters including the area of cultivated land, which agricultural crops will be included in the optimal solution (wheat, maize and sunflower, spring oats - control and spring canola - control, spring oats and spring rape - treated with biostimulants, with admissibility for distribution of different concentration of active substance).

The optimality criterion of the objective function, the constructed constraints and the set price values influence the results. Linear equations maximize profitable crops and minimize production costs.

Due to the listed reasons and imposed restrictive conditions in the optimization, wheat is planned to cover a minimum of 5,400 decares. This is the minimum restrictive condition for autumn cereal crops for crop rotation according to agronomic requirements (min. 45% of the crop rotation area). The entire amount of wheat is distributed over the minimum area set for autumn cereal crops. The stipulated maximum of 55% of the crop rotation area, or up to 6,600 decares, is not included in the solution of the task, because the mandatory inclusion of sunflower in the crop rotation is taken into account in the restrictive condition for the minimum size of the areas. In the optimal solution, he enters with 3,240 decares. In the remaining area of 3,360 decares, spring rape is included -

treated with chitosan - 500 mL daa^{-1}. A leading role in the distribution of these crops is played by those with a higher economic benefit for the farm. The optimization matrix does not include the distribution of the other spring rape treated with the other biostimulants.

Table 9. Production structure and economic results of application of biostimulants

Unknown	Name	daa	Number	BGN
x_1	Wheat (daa)	5,400		
x_2	Maize, (daa)	0		
x_3	Sunflower, (daa)	3,240		
x_4	Spring rape - control (daa)	0		
x_5	Spring rape - BS 1 Chitosan 500 mL daa^{-1}	3,360		
x_6	Spring rape - BS 2 Chitosan-2*500 mL daa^{-1}	0		
x_7	Spring rape - BS 3 Vermi compost extract 500 mL daa^{-1}	0		
x_8	Spring rape - BS 4 Vermi compost extract 2*500 mL daa^{-1}	0		
x_9	Spring rape - BS 5 Vermicomposting + nature-identical stretch regulator 500 mL daa^{-1}	0		
x_{10}	Spring rape BS 6 Vermicomposting + nature-identical stretch regulator 2*500 mL daa^{-1}	0		
x_{18}	Own arable land (daa)	1,000		
x_{19}	Leased arable land (daa)	11,000		
x_{20}	Permanently employed mechanics (no.)		4	
x_{21}	Permanently employed workers (no.)		2	
x_{22}	Income (BGN)			1,675,204.8
x_{23}	Material costs (BGN)			362,760
x_{24}	Labor costs (BGN)			108,000
x_{25}	Income (BGN)			1,312,444.8
x_{26}	Gross margin (BGN)			1,204,444.8
x_{27}	Fixed costs (BGN)			605,000
x_{28}	Profit (BGN)			599,444.8
x_{29}	Profit with subsidy (BGN)			971,444.8

Source: Authors' calculations, 2023.

The optimization model includes the maximum amount of land with sunflower, because it is economically profitable, and corn is dropped from the crop rotation.

During the development of the technical and economic regulations (TER), yields of agricultural crops were set, in accordance with biological production, depending on the region, the type of soil, with/without the presence of biostimulants, and different market prices of commodity crops. All this reflects on the income, income, gross margin and, accordingly, the profit of the various crops on the one hand, as well as on the agricultural economy as a whole, on the other.

In the solution of the task, it is possible to trace how the minimum and maximum limits are distributed, such as the restrictive condition for the area on which the use of biostimulants is allowed - min 3,360 decares and maximum 4,560 decares. The solution to the task only includes the spring rapeseed treated with chitosan 500 mL daa^{-1} in the minimum size of 3,360 daa of land, as economically the most profitable for the farm.

As a result, in the optimization model, all set restrictive conditions for achieving maximum economic effect - maximum gross margin and maximum profit - are fulfilled. In the solution of the problem, the optimal economic efficiency is achieved with a

Gross margin of BGN 1,204,444.8 or BGN 100.37 daa^{-1}, the realized profit without subsidy of BGN 599,444.8 (BGN 49.95 daa^{-1}) and with subsidy BGN 971,444.8, which is BGN 80.95 daa^{-1}.

Solution of the task, when the optimality criterion is set in the objective function as maximum profit (Table 10). When including fixed costs and the amount of subsidies per unit of planted area in the amount of BGN 31 ha^{-1}, the optimal solution does not change.

As a result of the subsidies, an increase in profit was generated from BGN 599,444.8 to BGN 971,444.8. The other attributes of the model remain unchanged.

Second option. Table 10 presents the results of the optimization, according to which a limit is set for minimum limits in which the cultivated land varies, but with maximum inclusion of the permissible area with the presence of crops treated with biostimulants.

Table 10. Variant when including only cultures treated in different concentrations of biostimulants. Production structure and economic results of application of biostimulants

Unknown	Name	daa	Number	BGN
x_1	Wheat (daa)	0		
x_2	Maize (daa)	0		
x_3	Sunflower (daa)	0		
x_4	Spring rape - control (daa)	0		
x_5	Spring rape - BS 1 Chitosan 500 mL daa^{-1}	12,000		
x_6	Spring rape - BS 2 Chitosan-2*500 mL daa^{-1}	0		
x_7	Spring rape - BS 3 Vermi compost extract 500 mL daa^{-1}	0		
x_8	Spring rape - BS 4 Vermi compost extract 2*500 mL daa^{-1}	0		
x_9	Spring rape - BS 5 Vermicomposting + nature-identical stretch regulator 500 mL daa^{-1}	0		
x_{10}	Spring rape BS 6 Vermicomposting + nature-identical stretch regulator 2*500 mL daa^{-1}	0		
x_{18}	Own arable land (daa)	1,000		
x_{19}	Leased arable land (daa)	11,000		
x_{20}	Permanently employed mechanics (no.)		4	
x_{21}	Permanently employed workers (no.)		2	
x_{22}	Income (BGN)			1,547,160
x_{23}	Material costs (BGN)			474,000
x_{24}	Labor costs (BGN)			108,000
x_{25}	Income (BGN)			1,073,160
x_{26}	Gross margin (BGN)			965,160
x_{27}	Fixed costs (BGN)			605,000
x_{28}	Profit (BGN)			360,160
x_{29}	Profit with subsidy (BGN)			732,160

Source: Authors' calculations, 2023.

Based on the set limiting conditions in the optimization, it is planned that the entire distribution of the sowing turnover area of 12,000 decares will be occupied by spring rape treated with chitosan 500 mL daa^{-1}. It is this solution that shows the variety of possible solutions of the proposed economic-mathematical model. The optimization model selects the most optimal solution according to the set parameters in the objective function

and offers such a distribution of the production structure, consistent with the restrictive conditions, different yield, market price, and the different economic efficiency of it.

In the optimization model, all set restrictive conditions are met to achieve maximum economic effect - maximum gross margin and maximum profit.

In the solution of the task, the optimal economic efficiency is achieved with a Gross margin of BGN 965,160, realized profit without subsidy of BGN 360,160 and with subsidy - in the amount of BGN 732,160.

In this option, the material costs increase from BGN 362,760 to BGN 474,000, due to the need to spray the rapeseed on the entire 12,000 decares area. Betting on this production in the agricultural economy, a decrease in income by BGN 128,044.80 is reported, or from BGN 1,675,204.8 it shrinks to BGN 1,547,160. This is a clear sign that treating crops with biostimulants in order to a good economic result is obtained, an increase in yield should be achieved in larger quantities. Apparently, the positive effect on yield, which is in the range (1–5% for 2021–2022) Theoretically, if their values are changed in the condition of the task, and this is completely possible and feasible, then the model after several iterations will give another optimization.

The working hypothesis that the applied BS significantly increases the production efficiency of the treated agricultural crops, but they do not have an analogous impact on the economic efficiency of the agricultural holding as a whole, was verified.

CONCLUSIONS

The influence of biostimulators on the economic efficiency of spring rape, as well as on the production structure of the agricultural holding, was carried out with an economic-mathematical model based on linear programming. The following conclusions can be drawn from the obtained results: On the one hand, the use of biostimulators in agriculture increases material costs and contributes to a higher yield and biometrics of spring rape. On the other hand, the proposed optimization model showed that the foliar treatment of agricultural crops with biostimulants is able to influence the production structure and the economic efficiency of the agricultural holding. And thirdly, the positive impact of biostimulants on yield does not always have a positive economic effect on the farm as a whole.

The resulting optimization is a kind of new approach for studying the economic efficiency in the use of biostimulants in agriculture. The proposed optimization model is a useful tool for accounting the economic efficiency of the effect of biostimulants not only for farmers, but also for politicians and management decision makers following the objectives of the Green Deal.

ACKNOWLEDGEMENTS. This work was supported by Project ‘Use of biostimulants in organic farming - assessment of contributions to the bioeconomy’, funded by Contract No. KP-06-N46 / 6 of 27.11.2020 from the Research Fund of the Ministry of Education and Science, Bulgaria. We are grateful to the Scientific Research Fund, Bulgaria.

REFERENCES

Belcheva, S. 1989. *Effect of biologically active substances on the seed productivity of alfalfa.* Dissertation thesis, Agricultural Academy, Sofia, Bulgaria (BG), 182 pp.

Bremmer, J., Gonzalez-Martinez, A., Jongeneel, R., Huiting, H., Stokkers, R. & Ruijs, M. 2021. Impact Assessment of EC 2030 Green Deal Targets for Sustainable Crop Production. *Wageningen, Wageningen Economic Research, Report* 2021–150. 70 pp.

Brown, P. & Saa, S. 2015. Biostimulants in agriculture. *Front. Plant Sci*. **6**, 671. doi: 10.3389/fpls.2015.00671

Bulgari, R., Franzoni, G. & Ferrante, A. 2019. Biostimulants application in horticultural crops under abiotic stress conditions. *Agronomy* **9**(6), 306.

Campobenedetto, C., Mannino, G., Beekwilder, J., Contartese, V., Karlova, R. & Bertea, C.M. 2021. The application of a biostimulant based on tannins affects root architecture and improves tolerance to salinity in tomato plants. *Sci. Rep.* **11**(1), 354. doi: 10.1038/s41598-020-79770-5

Chernikova, O., Mazhaysky, Yu., Buryak, S., Seregina, T. & Ampleeva, L. 2021. Comparative analysis of the use of biostimulants on the main types of soil. *Agronomy Research* **19**(S1), 711–720. doi: 10.15159/AR.21.075

Di Vaio, C., Testa, A., Cirillo, A. & Conti, S. 2021. Slow-release fertilization and Trichoderma harzianum-based biostimulant for the nursery production of young olive trees (Olea Europaea L.) *Agronomy Research* **19**(3), 1396–1405. doi: 10.15159/AR.21.143

Findura, P., Šindelková, I., Rusinek, R., Karami, H., Gancarz, M. & Bartoš, P. 2022. Determination of the influence of biostimulants on soil properties and field crop yields. *Int. Agrophys*. **36**, 351–359. doi: 10.31545/intagr/155955

Gedeon, S., Ioannou, A., Balestrini, R., Fotopoulos, V. & Antoniou, C. 2022. Application of Biostimulants in Tomato Plants (*Solanum lycopersicum*) to Enhance Plant Growth and Salt Stress Tolerance. *Plants* **11**(22), 3082. doi: 10.3390/plants11223082

Grabowska, A., Kunicki, E., Sekara, A., Kalisz, A. & Wojciechowska, R. 2012. The effect of cultivar and biostimulant treatment on the carrot yield and its quality. *Veg. Crops Res. Bull.* **77**, 37–48. doi: 10.2478/v10032-012-0014-1

Hurduzeu, G., Pânzaru, R.L., Medelete, D.M., Ciobanu, A. & Enea, C. 2022. The Development of Sustainable Agriculture in EU Countries and the Potential Achievement of Sustainable Development Goals Specific Targets (SDG 2). *Sustainability* **14**, 15798. doi: 10.3390/su142315798

Jongeneel, R.A., Silvis, H.J, Gonzalez-Martinez, A.R., Jager, J. 2021. The Green Deal: An assessment of impacts of the Farm to Fork and Biodiversity Strategies on the EU livestock sector. *Wageningen, Wageningen Economic Research, Report* 2021–130. 68 pp.

Kocira, S., Agnieszka Szparaga, A., Hara, P., Treder, K., Findura, P., Bartoš, P. & Filip. M. 2020. Biochemical and economical effect of application biostimulants containing seaweed extracts and amino acids as an element of agroecological management of bean cultivation. *Sci. Rep.* **10**, 17759. doi: 10.1038/s41598-020-74959-0

Li, J., Van Gerrewey, T. & Geelen, D. 2022. A Meta-Analysis of Biostimulant Yield Effectiveness in Field Trials. Front. *Plant Science* **13**, 836702. doi: 10.3389/fpls.2022.836702

Nemes, N. 2020. Comparative analysis of organic and non-organic farming systems: A critical assessment of farm profitability. *FAO Web side*. [cited May2020]. *https://www.fao.org/tempref/docrep/fao/011/ak355e/ak355e00.pdf*.

Nikolov, N., Ivanov, G. & Stefanov, L. 1994. Economic and mathematical modeling of agricultural production. *Sofia: Zemizdat.* (BG). Николов, Н., Иванов, Г., Стефанов, Л. 1994. Икономико-математическо моделиране на селскостопанското производство. *София: Земиздат* (in Bulgarian).

Rosegrant, M.W., Sulser, T.B. & Wiebe, K. 2022. Global investment gap in agricultural research and innovation to meet Sustainable Development Goals for hunger and Paris Agreement climate change mitigation. Front. *Sustain. Food Syst. Sec. Land, Livelihoods and Food Security*. Volume **6**, 965767. doi: 10.3389/fsufs.2022.965767

Rudnicki, R., Biczkowski, M., Wi´sniewski, Ł., Wi´sniewski, P., Bielski, S. & Marks-Bielska, R. 2023. Towards Green Agriculture and Sustainable Development: Pro-Environmental Activity of Farms under the Common Agricultural Policy. *Energies* **16**, 1770. doi: 10.3390/ en16041770

Sassine, Y.N., Sajyan, T.K., El Zarzour, A., Abdelmawgoud, A.M.R., Germanos, M. & Alturki, S.M. 2022. Integrative effects of biostimulants and salinity on vegetables: Contribution of bioumik and Lithovit®-urea50 to improve salt-tolerance of tomato. *Agronomy Research* **20**(4), 793–804. doi: 10.15159/AR.22.074

Szczepanek, M., Jaśkiewicz, B. & Kotwica, K. 2018. Response of barley on seaweed biostimulant application. *Research For Rural Development* **2**, 49–54. doi: 10.22616/rrd.24.2018.050

Wesseler, J. 2022. The EU's farm-to-fork strategy: An assessment from the perspective of agricultural economics. *Applied Economic Perspectives and Policy*, 1–18. doi: 10.1002/aepp.13239

Woziak, E., Blaszczak, A., Wiatrak, P. & Canady, M. 2020. Biostimulant mode of action: Impact of biostimulant on whole-plant. *In The Chemical Biology of Plant Biostimulants* (eds Geelen, D. & Xu, L.), 207–227 (Wiley, Hoboken, 2020).

https://www.mzh.government.bg/media/filer_public/2022/04/27/ra400_publicationcrops2021_preliminarydata.pdf

Agronomy Research **22**(2), 956–969, 2024
https://doi.org/10.15159/AR.24.068

Development and case study of an Industry 5.0 ready human-centric related brewing plant

T. Schlechter[1,*], P. Kopylov[2], J. Wegen[2], K. Manfredi[3], L. Nicoletti[3], A. Padovano[4], M. Cardamone[4], E. Francalanza[5] and M. Seidl[6,7]

[1]University of Applied Sciences Upper Austria, Stelzhamerstr. 23, AT4600 Wels, Austria
[2]EIT Manufacturing CLC North AB, Forskningsgången 6, SE41756 Gothenburg, Sweden
[3]CAL-TEK S.r.l., Contrada Cutura, 240, IT87036 Rende (CS), Italy
[4]University of Calabria, Energy and Mechanical Engineering (DIMEG), Department of Mechanical, Via P. Bucci - Edificio Cubo 46/C, IT87036 Arcavacata di Rende (CS), Italy
[5]University of Malta, Department of Industrial and Manufacturing Engineering, Msida MSD, MT2080, Malta
[6]Dietrachinger Privatbrauerei, Dietraching 24, AT5271 Moosbach, Austria
[7]Gerstl Bräu, Freiung 9/11, AT4600 Wels, Austria
[*]Correspondence: thomas.schlechter@ieee.org

Received: January 31st 2024; Accepted: June 21st 2024; Published: July 17th, 2024

Abstract. This article explores the transformative potential of learning factories in mecha- tronic systems development. Learning factories offer a dynamic, collaborative environment that bridges the gap between academia and industry, creating a mutu- ally beneficial ecosystem. The LEONARDO project aims to develop innovative teaching methods, materials and tools for human-centric industrial engineering and management education leveraging on an industry 5.0 replica of a brewing system. Brewing as a process can be considered as highly complex, while brewing as a procedure serves as a 'sexy vehicle' for appealing student's interest in industry 5.0 applications and human-centric production. The brewing process is and will increasingly be more automated and highly supervised. For the latter, modern implementations of sensors such as electronic nose, electronic tongue, and infrared spectroscopy are required to be installed on the brewing equipment. To efficiently use the sensor outputs, the produced signals need to be merged locally and pro- cessed adequately, researched and investigated deeply by the authors up-front with the results to be summarized. Furthermore, to enable the physical bridging of various involved institutions across Europe, connecting the relevant sites virtually presents another technological challenge. Adequate IoT equipment needs to be selected and included in the whole setup as well. Furthermore, an emphasis needs to be made on the human-centric approach, as well as data visualization. Each of the aforementioned pieces of technology need a thorough investigation along with a decent focus in integrating the puzzle pieces into the big picture which is the brewing plant. In this paper we describe the interaction along with the system integration strategies of the listed fields to enable a future proof industry 5.0 ready brewing plant, focusing on the human-centric approach demanded in the industry5.0 feature description.

Key words: digital factory, smart manufacturing, gamification, industry 5.0, human centricity.

INTRODUCTION

We are living in interesting and as well challenging times. The current generation has been and still is experiencing the fourth industrial revolution, incorporated in the term industry 4.0. The focus of industry 4.0 has mainly been the development and establishment of technologies among various fields (e.g., communication technology, AI, IoT, robotics, process engineering) to enable the 'Smart Manufacturing for the Future' (Demir et al., 2019; Froschauer et al., 2022). Although, while widely still many companies and countries struggle with digitization technologies, the next development stage of the industry, the fifth industrial revolution, already presents itself at our doors (Demir et al., 2019; Paschek et al., 2019). One key aspect of industry 5.0 is the human-centric approach, meaning focusing on the human as part of the industrial process - in many ways (Froschauer et al., 2021; Khan et al., 2023; Kopylov et al., 2024). While Paschek et al. (2019) provide a literature review based description of industry 4.0 and 5.0 in the context of a study analyzing the expected impact of the fifth industrial revolution on companies' business models, other publications focus on the technical interaction of humans and robots, so called human-robot co-working environments (Schönberger et al., 2018; Demir et al., 2019; Froschauer & Lindorfer, 2019; Emma-Ikata & Doyle-Kent, 2022; Ikumapayi et al., 2023). Fig. 1 illustrates the evolution of the industry from industry 1.0 to industry 5.0, impressively outlining the ever decreasing time intervals upon the arrival of the next revolutionary stage, while Fig. 2 illustrates the industry 5.0 triad, containing the three main corner stones of industry 5.0 as defined by the European Commission (European Commission (2021)).

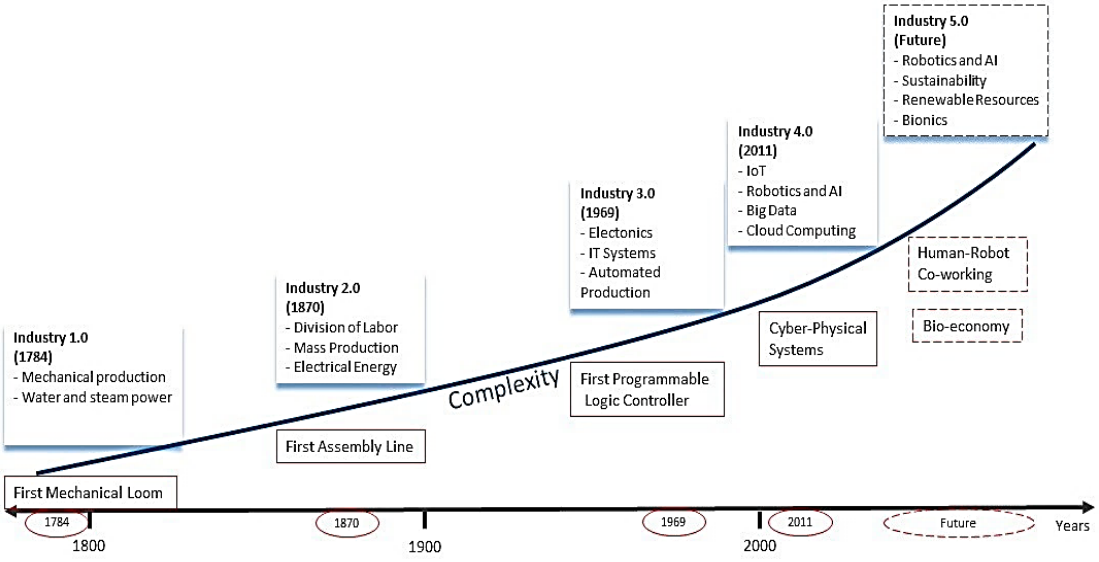

Figure 1. Roadmap from industry 1.0 to 5.0. (Demir et al., 2019).

As discussed by Zizic et al. (2022) and the literature review by Khan et al. (2023), instead of taking technology as the key player of the next industrial revolution, three different key drivers are set as the center of the industrial 5.0 paradigm by the European Commission (European Commission (2021)).

- The human-centric approach, which places human needs at the heart of the production process, asking what technology can do for workers and how can it be useful (Khan et al., 2023).
- Sustainability, which focuses on reuse, repurpose, and recycle of natural resources and reduce of waste and environmental impact (Saikia, 2023; Volpe et al., 2023).
- Resilience, which implies an introduction of robustness in industrial production. This robustness provides support through flexible processes and adaptable production capacities, especially when a crisis occurs (Pandey et al. (2023)).

As provided in an overview-like presentation by Demir et al. (2019), besides the technical challenges, also ethical issues are being discussed in the industry (Murphy et al. (2022); Emma-Ikata & Doyle-Kent (2022)), influence of industry 5.0 on the companies' culture(s) (Cillo et al. (2022)) and non-technical processes (Zizic et al. (2022)) like marketing as studied by Rajumesh (2023). Also, industry 5.0 does not only influence the companies and their employees, but will have significant impact on the whole society (Zizic et al. (2022)), e.g., describing and analyzing the correlation of consequences of 'Smart Manufacturing' towards a 'Digital Society' (Skobelev & Borovik, 2017; Martynov et al., 2019). This investigation shows the complexity of the industry 5.0 movement on the one side and the huge influencing potential, the immense scope of the latter on the overall society, on the other side.

Figure 2. Key corner stones of industry 5.0. (Zizic et al. (2022)).

To make all this happen in an efficient way, academia must be focused at as the initial source of knowledge gaining and spreading and, therefore, main responsible institution of advances and both technological and societal progress. A simple formulation or request may be, that involved parties are required to learn to work with robots (Demir et al., 2019). This does not only include the usage of robots and industry 5.0 approaches in education as discussed by Linert & Kopacek (2016) or Pozo et al. (2022) to foster technological enthusiasm and jump on the train of current youth's learning and studying paradigms, but incorporates a bridge building between industry and academia as, e.g., described by Lanz et al. (2019). The latter is also manifold referred to as learning factory, e.g., analyzed by Balve & Ebert (2019) in a retro-perspective evaluation of competence development based on graduates feedback, or by Doyle-Kent & Walsh Shanahan (2022) as a means of upskilling technical workers for industry 5.0. The essence each is to empower all relevant industrial employees from blue-collar workers (Cimino et al., 2023) to industrial engineers or production planners (Rannertshauser et al., 2022; Shah & Bharathi (2023)) to efficiently use the advantages of industry 5.0 achievements, focused not exclusively but essentially on the human-centric approach. Fig. 3 developed by Zizic et al. (2022) includes some of those findings, being training of the workers, customer as the designers (well-educated customer) and information based decision making,

closing the cycle of the interaction of academia (Rasmussen, 2012; Maijala et al., 2014; Zeidmane & Rubina, 2019), industry (Jørgensen, 2018), and entrepreneurship as one specific phase of industry (Põder et al., 2019), along with its influence towards a digital society (Skobelev & Borovik, 2017; Martynov et al. (2019); Motinho & Cavique, 2023).

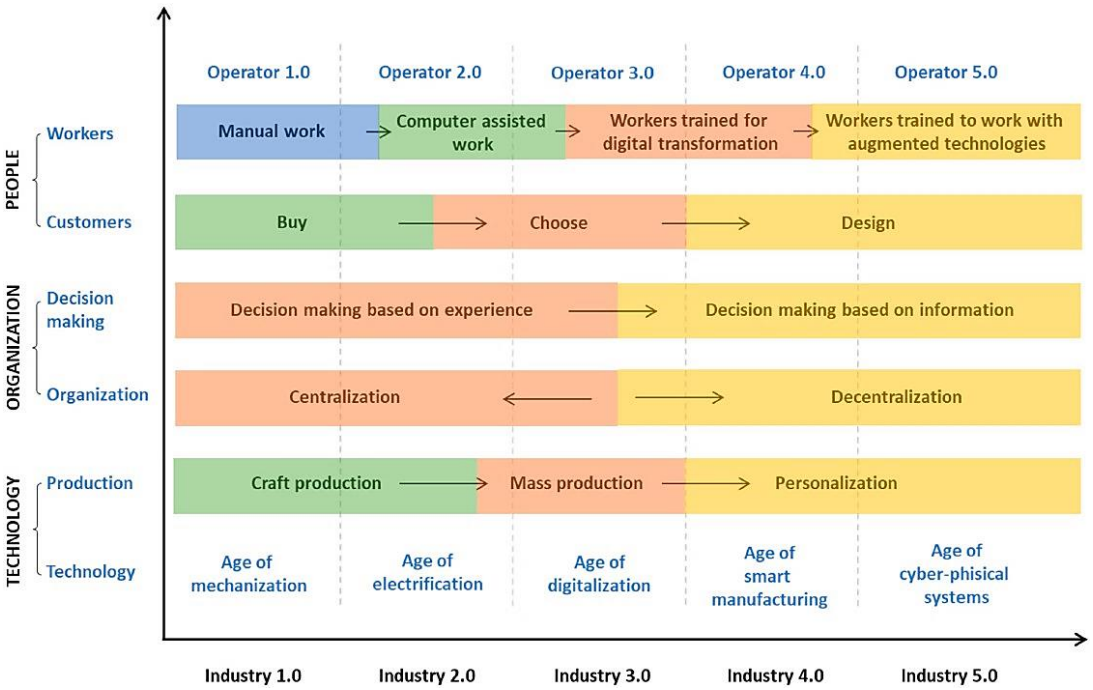

Figure 3. Transformations through the paradigms according to the important participants and segments of industries (Zizic et al., 2022).

The focus of this article is to grasp all of these points in the context of an open-access learning & experimentation factory, to be developed in the European Union funded Erasmus+ LEONARDO project (Padovano et al., 2023). The LEONARDO project aims to transform Industrial Engineering and Management (IEM) education by establishing innovative teaching methods, materials, and tools with a human-centric approach in the context of the industry 5.0 paradigm. In practice, the project will leverage an industry 5.0 replica of a brewing system as a hands-on learning environment for IEM students. LEONARDO will thus foster the entrepreneurial skills of IEM students by providing an applied learning environment to develop and test ideas. The brewing system called Learning and Experimenting open-Access Factory (LEAF) will facilitate innovative learning approaches as well as new teaching methods (Padovano et al., 2023). Some of the project partners already introduced the idea of a industry 5.0 ready brewing equipment as a business model in 2020 (Schlechter et al., 2020), aligned with some industry 5.0 corner stones like 'customer as the product designer' and the main concept of human-centricity. As well, current trends and technologies to modernize the current brewing community has been popular scientifically (Schlechter, 2023) and extensively (Vošahlík & Hart, 2021; Schlechter, 2024) discussed.

Essentially, this article will present the technical and academic infrastructure of the 'to- be' developed brewing plant as vehicle for the industry 5.0 educational open-access

factory example, which is currently implemented in one of the project partner locations (Wels, Austria), A second one, which is not focused on in this publication but contains similar functionality on a smaller scale, will be installed and further developed in the area of further project partners (Calabria, Italy).

The article is structured as follows. Section 2 provides a detailed system description of the hardware and software setup and requirements of the relevant brewing plant(s). The reader shall get an impression on what is existing, how does the existing setup need to be enhanced (automation, connectivity, additional sensors) and what are immediate and future use-cases for the developed setup. Section 3 provides an overview, how the technical setup is to be used in the project context and how it is anticipated to contribute to industry 5.0 training and execution. The relevant considered fields of interest along with potential teaching material are sketched. Section 4 presents an implementation architecture of the LEAF. Finally, Section 5 summarizes the findings.

System description and purpose

In this section the system design of the brewing plant used to fulfill the core topics of the LEONARDO project is described, starting from the currently existing system design via the necessary technological steps to be established towards the final anticipated knowledge platform delivering essential process data for educational purposes, vulgo the LEAF.

The Wels local LEAF brewing equipment installation will be carried out in a local small- scale brewery, the Gerstl Bräu (Der Brauereiführer (2024)). The advantage of this local brewery is, that a close relationship between the brewery (the brewery operator) and key players within the LEONARDO project at the University of Applied Sciences Upper Austria exists. Therefore, access of the brewery and therefore of the project related installations is guaranteed at all times. Fig. 4 shows an overview of the existing 10 hl brewing equipment in Wels, which will be extended by an automation unit and IoT components to enable remote access. The figure is of representative objective to underline the practical character of the given project and emphasize the actual implementation of the concept in a real brewery. In the picture the mash tank is shown, which in an other stage of the brewing process is as well used as wort cooker.

Figure 4. Gerstl brewery picture showing the mash tank.

Additionally, Fig. 5 illustrates the general overview of a professional brewing site taken from Wunderlich & Back (2009). This illustration represents as well the layout of the Gerstl Bräu (Der Brauereiführer (2024)) being a professional small-scale brewery with state of the art equipment found among all small to medium-size brewing sites. An overview of the study with relation to the human-centricity is given in Fig. 9 as well, showing the interaction of the human with various points of measurement in the brewing system and therefore brewing process.

In addition, as the Gerstl Bräu is a productive brewing plant, real life data of the brewing process will be available in continuous intervals and regularly, more than theoretically possible in an experimental setup. The overall project goals of LEONARDO will therefore be met more easily, complementing the to be installed 50 L experimental brewing equipment in Calabria and the 1,000 L operating brewing plant in Wels.

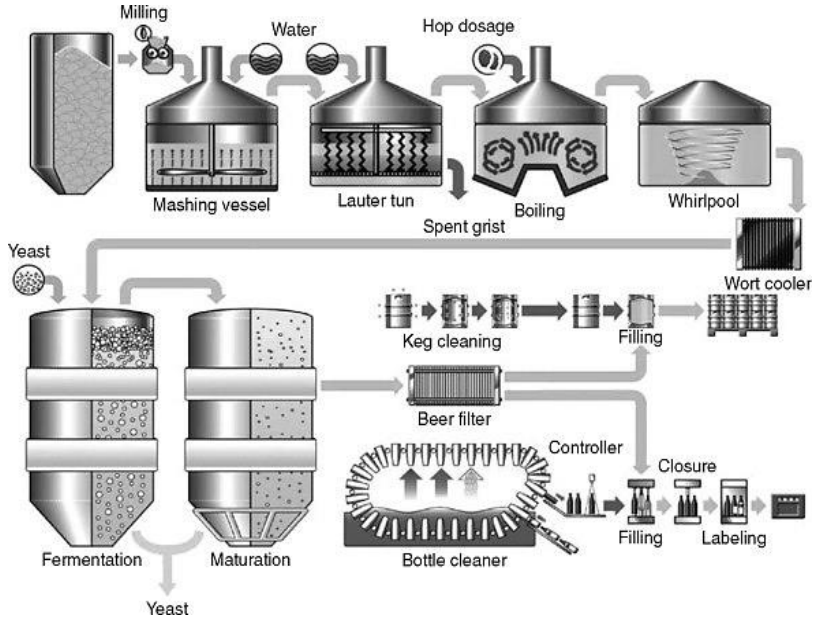

Figure 5. General overview of a typical brewing process.

Fig. 6 illustrates the rough basic system design of a brewing installation. Those include the main components like the various mashing, lautering, wort cooking and fermentation tanks, but as well needed pumps and valves to make the brewing process work. The illustrated setup should be seen as a rough overview to clarify the main technical challenges of the project fore-front enabling the to be setup innovative teaching concept.

The current installation is fully electrified, meaning, no manual valves need to be operated. The degree of automation, however, is limited. Therefore, the installation will be further developed towards a fully automated setup. The automation concept will be developed within the University of Applied Sciences Upper Austria, while the hardware installation (wiring, switch cabinet

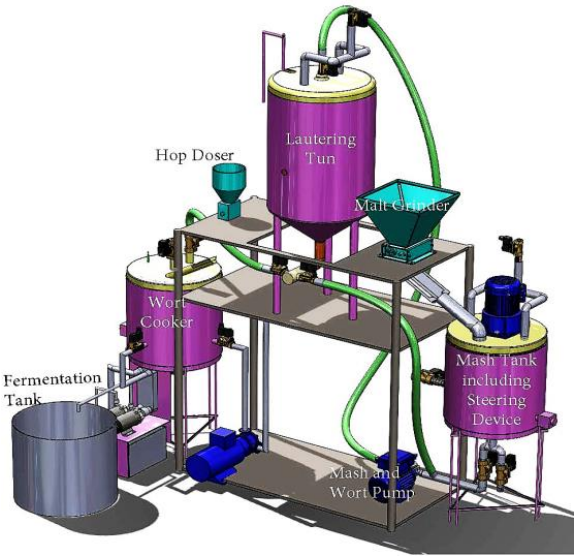

Figure 6. System design of the industry 5.0 brewing equipment.

installation, etc.) will be carried out by an electric professional. Fig. 7 shows the current control panel with manual operation, which will be extended by a second panel enabling full automation. To guarantee productive operation of the brewing plant at all times, the automated functionality will not replace the current installation but complement it.

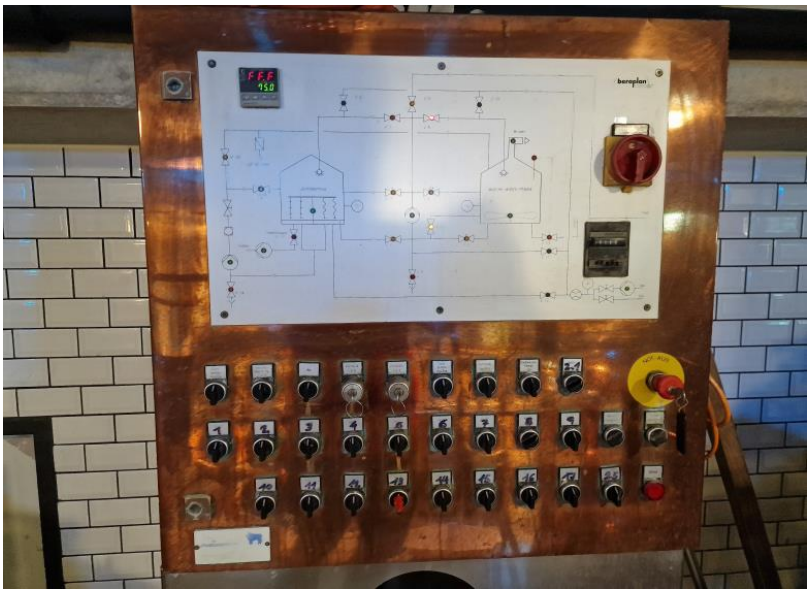

Figure 7. Gerstl brewery control unit.

Fig. 8 illustrates the additional components in an overview style.

As a follow up, IoT connectivity along with the integration of additional sensors is planned to be implemented. Those sensors include various temperature sensors for monitoring the homogeneity of the mash, an electronic nose as described in Schlechter (2024); Gonzalez Viejo et al. (2020), health parameter checks of the operator (e.g., heart beat rate, blood pressure, stress estimation, all using a fitness wrist band), NIR sensors, CO_2 sensors and many more. IoT connectivity is needed for several reasons.

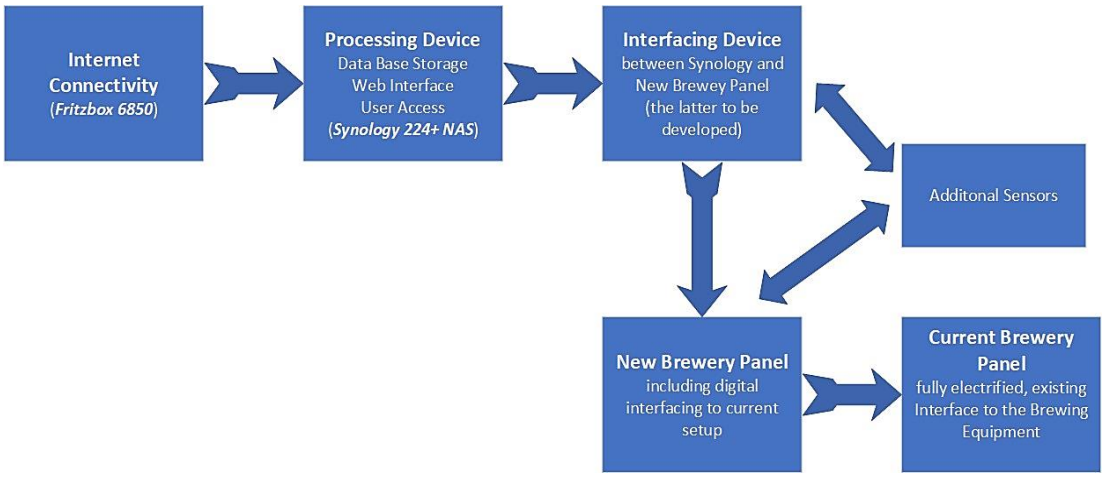

Figure 8. Block diagram of complete IoT implementation.

First, as one of the main features of the current project is remote accessibility, this connectivity needs to be established. This enables students using the to be developed industrial engineering educational concept in conjunction with the LEAF from everywhere in the world, given access is granted individually. Within the partner consortium of LEONARDO, human machine interfaces along with smart processing of gained information from the brewing process are developed. To feed those essential puzzle pieces of the final concept, the connectivity to the productive plant must be established. Secondly, to gather more relevant process data, additional sensors (in addition to standard sensors like temperature sensors, fraction sensors used for degree Plato measurements, fill level sensors, ...) will be added to the LEAF to enhance the functionality. Schlechter (2024) provided an extensive overview about the historical (Pearce et al., 1993; Gardner & Bartlett, 1994; Gardner et al., 1994; Gonzalez Viejo et al., 2020; Pornpanomchai & Suthamsmai, 2008 and current (Aouadi et al., 2020; Anisimov et al., 2021; Gonzalez Viejo et al., 2021; Seesaard & Wongchoosuk, 2022; Fuentes & Gonzalez Viejo, 2023; Kim et al., 2023; Liboà et al., 2023; Schlechter, 2023) technification development in the brewing branch. Already in 2020 Schlechter et al. (2020) proposed a concept in Agronomy Research on a business model with the LEONARDO project requirements - just not to use it for educational purposes, but for a real business. The outcome of this project may therefore be ulteriorly used in various fields, like innovation management, new product development, open innovation, entrepreneurship studies, etc. along with the training setup of industrial engineers which is the main scope of the LEONARDO project (Padovano et al., 2023). The efficient implementation of the proposed concept in addition will be supported by the Wels-local expertise in simulation workflow elaboration for complex automated system design, incorporated and described by Edlinger et al. (2023).

The system architectural review of the current system along with the required changes, adoptions, and extensions to the system given in this section acts as the base for the pedagogical approaches incorporating the final target of the LEONARDO project a stated by Padovano et al. (2023). The latter will be explained in more detail in Section 3.

Methodology and impact

In this section, the second meta-level of the given investigation and development will be sketched, which is more focused on the pedagogical objective as a main aim. Brewing, as a complex technological process, involves a nuanced blend of skills encompassing equipment operation, quality control, knowledge of biological and chemical processes, business acumen, and adept problem-solving. The application of a learning factory approach in the teaching context of the LEONARDO project serves as a noteworthy case study, exemplifying the effective use of this pedagogical concept in multidisciplinary settings.

LEONARDO establishes fruitful synergies with school education, adult education, Higher Education Institutions (HEI), and youth, and the project results can be exploited also in these fields, using the technical platform as an engaging platform to transport the learnings. For example, tools and materials developed for teaching industry 5.0 in higher education can also be incorporated into HEI programs. The project aims to understand future work qualifications in human-centric factories of the future, which will also be relevant to HEI, and create work-based learning opportunities at the LEAF Labs for

HEI students. This way, LEONARDO provides guidelines for developing and adapting HEI programs to meet the needs of the labour market and industry trends.

In terms of school education, LEONARDO will develop pedagogical approaches and materials, such as interactive simulations, videos, and multimedia resources, that high- school teachers can use to promote interest in STEM disciplines. LEAF lab managers and young people 'working' at the lab will act as ambassadors and mentors to inspire young people to pursue careers in the field, leveraging the beer brewing process as a motivation.

Specific connections will be established with high-schools that will be able to consider the LEAF lab as a venue for 'work experiences and internships' for highschool students. The upskilling pathways that LEONARDO will develop can also be applied in the field of adult education to reduce the skill gap and promote adult participation in learning. The education content and material can be also used by adult learning and guidance staff to improve their teaching methods. Digital and blended learning opportunities will be developed to offer a flexible learning offer not only for HEI students, but potentially also for adults, based on validation of acquired skills certified by micro-credentials or badges released at the end of a micro-courses carried out with the LEAF. Therefore, the LEAFs will become innovative local learning centres to attract and offer everyone in the community lifelong and life-wide learning opportunities. Finally, the adoption of a LEAF brewing system, which simulates real life, will enhance engagement and motivation of students. This makes the learning content more appealing as young people will be driven by the willingness to produce the beer, while at the same time, solving old and new problems related to H-IEM. This will promote young people's sense of initiative and entrepreneurship, creative learning and intercultural dialogue among all the people working at the LEAFs. Last but not least, given the affordability-by-design of the LEAF, the labs can be installed also at institutions that do not have large economic resources, thus giving marginalised young people in underdeveloped regions the opportunity to see with their own eyes how a human-centric production system works and creating the preconditions for their future employability by identifying the hard and soft skills and competences required for students to work in human-centric factories of the future (and become a workforce 5.0) and to define a pedagogical approach and curriculum design guidelines to support the teaching of the Industry 5.0 content via a combination of digital technologies, e.g., e-learning, in combination with/as well as the LEAF.

LEAF-as-a-service implementation architecture

As previously discussed LEAF is innovative as it is a small-scale but realistic replica of a brewing system which may be easily replicated. This provides an original and creative system compared to existing Learning Factory solutions, thus making education appealing for the younger generation. Furthermore, LEAF provides everyone the opportunity to access (even remotely), play and experiment their own ideas, in a LEAF- as-a-Service approach. This will allow the students to take active responsibility in the Industry 5.0 revolution. The concept of LEAF is based on the cloud based architectural setups, e.g., the Manufacturing-as-a-Service (MaaS) proposed by Rauschecker et al. (2011) and Factory-as-a-Service (FaaS) proposed by Hewa et al. (2023) approaches. By exposing the manufacturing capabilities and process to the user.

As illustrated in Fig. 9 the user, in this case an HEI student, may submit their customized brewing recipe to the LEAF. Through various IoT devices, such as smart sensors, Arduinos, Raspberry Pis, and HMIs, process information can be extracted from the LEAF. LEAF operator data may also be collected, through the use of smart watches or heart rate monitors. This information can be collected locally via an edge device, such as the Endian 4i Edge X. Pre-processing of data can be immediately carried out on site. In this way dimensionality reduction can be achieved through feature extraction and factor analysis. Machine Learning algorithms can then be deployed either at the edge or on the cloud to analyze the data and extract process related information. This can then be visualized through augmented devices such as tablets or VR goggles.

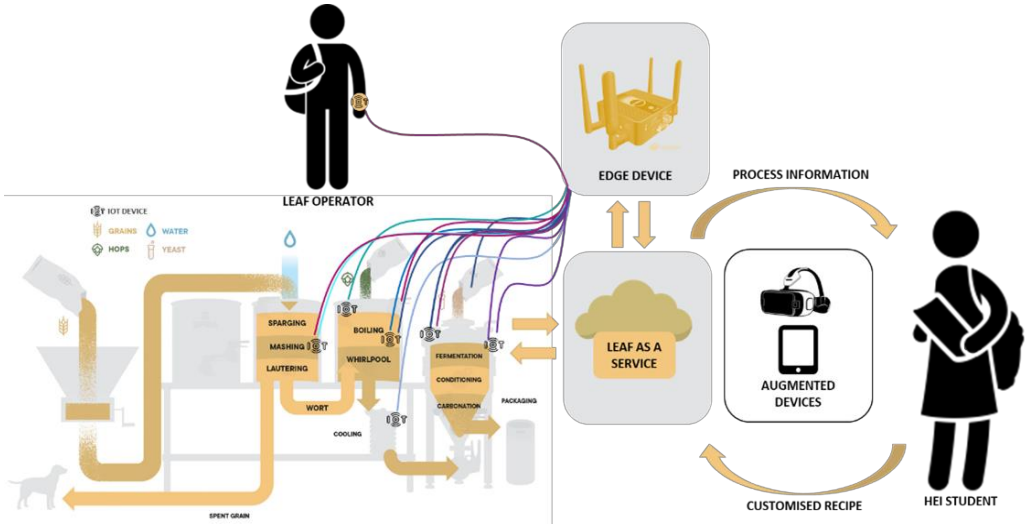

Figure 9. LEAF-as-a-Service Implementation Architecture.

By utilizing this LEAF-as-a-service architecture, this solution will provide remotely accessible services/apps for LEAF-based student game-based education. This will be developed in a way that students have access to practical, hands-on learning experiences that allow them to develop the skills and competences required for the workforce 5.0. This also supports the HEIs to be more resilient in terms of educational provision, since access to the LEAF facilities will be allowed remotely in case that laboratories and facilities are not accessible physically.

CONCLUSION

In this paper we presented the technical modification of a productive brewing plant involving all fields of action, in order to provide a solid technical base for a pedagogical concept towards higher education in the industry 5.0 human-centric approach, proposed by the European Commission (2021). We listed the technical setup along with potential enhancements on a current brewing system, focusing on the core features boosting the educational concept. The technical implementation will be used as a vehicle to train next generations' industrial engineers towards an efficient usage of industry 4.0 technology in a industry 5.0 concept, involving human-centricity, sustainability and resilience.

ACKNOWLEDGEMENT. This work is supported by the LEONARDO project, funded by the European Commission under the Erasmus+ programme KA-220 Cooperation Partnerships for Higher Education - No. 2023-1-IT02-KA220-HED-000164699. The views expressed belong to the author(s) alone and do not necessarily reflect the views of the European Union or the Erasmus+ National Agency -INDIRE. Neither the European Union nor the granting administration can be held responsible for them.

REFERENCES

Anisimov, D.S., Chekusova, V.P., Trul, A.A., Abramov, A.A., Borshchev, O.V., Agina, E.V. & Ponomarenko, S.A. 2021. Fully integrated ultra-sensitive electronic nose based on organic field-effect transistors. *Scientific Reports* **11**(10683). doi: 10.1038/s41598-021-88569-x

Aouadi, B., Zaukuu, J.-L.Z., Vitális, F., Bodor, Z., Fehér, O., Gillay, Z., Bazar, G. & Kovacs, Z. 2020. Historical Evolution and Food Control Achievements of Near Infrared Spectroscopy, Electronic Nose, and Electronic Tongue - Critical Overview. *Sensors* **20**(19), 5479.

Balve, P. & Ebert, L. 2019. Ex Post Evaluation of a Learning Factory - Competence Development Based on Graduates Feedback. In: 9th Conference on Learning Factories. *Procedia Manufacturing* **31**, Elsevier, 8–13. doi:10.1016/j.promfg.2019.03.002

Cillo, V., Gregori, G.L., Daniele, L.M., Caputo, F. & Bitbol-Saba, N. 2022. Rethinking companies' culture through knowledge management lens during Industry 5.0 transition. *Journal of Knowledge Management* **26**(10), Elsevier, 2485–2498. doi 10.1016/j.procs.2022.12.395

Cimino, A., Elbasheer, M., Longo, F., Nicoletti, L. & Padovano, A. 2023. Empowering Field Operators in Manufacturing: A Prospective Towards Industry 5.0. In: 4th International Conference on Industry 4.0 and Smart Manufacturing *Procedia Computer Science* **217**, Elsevier, 1948–1953. doi 10.1016/j.procs.2022.12.395

Demir, K.A., Döven, G. & Sezen, B. 2019. Industry 5.0 and Human-Robot Co- working. In: 3rd World Conference on Technology, Innovation and Entrepreneuship "Industry 4.0 focused Innovation, Technology, Entrepreneurship and Manufacture" June 21-23, 2019. *Procedia Computer Science* **158**, 688–695.

Der Brauereiführer (2024). Gerstl Bräu - "1. Welser Gasthausbrauerei". Small Scale Brewery. Available in: https://www.brauereifuehrer.com/wiki/Gerstl_Br%C3%A4u

Doyle-Kent, M. & Walsh Shanahan, B. 2022). The development of a novel educational model to successfully upskill technical workers for Industry 5.0: Ireland a case study. In: 21st IFAC Conference on Technology, Culture and International Stability TECIS 2022. *IFAC-PapersOnLine* **55**(39), 425–430.

Edlinger, R., Mitterhuber, U., Dumberger, S., Zouhar, D., Froschauer, R. & Nüchter, A. 2023. Integrated Simulation Workflow for Complex Automated System Design. In: *Proceedings of the Austrian Robotics Workshop 2023*, pp. 68–73.

Emma-Ikata, D. & Doyle-Kent, M. 2022. Industry 5.0 Readiness - Optimization of the Relationship between Humans and Robots in Manufacturing Companies in Southeast of Ireland. In: 21st IFAC Conference on Technology, Culture and International Stability TECIS 2022. *IFAC-PapersOnLine* **55**(39), 419–424. doi: 10.1016/j.ifacol.2022.12.071

European Commission (2021). Directorate General for Research and Innovation Industry. *5.0 - Towards a Sustainable, Human-Centric and Resilient European Industry*. Publications Office of the European Union: Luxemburg.

Froschauer, R., Kocher, A., Meixner, K., Schmitt, S. & Spitzer, F. 2022. Capabilities and Skills in Manufacturing: A Survey Over the Last Decade of ETFA. In: *IEEE International Conference on Emerging Technologies and Factory Automation, ETFA 2022*. United States. Institute of Electrical and Electronics Engineers Inc, 1–8.

Froschauer, R., Kurschl, W., Wolfartsberger, J., Pimminger, S., Lindorfer, R. & Blattner, J. 2021. A Human-Centered Assembly Workplace for Industry: Challenges and Lessons Learned. *Procedia Computer Science* **180**, 290–300.

Froschauer, R. & Lindorfer, R. 2019. Workflow-based programming of human-robot interaction for collaborative assembly stations. In *Proceedings of ARW & OAGM Workshop 2019*, OAGM & ARW Joint Workshop on Computer Vision and Robotics, 85–90.

Fuentes, S. & Gonzalez Viejo, C. 2023. *Novel use of e-noses for digital agriculture, food, and beverage applications*. Eds.: Gupta, R.K., Nguyen, T.A., Bilal, M. & Ahmadi, M. Nanotechnology-Based E-noses, Woodhead Publishing Series in Electronic and Optical Materials. Woodhead Publishing, 415–432.

Gardner, J.W. & Bartlett, P.N. 1994. A brief history of electronic noses. *Sensors and Actuators B: Chemical* **18**(1), 210–211.

Gardner, J.W., Pearce, T.C., Friel, S., Bartlett, P.N. & Blair, N. 1994. A multisensor system for beer flavour monitoring using an array of conducting polymers and predictive classifiers. *Sensors and Actuators B: Chemical* **18**(1), 240–243.

Gonzalez Viejo, C., Fuentes, S., Godbole, A., Widdicombe, B. & Unnithan, R.R. 2020. Development of a low-cost e-nose to assess aroma profiles: An artificial intelligence application to assess beer quality. *Sensors and Actuators B: Chemical* **308**, 127688.

Gonzalez Viejo, C., Fuentes, S. & Hernandez-Brenes, C. 2021. Smart Detection of Faults in Beers Using Near-Infrared Spectroscopy, a Low-Cost Electronic Nose and Artificial Intelligence. *Fermentation* **7**(3), 117.

Hewa, T., Porambage, P., Kovacevic, I., Weerasinghe, N., Harjula, E., Liyanage, M. & Ylianttila, M. 2023. Blockchain-Based Network Slice Broker to Facilitate Factory- As-a-Service. *IEEE Transactions on Industrial Informatics* **19**(1), 519–530.

Ikumapayi, O.M., Afolalu, S.A., Ogedengbe, T.S., Kazeem, R.A. & Akinlabi, E.T. 2023. Human-Robot Co-working Improvement via Revolutionary Automation and Robotic Technologies - An Overview. In: 4th International Conference on Industry 4.0 and Smart Manufacturing. *Procedia Computer Science* **217**, 1345–1353.

Jørgensen, M.H. 2018. Agricultural field production in an 'Industry 4.0' concept. *Agronomy Research* **16**(1), 94–102.

Khan, M., Haleem, A. & Javaid, M. 2023. Changes and improvements in Industry 5.0: A strategic approach to overcome the challenges of Industry 4.0. *Green Technologies and Sustainability* **1**(2), 100020.

Kim, B.J., Bonacchini, G.E., Ostrovsky-Snider, N.A. & Omenetto, F.G. 2023. Bimodal Gating Mechanism in Hybrid Thin-Film Transistors Based on Dynamically Reconfigurable Nanoscale Biopolymer Interfaces. *Advanced Materials* **35**(45), 2302062.

Kopylov, P., Wegen, J., Schlechter, T., Manfredi, K., Padovano, A., Cardamone, M., Nicoletti, L. & Francalanza, E. 2024. Leveraging Learning Factories for Mechatronic Systems Development: A Collaborative Approach. In: *19th International Conference on Computer Aided Systems Theory - Extended Abstracts*. Section: Mechatronic Product Development.

Lanz, M., Pieters, R. & Ghabcheloo, R. 2019. Learning environment for robotics education and industry-academia collaboration. Research. Experience. Education. 9th Conference on Learning Factories 2019 (CLF 2019), Braunschweig, Germany. *Procedia Manufacturing* **31**, 79–84.

Liboà, A., Genzardi, D., Núñez-Carmona, E., Carabetta, S., Di Sanzo, R., Russo, M. & Sberveglieri, V. 2023. Different Diacetyl Perception Detected through MOX Sensors in Real-Time Analysis of Beer Samples. *Chemosensors* **11**(2), 147.

Linert, J. & Kopacek, P. 2016. Robots for Education (Edutainment). In: 17th IFAC Conference on International Stability, Technology and Culture TECIS 2016. *IFAC- PapersOnLine* **49**(29), Elsevier, 24–29.

Maijala, P., Närvä, M. & Pasila, A. 2014. Farm-to-table concept: How the industry and commerce are integrated to the academic education system. *Agronomy Research* **12**(2), 673–680.

Martynov, V.V., Shavaleeva, D.N. & Zaytseva, A.A. 2019. Information Technology as the Basis for Transformation into a Digital Society and Industry 5.0. In: *International Conference "Quality Management, Transport and Information Security, Information Technologies" (IT&QM&IS)*, pp. 539–543. doi: 10.1109/ITQMIS.2019.8928305

Motinho, L. & Cavique, L. 2023. Philosophy of Artificial Intelligence and Its Place in Society, chapter Impact of Artificial Intelligence in Industry 4.0 and 5.0. *IGI Global* pp. 358–376.

Murphy, C., Carew, P.J. & Stapleton, L. 2022. Ethical Personalisation and Control Systems for Smart Human-Centred Industry 5.0 Applications. 21st IFAC Conference on Technology, Culture and International Stability TECIS 2022. *IFAC-PapersOnLine* **55**(39), 24–29.

Padovano, A., Francalanza, E., Schlechter, T., Kopylov, P., Wegen, J., Manfredi, K., Cardamone, M. & Nicoletti, L. 2023. LEONARDO - Learning & Experimentation OpeN-Access factoRy for inDustrial wOrkforce 5.0. https://www.uss-lab.it/projects/ leonardo/. Accessed 31.12.2023.

Pandey, S., Kiran, K., Parhi, S., Singh, A.K. & Jha, S.K. 2023. *Fostering Sustainable Development in the Age of Technologies*. Chapter Safety Management in the Era of Emerging Industrial Revolution: The Conceptualisation of Safety 4.0. Emerald Publishing Limited, Leeds, pp. 239–256. doi:10.1108/978-1-83753-060-120231017

Paschek, D., Mocan, A. & Draghici, A. 2019. Industry 5.0 - The expected impact of next industrial revolution. *In Thriving on future education, industry, business, and Society, Proceedings of the MakeLearn and TIIM International Conference*, Piran, Slovenia, pp. 15–17.

Pearce, T.C., Gardner, J.W., Friel, S., Bartlett, P.N. & Blair, N. 1993. Electronic nose for monitoring the flavour of beers. *Analyst* **118**(4), 371–377. Available in https://pdfs.semanticscholar.org/eb2a/34efea813776e4cec53c3192e1ad0f565375.pdf.

Pornpanomchai, C. & Suthamsmai, N. 2008. Beer classification by electronic nose. *In 2008 International Conference on Wavelet Analysis and Pattern Recognition ICWAPR*, Volume **1**, pp. 333–338.

Pozo, E., Patel, N. & Schrödel, F. 2022. Collaborative Robotic Environment for Educational Training in Industry 5.0 Using an Open Lab Approach. 13th IFAC Symposium on Advances in Control Education ACE 2022. *IFAC- PapersOnLine* **55**(17), 314–319.

Põder, A., Lemsalu, K., Nurmet, M. & Lehtsaar, J. 2019. Entrepreneurship education, entrepreneurship competencie sand entrepreneurial activities of alumni: A comparison between the engineering and other graduates of Estonian University of Life Sciences. *Agronomy Research* **17**(6), 2399–2416.

Rajumesh, S. 2023. Promoting sustainable and human-centric industry 5.0: a thematic analysis of emerging research topics and opportunities. *Journal of Business and Socio- economic Development* **4**(2), 111–126.

Rannertshauser, P., Kessler, M. & Arlinghaus, J.C. 2022. Human-centricity in the design of production planning and control systems: A first approach towards Industry 5.0. 10th IFAC Conference on Manufacturing Modelling, Management and Control MIM 2022. *IFAC-PapersOnLine* **55**(10), 2641–2646.

Rasmussen, M.D. 2012. Educational requirements to support research and innovation in Bioenergy. *Agronomy Research* **10**(S1, 205–209.

Rauschecker, U., Meier, M., Muckenhirn, R., Yip, A.L.K., Jagadeesan, A.P. & Corney, J.R. 2011. Cloud-based manufacturing-as-a-service environment for customized products. In *eChallenges e-2011 Conference, IIMC International Information Management Corporation*. Available in https://api.semanticscholar.org/CorpusID:55829322

Saikia, B. 2023. Fostering Sustainable Businesses in Emerging Economies. *Chapter Industry 5.0 - Its Role Toward Human Society: Obstacles, Opportunities, and Providing Human-Centered Solutions*. Emerald Publishing Limited, Leeds, pp. 109–126.

Schlechter, T. 2023. KI – Anwendungen in der Braubranche. *Brauwelt* **37–38**, 952–955. Available in https://brauwelt.com/de/themen/management/646074-ki---anwendungen-in-der-braubranche

Schlechter, T. 2024. Impact of AI on the Brewing Industry: A Comprehensive Summary. *Brewing Science* **77**(3–4), 18–32.

Schlechter, T., Froschauer, R. & Bronowicka-Schlechter, A. 2020. Towards a business and production engineering concept for individual beer brewing applying digitalization methodologies. *Agronomy Research* **18**(S1), 989–999.

Schönberger, D., Lindorfer, R. & Froschauer, R. 2018. Modeling Workflows for Industrial Robots Considering Human-Robot-Collaboration. In *Proceedings - IEEE 16th International Conference on Industrial Informatics*, INDIN 2018, pp. 400–405.

Seesaard, T. & Wongchoosuk, C. 2022. Recent Progress in Electronic Noses for Fermented Foods and Beverages Applications. *Fermentation* **8**(7), 302.

Shah, N. & Bharathi, S.V. 2023. Towards enhancing the students' employability for industry 5.0 through education 4.0. *AIP Conference Proceedings* **2869**(1), 050041.

Skobelev, P.O. & Borovik, S.Y. 2017. On the way from Industry 4.0 to Industry 5.0: From digital manufacturing to digital society. *Industry 4.0*, **2**(6), 307–311.

Volpe, M.D., Castro Peña, M.Y., Jaramillo-Gutiérrez, A. & Morris Molina, L.H. 2023. A Scientometric Overview of Industry 5.0: The Research Developments in the European Union. *Digitalization, Sustainable Development, and Industry 5.0*. Emerald Publishing Limited, Leeds., pp. 249–265.

Vošahlík, J. & Hart, J. 2021. Measurability of quality in fermentation process of rice wine by IoT in the field of industry 4.0. *Agronomy Research* **19**(S3), 1318–1324.

Wunderlich, S. & Back, W. 2009. 1 - Overview of Manufacturing Beer: Ingredients, Processes, and Quality Criteria. In Preedy, V.R., editor, *Beer in Health and Disease Prevention*, Academic Press, San Diego, pp. 3–16.

Zeidmane, A. & Rubina, T. 2019. Mathematics education for sustainable agriculture specialists. *Agronomy Research* **17**(1), 295–306.

Zizic, M.C., Mladineo, M., Gjeldum, N. & Celent, L. 2022. From Industry 4.0 towards Industry 5.0: A Review and Analysis of Paradigm Shift for the People, Organization and Technology. *Energies* **15**(14), 5221.

Agronomy Research **22**(2), 970–981, 2024
https://doi.org/10.15159/AR.24.082

Efficient maize cultivation: pre-sowing seed inoculation system - optimal nozzle pressure and diameter

M.S. Shelest[1], M.L. Shuliak[1], A.O. Butenko[2,*], O.M. Bakumenko[3], V.M. Zubko[1], O.M. Datsko[2], I.M. Masyk[2], V.M. Yatsenko[2], K.H. Sirovitskiy[1] and S.V. Rieznik[4]

[1]Sumy National Agrarian University, Faculty of Engineering and Technology, Department of Agroengineering, 160 H. Kondratieva Str., UA40021 Sumy, Ukraine
[2]Sumy National Agrarian University, Faculty of Agrotechnologies and Natural Resource Management, Department of Agrotechnologies and Soil Science, 160 H. Kondratieva Str., UA40021 Sumy, Ukraine
[3]Sumy National Agrarian University, Faculty of Agrotechnologies and Natural Resource Management, Department of Crop Protection, 160 H. Kondratieva Str., UA40021 Sumy, Ukraine
[4]State Biotechnological University, Faculty of Agronomy and Crop Protection, Department of Soil Science, 44 Alchevsky Str., UA61002 Kharkiv, Ukraine
[*]Correspondence: andb201727@ukr.net

Received: May 21st, 2024; Accepted: August 8th, 2024; Published: August 26th, 2024

Abstract. Inoculation, as a technological operation, is currently underestimated, yet it has repeatedly proven its effectiveness. Its application in production or scientific research typically leads to improvements in yield, grain quality, or plant biometric parameters under study. However, the inoculation process itself is not standardized by any legislative act, so farmers rely solely on recommendations from manufacturers of inoculants and carry out this operation using, so to say, makeshift means. Therefore, a system of at-planting inoculation has been developed, which involves conducting this operation directly in the field. Hence, the aim of this study was to investigate the parameters of pressure and nozzle diameter that would provide the optimal amount of inoculant on the seeds and would be as close as possible to the manufacturer's recommendations. To conduct the study, a system model was created in which nozzles with diameters of 0.2, 0.3, 0.4 and 0.5 mm were investigated under pressures of 3, 4, 5 and 6 atm. The optimal amount of working solution per 1 ton of seeds was calculated for conducting the operation in the usual way, and the amount of liquid reaching 1,000 maize seeds was determined. Thus, the optimal pressure and nozzle diameter were identified. With a pressure of 3 atm in the system, none of the nozzles provide the required amount of working fluid. A similar situation occurs with a nozzle diameter of 0.2 mm. However, at higher pressure in the system and with other nozzle diameters, it is still possible to provide the necessary amount of liquid. Therefore, for the at-planting inoculation system, it is advisable to use a pressure of 4 atm and a nozzle diameter of 0.4 mm.

Key words: 1,000-seed weight, *Zea mays*, planter, seeder, tilled crops, density, inoculation system, optimal operating parameters.

INTRODUCTION

Maize (*Zea mays L.*) is one of the most important crops worldwide and maximizing its productivity is imperative (Hegazy et al., 2014; Abo-Habaga et al., 2018). Currently, inoculation is an extremely relevant issue. The very term inoculation means settlement of beneficial microorganisms on the seed material in order to improve the germination properties of the seeds. More and more agricultural producers are considering growing organic products. Firstly, they are motivated by the price of organic products, which is usually significantly higher than that of products grown using conventional technologies (Balaji, 2016). Secondly, some, particularly farmers, are concerned about the state of the environment. Therefore, they use all possible means to increase crop productivity without using inorganic substances.

The effectiveness of inoculation has been proven for many crops and in different parts of the planet. For example, inoculation is considered most effective for leguminous crops, as nodular bacteria primarily inhabit the roots of these crops (Koliada et al., 2022; Michta et al., 2023). However, inoculation is carried out not only by bacterial organisms but also by arbuscular mycorrhiza (Kharchenko, 2019; Tanchyk, et al., 2021; Boymatova, 2022). However, inoculation is not only available for legumes but also for other crops. In particular, the positive effect of seed treatment with effective microorganisms has been proven for maize (Radchenko et al., 2022; Beltran-Medina et al., 2023), wheat (Gaspareto et al., 2023), rapeseed (Valetti et al., 2018), and others.

However, current inoculation methods are not perfect. For example, in the production scale of Ukrainian agricultural companies, inoculation is usually performed using seed treatment machines, such as auger, rotary, or chamber types, when it comes to wet inoculation (Bakhmat & Chinchyk, 2010; Moskalets & Moskalets, 2015). Another technical means used in production for seed treatment is concrete mixers. Alternatively, another way to inoculate seeds is to apply a working solution containing effective microorganisms directly into the furrow. A broader overview of possible methods and techniques is provided by Shelest., (2023). In general, it can be said that devices for inoculation are usually not specialized and cannot provide complete and quality treatment of planting material.

Therefore, the issue worth addressing in this article is the quality of seed treatment with inoculant. When applying it to the seed surface using such dubious methods, one should not expect to maintain the recommended dose of the preparation on the planting material, as specified by the manufacturers in their recommendations. For example, for the 'Bio-gel' preparation, it is stated that for pre-sowing seed treatment of grain and technical crops, it is advisable to apply 2 L t^{-1} of the preparation dissolved in 10 L of water (Application methods, 2015). Thus, it is assumed that this dose will provide the optimal amount of effective microorganisms on the seed surface and sufficient coverage with the preparation. However, when overloading the planting material, during transportation and unloading at-plantinging complex, there is a high probability that the layer of inoculant applied to the seeds will be lost.

There is also a question regarding the norm of inoculant application. A review of legislative or other regulatory documents did not reveal any examples of regulating the dosage of such substances. Therefore, one has to rely solely on the recommendations of inoculant manufacturers. In particular, the well-known Ukrainian company 'BTU-Center'

usually provides recommendations to use 2–3 liters of the preparation per ton (Inoculants BTU-CENTER, 2023). Typically, such a dosage is also proposed by other manufacturers.

Therefore, the aim of the study was to improve the adjustment of the at-planting inoculation system, which would allow for seed treatment in the optimal quantity up to the recommended dose of inoculants by manufacturers.

MATERIALS AND METHODS

To conduct research on seed inoculation in accordance with regulatory documentation, the recommended amount of inoculant was added to water at 20% of the water quantity. It is worth noting that the inoculant solution did not significantly affect the physico-mechanical properties of the working solution compared to water. It can be said that with such an amount of inoculant, its properties are almost identical to the physical properties of water. In particular, the density of water samples was 997 kg cm^{-3}, and the density of the working solution was 1,003 kg cm^{-3} (Fig. 1). Thus, the deviation in density is 0.6%, which can be attributed to the measurement error. Therefore, further experiments were conducted with water to save inoculant and eliminate its influence on the operation of the research equipment.

Figure 1. Density of water and working solution.

Experimental Stand

To conduct experiments at Sumy National Agrarian University, a model layout was created. Using the SolidWorks 2024 program, a sowing device was designed and printed on a 3D printer Flying Bear Ghost 5 for the main components. The model includes a tank (1) for the working solution, connected to the main pipeline (2) with a safety valve (3) and a filter (4). The working solution is delivered by a water pump (5) (Good PUMPs, 12V, 6A, 72W), through an analog pressure gauge (6) for the pressure control by a relief valve (7) (Ebowan DC 5 V G1/4, 12 MPA, China) and a two-way directional control valve (8). The solution is delivered to the nozzle (9) under a defined pressure (Fig. 2). The nozzle is mounted in the sowing tube at an angle of 17° relative to the plane on which the stand is located, and it is used for inoculation, i.e., spraying the working solution onto the planting material. The detailed structure of the system is presented in the work of Shelest et al. (2023). Therefore, this is how the device operates: when the stand is started, negative pressure is created in the seeding apparatus, which attaches the seed to the hole of the seeding disc. The seed is transported to the seed tube, where the pressure is turned off, and the seed begins to move along the tube in which the nozzle is located. The nozzle creates a conical spray on the seed path. Passing through this cut, the seed is covered with a working solution and falls out.

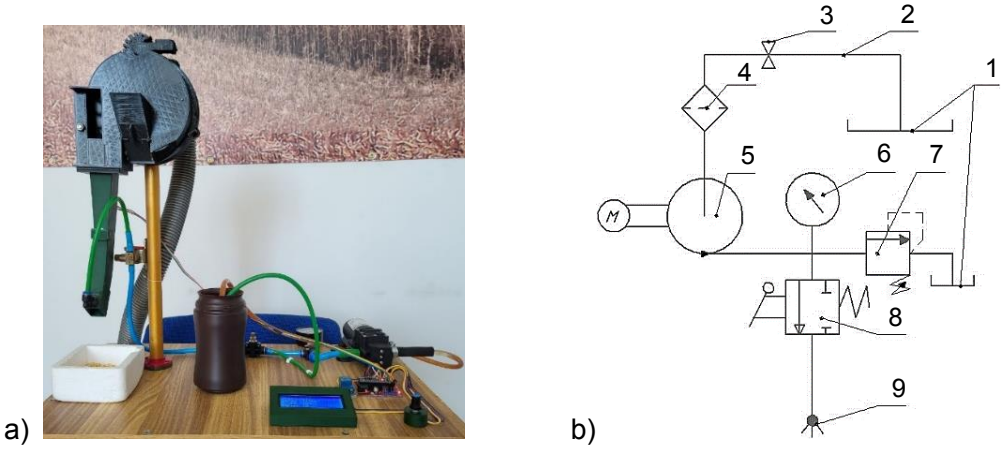

Figure 2. Model of the pre-sowing inoculation system, where a – prototype; b – hydraulic circuit of the inoculation system.

To spray the working solution and create the necessary droplet dispersion, TW6020, TW6030, TW6040 and TW6050 nozzles were used. The structure of the nozzle is shown in Fig. 3. The nozzle body (1) is made of stainless steel and contains an anti-drip valve (2), a spring (3), and a piston for mist formation (4). The nozzle head with a nozzle (5) works in tandem with the piston, ensuring uniform spraying. Nozzles with different nozzle diameters were used to vary the spray dispersion at different pressures.

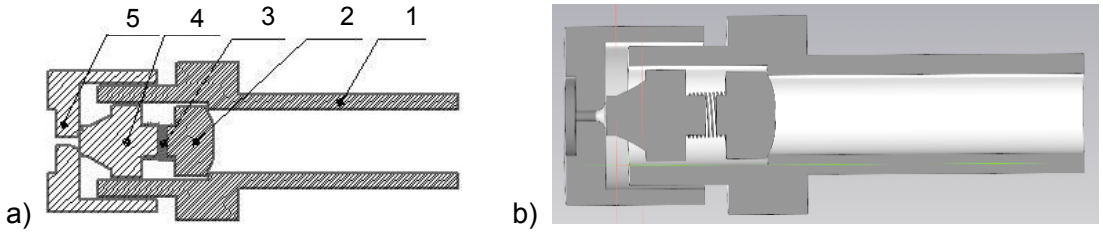

Figure 3. Structure of the nozzle, where a – schematic representation, b – 3D model.

Inoculation on the Stand

During the experiments, a two-factorial study was conducted. Table 1 presents the factors investigated during the experiment.

The tank was filled with water, the pressure was set using an electric regulator, then the at-planting inoculation system was activated, and the pressure was monitored using an analog pressure gauge. After reaching the required pressure and its stabilization, the nozzle was activated. During the study, a batch of 1,000 seeds was used, which were previously weighed on scales (Radwag, WLC 0.2/C/1, Poland) and placed in the sowing device. Then, sowing simulation together with seed treatment on the stand was performed. Thus, the seeds passed through the sowing tube

Table 1. Study Scheme

Factor	Indicator
Pressure (Factor A), atm	3, 4, 5, 6
Nozzle diameter (Factor B), mm	0.2 (2 in figures), 0.3 (3), 0.4 (4), 0.5 (5)

into the container for seed collection. To control the amount of liquid that reached the seeds, separately collected seed covered with liquid and liquid that did not adhere to the seeds were collected in a weighed container. Thus, results were obtained for each study variant, and the methodology was repeated for other pressures and nozzle sizes, with the main parameters of operation being recorded. Each experiment was repeated 10 times. The hybrid used for the study was Hemingway ES from Lidea company, with a declared seed weight of 1,000 seeds being 350 g. The actual seed weight slightly differed, so it was determined separately for each experimental variant.

Analysis of the Obtained Results

After obtaining the initial data, calculations were performed for their interpretation. The calculation of the optimal amount of inoculant that should reach the seeds in case of operation by the usual method is performed using the formula 1:

$$x_1 = \frac{a}{b} \times 1{,}000 \quad (1)$$

where x_1 is optimal dose of working solution according to the manufacturer's recommendations per 1,000 seeds, g; a is the dose of working solution per 1 ton of planting material, g; b is the number of seeds in 1 ton, pcs.

To determine the number of seeds in 1 ton of planting material, formula 2 was used.

$$b = \frac{10^9}{m_{1,000}} \times 1{,}000 \quad (2)$$

where $m_{1,000}$ is the mass of 1,000 seeds, g.

The obtained indicator serves as an estimate point for the study and indicates whether the given pressure and nozzle can be used in the at-planting inoculation system to ensure the optimal quality indicator of inoculant treatment.

Statistical data processing was performed using Statistica 10.0 and MS Excel. For determination of NDVI was used OneSoil program.

RESULTS AND DISCUSSION

The conducted research provided data indicating that the consumption of working fluid increases with increasing nozzle diameter at the specified pressure (Table 2).

Table 2. Average fluid consumption for treating 1,000 seeds at 3 atm pressure, g

Nozzle diameter, mm	Mean value, g	Minimum value, g	Maximum value, g	Dispersion, g^2	Standard deviation/SD
0.2	0.9	0.9	0.9	0.0	0.0
0.3	2.0	2.0	2.0	0.0	0.0
0.4	2.38	2.3	2.5	0.007	0.08
0.5	2.78	2.7	2.9	0.007	0.08

It is worth to mention that for the series of experiments, nozzles with diameters of 0.2 and 0.3 mm showed the most stable indicators which did not show any variations from the amount of liquid during each repetition all along of the experiment. For larger nozzle diameters, the indicator varied within 0.007 with a standard deviation of 0.08.

According to Eq. (1), the standard amount of working solution that should adhere to the seeds for each batch of 1,000 seeds was calculated based on the manufacturer's specifications. Fig. 4 clearly shows that at 3 atm pressure, the amount of working solution per 1,000 seeds cannot be provided by any of the nozzles compared to the standard value. At the same time, it is important to understand that introducing the next nozzle with a diameter of 0.6 mm could satisfy the requirement, but this would lead to an increase in the total fluid consumption, which is economically impractical. Incidentally, the total fluid consumption also increases with increasing nozzle diameter. For example, when using the optimal nozzle and pressure for a seeding density of 65 thousand seeds per ha, almost 5 tons of working solution will be used, while if a higher pressure will be used and a larger diameter of the nozzle, the required amount of working fluid will increase and will be 6.2 tons per ha. Accordingly, this will significantly affect the cost of growing products per hectare.

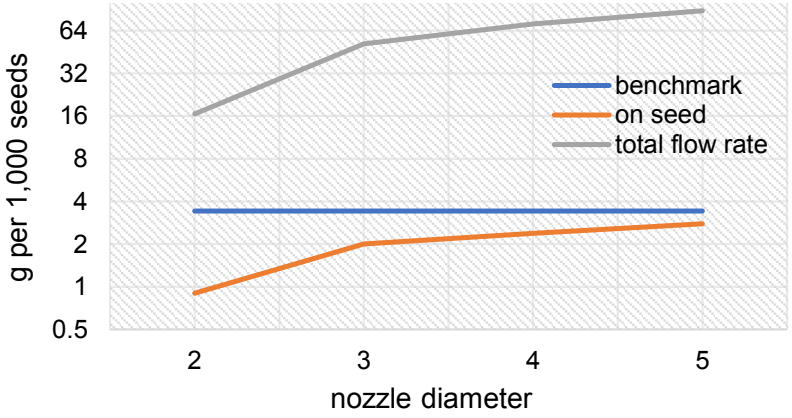

Figure 4. Working fluid consumption when using a pressure of 3 atm in the system.

When changing factor 'A' (Table 1), the research results presented in Table 3 were obtained. At a system pressure of 4 atm, the indicators have greater dispersion deviations and standard deviations compared to a pressure of 3 atm. This is due to the fact that the speed of the liquid spray has changed when it breaks up into droplets.

Table 3. Average fluid consumption for treating 1,000 seeds at 4 atm pressure, g

Nozzle diameter, mm	Mean value, g	Minimum value, g	Maximum value, g	Dispersion, g^2	Standard deviation/SD
0.2	1.1	1.1	1.2	0.003	0.05
0.3	2.6	2.3	2.9	0.08	0.28
0.4	3.2	2.9	3.9	0.14	0.38
0.5	3.7	3.1	4.3	0.32	0.56

Analysis of the research results allows stating that the consumption of working fluid at a pressure of 4 atm can meet the requirement for the standard liquid norm using nozzles with diameters of 0.4 and 0.5 mm. As seen from Fig. 5, the nozzle with a nozzle diameter of 0.2 mm, like the previous series of experiments, cannot achieve the standard liquid norm. The nozzle (with a diameter of 0.3 mm) is almost at the standard level, but

considering the conditions of real operation, it will not ensure the quality of the technological process execution. Its use will not meet the requirements for the uniformity of seed coverage with the working solution. Nozzles with diameters of 0.4 and 0.5 mm are capable of providing the required amount of working solution. However, with the increase in the amount of liquid covering the seeds, the total fluid consumption also increases. So, nozzles with diameters of 0.4 mm and 0.5 mm provide the required amount of working solution more reliably and with lower variability. The 0.4 mm nozzle, in particular, is identified as the most rational choice because it meets the standard treatment value with significantly lower total fluid consumption compared to the 0.5 mm nozzle. Therefore, the rational choice for use at-planting inoculation system is to choose a nozzle with a diameter of 0.4 mm. Using a nozzle that consumes more fluid than necessary is not economically practical. The 0.4 mm nozzle provides a balance between meeting the required liquid norm and minimizing fluid consumption, making it the most efficient choice.

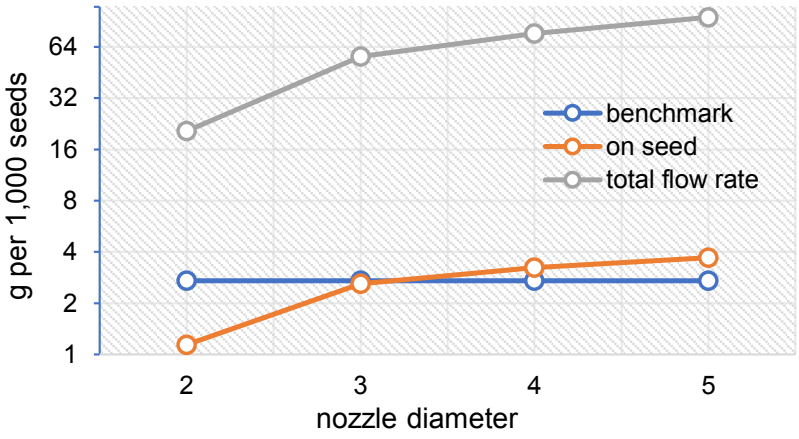

Figure 5. Working fluid consumption when using a pressure of 4 atm in the system.

With a pressure of 5 atm in the system, the dispersion and standard deviation indicators continue to increase. For the 0.2 mm nozzle, there is an increase in the spray rate compared to previous data (Table 4). At the same time, the consumption of working fluid for nozzles with diameters of 0.3 and 0.4 mm is significantly higher compared to the nozzle with a nozzle diameter of 0.2 mm. However, for the nozzle with a diameter of 0.5 mm, the amount of liquid on the seeds has decreased, which may be due to the increase in droplet size during spraying.

Table 4. Average fluid consumption for treating 1,000 seeds at 5 atm pressure, g

Nozzle diameter, mm	Mean value, g	Minimum value, g	Maximum value, g	Dispersion, g^2	Standard deviation/SD
0.2	1.64	1.1	2.0	0.11	0.33
0.3	4.18	3.2	5.7	0.85	0.92
0.4	4.5	3.2	5.6	1.23	1.11
0.5	3.14	2.6	3.8	0.21	0.46

From Fig. 6, it can be seen that the total consumption of the working fluid used for inoculation at a pressure of 5 atm has increased for all nozzles. Thus, the least amount spent was noted for the use of a 0.2 mm nozzle, and the highest, accordingly, for the 0.5 mm diameter nozzle.

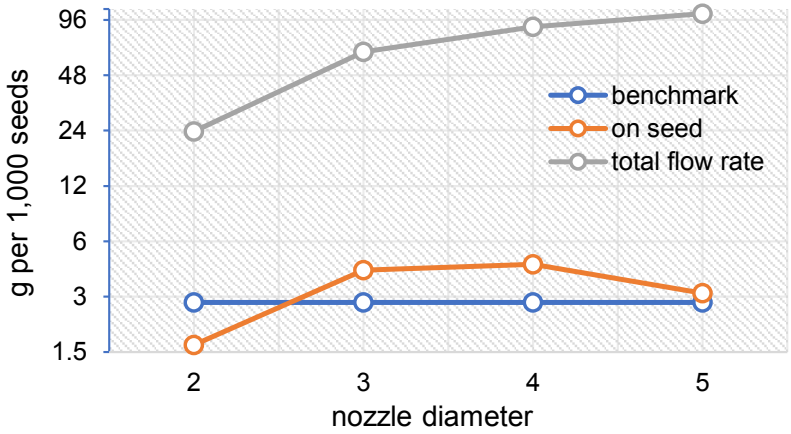

Figure 6. Working fluid consumption when using a pressure of 5 atm in the system.

At a pressure of 6 atm (Table 5), the fluid consumption for a 0.2 mm diameter nozzle doubles compared to the same diameter nozzle at 3 atm pressure (Table 2). However, the dispersion and standard deviation values indicate that the spray characteristics of the working fluid in it are the most stable compared to other nozzles. The 0.3 mm diameter nozzle has the highest dispersion and standard deviation values. The amount of working fluid for the 0.4 mm nozzle is lower compared to the previous one and has less variation in the indicators. For the 0.5 mm diameter nozzle, the fluid consumption significantly decreased and is almost at the same level as for a pressure of 5 atm, meaning that further increasing the pressure does not affect increasing the amount of liquid on the seeds, but only increases the total consumption of the working solution.

Table 5. Average fluid consumption for treating 1,000 seeds at 6 atm pressure, g

Nozzle diameter, mm	Mean value, g	Minimum value, g	Maximum value, g	Dispersion, g^2	Standard deviation/SD
0.2	1.86	1.8	1.9	0.003	0.05
0.3	5.18	3.6	6.8	1.56	1.24
0.4	4.92	3.9	6.1	0.84	0.91
0.5	3.24	3.0	3.5	0.03	0.19

From Fig. 7, it is clear that the total fluid consumption at a pressure of 6 atm in the system is highest compared to other series of experiments, and the trend of distribution of the amount of working solution from the smallest nozzle to the largest is maintained.

From the above data, it is clear that the nozzle diameter and system pressure at which it should operate can be determined. Thus, for a system pressure of 3 atm, none of the nozzles meets the requirement and does not provide the necessary amount of liquid

discharge onto the seeds, meaning that such pressure is insufficient for the system to work properly. At the same time, increasing the nozzle diameter to 0.6 mm makes no sense, as likely, the total amount of liquid during the nozzle operation will also increase, which is not economically feasible.

For a pressure of 4 atm, only 2 nozzles are capable of providing the standard treatment value for planting material, their diameter being 0.4 and 0.5 mm. The most rational option to use at-planting inoculation system is precisely the nozzle with a 0.4 mm diameter nozzle. Since the amount of liquid it can discharge exceeds the standard value, and the total consumption of working fluid is significantly lower than in nozzles with a diameter of 0.5 mm.

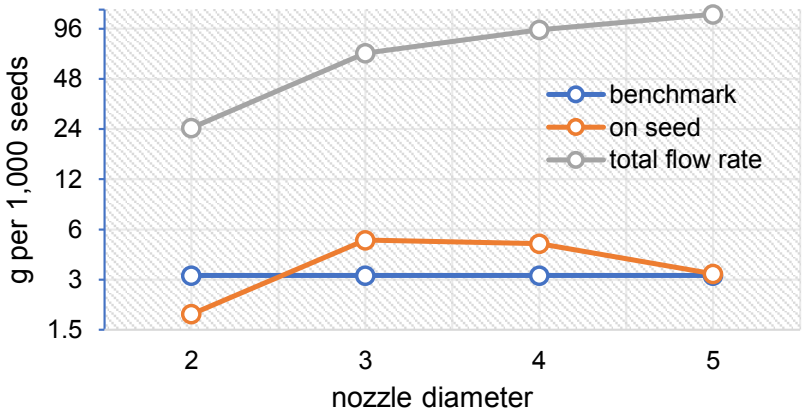

Figure 7. Working fluid consumption when using a pressure of 6 atm in the system.

Almost all nozzles, except for the one with a 0.2 mm diameter nozzle, can be used for incorporation at-planting inoculation system at a pressure of 5 atm. However, the consumption of working fluid for them significantly exceeds the option with a 0.4 mm diameter nozzle at a pressure of 4 atm. Moreover, the total fluid consumption of these nozzles at 5 atm pressure is also higher.

Similar results were obtained using a pressure of 6 atm in the system. Thus, nozzles with a nozzle diameter of 0.3–0.5 mm provide the standard value, but the indicators of working fluid consumption are significantly higher compared to the 0.4 mm nozzle and pressure in the system at 4 atm.

Therefore, it is rational to use a nozzle with a nozzle diameter of 0.4 mm at a pressure in the system of 4 atm, as it provides the standard value for the amount of liquid covering the seeds with the minimum total consumption of working fluid.

The study is limited by its focus on only four nozzle diameters and specific pressure conditions, which may not be representative of all possible scenarios. Additionally, the experiments were conducted under controlled laboratory settings and will only in spring of 2024 were tested in the field. That is why the investigated system was installed on the Elvorti Vega 8 Profi seeder (Fig. 8) with the and was used with nozzle diameter and pressures that were found to be most acceptable. As the field season is not over yet, the results of the experiment could not be highlighted yet. However, first impact of the developed system could be seen at the Fig. 9. The area of the field where the studied pre-sowing inoculation system was used is marked in green.

a) 

b) 

Figure 8. The view of the seeder, where a – reequipment of it with the pre-sowing inoculation system, b – work of the system in field conditions.

A similar system was invented by Chinese scientists. Although the system has some similarity in components and their arrangement, the use and location of the nozzle in the prototype (Wang et al., 2019) provides treatment of the row where the planting material is sown, not just the seeds. Therefore, the nozzle type (conical or sectorial) and the amount of liquid discharge by the nozzle per minute were investigated. A similar invention was made by scientists from India, whose aim was to measure the amount of working fluid that would be poured through nozzles with a nozzle diameter of 8, 10, and 12 mm (Lande & Mani, 2020). A similar system was developed by Manea et al. (2009) however, it does not involve getting the inoculant directly on the seeds. The task of this system is to introduce the inoculant directly into the soil. During the experiment, a lower pressure and only one nozzle diameter was used.

Figure 9. NDVI index of the research field.

However, scientists from Kharkiv have developed a slightly different system that can meet the need for inoculation, although they did not set such a task. Thus, a hydropneumatic seeder was created, which allows the planting material to be constantly in the liquid (Pastukhov et al., 2020). Nevertheless, this is not the first such planting complex that operates on this principle (Pill, 1991).

CONCLUSIONS

The developed system and technology of at-planting seed inoculation are capable of providing the necessary amount of inoculant on the seeds directly during sowing, thus eliminating the drawbacks of previous treatment.

The research results indicate that it is not advisable to use a nozzle with a nozzle diameter of 0.2 mm or less for the at-planting seed inoculation system, as they are unable to provide the standard working solution norm for 1,000 seeds.

Research has shown that it is rational to use a nozzle with a nozzle diameter of 0.4 mm at a pressure in the system of 4 atm. This nozzle is capable of providing the standard usage norm of the inoculant and preventing excessive use of the working fluid.

Future research should be conducted with the installation of a pre-sowing inoculation system on a planter and field testing of the system.

ACKNOWLEDGMENTS. We are thankful to the Czech government support provided by the Ministry of Foreign Affairs of the Czech Republics, which allowed this scientific cooperation to start within the project 'Empowering the Future of AgriScience in Ukraine: AgriSci – UA'.

REFERENCES

Abo-Habaga, M., Imara, Z. & Okasha, M. 2018. Development of a Combine Hoeing Machine for Flat and Ridged Soil. *Journal of Soil Sciences and Agricultural Engineering* **9**(12), 817–820. doi: 10.21608/jssae.2018.36548

Application methods. 2015. https://biogel.com.ua/product/application/?lang=en

Bakhmat, O.M. & Chinchyk, O.S. 2010. The effect of agrotechnical measures on soybean productivity in the Western region of Ukraine. *Feeds and Feed Production* **66**, 103–108.

Balaji, P. 2016. Consumers' willingness to pay (WTP) premium price for organic fruits and vegetables (OFV) in Western TamilNadu. *International journal of commerce and business management* **9**(1), 36–39. doi: 10.15740/HAS/IJCBM/9.1/36-39

Beltran-Medina, I., Romero-Perdomo, F., Molano-Chavez, L., Gutiérrez, A.Y., Silva, A.M.M. & Estrada-Bonilla, G. 2023. Inoculation of phosphate-solubilizing bacteria improves soil phosphorus mobilization and maize productivity. *Nutrient Cycling in Agroecosystems* **126**(1), 21–34. doi: 10.1007/s10705-023-10268-y

Boymatova, M. 2022. Inoculation of Soybeans with mycorrhizal Fungi in the Field of Central Asia. *Open Access Journal of Biomedical Science* **4**(1). doi: 10.38125/OAJBS.000393

Gaspareto, R.N., Jalal, A., Ito, W.C.N., Oliveira, C.E.D.S., Garcia, C.M.D.P., Boleta, E.H.M., Rosa, P.A.L., Galindo, F.S., Buzetti, S., Ghaley, B.B. & Filho, M.C.M.T. 2023. Inoculation with Plant Growth-Promoting Bacteria and Nitrogen Doses Improves Wheat Productivity and Nitrogen Use Efficiency. *Microorganisms* **11**(4), 1046. doi: 10.3390/microorganisms11041046

Hegazy, R.A., Abdelmotaleb, I.A., Imara, Z.M. & Okasha, M.H. 2014. Development and evaluation of small-scale power weeder. *Misr Journal of Agricultural Engineering* **31**(3), 703–728. doi: 10.21608/mjae.2014.98430

Inoculants BTU-CENTER. 2023. https://inoculants.btu-center.com/

Kharchenko, O., Zakharchenko, E., Kovalenko, I., Prasol, V., Pshychenko, O. & Mishchenko, Y. 2019. On problem of establishing the intensity level of crop variety and its yield value subject to the environmental conditions and constraints. *AgroLife Scientific Journal* **8**(1), 113–120.

Koliada, O., Bliznjuk, O., Masalitina, N., Belinska, A., Varankina, O. & Belykh, I. 2022. Case study of soybean inoculation with biotechnological preparations. *Integrated Technologies and Energy Saving* **3**, 3–11. doi: 10.20998/2078-5364.2022.3.01

Lande, S.D. & Mani, I. 2020. Design and development of pressurized aqueous fertilizer application system for seeder. *Agricultural Engineering Today* **44**(01), 12–19. doi: 10.52151/aet2020441.1514

Manea, D., Marin, E., Sorică, C. & Nedelcu, A. 2009. Mechanized Application of the Microbial Inoculants at Vegetable Plants Sowing. *Bulletin UASMV Agriculture* **66**(1), 381–386.

Michta, G.H., Da Silva, D.M., Lanzanova, L.S., Lanzanova, M.E., Redin, M., Guerra, D., De Souza, E.L. & Bohrer, R.E.G. 2023. Analysis of the importance of the inoculation technique in brazilian soybean crop. *Observatório de la economía Latinoamericana* **21**(6), 5126–5150. doi: 10.55905/oelv21n6-102

Moskalets, V.V. & Moskalets, T.Z. 2015. Formation of adaptive biocenetic relationships in phytocenoses of winter triticale in conditions of forest-steppe and poly-forest-steppe ecotypes. *Plant Varieties Studying and Protection* **1–2**, 54–60.

Pastukhov, V., Boiko, V., Tesliuk, H., Ulexin, V. & Kyrychenko, R. 2020. Study of seed agitation in the fluid of a hydropneumatic precision seeder. *Eastern-European Journal of Enterprise Technologies***5**(1), (107), 36–43. doi: 10.15587/1729-4061.2020.212517

Pill, W.G. 1991. Advances in Fluid Drilling. *HortTechnology* **1**(1), 59–65. doi: 10.21273/HORTTECH.1.1.59

Radchenko, M.V., Trotsenko, V.I., Butenko, A.O., Masyk, I.M., Hlupak, Z.I., Pshychenko, O.I., Terokhina, N.O., Rozhko, V.M. & Karpenko, O.Y. 2022. Adaptation of various maize hybrids when grown for biomass. *Agronomy Research* **20**(2), 404–413. doi: 10.15159/AR.22.028

Shelest, M.S. 2023. Modern systems of inoculation of seed material of row crops. *Bulletin of Sumy National Agrarian University. The Series: Mechanization and Automation of Production Processes* **3**(49), 90–97. doi: 10.32845/msnau.2022.3.13

Shelest, M., Kalnaguz, A., Datsko, O., Zakharchenko, E. & Zubko, V. (2023). System of pre-sowing seed inoculation. *Scientific Horizons* **26**(7). doi: 10.48077/scihor7.2023.140

Tanchyk, S., Litvinov, D., Butenko, A., Litvinova, O., Pavlov, O., Babenko, A., Shpyrka, N., Onychko, V., Masyk, I. & Onychko, T. 2021. Fixed nitrogen in agriculture and its role in agrocenoses. *Agronomy Research* **19**(2), 601–611. doi: 10.15159/AR.21.086

Valetti, L., Iriarte, L. & Fabra, A. 2018. Growth promotion of rapeseed (*Brassica napus*) associated with the inoculation of phosphate solubilizing bacteria. *Applied Soil Ecology* **132**, 1–10. doi: 10.1016/j.apsoil.2018.08.017

Wang, W., Wang, W., Jia, H., Zhuang, J. & Wang, Q. 2019. Effects of seed furrow liquid spraying device on sowing quality and seedling growth of maize. *International Journal of Agricultural and Biological Engineering* **12**(2), 68–74. doi: 10.25165/j.ijabe.20191202.3799

Agronomy Research **22**(2), 982–1000, 2024
https://doi.org/10.15159/AR.24.057

Spatial and temporal variability of enthalpy and its influence on the cloacal temperature of broilers

M.A.J.G. Silva[1], L.M.D. Santos[2], J.C.D. Ribeiro[1], M. Barbari[3], V. Becciolini[3], L.P. Naves[1] and P.F.P. Ferraz[2,*]

[1]Federal University of Lavras, Animal Science Department, Campus Universitário, PO Box 3037, Lavras, Minas Gerais, Brazil
[2]Federal University of Lavras, Agricultural Engineering Departament, Campus Universitário, PO Box 3037, Lavras, Minas Gerais, Brazil
[3]University of Firenze, Department of Agricultural, Food, Environmental and Forestry Science, Via San Bonaventura, 13, Firenze, Italy
[*]Correspondence: patrícia.ponciano@ufla.br

Received: January 15th, 2024; Accepted: June 5th, 2024; Published: June 20th, 2024

Abstract. Strategies aimed at mitigating heat stress conditions pose a challenge for the poultry industry operating in tropical climate zones. The primary aim of this research was to characterize and analyze the specific enthalpy of air (*h*, in kJ kg of dry air^{-1}) in a broiler house using geostatistical techniques. In addition, its relationship with the cloacal temperature ($t_{cloacal}$, °C) of the broilers was evaluated. The study was carried out in Lavras, Minas Gerais, Brazil. A total of 720 Cobb-500 broilers were raised from 1 to 42 days old. When the broilers were 7, 21, 35 and 42 days old, the dry bulb temperature (t_{db}, °C) and relative air humidity (RH, %) were recorded at 08:00 a.m. and 01:00 p.m. by seven sensors distributed throughout the installation, and $t_{cloacal}$ measured. Subsequently, *h* computed, and the data were examined through kriging interpolation. The $t_{cloacal}$ data were superimposed on the *h* maps of the facility. The spatial distribution of *h* inside the aviary (box) and temporal distribution (time and days) were characterized, and its variability was visualized. $T_{cloacal}$ was directly related to the spatial as well temporal distribution of *h*, providing information about the thermal influence on production environment and the physiological responses of broilers.

Key words: body temperature, geostatistics, heat stress, thermal comfort.

INTRODUCTION

In Brazil, intensive broiler production is conducted mainly in semiclimatized or climatized barns (Lima & Silva, 2019; Sans et al., 2021) due to the high cost of technological facilities with controlled environments. This suggests that ideal thermal comfort conditions are not always possible throughout the production cycle. As a result, the oscillations in the dry bulb temperature (t_{db}, °C) and relative air humidity (RH, %) inside poultry facilities can result in heat-stressed broilers, which represents a challenge

for industrial poultry farming, especially in tropical and subtropical regions (Liu et al., 2020; Abdel-Moneim et al., 2021).

According to Roushdy et al. (2018), chronic thermal stress (daily, 6 hours at 34 °C for three consecutive weeks) adversely influences feed intake and body weight gain among both Ross and Cobb broiler chickens. Castro Júnior & Silva (2021) reported that the rate of panting increased among broilers subjected to high temperatures (above 35 °C) as a strategy to enhance excess heat loss to the environment. This process corresponds to latent heat exchange, which depends on the RH. Thus, if the RH is high, this heat exchange process will be less efficient and may hinder thermoregulation of broilers (Castro Júnior & Silva, 2021).

For this reason, the reduced production performance due to heat stress has been associated with physiological and metabolic changes (Ahmed-Farid et al., 2021; Nawaz et al., 2021). According to Brown-Brandl et al. (2003), the physiological variable cloacal temperature ($t_{cloacal}$) is a suitable indicator of comfort or heat stress in broilers because it is directly related to the internal body temperature and is easy to measure.

Given the importance of the microclimate of the aviary for housed animals, the specific enthalpy of air (h, kJ kg of dry air^{-1}) is the only psychrometric variable that encompasses the concept of thermal energy in the environment, constituting the sum of the latent and sensible heat components, justifying its use for assessing the internal environment of poultry production due to the application of heat exchange physical concepts to animals and their environment (Queiroz et al., 2017; Castro Júnior & Silva et al., 2021).

Within this context, geostatistical techniques have been employed as efficient tools for evaluating thermal variables inside animal breeding facilities (Lopes et al., 2020; Faustino et al., 2021, Silva et al., 2021). Geostatistical analysis allows us to quantitatively characterize the spatial variability as much as the temporal variability in t_{db}, RH and h in installations, avoiding biased data interpretations and allowing the observation of spatial dependence through kriging maps (Oliveira et al., 2022). However, Sans et al. (2021) mentioned a lack of studies that include environmental (for example, h) and animal welfare ($t_{cloacal}$) indicators through geostatistical analysis and, when applied together, can allow the adoption of management strategies to improve animal welfare.

Silva et al. (2021) superimposed data of the respiratory rate and ear surface temperature of rabbits onto spatial distribution maps of the temperature and humidity index (THI) of a rabbit installation and concluded that the overlap between these datasets provided a viable alternative for evaluating environmental housing conditions and their impact on the physiological variables of these animals.

Therefore, the development of spatial distribution maps of h by kriging interpolation, as well as characterizing and evaluating its relationship with the physiological responses ($t_{cloacal}$) of broiler chickens, by applying the methodology of Silva et al. (2021), can be valuable for analyzing the environmental and physiological conditions of broilers due to the ease of interpretation of the developed maps and their application in the poultry industry. Thus, this strategy could provide an improvement in production rates, promote an increase in climate control management efficiency and facilitate the adjustment in daily equipment management in poultry facilities. Moreover, the reduction in production costs due to electricity savings contributes to more sustainable poultry farming (Coulombe et al., 2020).

Therefore, this study was conducted using geostatistical techniques to characterize and evaluate the psychrometric property *h* in a broiler installation, relating this factor to the $t_{cloacal}$ parameter of broilers by overlapping the collected data.

MATERIALS AND METHODS

The research was conducted in Brazil over 42 days, starting in August 2021 and ending in September 2021. Approval for the study was granted by the UFLA Ethics Committee for Animals Use (Protocol No. 006/2020). All the procedures performed with broilers were performed according to the guidelines recommended by this committee.

Experimental barn and broilers

The data for this experiment were obtained at a broiler farming facility situated within the Poultry Sector of the Animal Science Department at the Federal University of Lavras, Minas Gerais, Brazil (coordinates: 21° 14' S, 45° 00' W; altitude: 918 m). In accordance with the Köppen international classification system, the prevailing climate in this area can be categorized as Cwa, indicating a subtropical mesothermal climate with warm and rainy summers and cold and dry winters. The average air temperature is 22.5 °C during the hot season and 16.9 °C during the cold season (Sá Júnior et al., 2012).

The experimental semiclimatized barn is 44 m long and 6.35 m wide, exhibits a ceiling height of 2.90 m, is covered with asbestos tiles and has a concrete floor. Internally, the barn is divided into 30 boxes distributed on each side of the barn, totaling 60 boxes. Each box exhibits dimensions of 1.46 m (length) by 2.2 m (width) and is delineated by open wire meshing structures (4.19-mm wire thickness and 50-mm mesh). Between any two rows of boxes, there is a central corridor that is 44 m long and 1.95 m wide. Each box contains an incandescent lamp for heating (100 W and 220 V), a tubular feeder and a pendular drinker, and the floor is covered with wood shavings. Each side of the barn contains two fans (QLA85T6 model, Qualitas, São Paulo, Brazil) positioned approximately 1.70 m above the floor, with a diameter of 850 mm, a maximum flow of 15,000 m^3 h^{-1} and a rotation speed of 1,110 rpm. These fans can be manually activated when necessary. On the sides of the barn, there are curtains to manually control ventilation and incident sunlight reaching the broilers (Fig. 1, a, b).

One-day-old male Cobb-500 broiler chicks were acquired from a commercial hatchery and were individually weighed (43.0 ± 0.64 g). The experimental design comprised randomized blocks with the right and left sides of the shed defined as blocks. The broilers were distributed in six replicates (experimental units; boxes) of 15 broilers each, totaling 48 experimental units and 720 broilers.

During distribution, the first 24 boxes on each side of the barn were used, and the average weights of the broilers in each box were similar (646.0 ± 5.7 g). The broilers were provided corn and soybean meal (Table 1) designed in accordance with their nutritional needs for 1–7 days, 8–21 days, 22–35 days and 36–42 days of age (Cobb, 2019). The broilers were provided unrestricted access to both feed and water throughout the entire experimental duration (1–42 days of age). The light regime comprised 1 hour of darkness (1–7 days old), 8 hours of darkness (8–20 days old), 7 hours of darkness (21–35 days old) and 6 hours of darkness (36–42 days old), according to the lineage manual (Cobb, 2019).

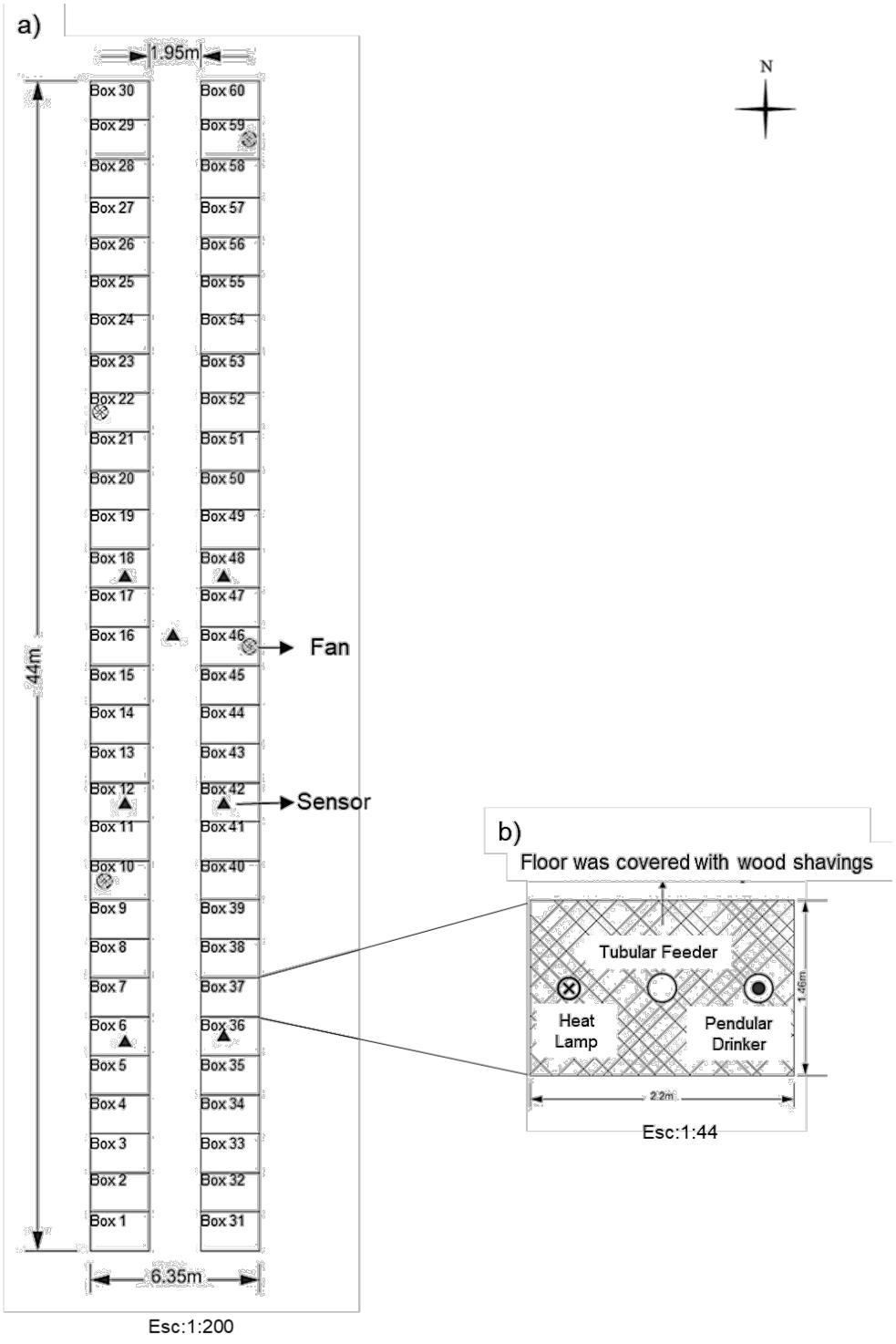

Figure 1. Diagram of the barn used: a) Location of boxes, sensors, and fans; b) Enlarged characterization of the box illustrating the floor type and the positions of the drinker, feeder and heat lamp.

Table 1. Ingredients and calculated nutritional composition (as-fed basis) of the basal diets provided to broilers in the different rearing periods

	Periods of broiler rearing (days of age)			
	1–7	8–21	22–35	36–42
Ingredients (g kg^{-1})				
Corn	562.60	614.55	624.82	645.15
Soybean meal, 45%	365.25	317.60	302.00	277.70
Soybean oil	25.60	24.20	33.29	37.60
Limestone	8.20	7.75	7.10	7.20
Dicalcium phosphate, 18.5%	18.75	17.50	15.45	15.60
Common salt	4.70	4.50	4.57	4.55
DL-Methionine, 99%	3.40	3.20	2.83	2.65
L-Lysine HCl, 99%	2.40	2.00	1.74	1.85
L-Threonine, 98.5%	1.10	0.70	0.20	0.20
Salinomycin, 12%	0.50	0.50	0.50	0.00
Choline chloride, 60%	0.50	0.50	0.50	0.50
Vitamin supplement [1]	1.00	1.00	1.00	1.00
Mineral supplement [2]	1.00	1.00	1.00	1.00
Nutritional composition				
AME (kcal kg^{-1})*	2,975	3,025	3,100	3,150
Crude protein (g kg^{-1})	214.91	196.60	189.52	180.07
Calcium (g kg^{-1})	9.04	8.41	7.61	7.61
Available phosphorus (g kg^{-1})	4.50	4.21	3.81	3.80
Sodium (g kg^{-1})	2.00	1.91	1.94	1.93
Digestible lysine (g kg^{-1})	12.22	11.21	10.22	9.72
Digestible methionine + cysteine (g kg^{-1})	9.13	8.54	8.03	7.63
Digestible threonine (g kg^{-1})	8.30	7.33	6.63	6.32
Digestible tryptophan (g kg^{-1})	2.42	2.18	2.10	1.97

*AME, Apparent metabolizable energy. [1] Levels per kg of supplement: folic acid 902.5 mg; pantothenic acid 12.0 g; biotin 77.0 mg; niacin 40.0 g; selenium 349.6 mg; vitamin A 8800,000.0 IU; vitamin B1 2499.0 mg; vitamin B12 16,200.0 mcg; vitamin B2 5,704.0 mg; vitamin B6 3998.4 mg; vitamin D3 3000000.0 IU; vitamin E 30000.0 IU; vitamin K3 2198.1 mg. [2] Levels per kg of supplement: copper 7000.0 mg; iron 50.0 g; iodine 1,500.0 mg; manganese 67.5 g; zinc 45.6 g.

Characterization of the thermal environment and measurement of the physiological response

Throughout the experiment, the curtains and heating lamps were manually controlled to maintain the internal temperature of the barn as elevated as possible between 9:00 a.m. and 5:00 p.m., ensuring that the value did not surpass an average of 32 °C during this period (Cheng et al., 2019). During the remaining hours of the day, the curtains, heating lamps, and fans were adjusted to maintain the temperature within the designated range for thermal comfort specific to each phase of broiler rearing, as outlined in the lineage manual (Cobb, 2019).

The t_{db} and RH values during broiler rearing were recorded by seven T/HR data loggers (Onset brand, HOBO, model H-08-003-02), which were located at a height compatible with the height of the broilers (0.30 m from the ground) (Curi et al., 2017); three loggers were placed on each side of the barn, and one was placed in the central corridor.

When the broilers were 7, 21, 35 and 42 days old, t_{db} and RH data were recorded at 08:00 a.m. and 01:00 p.m. by all seven sensors (Fig. 1, a, b). These four data collection days were established because they delineate the preinitial (1–7 days old), initial (8–21 days old), growth (22–35 days old) and final (36–42 days old) phases (Rostagno et al., 2017), including changes in feed formulations to satisfy the nutritional needs of the broilers (Table 1). The above two instances of recording were executed with the aim of detecting critical environmental conditions within the facility, following the adapted methodology by Andrade et al. (2022). Thus, *h* values were calculated from the environmental data registered by each sensor for each day (7-, 21-, 35- and 42-day-old broilers) and time (08:00 a.m. and 01:00 p.m.) using Eq. 1, as proposed by Albright (1990):

$$h = 1.006 \text{ x } t_{db} + \text{ W x } (2501 + 1.805 \text{ x } t_{db}) \quad (1)$$

where h is the enthalpy in kJ kg of dry air^{-1}; t_{db} is the dry bulb temperature in °C; and W is the humidity ratio or mixing ratio (W, kg of water vapor kg of dry air^{-1}) of air.

The blending proportion was determined using Eq. 2, which depends on the water vapor pressure (*ea*, kPa) and the atmospheric pressure at the location (P_{atm}, kPa).

$$\text{W} = \frac{0.622 \text{ x } e_a}{P_{atm} - e_a} \quad (2)$$

The local altitude used to calculate P_{atm} was 918 m.

Moreover, at the ages of 7, 21, 35, and 42 days, a single chicken per enclosure was chosen based on the average weight of the group (with a standard deviation of ± 3%), resulting in a total of 48 broilers. The cloacal temperatures ($t_{cloacal}$, °C) of the chosen broilers were assessed using a digital thermometer (model TH1027, G-TECH, Duque de Caxias, RJ, Brazil), with an accuracy of ± 0.2 °C, inserted into the cloaca for a duration of one minute.

Dataset

A dataset comprising unprocessed h (kJ kg of dry air^{-1}) and $t_{cloacal}$ (°C) data from Cobb-500 broilers at 7, 21, 35 and 42 days of age was created. Subsequently, the variability in h within the barn was analyzed via geostatistical analysis and kriging interpolation to obtain h maps for the aforementioned age periods, which were then correlated with the physiological variable $t_{cloacal}$.

Data partitioning method for model validation

The spatial and temporal dependence of the data of environmental variable h was analyzed by semivariogram adjustment using a classical estimator and the restricted maximum likelihood method (REML) (Ferraz et al., 2019a; Ferraz et al., 2020; Silva et al., 2021).

Due to the small dataset, the chosen method is suitable because, according to Ferraz et al. (2019a), the REML produces estimates with reduced bias when applied to small sample sizes. Despite the small amount of data collected, the number of points used in this study is sufficient. Furthermore, within this context, kriging predictors could provide the best linear unbiased predictions (BLUPs) (Lark, 2009; Slaets et al., 2021).

The most effective model adjusted for sentiment is a wave model, as elucidated in the description of Webster & Oliver (2007) (Eq. 3):

$$\hat{\gamma}(\mathrm{h}) = {C_0}^2 + \frac{a}{h}\sin\left(\frac{h}{a}\right)^4 \quad (3)$$

where h is the distance between the samples, C_0 is the nugget effect, and a is the interval.

After obtaining the model and estimated semivariance parameters, the model suitability was verified through cross validation (CV), which is a technique that allows the assessment of estimation errors by comparing the predicted values of the samples, as reported by Isaaks & Srivastava (1989).

The criteria for choosing a model based on the CV technique include considering mean error (ME) and reduced mean error (RE) values that are closer to zero; in addition, the lowest standard deviation of the mean errors (SDME) and the standard deviation of the reduced mean errors (SDRE) closest to one should be selected, according to the methodology of Ferraz et al. (2012). Thus, the model fitted in this study corroborates the findings of Santos et al. (2020) and Silva et al. (2021), as this model is better adapted to studies of environmental variables. After model fitting, the data were interpolated by ordinary kriging to allow the creation of maps and the visualization of the spatial and temporal distributions of h within the poultry house.

For geostatistical analysis, semivariogram function adjustment and data interpolation by the ordinary kriging method, R statistical software and the geoR package (Ribeiro Junior & Diggle, 2001) were employed. Moreover, spatial and temporal distribution maps of h data were generated using QGIS software version 2.14.15.

Finally, the $t_{cloacal}$ data obtained in the morning were superimposed onto maps of environmental data from the poultry facility.

RESULTS AND DISCUSSION

Table 2 indicates that the mean h value ranged from 33.69–53.63 kJ kg dry air^{-1}, considering the evaluation days and times. Table 3 indicates the ranges of t_{db} and RH relative to the thermal comfort of Cobb-500 broilers as a function of age, according to the lineage manual (Cobb, 2019), and the ranges of the variation in h calculated based on the ideal values of t_{db} and RH reported in the manual and obtained according to the equation proposed by Albright (1990).

When comparing the experimentally obtained and calculated ideal h values, it was observed that the h values recorded at 08:00 a.m. and 01:00 p.m. on days 7 and 21 (Table 2) were below the expected range, ranging from 61.08–70.26 kJ kg of dry air^{-1} on day 7 and from 53.77–53.83 kJ kg of dry air^{-1} on day 21 (Table 3). However, on day 35 at 01:00 p.m. and on day 42 at 08:00 a.m. and 01:00 p.m., when considering all the sensor measurements (Table 2), the h values exceeded the ideal ranges (Table 3) considered thermally comfortable for broilers. Furthermore, on day 35 at 08:00 a.m., the h values were 36.30 kJ kg of dry air^{-1} for sensor 2 and 36.75 kJ kg of dry air^{-1} for sensor 5. Notably, the h values were close to the comfortable range (36.38–36.63 kJ kg of dry air^{-1}) for rearing Cobb-500 broilers.

Table 2. The values of dry bulb temperature (t_{db}, °C), relative air humidity (RH, %) and specific enthalpy of air (*h*, in kJ kg of dry air^{-1}) at 08:00 a.m. and 1:00 p.m. recorded by sensors inside the conventional broiler house when the Cobb-500 broilers were 7, 21, 35 and 42 days old

8:00 a.m.					1:00 p.m.				
Day old	Sensors	t_{db}	RH	*h*	Day old	Sensors	t_{db}	RH	*h*
		°C	%	kg of dry air^{-1}			°C	%	kg of dry air^{-1}
7	1	20.76	62.65	45.95	7	1	27.92	31.90	47.25
	2	20.76	61.55	45.46		2	28.31	29.15	46.27
	3	20.76	61.05	45.24		3	28.11	30.85	46.99
	4	20.95	60.30	45.42		4	27.72	29.45	45.20
	5	20.19	68.00	46.69		5	27.72	32.20	47.00
	6	20.19	54.80	41.07		6	26.73	31.75	44.53
	7	20.76	66.70	47.75		7	26.93	37.40	48.53
21	1	20.95	50.10	40.90	21	1	32.35	23.70	50.87
	2	21.33	49.85	41.69		2	32.76	25.20	53.10
	3	20.95	56.00	43.50		3	32.14	23.90	50.58
	4	20.95	49.80	40.77		4	31.32	24.85	49.61
	5	20.00	59.25	42.46		5	31.32	23.60	48.60
	6	20.38	49.20	39.17		6	31.52	24.90	50.08
	7	20.57	59.25	43.94		7	30.71	24.20	47.80
35	1	22.10	36.40	37.27	35	1	31.93	25.00	51.06
	2	22.29	33.45	36.30		2	31.93	25.00	51.06
	3	22.10	36.90	37.50		3	31.93	25.00	51.06
	4	21.53	34.35	35.22		4	31.12	24.80	49.14
	5	21.52	37.85	36.75		5	30.92	24.30	48.31
	6	21.33	31.65	33.69		6	31.12	24.80	49.14
	7	21.53	41.70	38.48		7	31.32	23.85	48.80
42	1	21.52	66.50	49.87	42	1	26.54	44.15	51.80
	2	22.29	64.05	50.94		2	26.93	40.85	50.72
	3	21.90	66.95	51.21		3	26.54	42.40	50.70
	4	21.90	63.90	49.74		4	26.34	40.15	48.80
	5	21.90	69.60	52.49		5	26.34	44.80	51.68
	6	21.71	57.45	46.15		6	26.15	34.60	44.97
	7	21.52	74.45	53.63		7	25.76	49.75	53.12

Therefore, to better understand the influence of physical properties on the avian environment, *h* was calculated, with its values serving as a reference for decision-making. Although both t_{db} and RH are reference parameters for evaluating thermal stress in production animals, the change in the specific enthalpy of air (*h*, kJ kg of dry air^{-1}) can determine whether heat is released (exothermic) or absorbed (endothermic) during a given reaction (Correia & Oliveira, 2019).

Faustino et al. (2021) and Harada et al. (2021) suggested the psychrometric variable *h* for evaluating discomfort and animal ambience conditions since its calculation involves t_{db}, RH and atmospheric pressure, which are environmental variables normally available at meteorological stations. According to Pecoraro et al. (2024), for the productive performance of broiler chickens, in addition to the temperature within the comfort *h* range, adequate ranges of t_{db} and RH are necessary, especially at the final stages of rearing (21–42 days).

According to the information presented in Table 2, the *h* data exhibited variability throughout the analyzed period. However, this exploratory analysis does not provide a definitive assessment of the presence or absence of heterogeneity in both the spatial and temporal distributions of *h* within poultry houses, as described by Ferraz et al. (2019a). To address this issue, geostatistical analysis of *h* was conducted to systematically evaluate variability during the study period, following methods outlined in previous studies (Ferraz et al., 2020; Andrade et al., 2022; Oliveira et al., 2022).

Table 3. Relative air humidity (RH), dry bulb temperature (t_{db}) and specific enthalpy of air (*h*), which influence the thermal comfort of Cobb-500 broilers, as a function of age

Days old	RH (%)	t_{db} (°C)	*h* (kJ kg of dry air^{-1})
7	40–60	29–31	61.08–70.26
21	50–60	24–26	53.77–53.83
35	50–40	19–21	36.38–36.63
42	50–70	18–20	38.62–41.41

To enhance both quantitative and qualitative assessments of *h*, descriptive statistics and geostatistical techniques were employed. These methods aimed to provide crucial insights into the spatial distribution of each *h* class and to better understand the variability and impact of *h* within the investigated environment. Table 4 provides the model results and parameters derived from the experimental semivariograms adjusted for *h* in the poultry house on days 7, 21, 35, and 42 at 8:00 a.m. and 1:00 p.m.

Table 4. The REML method, wave model and the parameters estimated from experimental semivariograms applied to assess specific enthalpy of air (*h*, in kJ kg of dry air^{-1}) in a conventional barn utilized for raising Cobb-500 broilers

Days old	Hour	C_0*	C_1*	C_0+C_1*	a (m)*	DSD*		ME*	SDME*	RE*	SDRE*
7	8 a.m.	0.0	3.670	3.670	0.077	100%	strong	0.000	2.414	0.000	1.167
	1 p.m.	0.0	1.504	1.504	0.080	100%	strong	0.000	1.545	0.000	1.167
20	8 a.m.	0.0	2.322	2.322	0.145	100%	strong	0.000	1.920	0.000	1.167
	1 p.m.	0.0	2.557	2.557	0.667	100%	strong	0.000	2.015	0.000	1.167
35	8 a.m.	0.0	2.140	2.140	0.082	100%	strong	0.000	1.843	0.000	1.167
	1 p.m.	0.0	1.258	1.258	0.051	100%	strong	0.000	1.413	0.000	1.167
42	8 a.m.	0.0	4.775	4.775	0.078	100%	strong	0.000	2.753	0.000	1.167
	1 p.m.	0.0	5.997	5.997	0.078	100%	strong	0.000	3.086	0.000	1.167

* C0 – nugget effect; C1 – contribution; C0 + C1 – threshold; a – reach; DSD – degree of spatial dependence; ME – mean error; SDME – standard deviation of mean error; RE – reduced mean error; SDRE – standard deviation of reduced mean error.

The C_0 values for various days and times are provided in Table 4. As outlined by Ferraz et al. (2019a) and Santos et al. (2020), C_0 denotes the unexplained variability, considering the sampling distance as a significant parameter of the semivariogram. In other words, C_0 represents an unaccounted variable or random variance, typically attributable to measurement errors or variability in the measured property undetected at the sampling scale (Bhatti et al., 1991). Thus, for the purpose of comparing the magnitudes of the degree of spatial dependence (DSD) of the studied variable, the contributions of individual error were calculated, thereby expressing C_0 as a proportion of $C_0 + C_1$ (Table 4) (Trangmar et al.,1986).

Throughout the entire experimental period, C_0 equaled 0, indicating that the experimental error was practically null and that there was no significant variation at distances smaller than the sampling distance (Ferraz et al., 2019b), i.e., if the sensors were placed closer together, there would be no significant variation. Therefore, the sampling distance was suitable, and the experimental error was null when arranging the sensors to create a sampling network within the facility (Ferraz et al., 2019b).

Cajazeira & Assis Júnior (2011) characterized and geostatistically analyzed the spatial variations in the physical attributes of a Yellow Argisol across two soil layers. Surface maps were prepared using the kriging method. Their findings revealed that for the subsurface layer, the silt content exhibited a nugget effect close to 0%, suggesting a minimal experimental error. This indicates the insignificance of variable sampling at distances smaller than those employed. Thus, the results obtained by these authors corroborate the results of this study.

The reach values (a) of the semivariograms are significant for establishing the spatial dependence boundaries of *h,* as they represent the extent to which the sampling units exhibit correlations, as emphasized by Silva et al. (2021) and Oliveira et al. (2022). These parameters are instrumental in sampling design, aiding in identifying locations for environmental variable sampling, as described by McBratney & Webster (1983). The largest ranges (Table 4) were obtained on day 21 at 08:00 a.m. and 01:00 p.m. (0.145 and 0.667 m, respectively), while day 35 exhibited the lowest spatial continuity at 01:00 p.m. (0.051 m). Thus, it was found that the samples collected at distance a (Table 4), at which point the distance no longer influences the variable *h*, resulted in experimental semivariogram stability, which is agrees with the semivariogram behavior in the studies of Santos et al. (2020) and Silva et al. (2021).

The DSD was determined by assessing the ratio between C_0 and $C_0 + C_1$, following the classification proposed by Cambardella et al. (1994). In this classification, a DSD value is considered strong if the ratio between C_0 and $C_0 + C_1$ is $\leq 25\%$, moderate if the ratio is $> 25\%$ and $< 75\%$, weak if the ratio is $\geq 75\%$ and $<100\%$, and neutral if the ratio is equal to 100%. Notably, throughout the analysis period, the ratio between C_0 and $C_0 + C_1$ was $\leq 25\%$, and the DSD of the *h* variable could be considered strong.

According to Santos et al. (2020) and Silva et al. (2021), the strong DSD value of *h* obtained during the analysis period may be related to the wave model, which is better adapted to studies of environmental variables. In addition, on the analysis days and times, experimental semivariogram adjustment yielded ME and ER values close to zero, which conforms with the recommendations of Ferraz et al. (2012) and indicates the analysis quality and efficiency (Faraco et al., 2008) for assessing the comfort levels of animals in the production environment.

The obtained results suggested that the spatial distributions of the climatic attributes are not random since they exhibit strong DSD values, suggesting that geostatistical techniques are appropriate (Damasceno et al., 2019; Oliveira et al., 2019). Thus, the occurrence of spatial dependence allowed the interpolation of *h* data through kriging, which is commonly used to perform geostatistical mapping via spatial distribution maps (Damasceno et al., 2019).

Queiroz et al. (2017), Silva et al. (2021) and Andrade et al. (2022) suggested the use of isocolor maps of the spatial distribution of the THI and *h* in chicken, rabbit and dairy cattle production barns, respectively, with the objective of characterizing and identifying areas with different spatial variabilities in these environmental thermal

control indicators. According to the authors, this visual tool allows the identification of environmental conditions harmful to the thermal comfort of the animals and their timely correction.

With the use of the values derived from kriging, isocolor maps were generated, which show the spatial distribution of *h* within the poultry house. This allowed for examining the magnitude and variability in this variable throughout the experimental period within the facility (Fig. 2, a, b, c, d, e, f, g, h).

Fig. 2 shows that on days 7, 21, 35 and 42 at 08:00 a.m. (Fig. 2, a–d), *h* ranged from <35.1 to > 51.9 kJ kg of dry air^{-1}. In addition, on the same experimental days, at 01:00 p.m. (Fig. 2, e–h), *h* varied between 45.6 and 51.9 kJ kg of dry air^{-1}. Thus, the obtained *h* variability maps revealed that under the environmental conditions, the broilers were kept in boxes (with spatial variability) and throughout the experimental period (with temporal variability).

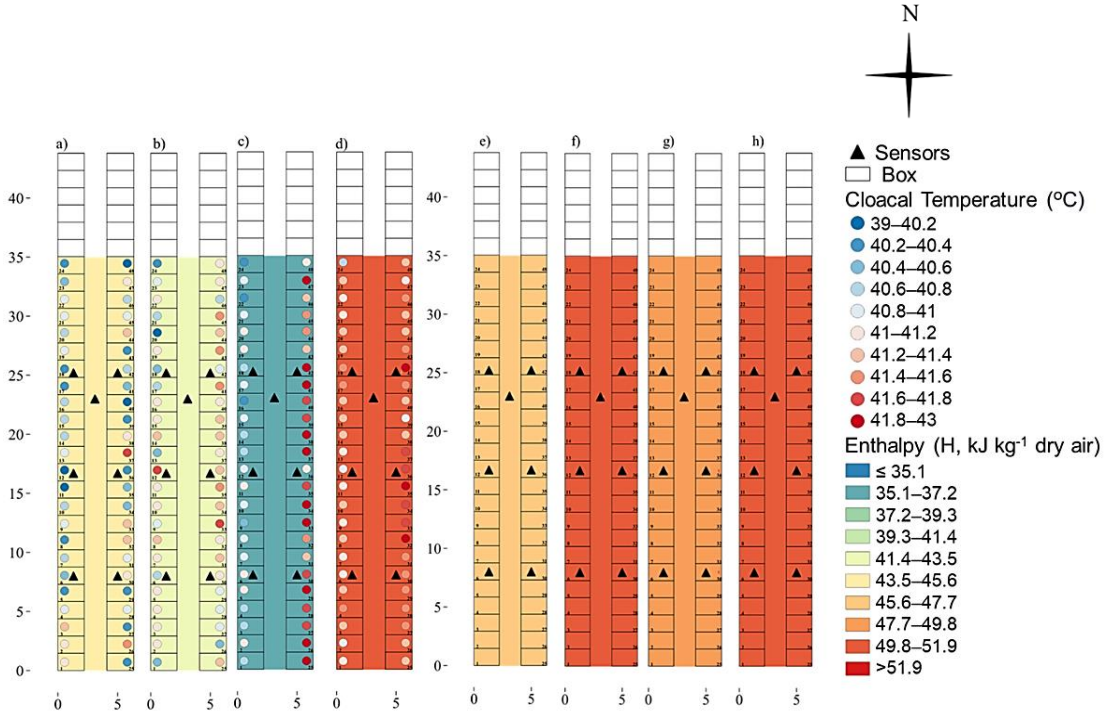

Figure 2. Spatial and temporal distribution of specific enthalpy of air (*h*, in kJ kg of dry air^{-1}) and cloacal temperature ($t_{cloacal}$, °C) in a conventional broiler house, according to the days and times studied: a) day 7, at 08:00 a.m.; b) day 21 at 08:00 a.m.; c) day 35 at 08:00 a.m.; d) day 42 at 08:00 a.m.; e) day 7 at 01:00 p.m.; f) day 21 at 01:00 p.m.; g) day 35 at 01:00 p.m.; and h) day 42 at 01:00 p.m.

On days 7 (Fig. 2, a, 4e) and 21 (Fig. 2, b, f), at both times, *h* ranged from 41.4–51.9 kJ kg of dry air^{-1}. The temperature in the entire poultry house was below the comfortable value for broilers in this age group (Table 3). Conversely, on day 35 at 01:00 p.m. (Fig. 2, g) and day 42 at 08:00 a.m. and 01:00 p.m. (Fig. 2, d, h), the thermal conditions inside the facility were high, with *h* varying between 47.7 and > 51.9 kJ kg of dry air^{-1}, demonstrating that during this period, the broilers may have experienced heat stress.

In Brazil, intensive broiler production is conducted mainly in semiclimatized or climatized barns (Lima & Silva, 2019; Sans et al., 2021). The type of semiclimatized barn used in our research is characterized by open sides, natural light complemented by artificial light, adjustable curtains and positive pressure fans, similar to the structure used in industrial commercially designed barns (Sans et al., 2021). There was transverse ventilation in the barn used in our study, and the curtains and fans were manually managed as necessary. Therefore, air exchange between the internal microenvironment of the barn and the external environment of the installation, as well as the limitations of the fans, may have contributed to the increase in enthalpy during this period.

Only on day 35 at 08:00 a.m. (Fig. 2, c) were the broilers exposed to thermal conditions (*h* varying between 35.1 and 37.2 kJ kg of dry air^{-1}) considered close to ideal for rearing, with *h* varying between 36.38 and 36.63 kJ kg of dry air^{-1} (Table 3).

Based on geostatistics analysis, it was noted that throughout the experimental duration (7, 21, 35 and 42 days old; 08:00 a.m. and 01:00 p.m.), there were variations in *h* (temporal variability) (Tables 2 and 4, Fig. 2, a–h) within the poultry house. The spatial variability, namely, the variations within the boxes in this study, was determined, as detailed in Table 2.

In Fig. 2, there was no variation in *h* between the boxes, and the scale used did not allow variation observation. This fact could be attributed to the number of samples collected, so studies are recommended to improve the distribution of sensors, studies should be conducted involving a greater number of sensors, and studies should be performed aimed at the direct identification of the spatial variability. However, understanding the spatial-temporal distribution of *h* within poultry houses is crucial for detecting potential fluctuations in the daily thermal conditions of the production microenvironment. This is significant because approximately ideal and consistent conditions are desirable to ensure that broilers can achieve their maximum productive performance throughout the housing period.

Sans et al. (2021) evaluated the spatial distributions of the environmental variables RH, t_{db}, air velocity, ammonia (NH_3) and carbon dioxide (CO_2) concentrations and illuminance in closed- and open-sided broiler chicken farms. The authors observed the heterogeneity in these variables within facilities using kriging maps, and it was demonstrated which indicators influenced the deterioration in the poultry house microclimate (higher temperatures and NH_3 and CO_2 concentrations). In this way, they could identify strategic points within the poultry house to manage the equipment to promote better ambience and minimize the occurrence of regions with little air exchange (dead spots), thus improving the quality and production of broiler batches. The authors also highlighted the importance of constant broiler welfare monitoring at key barn locations and the use of other environmental and physiological indicators for new observations of spatial distributions.

Within this context, the maps of the spatial and temporal distributions of *h* (Fig. 2, a–h) show different environmental conditions between the boxes, days and hours in the same broiler rearing barn. Therefore, the results demonstrated the need for greater control of the ambient temperature in the studied barn so that there is no compromise in the productive performance of future batches that will be housed in this facility. As such, the significance and practical utility of employing maps to visualize the spatial and temporal patterns of environmental variables are exemplified. Such maps are visual tools

to support decision-making so that critical welfare and management points can be quickly identified and corrected, thus allowing higher efficiency in climate control management and daily equipment adjustments in poultry facilities (Sans et al., 2021).

Moreover, understanding the impact of environmental factors on the physiological reactions of broilers to heat stress (Moghbeli Damane et al., 2018; Siddiqui et al., 2020) is necessary for understanding the adverse effects of unfavorable thermal conditions on organism functions. These effects include changes in the body antioxidant capacity, immunity, and intestinal morphology and physiology (Sahin et al., 2017; Song et al., 2018).

Fast-growing broilers, such as Cobb-500 broilers, exhibit a high central body temperature due to their increased metabolic activity resulting from targeting genetic selection programs for increased growth rates (Jahejo et al., 2016). During the last weeks of the production cycle, when energy metabolism is accelerated and heat dissipation is hampered by body warming, broilers are more susceptible to heat stress when exposed to high room temperatures (Awad et al., 2020). Notably, during the first two weeks of life, broilers are more susceptible to cold stress, whereas during the last two weeks, they are prone to heat stress, emphasizing the crucial need to prevent excessive exposure of broilers to elevated temperatures (Lara & Rostagno, 2013; Pecoraro et al., 2024).

When the room temperature exceeds the thermoneutral zone, broilers rely on physiological responses that aim to reduce heat production and/or increase the dissipation of excess heat to the environment (Castro Júnior & Silva et al., 2021). According to Brown-Brandl (2003), $t_{cloacal}$ is a suitable indicator of comfort or thermal stress due to its direct relationship with the central body temperature and ease of measurement. The ideal body temperature of broilers varies according to age, with values ranging from 39.6–40.6 °C for 0- to 7-day-old broilers, 40.0–41.1 °C for 8- to 21-day-old broilers, 41.2–41.7 °C for 22- to 35-day-old broilers and 41.2–41.6 °C for 36- to 42-day-old broilers (Marchini et al., 2007; Pires et al., 2020; Olgun et al., 2021).

Thus, the $t_{cloacal}$ values recorded on days 7, 21, 35 and 42 were superimposed onto the spatial maps of the environmental variable *h* in the poultry facility during the morning period (Fig. 2, a–h). Fig. 2, c, and d show that the $t_{cloacal}$ values of the broilers housed on the west side of the barn on days 35 and 42 ranged from 41.6–43 °C and 41.2–43 °C, respectively, in most boxes. These temperatures exceed what is considered ideal for broilers over the period considered ($t_{cloacal}$ at 35 days old = 41.2–41.7 °C; $t_{cloacal}$ at 42 days old = 41.2–41.6 °C). Conversely, when considering the broilers housed on the east side of the barn, on day 35 (Fig. 2, c), $t_{cloacal}$ values between 40.2 and 41.0 °C were recorded, which are below the values (41.2–41.7 °C) considered ideal for the age group, while only on days 21 (Fig. 2, b) and 42 (Fig. 2, d) were the broilers exposed to potentially comfortable conditions for their development, with $t_{cloacal}$ values ranging from 40.2–41.2 °C and 41.2–41.6 °C, respectively.

However, on day 7 (Fig. 2, a), in most boxes on the east side of the barn, the $t_{cloacal}$ values remained between 40.6 and 41.2 °C, demonstrating that during this period, the broilers may have experienced difficulty maintaining their body temperature, as *h* ranged from 43.5–45.6 kJ kg of dry air^{-1}, i.e., below the values recommended for the age group (*h* = 61.08–70.26 kJ kg of dry air^{-1}, Table 3). A factor that may have contributed to this finding is that barn heating was not enough to maintain the ideal conditions for the broilers on day 7. Thus, in the presence of cold stress, broilers strive to maintain

homeothermic conditions by increasing heat production and energy consumption (through feed) while minimizing heat loss, as noted by Hernandez et al. (2016).

It is important to highlight that the initial week of a broiler's life demands heightened care and attention from the producer. Errors in management during this phase, if recurrent, cannot be rectified later, impacting the ultimate performance of the broilers through delayed weight gain and/or the onset of diseases attributed to cold stress, as indicated by Tinôco et al. (2004). Recognizing the importance of warming the internal microenvironment of barns during the initial weeks of broiler life (Menegali et al., 2013), it is important to map the spatial distribution of *h* while incorporating physiological data from broiler chickens. This approach holds critical relevance in the animal-raising process, as it offers insights into the complex interactions between air properties and the physiological principles of animal thermoregulation. This method is both cost-effective and user-friendly, enabling adjustments in daily equipment management to enhance the thermal environment of the facility.

The observed values of $t_{cloacal}$ (Fig. 2, a, b, c, d) are consistent with the spatial and temporal distribution of *h* inside the barn (Fig. 2, a–h), and the physiological parameter $t_{cloacal}$ is directly related to the variation in *h*. This is due to the temporal distribution of *h* throughout the analysis period, demonstrating that the increase and/or reduction in *h* may have affected the ability of broilers to regulate their body temperature effectively.

During the experimental period, the broilers experienced thermal conditions outside their comfort range, posing an environmental challenge that, depending on its intensity and duration, could lead to a decline in their productive performance. It is widely acknowledged that thermoneutral environments allow animals to manifest their maximum genetic potential due to the lower energy deviation in thermoregulatory processes (Moghbeli Damane et al., 2018; Goo et al., 2019; Ahmed-Farid et al., 2021).

According to Awad et al. (2018) and Liu et al. (2020), a meta-analysis revealed adverse effects when broilers occurred outside their thermal comfort range. These effects include reduced body weight gain (GWG, g), diminished feed intake, and an elevated feed conversion rate (FC, g g^{-1}) in live broilers, ultimately leading to a subpar meat quality. In addition, adverse effects on the intestinal microbiome were detected in broilers under heat stress (Song et al., 2018). Therefore, to mitigate the harmful consequences of environmental stress, strategies for alleviating the impact of temperature on production and reducing economic losses in the poultry industry are urgently needed (Liu et al., 2020).

Therefore, studies have actively advanced new technologies for assessing thermal stress among broiler chickens. These studies focused on microclimatic air variables, with a particular emphasis on psychrometric properties such as t_{db} and RH (Sans et al., 2021; Cho et al., 2022). Although both t_{db} and RH are key parameters for assessing thermal stress in production animals, *h* is the only psychrometric parameter that comprehensively embodies the notion of thermal energy within the environment. Notably, *h* represents the combined latent and sensible heat, justifying its application considering these fundamental principles of heat exchange between animals and their surroundings (Castro Júnior & Silva, 2021; Pecoraro et al., 2024).

Britto (2010) described the possibility of devising strategies for environmental control based on the variation in psychrometric properties within a specific system (from sampling P to P'). Under this scenario, geostatistical analysis could aid in visualizing psychometric parameter variations by employing kriging maps. This tool

enables the differentiation and visualization of areas with variations in microclimatic attributes across space, such as *h*. This tool could help in identifying problematic areas within poultry houses, as described by Sans et al. (2021) and Queiroz et al. (2017).

It is crucial to highlight that productivity and financial and animal welfare indexes can be improved when the use of electrical equipment, such as lamps, fans, evaporative cooling systems, exhaust fans and/or sprinklers, is optimized to promote better ambience. Moreover, electricity savings contribute to more sustainable poultry farming (Coulombe et al., 2020).

Sans et al. (2021) mentioned the lack of studies that include environmental indicators (for example, *h*) and well-being-related indicators ($t_{cloacal}$) of animals that can be assessed through geostatistical analysis, and their combined use could facilitate the implementation of strategies to enhance broiler production.

In summary, the utilization of spatial distribution maps for *h* enables the provision of more precise information to producers regarding variations in thermal conditions during broiler housing. This facilitates increased efficiency in climate control management and adjustments in daily operational management of equipment in poultry facilities, particularly those in areas with tropical climates.

CONCLUSIONS

The geostatistical analysis technique allowed verification of the occurrence of spatial and temporal variabilities in *h* in a conventional poultry barn, demonstrating that broilers possibly experienced thermal discomfort due to *h* oscillation.

Notably, $t_{cloacal}$ was directly related to the spatial distribution of *h*, highlighting the importance of interventions aimed at improving the ambient temperature for subsequent batches of broilers to be housed in the same facility.

Therefore, the optimization of data collection of microclimatic variables within poultry facilities (use of more sensors) and measurements of physiological variables of broiler chickens in real time would be necessary to enhance the database and the accuracy of this methodology in future studies. This would improve the information provided to producers and help them identify variations in the thermal environment and facilitate changes in daily equipment operation at poultry facilities.

ACKNOWLEDGEMENTS. The authors would like to thank the Federal University of Lavras, where the experiment was performed. JCDR thanks the scholarship provided by the CNPq. LPN thanks the research productivity grant provided by CNPq (protocol number 312436/2020-3).

REFERENCES

Abdel-Moneim, E., Abdel-Moneim, A.M., Shehata, R.E.K., Vinod, K.P., Nashaat, S.I, Abdelkawy, A. El-G., Sami, A.A., Salah, A.G., Noura, M.M., Ahmed, M.E., Mohamed, A.E., Magda, M.W. & TArek, A.E. 2021. Nutritional manipulation to combat heat stress in poultry–A comprehensive review. *Journal of Thermal Biology* **98**, 102915. doi: 10.1016/j.jtherbio.2021.102915

Ahmed-Farid, O.A., Ayman, S.S, Mohamed, A.N. & Mahmoud, S. El-Tarabany. 2021. Effects of Chronic Thermal Stress on Performance, Energy Metabolism, Antioxidant Activity, Brain Serotonin, and Blood Biochemical Indices of Broiler Chickens. *Animals* **11**(9), 2554. doi: https://doi.org/10.3390/ani11092554

Albright, L.D. 1990. *Environment control for animals and plants*. American Society of Agricultural Engineers Michigan. 1.ed. St Joseph: Michigan, 453 pp.

Andrade, R.R., Tinôco, I.F.F., Damasceno, F.A., Ferraz, G.A.S., Freitas, L.C.S.R., Ferreira, C.F.S., Barbari, M. & Teles Junior, C.G.S. 2022. Spatial analysis of microclimatic variables in compost-bedded pack barn with evaporative tunnel cooling. *Anais da Academia Brasileira de Ciências* **94**, e20210226. doi: 10.1590/0001-3765202220210226

Awad, E.A., Idrus, Z., Soleimani Farjam, A., Bello, A.U. & Jahromi, M.F. 2018. Growth performance, duodenal morphology and the caecal microbial population in female broiler chickens fed glycine-fortified low protein diets under heat stress conditions. *British Poultry Science* **59**(3), 340–348. doi: 10.1080/00071668.2018.1440377

Awad, E.A., Najaa, M., Zulaikha, Z.A., Zulkifli, I. & Soleimani, A.F. 2020. Effects of heat stress on growth performance, selected physiological and immunological parameters, caecal microflora, and meat quality in two broiler strains. *Asian-Australasian Journal of Animal Sciences* **33**, 5778–787. doi: 10.5713/ajas.19.0208

Bhatti, A.U., Mulla, D.J. & Frazier, B.E. 1991. Estimation of soil properties and wheat yields on complex eroded hills using geostatistics and thematic mapper images. *Remote Sensing of Environment* **37**(3), 181–191. doi: 10.1016/0034-4257(91)90080-P

Britto, J.F.B. 2010. Considerations about psychrometrics. *Revista SBCC* **45**, 35–41 (in Portuguese).

Brown–Brandl, T.M., Yanagi, T., Xin, H., Gates, R.S., Bucklin, R.A. & Ross, G.S. 2003. A new telemetry system for measuring core body temperature in livestock and poultry. *Applied Engineering in Agriculture* **19**(5), 583. doi: 10.13031/2013.15316

Cajazeira, J.P. & Assis Júnior, R.N.D. 2011. Spatial variability of the primary fractions and aggregate of an Ultisol in the state of Ceará, Brazil. *Revista Ciência Agronômica* **42**, 258–267 (in Portuguese).

Cambardella, C.A., Moorman, T.B., Novak, J.M., Parkin, T.B., Karlen, D.L., Turco, R.F. & Konopka, A.E. 1994. Field-scale variability of soil properties in central Iowa soils. *Soil Science Society of America Journal* **58**(5), 1501–1511. doi: 10.2136/sssaj1994.03615995005800050033x

Castro Júnior, S.L. & Silva, I.J.O.D. 2021. The specific enthalpy of air as an indicator of heat stress in livestock animals. *International Journal of Biometeorology* **65**, 149–161. doi: 10.1007/s00484-020-02022-8

Cheng, Y.F., Chen, Y.P., Chen, R., Su, Y., Zhang, R.Q., He, Q.F., Wang, K., Wen, C. & Zhou, Y.M. 2019. Dietary mannan oligosaccharide ameliorates cyclic heat stress-induced damages on intestinal oxidative status and barrier integrity of broilers. *Poultry Science* **98**(10), 4767–4776. doi: 10.3382/ps/pez192

Cho, J.H., Lee, I.B., Lee, S.Y., Park, S.J., Jeong, D.Y., Decano-Valentin, C.& Lee, S.J. 2022. Development of Heat Stress Forecasting System in Mechanically Ventilated Broiler House Using Dynamic Energy Simulation. *Agriculture* **12**(10), 1666. doi: 10.3390/agriculture12101666

Cobb. 2019 Broiler-Guide. *Broiler Management Manual Cobb-500*. COBB-VANTRESS, pp.112.

Correia, J.J. & Oliveira, W.C.A. 2019. Definition of enthalpy in textbooks. Binacional Magazine Brazil-Argentina: *Dialogue between Sciences* **8**, 327–353. doi: https://doi.org/10.22481/rbba.v8i1.4912 (in Portuguese).

Coulombe, F., Rousse, D.R. & Paradis, P.L. 2020. CFD simulations to improve air distribution inside cold climate broiler houses involving heat exchangers. *Biosystems Engineering* **198**, 105–118. doi: 10.1016/j.biosystemseng.2020.07.015

Curi, T.M.R.D.C., Conti, D., Vercellino, R.D.A., Massari, J.M., Moura, D.J.D., Souza, Z.M.D. & Montanari, R. 2017. Positioning of sensors for control of ventilation systems in broiler houses: a case study. *Scientia Agricola* **74**, 101–109. doi: 10.1590/1678-992x-2015-0369

Damasceno, F.A., Oliveira, C.E.A., Ferraz, G.A.S., Nascimento, J.A.C., Barbari, M. & Ferraz, P.F.P. 2019. Spatial distribution of thermal variables, acoustics and lighting in compost dairy barn with climate control system. *Agronomy Research* **17**, 385–395. doi: 10.15159/AR.19.115

Faraco, M.A., Uribe-Opazo, M.A., Silva, E.A.A.D., Johann, J.A. & Borssoi, J.A. 2008. Selection criteria of spatial variability models used in thematical maps of soil physical attributes and soybean yield. *Revista Brasileira de Ciência do Solo* **32**, 463–476. doi: 10.1590/S0100-06832008000200001 (in Portuguese).

Faustino, A.C., Turco, S.H., Silva Junior, R.G., Miranda, I.B., Anjos, I.E. & Lourençoni, D. 2021. Spatial variability of enthalpy and illuminance in free-range broiler sheds. *Revista Brasileira de Engenharia Agrícola e Ambiental* **25**, 340–344. doi: 10.1590/1807-1929/agriambi.v25n5p340-344

Ferraz, G.A.S., Silva, F.M.D., Carvalho, L.C., Alves, M.D.C. & Franco, B.C. 2012. Spatial and temporal variability of phosphorus, potassium and of the yield of a coffee field. *Engenharia Agrícola* **32**, 140–150. doi: 10.1590/S0100-69162012000100015 (in Portuguese).

Ferraz, P.F., Ferraz, G.A., Damasceno, F.A., Moura, R.S.D., Silva, M.A.J.G. & Rodrigues, R.D.L. 2019a. Spatial variability of enthalpy in rabbit house with and without ridge vent. *Revista Brasileira de Engenharia Agrícola e Ambiental* **23**, 126–132. doi: 10.1590/1807-1929/agriambi.v23n2p126-132

Ferraz, P.F.P., Ferraz, G.A.S., Schiassi, L., Nogueira, V.H.B., Barbari, M. & Damasceno, F.A. 2019b. Spatial variability of litter temperature, relative air humidity and skin temperature of chicks in a commercial broiler house. *Agronomy Research* **17**(2), 408–417. doi: 10.15159/AR.19.112

Ferraz, P.F.P., Gonzalez, V.C., Ferraz, G.A.S., Damasceno, F.A., Osorio, J.A.S. & Conti, L. 2020. Assessment of spatial variability of environmental variables of a typical house of laying hens in Colombia: Antioquia state Case. *Agronomy Research* **18**, 1244–1254. doi: 10.15159/AR.20.099

Goo, D., Kim, J.H., Park, G.H., Delos Reyes, J.B. & Kil, D.Y. 2019. Effect of heat stress and stocking density on growth performance, breast meat quality, and intestinal barrier function in broiler chickens. *Animals* **9**(3), 107. doi: 10.3390/ani9030107

Harada, É.S., Montanhani, M.E.S., Bueno, L.G.deF., Mollo Neto, M., Souza, S.R.L.de & Fonseca, R.da. 2021. Enthalpy-based decision trees for comfort assessment for light layers in tropical climates. *Research, Society and Development* **10**, 1–10. doi: https://doi.org/10.33448/rsd-v10i3.13354 (in Portuguese).

Hernandez, R.O., Tinoco, I.F., Osorio, S.J.A., Mendes, L.B. & Rocha, K.S. 2016. Thermal environment in two broiler barns during the first three weeks of age. *Revista Brasileira de Engenharia Agrícola e Ambiental* **20**, 256–262. doi: 10.1590/1807-1929/agriambi.v20n3p256-262

Isaaks, E.H. & Srivastava, R.M. 1989. *Applied geostatistics*. New York: Oxford University, 561 pp.

Jahejo, A.R., Rajput, N., Rajput, N.M., Leghari, I.H., Kaleri, R.R., Mangi, R.A. & Pirzado, M.Z. 2016. Effects of heat stress on the performance of Hubbard broiler chicken. *Cells, Animal and Therapeutics* **2**(1), 1–5.

Lara, L.J. & Rostagno, M.H. 2013. Impact of heat stress on poultry production. *Animals* **3**(2), 356–369. doi: 10.3390/ani3020356

Lark, R.M. 2009. Kriging a soil variable with a simple nonstationary variance model. *Journal of Agricultural, Biological, and Environmental Statistics* **14**, 301–321. doi: 10.1198/jabes.2009.07060

Lima, V.A. & Silva, I.J.O. 2019. Poultry farming and laying in Brazil overcomes its challenges with technology and in a sustainable way. *In*: Hartung, J., Paranhos da Costa, M., Perez, C. (Eds.), Animal welfare in Brazil and Germany: responsibility and sustainability. GRAFTEC Gráfica e Editora Ltda, pp. 116–123 (in Portuguese).

Liu, L., Ren, M., Ren, K., Jin, Y. & Yan, M. 2020. Heat stress impacts on broiler performance: a systematic review and meta-analysis. *Poultry Science* **99**(11), 6205–6211. doi: 10.1016/j.psj.2020.08.019

Lopes, I., Silva, M.V.D., Melo, J.M.D., Montenegro, A.A.D.A. & Pandorfi, H. 2020. Geostatistics applied to the environmental mapping of aviaries. *Revista Brasileira de Engenharia Agrícola e Ambiental* **24**(6), 409–414.

Marchini, C.F.P., Silva, P.L., Nascimento, M.R.B.M. & Tavares, M. 2007. Respiratory frequency and cloacal temperature in broiler chickens submitted to high cyclic ambient temperature. *Arch Vet Sci* **12**(1).

Mcbratney, A.B. & Webster, R. 1983. How many observations are needed for regional estimation of soil properties? *Soil Science* **135**(3), 177–183.

Menegali, I., Tinoco, I.F., Carvalho, C.D., Souza, C.D.F. & Martins, J.H. 2013. Behavior of environmental variables on minimum ventilation systems for the production of broiler chickens. *Revista Brasileira de Engenharia Agrícola e Ambiental* **17**, 106–113. doi: 10.1590/S1415-43662013000100015

Moghbeli Damane, M., Barazandeh, A., Sattaei Mokhtari, M., Esmaeilipour, O. & Badakhshan, Y. 2018. Evaluation of body surface temperature in broiler chickens during the rearing period based on age, air temperature and feather condition. *Iranian J. Appl. Anim. Sci.* **8**(3), 499–504.

Nawaz, A.H., Amoah, K., Leng, Q.Y., Zheng, J.H., Zhang, W.L. & Zhang, L. 2021. Poultry response to heat stress: Its physiological, metabolic, and genetic implications on meat production and quality including strategies to improve broiler production in a warming world. *Frontiers in Veterinary Science* **8**, 699081. doi: 10.3389/fvets.2021.699081

Olgun, O., Abdulqader, A.F. & Karabacak, A. 2021. The importance of nutrition in preventing heat stress at poultry. *World's Poultry Science Journal* **77**(3), 661–678. doi: 10.1080/00439339.2021.1938340

Oliveira, C.E.A., Damasceno, F.A., Ferraz, P.F.P., Nascimento, J.A.C., Ferraz, G.A.S. & Barbari, M. 2019. Geostatistics applied to evaluation of thermal conditions and noise in compost dairy barns with different ventilation systems. *Agronomy Research* **17**, 783–796. doi: 10.15159/AR.19.116

Oliveira, C.E.A., Tinôco, I.D.F.F., Damasceno, F.A., Oliveira, V.C.D., Ferraz, G.A.E.S., Sousa, F.C.D., Andrade, R.R. & Barbari, M. 2022. Mapping of the Thermal Microenvironment for Dairy Cows in an Open Compost-Bedded Pack Barn System with Positive-Pressure Ventilation. *Animals* **12**(16), 2055. doi: 10.3390/ani12162055

Pires, G.A., Cordeiro, M.B., Do Nascimento, A.M., Da Costa Rodrigues, S.F., Da Silva Correia, F.C., De Freitas, H.J. & De Souza, E.M. 2020. Physiological responses of broiler chickens reared under the environmental conditions of Rio Branco –Acre.*Medicina Veterinária* (UFRPE) **14**(3), 210–219 (in Portuguese).

Pecoraro, C.A., Gonçalves, J.C., Nunes, E.H., Bumbieris Junior, V.H., Tavares Filho, J. & Miranda, K.O.daS. 2024. Enthalpy as a thermal comfort index in broiler poultry production. *Revista Brasileira De Engenharia Agrícola E Ambiental* **28**(1), e270399. https://doi.org/10.1590/1807-1929/agriambi.v28n1e270399

Queiroz, M.L.D.V., Barbosa, J.A.D., Sales, F.A.D.L., Lima, L.R.D. & Duarte, L.M. 2017. Spatial variability in a broiler shed environment with fogging system. *Revista Ciência Agronômica* **48**, 586–595 (in Portuguese).

Ribeiro Junior, P.J. & Diggle, P.J. 2001 *GeoR: a package for geostatistical analysis*. R-News, pp. 14–18.

Rostagno, H.S., Albino, L.F.T., Hannas, M.I., Donzele, J.L., Sakomura, N.K., Perazzo, F.G., Saraiva, A., Teixeira, M.L, Rodrigues, P.B., Oliveira, R.F., De Toledo Barreto, S.L. & Brito, C.O. 2017. *Brazilian Tables for Poultry and Swine-Composition of Feedstuffs and Nutritional Requirements*, Viçosa, mg, Brazil, 403 pp.

Roushdy, E.M., Zaglool, A.W. & El-Tarabany, M.S. 2018. Effects of chronic thermal stress on growth performance, carcass traits, antioxidant indices and the expression of HSP70, growth hormone and superoxide dismutase genes in two broiler strains. *J. Therm. Biol*. **74**, 337–343. doi: 10.1016/j.jtherbio.2018.04.009

Sá Júnior, A., Carvalho, L.G., Silva, F.F. & Alves, M.C. 2012. Application of the Köppen classification for climatic zoning in the state of Minas Gerais, Brazil. *Theoretical and Applied Climatology* **108**, 1–7.

Sahin, N., Hayirli, A., Orhan, C., Tuzcu, M., Akdemir, F.A.T.I.H., Komorowski, J.R. & Sahin, K. 2017. Effects of the supplemental chromium form on performance and oxidative stress in broilers exposed to heat stress. *Poultry Science* **96**(12), 4317–4324. doi: 10.3382/ps/pex249

Sans, E.C.O., Vale, M.M., Vieira, F.M.C., Vismara, E.S. & Molento, C.F.M. 2021. In-barn heterogeneity of broiler chicken welfare in two industrial house designs and two seasons in Southern Brazilian subtropical climate. *Livestock Science* **250**, 104569. doi: 10.1016/j.livsci.2021.104569

Santos, L.M., Ferraz, G.A., Batista, M.L., Martins, F. & Barbosa, B.D. 2020. Characterization of noise emitted by a low-profile tractor and its influence on the health of rural workers. *Anais da Academia Brasileira de Ciências* **92**, 1–10. doi: 10.1590/0001-3765202020200460

Siddiqui, S.H., Kang, D., Park, J., Khan, M. & Shim, K. 2020. Chronic heat stress regulates the relation between heat shock protein and immunity in broiler small intestine. *Scientific Reports* **10**(1), 18872. doi: 10.1038/s41598-020-75885-x

Silva, M.A.J.G., Ferraz, P.F.P., Santos, L.M.D., Ferraz, G.A.E.S., Rossi, G. & Barbari, M. 2021. Effect of the spatial distribution of the temperature and humidity index in a New Zealand white rabbit house on respiratory frequency and ear surface temperature. *Animals* **11**(6), 1657. doi: 10.3390/ani11061657

Slaets, J.I., Boeddinghaus, R.S. & Piepho, H.P. 2021. Linear mixed models and geostatistics for designed experiments in soil science: Two entirely different methods or two sides of the same coin? *European Journal of Soil Science* **72**(1), 47–68. doi: 10.1111/ejss.12976

Song, Z.H., Cheng, K., Zheng, X.C., Ahmad, H., Zhang, L.L. & Wang, T. 2018. Effects of dietary supplementation with enzymatically treated Artemisia annua on growth performance, intestinal morphology, digestive enzyme activities, immunity, and antioxidant capacity of heat-stressed broilers. *Poultry Science* **97**(2), 430–437. doi: 10.3382/ps/pex312

Tinôco, I.D.F., Figueiredo, J.L.A., Santos, R.C., Silva, J.D. & Pugliesi, N.L. 2004. Placas porosas utilizadas em sistemas de resfriamento evaporativo. *Engenharia na Agricultura* **12**(1), 17–23.

Trangmar, B.B., Yost, R.S. & Uehara, G. 1986. Application of geostatistics to spatial studies of soil properties. *Advances in Agronomy* **38**, 45–94. doi: 10.1016/S0065-2113(08)60673-2

Webster, R. & Oliver, M.A. 2007. *Geostatistics for environmental scientists*. John Wiley & Sons, 317 pp.

Agronomy Research **22**(2), 1001–1015, 2024
https://doi.org/10.15159/AR.24.055

IGF1 and IGF2 gene polymorphisms are associated with the feed efficiency of fattened lambs in Latvian sheep breads

I. Trapina[1,*], S. Plavina[1], N. Krasņevska[1], J. Paramonovs[1], D. Kairisa[2] and N. Paramonova[1]

[1]Genomics and Bioinformatics, Institute of Biology of the University of Latvia, Jelgava str. 3, LV-1004 Riga, Latvia
[2]Institute of Agrobiotechnology, Faculty of Agriculture, Latvian University of Life Sciences and Technologies, Liela Street 2, LV-3001 Jelgava, Latvia
[*]Correspondence: ilva.trapina@lu.lv

Received: January 30th, 2024; Accepted: May 29th, 2024; Published: June 20th, 2024

Abstract. Feed efficiency is an economically important indicator in sheep farming. The most effective technology for selecting the best feed-efficient lambs for breeding is marker association selection of genetic variations in the sheep genome as potential biomarkers. In tissue growth and differentiation, insulin-like growth factors (IGFs) play a major role: IGF1 mediates the effects of growth hormone, and IGF2 is a growth regulator, regulating skeletal muscle growth. The study aims to find possible molecular markers for feed efficiency indicators in IGF1 and IGF2 genes for Latvian sheep breeds. The exonic regions of the IGF1 and IGF2 genes were sequenced for the first time in the genomic DNA of 76 controlled, intensively fattened lambs, to search for possible genetic biomarkers. Seven polymorphic loci in the IGF1 gene and sixteen in the IGF2 gene were detected. Statistically significant associations of the IGF1 SNP rs600896367 were found with residual indicators: Residual feed intake, Residual weight gain (RWG), and Residual intake and body weight gain (RIG), and with feed efficiency and feed conversion ratio in the overall group of samples. Additionally, IGF2 SNPs New_7 and rs429576107 exhibited associations with RWG and RIG specifically in the Latvian dark-head sheep group. On average, effect of the IGF1 SNP on associated feed efficiency residuals is 3.9%, with the most pronounced impact observed in RFI. In contrast, the influence of IGF2 SNPs is comparatively lower. Our results indicate that rs600896367 and New7/rs429576107 are potential molecular markers for marker-assisted selection in sheep breeding for residual feed efficiency indicators.

Key words: breeding, fattening, feed efficiency, insulin-like growth factor, Latvian sheep, polymorphisms.

INTRODUCTION

Sheep breeding plays an important role in meeting the needs of rural populations through the supply of meat (Kumar et al., 2023). According to Eurostat, the sheep population in Latvia was 112.21 thousand in 2017, but decreased to 87.32 thousand in 2022 (Eurostat, 2023a). Sheep and goat meat production in Latvia was 0.47 thousand tons in 2022, and 0.43 thousand tons in 2017 (Eurostat, 2023b). The number of sheep

has been decreasing in recent years, therefore, improving the growth, production, and reproduction performance of Latvian sheep breeds a necessary need. There are currently ten sheep breeding programs in Latvia (LAAA, 2022) which include regularly controlled trials of fattening ram offspring to evaluate them.

In sheep breeding, more precisely, in fattening sheep for meat production, a large part of the daily costs are the feed costs; one of the possibilities for reducing them is to breed animals with higher feed efficiency (Berry & Crowley, 2013; Lima et al., 2017). For farmers to have access to higher feed efficiency animals, it is necessary to carry out breeding work with a specific goal - to increase the feed efficiency of the breeds (Wakchaure et al., 2015). Feed efficiency indicators include Feed efficiency (FE), Feed conversion ratio (FCR), Relative growth rate (RGR), Kleiber ratio (KR), Residual feed intake (RFI), Residual weight gain (RWG), and Residual intake and body weight gain (RIG), reduced the ratio of average weight gain and amount of feed required what in final reduce production costs (Berry & Crowley, 2013).

The inheritance value of feed efficiency indicators varies among different breeds and ranges from 0.10 to 0.45. However, traits inherited from parents represent genetic variations in the genome, the combinations of which determine the quality of feeding efficiency parameters (Chacko Kaitholil et al., 2024). It is considered that feeding efficiency is a combinative trait controlled by a large number of genes, as well as environmental influences (Rosa, 2015). One of the very effective technologies for selecting the best feed-efficient lambs for breeding is marker association selection (MAS) of genetic variations in the sheep genome, as potential biomarkers for defining this economically important performance trait (Wakchaure et al., 2015).

Studies suggest that molecular markers associated with feed efficiency may be genetic variations in genes involved in various metabolic processes (Chacko Kaitholil et al., 2024). In tissue growth and differentiation, insulin-like growth factors (IGFs) play a major role. Insulin-like growth factor 1 (IGF1) mediates the effects of growth hormone. Polymorphism in the IGF1 is reported to affect growth and production traits in several livestock species (Li et al., 2021). Several studies investigate the effect of polymorphisms in 5'UTR or intron regions of the IGF1 gene on growth characteristics in different sheep breeds (Li et al., 2021). In the 5'UTR region were found SNPs associated with growth traits in Makui (Hajihosseinlo et al., 2013) and Makooei sheep (Negahdary et al., 2013), but not in Hulun Buir sheep (Ding et al., 2022), Polish Pomeranian coarse-wool sheep (Proskura & Szewczuk, 2014) or Palu sheep (Malewa & Awaluddin, 2022).

Insulin-like growth factor 2 (IGF2), growth regulator A, or somatomedin A, regulates feta development and skeletal muscle growth (Wei et al., 2018; Zhao et al., 2024), and acts as a growth factor, as an autocrine signal to promote muscle cell growth and differentiation by increasing the expression of MyoD and myogenin (Wei et al., 2018). There are important studies on the association of polymorphisms of IGF*2* with feed efficiency in cows and pigs, but the limited number of studies on this topic relates to the sheep genome. There is a study on the association of five SNPs in the 5'UTR region with body weight indices in 6-12-month-old Chinese Tibetan sheep (Zhao et al., 2024).

Elucidation of the molecular mechanisms of the feed efficiency trait, in the context of the genes involved and their polymorphisms, is important for farm profitability, environmental cleanliness, and breeding assistance (Zhang et al., 2023). Therefore, the discovery of genes and genetic variations underlying feed efficiency is an important breeding strategy in sheep farming. At the same time, it is important to consider the

differences between the mechanisms or effects of genes and their variations in their influence on the studied productive tract in different breeds (Chacko Kaitholil et al., 2024). In sheep, only a few genomic variations associated with feed efficiency have been identified because it was difficult to accurately record individual feed intake in group-reared herds (Zhang et al., 2023). Our study provides an opportunity to search for genomic variations of sheep breeds bred in Latvia related to feed efficiency indicators, as the lambs have been reared under controlled conditions with intensive fattening. Feed efficiency parameters analysed in lambs can be used as an economical and rapid breeding tool.

Currently, there is a lack of studies that have examined the sequence of the IGFs genes and its potential impact on sheep breeds specifically bred in Latvia, including the national breed known as the Latvian Darkh-Head (LT; Latvijas tumšgalve). This study attempted to determine the distribution of the SNPs of the IGF1 and IGF2 genes in six most popular Latvian sheep breeds. Additionally, it sought to analyse the potential functions of these genetic variants under standardised feeding settings. The study aims to analyse for the first time the sequences of the exon region of the IGF1 and IGF2 genes in lambs of breeds bred in Latvia, as well as to find out the possible relationship of polymorphisms in both gene regions with feed efficiency indicators in intensively fattened lambs of Latvian sheep breeds. Science-based knowledge of statistically significant associations between gene polymorphisms and feed efficiency indicators can be used as an economical and rapid breeding tool to promote sheep breeding with higher feed efficiency indicators. In this way, breeders can systematically improve the sheep breed with each generation by using MAS in future.

MATERIALS AND METHODS

Animals of intensive fattening

76 lambs from six breeds: Latvian dark-head (48 lambs), Merinolandschaf (MSL; 8 lambs), Île de France (IF; 6 lambs), Charollais (CH; 3 lambs), Dorper (DOR; 5 lambs) and Texel (TE; 6 lambs), were included in controlled fattening from March to October 2022. This study was carried out in cooperation with the Latvian Sheep Breeders' Association at the ram breeding control station including in a specific group, all Latvia's most frequently grown varieties with an approximate proportional distribution. Lambs were fattened for 66.38 ± 11.05 days with an interval of 44 to 83 days.

According to the fattening control technique (LAAA, 2022), all offspring from the same ram were fattened together in an enclosure with an approximate area of 4 square metres. The pen was equipped with a detachable container for blended concentrate and a grated container for hay. Straw is used as bedding. Once each batch of lambs is finished, the cage is meticulously sanitised. The structure incorporates natural ventilation through ceiling apertures and windows equipped with insect-proof screens. The housing of animals during the research adhered to animal welfare requirements. The health of the animals during fattening is monitored by a certified veterinarian of the Latvian Association of Sheep Breeders. No health problems were reported during this fattening.

Information on the intensive fattening of lambs and the calculation of feed efficiency indicators is described in previous publications (Trapina et al., 2023a, 2023b). Feed efficiency, Feed conversion rate, Relative growth rate, Kleiber coefficient, and residuals: Residual feed intake, Residual weight gain, and Residual intake and live

weight gain were calculated using previously published formulas (Berry & Crowley, 2013; Lima et al., 2017; Trapina et al., 2023b).

DNA sequencing and SNP identification

At the end of the fattening or 24 h fasting before slaughter, blood samples from the jugular vein were taken from each lamb for genomic DNA extraction with a kit for genomic DNA extraction (Fermentas, Lithuania). DNA quality and quantity were determined using agarose gel electrophoresis and spectrophotometry.

IGF1 and IGF2 gene exons, including at least 100 bp of introns of each end, were sequenced using the Illumina MiSeq DNA (Illumina, USA) sequencing system. By using Geneious Prime® 2023.2.1 (https://www.geneious.com), clean reads were mapped to the sheep reference genome (GCF_016772045.1_ARS-UI_Ramb_v2.0, NCBI), and variable loci were detected.

Statistiscal analyses

Single-locus genotypes and allele frequencies were estimated by direct counting. Mean and standard error (*SEM*) of feed efficiency indicators of the group of the single-locus genotype were calculated from the measurement data. Appropriate statistical tests (*T-tests, ANOVA, Kruskal-Wallis, or Median test*) were used to determine the magnitude of the difference between genotype group data depending on data normality and/or homogeneity of variances in all 76 samples and 48 LT sample group. A significant result was defined as $P < 0.05$.

All haplotypes of the collection samples were created with the software DnaSP6.12.03 (www.ub.edu/dnasp/) (Rozas et al., 2017), but linkage disequilibrium (LD) analysis was performed twice: with DnaSP 6.12.03 and with Haploview 4.1. (Barrett et al., 2005)

Possible statistically associated genotype effects on feed efficiency were determined using *General Lineal Model* analysis. The *GLM* equation as individual covariates were included breed affiliation, birth weight, and IGF1 or IGF2 gene-associated SNP genotypes. In *GLM*, the possible significance of the interaction between variables was tested to include or not include them in the model. The *GLM* analysis was performed with/without SNP information including.

Analytical statistics were performed with SPSS v.25 (IBM Corp., 2017).

RESULTS AND DISCUSSION

Polymorphism detection and genetic diversity of IGF1 and IGF2 genes

The latest and most complete sequence ARS_UI_Ramb_v2.0 (breed: Rambouillet, France) of the sheep (*Ovis aries*) genome can be found in the NCBI database (https://www.ncbi.nlm.nih.gov/), which was posted there in 2022 (Davenport et al., 2022). This sequence information was used when analysing and comparing the sequences of samples of Latvian sheep breeds obtained in the study. However, since 2017, the NCBI database no longer stores information on animal (non-human) genome variations. Therefore, variation information was obtained from the Ensembl database (www.ensembl.org), which has a large amount of information but uses an older and non-updated sheep genome sequence. Accordingly, the localisation of variation in genes is determined by the ARS_UI_Ramb_v2.0 sequence.

The IGF1 gene is located on the 3rd chromosome (NC_056056) on the negative strand. The Ensembl database lists five transcripts, but the UniProt protein P10763 (www.uniprot.org) is annotated to ENSOART00020015334.2 with four exons of 154 amino acids. The database contains information on 1,084 allelic variations or polymorphisms for a given transcript. Of these polymorphisms, seven (7) SNPs were variable in Latvian sheep samples, including two SNPs in the second exon in the active protein region (Fig. 1, A).

The IGF2 gene is located on the 21st chromosome (NC_056074.1). The UniProt protein P10764 is annotated to the one (ENSOART00020011909.2) of three transcripts of the Ensembl database, a transcript containing five (5) exons. In the case of a particular transcript, the database contains information on 116 allelic variations or polymorphisms. Of these polymorphisms, nine (9) SNPs were found to be variable in Latvian sheep samples, including three SNPs localised in exons (Fig. 1, B). In addition to the IGF2 gene, seven previously unknown variable loci were found.

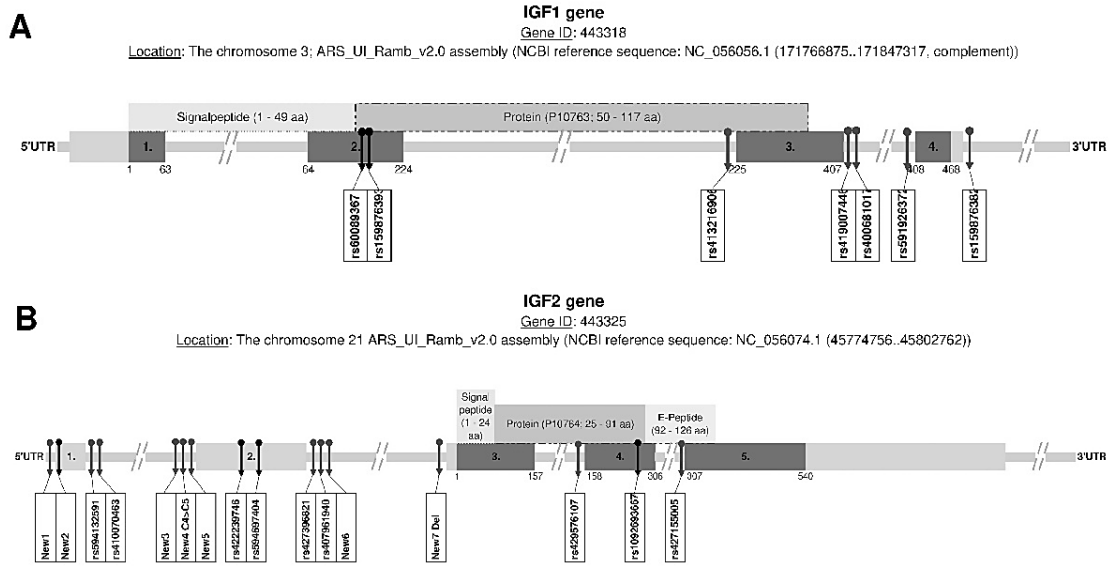

Figure 1. Gene IGF1 (A) and IGF2 (B) structure of exon regions with polymorphisms (arrows) found in Latvian sheep bread samples. The numbers below the exons reflect the numbering of nucleotides in the cDNA, starting with the first ATG number (according to NCBI database, https://www.ncbi.nlm.nih.gov/).

In the case of the IGF1 gene, a group of three polymorphisms with complete linkage disequilibrium (LD; D' = 1.00; r = 1.00) was found among the seven SNPs, while in the IGF2 gene, a total of two LD groups with two SNPs each were found (Fig. 2). Accordingly, only one SNP from each group was included in the association analysis. Complete LD group in the IGF1 gene were formed by rs413216906, rs419007446, and rs400681017, but in the case of IGF*2*, two new polymorphisms generated blocks with two known SNP: New2 with rs410070463 and New7 with rs429576107. In the IGF1 LD block, the haplotype from the common alleles of all three SNPs occurs in 86.80% of lambs' DNA samples examined, and the haplotype from the rare alleles is 13.20%, respectively.

Also, in the LD blocks of the IGF2 gene, haplotypes are formed from frequent and rare alleles. In the first block, formed from New2 and rs410070463, the haplotype of the most frequent alleles is present in 96.70% of investigated Latvian lambs, and the second block - 85.50%, respectively. SNPs inside LD blocks are examined together.

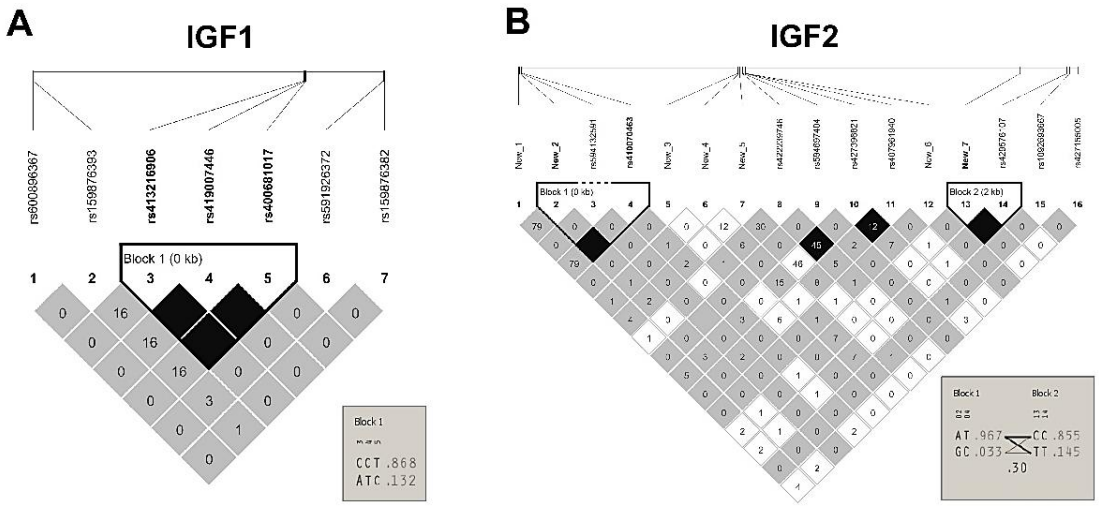

Figure 2. Linkage disequilibrium analysis of polymorphisms of (A) IGF1 and (B) IGF2 genes. The colour of the square indicates the value of D' (black - 1.00; white 0.00), and the value in the square is the value of r2 *100.

Information on LD for IGF1 gene SNPs is limited. For Hulun Buir sheep (Ding et al., 2022) were analysed three IGF1 SNPs, with no significant LD. Additionally, for Santa Inês lambs (Machado et al., 2020) two LD blocks of 11 SNPs were identified in the Intron 1 region. In Chinese Tibetan sheep, an LD including several SNPs was also identified in the 3'UTR region of the IGF2 gene (Zhao et al., 2024).

According to results of genotyping (Table 1), for all SNPs of the IGF1 gene, except rs159876393, the most common genotype in Latvian sheep samples is the homozygous genotype of the common allele.

For three SNPs: rs600896367, rs591926372, and rs159876382, no homozygous form of the rare allele was detected. Also, in cases of rs600896367 and rs159876382, all samples of Latvian dark-head (LT) were monozygotic, but in the case of rs591926372 - no LT breed samples were monozygotic.

Genotyping analysis by the International Sheep Genome Consortium International Sheep Genomics Consortium (ISGC, https://www.sheephapmap.org/) also failed to detect the homozygous form of the rare allele for rs600896367. The homozygous form of the rare allele was detected in Coopworth sheep for rs591926372 and one for the Wiltshire sheep sample at rs159876382.

A large difference was found between the IGF1 rs159876393 genotype distribution of the LT breed and other variety breeds (Table 1). In the case of the LT breed, 54.17% of the lambs were found to have the heterozygous form, which was found in only 16.67% of animals of the other Latvian breeds. In ISGC genotyping, the heterozygous genotype was detected most frequently (39.06%).

Table 1. Frequency (%) of genotypes of polymorphisms of IGF1 gene of sheep of Latvian breeds

Gene	Polymorphisms		Group of sheep (n)			Statistical
	ID number Alleles*	Genotype	All (76)	LT (48)	Other (28)	analyses (*P*)
IGF1	rs600896367	GG	97.37	100.00	92.86	0.06
	c.147G>A	GA	2.63	0.00	4.17	
	p.Ala=	AA	0.00	0.00	0.00	
	rs159876393	TT	38.16	22.92	64.29	1.43×10^{-3}
	c.153T>C	TC	44.74	54.17	16.67	
	p.Pro51=	CC	17.11	22.92	4.17	
	LD1^	CC/CC/TT	77.63	68.75	92.86	4.65×10^{-2}
		CA/CT/TC	18.42	25.00	4.17	
		AA/TT/CC	3.95	6.25	0.00	
	rs591926372	TT	89.47	83.33	100.00	2.23×10^{-2}
	c.408-54T>C	TC	10.53	16.67	0.00	
		CC	0.00	0.00	0.00	
	rs159876382	CC	96.05	100.00	89.29	2.07×10^{-2}
	c.468+72G>G	CG	3.95	0.00	6.25	
		GG	0.00	0.00	0.00	

n – Sample number in group; * – Nucleotides in position in gene cDNA: common allele (1) to Rear allele (2) as second; *P* – the statistical significance between LT (Latvina dark-head) and other group; LD1^ – SNP rs413216906 (c.225-47C>A), rs419007446 (c.407+7C>T) and rs400681017 (c.407+88T>C).

An LD block of three SNPs was identified as having combinations of genotypes included rear allele only in the LT breed, but not in lambs from other Latvian breeds. Accordingly, about six times more samples of LT heterozygotes were identified.

From these analysed SNPs of the IGF1 gene, we have found that rs600896367 has been analysed in Hulun Buir sheep (Ding et al., 2022). The results are similar to ours because, in Hulun Buir, sheep were found in only 0.02% of heterozygote samples and without rear homozygote samples. SNP rs159876393 and one of LD block - rs413216906 have been analysed in Hulun Buir sheep (Ding et al., 2022) and New Zealand Romney sheep (Li et al., 2021).

Genotype distribution related to rs413216906 heterozygotes in Hulun Buir sheep concerning LT sheep was found to be similar, however, with the higher prevalence of common allele homozygotes. The rs159876393 genotype distribution is more similar to the common cohort of all Latvian breeds (Ding et al., 2022).

The locus rs159876393 genotype distribution in the Zealand Romney sheep (Li et al., 2021) and the distribution in the LT sheep breed are similar, with a definite presence of 50% heterozygous samples in both cases. On the other hand, with almost 85% showing the common allele for rs413216906, the allele results are more similar to the total eksperimantal group of Latvian lambs.

In the case of 16 SNP polymorphisms of the IGF2 gene, the 15 most common genotypes were determined to be homozygous for common alleles (Table 2).

A deviation occurs with the SNP rs407961940, where the most frequent genotype corresponds to an allele that is not present in the reference sequence or a homozygous genotype of a mutant, usually rare, allele. Furthermore, this scenario is observed in samples from both the LT variety and for samples of other Latvian varieties. There is no information on the genotypic distribution of this SNP in the database, nor is there any scientific publication.

Table 2. Frequency (%) of genotypes of polymorphisms of IGF2 gene of sheep of Latvian breeds

Gene	Polymorphisms		Group of sheep (n)			Statistical
	ID number Alleles*	Genotype	All (76)	LT (48)	Other (28)	analyses (*P*)
IGF2	New_1	AA	94.74	91.67	100.00	0.12
	c.1-21654A>G	AG	5.26	8.33	0.00	
		GG	0.00	0.00	0.00	
	LD1^	AA/TT	93.42	91.67	96.43	0.42
		AG/TC	6.58	8.33	3.57	
		GG/CC	0.00	0.00	0.00	
	rs594132591	GG	98.68	100.00	96.43	0.19
	c.1-21538G>A	GA	1.32	0.00	3.57	
		AA	0.00	0.00	0.00	
	New_3	GG	94.74	93.75	96.43	0.51
	c.1-12231G>A	GA	2.63	4.17	0.00	
		AA	2.63	2.08	3.57	
	New_4	C4C4	63.16	66.67	57.14	0.69
	c.1-12148C4 > C5	C4C5	13.16	12.50	14.29	
		C5C5	23.68	20.83	28.57	
	New_5	CC	56.58	62.50	46.43	0.29
	c.1-12148C>T	CT	14.47	10.42	21.43	
		TT	28.95	27.08	32.14	
	rs422239746	GG	73.68	77.08	67.86	0.26
	c.1-12032G>A	GA	13.16	14.58	10.71	
		AA	13.16	8.33	21.43	
	rs594697404	CC	98.68	100.00	96.43	0.19
	c.1-11998C>T	CT	1.32	0.00	3.57	
		TT	0.00	0.00	0.00	
	rs427396821	CC	43.42	45.83	39.29	0.26
	c.1-11887C>T	CT	43.42	45.83	39.29	
		TT	13.16	8.33	21.43	
	rs407961940	AA	5.26	6.25	3.57	0.14
	c.1-11886A>G	AG	26.32	18.75	39.29	
		GG	68.42	75.00	57.14	
	New_6	CC	92.11	87.50	100.00	0.051
	c.1-11882C>T	CT	7.89	12.50	0.00	
		TT	0.00	0.00	0.00	
	LD2#	CC/CC	73.68	75.00	71.43	0.90
		C-/CT	23.68	22.92	25.00	
		--/TT	2.63	2.08	3.57	
	rs1092693667	CC	98.68	100.00	96.43	0.19
	c.258C>A	CA	1.32	0.00	3.57	
	p.Ala86=	AA	0.00	0.00	0.00	
	rs427155005	CC	77.63	72.92	85.71	0.20
	c.307-15C>T	CT	22.37	27.08	14.29	
		TT	0.00	0.00	0.00	

n – Sample number in group; * – Nucleotides in position in gene cDNA: common allele (1) to Rear allele (2) as second; *P* – the statistical significance between LT (Latvina dark-head) and other group; LD1^ – SNP New_2 (c.1-21608A>G) and rs410070463 (c.1-21466T>C); LD2#: New_7 (c.1-75DelC) and rs429576107 (c.158-29C>T).

Four of all analysed IGF2 gene SNPs (rs594132591, New_3, rs594697404 and rs1092693667) can be considered rare, as the frequency of rare genotypes for all samples together is less than 5%.

Among 16 specific genetic variations analyzed in DNA samples of Latvian sheep breeds, seven single nucleotide polymorphisms (SNPs) have not been documented or described in any previous studies. Among these SNPs, one (New_3 G>A) is a rare SNP (frequency of rare genotypes <5%), but with all three possible genotypes; other three new SNPs have high genetic variability found specifically in the LT variety samples.

When comparing the genetic diversity of Latvian sheep breed samples with the genotype distributions from the ISGC project, notable differences arise, particularly in the occurrence of homozygous genotypes for rare alleles. Three SNPs exhibited significant distinctions, with the homozygous genotype of the rare allele being absent in Latvian samples but present in the ISGC samples, with a rarity of around 1%, primarily in specific breeds. This variance may be attributed to our study's smaller sample size. In cases where the homozygous genotype of the rare allele was detected in ISGC samples, it was rare - around 1%, and only in specific breeds. However, for one SNP, the homozygous genotype of the rare allele was not detected in ISGC samples but was found in 13.16% of Latvian sheep samples, specifically in the LT, TE, MSL, and DOR breeds, excluding IF and CH breeds.

IGF2 gene polymorphisms have been infrequently examined in previous studies. Presently, information is limited to a single study on SNP analysis within the 3'UTR region of the IGF2 gene in Chinese Tibetan sheep (Zhao et al., 2024). Contrastingly, other investigations of IGF2 have predominantly focused on the protein's functional aspects (Chen et al., 2008; Wei et al., 2018).

In contrast to the SNP distribution observed in the IGF1 gene, the variation in the IGF2 gene is significantly smaller in Latvian sheep breeds, particularly between LT and other breeds.

Associations with Feed Efficiency indicators

IGF1 gene SNP rs600896367 was statistically significantly associated (Fig. 3) with Feed efficiency, Feed conversion ratio and residual indicators: Residual feed intake, Residual weight gain and Residual intake and body weight gain in the overall Latvian sheep group. Sheep with SNP rs600896367 heterozygote GA genotype showed on average a need for less than 1.60 kg dry material intake to gain 1 kg of body weight ($P = 2.97\times10^{-2}$), and the gain from 1 kg of dry material intake was greater on average for 90 grams ($P = 1.57\times10^{-3}$) than sheep with the homozygous GG genotype of the common allele (Fig. 3, A). In the case of a particular SNP, no homozygote of the rare allele was detected either among Latvian sheep breeds or in the ISGC study.

Sheep with SNP rs600896367 heterozygote GA genotype had negative RFI ($P = 4.47\times10^{-5}$) and positive RWG ($P = 2.22\times10^{-3}$) compared to sheep with the most common CC genotype (Fig. 3, A). The obtained differences also add up to a statistically significant RIG difference: -0.13 for sheep with GG genotype versus 4.80 for sheep with GA genotype. The findings suggest that sheep with the GA genotype are not only economically superior when assessed individually based on RWG and RFI but also according to the RIG index. (Fig. 3, C). The variation in RIG index among lambs with different genotypes exceeds 4.5-fold, indicating that lambs with the heterozygous GA genotype require a shorter feeding time (i.e. faster ADG) and a lower daily feed

intake compared to what is expected, considering potential differences in maintenance (i.e., BW) requirements (Berry & Crowley, 2012).

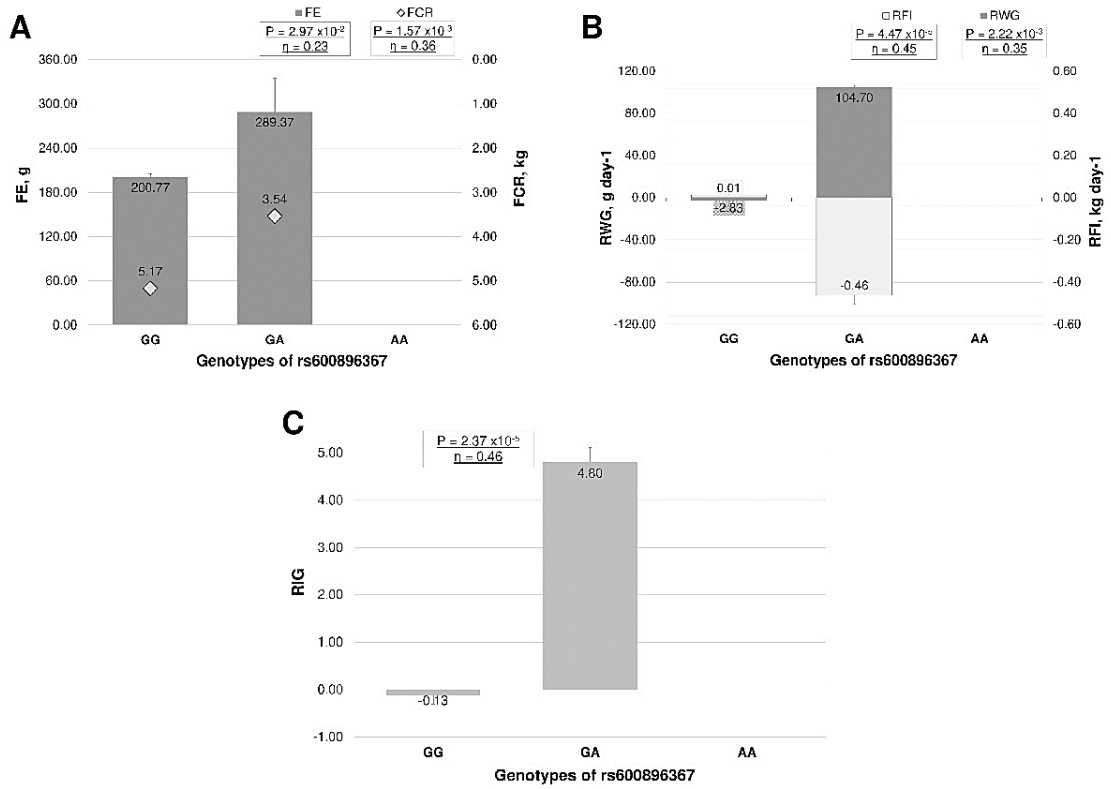

Figure 3. Gene IGF1 SNP rs600896367 association with (A) Feed efficiency (FE) and Feed conversion ratio (FCR), (B) Residual feed intake (RFI) and Residual weight gain (RWG) and (C) Residual intake and body weight gain (RIG) in the overall Latvian sheep. *P* – the statistical significance of mean with *ANOVA* or *T-test* test; η – a measure of association.

In our study, the relationship between IGF1 gene polymorphisms and feed efficiency indicators is analysed for the first time. In the case of the IGF1 gene, we have identified a potential marker that is probably unrelated to a specific sheep breed. Previous studies have presented divergent findings concerning the correlation between variations in the IGF1 gene and growth traits in sheep. Specifically, there are findings on the association of the IGF1 gene with weight gain during various periods of growth in Makooei sheep (Hajihosseinlo 2013; Negahdary et al., 2013), Munjalai sheep (Kumar et al., 2023), Barki and Farafra sheep (Darwish et al., 2023), Turkey meat sheep breeds (Kader Esen & Esen, 2023), Hulun Buir sheep (Ding et al., 2022), New Zealand Romney lambs (Li et al., 2021). Simultaneously, certain studies (Proskura & Szewczuk, 2014; Malewa & Awaluddin, 2022; Kumar et al., 2023) have reported a lack of association between various IGF1 polymorphisms and parameters that characterize sheep growth.

In current study, IGF2 gene LD2 block with SNPs New_7 and rs429576107 were found in statistically significant associations with RWG ($P = 4.46\times10^{-2}$) and RIG ($P = 4.06\times10^{-2}$) in the Latvian dark-head sheep, but the association with RFI was borderline statistically significant (Fig. 4). Association analysis indicates that 75% of all

LT lambs carry the desired more common genotype CC/CC of LD2 block, with mean RWG and RFI scores three times better than those of heterozygous or rare allele homozygous genotypes (Fig. 4, A). Lambs harboring the LD2 block genotype CC/CC exhibit a threefold increase in RIG compared to lambs with other genotype variations (Fig. 4, B). This justifies a statistical correlation not only with RWG but also with RFI.

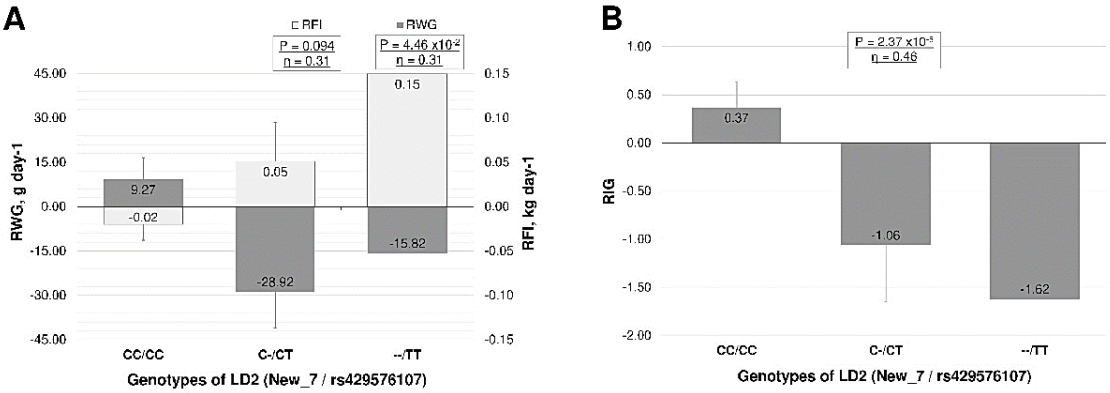

Figure4. Gene IGF2 LD block of two SNP: New_7 / rs429576107, association with (A) Residual feed intake (RFI) and Residual weight gain (RWG) and (B) Residual intake and body weight gain (RIG) in the overall Latvian sheep. *P* – the statistical significance of mean with *ANOVA* or *T-test* test; η – a measure of association.

Research on the IGF2 gene and its polymorphisms in sheep breeds is limited. Zhao et al. (2024) found three 5'UTR region SNPs associated with body weight indices in 6-12-month-old Chinese Tibetan sheep.

The current study suggests an association between IGF1 and IGF2 gene polymorphisms and feed efficiency indicators implying their potential use as genetic markers in marker-assisted selection for the breed improvement of Latvian sheep. Especially, for consumer demand for lamb meat (up to 8 months; pre-slaughter weight between 40 and 55 kg), RIG is an indicator recommended for use as a sheep classifier with the aim of higher feed efficiency with higher weight gain (Gurgeira et al., 2022). The statistically significant association of SNPs with RIG indicates that using the polymorphism as a molecular marker in the MAS process, it is possible to improve the economic performance of lambs, considering that the improvement in the efficiency for RIG indicator leads to a reduced DMI and increased ADG (do Nascimento et al., 2020).

Prediction of value of feeding efficiency indicators

The GLM analysis was used to determine SNPs' statistically significant effect size on feed efficiency indicators. The evidence strongly indicates that choosing a ram recognized by sheep breeding specialists and utilized in breeding significantly impacts (R^2 approximately 70–75%) the prediction of feed efficiency indicators. However, the productivity parameters of the ram at the age around 5–6 months (the age of lambs at the finish of fattening in our study) are not always known, which prevents the use of ram indicators in lambs' prediction algorithms. Accordingly, we did not use rams as an influencing variable in the prediction models. In this way, we were able to determine the significance level of the SNP effect.

The GLM analysis included variables detectable at lamb birth: breed affiliation, birth weight, number of lambs in the litter, and genotype of the statistically significant SNP. When analysing the effect of IGF1 gene SNPs, all samples and all six sheep breeds were used, but in the case of IGF2 gene SNPs, the analysis was performed only on LT samples. In addition, the analysis found the best GLM model with the largest R^2 value, considering the main effect and interaction of each variable.

When creating prediction algorithms using the *GLM* method, it was observed that the IGF1 gene SNP reached statistical significance in the RFI and RIG prediction models. However, it was not possible to create a statistically significant model for the FCR parameter (Table 3). For the FE and RWG parameters, a statistically significant model with the highest R^2 or coefficient of determination was developed, however, none of the included variables demonstrated statistical significance.

The most substantial distinction in the value of R^2 for prediction models, whether including or not including the IGF1 gene SNP rs600896367 was identified in RFI prediction. This presence of this difference allowed for the creation of a model with the highest R^2.

Table 3. The General Linear Model analysis of statistically significant polymorphisms of IGF1 and IGF2 genes

Feed efficiency indicators	Model*	Adjusted R^2		
		with SNP	without SNP	difference
	IGF1 gene SNPrs600896367			
FE	IGF1 SNP + BirthNr + Breed + BWbirth	0.119	0.106	0.013
FCR	No significant modele	-	-	-
RWG	IGF1 SNP + BirthNr*Breed*BWbirth	0.185	0.172	0.013
RFI	**IGF1 SNP** + BirthBW + **Breed*BirthNr**	0.502	0.425	0.077
RIG	**IGF1 SNP** + BirthNr + **Breed*BWbirth**	0.350	0.297	0.053
	IGF2 gene SNPs New_7 / rs42957610			
RWG	**IGF2 SNPs** + BirthNr	0.135	n.s.	-
RIG	**IGF2 SNPs**	0.094	n.s.	-

* – in statistically significant ($P < 0.05$) model in bold statistically significant ($P < 0.05$) variables; BirthNr – number of lambs in litter; BWbirth – body weight at birth. n.s. – no significant results.

The *GLM* including SNP rs600896367 explained 50.2% of the determination ($R^2 = 0.50$) for the RFI parameter, while the model without it explained 42.5% ($R^2 = 0.425$), indicating a 7.7% increase in the explained proportion for FE and RWG. Inclusion of SNP rs600896367 in *GLM* changed the explained proportion by 1.3% for RFI and 5.3% for RIG. These data establish the significance of the rs600896367 SNP of the IGF1 gene in determining feed efficiency parameters.

SNPs New 7 and rs42957610 of the IGF2 gene have a significantly lower effect on RWG and RIG prediction, and the significance of lamb birth weight was not identified in GLM analysis.

Constructing a GLM, a statistically significant model was achieved for RWG, incorporating IGF2 SNPs New_7 and rs42957610 along with the number of lambs born in a litter. However, a statistically significant model for RIG was established only by including genotypes of the SNPs New_7 and rs42957610 together. For both indicators

of feed efficiency, the explanatory part with the specific GLMs did not reach greater than 15% ($R^2 < 0.15$), indicating a relatively small impact of SNPs on these parameters.

Although the utilization of gene polymorphisms as molecular markers in sheep breeding is not widespread, there are studies that incorporate genomic DNA variations into the estimation of breeding values (EBV). For instance, researchers like Carracelas et al. (2022) and Kaseja et al. (2023) have explored Best Linear Unbiased Prediction (BLUP) models, applying DNA variations obtained from SNP arrays containing thousands of SNPs. However, such models do not analyse the individual effect of each SNP.

The importance of SNPs of the IGF1 and IGF2 in determining feed efficiency has been established. Consideration must be given to the fact that indicators of feed efficiency are often characterized by multilocus traits, with complex molecular mechanisms influenced by various factors (Zhang et al., 2023). Consequently, while each SNP may have minimal significance, their common influences effect remains significant in understanding and improving feed efficiency traits. Further research is needed to verify the obtained results in an additional group of samples and to clarify the possibility of IGF1 and IGF2 gene SNPs as molecular markers and it use in MAS.

CONCLUSIONS

The first sequencing of the exon region of the IGF1 and IGF2 genes in DNA samples of lambs from Latvian sheep breeds revealed known seven polymorphisms in the IGF1 gene and 16, including seven not reported, in the IGF2 gene.

Genetic variability of sheep samples of Latvian national breed Latvian dark-head differs from other varieties for the IGF1 gene, but the distribution is similar for the *IGF2*.

IGF1 gene SNP rs600896367 (c.147G>A) is statistically significantly associated with Feed efficiency, Feed conversion ratio and residual indicators: Residual feed intake, Residual weight gain and Residual intake and body weight gain, in the overall Latvian sheep group, but IGF2 gene LD2 block with SNPs New_7 (c.1-75DelC) and rs429576107 (c.158-29C>T) is statistically significant associations with RWG and RIG in the Latvian dark-head sheep.

The General Linear Model analysis showed that the SNP rs600896367, alongside with birth body weight, lamb breed, and birth number, explains 50.2% ($R^2 = 0.50$) of the Residual Feed Intake of intensive fattening. The potential individual impact of this SNP is estimated to be approximately 7.7%. In contrast, the LD2 block of the IGF2 gene, with SNPs New_7 and rs429576107 included, contributes to around 10% of the Residual Weight Gain.

Our results indicate that rs600896367 of the IGF1 gene and New7/rs429576107 of the IGF2 gene are potential molecular markers for marker-assisted selection in sheep breeding for residual feed efficiency indicators.

ACKNOWLEDGEMENTS. The study was funded by the LZP-2021/1-0489 project: 'Development of an innovative approach to identify biological determinants involved in the between-animal variation in feed efficiency in sheep farming'.

REFERENCES

Barrett, J.C., Fry, B., Maller, J. & Daly, M.J. 2005. Haploview: Analysis and visualisation of LD and haplotype maps. *Bioinformatics* **21**(2), 263–265. doi: 10.1093/bioinformatics/bth457

Berry, D.P. & Crowley, J.J. 2012. Residual intake and body weight gain: A new measure of efficiency in growing cattle. *Journal of Animal Science* **90**(1), 109–115. doi: 10.2527/jas.2011-4245

Berry, D.P. & Crowley, J.J. 2013. CELL BIOLOGY SYMPOSIUM: Genetics of feed efficiency in dairy and beef cattle1. *Journal of Animal Science* **91**(4), 1594–1613. doi: 10.2527/jas.2012-5862

Carracelas, B., Navajas, E.A., Vera, B. & Ciappesoni, G. 2022. SNP arrays evaluation as tools in genetic improvement in Corriedale sheep in Uruguay. *Agrociencia Uruguay* **26**(2). doi: 10.31285/AGRO.26.998

Chacko Kaitholil, S.R., Mooney, M.H., Aubry, A., Rezwan, F. & Shirali, M. 2024. Insights into the influence of diet and genetics on feed efficiency and meat production in sheep. *Animal Genetics* **55**(1), 20–46. doi: 10.1111/age.13383

Chen, R.L., Kassem, N.A., Sadeghi, M. & Preston, J.E. 2008. Insulin-Like Growth Factor-II Uptake Into Choroid Plexus and Brain of Young and Old Sheep. *The Journals of Gerontology: Series A* **63**(2), 141–148. doi: 10.1093/gerona/63.2.141

Darwish, A.M., Abdelhafez, M.A., Abdel-Hamid, Z.G., Othman, S.I., Mohamed, I.E. & Allam, A.A. 2023. Correlation analysis between polymorphism of leptin and IGFI genes and body measurements in Barki and Farafra sheep. *Beni-Suef University Journal of Basic and Applied Sciences* **12**(1), 119. Doi: 10.1186/s43088-023-00450-0

Davenport, K.M., Bickhart, D.M., Worley, K., Murali, S.C., Salavati, M., Clark, E.L., Cockett, N.E., Heaton, M.P., Smith, T.P.L., Murdoch, B.M. & Rosen, B.D. 2022. An improved ovine reference genome assembly to facilitate in-depth functional annotation of the sheep genome. *GigaScience* **11**, giab096. Doi: 10.1093/gigascience/giab096

Ding, N., Tian, D., Li, X., Zhang, Z., Tian, F., Liu, S., Han, B., Liu, D. & Zhao, K. 2022. Genetic Polymorphisms of IGF1 and IGF1R Genes and Their Effects on Growth Traits in Hulun Buir Sheep. *Genes* **13**(4), 666. doi: 10.3390/genes13040666

do Nascimento, E.M., Maggioni, H., Bach, C.I.S., do Nascimento, W.G., Fernandes, S.R. & Garcez Neto, A.F. 2020. Residual intake and body weight gain on the performance, ingestive behaviour, and characteristics of longissimus muscle of Dorper × Santa Inês lambs. *Small Ruminant Research* **192**, 106248. doi: 10.1016/j.smallrumres.2020.106248

Eurostat, 2023a. https://ec.europa.eu/eurostat/databrowser/view/APRO_MT_LSSHEEP/default/table?lang=en Accessed 05.12.2023.

Eurostat, 2023b. https://ec.europa.eu/eurostat/databrowser/product/view/tag00045 Accessed 05.12.2023.

Gurgeira, D.N., Crisóstomo, C., Sartori, L.V.C., de Paz, C.C.P., Delmilho, G., Chay-Canul, A.J., Bedoya, H.J.N., Vega, W.H.O., Bueno, M.S. & da Costa, R.L.D. 2022. Characteristics of growth, carcass and meat quality of sheep with different feed efficiency phenotypes. *Meat Science* **194**, 108959. doi: 10.1016/j.meatsci.2022.108959

Hajihosseinlo, A., Hashemi, A., Razavi-Sheshdeh, S. & Pirany, N. 2013. Association of the polymorphism in the 5' flanking region of the ovine IGF-I gene with growth and development traits in Makui sheep of Iran. *European Journal of Zoological Research* **2**, 19–24.

IBM Corp. Released 2017. IBM SPSS Statistics for Windows, Version 25.0. Armonk, NY: IBM Corp.

Kader Esen, V. & Esen, S. 2023. Association of the IGF1 5′UTR Polymorphism in Meat-Type Sheep Breeds Considering Growth, Body Size, Slaughter, and Meat Quality Traits in Turkey. *Veterinary Sciences* **10**(4), 270. doi: 10.3390/vetsci10040270

Kaseja, K., Mucha, S., Smith, E., Yates, J., Banos, G. & Conington, J. 2023. Including genotypic information in genetic evaluations increases the accuracy of sheep breeding values. *Journal of Animal Breeding and Genetics* **140**(4), 462–471. doi: 10.1111/jbg.12771

Kumar, S., Dahiya, S.P., Magotra, A., Ratwan, P. & Bangar, Y. 2023. Influence of single nucleotide polymorphism in the IGF-1 gene on performance and conformation traits in Munjal sheep. *Zygote* **31**(1), 70–77. doi: 10.1017/S0967199422000545

LAAA. 2022. Genealogy programs. https://www.laaa.lv/lv/skirnes-saimniecibas/ciltsdarba-programmas/ Accessed 29.11.2022.

Li, S., Zhou, H., Zhao, F., Fang, Q., Wang, J., Liu, X., Luo, Y. & Hickford, J.G.H. 2021. Nucleotide Sequence Variation in the Insulin-Like Growth Factor 1 Gene Affects Growth and Carcass Traits in New Zealand Romney Sheep. *DNA and Cell Biology* **40**(2), 265–271. doi: 10.1089/dna.2020.6166

Lima, N.L.L., Ribeiro, C.R. de F., de Sá, H.C.M., Leopoldino Júnior, I., Cavalcanti, L.F.L., Santana, R.A.V., Furusho-Garcia, I.F. & Pereira, I.G. 2017. Economic analysis, performance, and feed efficiency in feedlot lambs. *Revista Brasileira de Zootecnia* **46**(10), 821–829. doi: 10.1590/S1806-92902017001000005

Machado, A.L., Meira, A.N., Jucá, A. de F., Azevedo, H.C., Muniz, E.N., Coutinho, L.L., Mourão, G.B., Pedrosa, V.B. & Pinto, L.F.B. 2020. Variants in GH, IGF1, and LEP genes associated with body traits in Santa Inês sheep. *Scientia Agricola* **78**, e20190216. https://doi.org/10.1590/1678-992X-2019-0216

Malewa, A.Dg. & Awaluddin, A. 2022. Polymorphisms of Palu Sheep IGF-1 Gene and Their Relationship with Skeletal Growth. *Tropical Animal Science Journal* **45**(1), 9–15. doi: 10.5398/tasj.2022.45.1.9

Negahdary, M., Hajihosseinlo, A. & Ajdary, M. 2013. PCR-SSCP Variation of IGF1 and PIT1 Genes and Their Association with Estimated Breeding Values of Growth Traits in Makooei Sheep. *Genetics Research International* **2013**, 1–6. https://doi.org/10.1155/2013/272346

Proskura, W. & Szewczuk, M. 2014. The Polymorphism in the IGF1R Gene is Associated with Body Weight and Average Daily Weight Gain in Pomeranian Coarsewool Ewes. *Pakistan Veterinary Journal* **34**, 514–517.

Rosa, G.J.M. 2015 Basic Genetic Model for Quantitative Traits. In Khatib, H. (eds) *Molecular and Quantitative Animal Genetics*. John Wiley & Sons, Inc., Hoboken, New Jersey, 33–37.

Rozas, J., Ferrer-Mata, A., Sánchez-DelBarrio, J.C., Guirao-Rico, S., Librado, P., Ramos-Onsins, S.E., Sánchez-Gracia, A. 2017. DnaSP 6: DNA Sequence Polymorphism Analysis of Large Datasets. *Mol. Biol. Evol*. **34**, 3299–3302. doi: 10.1093/molbev/msx248

Trapina, I., Kairisa, D. & Paramonova, N. 2023a. Comparison of sire rams of the Latvian Dark-Head breed according to feed efficiency indicators as the beginning of genomic breeding research. *Agronomy Research* **21**(S2), 611–622. doi: 10.15159/AR.23.030

Trapina, I., Kairisa, D. & Paramonova, N. 2023b. Feed efficiency indicators and hormones related to nutrient metabolism in intensive fattened lambs of sire rams of different sheep breeds in Latvia. *Agronomy Research* **21**(S2), 598–610. doi: 10.15159/AR.23.031

Wakchaure, R., Ganguly, S., Praveen, P.K., Kumar, A., Sharma, S. & Mahajan, T. 2015. Marker Assisted Selection (MAS) in Animal Breeding: A Review. Journal of Drug *Metabolism & Toxicology* **6**(5), e127. doi: 10.4172/2157-7609.1000e127

Wei, C., Wu, M., Wang, C., Liu, R., Zhao, H., Yang, L., Liu, J., Wang, Y., Zhang, S., Yuan, Z., Liu, Z., Hu, S., Chu, M., Wang, X. & Du, L. 2018. Long Noncoding RNA Lnc-SEMT Modulates IGF2 Expression by Sponging miR-125b to Promote Sheep Muscle Development and Growth. *Cellular Physiology and Biochemistry* **49**(2).

Zhang, D., Li, X., Li, F., Zhang, X., Zhao, Y., Zhang, Y., Ma, Z., Tian, H., Weng, X. & Wang, W. 2023. Genome-wide association study identifies novel loci associated with feed efficiency traits in Hu lambs1. *Journal of Integrative Agriculture.* doi: 10.1016/j.jia.2023.10.011

Zhao, X., Yan, J., Chu, H., Wu, Z., Li, W., Zhang, Q., Zhang, Y., Guo, Y. & Fan, Z. 2024. The polymorphism of the ovine insulin like growth factor-2 (IGF2) gene and their associations with growth related traits in Tibetan sheep. *Tropical Animal Health and Production* **56**(1), 19. doi: 10.1007/s11250-023-03858-z

Agronomy Research **22**(2), 1016–1025, 2024
https://doi.org/10.15159/AR.24.084

Study of heat exchange processes in the cooling system of a poultry house with side ventilation

V. Trokhaniak[1], Y. Nasieka[1,2], Ye. Ihnatiev[3,4], O. Synyavskiy[1], O. Skliar[4] and J. Olt[3,*]

[1]National University of Life and Environmental Sciences of Ukraine, 15 Heroyiv Oborony Str., UA03041 Kyiv, Ukraine
[2]V.Ye. Lashkaryov Institute of Semiconductor Physics of NAS of Ukraine, 45 Nauky Av., UA02000 Kyiv, Ukraine
[3]Estonian University of Life Sciences, Institute of Forestry and Engineering, 56 Kreutzwaldi Str., EE1006 Tartu, Estonia
[4]Dmytro Motornyi Tavria State Agrotechnological University, 66 Zhukovsky Str., UA69600 Zaporizhzhia, Ukraine
[*]Correspondence: jyri.olt@emu.ee

Received: May 21st, 2024; Accepted: August 6th, 2024; Published: August 26th, 2024

Abstract. Modern systems for cooling the supply air in poultry houses are based on the use of spraying or evaporative systems. Both systems rely on the principle of adiabatic cooling, where water transitions from a liquid to a gaseous state through free evaporation, allowing for the reduction of the temperature of the external heated air in poultry premises. The objective of the research study was development of theoretical basis for using new method of cooling the outside air in poultry house ventilation systems is proposed, based on the use of water from underground wells and recuperative heat exchangers to cool the supply air. This method enables the reduction of the outside air temperature without increasing its relative humidity, unlike water spraying cooling systems, for example. Numerical modeling was conducted to obtain velocity fields, temperatures, and pressure differentials in the air environment of the poultry house. The results show that the air temperature exiting the heat exchangers at 20 °C is heated up to 26.6 °C inside the poultry house. Thus, the temperature of the supply air with this cooling system does not exceed permissible norms. The velocities and pressure differentials are sufficient to ensure that the air exiting the supply valves reaches the middle of the poultry house.

Key words: computational fluid dynamics (CFD), heat exchanger; lateral ventilation system, recuperation, thermal regime.

INTRODUCTION

The traditional cooling system used in poultry houses to maintain regulated indoor microclimate is direct evaporative cooling (DEC) (Hoff, 2018; Liang et al., 2020; Boltyanska et al., 2022). In these systems, 100% fresh outside air is drawn through evaporative cooling pads on the lateral walls to meet heat and air quality constraints

(Raza et al., 2020). Consequently, the air temperature is reduced while simultaneously increasing moisture content. Moreover, DEC elevates the humidity of the supply air, thereby reducing heat loss from the birds (Rozenboim et al., 2007). Apart from thermal stress, high humidity indoors leads to other adverse health consequences, as it increases the amount of ammonia emitted from poultry litter (Kristensen & Wathes, 2000). This results in decreased feed consumption and egg production by the birds, as well as increased mortality rates, leading to reduced productivity and profitability within the industry.

Modern cooling systems for supply air in poultry houses (Donald, 2012; Czarick & Fairchild, 2014) are based on the use of spraying or evaporative systems. Both systems rely on the principle of adiabatic cooling (Hui et al., 2018), where water transitions from a liquid to a gaseous state through free evaporation, allowing for the reduction of the temperature of the external heated air in poultry premises.

The second method involves spraying devices such as nozzles or disk sprayers, which produce an aerosol or spray containing small water droplets (Kim et al., 2008). Nozzles come in two types: low-pressure and high-pressure water systems. When using the nozzle method for air cooling, it is necessary to have a special water treatment system - purification, filtration, etc., as high salt content quickly impairs the operation of the nozzles. Additionally, operating such systems requires significant electricity consumption.

Drawbacks of the cassette method include high aerodynamic resistance and high installation costs. Additionally, a disadvantage of this method is the clogging of cassette channels with dust during operation. It should be noted that mold forms on the clogged surface of the cassette, introducing components into the supply air, which, in high humidity conditions, contributes to the onset of various diseases in poultry. In case of untimely cleaning of the cassettes, algae may grow on their surfaces. These factors prompt frequent replacement of cassettes as early as the first year of operation. The maximum service life of cassettes does not exceed 10 years and depends on water quality, preventive maintenance, and operational regime. The effectiveness of cassette cooling also largely depends on the airtightness of the poultry house.

In this research was used methods of computational fluid dynamics (CFD). It is a branch of fluid mechanics that uses numerical analysis and algorithms to solve and analyze problems involving fluid flows. CFD is widely used in various engineering fields to simulate the behavior of fluids (liquids and gases) in and around objects.

The main problem identified in this research is the inefficiency and associated issues with traditional and modern cooling systems in poultry houses. Specifically, traditional direct evaporative cooling (DEC) systems, while reducing air temperature, increase humidity levels, leading to thermal stress, adverse health effects, reduced feed consumption, lower egg production, and higher mortality rates among poultry. Modern cooling systems using spraying or evaporative methods also have significant drawbacks, such as high aerodynamic resistance, high installation and maintenance costs, clogging of channels, mold and algae growth, and substantial electricity consumption. These issues highlight the urgent need for a more effective, sustainable cooling system that can maintain an optimal microclimate in poultry houses without the negative impacts associated with increased humidity and high maintenance requirements.

Given these numerous challenges faced by the poultry industry, the ability to create a suitable and sustainable cooling system for poultry houses in Ukraine is a pressing necessity.

The purpose of the study was to develop a theoretical basis for use of a new method of cooling outside air in ventilation systems of poultry houses, based on use of water from underground wells and recuperative heat exchangers to cool the supply air.

MATERIALS AND METHODS

In poultry houses, a lateral cooling system is proposed for the summer period when the outside air temperature reaches 27 °C (Rozenboim et al., 2007). Heat exchangers are installed on the supply air valves on the exterior side of the poultry house. Groundwater is used as the coolant. Previous studies by the authors (Trokhaniak et al., 2023a), which focused on developing heat exchangers for such a cooling system, have provided detailed insights. The required water flow and all other parameters of the heat exchanger are presented in this article. Analyzing the results, it is projected that through these heat exchangers, the external warm air will pass and be cooled down to 20 °C. The poultry house contains 41,000 birds, each weighing 3 kg, of a meat breed kept on the floor. The poultry serves as a heat source, modeled as a first-kind boundary condition with a temperature of +41 °C. The bedding on the concrete floor was not accounted for in this model. Future research will include modeling the bedding as a porous zone, addressing gas emissions from it, and performing air composition analysis using species transport models.

Additionally, based on previous studies by the authors (Trokhaniak et al., 2023b, 2023c), exhaust fans, totaling 4 units for half of the poultry house, are installed on the lateral wall with a combined airflow rate of 42.8 kg s^{-1}. This airflow volume is sufficient for removing excess heat from the poultry house. Also considered are the supply air valves, positioned at a height of 0.21 m above the floor level. The spoiler angle over the valve is set at 73 degrees, with a spoiler length of 0.2 m. The nearby valves to the fans are closed, specifically: 9–10, 17–18, 25–26, and 33–34. Thus, 32 valves are utilized for half of the poultry house. The Air Inlet Valve 3000-VFG valves have a width of 0.86 m, and their opening height is 0.09 m.

The poultry house has dimensions of 120×21 meters and a height of 5.3 meters, the total volume of the poultry house is 5,234.4 m^3. To reduce the use of computational resources, a 'symmetry' boundary condition was applied. Consequently, the width of the poultry house is 10.5 meters. The floor is made of concrete 0.1 m thick, with polystyrene insulation 0.05 m thick above and below it. At positions 2 m from the walls, the thickness of the thermal insulation material is increased to 0.1 m. Assuming the temperature is 10 °C. The walls are constructed as three-layered, with concrete 0.06 m thick on both sides, and polystyrene insulation 0.1 m thick in between. For simplicity in the model, the ceiling is also constructed as three-layered, with concrete on both sides and Izovat 30 thermal insulation material 0.1 m thick in between. Boundary conditions of the third kind (Fig. 1) with a temperature of 40 °C and a heat transfer coefficient of 10 W $(m^2\ K)^{-1}$ were applied to all exterior walls and the ceiling. Assuming low wind speeds were observed at the poultry house location.

The geometry of the poultry house was created in ANSYS Design Modeler 2023 R1, and boundary conditions were set. Then, the geometry was transferred to ANSYS Meshing 2023 R1 for mesh generation. Meshing was performed using the CutCell method. The minimum face size is 0.015 m, and the maximum face size is 0.12 m. For the supply air valves and exhaust fans, the mesh was refined with minimum element sizes of 0.01 m and 0.04 m, respectively. Mesh refinement was applied for more accurate

results at the inlet and outlet of the poultry house. As a result, the orthogonal quality of the mesh is 0.214, with a total of 4,485,116 elements and 4,854,992 nodes.

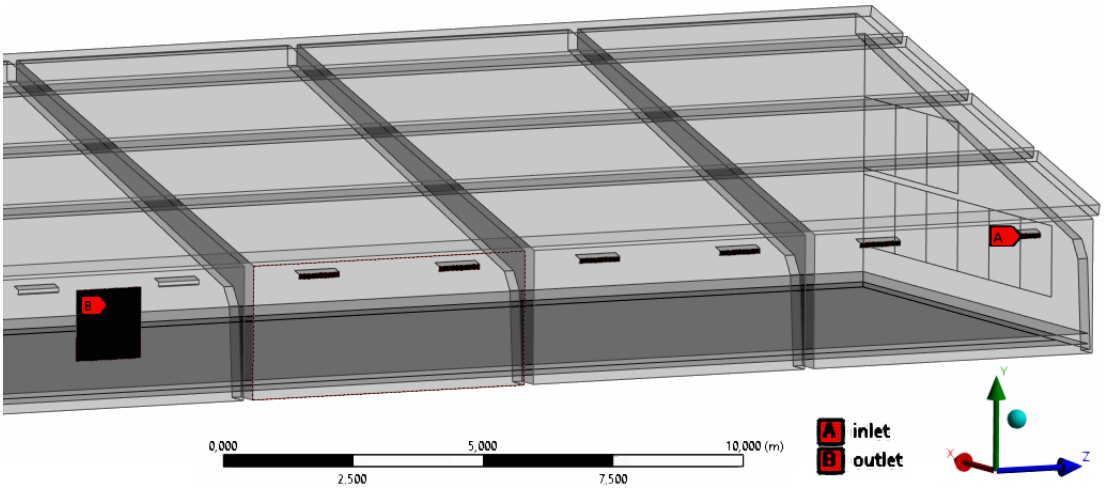

Figure 1. 3D model of the poultry house.

Numerical simulations were conducted directly in ANSYS Fluent 2023 R1. The model employed the Navier-Stokes equations (Trokhaniak & Klendii, 2018), the standard k-ε turbulence model, and the Discrete Ordinates radiation model (ANSYS). The methodology of mathematical modeling in the technical field of agriculture and in determining microclimate parameters is detailed in (Kaletnik et al., 2020; Kic, 2016). Certain aspects of this methodology can be applied in this study. The modeling was conducted as steady-state.

RESULTS AND DISCUSSION

Figs 2–3 depict the results of numerical modeling of the poultry house at four sections along the length of the building - 10.25 m, 43.25 m, 74.75 m, and 109.25 m along the *xy* axis. The first and second sections correspond to the midpoint of the 4th supply air valve and the 15th valve, respectively. The third section is located at the 3rd exhaust fan (between the 25th and 26th supply air valves). The fourth section is in the middle of the 37th supply air valve. Along the length of the poultry house, there are 40 supply air valves, out of which 32 are in use.

On sections 1, 2, and 4, flow lines in the poultry house are displayed (see Fig. 2, a; b; d). It is observed that the valves and spoilers are strategically positioned. The airflow exits the valves at a velocity of 14.36 m s^{-1}. Upon reaching nearly the middle of the poultry house, it descends, losing velocity, towards the birds. Between the swift airflow and the birds, a large vortex is formed, which provides fresh air delivery to the birds. In the upper part of the poultry house, along the centerline, a small air vortex is created due to the specific construction of the poultry house. Additionally, there is a separation of the airflow due to its intensive supply. This results in turbulence in the airflow and intense mixing of fresh air with exhaust air in these sections. At certain points, near the

inlet of the supply air valves, the maximum airflow velocity reaches up to 14.62 m s^{-1}. The pressure at the inlet of the supply air valves reaches 124.3 Pa.

In turn, at the exhaust fans (see Fig. 2, c), the air velocity is 6.13 m·s^{-1}. The air is uniformly removed from the poultry house. The pressure at the outlet is –3.31 Pa.

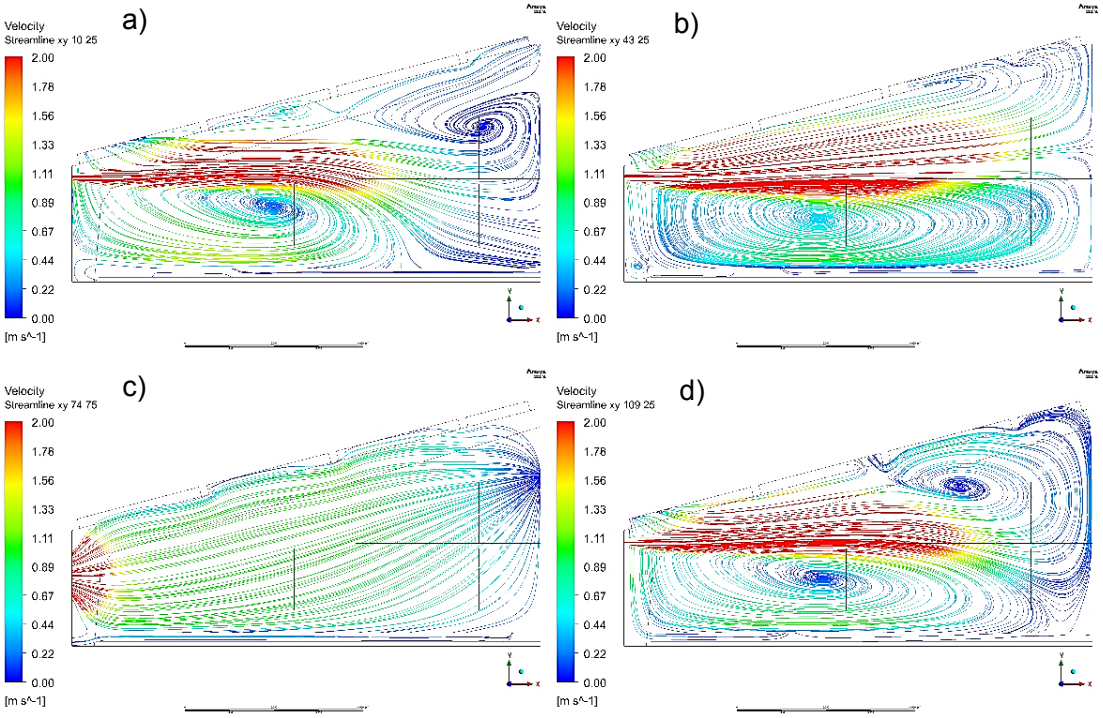

Figure 2. Flow lines (m·s^{-1}) in the poultry house along the xy axis at distances from the front end wall: a – 10.25 m; b – 43.25 m; c – 74.75 m; d – 109.25 m.

In Fig. 3, the temperature distribution at various sections in the poultry house is presented. It can be observed that the cooled air from the heat exchangers at a temperature of 20 °C (Fig. 3, a, b, d) is directed from the valves into the poultry house. After traveling approximately 1.5 m, it heats up, and the cold airflow disperses throughout the space. The average temperature in these sections ranges from 24.44 to 26.11 °C.

Considering the large length of the poultry house, there is a temperature stagnation zone near the wall at 1.5 m (Fig. 3, b) and 0.5 m (Fig. 3, c), where temperatures range from 28 to 32 °C. The model assumes that the birds are not located within 0.5 m from the wall. Therefore, only a very small amount of birds will experience some discomfort (Fig. 3, b). Near the ceiling, at a short distance of about 0.1 m, temperatures range from 28 to 40 °C. These elevated temperatures are due to the high outside air temperature (40 °C) and the intensity of solar radiation. Fig. 3, c depicts the temperature field at the level of the 3rd exhaust fan. The temperature in this area is slightly higher, ranging from 26.82 to 27.35 °C. This is because there is no supply of cooled air in this area. The heated air enters the exhaust fan removal area, where the temperature at the outlet is 26.84 °C.

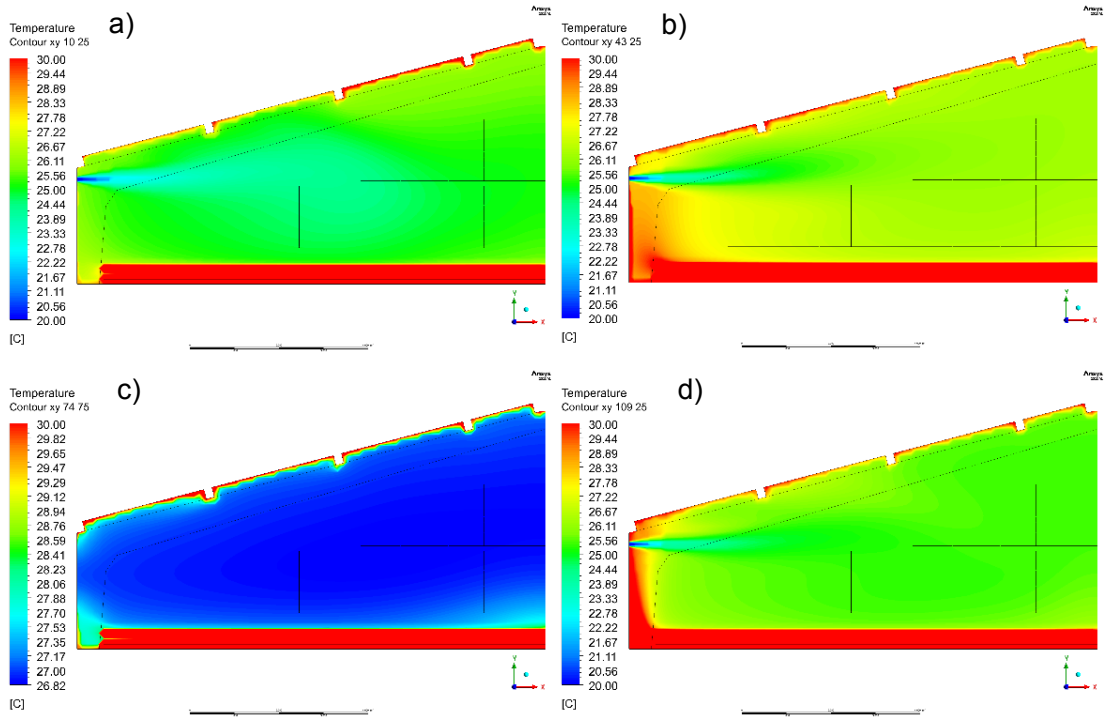

Figure 3. Temperature losses (°C) in the poultry house along the *xy* axis at distances from the front end wall: a – 10.25 m; b – 43.25 m; c – 74.75 m; d – 109.25 m.

In Fig. 4, the velocity field (Fig. 4, a) and the temperature field (Fig. 4, b) at a height of 0.7 m from the floor level are presented. These results are the most interesting and important since the birds are housed on the floor. Considering the technical standards for poultry management, the air velocity near the birds should not exceed 2 m·s^{-1}. Therefore, the results in Fig. 4, a are shown within the range of 0–2 m·s^{-1}. Considering the results presented in Figure 3 and the high air velocities at the inlet of the supply air valves, which reach 14.62 m·s^{-1}, only in small areas does the air velocity exceed 2 m·s^{-1}. The average air velocity in the section (see Fig. 4, a) is 0.74 m·s^{-1}, and the pressure is 0.599 Pa. These results demonstrate the effectiveness of the ventilation system in the poultry house.

The air temperature near the birds during the hot period of the year should not exceed 28 °C. Considering the results of the numerical modeling (see Fig. 4, b), the air temperature exceeding 28 °C occupies an area of no more than 7.8%. This demonstrates sufficient efficiency of the poultry house cooling system. Slightly lower air temperatures are observed on the rear and frontal sides of the poultry house, starting from 24.68 °C. The average temperature across the entire area of the poultry house at a height of 0.7 m from the floor level is 26.55 °C.

On Fig. 5, the airflow velocity distribution within the 3D poultry house is depicted, ranging 0–2 m·s^{-1}. As observed, the valves operate efficiently by delivering fresh, cooled air into the center of the poultry house. The two nearest valves to the fans are closed.

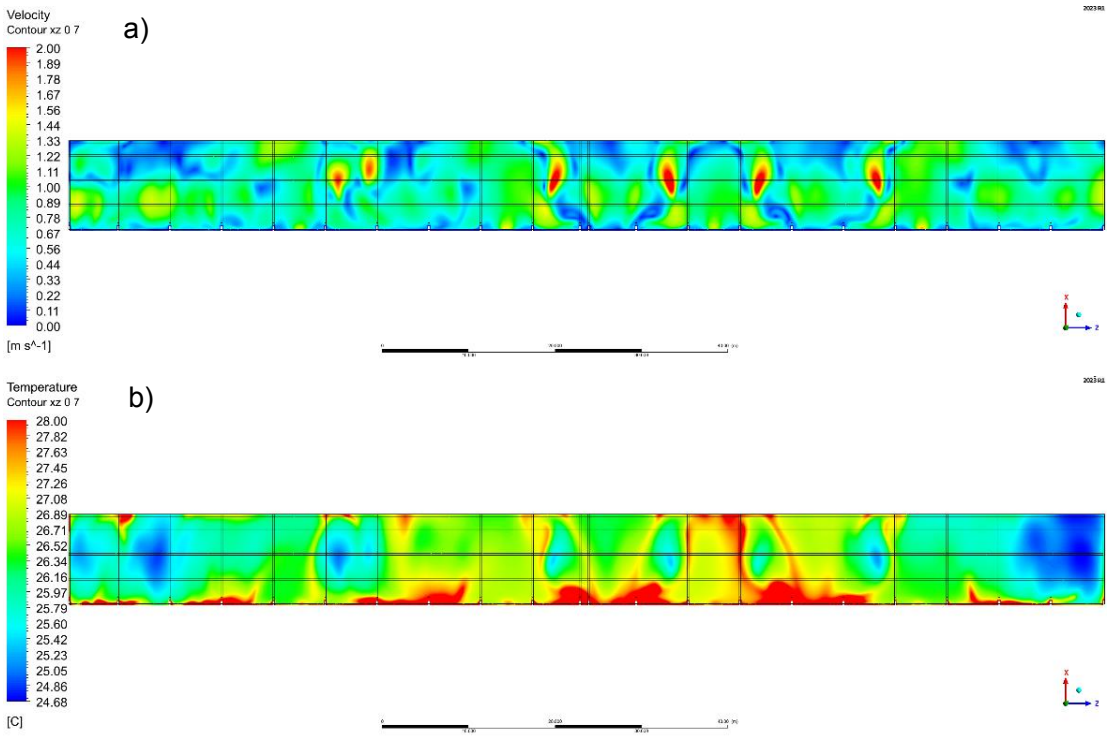

Figure 4. Velocity field, $m \cdot s^{-1}$ (a), and temperature field, °C (b), in the poultry house along the *zx* axis at a height of 0.7 m from the floor level.

However, there is a certain attenuation and downward airflow at valves 11, 16, 19, 24, 27, and 32 (see Fig. 5). This phenomenon is ultimately observable in Fig. 4, a as well. This phenomenon is not observed at valves 8 and 35 because there are no fans directing airflow towards the frontal and rear walls from these valves. The airflow exiting from valves 1–8 and 35–40 exhibits a more uniform airflow pattern.

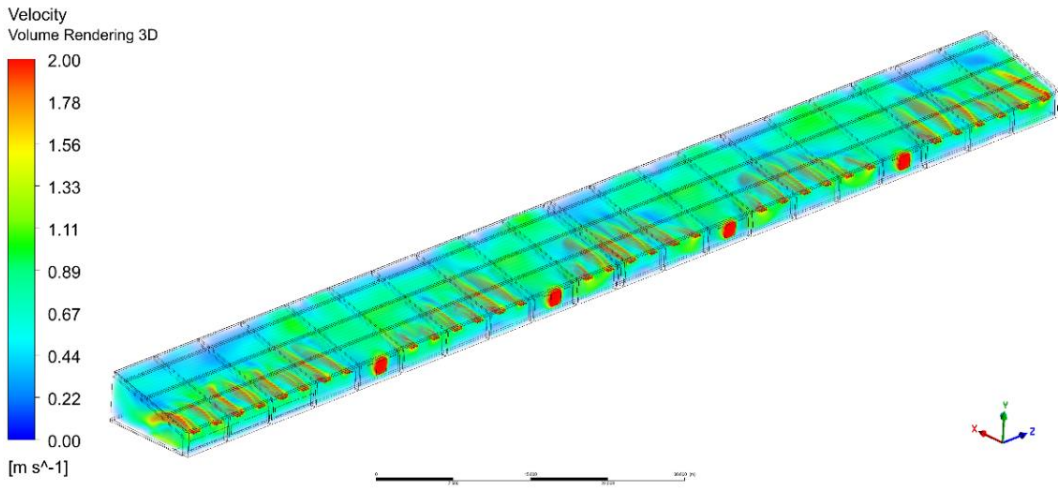

Figure 5. Visualization of the volumetric airflow distribution in the poultry house ranging from 0 to 2 $m \cdot s^{-1}$.

In Fig. 6, b, the temperature distribution along the *zy* axis at a distance of 5.25 m from the side wall is depicted. As a result of numerical modeling, several elevated temperatures exceeding 28 °C were identified near the third exhaust fan and the ceiling. However, such stagnant temperature zones are insignificant and do not significantly affect the main flock of birds.

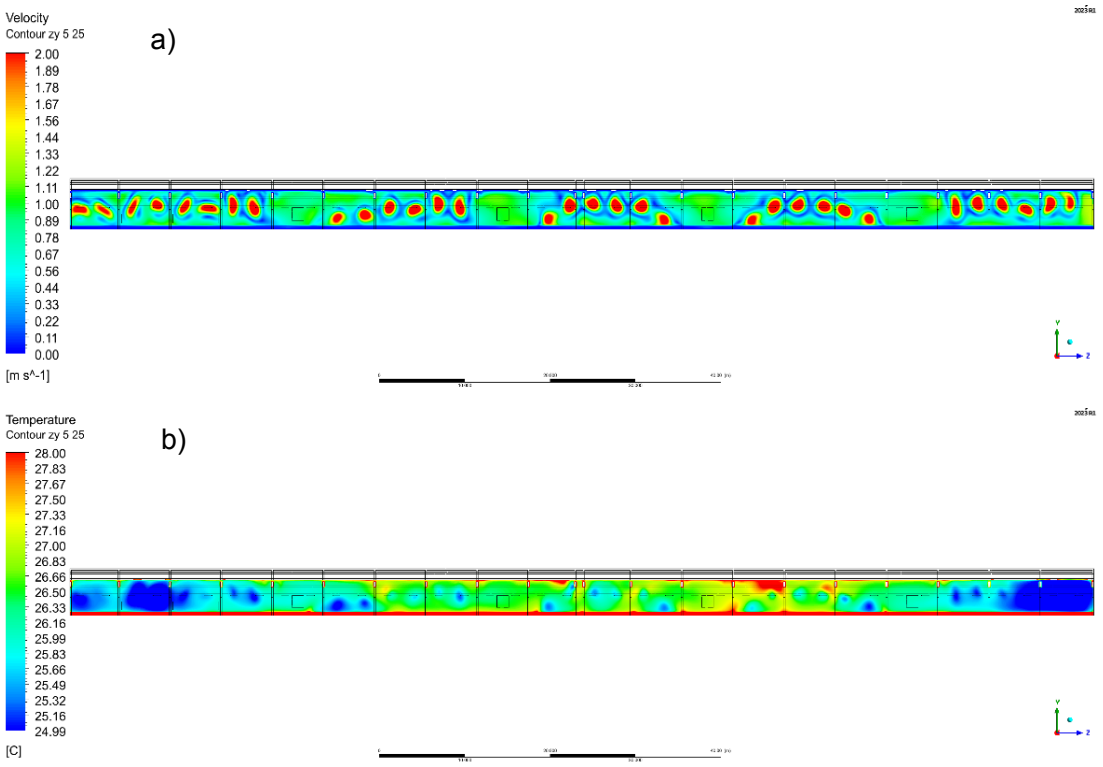

Figure 6. Velocity field, $m \cdot s^{-1}$ (a), and temperature field, °C (b), in the poultry house along the *zy* axis at 5.25 m from the side wall.

The modeling of the air environment in the poultry house demonstrated the efficiency of the proposed cooling system. The research results show a more stable relative humidity compared to those proposed by other authors (Donald, 2012; Czarick & Fairchild, 2014), which are based on spraying or adiabatic cooling (Hui et al., 2018). Cooling systems from different authors are accompanied by a significant increase in humidity, which ultimately leads to poultry diseases, mortality, and decreased production output in poultry farms (Ishchenko et al., 2019).

The use of evaporative cooling pads (Hoff, 2018; Liang et al., 2020; Boltyanska et al., 2022) also increases humidity in poultry houses. Additionally, it requires extra water treatment and excessive water consumption to maintain the microclimate in proper conditions.

All the above-mentioned cooling systems share common drawbacks: increased humidity in the poultry house, high water usage, and ultimately, reduced productivity of poultry farms (Wang et al., 2019). However, all these cooling methods perform their function despite these significant negative aspects. In the proposed cooling system, poultry will be in comfortable conditions, as much as possible.

The article is theoretical in nature; however, the authors conducted preliminary experimental investigations to validate the obtained results. Based on these preliminary studies, it can be stated that the proposed model is expected to have deviations of up to 12% from real data (Trokhaniak et al., 2019).

The research conducted in the poultry building is intricately linked to animal welfare. The primary motivation behind this research, as presented in the article, is to analyze energy inputs and the changes in microclimatic conditions within the building, with a significant focus on air flow dynamics. However, the underlying and critical objective of these analyses is to improve the welfare of the birds housed in these facilities.

The proposed system for cooling outside air in ventilation systems of poultry houses affects the health of birds as it provides: temperature regulation; humidity control and air quality improvement.

The results of this research have the potential to bring about significant improvements in poultry welfare. By addressing both the microclimatic conditions and energy efficiency, the study offers practical solutions that can be implemented to create a more sustainable and humane environment for poultry. This not only benefits the birds but also enhances productivity and profitability for poultry farmers, aligning economic and welfare goals.

CONCLUSIONS

1. The numerical modeling results investigated the cooling system during the hot period of the year with an outside air temperature of 30 °C in a 3D model of half of the poultry house. A new cooling system for poultry houses was proposed using heat exchange equipment, which would output air at a temperature of 20 °C. Groundwater is suggested as the cooling medium.

2. Velocity fields were obtained at various locations within the room along the xy- axis. The effectiveness of the placement of supply vents and spoilers above them was demonstrated. Fresh air flow exiting the vents at a speed of 14.36 m s^{-1} reached the center of the room, ensuring its quality. The temperature in these areas averaged between 24.44 and 27.35 °C, not exceeding the limit of 28 °C during the hot period of the year. Analyzing the results of the numerical modeling at a height of 0.7 m from the floor level, it was concluded that discomfort would be experienced by no more than 7.8% of the birds with the proposed cooling system. The average velocity was 0.74 m s^{-1}, with an air temperature of 26.56 °C. Only in certain areas did the temperature exceed 28 °C.

ACKNOWLEDGEMENTS. Supported by Education and Science of Ukraine projects of scientific works of young scientists (Kyiv), Project No. 110/1M-pr-2022.

REFERENCES

Boltyanska, N., Podashevskaya, H., Skliar, O., Sklyar, R. & Boltianskyi, O. 2022. Problems of implementation of digital technologies in animal husbandry. *CEUR Workshop Proceedings* **3109**, pp. 75–82.

Czarick, M. & Fairchild, B. 2014. Plastic cooling pads are found to be less efficient comparing to paper cool pads. *Poultry Housing Tips* **24**(8), College of Agricultural and Environmental Sciences, Georgia, USA, 64–69.

Donald, J.O. 2012. *Technology of microclimate of broiler house*. Aviagen Brands. Huntsville, USA, 24 pp.

Ishchenko, K.V., Palii, A.P., Kis, V.M., Petrov, R.V., Nagorna, L.V., Dolbanosova, R.V. & Paliy, A.P. 2019. Investigation of microclimate parameters for the content of toxic gases in poultry houses during air treatment in the scrubber with the use of various fillers. *Ukrainian Journal of Ecology* **9**(2), 74–80.

Hoff, S.J. 2018. HVAC *Techniques for Modern Livestock and Poultry Production Systems*. In book: HVAC Systems. IntechOpen, pp. 170. doi: 10.5772/intechopen.78785

Hui, X., Li, B.M., Xin, H.W., Zheng, W.C., Shi, Z.X., Yang, X. & Zhao, S.M. 2018. New control strategy against temperature sudden-drop in the initial stage of pad cooling process in poultry houses. *International Journal of Agricultural and Biological Engineering* **11**(1), Beijing, China, 66–73. doi: 10.25165/j.ijabe.20181101.2479

Kaletnik, H., Sevostianov, J., Bulgakov, V., Holovach, I., Melnik, V., Ihnatiev, Ye., Olt, J. 2020. Development and examination of high-performance fluidisedbed vibration drier for processing food production waste. *Agronomy Research* **18**(4), 2391–2409. doi:10.15159/AR.20.234

Kic, P. 2016. Microclimatic conditions in the poultry houses. *Agronomy Research* **14**(1), 82–90.

Kim, K., Yoon, J.Y., Kwon, H. J., Han, J.H., Son, J.E., Nam, S.W. & Lee, I.B. 2008. 3-D CFD analysis of relative humidity distribution in greenhouse with a fog cooling system and refrigerative dehumidifiers. *Biosystems Engineering* **100**(2), San Diego, USA, 245–255.

Kristensen, H.H. & Wathes, C. M. 2000. Ammonia and poultry welfare: a review. *World's Poult Sci J*. **56**(3), 235–245.

Liang, Y., Tabler, G.T. & Dridi, S. 2020. Sprinkler technology improves broiler production sustainability: from stress alleviation to water usage conservation: A mini review. *Front Veterinary Sci.* **7**, 689.

Raza, H.M.U., Ashraf, H., Shahzad, K., Sultan, M., Miyazaki, T. and Usman, M. 2020. Investigating applicability of evaporative cooling systems for thermal comfort of poultry birds in Pakistan. *Appl Sci*. **10**(13), 4445. doi: 10.3390/app10134445

Rozenboim, I., Tako, E., Gal-Garber, O., Proudman, J.A. & Uni, Z. 2007. The effect of heat stress on ovarian function of laying hens. *Poult Sci.* **86** (8), 1760–1765.

Trokhaniak, V., Gorobets, V., Shelimanova, O. & Balitsky, A. 2023a. Research of thermal and hydrodynamic flows of heat exchangers for different air cooling systems in poultry houses. *Machinery & Energetics* **14**(1), 6878. doi: 10.31548/machinery/1.2023.68

Trokhaniak, V., Ivanovs, S., Nasieka, Yu., Chernysh, O., Aboltins, A., Ihnatiev, Y. & Synyavskiy, O. 2023b. Usage of CFD for research on lateral ventilation system in poultry house. *Engineering for Rural Development* **22**, 582−587. doi: 10.22616/ERDev.2023.22.TF120

Trokhaniak, V. & Klendii, O. 2018. Numerical simulation of hydrodynamic and heat-mass exchange processes of a microclimate control system in an industrial greenhouse. *Bulletin of the Transilvania University of Brasov, Series II: Forestry, Wood Industry, Agricultural Food Engineering* **11**(60), 171–184.

Trokhaniak, V.I., Rutylo, M.I., Rogovskii, I.L., Titova, L.L., Luzan, O.R. & Bannyi, O.O. 2019. Experimental studies and numerical simulation of speed modes of air environment in a poultry house. *INMATEH – Agricultural Engineering* **59**(3), 9−18. doi: 10.35633/INMATEH-59-01

Trokhaniak, V.I., Spodyniuk, N.A., Lendiel, T.I., Luzan, P.H., Mishchenko, A.V., Tarasenko, S.V., Popa, L. & Ionita, C. 2023c. Investigation of an improved side ventilation system in a poultry house using CFD. *INMATEH-Agricultural Engineering* **69**(1), 121–130. doi: 10.35633/inmateh-69-11

Wang, Y., Zheng, W., Li, B. & Li, X. 2019. A New ventilation system to reduce temperature fluctuations in laying hen housing in continental climate. *Biosystems Engineering* **181**, 52–62.

Agronomy Research **22**(2), 1026–1070, 2024
https://doi.org/10.15159/AR.24.086

Potential of oilseed radish (*Raphanus sativus* l. var. *oleiformis* Pers.) as a multi-service cover crop (MSCC)

Y. Tsytsiura*

Vinnytsia National Agrarian University, Faculty of Agronomy, Horticulture and Plant protection, Soniachna street, 3, UA21008 Vinnytsia, Ukraine
*Correspondence: yaroslavtsytsyura@ukr.net, yaroslav301974@gmail.com

Received: May 4th, 2024; Accepted: August 13th, 2024; Published: September 5th, 2024

Abstract. The possibility of oilseed radish use as multi-service cover crop (MSCC) during the ten-year period for spring and summer sowing was investigated. A comprehensive approach to assessing the formation of aboveground and root biomass by biochemical analysis with a comprehensive assessment of the factors that determine the quality, manufacturability and agricultural value of the crop was methodically applied. The actual agricultural value from the point of view of the possible use of oilseed radish as a cover, intermediate, green manure, fodder crop and an additional source for biogas production was analyzed.
A multi-year data set based on 8 indicators of the formed plant mass, 17 basic indicators of biochemical composition, and 12 derived indicators of ratios and accumulation was formed. Based on the criterion evaluation and comparison of the long-term data set with similar indicators for cruciferous species used as a multi-service cover crop, oilseed radish was classified as a crop with high adaptive bioorganic potential. This was confirmed by the application of the Multi-criteria decision aiding (MCDA) method. The use of this method proved the possibility of multi-purpose use of oilseed radish as a multi-service cover crop on soils with medium fertility potential for unstable moisture conditions. The order of increasing importance of the direction of critical use of oilseed radish in the spring sowing period was: 'Catch crop' (Consistency index 0.188) - 'Biogas' (0.226) - 'Fodder' (0.370) - 'Green manure' (0.340) - 'Cover crop' (0.431). A similar order for the summer sowing period was: 'Cover crop' (0.244) - 'Catch crop' (0.305) - 'Biogas' (0.357) - 'Fodder' (0.407) - 'Green manure' (0.415).

Key words: criteria of multipurpose use, biogas, green manure, forage intermediate crops, catch crop.

INTRODUCTION

The dynamic growth of soil degradation against the background of a general shortage of classical organic fertilizers and rising prices for mineral fertilizers lead to a constant search for technological alternatives in the agricultural sector of the economy (Kaletnik et al., 2019, 2020; Honcharuk et al., 2023, Tokarchuk et al., 2023; Honcharuk & Yemchyk, 2024). A widely recognized alternative for the formation of environmentally sustainable and balanced soil use is the use of intermediate crops for multiple purposes. Intermediate crops are used for various purposes: biologization of agrotechnologies, soil

rehabilitation and conservation, a source of organic recycling fertilization systems (green manure), biomass for feed and bioenergy use (Couëdel et al., 2019; Dzvene et al., 2023). The global market for such crops has a pronounced positive growth trend. The Green Manure Global Market Report 2024 (2023) notes that the green manure market size has grown strongly in recent years. It will grow from $2.17 billion in 2023 to $2.33 billion in 2024 at a compound annual growth rate of 7.6%. The growth in the historical period can be attributed to organic farming practices, soil health awareness, crop rotation practices, government support and subsidies, crop diversification, water conservation, and reduced environmental impact. The green manure market size is expected to see strong growth in the next few years. It will grow to $3.07 billion in 2028 at a compound annual growth rate of 7.1%. The growth in the forecast period can be attributed to climate change adaptation, regenerative agriculture practices, consumer demand for sustainable agriculture, integration in precision agriculture, enhanced soil microbial activity, water quality management. Major trends in the forecast period include the integration of leguminous and cruciferous cover crops, no-till and reduced-till farming systems, innovations in cover cropping.

Based on this, the concept of multi-service cover crop (MSCC) was formulated (Justes & Richard, 2017). It involved the search, selection, and combination of crops in crop rotation that are characterized by unpretentiousness to the terms of use, high intensity and volume of accumulation of aboveground and underground biomass of appropriate biochemical quality and rates of mineralization in the soil and suitability for anaerobic fermentation processes (Couëdel et al., 2019; Lucadamo et al., 2022; Scavo et al., 2022). A significant part of the MSCC system is represented by the use of intermediate crops to prevent organic matter deficiency in soils under different fertilization options through their use as green manure (Boselli et al., 2020; Guinet et al., 2023). The relevance of green manure in the MSCC system is due to the shortage of organic fertilizers due to changes in the management of farm animals and the conversion of modern livestock complexes to schemes for processing manure waste into biogas (Pan et al., 2021), as well as the transition to minimized and zero tillage technologies (Boselli et al., 2020). In this regard, green manure has been evaluated as an effective resource for replenishing organic matter in the soil both from the point of view of optimizing the modes of its humification and accumulation of organic carbon in general (Lei et al., 2022; Lee et al., 2023). It also realized a positive impact on the complex of soil properties (Chen et al., 2020; Ansari et al., 2022; Israt & Parimal, 2023). The implementation of MSCC contributed to the agro-ecological sustainability of agro-landscapes by such factors as pollination of plants, support of wild fauna, as well as providing a more attractive aesthetic appearance due to the optimized filling of ecological niches of fauna and flora of the territories (Justes & Richard, 2017). The selection of potential candidate crops that correspond to the MSCC principles should be based on the study of basic eligibility criteria (Couëdel et al., 2019; Singh et al., 2023).

Given the relevance of these issues, the purpose of the ten-year research cycle was to determine the bioproductive potential of oilseed radish (*Raphanus sativus* L. var. *oleiformis* Pers.) on gray forest soils from the point of view of compliance with MSCC criteria, taking into account the preliminary data of a comprehensive assessment of its morphological and bioproductive potential (Tsytsiura, 2019, 2020, 2021, 2022; 2023a, 2023b, 2023c).

MATERIALS AND METHODS

The research was carried out during 2014–2023 at the experimental field of Vinnytsia National Agrarian University (N 49°11′31″, E 28°22′16″.) on Grey and Dark Gray forest soils (Greyi-Luvic Phaeozems (Phaeozems Albic, Dark Gray Podzolic Soils) according to WRB (IUSS, 2015)) Haplic Greyzems according to FAO (IUSS, 2015)) of silty clay loamy texture (sicl) (fluctuations in the content of fractions for the horizon 0–30 cm: sand 12.03–14.32, silt 55.86–57.79 and clay 29.35–30.21). The agrochemical potential of the soil for layer 0–30 cm was determined with the standards for analytical laboratory methods (Sparks et al., 1996) and had the following average indicators for the research period: humus content: 2.68%, easily hydrolyzed nitrogen 81.5 mg kg^{-1} of soil, mobile phosphorus 176.1 mg kg^{-1} of soil, exchangeable potassium 110.8 mg kg^{-1} of soil, pH_{KCl} 5.8, hydrolytic acidity 3.29 mg-equivalent 100 g^{-1} of soil. The soil fertility potential based on the presented agrochemical properties was estimated as average (according to Sanchez et al., 1982).

The variety of oilseed radish 'Zhuravka' was used. Sowing was carried out on an unfertilized background with a seeding rate of 2.5 million seeds ha^{-1} using the conventional row method (row spacing of 15 cm). This sowing option corresponded to the variant of fodder–green manure use of oilseed radish (Tsytsiura, 2020). Two systems of using oilseed radish as an intermediate crop for multiple purposes were investigated:

I. The system of early spring sowing (first-second decade of April) after intermediate cultivation to a depth of 8–10 cm with leveling against the background of autumn plowing at 20–22 cm. The date of phenological achievement of the optimal phase of multicomponent use of oilseed radish biomass (flowering stage (BBCH 64-67) was in the second-third decade of June.

II. The system of summer sowing (the second–third decade of July) immediately after harvesting the predecessor with intermediate combined tillage (flat cutter + rotary loosening with leveling) to a depth of 12–14 cm. The date of flowering stage (BBCH 64-67) was in the second or third decade of October.

The sowing date of the first variant was determined at the early stage of physical ripeness of the soil. For the second variant, the soil moisture indicator was used. It was based on the date of the nearest precipitation with an intensity of at least 5 mm (according to the recommendations of Florentín et al. (2010)). The optimality of the phase of leaf and stem mass use was determined taking into account the combination of maximum individual plant productivity and relevant quality indicators for effective variant of biofumigant and green manure use of oilseed radish under conditions of unstable moisture in different soil zones according to Alonso-Ayuso et al. (2014) and Duff et al. (2020).

The experimental plots were formed in quadruplicate using the method of small plot randomization (total plot area 35 m^2, accounting area 25 m^2).

To control the number of weeds, a mixture of herbicides was used in the rosette phase (BBCH 20–22) 'Galera 334', aqueous solution (clopyralid, 267 g L^{-1} + picloram, 67 g L^{-1}), 0.3 L ha^{-1} - against dicotyledonous weeds; 'Select', emulsion concentrate (clethodim, 120 g L^{-1}), 0.7 L ha^{-1} - graminicide. To control the number of cruciferous fleas (*Phyllotreta atra* F., *Phyllotreta nemorum* L., *Phyllotreta undulata* Kutsch, *Phyllotreta nigripes* F.) common in the agrocenosis of oilseed radish (Tsytsiura, 2024),

the insecticide 'Bliskavka' (emulsion concentrate, alphacypermethrin 100 g L^{-1}) was applied at 0.2 L ha^{-1} in the phase of cotyledons–first true leaves (BBCH 10-12).

Stage growth was recorded using the Biologische Bundesanstalt, Bundessortenamt und CHemische Industrie (BBCH) scale (Test Guidelines, 2017).

Accounting of aboveground plant biomass (BM). It was carried out at the full flowering stage (BBCH 64-67) in 4 randomized plots by the method of trial plots of 1 m^2 in each replication (16 plots in total) with subsequent weighing using a laboratory scale YP50002 (5 kg) with a discretion of 0.01 g. Prior to weighing and subsequent field and laboratory manipulations, any non-native plant impurities were removed from the sample. Some of the accounting plots were selected with the condition that the perimeter of the aboveground biomass accounting coincided with the system of monolithic analysis of the formed root systems.

The ground cover (GC) was monitored during the entire crop cycle for both variants of oilseed radish use. The indicator was recorded starting from the phenophase of true leaf formation (BBCH 12–13) with an interval of 5 days until the flowering phase (BBCH 64-67). To account for GC, we used the methodology of Ramirez-Garcia et al. (2012), which was based on digital pictures of the marked surface taken from a perspective at a 1.5 m height. The images were taken with a Canon EOS 750D Kit + Canon EF 50 mm f/1.8 STM processed using SigmaScan Pro 5® software. CurveExpert Professional v. 2.7.3 (Hyams Development) was used to estimate the GC dynamics according to the recommendations of Bodner et al. (2010).

Assessment of the formation of plant root biomass (RBM) of oilseed radish was carried out at a similar phenophase as for the assessment of the formation of aboveground plant biomass by the monolith method according to the recommendations of Wahlström et al. (2015). Separation of the root mass in the monolithic profile was carried out by washing on a column of sieves (laboratory sieves of woven wire mesh: 4.0 mm, 2.0 mm, 1.0 mm, 0.5 mm and 0.25 mm). The selected roots were stored in closed plastic containers at 5 °C. The washed and selected root were air-dried for 24 h and then weighed on a laboratory balance (3,100 g/0.01 g) WALCOM LB3002 (± 0.01 g).

The root system productivity coefficient was calculated according to Poorter et al. (2012) as the ratio of crude (dry) aboveground plant biomass to the mass of formed roots. The proportion of root residues in the total plant biomass was determined as the ratio of root mass to aboveground plant mass expressed in %.

Chemical analysis of leaf biomass. All laboratory chemical analyzes were carried out in quadruplicate with the determination of the basic components of biochemical analysis expressed on an absolutely dry weight basis (according to Undersander et al., 1993).

The dry matter (DM) and organic dry matter (ODM) contents were measured by drying in an oven at 105 °C and then ashing the dried sample at 550 °C. The resulting dried samples were re-weighed and ground using a Vilitek VLM-16 800 g 2,200 mL electrostatic laboratory mill.

The ash content (AOAC Official Method 942.05) was based on the gravimetric loss by heating to 600 °C for a period of two hours.

Crude fiber (CFb) (AOAC Official Method 978.10) is determined gravimetrically as the residue remaining after the acid and alkaline digestions.

Dietary fiber content (DFb) was calculated as the difference between NDF-ADL (according to Quemada & Cabrera, 1995).

The crude fat content (CF) (AOAC Official Method 2003.05) was determined by using the Randall modification of the standard Soxhlet extraction.

Determination of total nitrogen content (TNC) (AOAC Official Method 978.04) by the Kjeldahl method in dry biomass was performed using the KjeLROC Kd-310 analyzer (ISO 17025). For accounting of nitrogen-containing compounds in the Kjeldahl method, a preliminary solution reduction was used (Undersander et al., 1993).

Total crude protein (CP) (AOAC Official Method 990.03 and AOAC Official Method 978.04) was calculated as the nitrogen content multiplied by the standard conversion factor of 6.25.

The content of total organic carbon (TOC) was determined using a laboratory analyzer of total organic carbon of the TOC-LCPH series according to the standard protocol for low-temperature thermocatalytic oxidation of plant material.

Neutral Detergent Fibre (NDF) was determined using AOAC Official Method 2002-04 by neutral detergent solution and heat.

Acid Detergent Fibre (ADF) was determined gravimetrically as the residue remaining after acid detergent extraction (by AOAC Official Method 973.18).

Analysis of tissue for Acid Detergent Lignin (ADL) followed the ADF-Sulfuric Lignin method (Rowland & Roberts, 1994 (AOAC Official Method 973.18) in view of Sluiter et al. (2004)).

Cellulose was considered to be represented by the difference between ADF and ADL, and hemicellulose was the difference between NDF and ADF according to the Van Soest method (Van Soest et al., 1991; FOSS, 2018).

Nitrogen-free extracts (NfE) were calculated as the difference between the content of 100% dry matter and the content of CP, CFb, CF and CA (Undersander et al., 1993).

Carbohydrates (CH) determined by the amount of NfE + CFb (according to Weende method (FOSS, 2018)).

The C/N ratio was calculated as the ratio of Total Organic Carbon (TOC) to Total Nitrogen Content (TNC) (Anzola-Rojas et al., 2014).

The crop residue quality (RQ) was calculated as the sum of its labile (100-NDF) and cellulose like (ADF-ADL) decomposable fraction (Quemada & Cabrera, 1995).

Glucosinolate content (GSL) was determined on frozen plant by high performance liquid chromatography according to standard methods (ISO 9167:2019 (2019)) in view of Arguello et al. (1999).

The content of total phosphorus and potassium in plants was determined according to Method of measurement 31-497058-019-200531-497058-019-2005.

Calcium in plant material was determined by the complexometric method (in modification of Nielsen, 2010).

Sulfur content was determined in accordance with AOAC 923.01-1923.

Comparable conversion of oilseed radish biomass by total NPK accumulation in cattle manure was carried out to the average chemical composition of manure (an orientation to manure with a dry matter content of 10–15% in comparison to similar matter content of the biomass of oilseed radish plants) at a standard concentration of N 3.2 g kg^{-1}, P 2.0 g kg^{-1}, K 3.8 g kg^{-1}) according to the statistics provided Brown (2021) and Composts & Fertilizers (2023).

Multi-criteria decision aiding (MCDA) was used for the analysis according to Ramirez-Garcia et al. (2015). The initial criteria were: ground cover (GCmax, in % at 60 days after sowing), the biomass at the end of the experiment (BM, kg m^{-2}), the C:N

ratio, the N uptake (N_{upt}, g m^{-2} (calculated according to Gastal & Lemaire (2002) and Letey et al. (1982)), the residue quality (RQ, g kg^{-1}_{DM}), glucosinolate productivity (GSL, mmol m^{-2}), the fiber content (CFb, g kg^{-1}_{DM}) and the dietary fiber content (DFb, g kg^{-1}_{DM} for the direction of use 'fodder crop'). Based on the formed system, 70 R_{ij} outcomes were obtained. The internal coefficients of importance of each factor were determined on the basis of the fundamental scale according to Saaty & Vargas (2012). The MCDA procedure was carried out in the analysis subsystem according to the Analytic Hierarchy Process (AHP), Technique for Order Preference by Similarity to Ideal Solution (TOPSIS) with the recommendations of Rao (2007), Ramirez-Garcia et al. (2015) and El Amine et al. (2016).

The analysis of weather conditions and the level of their variability for the period 2014–2023 was based on the hydrothermal coefficient (*HTC*) (Eq.):

$$HTC = \frac{\sum R}{0.1 \times \sum t_{>10}} \quad (1)$$

where $\sum R$ – the sum of precipitation (mm) over a period with temperatures above 10 °C; $\sum t_{>10}$ – the sum of effective temperatures over the same period. Ranking of *HTC* values: *HTC* > 1.6 – excessive humidity; *HTC* 1.3–1.6 – humid conditions; *HTC* 1.0–1.3 – moderately dry conditions; *HTC* 0.7–1.0 – dry conditions; *HTC* 0.4–0.7 – very dry conditions.

The De Martonne Aridity Index (I_{DM}) (according to Moral et al., 2016) was used to characterize the arid/humid conditions of a territory for a month according to Eq. (2):

$$I_{DM} = \frac{12P_m}{T_m + 10}, \quad (2)$$

where P_m and T_m are the precipitation volume and mean air temperature in the corresponding month, respectively.

According to the I_{DM} values calculated using the equation above, the climate of a region can be classified (type of climate according to the De Martonne aridity index (I_{DM}, adapted after Baltas, 2007) Arid $I_{DM} < 10$; Semi-Arid $10 \leq I_{DM} < 20$; Mediterranean $20 \leq I_{DM} < 24$; Semi-humid $24 \leq I_{DM} < 28$; Humid $28 \leq I_{DM} < 35$; Very Humid $35 \leq I_{DM} \leq 55$; Extremely humid $I_{DM} > 55$.

The evapotranspiration was calculated using Eq. (3) (according Latief et al. (2017)):

$$E = 0.0018 \times (25 + t)^2 \times (100 - a), \quad (3)$$

where *E* is the evapotranspiration of plants for a certain period, mm; *t* is the average air temperature for the period °C; *a* is the average air humidity for the analyzed period, %.

The Vysotsky-Ivanov humidification coefficient (K_h) was determined by Eq. (4) according to Latief et al. (2017):

$$K_h = \frac{P}{E}, \quad (4)$$

where K_h – moisture coefficient; *P* – amount of precipitation for the analyzed period, mm; *E* – evaporation for the analyzed period, mm. The different degrees of moisture is carried out according to gradation: $K_h > 1.0$ – territory (time period) with excessive moisture, K_h close to 1 – optimal moisture, K_h = 1.0–0.6 – unstable moisture, K_h = 0.6–0.3 – insufficient hydration.

Table 1. Estimation of the values of hydrothermal regimes of the period of vegetation of oilseed radish for the variant of spring and summer sowing, 2014–2023

Year	Precipitation, mm (IV–VI)	*t_{aver}, °C (IV–VI)	Months of the growing season								
			IV			V			VI		
			HTC	I_{DM}	K_h	*HTC*	I_{DM}	K_h	*HTC*	I_{DM}	K_h
Spring sowing											
2014	339.6	13.84	0.725	45.7	1.18	3.928	88.9	2.11	1.545	34.8	0.83
2015	142.3	14.36	0.645	37.3	0.78	0.917	20.6	0.41	0.715	16.9	0.27
2016	193.4	15.06	0.296	21.6	0.44	0.489	40.4	0.99	1.265	29.9	0.75
2017	125.1	14.07	3.919	39.2	0.75	0.777	16.8	0.34	0.504	11.9	0.22
2018	170.8	16.38	0.290	10.8	0.19	0.308	7.2	0.12	4.404	103.7	2.31
2019	398.5	15.39	0.565	33.5	0.72	4.902	111.0	3.29	1.682	41.4	0.96
2020	343.8	13.67	0.091	36.4	0.50	5.327	106.4	3.18	1.548	37.3	0.89
2021	282.8	13.26	0.233	38.8	0.96	3.125	66.7	1.64	1.679	39.8	1.00
2022	242.1	14.30	0.563	57.4	2.33	1.430	31.3	0.79	1.496	36.1	0.85
2023	239.8	14.18	1.543	91.5	3.33	0.085	1.9	0.04	1.640	38.9	0.87

Year	Precipitation, mm (VII–X)	*t_{aver}, °C (VII-X)	Months of the growing season												*t_{aver}, °C	Precipitation amount mm**
			VII			VIII			IX			X				
			HTC	I_{DM}	K_h	*HTC*	I_{DM}	K_h	*HTC*	I_{DM}	K_h	*HTC*	I_{DM}	K_h		
Summer sowing																
2014	250.8	15.4	1.312	32.7	0.77	1.049	26.0	0.51	1.252	25.7	0.56	1.770	35.8	0.93	–	–
2015	160.8	16.6	0.321	8.1	0.14	0.124	3.1	0.05	1.184	26.8	0.63	3.039	49.4	1.25	0.2	245.5
2016	212.7	15.6	1.056	26.5	0.55	0.898	22.0	0.43	0.014	2.5	0.05	0.548	63.4	2.45	9.5	256.1
2017	318.0	16.0	1.524	37.5	0.72	0.819	20.7	0.38	3.100	61.2	1.57	1.065	30.0	1.26	-0.6	325.7
2018	273.4	16.4	2.158	53.4	1.63	0.585	14.6	0.30	1.378	27.2	0.71	0.873	27.6	0.95	-0.4	323.7
2019	161.7	16.0	1.013	24.4	0.56	0.237	5.9	0.11	0.994	20.7	0.42	0.383	27.4	0.93	0.0	271.0
2020	245.4	17.6	0.589	14.7	0.31	0.527	13.2	0.22	0.859	27.5	0.54	2.544	60.6	3.05	2.9	200.5
2021	176.9	15.4	0.782	20.1	0.45	1.459	35.7	0.91	0.705	17.6	0.51	0.000	1.7	0.04	-0.3	356.1
2022	436.6	16.0	0.900	22.4	0.58	1.712	43.1	1.06	4.960	98.1	2.60	3.167	51.4	1.50	1.2	216.9
2023	247.1	18.3	1.414	35.8	0.82	0.652	16.9	0.36	1.015	23.4	0.63	1.025	29.9	0.93	2.2	278.0
															–	–

* – the mean daily average temperature (°C); ** – the amount of precipitation (mm) for the period November of the previous year – March of the following year.

A generalized assessment of the hydrothermal regimes of the oilseed radish vegetation period within the years of research presented in Table 1. According to the general classification of the hydrothermal regime of the territories (Latief et al., 2017), the study

period was characterized as conditions of unstable moisture. Taking into account the optimal parameters for the growth processes of oilseed radish plants according to our previous long-term estimates (Tsytsiura, 2020) and the grouping classification by De Martonne Aridity Index (I_{DM}) and Vysotsky-Ivanov humidification coefficient (K_h), the years of research were placed in the following order of increasing favorability of growth processes for the conditions of spring sowing: 2017–2015–2016–2018–2021–2022–2023–2014–2020–2019. For the conditions of the summer sowing period, a similar series was as follows: 2015–2021–2019–2016–2023–2014–2020–2018–2017–2022.

Statistical processing. The indicators of variation statistics were determined using the generally accepted calculation method in the statistical software Statistica 10 (StatSoft - Dell Software Company, USA) and Past 4.13 software (Øyvind Hammer, Norway).

An arithmetic mean ($\overline{x}$), standard deviation ($\pm SD$) and coefficient of variation (CV) were used for statistical evaluation of the obtained average values.

Moreover, a Spearman's correlation test was used for a statistical level of $p < 0.05$ and $p < 0.01$. The data obtained were analyzed using the analysis of ANOVA (Wong, 2018). Tukey HSD Test in R (version R statistic i386 3.5.3) on the 95% family-wise confidence level were used. The coefficient of determination (R^2) and adjusted coefficient of determination (R^2_{adj}) was used for statistically assess the correlation in accordance with Snecdecor & Cochran (1991).

The Chaddock scale (1925) was used to estimate R^2 (R^2 of 0.1–0.3 indicated a weak relationship; 0.3–0.5 moderate; 0.5–0.7 significant; 0.7–0.9 high; 0.9–0.99 very high).

The degree of correlations was estimated by the value of the coefficient of determination (d_{xy}) (Eq. 5) and the use of the method of correlation graph in two interpretations (G and G') (Eqs 6 and 7):

$$d_{yx} = r_{ij}^2 \times 100 \quad (5)$$

$$G = \sum_{|r_{ij}| \geq \alpha} |r_{ij}| \quad (6)$$

$$G' = \left(\sum_{|r_{ij}| \geq \alpha} |r_{ij}| \right) / n \quad (7)$$

where r_{ij} is the correlation coefficient between the i-th and j-th indicator. Only reliable number (n) of correlation coefficients were used in the calculation.

RESULTS AND DISCUSSION

During the ten-year period of study, the average value of the formed aboveground biomass (BM) at the spring sowing date was 24.04 t ha^{-1} with an interannual variation of 30.55% and the root biomass (RBM) was 8.70 t ha^{-1} and 44.70%.

At the summer sowing date, similar indicators were 18.34 t ha^{-1} (32.80%) and 5.50 t ha^{-1} (38.95%) (Fig. 1). The formation of these indicators in dry matter had certain differences, while maintaining the same nature of fluctuations within the years of study.

The average long-term dry matter content in aboveground biomass during the summer sowing period was 2.55% higher for aboveground biomass and 1.21% higher for root biomass compared to the spring sowing period.

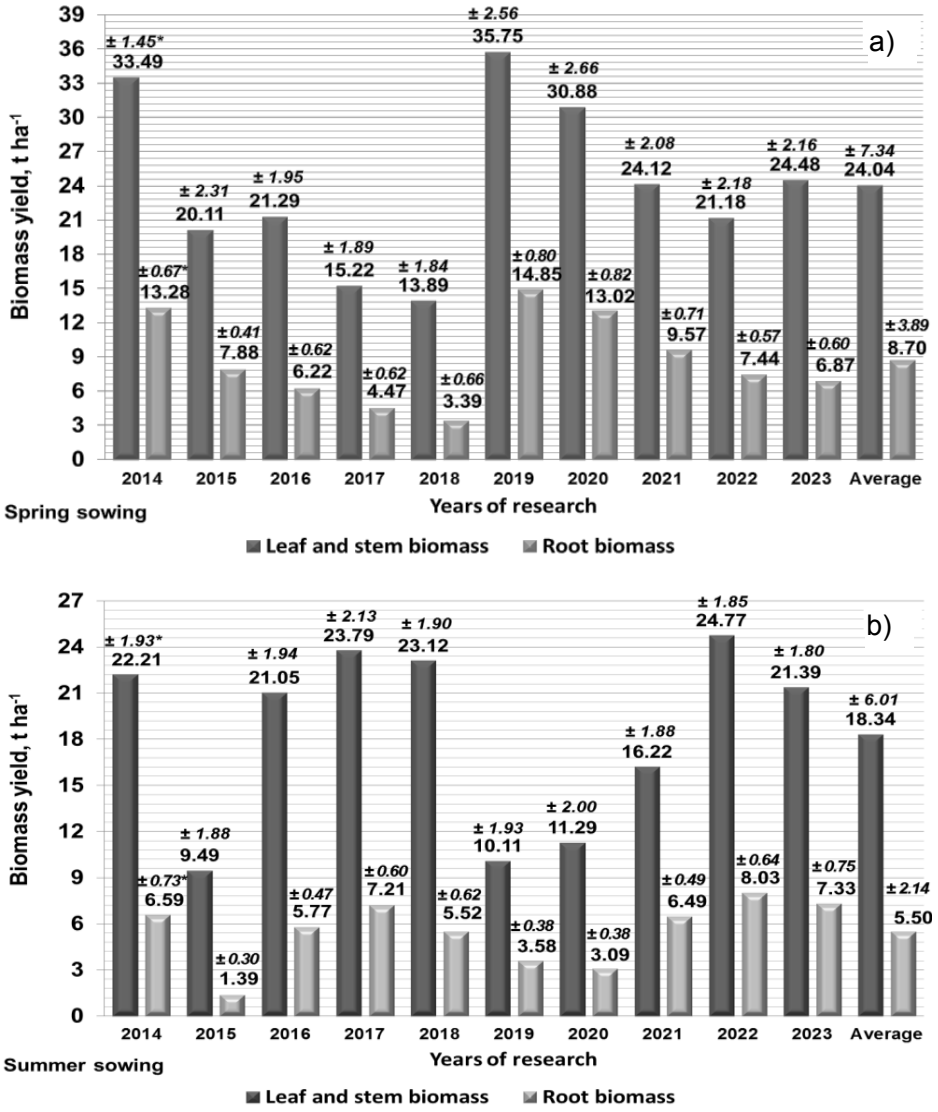

Figure 1. Formed aboveground and root biomass of oilseed radish plants for spring (a) and summer (b) sowing, t ha^{-1} ($LSD_{05\ spring}$BM 1.39 $LSD_{05\ spring}$RBM 1.15; $LSD_{05\ summer}$BM 1.29, $LSD_{05\ summer}$RBM 0.60), 2014–2023. * – Standard deviation

In terms of dry matter, the average level of aboveground biomass was 3.10 t ha^{-1} (23.59% interannual variation) and 1.82 t ha^{-1} (40.86%) for the root biomass produced in the spring sowing date, and 2.82 t ha^{-1} (27.51%) and 1.24 t ha^{-1} (38.75%) in the summer sowing date (Fig. 2). As a result, the total bioproductivity of oilseed radish (the sum of aboveground and root biomass) during the spring sowing period was 32.74 t ha^{-1} in raw weight (34.06% of interannual variability) and 4.92 t ha^{-1} in dry matter (29.47%). These indicators are 8.90 and 0.86 t ha^{-1} lower than the average for the summer sowing date.

The high level of interannual variation is explained by the reaction of oilseed radish plants and the variability of hydrothermal regimes of its vegetation period for both sowing dates during the research period (Table 1). According to the coefficient of variation (*CV*), the variability of precipitation during the evaluation period was 48.24%, average daily temperature 27.46%, *HTC* (K_h) 68.11%, I_{DM} 58.93%. Based on the statements of Latief et al. (2017), such heterogeneity of hydrothermal regimes maked it possible to assess the stress response of oilseed radish plants with high reliability from the point of view of MSCC indicators.

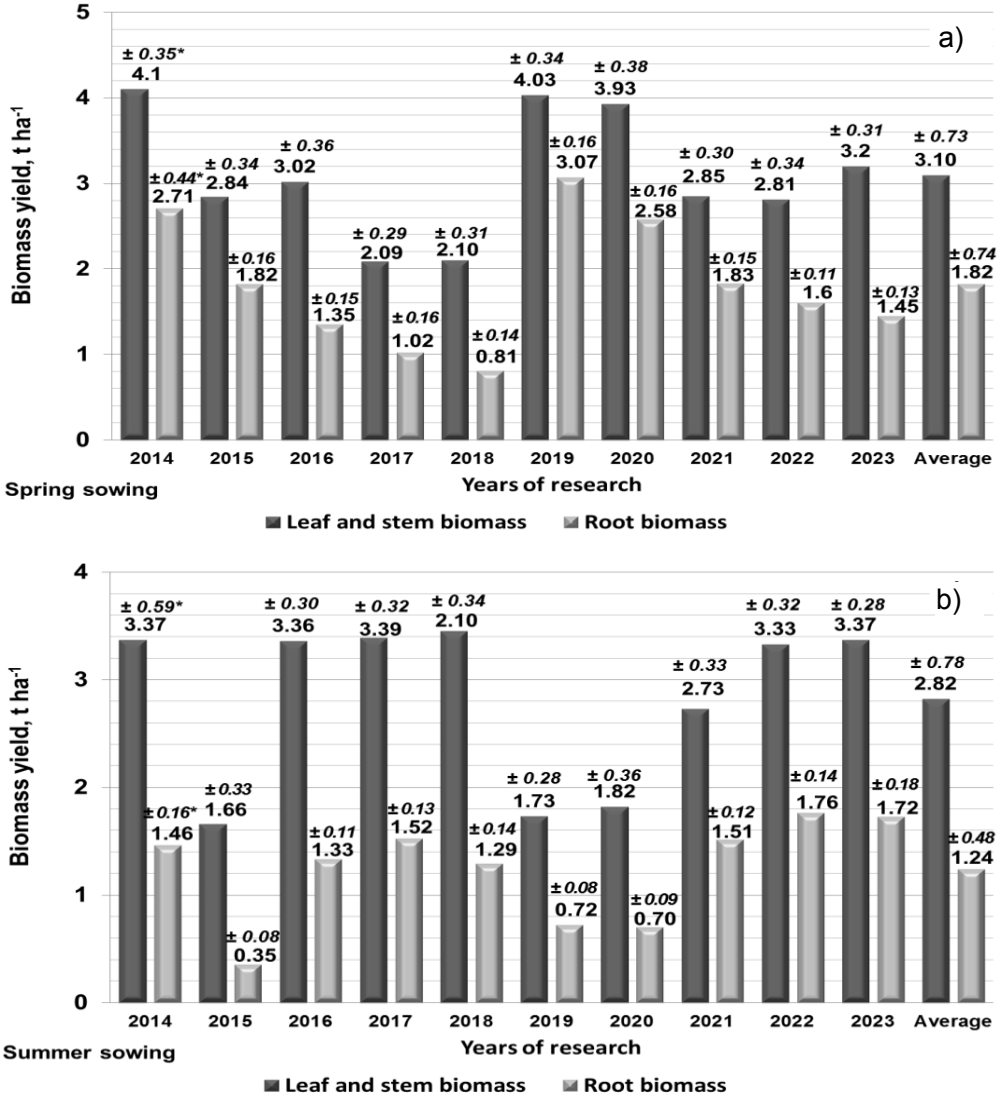

Figure 2. Formed aboveground and root biomass of oilseed radish plants in transformation to dry matter (DM) for spring (a) and summer (b) sowing, t ha^{-1} ($LSD_{05\ spring}$BM 0.24 $LSD_{05\ spring}$RBM 0.26; $LSD_{05\ summer}$BM 0.27, $LSD_{05\ summer}$RBM 0.13), 2014–2023. * – Standard deviation.

It was useful to evaluate the achieved level of bioproductivity of oilseed radish in comparison with other cruciferous species used as intermediate crops in the system of existing agrotechnological solutions.

In the study of Bhogal et al. (2019), the technological interval of oilseed radish biomass yield ranges from 15 to 45 t ha^{-1} depending on soil and climatic conditions. According to the study Quintarelli et al (2022), oilseed radish was classified as a high-yielding cover crop for conditions of sufficient moisture. A number of researchers had noted its sufficient level of adaptability for cultivation in various intermediate technological schemes with different sowing dates right up to August 15 with an average bioproductivity level above 15 t ha^{-1} (White et al., 2016; Wollford & Jarvis 2017; Lövgren, 2022). For conditions of unstable moisture, the yield of aboveground biomass of such crops as white mustard, spring rape, fodder radish (var. Tillage radish (Daikon radish) was in the range of 12–27 t ha^{-1}. For winter rape (for using its biomass in the early summer period) the yield of aboveground biomass was 25–60 t ha^{-1}. The formed underground (root) biomass for the same group of crops was 5–15 t ha^{-1} and 12–25 t ha^{-1}. A high sensitivity of these cruciferous species to the moisture regime, especially during the summer sowing period for unstable moisture conditions was most pronounced (Clark, 2008; Ramirez-Garcia et al., 2012; Ugrenović et al., 2019; Safaei et al. 2022; Ţiţei, 2022).

For conditions of sufficient moisture the achievable levels of the formed aboveground biomass of cruciferous crops was in the range of 12–30 t ha^{-1} de Ruiter et al., 2009; Pekarek et al., 2013; Sousa et al., 2019; Simeão et al., 2023). Rapid growth rates of aboveground biomass of oilseed radish in 40 days after full germination of plants and the concomitant formation of root biomass (with the share of root biomass in total phytomass 18–50%) was noted (Kemper et al., 2020). Based on these results, oilseed radish should be attributed to highly productive crops with developed adaptive mechanisms of plant biomass formation.

On the other hand, the observed high level of variation of the hydrothermal conditions indicator showed a significant role in the realization of oilseed radish plants bioproductivity. If take into account the declared maximum productive potential of the varieties of this crop grown in Ukraine (Tsytsiura 2023c.) at the applied sowing rate up to 50 t ha^{-1} in spring and up to 35 t ha^{-1} in summer sowing, the level of realization of its potential in our studies was varied 27.8–70.0% in spring sowing and 27.1–70.8% in summer sowing. The close interval of realization of bioproductivity at radically different sowing dates was showed the presence of characteristic mechanisms of pre-adaptation to variable heterodynamic environmental conditions in the plant (Borgogno et al., 2009). Based on this oilseed radish can be recommended for the system of different terms of use in the variants of intermediate sowing between the main crops in the rotation of spring and winter groups of crops.

The level of adaptability of a plant with a focus on the formed aboveground and root biomass can be concluded by analyzing different variants of the relationship between these indicators. The efficiency of multipurpose use of field crops was determined by the productivity of its root system which used as a productivity coefficient of the share of root biomass in the formed plant biomass (Williams et al., 2013; Thorup-Kristensen & Kirkegaard, 2016). For oilseed radish, during the study period, the root system productivity coefficient for crude biomass was 2.97 (20.33%) for spring and 3.63 (33.69%) for summer sowing. In terms of dry matter, the index was 1.83 (22.82%) and 2.51 (33.53%) respectively. The inverse ratio of root mass to aboveground mass for spring sowing was 0.35 (crude biomass) and 0.57 (in dry matter) with an interannual variation of 18.67–21.24%. For the summer sowing period, the same indicators were

0.30 (22.98%), 0.43 (23.63%) respectively. This level of ratio indicated the rapid growth rates of oilseed radish plants for both parts of the plants with parity development of the aboveground mass and the presence of a sensitive stress response to deteriorating soil conditions in terms of moisture, aeration, etc (according to the statement of Bláha (2021)). The inertia of the growth of the aboveground part at termination the growth of the underground part was proved. It was confirmed by a decrease in the level of interannual variation of the ratio of root biomass to aboveground biomass with a coefficient of 1.88 for the spring sowing and 1.54 for the summer sowing. This inertia, which determined the preservation of the intensity of growth processes due to the more pronounced stress resistance of the root system (noted in cruciferous species by Ahmad et al. (2012)) allowed oilseed radish to adapt to medium-long periods of aridization and to form an aboveground plant biomass at the level of 50% compared to normal hydrothermal conditions. Such features were formed in the conditions in 2015 for both sowing dates and in 2017 with spring sowing (Table 1). At the same time, should expect an intensification of the growth rate decline with the deterioration of hydrothermal regimes of plant vegetation both from the standpoint of aboveground conditions and soil conditions (Williams et al., 2013; Agathokleous et al., 2019; Kul et al., 2021).

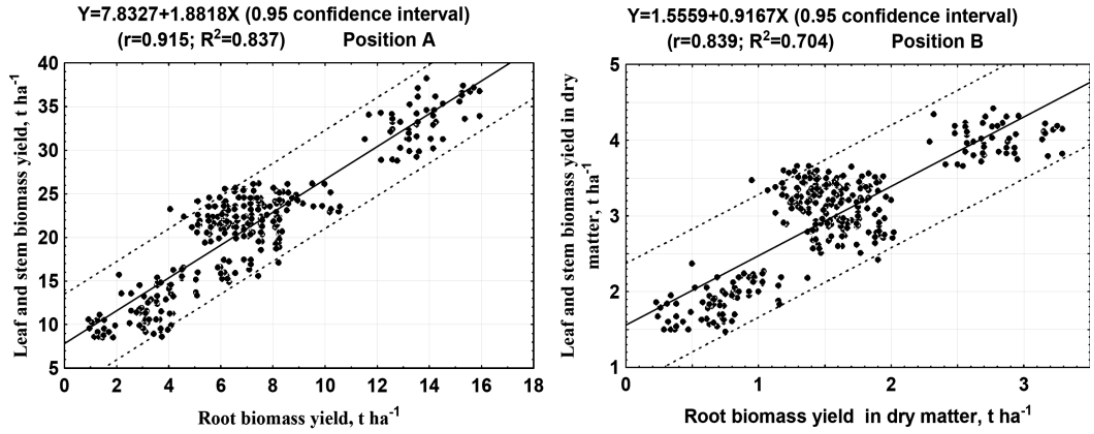

Figure 3. Relationship between aboveground biomass yield and formed root biomass in oilseed radish, 2014–2023 (in a single data system of replication–year–sowing date*;* position A – in raw mass, position B – in dry matter).

It was confirmed by a certain discrepancy between the abscissa and ordinate interval of the graphical display of the data set with 4 units of abscissa correspond to 15 units of ordinate in the version of the data on crude plant biomass and 2 and 3.5 units for dry matter, respectively (Fig. 3). The discrepancy in the axial graphical dynamics of the comparison explained by the difference between the dry matter content of aboveground and root biomass. Such features based on the research of Gan et al. (2009), Benjamin et al. (2014), Bacher et al. (2021) and Kou et al. (2022), confirmed the high adaptive potential of oilseed radish with the possibility of its cultivation as an intermediate crop, especially in summer sowing terms with the existing stressful hot periods characteristic. In addition, the determined parity of the aboveground part of oilseed radish plants in comparison with their root part indicates, taking into account the study of Lopez et al.

(2023), proved a high positive response of oilseed radish on additional mineral nutrition and a high level of accumulation of macro and microelements in the formed biomass.

This fact was valuable in view of the possibility of green manure application of oilseed radish as one of the components of the MSCC system.

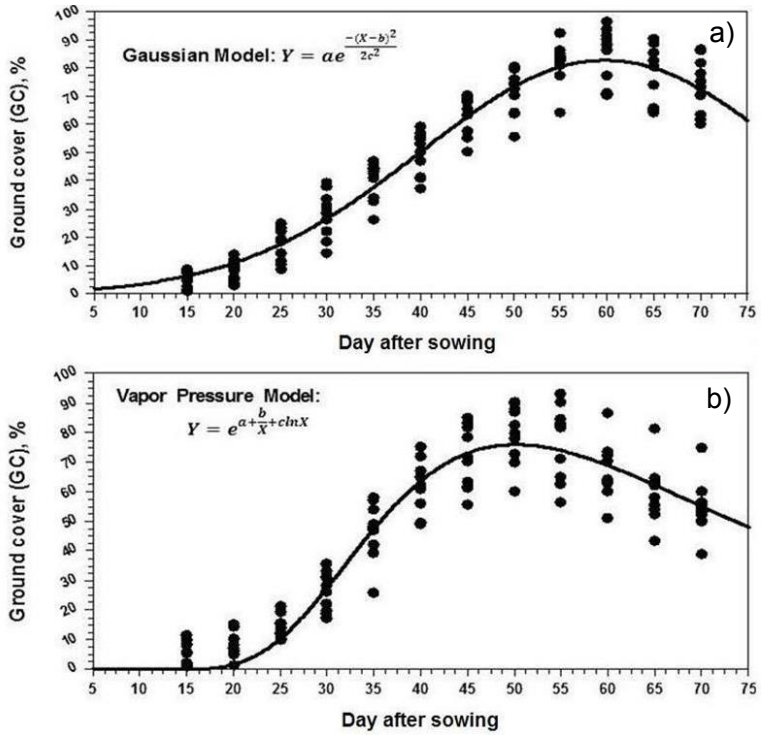

Figure 4. Graphical model with statistical evaluation parameters for the indicator 'Ground cover' (GC) in oilseed radish (vertical marks on the dates of accounting – indicator values in the experimental interval 2014–2023). The position a – variant of the spring sowing season: Coefficient Data: $a = 82.460$; $b = 59.729$; $c = 19.640$; $r = 0.967$; $R^2 = 0.936$; $R^2_{adj} = 0.919$; $S = 7.453$; $RMSE = 71.129$; $RRMSE = 7.545$; $PE = 0.843$; $p < 0.001$. The position b – variant of the summer sowing period: Coefficient Data: $a = 37.471$; $b = -335.487$; $c = -6.761$; $r = 0.956$; $R^2 = 0.915$; $R^2_{adj} = 0.902$; $S = 7.912$; $RMSE = 83.707$; $RRMSE = 9.123$; $PE = 0.796$; $p < 0.001$.

The obtained data on the bioproductive realization of oilseed radish growth processes allowed to further characterize an important component of 'ground cover' (GC) (Fig. 4) as a significant MSCC evaluation criteria. The optimal estimate of this indicator should be at least 70% for the potentially possible period before the optimal phenological date of use (Bodner et al., 2010; Tixier et al., 2010; Ramírez-García et al., 2015). For both sowing dates, an exponential dependence with certain mathematical differences from the commonly used Gompertz function with an asymptote of growth to the maximum GC index was established (Tjørve & Tjørve, 2017). Based on the analysis of the data presented and on the basis of previous studies on the patterns of formation of the leaf apparatus of oilseed radish (Tsytsiura, 2020a), the interval of intensive GC growth in the phenological interval from the beginning of flowering (BBCH 50–52) to its completion (BBCH 68–69) was determined. It should be noted a number of features of the dynamics of GC formation in oilseed radish. One of its was an intensive decrease

due to leaf death on 55–75 days after sowing (which is confirmed by power expressions in the equations in Fig. 4 $X2c^{-2}$ and $2bxc^{-2}$ for spring sowing and bx^{-1} for summer sowing wich was consistent with the findings of Werker & Jaggard (1997)). The another feature was reaching the maximum level of GC on 60 days after sowing in the spring sowing 83.69% (with fluctuations in the range of 71.23–93.67 and on 50 days in the summer sowing 79.94% (60.27–90.36%).

For the summer sowing, both more intensive growth and more intensive decline in the dynamics of GC were determined. On the 70th day after sowing, the GC index was 73.77% (with an interannual variation of 22.43%) for spring and 50.74% (29.93%) for summer sowing. The duration of reaching the maximum value of the GC index in the summer sowing was significantly shorter than in the spring sowing variant. The dynamics of its decrease in the post-peak period was also significantly higher. Based on the data for the summer sowing, the optimal variant of oilseed radish use for the 'cover crop' function was in the period 45–55 days after sowing. For the spring sowing variant it was possible to prolong up to 70 days after sowing.

Table 2. Pearson's correlation coefficients of dependence of oilseed radish bioproductivity parameters on hydrothermal parameters of the growing season (for a joint system of matching sowing dates-repetitions-years (N=160))

1	2	3	4	5	6	7	8	9	10	11
1	-0.40	0.49	0.91	0.96	0.91	0.95	0.95	0.96	-0.51	0.52
2		-0.02	-0.71	-0.62	-0.71	-0.44	-0.53	-0.48	0.51	-0.54
3			0.29	0.37	0.29	0.52	0.36	0.49	-0.35	0.28
4				0.99	1.00	0.87	0.93	0.90	-0.57	0.61
5					0.99	0.91	0.96	0.94	-0.56	0.60
6						0.87	0.93	0.90	-0.57	0.61
7							0.94	0.99	-0.41	0.40
8								0.97	-0.63	0.66
9									-0.49	0.49
10										-0.96
**7.56	4.96	3.46	7.78	7.90	7.78	7.30	7.86	7.61	5.56	5.67
***0.69	0.45	0.31	0.71	0.72	0.71	0.66	0.71	0.69	0.51	0.52

r = |0|–|0.4| No or weak correlation; r = |0.4|–|0.7| Moderate correlation; r = |0.7|–|1.0| Strong correlation. 1=Precipitation (mm); 2 = Average daily temperature (°C); 3=Air humidity (%); 4 = *HTC*; 5=I_{DM}; 6 = K_h; 7 = Leaf and stem biomass yield (t ha^{-1}); 8=Root biomass yield (t ha^{-1}); 9 = Total plant biomass (t ha^{-1}); 10 =Root system productivity coefficient (in dry matter); 11 = Share of root residues in total dry biomass of plants (%); ** Graf G; *** Graf G'. Significance level of $p < 0.05$, the interval r = 0.15–0.19, for $p < 0.01$ r = 0.20–0.25, for $p < 0.001$ $r > 0.25$.

The correlation analysis confirmed the above conclusions about the role of hydrothermal conditions in the possible level of achievement of the total bioproductivity of oilseed radish plants (Table 2). According to the value of the correlation graph of the first type (Graf G), the formation of both aboveground and underground (root) biomass of oilseed radish plants had the highest total dependence of modular numerical values of correlation coefficients from the position of plant weight characteristics (interval Graf G 7.30–7.61). Among the hydrothermal factors of the growing season, hydrometeorological coefficients such as *HTC*, I_{DM}, K_h were maximum (average Graf $G > 7.70$). The amount of precipitation played a more significant role in the system of formation of the total bioproductivity of plants than the level of average daily temperature (ratio coefficient 1.52) and relative humidity (ratio coefficient 2.18). According to the values of the

correlation graph of the second type (Graf G'), the coefficient of determination was 51.84% for the Aridity Index (I_{DM}), 50.41% for the hydrothermal coefficient (*HTC*) and the humidification coefficient (K_h), 47.6% for the amount of precipitation, 20.3% for the average daily temperature and 9.6% for the relative humidity. The determining factor in the formation of the total bioproductivity of oilseed radish plants was the total moisture supply during of its vegetation period and the processes of change of this indicator in relation to evaporation, temperature dynamics and the rate of its growth. The determined lower dependence on the average daily temperature gave grounds to assert its adaptive resistance to low temperatures and the possibility of initiating growth processes in the early and ultra-early periods of the sowing dates. The direction of the dependence showed that the level of total biomass of oilseed radish plants with a high level of predicted probability will increase with increasing precipitation (d_{yx} = 92.2%) and high values of hydrothermal coefficients and ratios (d_{yx} = 81.0–88.4%). It should be noted that oilseed radish had certain advantages in terms of climate adaptation indicators in comparison obtained dependencies with the model parameters wich were included in the predictive models of biomass formation for spring and winter rape, white mustard in variants of its multiple use (Dorsainvil et al., 2005; Jing et al., 2016; Asgari et al., 2021).

The ability to intensive growth processes of oilseed radish plants at lower temperatures had already been noted. Over the 10-year period of research, the average daily air temperature was 14.5 °C for the period April–June (Table 1). Such level of temperature for white mustard and spring rape will already contribute to a decrease in the rate of growth processes and the size of the formed generative part of plants (Ahmad, 2017). The higher levels of dependence for relational quantities (ratios, coefficients) in comparison with the basic climatic parameters on oilseed radish was proved a more complex hierarchy of dependencies between the bioproductivity of oilseed radish plants and the climatic parameters of its growing season. Oilseed radish had a rather flexible adaptive mechanism that distinguished it from other cruciferous plants in terms of the possibility of using it in the MSCC system. This was also confirmed by research Akbarzadeh & Katsikas (2021).

From the point of view of assessing the value of the respective crop for its use in green manure, reclamation (rehabilitation of degraded soils) and biogas potential, it was important to assess the biochemical composition of the formed biomass. The results of such studies was presented in Tables 3 and 4. To estimate and determine the average biochemical portfolio of oilseed radish, gradations of estimates of a number of cruciferous crops were applied in the studies of Ayres & Clements (2002), Azam et al. (2013), Villalobos & Brummer (2013), Winkler (2017), Bell et al. (2020), Keim et al. (2020), Castillo-Umaña et al. (2020), Bakker et al. (2021), Omokanye et al. (2021), Sánchez et al. (2023). Based on these studies, the formed aboveground biomass of oilseed radish plants attributed as a high-protein (CP = 12–23%$_{DM}$) with an increase in summer sowing variant. The average perennial ratio content CP between summer and spring sowing 1.23. The high fat content (CF > 3.0%$_{DM}$) also actualized the leaf and stem mass of oilseed radish as a fodder crop. The high ash content (CA > 12%$_{DM}$) against the background of high phosphorus, potassium, calcium and sulfur (based on the conclusions of Abe (1984), Justes & Richard, 2017) allowed to attribute the leaf mass simultaneously for fodder and green manure purposes.

Table 3. Chemical composition of oilseed radish leaf and stem mass in spring sowing for flowering stage (BBCH 64-67), 2014–2023

Year	Organic dry matter (ODM) (%DM)*		Crude protein (CP) (%DM)		Crude fat (CF) (%DM)		Crude fibre (CFb) (%DM)		Crude ash (CA) (%DM)		NDF (%DM)		ADF (%DM)		ADL (%DM)	
	$\overline{x}$	**SD	$\overline{x}$	SD	$\overline{x}$	SD	$\overline{x}$	SD	$\overline{x}$	SD	$\overline{x}$	SD	$\overline{x}$	SD	$\overline{x}$	SD
2014	87.29	2.50	17.55	2.78	3.02	0.24	19.22	0.64	12.71	0.59	36.91	0.52	24.12	0.42	5.85	0.12
2015	85.41	1.82	15.08	1.91	5.55	0.40	23.07	0.65	14.59	0.45	40.12	0.29	31.24	0.59	4.77	0.14
2016	86.72	1.74	14.29	1.29	3.89	0.16	21.75	0.42	13.28	0.57	36.88	0.42	25.09	0.51	3.89	0.21
2017	84.89	2.47	15.91	1.85	5.09	0.49	23.24	0.30	15.11	0.19	38.09	0.35	28.57	0.57	4.05	0.12
2018	85.95	1.88	15.12	0.56	4.53	0.10	21.52	1.00	14.05	0.27	36.17	0.28	26.62	0.39	3.35	0.09
2019	87.48	1.59	19.17	0.84	3.01	0.31	19.17	0.87	12.52	0.76	34.02	0.19	22.19	0.25	3.58	0.11
2020	87.12	2.13	14.19	1.25	3.28	0.12	20.97	0.83	12.88	0.24	35.39	0.44	24.97	0.39	3.37	0.15
2021	87.39	1.72	12.75	0.83	3.59	0.45	21.83	0.43	12.61	0.34	36.41	0.25	25.17	0.47	4.02	0.07
2022	87.73	0.81	14.56	1.27	3.87	0.66	22.19	0.58	12.27	0.81	37.58	0.57	25.91	0.21	3.81	0.18
2023	86.32	1.49	17.02	1.01	3.94	0.20	22.29	0.87	13.68	0.54	35.89	0.39	24.11	0.33	3.96	0.13
$\bar{X}$	86.63	0.96	15.56	1.89	3.98	0.85	21.53	1.40	13.37	0.96	36.75	1.65	25.80	2.54	4.07	0.75
***R_{min}	1.17–1.33	–	0.55–1.08	–	0.47–0.58	–	0.81–1.09	–	0.63–0.82	–	0.81–0.97	–	0.88–1.05	–	0.13–0.21	–
LSD_{05}	1.29	–	0.87	–	0.52	–	1.00	–	0.75	–	0.90	–	0.93	–	0.16	–

Year	Cellulose (%DM)	Hemicellulose (%DM)	TNC (%DM)		TOC (%DM)		Phosphorus (%DM)		Potassium (%DM)		Calcium (%DM)		Sulfur (%DM)		GSL μmol g^{-1} DM	
	$\overline{x}$	$\overline{x}$	$\overline{x}$	SD	$\overline{x}$	SD	$\overline{x}$	SD	$\overline{x}$	SD	$\overline{x}$	SD	$\overline{x}$	SD	$\overline{x}$	SD
2014	18.27	12.79	2.81	0.44	38.25	0.57	0.54	0.06	2.71	0.11	1.07	0.14	0.32	0.06	12.08	0.45
2015	26.47	8.88	2.41	0.31	40.22	0.81	0.62	0.05	3.96	0.19	0.97	0.12	0.42	0.09	13.52	0.43
2016	21.20	11.79	2.29	0.21	39.14	0.48	0.77	0.17	4.74	0.24	1.00	0.10	0.50	0.10	14.51	0.37
2017	24.52	9.52	2.55	0.30	41.12	0.65	0.85	0.08	5.72	0.38	1.15	0.15	0.59	0.11	16.08	0.87
2018	23.27	9.55	2.42	0.09	39.77	0.78	0.69	0.07	3.74	0.20	1.03	0.08	0.52	0.06	15.56	0.57
2019	18.61	11.83	3.07	0.13	37.14	1.14	0.52	0.05	2.25	0.11	0.81	0.18	0.35	0.12	11.89	0.44
2020	21.60	10.42	2.27	0.20	40.09	0.43	0.63	0.08	4.08	0.16	0.92	0.07	0.35	0.05	12.44	0.60
2021	21.15	11.24	2.04	0.13	37.95	0.73	0.48	0.09	2.87	0.37	0.93	0.17	0.39	0.05	12.77	0.40
2022	22.10	11.67	2.33	0.20	38.44	0.46	0.51	0.03	3.03	0.10	0.89	0.10	0.41	0.08	13.84	0.52
2023	20.15	11.78	2.72	0.16	38.89	0.42	0.61	0.06	3.19	0.31	0.82	0.07	0.34	0.09	12.97	0.59
$\bar{X}$	21.73	10.95	2.49	0.30	39.10	1.21	0.62	0.12	3.63	1.04	0.96	0.11	0.42	0.09	13.57	1.44
R_{min}	–	–	0.20–0.39	–	0.89–1.05	–	0.09–0.14	–	0.25–0.39	–	0.15–0.20	–	0.10–0.14	–	0.19–0.36	–
LSD_{05}	–	–	0.34	–	0.98	–	0.12	–	0.34	–	0.18	–	0.12	–	0.23	–

*The indicator of transformation between %DM and g kg^{-1}_{DM} = %DM x 10.**SD – standard deviation; ***Tukey's test (R_{min} for $p_{adj} < 0.05$).

Table 4. Chemical composition of oilseed radish leaf and stem mass in summer sowing for flowering stage (BBCH 64-67), 2014–2023

Year	Organic drymatter (ODM) (%DM)*		Crude protein (CP) (%DM)		Crude fat (CF) (%DM)		Crude fibre (CFb) (%DM)		Crudeash (CA) (%DM)		NDF (%DM)		ADF (%DM)		ADL (%DM)	
	$\overline{x}$	**SD	$\overline{x}$	SD	$\overline{x}$	SD	$\overline{x}$	SD	$\overline{x}$	SD	$\overline{x}$	SD	$\overline{x}$	SD	$\overline{x}$	SD
2014	85.08	0.99	17.44	1.31	4.17	0.82	23.32	0.82	14.92	0.90	42.31	0.52	29.89	0.42	6.12	0.12
2015	83.79	0.87	14.88	1.61	5.82	0.62	26.72	0.70	16.21	0.72	46.12	0.29	33.17	0.59	6.61	0.14
2016	84.08	1.78	18.38	2.15	4.40	0.40	23.89	0.61	15.92	0.33	42.87	0.42	30.05	0.51	6.18	0.21
2017	85.36	3.32	19.88	2.00	4.29	0.33	22.97	0.75	14.64	0.60	41.92	0.35	29.19	0.57	5.74	0.12
2018	84.80	1.71	20.75	2.42	4.78	1.09	23.69	0.99	15.20	0.63	42.30	0.28	29.68	0.39	5.92	0.09
2019	83.21	1.13	16.13	1.65	5.02	0.48	25.33	1.03	16.79	0.35	44.35	0.19	31.87	0.25	6.48	0.11
2020	84.63	0.74	20.44	1.39	4.55	0.79	24.17	0.85	15.37	1.11	44.11	0.44	31.05	0.39	6.25	0.15
2021	83.56	1.93	19.31	1.52	4.72	0.28	24.85	0.64	16.44	0.86	44.55	0.25	31.27	0.47	6.29	0.07
2022	85.03	0.67	22.94	3.26	4.08	0.65	22.51	0.79	14.97	0.44	42.37	0.57	28.97	0.21	5.52	0.18
2023	84.42	0.54	21.44	3.13	4.27	0.32	23.92	0.64	15.58	0.92	43.09	0.39	30.34	0.33	6.09	0.13
$\bar{X}$	84.40	0.71	19.16	2.48	4.61	0.52	24.14	1.23	15.60	0.71	43.40	1.34	30.55	1.30	6.12	0.33
***R_{min}	0.81–0.96	–	1.05–1.28	–	0.82–0.96	–	0.92–1.19	–	0.88–1.12	–	0.99–1.36	–	1.53–1.81	–	0.32–0.48	–
LSD_{05}	0.92	–	1.14	–	0.91	–	1.14	–	1.05	–	1.24	–	1.64	–	0.37	–
Year	Cellulose (%DM)	Hemicellulose (%DM)	TNC (%DM)		TOC (%DM)		Phosphorus (%DM)		Potassium (%DM)		Calcium (%DM)		Sulfur (%DM)		GSL mmol g^{-1} DM	
	$\overline{x}$	$\overline{x}$	$\overline{x}$	SD	$\overline{x}$	SD	$\overline{x}$	SD	$\overline{x}$	SD	$\overline{x}$	SD	$\overline{x}$	SD	$\overline{x}$	SD
2014	23.77	12.42	2.79	0.21	41.03	1.34	0.57	0.09	3.52	0.36	1.07	0.17	0.41	0.11	18.55	1.04
2015	26.56	12.95	2.38	0.26	39.82	1.31	0.71	0.10	4.71	0.20	1.13	0.26	0.68	0.06	21.58	1.56
2016	23.87	12.82	2.94	0.34	40.59	1.78	0.67	0.07	3.89	0.14	1.09	0.29	0.39	0.04	18.19	1.09
2017	23.45	12.73	3.18	0.32	38.51	0.79	0.59	0.09	3.33	0.46	0.92	0.18	0.35	0.06	17.92	0.60
2018	23.76	12.62	3.32	0.39	38.09	1.71	0.65	0.07	4.35	0.16	0.85	0.09	0.53	0.04	21.02	0.53
2019	25.39	12.48	2.58	0.26	40.87	0.82	0.78	0.07	4.98	0.15	1.28	0.23	0.56	0.17	21.19	0.56
2020	24.80	13.06	3.27	0.22	38.44	0.85	0.54	0.06	3.39	0.23	1.09	0.15	0.47	0.05	19.75	0.52
2021	24.98	13.28	3.09	0.24	41.29	0.76	0.64	0.09	3.57	0.34	1.05	0.09	0.59	0.07	21.53	0.70
2022	23.45	13.40	3.67	0.52	38.98	1.73	0.52	0.03	3.05	0.20	0.67	0.18	0.31	0.09	17.17	0.63
2023	24.25	12.75	3.43	0.50	39.15	0.89	0.59	0.08	3.82	0.40	0.95	0.11	0.49	0.09	20.09	0.47
$\bar{X}$	24.43	12.85	3.07	0.40	39.68	1.20	0.63	0.08	3.86	0.63	1.01	0.17	0.48	0.12	19.70	1.64
***R_{min}	–	–	0.41–0.53	–	1.73–1.95	–	0.07–0.15	–	0.32–0.44	–	0.21–0.32	–	0.08–0.15	–	0.31–0.54	–
LSD_{05}	–	–	0.49	–	1.82	–	0.11	–	0.41	–	0.27	–	0.12	–	0.43	–

*The indicator of transformation between %DM and g kg^{-1}_{DM} = %DM x 10. **SD – standard deviation; ***Tukey's test (R_{min} for $p_{adj} < 0.05$).

On the basis of this, it was also established possibility of the recycling of nutrients through the system of its return to the soil as green fertilizers in the form of oilseed radish biomass. The relatively high cellulose content at the flowering stage in spring (> 18%$_{DM}$) and summer sowing (> 23%$_{DM}$) against the background of the previously noted features of accelerated plant development ('biological aging') confirmed a steady trend of reducing the quality biochemical parameters of plant mass in later phases of the growing. This was confirmed by comparing the content of not only cellulose but also the constituent derivatives NDF, ADF and ADL. This is also confirmed in a number of studies on other cruciferous plant species (Azam et al., 2013; Herrmann et al., 2016; Bell et al., 2020). It was also indicated by a 1.5-fold increase in lignin content in plant mass (in the form of ADL) when comparing summer and spring sowing dates. Such a stable trend allowed to determine the peculiarities of oilseed radish biomass formation at different sowing dates. For the spring sowing, against the background of lower average daily temperatures and slow growth rates, the process of protein complex formation under the lower stressful temperature conditions, which (according to the studies of Sharma & Dubey (2019), Zhou et al. (2023)), contributed to the formation of plant tissues with a higher level of organic matter and water content with lower fiber, cellulose, protein and ash content. For the summer sowing, when plants formed at significantly higher levels of average daily temperature and more stressful conditions of hydrothermal vegetation regime (Table 1), biochemical processes had the reverse nature. A similar system of correlations was noted for white mustard at different periods of its use (Ţiţei (2022)) and some representatives of the radish genus (Ayres & Clements, 2002). This is also confirmed by the results of comparing the main biochemical components for the spring sowing with similar long-term averages of the summer one. The obtained coefficients of this ratio in the interval of research years for ODM 1.03–1.11, CP 0.77–0.85, CF 0.74–0.88, CFb 0.79–0.89, ADL 0.59–0.71, Cellulose 0.81–0.89, Hemicellulose 0.73–0.85, TNC 0.74–0.85, TOC 0.91–0.99, P 0.89–0.98, K 0.85–0.94, Ca 0.87–0.95, S 0.79–0.90, GSL 0.82–0.88. As a result, in view of a number of studies (Clark 2008; Hansen et al., 2021, 2022; Jauhiainen 2022; Launay et al., 2022; Fajobi et al., 2023; Lallement et al., 2023; Lymperatou et al., 2023; Manyi-Lohn & Lues, 2023), the leaf mass of oilseed radish of different sowing dates will have different criterion evaluation in the MSCC system.

At the same time, due to the increasing stress of general environmental factors, the overall variability of the obtained average values in terms of years of research was also increasing. The coefficient of variation of the average for the general data set for the summer sowing of oilseed radish had an average growth coefficient of 1.21 compared to the indicators of the spring sowing. Such features lead to an increase in the variable component in assessing the effectiveness of the use of the obtained oilseed radish biomass for the criterion goals of the MSCC system.

It should also be noted that based on studies oilseed radish in the management system as a cover crops for different purposes (Herrmann et al., 2016; Blume et al., 2020; Gamba et al., 2021; Hansen et al. 2021; Lövgren, 2022; Olofsson & Ernfors, 2022; Kemper et al., 2023), the results of biochemical evaluation presented in Tables 3–4 have certain differences. The CP content at the spring sowing was 0.9–1.5% $_{DM}$ lower than at the summer sowing and did not reach 25–27%$_{DM}$ noted in the above studies. The content of lignin, cellulose and its derivatives was 3.8–7.7%$_{DM}$ higher than in the estimates of Herrmann et al. (2016) and Hansen et al. (2021). The total organic carbon (TOC) content

had a relatively stable value with fluctuations in the range of 38–42%$_{DM}$, although in the study by Hansen et al. (2021) its had a narrower interval of 39–40%$_{DM}$. In the study of Gamba et al. (2021) its level of 35–44%$_{DM}$ was noted. The detail of the content of the main elements (nitrogen, phosphorus and potassium) was estimated for two seasons with different weather conditions in the study by Hansen et al. 2021. In comparison with the data of this study, for oilseed radish on gray forest soils under conditions of unstable moisture, the phosphorus content was found 0.13–0.33%$_{DM}$ higher, the potassium content was 0.72–1.12%$_{DM}$ lower, and the calcium content was 0.15–0.24%$_{DM}$ higher. The nitrogen content was less by 0.18–0.35%$_{DM}$. In comparison with other cruciferous plant species were determined: CP content by 3.4–8.7%$_{DM}$ lower, CF content by 1.3–2.4%$_{DM}$ higher, CFb content by 1.9–6.1%$_{DM}$ lower, CA content by 1.7–2.2%$_{DM}$ lower, ADL content by 0.7–2.5%$_{DM}$ lower, potassium content by 1.8–3.7%$_{DM}$ higher, phosphorus content by 0.12–0.22%$_{DM}$ lower and sulfur content by 0.27–0.35%$_{DM}$ lower (Swarcewicz et al., 2013; Li et al., 2019; Abdallah et al., 2020;, Liu et al., 2020; Tian & Deng, 2020; Wang et al., 2022; Jacob et al., 2022; Rajković et al., 2022; Ţiţei, 2022; Oliveira & Słomka, 2021; Shitophyta et al., 2023; Israt & Parimal, 2023).

The content of glucosinolates (GSL) is important in the MSCC criterion system in such areas as ‘cover crop’, ‘catch crop’, ‘green manure’. Glucosinolates provide the effect of biofumigation through the formation of active components as a result of the decomposition of the leaf and stem mass of cruciferous species that has been worked into the soil. Biofumigation contributes to reduce the germination of weed seeds, soil fungicidal effect against a number of harmful pathogens and reduction of soil pests, in particular, various species of nematodes due to soil transformation of glucosinolates into isothiocyanates (ITC) (Sang et al., 1984; Kirkegaard & Sarwar, 1998; Śmiechowska et al., 2010; Edwards & Ploeg, 2014; Sarıkamıs et al., 2017; Blažević et al., 2020; Yan et al., 2023; Redha et al., 2023).

The presence of glucosinolates at certain concentration levels is desirable for intermediate cover crops, especially in summer sowing, to control a number of entomophages and diseases, which guarantees the necessary level of plant survival and the appropriate technological planting density and bioproductivity (McDowell et al., 2008; Zachariah, 2011; Bohinc et al., 2013; Bhandari et al., 2015; Perniola et al., 2019; Andini, 2020; Ait Kaci Ahmed et al., 2022; Abdel-Massih et al., 2023; Tsytsiura, 2024).

At the same time, the high concentration of glucosinolates significantly narrowed the use of crop in the MSCC system as a ‘fodder crop’, reducing the feed value of the plant and can cause poor compatibility and a number of disorders in animals (Prieto et al., 2019).

High concentration of glycosinolates also reduced the efficiency of such a direction as ‘biogas crop’ due to the inhibition of the intensity of anaerobic fermentation of the resulting leaf-stem mass (Cleemput, 2011; Al Seadi et al., 2013; Herrmann et al., 2016; Tsytsiura 2023b). The content of glucosinolates is also important for cruciferous crops used as ‘catch crops’. It has been established that these compounds was involved in the formation of plant stress responses to abiotic factors. Its intensive growth had a high levels of significant correlation with the increase in the overall stress of the growing season by climatic parameters. It is especially important for intermediate crops that are often grown in the summer–autumn period with increasingly stressful environmental conditions (Chowdhury, 2022; Lei et al., 2022; Zhang et al., 2022).

Long-term assessment of the direct and derived glucosinolate potential of cruciferous plants proved high interspecific variability of their content as well as high variability of concentration in the aboveground parts of the plant depending on the phenological phase of development and abiotic environmental conditions (Sang et al., 1984; Kirkegaard & Sarwar, 1998; Bellostas et al., 2004; Ciska et al., 2008; Velasco et al., 2008; Edwards & Ploeg, 2014; Bhandari et al., 2015; Yi et al., 2016; Ricardo et al., 2018; Liu et al., 2020; Wu et al., 2021; Mocniak et al., 2023; Iwar et al., 2024). The total content of glucosinolates and different cruciferous plant species ranged from 1.97 to 140.9 μmol g^{-1}_{DM} with a maximum concentration in seeds and generative parts and a minimum in the early stages of vegetation in leaves and roots. It was noted (Velasco et al., 2008) that the concentration of glucosinolates among the cruciferous groups was maximum for leafy cruciferous plants (up to 26 μmol g^{-1}_{DM}), lower values were noted for the group of fodder cruciferous plants (up to 24 μmol g^{-1}_{DM}). The classical oilseed cruciferous plants had the lowest level of this indicator (12–16 μmol g^{-1}_{DM}). In the study by Bhandari et al. (2015), The lowest GSL conyent were observed in radish genus across all tissues examined (18–40 μmol g^{-1}_{DM}).

The long-term average GSL content in the aboveground biomass of oilseed radish was 13.57 μmol g^{-1}_{DM} (*CV* 8.32%) in spring and 19.70 μmol g^{-1}_{DM} (*CV* 10.58%) in summer sowing. It was confirmed the increase in its concentration with an increase in the overall stress of the growing season. In various studies on oilseed radish at the flowering stage, the level of glucosinolates was in the range of 9–41 μmol g^{-1}_{DM} and was 1.2–1.5 times higher in inflorescences compared to leaves and stem (Gimsing & Kirkegaard, 2006; Bohinc et al., 2013; Duff et al., 2020). For white mustard the average GSL content (on average per plant) for the flowering phase was in the range of 11–56 μmol g^{-1}_{DM} (Sang et al., 1984; Kirkegaard & Sarwar, 1998; Bohinc et al., 2013; Ciska et al., 2008; Tian & Deng, 2020). For spring rape GSL content was 9–44 μmol g^{-1}_{DM} (Sang et al., 1984; Birch et al., 1992). For winter rape this indicator was at the level of 8–51 μmol g^{-1}_{DM} (Sang et al., 1984; Milford & Evans, 1991; Kirkegaard & Sarwar, 1998; Ciska et al., 2008; Yasumoto et al., 2010; Bohinc et al., 2013; Salisbury et al., 2018). The long-term data of the GSL content in oilseed radish (Table 3–4) allowed to classify it as a cruciferous crops with high biofumigation potential for both spring and summer use.

The biofumigation potential of oilseed radish was also confirmed by the value of glucosinolate productivity for both sowing dates (Table 5). The obtained values was in the range of 32.7–49.5 mol ha^{-1} (with an interannual *CV* of 15.1%) for spring sowing and 36.0–72.5 mol ha^{-1} (24.9%) for summer sowing. This result was positively correlated with the study of Duff et al. (2020). It was noted the effective level of GSL content for achieving multiple goals of soil biofumigation by green manure in the case of spring and summer sowing, depending on the type of cruciferous plants in the range of 30–105 mol ha^{-1}. The interval of 60–105 mol ha^{-1} was achieved by using different types of mustard (White mustard (*Sinapis alba*), Ethiopian mustard (*Brassica carinata*), Indian mustard (*Brassica juncea*), Fodder mustard (*Brassica napus*), Black mustard (*Brassica nigra*)) in pure sowings or in various mixtures with radishes (such species-specific trademarks as ‘Tillage Radish’, ‘Terranova Radish’, ‘Black Jack Radish’).

Table 5. The main indicators of quality of oilseed radish aboveground biomass for different terms of sowing, 2014–2023

Year	C/N ratio				C/P ratio				C/S ratio				Carbohydrates (CH) (%$_{DM}$)			
	*SprS		SumS		SprS		SumS		SprS		SumS		SprS		SumS	
	$\overline{x}$	**SD	$\overline{x}$	SD	$\overline{x}$	SD	$\overline{x}$	SD	$\overline{x}$	SD	$\overline{x}$	SD	$\overline{x}$	SD	$\overline{x}$	SD
2014	13.94	2.80	14.77	1.18	71.41	7.27	73.59	13.45	122.24	19.90	106.69	34.14	66.71	3.37	64.43	1.33
2015	16.86	1.81	16.86	1.60	65.12	4.58	57.06	9.16	98.68	18.50	58.94	5.65	64.80	2.05	65.01	1.98
2016	17.20	1.67	13.99	2.18	53.27	14.66	61.25	8.23	80.55	15.57	105.36	15.79	68.52	1.90	62.44	1.95
2017	16.28	1.83	12.21	1.35	48.70	4.49	66.25	9.09	71.71	14.05	112.41	18.62	63.86	2.49	62.45	2.22
2018	16.45	0.71	11.58	1.41	58.20	7.29	59.08	6.73	77.13	7.97	72.27	7.92	66.30	0.83	60.60	1.90
2019	12.12	0.86	15.97	1.73	72.13	8.98	52.73	4.93	115.31	35.43	80.62	33.69	65.28	1.71	63.31	1.97
2020	17.75	1.37	11.81	1.03	64.30	7.13	71.70	6.70	116.73	19.14	82.29	6.68	69.65	1.37	61.08	1.45
2021	18.67	1.44	13.42	1.06	80.82	12.41	65.64	10.32	98.56	14.00	70.80	9.22	71.05	0.81	60.88	1.57
2022	16.59	1.48	10.84	2.11	75.56	4.00	75.03	2.14	96.60	18.90	134.31	40.91	69.30	1.00	59.18	2.97
2023	14.34	0.96	11.58	1.51	64.24	6.67	67.15	8.31	120.76	31.85	82.23	17.63	65.38	1.71	59.93	3.24
$\bar{X}$	16.02	2.36	13.30	2.40	65.37	12.13	64.95	10.23	99.83	25.78	90.59	29.80	67.08	2.83	61.93	2.63
LSD_{05}	2.30	–	2.05	–	5.79	–	3.89	–	12.81	–	10.55	–	2.71	–	3.08	–

Year	Residue quality (RQ) (%$_{DM}$)				Accumulation in aboveground biomass (kg ha^{-1})											
					Nitrogen***				Phosphorus				Potassium			
	SprS		SumS		SprS		SumS		SprS		SumS		SprS		SumS	
	$\overline{x}$	SD	$\overline{x}$	SD	$\overline{x}$	SD	$\overline{x}$	SD	$\overline{x}$	SD	$\overline{x}$	SD	$\overline{x}$	SD	$\overline{x}$	SD
2014	81.36	0.82	81.46	0.88	114.6	15.27	93.94	11.22	22.14	2.70	19.50	5.27	111.15	9.64	118.21	12.98
2015	86.35	0.84	80.44	0.72	68.34	8.05	39.51	4.58	17.62	1.71	11.88	2.50	112.56	9.22	78.38	7.71
2016	84.32	0.98	81.00	1.33	69.32	8.38	98.71	14.96	23.19	4.95	22.32	0.16	143.27	10.32	130.87	15.65
2017	86.43	0.65	81.53	1.84	53.28	6.04	108.00	12.61	17.76	1.65	20.04	3.26	119.68	10.73	113.53	20.25
2018	87.10	1.15	81.46	0.78	51.08	9.02	114.45	14.26	14.58	3.01	22.42	2.64	78.54	10.69	150.09	11.32
2019	84.59	0.88	81.04	0.78	123.8	10.91	44.75	5.09	21.05	3.56	13.56	1.81	90.61	5.69	86.49	7.42
2020	86.21	1.08	80.69	0.68	89.21	8.25	59.46	6.82	24.79	3.46	9.77	0.74	160.26	4.34	61.51	5.40
2021	84.74	1.33	80.43	0.52	58.03	4.48	84.48	10.67	13.88	4.07	17.56	3.53	81.32	8.28	97.64	13.52
2022	84.52	1.07	81.08	0.71	65.62	7.09	122.58	21.80	14.35	1.12	17.28	1.17	85.26	4.59	101.62	10.79
2023	84.26	1.39	81.16	0.98	87.14	5.89	115.51	17.38	19.50	1.36	19.79	1.68	101.96	6.37	129.07	18.97
$\bar{X}$	84.99	1.83	81.03	0.95	78.04	25.40	88.14	31.25	18.88	4.57	17.41	4.80	108.46	25.52	106.74	22.25
LSD_{05}	1.50	–	2.17	–	8.69		9.73		4.33		3.86		8.77		10.72	

Year			2014	2015	2016	2017	2018	2019	2020	2021	2022	2023	$\bar{X}$	LSD_{05}
Ca accumulation (kg ha^{-1})		SprS	44.05	27.48	30.27	24.04	21.75	32.28	36.17	26.79	25.05	26.31	29.42	3.69
		SumS	36.27	18.69	36.90	31.04	29.24	22.09	19.72	28.81	22.10	32.03	27.69	4.27
S accumulation (kg ha^{-1})		SprS	13.18	11.89	15.15	12.31	11.00	14.29	13.78	11.10	11.52	10.82	12.50	2.34
		SumS	14.09	11.32	13.02	11.87	18.24	9.75	8.51	16.19	10.36	16.53	12.99	3.82
GSL productivity (mol ha^{-1})		SprS	49.5	38.4	43.8	33.6	32.7	47.9	48.9	36.4	38.9	41.5	41.2	0.17
		SumS	62.5	35.8	61.1	60.8	72.5	36.7	36.0	58.8	57.2	67.7	54.9	0.35
Equivalent cattle manure, t ha^{-1}		SprS	23.0	18.9	22.8	18.9	13.7	21.7	26.1	13.9	15.2	19.6	23.0	–
		SumS	22.0	12.6	24.3	23.1	28.1	14.2	12.5	19.2	23.1	25.6	22.0	–

*SprS – Spring sowing; SumS – Summer sowing. **SD – standard deviation; *** transformation from kg ha^{-1} to g m^{-2} by dividing the value by 10.

At the achieved level of glucosinolate accumulation, the studied species of oilseed radish (*Raphanus sativus* L. var. *oleiformis* Pers.) can be effectively used at both sowing dates in the soil rehabilitation system through the process of green manure biofumigation. The issue of combining oilseed radish with other cruciferous species under conditions of unstable moisture should be further investigated in the future.

It was noted (Couëdel et al., 2019) that the biochemical assessment of the leaf mass of plants used as cover crops for multipurpose use requires a system of appropriate ratios that determine the processes of decomposition, mineralization, accumulation and the predicted intensity of anaerobic fermentation. These ratios was widely used by the scientific community and proposed in the analysis of Hansen et al. (2021), Thiébeau et al. (2021), Hansen et al. (2022), Quintarelli et al. (2022), Allam et al. (2023), Yousefi et al. (2024). The results of this assessment was presented in Table 5.

According to a number of studies (Kriaučiūnienė et al., 2012; Jahanzad et al., 2016; Sousa et al., 2019; Liu et al., 2020; Toleikiene et al., 2020; Dorissant et al., 2022; Silva et al., 2023), the C/N ratio is decisive in the decomposition rate of green manure. The biomass of oilseed radish at the interval value of C/N ratio 8.73–20.11 with interannual variation of 12.3% for spring sowing and 15.4% for summer sowing (Table 5) was fully compliant to the criteria of 'fodder crop' and 'green manure'. It was predicted to ensure rapid decomposition of its raw biomass in the soil, especially under conditions of sufficient moisture supply against the background of high average daily temperatures. These values also indicated a significant proportion of leaves and inflorescences in the total biomass of oilseed radish, especially at the summer sowing date. Such conclusions was confirmed by the findings of Kriaučiūnienė et al. (2012) on the decomposition rates of different parts of cruciferous plant species. It should also be noted that in the case of summer sowing of oilseed radish, according to a number of studies (Wadman & de Haan, 1997; Hadas et al., 2004; Flores-Sánchez et al., 2016; Drost et al., 2019; Salume et al., 2020) decomposition rates will have predictably slower due to the significantly lower temperature during the period of direct use of biomass in the form of green manure (Table 1). The optimal value of C/N ratio, which provides a positive ratio between the rate of decomposition and subsequent humus accumulation and immobilization of mineral nutrients, was range from 13 to 25 depending. Actually, this indicator depends from the weather conditions, soil type and the nature of the use of the corresponding cover crop (Wadman & de Haan, 1997). It was also positively correlates with C/N ratio in classical cattle manure 16.6–25.0 (Pan et al., 2021). The biomass of oilseed radish formed during spring sowing had a higher degree of compliance with these intervals for green manure use. Its use can be optimized by using oilseed radish in mixed crops with cereals and legumes, as well as using additional plant materials for combined green manure (e.g. straw) (according to the recommendations of Couëdel et al. (2019) and Hansen et al. (2021)).

The determined long-term average C/N ratio also allowed to classify oilseed radish as a candidate for the 'fodder crop' in the MSCC system.

The value of the C/N indicator was considered from the standpoint of increased protein content, i.e. higher total nitrogen content with optimization of fiber and non-nitrogenous compounds (lower carbon content). As a result, the optimal value of the C/N ratio was in the range of 8–15 (Li & Zhou, 2002).

It has been noted that the optimal C/N ratio for anaerobic biomass dehydration in biogas production technologies was in the range of 20–30 with an interval of possible technological deviations from 10 to 40 (Guarino et al., 2016; Herrmann et al., 2016; Dębowski et al., 2022; Manyi-Loh. & Lues, 2023; Tsytsiura, 2023a). At low values of the C/N ratio, the concentration of the ammonium form of nitrogen increased significantly and the microbial process of anaerobic fermentation was inhibited (Cerón-Vivas et al., 2019; Choi et al., 2020). Based on this, the most appropriate option for oilseed radish would be the use of pre-prepared biomass both through silage and through co-fermentation of fresh mass with other plant or organic resources as well as the use of cofermentation and inoculum (Carvalho et al., 2011; Wang et al., 2012; Herrmann et al., 2016; Oliveira & Słomka, 2021). It was proved that silage fermentation of oilseed radish leaf and stem mass allowed to increase the C/N ratio by 3–6 units depending on the phenological phase of plants during the formation of silage mass and the use of inoculum. It was helped to optimize the accumulation curve of the generated biomethane and intensified the digestion process (Tsytsiura, 2023c). It should be noted that C/N ratio for other cruciferous crops used in MSCC variants at the flowering stage was in the range of 12–23 for spring sowing and 10–18 for summer sowing (Herrmann et al., 2016; Li et al., 2019; Blume et al., 2020; Keim et al., 2020; Liu et al., 2020; Hansen et al., 2021; Ţiţei, 2022). Such results confirmed the high potential of oilseed radish in the MSCC criterion system in comparison with the already widely used cruciferous crops.

It was also important to evaluate the C/P ratio, which was characterized the relationship between soil immobilization of mobile phosphorus forms and the efficiency of its replenishment by biomass introduced into the soil. This ratio affects the nature of the microbiological decomposition of green manure, especially in soils depleted in mobile phosphorus forms (Ngatia et al., 2014; Nobile et al., 2019). The optimal option for green manure application of the formed biomass was a high phosphorus content and low C/P ratio (Rinasoa et al., 2022). This ensured the maintenance of intensive rates of biomass decomposition in the soil with a positive balance of phosphorus release (Amy et al., 2024). According to this criterion, the leaf and stem mass of oilseed radish responded the required disparity between the phosphorus content and its ratio to organic carbon with a long-term average value about 70 with an interannual variation of 15.3% for spring and 11.34% for summer sowing. At the same time, the difference between the average long-term value for both sowing dates was not significant. It is interesting to note that in cereal green manure, this ratio was 115–140. In legumes green manure was 110–125 (Hansen et al., 2021). Based on this the oilseed radish will be effective for green manuring of soils poor in mobile phosphorus and in options for restoring a positive phosphorus balance in soils under organic fertilization systems.

Important for assessing the biofumigation potential of plants was the C/S ratio. It was a relative indicator of the presence of glucosinolates in plant biomass, since the biochemical composition of some chemical compounds belonging to this group of substances is sulfur-containing (De Kok et al., 2012; Pekarek et al., 2013; Galaup, 2018; Couëdel et al., 2019; Duff et al., 2020). It has been established that an effective green manure option with an overall biofumigation effect is possible at a C/S ratio of no more 120 (Kirkegaard & Sarwar, 1998; Zachariah, 2011). For oilseed radish this indicator was in the range of 71–122 for spring sowing and 59–134 for summer sowing. That was corresponded to the requirements of an effective biofumigation process for green manure

use of the formed biomass. During the summer sowing period, this indicator had a 1.36 times higher level of interannual variation than during the spring sowing period (25.6%) and significantly lower than its long-term average value by 9.24 units. This character of the formation of the indicator was explained by the lower proportion of the generative part and the larger proportion of leaves, which, given the data on the content of glucosinolates in different parts of cruciferous plants and naturally reduces the content of sulfur-containing compounds in the formed biomass (Bohinc et al., 2013; Perniola et al., 2019). This was confirmed by comparing the maximum C/S value of 134.31 for the conditions of summer sowing in 2022, for which the highest amount of precipitation of 436.6 mm at moderate temperature was recorded in this period (Table 1).

The criterion value of the leaf-stem aboveground mass of oilseed radish in the MSCC system was also confirmed by the level of carbohydrates (CH), which determined the dynamics of mass decomposition in terms of released substances and its subsequent positive effect on the microbiological activity of the soil and the promotion of its self-aggregation (Liu et al., 2020; Israt & Parimal, 2023). From this point of view, CH content in oilseed radish mass in the range of 55–60%$_{DM}$ characterized it as suitable for effective green manure utilization. It had also proved that carbohydrates are energy-providing feed components composed of carbon, hydrogen, and oxygen. They should make up about 75%$_{DM}$ of an animal's diet (Navarro et al., 2019). According to this indicator, the biomass of oilseed radish with a carbonate content of up to 50–70%$_{DM}$ needs to be improved in terms of the desired compatible use. For this effective will be the use cereals and legumes, which is confirmed in a number of studies (Ayres & Clements, 2002; Mbambalala et al., 2023; Sánchez et al., 2023).

It is argued that biomass, particularly agricultural residues and biomass rich in structural carbohydrates, offers significant potential for sustainable biogas production (Venslauskas et al., 2024). At the same time, for most crops with high biogas production potential, the CH content should reach 65–75%$_{DM}$ (Herrmann et al., 2016). Based on these statements, the biomass of oilseed radish formed by the plant during the spring sowing period with an average long-term carbonate content of 67.08%$_{DM}$ was technologically more suitable for biogas production than the same during the summer sowing period, which is consistented with the results of our previous studies (Tsytsiura, 2023a).

To evaluate the possibility of effective use of oilseed radish leaf mass in the form of mulching with spreading of the chopped mass on the soil surface (Duff et al. 2020; Nithisha et al. 2022), the residue quality (RQ) index in the traditional variation (Quemada & Cabrera, 1995) was adapted. The obtained long-term average RQ index was 84.99%$_{DM}$ for spring and 81.03%$_{DM}$ for summer sowing. This was close to the value of the indicator for other cruciferous plant species (Bajgai et al., 2014, Thiébeau et al., 2021; Sharma et al., 2022). It was also proved the potential use of oilseed radish biomass for green mulching in the system of creating a protective mulching layer in the variants of bioconservation agriculture. This type of technological solution for oilseed radish mass is predicted to be more efficient when using plant biomass grown in the spring sowing period.

The study of the indicators of accumulation of the main nutrients in the formed biomass of oilseed radish was comparabled to their concentration noted in Tables 3–4. The average long-term ratio of content and accumulation in the aboveground biomass of

N:P:K:Ca:S was established in the following expression (with indication of the range of values) 1.00 (0.65–1.59):0.24 (0.18–0.40):1.39 (1.04–2.05):0.38 (0.28–0.56):0.16 (0.14–0.19) for spring sowing and 1.00 (0.51–1.39):0.20 (0.11–0.25):1.21 (0.70–1.70):0.31 (0.21–0.42):0.15 (0.10–0.21) for the summer sowing. To compare the intensity of accumulation of individual elements (based on the generalization of De Kok et al., 2012; Szczepanek & Siwik-Ziomek, 2019; Franzen, 2023; Yahbi et al., 2024) this ratio of N:P:K:Ca:S for rapeseed was in the range of 0.9–1.7:0.4–0.7:1.4–2.2:0.45–0.75:0.18–0.55. The same ratio for different mustard species was 0.8–1.2:0.3–0.6:1.2–1.6:0.40–0.65:0.24–0.60. For other types of cruciferous plants used in the system of intermediate green manure (for example*, Barbarea vulgaris* L.) this ratio was in the range of 0.6–1.1:0.2–0.6:1.1–1.3:0.25–0.50:0.18–0.32. In summary, the oilseed radish was characterized by similar features in the accumulation of basic nutrients as for widely used rapeseed and mustard in the MSCC system.

Based on the determined ratios, the intensity of growth processes for the formation of oilseed radish leaf and stem mass will be predicted to be high with sufficient soil supply of available forms of nitrogen and potassium. As for phosphorus, (according to the findings of Weih et al. (2018)), the critical period of consumption of this element for oilseed radpsh will be at the early stages of the growing.

At the same time, in terms of the direction and use of 'catch crop' in the MSCC system, according to the 'N uptake' indicator, oilseed radish showed significantly lower levels of nitrogen removal over the ten-year evaluation period compared to the predicted levels of this indicator for already noted widely used crops such as rapeseed and mustard. The determined nature of accumulation also showed a high positive response of oilseed radish to additional mineral nutrition, especially during the period of active growth of vegetative mass, which according corresponded to 30–35 days after sowing for spring and 25 days after sowing for summer sowing (Fig. 4).

According to the accumulation of phosphorus and calcium in comparison with niche cruciferous crops, oilseed radish was classified as a species with intensive accumulation of these elements (based on the gradation of Wallace & Mueller, 1980).

Based on the above, the established high levels of productivity of oilseed radish at lower levels of consumption of the main elements to ensure this productivity allowed to recommend it for the system of saturating multi-term crops in the links of typical crop rotations with the criterion of 'catch crop' and 'green manure'. This statement is consistented with the findings of Grzebisz et al. (2022, 2023). This was also confirmed by the results of equivalent transformation of the formed aboveground mass of oilseed radish in terms of the content of organic and dry matter in cattle manure. Such conversion, which provided an average perennial rate of more than 20 t ha^{-1} and taking into account the study by Carr et al. (2020), proved the effectiveness of using oilseed radish at both sowing dates in the system of bioorganic fertilization technologies.

It is important to note that the characterized basic indicators and correlations (according to Ramírez-García et al. (2015)) that determine the belonging to different niche areas in the MSCC system for oilseed radish formed a regression system of dependencies. The most significant are presented in Table 6. It was found that the quality of plant residues (RQ) decreased with both an increase in precipitation and an increase in temperature. This was explained by the intensification of vegetative growth processes

with a slowdown in qualitative biochemical transformations characteristic of natural physiological aging. At the same time, an increase in temperature will ensure an increase in the content of lignin derivatives and an increase in precipitation will cause a general decrease in the components of NDF and ADL. In interaction, this will form plant residues with rapid rates of aerobic decay and reduce its quality in terms of bio-cycling of its components. This character was consistented with the determined dependencies between RQ and hydrothermal ratios – the aridity coefficient I_{DM} and the moisture coefficient K_h. Similar results were obtained in the studies of Bajgai et al. (2014).

Table 6. Multiple regression dependence between hydrothermal conditions of vegetation and indicators of value of aboveground mass of oilseed radish according to the criteria of multi-service cover crop (MSCC) (average data for 2014–2023)

Qualitative indicator	Equation of dependence	Parameters of the equation		Statistical evaluation of components				
		x	y	Multiple R	Multiple $R^2_{(adj.)}$	F	$df1$, $df2$	p
RQ	RQ = 92.503-0.00995x-0.4975y	Precipitation (mm)	Average daily temperature (°C)	0.873	0.735	27.334	2.170	< 0.001
C/N	C/N = 24.5149-0.0189x-0.4478y			0.788	0.576	13.891	2.170	< 0.001
N_{upt}	N_{upt} = -7.040+0.1394x+1.3556y			0.850	0.689	22.058	2.170	< 0.001
CFb	CFb = 21.851-0.0152x-0.1937y			0.862	0.713	24.599	2.170	< 0.001
GC	GC = 84.205+0.0934x-1.343y			0.821	0.636	17.625	2.170	< 0.001
GSL	GSL = 12.918-0.0147x+0.1731y			0.806	0.609	15.773	2.170	< 0.001
RQ	RQ = 84.268-1.5649x+10.285y	I_{DM}	K_h	0.738	0.545	10.188	2.170	< 0.05
C/N	C/N = 17.569-2.151x+13.344y			0.854	0.729	22.823	2.170	< 0.001
N_{upt}	N_{upt} = 13.420+9.622x-54.875y			0.921	0.831	47.785	2.170	< 0.001
CFb	CFb = 25.222-0.1074x-0.7081y			0.815	0.625	16.785	2.170	< 0.001
GC	GC = 62.557-1.1471x+16.155y			0.895	0.707	21.789	2.170	< 0.001
GSL	GSL = 15.779-0.0079x-1.2605y			0.783	0.612	19.446	2.170	< 0.001

The C/N ratio also decreased with an increase in both precipitation and average daily temperature. This was consistented with the previously mentioned theory of stress proteins and an increase in the content of nitrogenous compounds. In the case of precipitation it was determined by decrease in the rate of physiological aging with the formation of an increased nitrogen content in late phenostages.

In the case of temperature, a stress response system was formed in the form of an increased content of stress proteins and, accordingly, a higher concentration of nitrogen in biomass. Against the background of the previously mentioned stable organic carbon content, this ultimately reduced the value of the C/N ratio. At the same time, the negative forming direction in the equation of the aridity index (I_{DM}) and the positive forming direction for the moisture coefficient (K_h) indicated a more important role of the precipitation to evapotranspiration ratio than precipitation to the sum of temperatures. In the first case, this contributed to the accumulation of both organic carbon and nitrogen compounds and was consistented with the estimates of Agren & Weih (2012). It was also conformed by the presented results of regression dependencies for the resultant component N_{upt}. For the indicator of soil coverage 'GC', the peculiarities of the formation of the indicator for oilseed radish were confirmed. It was found an increase in its value with an increase in precipitation and a decrease in evaporation in terms of the

value of the moisture coefficient (K_h) and a decrease in the average daily air temperature. This was consistented with all the dependencies that determined the intensity of growth processes in the dynamics (Fig. 4) and with the conclusions of a number of studies (Ramirez-Garcia et al., 2012; Ugrenović et al., 2019; Kashyap et al., 2023).

The regression analysis proved a positive formative effect of the increase in average daily temperatures and a negative formative effect of precipitation on the accumulation of glucosinolates. The GSL content was consistented with a significantly higher concentration of its in the biomass of oilseed radish during the summer sowing period, especially under conditions of moisture deficit against the background of intensively increasing average daily temperatures. The GSL content was positively correlated with similar studies on other cruciferous crops (Milford & Evans, 1991; del Carmen Martínez-Ballesta et al., 2013, Bellec et al., 2023; Ben Ammar et al., 2023).

An important component in assessing the belonging of oilseed radish to the MSCC system is an attribute assessment of the component coefficients of the resulting equations of the corresponding conceptual direction of use. For scientific detailing and substantiation of the selected attributes, a systematization of a number of studies that directly or indirectly relate to the issues of MSCC formation was applied. The results of this generalization are presented in Table 7.

The formed array of initial data on the importance of the studied attributes in the formation of the direction of use of oilseed radish allowed to obtain its normalized matrix (Table 8).

The conditions of 2014 and 2023 were recognized as ensuring the maximum realization of the possibility of multicomponent use of aboveground biomass of oilseed radish in all defined areas. In contrast, the conditions of 2015 and 2017 had a significant lowest level of criterion realization. In the system of evaluation of individual attributes, its importance was confirmed on the basis of the systematization of the results of long-term studies. Aaccording to this studies, the indicator of the amount of formed aboveground biomass was dominant in the context of all studied areas of use of oilseed radish. The the fiber content or its dietary form was in the last ranking place.

The significance of the difference within the years of evaluation was minimal for the attributes ‘GSL’, ‘CFb’ and ‘RQ’, which was associated with the different directions of the identified trends of its formation for different uses in the MSCC system and was positively consistented with the data of Ramírez-García et al. (2015).

The results of the multicriteria analysis within different sowing dates established the final sums of normalized and weight-adjusted attributes (Table 9). Accordingly, it was determined that different sowing dates of oilseed radish have different years of optimality for a particular use. The maximum number of maximum values of the adjusted coefficients was observed for the conditions of 2019 for the spring sowing period and for the conditions of 2022 for the summer sowing period. On this basis the possibility of involving oilseed radish as an effective candidate for crops of the MSCC system was determined.

The sowing dates influenced the assessment of the efficiency of use, which is confirmed by the average normalized index for this attribute in the array of years of study. Shifting the sowing dates of oilseed radish from spring to summer increased the efficiency of its use in the such criterion area as ‘Green manure’, ‘Fodder’ and ‘Catch crop’ (increase in the rating position by 1–2 levels).

Table 7. Intensity of importance of the normalized attributes on fundamental scale in oilseed radish as the multi-service cover crop (MSCC) utility functions assigned by the decision makers based on analysis of publications for both sowing dates

Use	GC*	BM	C/N	N_{upt}	RQ	GSL	CFb	Attributes selected based on the analysis of publications
Cover crop	5	2	1	1	3	3	1	Snapp et al., 2005; Clark, 2008; Bodner et al., 2010; Tixier et al., 2010; Bangarwa et al., 2011; Zachariah, 2011; Justes et al., 2012; Gieske, 2013; Ramírez-García et al., 2015a; White et al., 2016; Wendling et al., 2016; Wollford & Jarvis, 2017; Warren, 2017; Couedel et al., 2018, 2019; Tribouillois et al., 2018; Bhogal et al., 2019; Toom et al., 2019; Ugrenović et al., 2019; Chapagain et al., 2020; Duff et al., 2020; Norberg & Aronsson, 2020; Hansen et al., 2021; Lövgren, 2022; Quintarelli et al., 2022; Ait Kaci Ahmed et al., 2022; Restovich et al., 2022
	**+	+	+	-	+	+	+	
Catch crop	2	2	1	2	2	3	1	Snapp et al., 2005; Molinuevo-Salces et al., 2014; Gieske, 2013; Alonso-Ayuso et al., 2014; Ramírez-García et al., 2015, 2015a; White et al., 2016; Wendling et al., 2016; Wollford & Jarvis, 2017; Warren, 2017; Couedel et al., 2018, 2019; Bhogal et al., 2019; Sieling et al., 2019; Toom et al., 2019; Chapagain et al., 2020; Duff et al., 2020; Hansen et al., 2021; Lövgren, 2022; Restovich et al., 2022
	+	+	-	-	+	+	+	
Green manure	3	5	2	3	5	7	3	Kirkegaard & Sarwar, 1998; Eberlein et al., 1998; Gimsing & Kirkegaard, 2006; Clark, 2008; Florentín, 2010; Bangarwa et al., 2011; Zachariah, 2011; Ramírez-García et al., 2015; Flores-Sánchez et al., 2016; Stubbs & Kennedy, 2017; Galaup, 2018; Hu et al., 2018; Heuermann et a., 2019; Li et al., 2019; Liu et al., 2020; Salume et al., 2020; Lövgren, 2022; Ait Kaci Ahmed et al., 2022; Lei et al., 2022; Jie, 2022; Jauhiainen, 2022; Wang et al., 2022; Israt & Parimal, 2023; Källén, 2023;
	+	+	-	-	+	+	-	
Fodder	3	5	3	3	1	7	5	Gustine & Jung, 1985; Capecka & Libik, 1998; Westwood & Mulcock, 2012; Ramírez-García et al., 2015, 2015a; Winkler, 2017; FOSS. 2018; Duff et al., 2020; Kılıç et al., 2021; Olofsson & Ernfors, 2022; Abdelrahman et al., 2022; Safaei et al., 2022; Jie, 2022; Ţiţei, 2022
	+	+	-	+	+	-	+	
Biogas	3	5	5	3	5	5	3	Chen et al., 2008; Cleemput, 2011; Herout et al., 2011; Murphy et al., 2011; Carvalho et al., 2011; Al Seadi et al., 2013; Molinuevo-Salces et al., 2013; Dandikas et al., 2014; Carvalho et al., 2014; Herrmann et al., 2014, 2016; Guarino et al., 2016; Einarsson & Persson, 2017; Maier et al., 2017; Martínez-Gutiérrez, 2018; Cerón-Vivas et al., 2019; Choi et al., 2020; Liu et al., 2020; Oliveira & Słomka, 2021; Launay et al., 2022; Jauhiainen, 2022; Fajobi et al., 2023; Lallement et al., 2023; Lymperatou et al., 2023; Manyi-Lohn & Lues, 2023; Shitophyta et al., 2023
	+	+	+	+	+	-	-	

Equations with attribute for uses (desirable trend of formation: growth '+', decline '-')	
Cover crop	$5GC + 2BM + C/N - N_{upt} + 3RQ + 3GSL + CFb$
Catch crop	$2GC + 2BM - C/N - 2N_{upt} + 2RQ + 3GSL + CFb$
Green manure	$3GC + 5BM - 2C/N - 3N_{upt} + 5RQ + 7GSL - 3CFb$
Fodder	$3GC + 5BM - 3C/N + 3N_{upt} + RQ - 7GSL + 5DFb$***
Biogas	$3GC + 5BM + 5C/N + 3N_{upt} + 5RQ - 5GSL - 4CFb$

*GC: ground cover (% at 60 days after sowing); BM: biomass reached at the end of the experiment (kg m^{-2}); CN: C/N ratio; N_{upt}: N uptake (g m^{-2}); RQ: residue quality (g kg^{-1}_{DM}); CFb: fiber content (g kg^{-1}_{DM}); DFb: dietary fibre content (g kg^{-1}_{DM}); GSL: glucosinolate productivity (mmol m^{-2}). **desirable trend of formation: growth '+', decline '-' ***DFb only for the 'fodder crop' direction.

Table 8. Average of normalized values for 7 attributes of oilseed radish evaluation as multi-service cover crop functions (MSCC), 2014–2023 (averaged for the complete data set, directions of use–sowing dates)

Year	GC*	BM	C/N	N_{upt}	RQ	GSL	CFb (DFb**)	Amount	Rating
2014	0.213^{a}	0.268^{b}	0.129^{c}	0.069^{b}	0.072^{b}	0.086^{b}	0.057^{c}	0.897	1
2015	0.128^{f}	0.196^{h}	0.118^{e}	0.064^{d}	0.075^{a}	0.089^{a}	0.061^{b}	0.730	9
2016	0.179^{c}	0.231^{e}	0.120^{e}	0.069^{b}	0.075^{a}	0.088^{a}	0.062^{a}	0.824	6
2017	0.151^{h}	0.208^{g}	0.123^{d}	0.070^{b}	0.076^{a}	0.089^{a}	0.064^{a}	0.782	8
2018	0.154^{g}	0.214^{f}	0.125^{d}	0.075^{a}	0.075^{a}	0.089^{a}	0.064^{a}	0.796	7
2019	0.168^{e}	0.278^{a}	0.136^{a}	0.067^{c}	0.073^{b}	0.088^{a}	0.057^{c}	0.868	3
2020	0.167^{e}	0.262^{c}	0.120^{e}	0.063^{d}	0.074^{a}	0.088^{a}	0.060^{b}	0.834	5
2021	0.159^{f}	0.263^{c}	0.117^{f}	0.069^{b}	0.076^{a}	0.089^{a}	0.060^{b}	0.834	5
2022	0.172^{d}	0.270^{b}	0.127^{c}	0.073^{a}	0.076^{a}	0.088^{a}	0.061^{b}	0.867	4
2023	0.185^{b}	0.262^{c}	0.132^{b}	0.071^{b}	0.076^{a}	0.088^{a}	0.060^{b}	0.873	2
Average	0.168	0.245^{d}	0.125^{d}	0.069^{b}	0.075^{a}	0.088^{a}	0.061^{b}	–	–
Rating	2	1	3	6	5	4	7	–	–

* GC: ground cover (% at 60 days after sowing); BM: biomass reached at the end of the experiment (kg m^{-2}); CN: C/N ratio; N_{upt}: N uptake (g m^{-2}); RQ: residue quality (g kg^{-1}_{DM}); CFb: fiber content (g kg^{-1}_{DM}); DFb: dietary fibre content (g kg^{-1}_{DM}); GSL: glucosinolate productivity (mmol m^{-2}). **DFb for the direction use only for 'fodder crop' direction.

Table 9. Sum of normalized values multiplied by the weighting coefficients for 7 attributes attained by each use oilseed radish as multi-service cover crop functions (MSCC), 2014–2023

Year of research	Direction of use in the concept of MSCC										Rating by MSCC
	Cover crop		Catch crop		Green manure		Fodder		Biogas		
	*SprS	SumS	SprS	SumS	SprS	SumS	SprS	SumS	SprS	SumS	
2014	0.82^{d}	0.86^{b}	0.95^{b}	0.85^{d}	0.88^{b}	0.91^{c}	0.96^{b}	0.91^{c}	0.95^{b}	0.88^{c}	1
2015	0.82^{d}	0.84^{c}	0.73^{g}	0.72^{f}	0.75^{f}	0.62^{h}	0.76^{g}	0.60^{g}	0.75^{g}	0.59^{g}	10
2016	0.83^{d}	0.82^{d}	0.76^{d}	0.83^{e}	0.80^{e}	0.89^{d}	0.79^{f}	0.89^{c}	0.78^{f}	0.87^{c}	7
2017	0.82^{d}	0.73^{g}	0.68^{h}	0.83^{e}	0.80^{e}	0.87^{e}	0.65^{i}	0.87^{d}	0.65^{i}	0.87^{c}	9
2018	0.83^{d}	0.79^{e}	0.63^{i}	0.87^{c}	0.80^{e}	0.89^{d}	0.70^{h}	0.88^{c}	0.69^{h}	0.93^{b}	8
2019	0.79^{e}	**0.89^{a}**	**0.98^{a}**	0.82^{e}	**0.91^{a}**	0.76^{g}	**0.99^{a}**	0.73^{f}	**0.99^{a}**	0.72^{f}	4
2020	0.87^{b}	0.78^{f}	0.86^{c}	0.82^{e}	0.85^{c}	0.79^{f}	0.90^{c}	0.80^{e}	0.90^{c}	0.76^{e}	6
2021	**0.93**^{a}	0.84^{c}	0.74^{g}	0.86^{d}	0.82^{d}	0.87^{e}	0.80^{e}	0.87^{d}	0.80^{e}	0.85^{d}	5
2022	0.85^{c}	0.80^{e}	0.77^{f}	0.90^{b}	0.83^{d}	**0.99^{a}**	0.82^{e}	**0.99^{a}**	0.81^{e}	**0.98^{a}**	3
2023	0.82^{d}	0.81^{d}	0.84^{c}	**0.93^{a}**	0.85^{c}	0.93^{b}	0.88^{d}	0.94^{b}	0.87^{d}	0.94^{b}	2
Average	0.838^{a}	0.816^{d}	0.794^{d}	0.843^{b}	0.829^{b}	0.852^{a}	0.825^{b}	0.849^{a}	0.819^{c}	0.839^{b}	– –
Rating by use	1	5	5	3	2	1	3	2	4	4	– –
Consistensy index (CI)*	0.431	0.244	0.188	0.357	0.340	0.415	0.370	0.407	0.226	0.305	–

*SprS – Spring sowing; SumS – Summer sowing. In bold, the maximum values, and in italics, the minimum. Case letters indicate statistical differences ($p < 0.05$); *the indicator is a component of the scheme of Analytic Hierarchy Process (AHP) according to Saaty & Vargas (2012).

The positions in the criterion of 'Biogas' use remained unchanged. Its use in the direction of 'Cover crop' was significantly lower (decrease in the rating by 4 positions). Such changes, taking into account the saturating and intermediate nature of the summer

sowing of oilseed radish, proved the technological potential of its use in a wide period of time in the MSCC system. It was also found that the rating by the direction of use depended on the conditions of the year. For example, for the conditions of 2018 and 2023, the direction 'Biogas' during the summer sowing period had the first rating among other directions of use with an average fourth position in the consolidated data set. Similar trends were found for other uses. This confirmed conclusions about the role of hydrothermal regimes of the growing season in shaping compliance with MSCC criteria.

CONCLUSIONS

According to the results of a multi-year study cycle, oilseed radish showed high productivity and adaptability. On soils of medium fertility potential with an unfertilized background, its average total bioproductive potential (leaf + root mass) in dry matter over 50–60 days of vegetation was 4.92 t ha^{-1} in spring and 4.06 t ha^{-1} in summer sowing. According to the results of a long-term integrated assessment of the biochemical portfolio of oilseed radish leaf mass, it was classified as a high-protein crop (crude protein content 15–23%$_{DM}$) with a high fat content (3.2–5.8%$_{DM}$) and an average content of cellulose-derived components (20–24%$_{DM}$). This maked it possible to recommend it for cultivation in a wide range of intermediate sowing options and to form a fodder- green manure and green manure-bioenergy agrocenosis in areas of a wide climatic spectrum. According to the ash content and the content of basic macro and microelements, its use as a green manure was equivalent to an average of 20 t ha^{-1} of cattle manure. Its biofumigation potential in terms of glucosinolates content of 41.2–54.90 mol ha^{-1} will guarantee a high efficiency in different variants of soil biofumigation technologies.

Using the above data block with the application of Multi-criteria decision aiding (MCDA), the possibility of multi-purpose use of oilseed radish in the criterion system of multi-service cover crop (MSCC) was proved. The order of decreasing technological significance of oilseed radish for the conditions of unstable hydrothermal regime on soils with an average level of fertility (averaged for spring and summer sowing dates) was the following: 'Green manure' - 'Fodder' - 'Cover crop' - 'Biogas' - 'Catch crop'.

REFERENCES

Abdallah, I., Yehia, R. & Kandil, M.Ah. 2020. Biofumigation potential of Indian mustard (Brassica juncea) to manage Rhizoctonia solani. *Egyptian Journal of Biological Pest Control* **30**. 99 doi: 10.1186/s41938-020-00297-y

Abdel-Massih, R.M., Debs, E., Othman, L., Attieh, J. & Cabrerizo, F.M. 2023. Glucosinolates, a natural chemical arsenal: More to tell than the myrosinase story. *Frontiers in Microbiology* **14**, 1130208. doi: 10.3389/fmicb.2023.1130208

Abdelrahman, M., Wang, W., Lv, H., Di, Z., An, Z., Lijun, W., Shaukat, A., Bo, W., Guangsheng, Z., Liguo, Y. & Guohua, H. 2022. Evaluating the Effect of Forage Rape (*Brassica napus*) Ensiling Kinetics on Degradability and Milk Performance as Non-conventional Forage for Dairy Buffalo. *Frontiers in Veterinary Science* **9**, 926906. doi: 10.3389/fvets.2022.926906

Abe, A. 1984. Assessment of the Quality of Forage from Its Chemical Composition and Application to Feeding Program. *Tropical agriculture research series: proceedings of a symposium on tropical agriculture researches* **18**, 133–150.

Agathokleous, E., Belz, R.G., Kitao, M., Koike, T. & Calabrese, E.J. 2019. Does the root to shoot ratio show a hormetic response to stress? An ecological and environmental perspective. *Journal of Forestry Research* **30**, 1569–1580. doi: 10.1007/s11676-018-0863-7

Agren, G.I. & Weih, M. 2012. Plant stoichiometry at different scales: Element concen-tration patterns reflect environment more than genotype. *New Phytologist* **194**, 944–952.

Ahmad, P. 2017. Oilseed Crops. Yield and Adaptations under Environmental Stress. John Wiley & Sons Ltd, The Atrium, Southern Gate, Chichester, West Sussex, PO19 8SQ, UK, 310 pp.

Ahmad, P., Bhardwaj, R. & Tuteja, N. 2012. Plant signalling under abiotic stress environment. In: *Ahmad P, Prasad MNV (eds) Environmental adaptations and stress tolerance of plants in the era of climate change*. Springer, New York, pp. 297–323. doi: 10.1007/ 978-1-4614-0815-4

Ait Kaci Ahmed, N., Galaup, B., Desplanques, J., Dechamp-Guillaume, G. & Seassau, C. 2022. Ecosystem Services Provided by Cover Crops and Biofumigation in Sunflower Cultivation. *Agronomy* **12**, 120. doi: 10.3390/agronomy12010120

Akbarzadeh, A & Katsikas, S. 2021. Identifying and Analyzing Dependencies in and among Complex Cyber Physical Systems. *Sensors* **21**(5), 1685. doi: 10.3390/s21051685

Al Seadi, T., Rutz, D., Janssen, R. & Drosg, B. 2013. Biomass resources for biogas production. In: *The biogas handbook*: Science, production and applications, pp. 19–51.

Allam, M., Radicetti, E., Ben Hassine, M., Jamal, A., Abideen, Z. & Mancinelli, R. 2023. A Meta-Analysis Approach to Estimate the Effect of Cover Crops on the Grain Yield of Succeeding Cereal Crops within European Cropping Systems. *Agriculture* **13**(9), 1714. doi: 10.3390/agriculture13091714

Alonso-Ayuso, M., Gabriel, J.L. & Quemada, M. 2014. The kill date as a management tool for cover cropping success. *PLoS ONE* **9**, e109587.

Amy, C., Avice, J-C., Laval, K., Trinsoutrot-Gattin, I. & Bressan, M. 2024. The Importance of Considering Levels of P and N Fertilization to Promote Beneficial Interaction between Rapeseed and Phosphate-Solubilizing Bacteria. *Agronomy* **14**(2), 334. doi:10.3390/agronomy14020334

Andini, S. 2020. *Antimicrobial isothiocyanates from Brassicaceae glucosinolates Analysis, reactivity, and quantitative structureactivity relationships*. PhD thesis. Wageningen University, Wageningen, The Netherlands, 208 pp.

Ansari, M.A., Choudhury, B.U., Layek, J., Das, A., Lal, R. & Mishra, V.K. 2022. Green manuring and crop residue management: Effect on soil organic carbon stock, aggregation, and system productivity in the foothills of Eastern Himalaya (India). *Soil Tillage Research* **218**, 105318. doi: 10.1016/j.still.2022.105318

Anzola-Rojas, M.D.P., Gonçalves da Fonseca, S., Canedo da Silva, C., Maia de Oliveira, V. & Zaiat, M. 2014. The use of the carbon/nitrogen ratio and specific organic loading rate as tools for improving biohydrogen production in fixed-bed reactors. *Biotechnology Reports* **4**(5), 46–54. doi: 10.1016/j.btre.2014.10.010

Arguello, L.G., Sensharma, D.K., Qiu, F., Nurtaeva, A. & Rassi, Z.E. 1999. High-Performance Liquid-Phase Separation of Glycosides Analytical and Micropreparative HPLC Combined with Spectroscopic and Enzymatic Methods for Generating a Glucosinolate Library. *Journal of AOAC INTERNATIONAL* **82**(5), 1115–1127. doi:10.1093/jaoac/82.5.1115

Asgari, A., Darzi-Naftchali, A., Nadi, M. & Saberali, S.F. 2021. Improvement in canola yield and growth indices and water-use efciency with subsurface drainage in a humid climate. *Paddy Water Environment* **19**(1), 23–33.

Ayres, L. & Clements, B. 2002. Forage brassicas – quality crops for livestock production. *Agfact P2* **1**, 1–3.

Azam, A., Khan, I., Mahmood, A. & Hameed, A. 2013. Yield, chemical composition and nutritional quality responses of carrot, radish and turnip to elevated atmospheric carbon dioxide. *Journal of the Science of Food and Agriculture* **93**, 3237–3244.

Bacher, H., Sharaby, Y., Walia, H. & Peleg, Z. 2021. Modifying root/shoot ratios improves root water influxes in wheat under drought stress. *bioRxiv*, 455065. doi: 10.1101/2021.08.04.455065

Bajgai, Y., Kristiansen, P., Hulugalle, N. & McHenry, M. 2014. Effect of residue management and conventional and organic soil management systems on crop yields and weed biomass. *Acta Horticulturae* **1018**, 227–234. doi: 10.17660/ActaHortic.2014.1018.23

Bakker, C., Hite, L., Wright, C., Smart, A., Dinh, T., Blair, A., Underwood, K. & Grubbs, J.K. 2021. Impact of feeding cover crop forage containing brassicas to steers during backgrounding on palatability attributes of beef strip steaks. *Foods* **10**, 1250.

Baltas, E. 2007. Spatial Distribution of Climatic Indices in Northern Greece. *Meteorological Applications* **14**, 69–78. doi: 10.1002/met.7

Bangarwa, S.K., Norsworthy, J.K., Mattice, J.D. & Gbur, E.E. 2011. Glucosinolate and Isothiocyanate Production from Brassicaceae Cover Crops in a Plasticulture Production System. *Weed Science* **59**(2), 247–254. doi:10.1614/WS-D-10-00137.1

Bell, L.W., Watt, L.J. & Stutz, R.S. 2020. Forage brassicas have potential for wider use in drier, mixed crop–livestock farming systems across Australia. *Crop Pasture Science* **71**, 924–943.

Bellec, L., Cortesero, A.M., Marnet, N., Faure, S. & Hervé, M.R. 2023. Age-specific allocation of glucosinolates within plant reproductive tissues. *Plant Science* **331**, 111690. doi: 10.1016/j.plantsci.2023.111690.

Bellostas, N., Sørensen, J.C. & Sørensen, H. 2004. Qualitative and quantitative evaluation of glucosinolates in cruciferous plants during their life cycles. *Agroindustria* **3**(3), 5611.

Ben Ammar, H., Arena, D., Treccarichi, S., Di Bella, M.C., Marghali, S., Ficcadenti, N., Lo Scalzo, R. & Branca, F. 2023. The Effect of Water Stress on the Glucosinolate Content and Profile: A Comparative Study on Roots and Leaves of *Brassica oleracea* L. Crops. *Agronomy* **13**, 579. doi: 10.3390/ agronomy13020579

Benjamin, J., Nielsen, D., Vigil, M., Mikha, M. & Calderon, F. 2014. Water Deficit Stress Effects on Corn (*Zea mays* L.) Root:Shoot Ratio. *Open Journal of Soil Science* **4**, 151–160. doi: 10.4236/ojss.2014.44018

Bhandari, S.R., Jo, J.S. & Lee, J.G. 2015. Comparison of Glucosinolate Profiles in Different Tissues of Nine Brassica Crops. *Molecules* **20**(9) 15827–15841. doi: 10.3390/molecules200915827

Bhogal, A., White, C. & Morris, N. 2019. *Project Report №. 620 Maxi Cover Crop: Maximising the benefits from cover crops through species selection and crop management*. AHDB Cereals & Oilseeds is a part of the Agriculture and Horticulture Development Board (AHDB). 111 pp.

Birch, A.N., Wynne Griffiths, D., Hopkins, R., Macfarlane smith, W.H. & McKinlay, R. 1992. Glucosinolate responses of swede, kale, forage and oilseed rape to root damage by turnip root fly (Delia floralis) larvae. *Journal of the Science of Food and Agriculture* **60**, 1–9.

Blažević, I., Montaut, S., Burčul, F., Olsen, C.E., Burow, M., Rollin, P. & Agerbirk, N. 2020. Glucosinolate structural diversity, identification, chemical synthesis and metabolism in plants. *Phytochemistry* **169**, 112100. doi: 10.1016/j.phytochem.2019.112100

Blume, R.Y., Lantukh, G.V., Levchuk, I.V., Lukashevych, K.M., Rakhmetov, D.B. & Blume, Y.B. 2020. Evaluation of potential biodiesel feedstocks: camelina, turnip rape, oilseed radish and Tyfon. *The Open Agriculture Journal* **14**, 299–320. doi: 10.2174/1874331502014010299

Bláha, L. 2021. Importance of Root-Shoot Ratio for Crops Production: A Review. *Current Topics in Agricultural Sciences* **1**, 37–49. doi: 10.9734/bpi/ctas/v1/12112D

Bodner, G., HImmelbauer, M., Loiskandl, W. & Kaul, H.-P. 2010. Improved evaluation of cover crop species by growth and root factors. *Agronomy for Sustainable Development* **30**, 455–464. doi: 10.1051/agro/2009029

Bohinc, T., Košir, I.J. & Trdan, S. 2013. Glucosinolates as arsenal for defending Brassicas against cabbage flea beetle (Phyllotreta spp.) attack. *Zemdirbyste-Agriculture* **100** (2), 199–204. doi: 10.13080/z-a.2013.100.026

Borgogno, F., D'Odorico, P., Laio, F. & Ridolfi, L. 2009. Mathematical models of vegetation pattern formation in ecohydrology. *Reviews of Geophysics* **47**, RG1005. doi: 10.1029/2007RG000256.

Boselli, R., Fiorini, A., Santelli, S., Ardenti, F., Capra, F., Maris, S.C. & Tabaglio, V. 2020. Cover crops during transition to no-till maintain yield and enhance soil fertility in intensive agro-ecosystems. *Field Crops Research* **255**, 107871. doi: 10.1016/j.fcr.2020.107871

Brown, C. 2021. Available Nutrients and Value for Manure from Various Livestock Types. *Factsheet № 21077*. AGDEX 538. Ministry of Agriculture, Food and Rural Affairs. Queen's Printer for Ontario. 10 pp.

Capecka, E. & Libik, A. 1998. Quality differences between radish (*Raphanus sativus* l.) cultivars determine the possibilities of their use. *Acta Horticultural* **459**, 89–96. doi: 10.17660/ActaHortic.1998.459.8

Carr, P.M., Cavigelli, M.A., Darby, H., Delate, K., Eberly, J.O., Fryer, H.K., Gramig, G.G., Heckman, J.R., Mallory, E.B., Reeve, J.R., Silva, E.M., Suchoff, D.H. & Woodley, A.L. 2020. Green and animal manure use in organic field crop systems. *Agronomy Journal* **112**, 648–674. doi: 10.1002/agj2.20082

Carvalho, L., Di Berardino, S. & Duarte, E. 2011. Biogas production from mediterranean crop silages. *Proceedings Sardinia 2011*. Thirteenth International Waste Management and Landfill Symposium S. Margherita di Pula, Cagliari, Italy; 3–7 October 2011. URL: https://repositorio.lneg.pt/bitstream/10400.9/1452/1/Artigo%20Sardenha%202011-crop-digestion.pdf (accessed on 06 February 2024)

Castillo-Umaña, M., Balocchi, O., Pulido, R., Sepúlveda-Varas, P., Pacheco, D., Muetzel, S., Berthiaume, R. & Keim, J.-P. 2020. Milk production responses and rumen fermentation of dairy cows supplemented with summer brassicas. *Animal* **14**, 1684–1692.

Cerón-Vivas, A., Cáceres, K.T., Rincón, A. & Cajigas, A.A. 2019. Influence of pH and the C/N ratio on the biogas production of wastewater. *Revista Facultad de Ingeniería Universidad de Antioquia* **92**, 88–95. doi: 10.17533/udea.redin.20190627

Chaddock, R.E. 1925. *Principles and Methods of Statistics* (1st Edition), Houghton Miffin Company. The Riverside Press, Cambridge, 471 pp.

Chapagain, T., Lee, E.A. & Raizada, M.N. 2020. The Potential of Multi-Species Mixtures to Diversify Cover Crop Benefits. *Sustainability* **12**(5), 2058. doi: 10.3390/su12052058

Chen, S., Zhang, X., Shao, L., Sun, H., Niu, J. & Liu, X. 2020. Effects of straw and manure management on soil and crop performance in North China plain. *Catena* **187**, 104359. doi: 10.1016/j.catena.2019.104359

Chen, Y., Cheng, J. J. & Creamer, K. 2008. Inhibition of anaerobic digestion process: A review. *Bioresource Technology* **99**, 4044–4064. doi: 10.1016/j.biortech.2007.01.057

Choi, Y., Ryu, J. & Lee, S.R. 2020. Influence of carbon type and carbon to nitrogen ratio on the biochemical methane potential, pH, and ammonia nitrogen in anaerobic digestion. *Journal of Animal Science and Technology* **62**(1), 74–83. doi: 10.5187/jast.2020.62.1.74

Chowdhury, P. 2022. Glucosinolates and Its Role in Mitigating Abiotic and Biotic Stress in Brassicaceae. In: Plant Stress Physiology - Perspectives in Agriculture. *IntechOpen*, 14 pp. doi: 10.5772/intechopen.102367

Ciska, E., Honke, J. & Kozłowska, H. 2008. Effect of light conditions on the contents of glucosinolates in germinating seeds of white mustard, red radish, white radish, and rapeseed. *Journal of Agricultural and Food Chemistry* **56**(19), 9087–9093. doi: 10.1021/jf801206g.

Clark, A. 2008. *Managing cover crops profitably*. DIANE Publishing (3rd ed.), 248 pp.

Cleemput, S. 2011. *Breeding for a reduced glucosinolate content in the green mass of rapeseed to improve its suitability for biogas production*. PhD Thesis. Georg-August-Universität Göttingen, 104 pp. doi: 10.53846/goediss-1837

Composts & Fertilisers. 2023. NPK Nutritional Values of Animal Manures & Compost Etc. Available online: https://www.allotment-garden.org/composts-fertilisers/npk-nutritional-values-animal-manures-compost/#google_vignette (accessed on 06 February 2024).

Couedel, A. 2018. Analysis of performances of crucifers-legumes cover crop mixtures to provide multiple-ecosystem services. *Agricultural sciences*. Institut National Polytechnique de Toulouse -INPT, 197 pp.

Couëdel, A., Kirkegaard, J., Alletto, L. & Justes, É. 2019. Cruciferlegume cover crop mixtures for biocontrol: Toward a new multiservice paradigm. *Advances in Agronomy* **157**, 55–139. doi: 10.1016/bs.agron.2019.05.003

Dandikas, V., Heuwinkel, H., Lichti, F., Drewes, J.E. & Koch, K. 2014. Correlation between biogas yield and chemical composition of energy crops. *Bioresource Technology* **174**, 316–320. doi: 10.1016/j.biortech.2014.10.019

De Kok, L.J., Tausz, M., Hawkesford, M.J., Hoefgen, R., McManus, M.T., Norton, R.M., Rennenberg, H., Saito, K., Schnug, E. & Tabe, L. 2012. *Sulfur Metabolism in Plants: Mechanisms and Applications to Food Security and Responses to Climate Change*; Springer: Dordrecht, The Netherlands, 284 pp.

de Ruiter, J., Wilson, D., Maley, S., Fletcher, A., Fraser, T., Scott, W., Berryman, S., Dumbleton, A. & Nichol, W. 2009. *Management practices for forage brassicas*. Forage rassica development group, 7 pp.

del Carmen Martínez-Ballesta, M., Moreno, D.A. & Carvajal, M. 2013. The Physiological Importance of Glucosinolates on Plant Response to Abiotic Stress in Brassica. *International Journal of Molecular Sciences* **14**, 11607–11625 doi:10.3390/ijms140611607

Dorissant, L., Brym, Z.T. & Swartz, S. 2022. Residue decomposition dynamics in mixed ratios of two warm-season cover crops. *Agrosystems, Geosciences & Environment* **5**, e20311. https://doi.org/10.1002/agg2.20311

Dorsainvil, F., Durr, C.C., Justes, E.E. & Carrera, A. 2005. Characterisation and modelling of white mustard (Sinapis alba L.) emergence under several sowing conditions. *European Journal of Agronomy* **23** (2) 146–158. doi: 10.1016/j.eja.2004.11.002⟩

Drost, S.M., Rutgers, M., Wouterse, M., de Boer, W. & Bodelier, P.L.E. 2019. Decomposition of mixtures of cover crop residues increases microbial functional diversity. *Geoderma* **114060**. doi: 10.1016/j.geoderma.2019.114060

Duff, J., van Sprang, C., O'Halloran, J. & Hall, Z. 2020. *Guide to Brassica Biofumigant Cover Crops Managing soilborne diseases in vegetable production systems*. Horticulture Innovation through VG16068 Optimising cover cropping for the Australian vegetable industry. State of Queensland. Department of Agriculture and Fisheries 40 pp.

Dzvene, A.R., Tesfuhuney, W.A., Walker, S. & Ceronio, G. 2023. Management of Cover Crop Intercropping for Live Mulch on Plant Productivity and Growth Resources: A Review. *Air, Soil and Water Research* **16**. doi:10.1177/11786221231180079

Dębowski, M., Kazimierowicz, J., Zieliński, M. & Bartkowska, I. 2022. Co-Fermentation of Microalgae Biomass and Miscanthus × giganteus Silage-Assessment of the Substrate, Biogas Production and Digestate Characteristics. *Applied Sciences* **12**(14), 7291. doi: 10.3390/app12147291

Eberlein, C.V., Morra, M.J., Guttieri, M.J., Brown, P.D. & Brown, J. 1998. Glucosinolate Production by Five Field-Grown Brassica napus Cultivars Used as Green Manures. *Weed Technology* **12**(4), 712–718. doi:10.1017/S0890037X00044596

Edwards, S. & Ploeg, A. 2014. Evaluation of 31 potential biofumigant brassicaceous plants as hosts for three meloiodogyne species. *Journal of Nematology* **46**(3), 287–295.

Einarsson, R & Persson, U.M. 2017. Analyzing key constraints to biogas production from crop residues and manure in the EU–A spatially explicit model. *PLoS ONE* **12**(1), e0171001. doi: 10.1371/journal.pone.0171001

El Amine, M., Pailhès, J. & Perry, N. 2016. Selection and use of a multi-criteria decision aiding method in the context of conceptual design with imprecise information: Application to a solar collector development. Concurrent Engineering: *Research and Applications* **24**(1), 35–47. doi: 10.1177/1063293X15613838

Fajobi, M.O., Lasode, O.A., Adeleke, A.A., Ikubanni, P.P. & Balogun, A.O. 2023. Prediction of Biogas Yield from Codigestion of Lignocellulosic Biomass Using Adaptive Neuro-Fuzzy Inference System (ANFIS) Model. *Journal of Engineering* **Article ID 9335814**. doi: 10.1155/2023/9335814

Florentín, M.A., Peñalva, M., Calegari, A., Translated, R.D. & Mcdonald, M.J. 2010. *Green Manure/Cover Crops and Crop Rotation in Conservation Agriculture on Small Farms*. Integrated Crop Management: Rome, Italy, **12**, 97 pp.

Flores-Sánchez, D., Pastor, A., Rossing, W.A.H., Kropff, M.J. & Lantinga, E.A. 2016. Decomposition, N contribution and soil organic matter balances of crop residues and vermicompost in maize-based cropping systems in southwest Mexico. *Journal of Soil Science and Plant Nutrition* **16**(3), 801–817.

FOSS. 2018. Fibre analysis of animal feed Crude fibre, neutral detergent fibre and acid detergent fibre – the standards and the automation options. eBook. Available online: https://www.fossanalytics.com/-/media/files/documents/papers/laboratories-segment/ebook-fibre-analysis-of-animal-feed-gb.ashx (accessed on 06 February 2024).

Franzen, D.W. 2023. Fertilizing Canola and Mustard. SF1122. URL: https://www.ndsu.edu/agriculture/extension/publications/fertilizing-canola-and-mustard (date of access April 25, 2024).

Galaup, B. 2018. Assessment of the potential of biotic regulation by Brassica cover-crops used as biofumigants. Case of Verticillium dahliae affecting Sunflower crop in southwestern France. Mster Thesis. Norwegian University of Life Science. 42 pp.

Gamba, M., Asllanaj, E., Raguindin, P.F., Glisic, M., Franco, O.H., Minder, B., Bussler, W.W., Metzger, B., Kern, H.J. & Muka, T. 2021. Nutritional and phytochemical characterization of radish (*Raphanus sativus*): A systematic review. *Trends in Food Science & Technology* **113**, 205–218.

Gan, Y.T., Campbell, C.A., Janzen, H.H., Lemke, R., Liu, L.P., Basnyat, P. & McDonald, C.L. 2009. Root mass for oilseed and pulse crops: Growth and distribution in the soil profile. *Canadian Journal of Plant Science* **89**, 883–893.

Gastal, F. & Lemaire, G. 2002. N uptake and distribution in crops: an agronomical and ecophysiological perspective. *Journal of Experimental Botany* **53** (370), 789–799. doi: 10.1093/jexbot/53.370.789

Gieske, M.F. 2013. *Radish and other brassica cover crop effects on nitrogen availability and weed management*. PhD Thesis. University of Minnesota Digital Conservancy, 122 pp.

Gimsing, A.L. & Kirkegaard, J.A. 2006. Glucosinolate and isothiocyanate concentration in soil following incorporation of Brassica biofumigants. *Soil Biology and Biochemistry* **38**, 2255–2264.

Green Manure Global Market Report 2024. By Type (Leguminous, Non Leguminous), By Source (Dhaincha, Sesbania, Sunhemp, Other Sources), By Application (Grains And Cereals, Pulses And Oilseeds, Fruits And Vegetables, Other Applications) - Market Size, Trends, And Global Forecast 2024–2033. URL: https://www.thebusinessresearchcompany.com/report/green-manure-global-market-report (date of access April 25, 2024).

Grzebisz, W., Diatta, J., Barłóg, P., Biber, M., Potarzycki, J., Łukowiak, R., Przygocka-Cyna, K. & Szczepaniak, W. 2022. Soil Fertility Clock – Crop rotation as a paradigm in nitrogen fertilizer productivity control. *Plants* **11**, 2841.

Grzebisz, W., Zielewicz, W. & Przygocka-Cyna, K. 2023. Deficiencies of Secondary Nutrients in Crop Plants – A Real Challenge to Improve Nitrogen Management. *Agronomy* **13**(1), 66. doi:10.3390/agronomy13010066

Guarino, G., Carotenuto, C., Di Cristofaro, F., Papa, S., Morrone, B. & Minale, M. 2016. Does the C/N ration really affect the biomethane yield? a three years investigation of buffalo manure digestion. *Chemical Engineering Transactions* **49**, 463–468. doi: 10.3303/CET1649078

Guinet, M., Voisin, A-S. & Nicolardot, B. 2023. Potential C and N Mineralisation of Shoot and Root Residues from Ten Grain Legume Species As Related to their Biochemical Characteristics. *World Journal of Agriculture and Soil Science* **8**(4), WJASS.MS.ID.000691.

Gustine, D.L. & Jung, G.A. 1985. Influence of some management paramters on glucosinolate levels in Brassica forage. *Agronomy Journal* **77**, 593–597. doi: 10.2134/agronj1985.00021962007700040020x

Hadas, A., Kautsky, L., Goek, M. & Kara, E.E. 2004. Rates of decomposition of plant residues and available nitrogen in soil, related to residue composition through simulation of carbon and nitrogen turnover. *Soil Biology and Biochemistry* **36**(2), 255–266. doi: 10.1016/j.soilbio.2003.09.012

Hansen, V., Eriksen, J. & Jensen, L.S. 2021. Towards integrated cover crop management: N, P and S release from aboveground and belowground residues. *Agriculture, Ecosystems & Environment* **313**. doi: 10.1016/j.agee.2021.107392

Hansen, V., Müller-Stöver, D. & Magid, J. 2022. Green manure crops for low fertility soils URL: https://orgprints.org/id/eprint/37832/1/poster_Veronika%20Hansen.pdf (date of access April 25, 2024).

Herout, M., Malaťák, J., Kučera, L. & Dlabaja, T. 2011. Biogas composition depending on the type of plant biomass used. *Research in Agricultural Engineering* **57**, 137–143.

Herrmann, C., Idler, C. & Heiermann, M. 2016. Biogas crops grown in energy crop rotations: Linking chemical composition and methane production characteristics. *Bioresource Technology* **206**, 23–35. doi: 10.1016/j.biortech.2016.01.058

Herrmann, C., Prochnow, A., Heiermann, M. & Idler, C. 2014. Biomass from landscape management of grassland used for biogas production: effects of harvest date and silage additives on feedstock quality and methane yield. *Grass Forage Science* **69**, 549–566. doi: 10.1111/gfs.12086

Heuermann, D., Gentsch, N., Boy, J., Schweneker, D., Feuerstein, U., Groß, J., Bauer, B., Guggenberger, G. & von Wirén, N. 2019. Interspecific competition among catch crops modifies vertical root biomass distribution and nitrate scavenging in soils. *Scientific Reports* **9**(1), 11531. doi: 10.1038/s41598-019-48060-0

Honcharuk, I., Tokarchuk, D., Gontaruk, Y. & Hreshchuk, H. 2023. Bioenergy recycling of household solid waste as a direction for ensuring sustainable development of rural areas. *Polityka Energetyczna – Energy Policy Journal* **26**(1), 23–42. doi: 10.33223/epj/161467

Honcharuk, I.V. & Yemchyk, T.V. 2024. Waste-free biofuel production technologies as a way to the European Green Deal. *Polityka Energetyczna – Energy Policy Journal* **27**(1), 81–94. doi: 10.33223/epj/175284

Hu, T., Olesen, J.E., Christensen, B.T. & Sørensen, P. 2018. Release of carbon and nitrogen from fodder radish (Raphanus sativus) shoots and roots incubated in soils with different management history. *Acta Agriculturae Scandinavica, Section B – Soil & Plant Science* **68**(8), 749–756. doi: 10.1080/09064710.2018.1480730

Israt, I.J. & Parimal, B.K. 2023. Residual Effect of Green Manure on Soil Properties in Green Manure-Transplant Aman-Mustard Cropping Pattern. *Indian Journal of Agricultural Research* **57**(1), 67–72. doi: 10.18805/IJARe.AF-696

IUSS Working Group WRB. 2015. International Soil Classification System for Naming Soils and Creating Legends for Soil Maps. *World Reference Base for Soil Resources* 2014, Update 2015, 106 pp.

Iwar, K., Desta, K.T., Ochar, K. & Kim, S-H. 2024. Unveiling Glucosinolate Diversity in Brassica Germplasm and In Silico Analysis for Determining Optimal Antioxidant Potential. *Antioxidants* **13**(3), 376. doi: 10.3390/antiox13030376

Jacob, G.A., Prabhakaran, S.P.S., Swaminathan, G. & Joseyphus, R.J. 2022. Thermal kinetic analysis of mustard biomass with equiatomic iron-nickel catalyst and its predictive modeling. *Chemosphere* **286**(Pt 3), 131901. doi: 10.1016/j.chemosphere.2021.131901

Jahanzad, E., Barker, A.V., Hashemi, M., Eaton, T. & Sadeghpour, A. 2016. Nitrogen release dynamics and decomposition of buried and surface cover crop residues. *Agronomy Journal* **108**, 1735–1741. doi: 10.2134/agronj2016.01.0001

Jauhiainen, M. 2022. *Grass Silage as a Feedstock for a Biogas Plant – A feasibility study and development of a cost calculation tool*. PhD Thesis. Savonia University of Applied Sciences, 69 pp.

Jie, O.Y. 2022. *Comparison of nutritional composition, antiinflammatory and antioxidative activities between the raw and boiled Raphanus sativus subsp. longipinnatus roots. PhD thesis*. Universiti Tunku Abdul Rahman. 74 pp.

Jing, Q., Shang, J., Qian, B., Hoogenboom, G., Hufman, T., Liu, J., Ma, B.L., Geng, X., Jiao, X., Kovacs, J. & Walters, D. 2016. Evaluation of the CSM-CROPGRO-Canola Model for Simulating Canola Growth and Yield at West Nipissing in Eastern Canada. *Agronomy Journal* **108**(2), 1–10.

Justes, E. & Richard, G. 2017. Contexte, Concepts et Definition des cultures intermediaires multiservices. *Innovations Agronomiques* **62**, 17–32.

Justes, E.E., Rechauchère, O. & Chemineau, P. 2012. The use of cover crops to reduce nitrate leaching: Effect on the water and nitrogen balance and other ecosystem services. *INRA*. 8 pp.

Kaletnik, G., Honcharuk, I. & Okhota, Yu. 2020 The Waste Free Production Development for the Energy Autonomy Formation of Ukrainian Agricultural Enterprises. *Journal of Environmental Management and Tourism* **3**(43), 513–522. doi:10.14505/jemt.v11.3(43).02

Kaletnik, H., Pryshliak, V. & Pryshliak, N. 2019. Public Policy and Biofuels: Energy, Environment and Food Trilemma. *Journal of Environmental Management and Tourism* (Volume **X**, Summer), **3**(35), 479–487. doi: 10.14505/jemt.v10.3(35).01

Kashyap, A., Kumari, S., Garg, P., Kushwaha, R., Tripathi, S., Sharma, J., Gupta, N.C., Kumar, R.R., Yadav, R. & Vishwakarma, H. 2023. Indexing Resilience to Heat and Drought Stress in the Wild Relatives of Rapeseed-Mustard. *Life* **13**(3), 738. doi: 10.3390/life13030738

Keim, J., Daza, J., Beltrán, I., Balocchi, O., Pulido, R., Sepúlveda-Varas, P., Pacheco, D. & Berthiaume, R. 2020. Milk production responses, rumen fermentation, and blood metabolites of dairy cows fed increasing concentrations of forage rape (Brassica napus ssp. Biennis). *Journal of Dairy Science* **103**, 9054–9066.

Kemper, R., Bublitz, T.A., Müller, P., Kautz, T., Döring, T.F. & Athmann, M. 2020. Vertical root distribution of different cover crops determined with the profile wall method. *Agriculture* **10**, 503. doi: 10.3390/agriculture10110503

Kemper, R., Döring, T.F., Legner, N., Meinen C. & Athmann, M. 2023. Oilseed radish, winter rye and crimson clover: root and shoot performance in cover crop mixtures. *Plant Soil*. URL: https://link.springer.com/article/10.1007/s11104-023-06240-y#citeas (Access April 25, 2024) doi: 10.1007/s11104-023-06240-y

Kirkegaard, J.A. & Sarwar, M. 1998. Biofumigation potential of brassicas: I. Variation in glucosinolate profiles of diverse field-grown brassicas. *Plant and Soil* **201**(1), 71–89.

Kou, X, Han, W. & Kang, J. 2022. Responses of root system architecture to water stress at multiple levels: A meta-analysis of trials under controlled conditions. *Frontiers Plant Science* **13**, 1085409. doi: 10.3389/fpls.2022.1085409

Kriaučiūnienė, Z., Velička, R. & Raudonius, S. 2012. The infuence of crop residues type on their decomposition rate in the soil: a litterbag study. *Zemdirbyste* **99**, 227–236.

Kul, R., Ekinci, M., Turan, M., Ors, S. & Yildirim, E. 2021. How Abiotic Stress Conditions Affects Plant Roots. *IntechOpen*. URL: https://www.researchgate.net/publication/348208107_How_Abiotic_Stress_Conditions_Affects_Plant_Roots (Access April 20, 2024) doi: 10.5772/intechopen.95286

Källén, A.S. 2023. *Underlying mechanisms behind nitrous oxide emissions in oilseed radish, Raphanus sativus var. oleiformis, and Phacelia tanacetifolia*. Independent Project in Biology, A2E. Swedish University of Agricultural Sciences, SLU, 49 pp.

Kılıç, Ü., Erişek, A., Garipoğlu, A., Ayan, İ. & Önder, H. 2021. The effects of different forage types on feed values and digestibilities in some brassica fodder crops. *Turkish Journal of Agricultural and Natural Sciences* **8**(1), 94–102. doi: 10.30910/turkjans.747031

Lallement, A., Peyrelasse, C., Lagnet, C., Barakat, A., Schraauwers, B., Maunas, S. & Monlau, F. 2023. A Detailed Database of the Chemical Properties and Methane Potential of Biomasses Covering a Large Range of Common Agricultural Biogas Plant Feedstocks. *Waste* **1**(1), 195–227. doi: 10.3390/waste1010014

Latief, A., Raihana, K.H., Sabah, P. & Syed, S.M. 2017. *Experimental Agrometeorology: A Practical Manual*. Cham: Springer International Publishing, 159 pp.

Launay, C., Houot, S., Frédéric, S., Girault, R., Levavasseur, F., Marsac, S. & Constantin, J. 2022. Incorporating energy cover crops for biogas production into agricultural systems: benefits and environmental impacts. A review. *Agronomy for Sustainable Development* **42**, 57. doi: 10.1007/s13593-022-00790-8

Lee, C.-R., Kim, S.H., Oh, Y., Kim, Y.J. & Lee, S.-M. 2023. Effect of Green Manure on Water-Stable Soil Aggregates and Carbon Storage in Paddy Soil. *Korean Journal of Soil Science and Fertilizer* **56**(2), 191–198. doi:10.7745/KJSSF.2023.56.2.191

Lei, B., Wang, J. & Yao, H. 2022. Ecological and environmental benefits of planting green manure in paddy fields. *Agriculture* **12**(2), 223. doi: 10.3390/agriculture12020223

Letey, J., Jarrell, W.M. & Valoras, N. 1982. Nitrogen and water uptake patterns and growth of plants at various minimum solution nitrate concentrations. *Journal of Plant Nutrition* **5**(2), 73–89. doi: 10.1080/01904168209362939

Li, S., Yu, W., Liu, X. & Wang, M. 2020. Analysis of root system architecture affected by swarming behavior. *Journal of Horticultural Research* **28**(1), 1–12. doi: 10.2478/johr-2020-0006

Li, W.G.M., Yang, X.X., Huang, C.G., Xue, N.W., Xia, Q., Liu, X.L., Zhang, X.Q., Yang, S., Yang, Z.P. & Gao, Z.Q. 2019. Effects of rapeseed green manure on soil fertility and bacterial community in dryland wheat field. *Agricultural Sciences in China* **52**, 2664–2677.

Li, Z.Y. & Zhou, D. 2002. Optimization of C/N ratio preparation of protein-rich and multi-enzymes feed thallus through synergic fermentation of mixed distillers' grains. *Journal of Environmental Sciences (China)* **14**(1), 141–144.

Liu, X.H., Zhou, X., Deng, L.C., Fan, L.Y., Qu, L. & Li, M. 2020. Decomposition characteristics of rapeseed green manure and effect of nutrient release on soil fertility. *Hunan Agricultural Science* **416**, 39–44.

Lopez, G., Ahmadi, S.H., Amelung, W., Athmann, M., Ewert, F., Gaiser, T, Gocke, M.I., Kautz, T., Postma, J., Rachmilevitch, S., Schaaf, G., Schnepf, A., Stoschus, A., Watt, M., Yu, P. & Seidel, S.J. 2023. Nutrient deficiency effects on root architecture and root-to-shoot ratio in arable crops. *Frontiers Plant Science* **13**, 1067498. doi: 10.3389/fpls.2022.1067498

Lucadamo, E.E., Holmes, A.A., Wortman, S.E. & Yannarell, A.C. 2022. Post-termination Effects of Cover Crop Monocultures and Mixtures on Soil Inorganic Nitrogen and Microbial Communities on Two Organic Farms in Illinois. *Frontiers Soil Science* **2**, 824087. doi: 10.3389/fsoil.2022.824087

Lymperatou, A., Engelsen, T.K., Skiadas, I.V. & Gavala, H.N. 2023. Prediction of methane yield and pretreatment efficiency of lignocellulosic biomass based on composition. *Waste Management* **155**, 302–310. doi: 10.1016/j.wasman.2022.10.040

Lövgren, E. 2022. *Complete removal of biomass from oilseed radish as a cover crop decreased nitrous oxide emissions*. Master's degree project. Swedish University of Agricultural Sciences, 46 pp.

Maier, S., Szerencsits, M. & Shahzad, K. 2017. Ecological evaluation of biogas from catch crops with Sustainable Process Index (SPI). *Energy, Sustainability and Society* **7**, 4. doi: 10.1186/s13705-017-0106-3

Manyi-Loh, C.E. & Lues, R. 2023. Anaerobic Digestion of Lignocellulosic Biomass: Substrate Characteristics (Challenge) and Innovation. *Fermentation* **9**(8), 755. doi: 10.3390/fermentation9080755

Martínez-Gutiérrez, E. 2018. Biogas production from different lignocellulosic biomass sources: advances and perspectives. *Biotechnology* **8**(5), 233. doi: 10.1007/s13205-018-1257-4

Mbambalala, L., Rani, Z.T., Mpanza, T.D.E., Mthana, M.S., Ncisana, L. & Mkhize, N.R. 2023. Fodder Radish as a Potential Alternative Feed Source for Livestock in South Africa. *Agriculture* **13**(8), 1625. doi: 10.3390/agriculture13081625

McDowell, N., Pockman, W.T., Allen, C.D., Breshears, D.D., Cobb, N., Kolb, T., Plaut, J., Sperry, J., West, A., Williams, D.G. & Yepez, E.A. 2008. Mechanisms of plant survival and mortality during drought: why do some plants survive while others succumb to drought? *New Phytologist* **178**, 719–739. doi: 10.1111/j.1469-8137.2008.02436.x

Milford, G.F.J. & Evans, E.J. 1991. Factors Causing Variation in Glucosinolates in Oilseed Rape. *Outlook on Agriculture* **20**(1), 31–37. doi: 10.1177/003072709102000107

Mocniak, L.E., Elkin, K.R., Dillard, S.L., Bryant, R.B. & Soder, K.J. 2023. Building comprehensive glucosinolate profiles for brassica varieties. *Talanta* **251**, 123814. doi: 10.1016/j.talanta.2022.123814

Molinuevo-Salces, B., Larsen, S. U., Ahring, B. K. & Uellendahl, H. 2013. Biogas from Italian ryegrass and oil seed radish: Effect of nitrogen application on biomass yield and methane production. Poster presented at 21st European Biomass Conference and Exhibition, Copenhagen, Denmark. URL: https://core.ac.uk/download/pdf/60543231.pdf (date of application 22.08.2023).

Molinuevo-Salces, B., Larsen, S.U., Ahring, B.K. & Uellendahl, H. 2014. Biogas production from catch crops: a sustainable agricultural strategy to increase biomass yield by coharvest of catch crops and straw. In *22nd European Biomass Conference and Exhibition* (EU BC&E 2014 - Hamburg, Germany. 5 pp.

Moral, F.J., Rebollo, F.J., Paniagua, L.L., García-Martín, A. & Honorio, F. 2016. Spatial Distribution and Comparison of Aridity Indices in Extremadura, Southwestern Spain. *Theoretical and Applied Climatology* **126**, 801–814. doi: 10.1007/s00704-015-1615-7

Murphy, J., Braun, R., Weiland, P. & Wellinger, A. 2011. Biogas from Crop Digestion. Task 37 - Energy from Biogas. *IEA Bioenergy*, 24 pp.

Navarro, D.M.D.L., Abelilla, J.J. & Stein, H.H. 2019. Structures and characteristics of carbohydrates in diets fed to pigs: a review. *Journal of Animal Science and Biotechnology* **10**, 39. doi: 10.1186/s40104-019-0345-6

Ngatia, L.W., Reddy, K.R., Nair, P.R., Pringle, R.M., Palmer, T.M. & Turner, B.L. 2014. Seasonal patterns in decomposition and nutrient release from East African savanna grasses grown under contrasting nutrient conditions. *Agriculture, Ecosystems & Environment* **188**, 12–19.

Nielsen, S.S. 2010. *Complexometric Determination of Calcium*. In: Nielsen, S.S. (eds) Food Analysis Laboratory Manual. Food Science Texts Series. Springer, Boston, MA., 61–67. doi: 10.1007/978-1-4419-1463-7_8

Nithisha, A., Bokado, K. & Charitha, K.S. 2022. Mulches: Their impact on the crop production. *The Pharma Innovation Journal* **11**(7), 3597–3603.

Nobile, C., Houben, D., Michel, E., Firmin, S., Lambers, H., Kandeler, E. & Faucon, M.-P. 2019. Phosphorus-acquisition strategies of canola, wheat and barley in soil amended with sewage sludges. *Science Reports* **9**, 14878. doi: 10.1038/s41598-019-51204-x

Norberg, L. & Aronsson, H. 2020. Effects of cover crops sown in autumn on N and P leaching. *Soil Use and Management* **36**(2), 200–211. doi: https://doi.org/10.1111/sum.12565

Oliveira, W.K. & Słomka, A. 2021. Assessment of the Biogas Yield of White Mustard (Sinapis alba) Cultivated as Intercrops. *Journal of Ecological Engineering* **22**(7), 67–72. doi: 10.12911/22998993/138815

Olofsson, F. & Ernfors, M., 2022. Frost killed cover crops induced high emissions of nitrous oxide. *Science Total Environment* **837**, 155634. doi: 10.1016/j. scitotenv.2022.155634.

Omokanye, A., Hernandez, G., Lardner, H.A., Al-Maqtari, B., Gill, K.S. & Lee, A. 2021. Alternative forage feeds for beef cattle in Northwestern Alberta, Canada: Forage yield and nutritive value of forage brassicas and forbs. *Journal of Applied Animal Research* **49**, 203–210.

Pan, D., Tang, J., Zhang, L., He, M. & Kung, C. 2021. The impact of farm scale and technology characteristics on the adoption of sustainable manure management technologies: Evidence from hog production in China. *Journal of Cleaner Production* **280**, 1243–1250. doi: 10.1016/j.jclepro.2020.124340

Pekarek, R.A., Hoyt, G., Monks, D. & Jennings, K. 2013. Biomass Production of Biofumigant Cover Crops – 'Caliente' Mustard and Oilseed Radish. *NC State Extension Publications*. AG-782. URL: https://content.ces.ncsu.edu/biomass-production-of-biofumigant-cover-crops-caliente-mustard-and-oilseed-radish (date of access April 21, 2024).

Perniola, O.S., Chorzempa, S.E., Staltari, S. & Molina, M. del C. 2019. Biofumigación con Brassica juncea: efecto sobre la flora arvense. *Revista De La Facultad De Agronomía* **118**(1), 25–35. doi: 10.24215/16699513e003

Poorter, H., Niklas, K.J., Reich, P.B., Oleksyn, J., Poot, P. & Mommer, L. 2012. Biomass allocation to leaves, stems and roots: meta-analyses of interspecific variation and environmental control. *New Phytologist* **193**, 30–50. doi: 10.1111/j.1469-8137.2011.03952.x

Prieto, M., López, C.J. & Simal-Gandara, J. 2019. Glucosinolates: Molecular structure, breakdown, genetic, bioavailability, properties and healthy and adverse effects. *Advances in Food and Nutrition Research* **90**, 305–350.

Quemada, M. & Cabrera, M.L. 1995. Carbon and nitrogen m ineralized from leaves and stem s of 4 cover crops. *Soil Science Society of America Journal* **59**, 471–477.

Quintarelli, V., Radicetti, E., Allevato, E., Stazi, S.R., Haider, G., Abideen, Z., Bibi, S., Jamal, A. & Mancinelli, R. 2022. Cover Crops for Sustainable Cropping Systems: A Review. *Agriculture* **12**, 2076. doi: 10.3390/agriculture12122076

Rajković, D., Marjanović Jeromela, A., Pezo, L., Lončar, B., Zanetti, F., Monti, A. & Kondić Špika, A. 2022. Yield and Quality Prediction of Winter Rapeseed–Artificial Neural Network and Random Forest Models. *Agronomy* **12**(1), 58. doi: 10.3390/agronomy12010058

Ramirez-Garcia, J., Almendros, P. & Quemada, M. 2012. Ground cover and leaf area index relationship in a grass, legume and crucifer crop. *Plant, Soil and Environment* **58**, 385–390.

Ramírez-García, J., Carrillo, J.M., Ruiz, M., Alonso-Ayuso, M. & Quemada, M. 2015. Multicriteria Decision Analysis Applied to Cover Crop Species and Cultivars Selection. *Field Crops Research* **175**, 106–115.

Ramírez-García, J., Gabriel, J.L., Alonso-Ayuso, M. & Quemada, M. 2015a. Quantitative characterization of five cover crop species. *The Journal of Agricultural Science* **153**, 1174–1185. doi:10.1017/S0021859614000811

Rao, R.V. 2007. *Decision Making in the Manufacturing Environment, Using Graph Theory and Fuzzy Multiple Attribute Decision Making Methods*. Springer: Berlin/Heidelberg, Germany, 294 pp.

Redha, A.A., Torquati, L., Langston, F., Nash, G.R., Gidley, M.J. & Cozzolino, D. 2023. Determination of glucosinolates and isothiocyanates in glucosinolate-rich vegetables and oilseeds using infrared spectroscopy: A systematic review. *Critical Reviews in Food Science and Nutrition* **10**, 1–17. doi: 10.1080/10408398.2023.2198015

Restovich, S.B., Andriulo, A.E. & Portela, S.I. 2022. Cover crop mixtures increase ecosystem multifunctionality in summer crop rotations with low N fertilization. *Agronomy for Sustainable Development* **42**, 19. doi: 10.1007/s13593-021-00750-8

Ricardo, L.L., Bernardi, D.I., Mantovanelli, G.C., Moreno, B.P., Mito, M.S., Silva, A.A., Oliveira, R.S., Iwamoto, E.L., Sarragiotto, M.H. & Baldoqui, D.C. 2018. Phytochemical investigation and phytotoxic activity of aerial parts of oilseed radish (*Raphanus sativus* var. *oleifer* Stokes). *Biochemical Systematics and Ecology* **78**, 52–58. doi: 10.1016/j.bse.2018.03.009

Rinasoa, S., Nishigaki, T., Rabeharisoa, L., Tsujimoto, Y. & Rakotoson, T. 2022. Organic materials with high P and low C:P ratio improve P availability for lowland rice in highly weathered soils: Pot and incubation experiments. *Journal of Plant Nutrition and Soil Science* **185**, 475–485. doi: 10.1002/jpln.202100266

Rowland, A.P. & Roberts, J.D. 1994. Lignin and cellulose fractionation in decomposition studies using acid-detergent fibre methods. *Communications in Soil Science and Plant Analysis* **25**(3–4), 269–277. doi: 10.1080/00103629409369035

Saaty, T.L. & Vargas, L.G. 2012. *Models, Methods, Concepts & Applications of the Analytic Hierarchy Process*. Second Edition. Springer New York Heidelberg Dordrecht London, 345 pp.

Safaei, A.R., Rouzbehan, Y. & Aghaalikhani, M. 2022. Canola as a potential forage. *Translational Animal Science* **6**(3), txac100. doi: 10.1093/tas/txac100.

Salisbury, P.A., Potter, T.D., Gurung, A.M., Mailer, R.J. & Williams, W.M. 2018. Potential impact of weedy Brassicaceae species on oil and meal quality of oilseed rape (canola) in Australia. *Weed Research* **58**(3), 200–209. doi: 10.1111/wre.12296.

Salume, J.A., Oliveira, R.A., Sete, P.B., Comin, J.J., Ciotta, M.N., Lourenzi, C.R., Soares, C.R.F.S., Loss, A., Carranca, C., Giacomini, S.J., Boitt, G. & Brunetto, G. 2020. Decomposition and nutrient release from cover crop residues under a pear orchard. *Revista Brasileira de Ciências Agrárias* **43**, 72–81.

Sanchez, P.A., Cuoto, W. & Boul, S.W. 1982. The fertility capability soil classification system; interpretation application and modification. *Geoderma* **27**, 238–309.

Sang, J.P., Minchinton, I.R., Johnstone, P.K. & Truscott, R.J.W. 1984. Glucosinolate profiles in the seed, root and leaf tissue of cabbage, mustard, rapeseed, radish and swede. *Canadian Journal of Plant Science* **64**(1), 77–93. doi: 10.4141/cjps84-011

Sarıkamıs, G., Aydınlı, G. & Mennan, S. 2017. Glucosinolates in some brassica species as sources of bioactive compounds against root knot nematodes. *International Journal of Advanced Research* **5**, 271–278. doi: 10.21474/IJAR01/5530

Scavo, A., Fontanazza, S., Restuccia, A., Pesce, G.R., Abbate, C. & Mauromicaleet, G. 2022. The role of cover crops in improving soil fertility and plant nutritional status in temperate climates. A review. *Agronomy for Sustainable Development* **42**(5), 93. doi: 10.1007/s13593-022-00825-0ff.ffhal-04201630

Sharma, P. & Dubey, R.S. 2019. Protein Synthesis by Plants Under Stressful Conditions. In: *Handbook of Plant and Crop Stress, Fourth Edition*. CRC Press, 45 pp.

Sharma, S., Kaur, S., Parkash Choudhary, O., Singh, M., Al-Huqail, A.A., Ali, H.M., Kumar, R. & Siddiqui, M.H. 2022. Tillage, green manure and residue retention improves aggregate-associated phosphorus fractions under rice–wheat cropping. *Scientific Reports* **12**, 7167. doi: 10.1038/s41598-022-11106-x

Shitophyta, L.M., Putri, S.R., Salsabiella, Z.A., Budiarti, G.I., Rauf, F. & Khan, A. 2023. Theoretical Biochemical Methane Potential Generated by the Anaerobic Digestion of Mustard Green Residues in Different Dilution Volumes. *Polish Journal of Environmental Studies* **32**(5), 4799–4804. doi: 10.15244/pjoes/162690

Sieling, K. 2019. Improved N transfer by growing catch crops – a challenge. *Journal für Kulturpflanzen* **71**(6), 145–160. doi: 10.5073/JfK.2019.06.01

Silva, G.O.A., Southam, G. & Gagen, E.J. 2023 Accelerating soil aggregate formation: a review on microbial processes as the critical step in a post-mining rehabilitation context. *Soil Research* **61**(3), 209–223. doi: 10.1071/SR22092

Simeão, R.M., Silva, D.D., Santos, F.C., Vilela, L., Silveira, M.C.T., Resende, A.C. & Albuquerque, P.E.P. 2023. Adaptation and indication of forage crops for agricultural production in sandy soils in western Bahia State, Brazil. *Acta Scientiarum. Agronomy* **45**, e56144. doi: 10.4025/actasciagron.v45i1.56144

Singh, D., Devi, K.B., Ashoka, P., Bahadur, R., Kumar, N., Devi, O.R. & Shahni, Y.S. 2023. Green Manure: Aspects and its Role in Sustainable Agriculture. *International Journal of Environment and Climate Change* **13**(11), 39–45. doi: 10.9734/ijecc/2023/v13i113142

Snapp, S.S., Swinton, S.M., Labarta, R., Mutch, D., Black, J.R., Leep, R., Nyiraneza, J. & O'neil, K. 2005. Evaluating cover crops for benefits, costs and performance within cropping system niches. *Agronomy Journal* **97**(1), 322–332. doi: 10.2134/ agronj2005.0322a

Snecdecor, G.W. & Cochran, W.G. 1991. *Statistical Methods, 8th Edition*. Wiley-Blackwell, 524 pp.

Sousa, D.C., Medeiros, J.C., Lacerda, J.J.J., Rosa, J.D., Boechat, C.L., Sousa, M.N. G., Mafra, A.L. 2019. Dry mass accumulation, nutrients and decomposition of cover plants. *Journal of Agricultural Science* **11**(5), 152–160. doi: https://doi.org/10.5539/jas.v11n5p152

Sparks, D.L., Page, A.L., Helmke, P.A., Loeppert, R.H., Soltanpour, P.N., Tabatabai, M.A., Johnston, C.T. & Sumner, M.E. 1996. *Methods of Soil Analysis*, Part 3: Chemical Methods. Soil Science Society of America, Inc., American Society, 1424 pp.

Stubbs, T. & Kennedy, A.C. 2017. Prediction of Canola Residue Characteristics Using Near-Infrared Spectroscopy. *International Journal of Agronomy*, 4813147, 1–9. doi: 10.1155/2017/4813147

Swarcewicz, M., Adaszynska, M. & Wrzesinska, E. 2013. Chemical Composition of Macerated Plant Parts of White Mustard Sinapis alba. *Chemistry of Natural Compounds* **49**, 557–558. doi: 10.1007/s10600-013-0671-4

Szczepanek, M & Siwik-Ziomek, A.P 2019. K Accumulation by Rapeseed as Affected by Biostimulant under Different NPK and S Fertilization Doses. *Agronomy* **9**(9), 477. doi: 10.3390/agronomy9090477

Sánchez, R.D.G., Sánchez, D.J.I., Ochoa, M.E., González Cifuentes, A.I., Reyes González, A. & Hernández, R.K. 2023. Yield and nutritional value of forage brassicas compared to traditional forages. *Revista Mexicana de Ciencias Pecuarias* **14**, 237–247.

Śmiechowska, A., Bartoszek, A. & Namieśnik, J. 2010. Determination of glucosinolates and their decomposition products-indoles and isothiocyanates in cruciferous vegetables. *Critical Reviews in Analytical Chemistry* **40**, 202–216. doi: 10.1080/ 10408347.2010.490489

Test Guidelines for the conduct of tests for distinctness. uniformity and stability of Fodder Radish (*Raphanus sativus* L. var. *oleiformis* Pers.). 2017. Geneva, 23 pp.

Thiébeau, P., Jensen, L.S., Ferchaud, F. & Recous, S. 2021. Dataset of biomass and chemical quality of crop residues from European areas. *Data in Brief* **37**, 1–8. doi: 10.1016/j.dib.2021.107227ff

Thorup-Kristensen, K. & Kirkegaard, J. 2016. Root system-based limits to agricultural productivity and efficiency: the farming systems context. *Annals Bottany* **118**(4), 573–592. doi: 10.1093/aob/mcw122

Tian, Y. & Deng, F. 2020. Phytochemistry and biological activity of mustard (Brassica juncea): a review. *CyTA – Journal of Food* **18**(1), 704–718. doi: 10.1080/19476337.2020.1833988

Tixier, P, Lavigneb, C., Álvareza, S., Gauquierb, A., Blancharda, M.G., Ripochea, A. & Acharda, R. 2010. Model evaluation of cover crops, application to eleven species for banana cropping systems. *European Journal of Agronomy* **34**(2), 53–61. doi: 10.1016/j.eja.2010.10.004

Tjørve, K.M.C. & Tjørve, E. 2017. The use of Gompertz models in growth analyses, and new Gompertz-model approach: An addition to the Unified-Richards family. *PLoS One* **12**(6), e0178691. doi: 10.1371/journal.pone.0178691

Tokarchuk, D., Pryshliak, N., Yaremchuk, N. & Berezyuk, S. 2023. Sorting, Logistics and Secondary Use of Solid Household Waste in Ukraine on the Way to European Integration. *Ecological Engineering and Environmental Technology* **24**(1), 207–220. doi: 10.12912/27197050/154995

Toleikiene, M., Arlauskiene, A., Fliesbach, A., Iqbal, R., Sarunaite, L. & Kadziuliene, Z. 2020. he decomposition of standardised organic materials in loam and clay loam arable soils during a non-vegetation period. *Soil and Water Research* **15**(3), 181–190. doi: 10.17221/31/2019-swr

Toom, M., Talgre, L., Pechter, P., Narits, L., Tamm, S. & Lauringson, E. 2019. The effect of sowing date on cover crop biomass and nitrogen accumulation. *Agronomy Research* **17**(4), 1779–1787. doi: https://doi.org/10.15159/AR.19.164

Tsytsiura, Y. 2022. The influence of agroecological and agrotechnological factors on the generative development of oilseed radish (*Raphanus sativus* var. *oleifera* Metzg.). *Agronomy Research* **20**(4), 842–880. doi: 10.15159/ar.22.035

Tsytsiura, Y. 2023a. Estimation of biomethane yield from silage fermented biomass of oilseed radish (*Raphanus sativus* L. var. *oleiformis* Pers.) for different sowing and harvesting dates. *Agronomy Research* **21**(2), 940–978. 10.15159/AR.23.101

Tsytsiura, Y 2024. Ecological Approach to the Identication of the Degree of Phytophage Damage Based on Chlorophyll Fluorescence Induction in Oilseed Radish (*Raphanus sativus* L. var. *oleiformis* Pers.). *Journal of Ecological Engineering* **25**(2), 227–243. doi: 10.12911/22998993/176983

Tsytsiura, Y. 2020a. Formation and determination of the individual area of oilseed radish leaves in agrophytocenosises of different technological construction. *Agronomy Research* **18**(3), 2217–2244. doi: 10.15159/AR.20.219

Tsytsiura, Y. 2023b. Evaluation of oilseed radish (*Raphanus sativus* l. var. *oleiformis* Pers.) oil as a potential component of biofuels. *Engenharia Agrícola, Jaboticabal* **43**(Special issue), e20220137. doi: 10.1590/1809-4430-Eng.Agric.v43nepe20220137/2023.

Tsytsiura, Y. 2023c. Assessment of the relation between the adaptive potential of oilseed radish varieties (*Raphanus sativus* L. var. *oleiformis* Pers.) and chlorophyll fluorescence induction parameters. *Agronomy Research* **20**(1), 193–221. doi: 10.15159/AR.23.001

Tsytsiura, Y.H. 2019. Evaluation of the efficiency of oilseed radish agrophytocoenosis construction by the factor of reproductive effort. *Bulgarian Journal of Agricultural Science* **25**(6), 1161–1174.

Tsytsiura, Y.H. 2020. Modular-vitality and ideotypical approach in evaluating the efficiency of construction of oilseed radish agrophytocenosises (*Raphanus sativus* var. *oleifera* Pers.). *Agraarteadus* **31**(2), 219–243. doi: 10.15159/jas.20.27

Tsytsiura, Y.H. 2021. Matrix quality variability of oilseed radish (Raphanus sativus l. var. oleiformis Pers.) and features of its formation in technologically different construction of its agrophytocenosis. *Agronomy Research* **19**(1), 300–326 doi: 10.15159/ar.21.003

Ugrenović, V., Filipović, V., Jevremović, S., Marjanović, J.A., Popović, V., Buntić, A. & Delić, D. 2019. Effect of Brassicaceae as cover crops. *Selekcija i semenarstvo* **25**(2), 1–8. doi: 10.5937/SelSem1902001U (in Serbian).

Undersander, D., Mertens, D.R. & Thiex, N. 1993. *Forage analyses*. Procedures. National Forage Testing Association, 139 pp.

Van Soest, P.J., Robertson, J.B. & Lewis, B.A., 1991. Methods for dietary fiber, neutral detergent fiber, and nonstarch polysaccharides in relation to animal nutrition. *Journal of Dairy Science* **74**, 3583–3597. doi: 10.3168/jds.S0022-0302(91)78551-2

Velasco, P., Soengas, P., Vilar, M., Cartea, M.E. & del Rio, M. 2008. Comparison of glucosinolate profiles in leaf and seed tissues of different Brassica napus crops. *Journal of the American Society for Horticultural Science* **133**(4), 551–558. doi: 10.21273/JASHS.133.4.551

Venslauskas, K., Navickas, K., Rubežius, M., Žalys, B. & Gegeckas, A. 2024. Processing of Agricultural Residues with a High Concentration of Structural Carbohydrates into Biogas Using Selective Biological Products. *Sustainability* **16**(4), 1553. doi: 10.3390/su16041553

Villalobos, L. & Brummer, J. 2013. Evaluation of Brassicas for fall forage. In *Proceedings of theWestern States Alfalfa and Forage Symp*, Reno, NV, USA, 17–31.

Wadman, W.P. & de Haan, S. 1997. Decomposition of organic matter from 36 soils in a long-term pot experiment. *Plant and Soil* **189**(2), 289–301.

Wahlström, E.M., Hansen, E.M., Mandel, A., Garbout, A., Kristensen, H.L. & Munkholm, L.J. 2015. Root development of fodder radish and winter wheat before winter in relation to uptake of nitrogen. *European Journal of Agronomy* **71**, 1–9. doi:10.1016/J.EJA.2015.07.002

Wallace, A. & Mueller, R.T. 1980. Calcium uptake and distribution in plants. *Journal of Plant Nutrition* **2**, 247–256.

Wang, X., Ma, H., Guan, C. & Guan, M. 2022. Decomposition of Rapeseed Green Manure and Its Effect on Soil under Two Residue Return Levels. *Sustainability* **14**, 11102. doi: 10.3390/ su141711102

Wang, X., Yang, G., Feng, Y., Ren, G. & Han, X. 2012. Optimizing feeding composition and carbon-nitrogen ratios for improved methane yield during anaerobic co-digestion of dairy, chicken manure and wheat straw. *Bioresource Technology* **120**, 78–83. doi: 10.1016/j.biortech.2012.06.058

Warren, J., Meeks, K. & Edwards, J.. 2017. Benefits of using cover crops in Oklahoma no-till. *Bull. PSS-2161*. Oklahoma Cooperative Extension Service. Oklahoma State University. Stillwater, OK, 41 pp.

Weih, M., Hamner, K. & Pourazari, F. 2018. Analyzing plant nutrient uptake and utilization efficiencies: Comparison between crops and approaches. *Plant Soil* **430**, 7–21.

Wendling, M., Büchi, L., Amossé, C., Sinaj, S., Walter, A. & Charles, R. 2016. Influence of root and leaf traits on the uptake of nutrients in cover crops. *Plant and Soil* **409**(1–2), 419–434.

Werker, A.R. & Jaggard, K.W. 1997. Modelling asymmetrical growth curves that rise and then fall: applications to foliage dynamics of sugar beet (*Beta vulgaris* L.). *Annals of Botany* **79**, 657–665.

Westwood, C.T. & Mulcock, H. 2012. Nutritional evaluation of five species of forage brassica. *Journal of New Zealand Grasslands* **74**, 31–38.

White, C.A., Holmes, H.F., Morris, N.L. & Stobart, R.M. 2016. *A review of the benefits, optimal crop management practices and knowledge gaps associated with different cover crop species*. Research Review №. 90. AHDB Cereals & Oilseeds, 90 pp.

Williams, J.D., McCool, D.K., Reardon, C.L., Douglas, C.L., Albrecht, S.L. & Rickman, R.W. 2013. Root:shoot ratios and belowground biomass distribution for Pacific Northwest dryland crops. *Journal of Soil and Water Conservation* **68**(5), 349–360. doi: 10.2489/jswc.68.5.349

Winkler, O.R.T. 2017. *Agronomic studies of forage brassicas as full-season and cover crops for grazing in North Dakota*. PhD Thesis. North Dakota State University, 219 pp.

Wollford, A.R. & Jarvis, P.E. 2017. *Cover, catch and companion crops. Benefits, challenges and economics for UK growers*. Game & Wildlife Trust The Allerton Project, 28 pp.

Wong, J. 2018. *Handbook of statistical analysis and data mining applications*. Cambridge, Academic Press. 589 pp.

Wu, X., Huang, H., Childs, H., Wu, Y., Yu, L. & Pehrsson, P.R. 2021. Glucosinolates in Brassica Vegetables: Characterization and Factors That Influence Distribution, Content, and Intake. *Annual Review of Food Science and Technology* **12**(1), 485–511. doi: 10.1146/annurev-food-070620-025744

Yahbi, M., Keli, A., El Alami, N., Nabloussi, A., Maataoui, A. & Daoui, K. 2024. Chemical composition and quality of rapeseed meal as affected by genotype and nitrogen fertilization. *OCL* **31**, 5. doi: 10.1051/ocl/2024004

Yan, C., Huang, Y., Zhang, S., Cui, L., Jiao, Z., Peng, Z., Luo, X., Liu, Y. & Qiu, Z. 2023. Dynamic profiling of intact glucosinolates in radish by combining UHPLC-HRMS/MS and UHPLC-QqQ-MS/MS. *Frontiers Plant Science* **14**, 1216682. doi: 10.3389/fpls.2023.1216682

Yasumoto, S., Matsuzaki, M., Hirokane, H. & Okada, K. 2010. Glucosinolate Content in Rapeseed in Relation to Suppression of Subsequent Crop. *Plant Production Science* **13**(2), 150–155. doi: 10.1626/pps.13.150

Yi, G., Lim, S., Chae, W.B., Park, J.E., Park, H.R., Lee, E.J. & Huh, J.H. 2016. Root Glucosinolate Profiles for Screening of Radish (*Raphanus sativus* L.) Genetic Resources. *Journal of Agricultural and Food Chemistry* **64**(1), 61–70. doi: 10.1021/acs.jafc.5b04575

Yousefi, M., Dray, A. & Ghazoul, J. 2024. Assessing the effectiveness of cover crops on ecosystem services: a review of the benefits, challenges, and trade-offs. *International Journal of Agricultural Sustainability* **22**(1), 2335106 doi: 10.1080/14735903.2024.2335106

Zachariah, H. 2011. *Potential of three brassica cover crops for biofumigation in the field and the relationship between soil myrosinase and biofumigation efficacy*. PhD Thesis. Clemson University. TigerPrints. 1248, 136 pp.

Zhou, P., Graether, S.P., Hu, L. & Zhang, W. 2023. Editorial: The role of stress proteins in plants under abiotic stress. *Frontiers in Plant Science* **4**(14), 1193542. doi: 10.3389/fpls.2023.1193542

Ţiţei, V. 2022. The quality of fresh and ensiled biomass from white mustard, Sinapis alba, and its potential uses. *Scientific Papers. Series A. Agronomy* **1**(65), 559–566.

INSTRUCTIONS TO AUTHORS

Papers must be in English (British spelling). Authors are strongly urged to have their manuscripts reviewed linguistically prior to submission. Contributions should be sent electronically. Papers are considered by referees before acceptance. The manuscript should follow the instructions below.

Structure: Title, Authors (initials & surname; an asterisk indicates the corresponding author), Authors' affiliation with postal address (each on a separate line) and e-mail of the corresponding author, Abstract (up to 250 words), Key words (not repeating words in the title), Introduction, Materials and methods, Results and discussion, Conclusions, Acknowledgements (optional), References.

Layout, page size and font

- Use preferably the latest version of **Microsoft Word**, doc., docx. format.
- Set page size to **ISO B5 (17.6×25 cm)**, all **margins at 2 cm**. All text, tables, and figures must fit within the text margins.
- Use single line spacing and **justify the text**. Do not use page numbering. Use **indent 0.8 cm** (do not use tab or spaces instead).
- Use font Times New Roman, point size for the title of article **14 (Bold)**, author's names 12, core text 11; Abstract, Key words, Acknowledgements, References, tables, and figure captions 10.
- Use *italics* for Latin biological names, mathematical variables and statistical terms.
- Use single ('…') instead of double quotation marks ("…").

Tables

- All tables must be referred to in the text (Table 1; Tables 1, 3; Tables 2–3).
- Use font Times New Roman, regular, 10 pt. Insert tables by Word's 'Insert' menu.
- Do not use vertical lines as dividers; only horizontal lines (1/2 pt) are allowed. Primary column and row headings should start with an initial capital.

Figures

- All figures must be referred to in the text (Fig. 1; Fig. 1 A; Figs 1, 3; Figs 1–3). Use only black and white or greyscale for figures. Avoid 3D charts, background shading, gridlines and excessive symbols. Use font **Arial, 10 pt** within the figures. Make sure that thickness of the lines is greater than 0.3 pt.
- Do not put caption in the frame of the figure.
- The preferred graphic format is Excel object; for diagrams and charts EPS; for half-tones please use TIFF. MS Office files are also acceptable. Please include these files in your submission.
- Check and double-check spelling in figures and graphs. Proof-readers may not be able to change mistakes in a different program.

References

- **Within the text**

In case of two authors, use '&', if more than two authors, provide first author 'et al.':

Smith & Jones (2019); (Smith & Jones, 2019);

Brown et al. (2020); (Brown et al., 2020)

When referring to more than one publication, arrange them by following keys: 1. year of publication (ascending), 2. alphabetical order for the same year of publication:

(Smith & Jones, 2019; Brown et al., 2020; Adams, 2021; Smith, 2021)

- **For whole books**

Name(s) and initials of the author(s). Year of publication. *Title of the book* (*in italics*). Publisher, place of publication, number of pages.

Behera, K.B. & Varma, A. 2019. *Bioenergy for Sustainability and Security*. Springer International Publishing, Cham, pp. 1–377.

- **For articles in a journal**

Name(s) and initials of the author(s). Year of publication. Title of the article. *Abbreviated journal title* (*in italic*) volume (in bold), page numbers.

Titles of papers published in languages other than English, should be replaced by an English translation, with an explanatory note at the end, e.g., (in Russian, English abstr.).

Bulgakov, V., Adamchuk, V., Arak, M. & Olt, J. 2018. The theory of cleaning the crowns of standing beet roots with the use of elastic blades. *Agronomy Research* **16**(5), 1931–1949. doi: 10.15159/AR.18.213

Doddapaneni, T.R.K.C., Praveenkumar, R., Tolvanen, H., Rintala, J. & Konttinen, J. 2018. Techno-economic evaluation of integrating torrefaction with anaerobic digestion. *Applied Energy* **213**, 272–284. doi: 10.1016/j.apenergy.2018.01.045

- **For articles in collections:**

Name(s) and initials of the author(s). Year of publication. Title of the article. Name(s) and initials of the editor(s) (preceded by In:) *Title of the collection (in italics)*, publisher, place of publication, page numbers.

Yurtsev, B.A., Tolmachev, A.I. & Rebristaya, O.V. 2019. The floristic delimitation and subdivisions of the Arctic. In: Yurtsev, B.A. (ed.) *The Arctic Floristic Region*. Nauka, Leningrad, pp. 9–104 (in Russian).

- **For conference proceedings:**

Name(s) and initials of the author(s). Year of publication. Name(s) and initials of the editor(s) (preceded by In:) *Proceedings name (in italics)*, publisher, place of publishing, page numbers.

Ritchie, M.E. & Olff, H. 2020. Herbivore diversity and plant dynamics: compensatory and additive effects. In: Olff, H., Brown, V.K. & Drent R.H. (eds) *Herbivores between plants and predators. Proc. Int. Conf. The 38th Symposium of the British Ecological Society*, Blackwell Science, Oxford, UK, pp. 175–204.

Please note

- Use '.' (not ',') for decimal point: 0.6 ± 0.2; Use ',' for thousands – 1,230.4;
- Use '–' (not '-') and without space: pp. 27–36, 1998–2000, 4–6 min, 3–5 kg
- With spaces: 5 h, 5 kg, 5 m, 5 °C, C : D = 0.6 ± 0.2; $p < 0.001$
- Without space: 55°, 5% (not 55 °, 5 %)
- Use 'kg ha^{-1}' (not 'kg/ha');
- Use degree sign ' ° ' : 5 °C (not 5 ^{O}C).